

UNIVERSITE PARIS DESCARTES
FACULTE DE MEDECINE PARIS DESCARTES

THESE
pour obtenir le grade de
DOCTEUR
en Sciences de la Vie et de la Santé
Ecole Doctorale GC2ID
Discipline: Immunologie

présentée et soutenue par madame
Niloufar KAVIAN, épouse TESSLER

le 20 juin 2012

**Activation fibroblastique et nouvelles
approches thérapeutiques dans la
Sclérodermie systémique**

Jury

Président : Mme le Pr M-C. Béné

Directeur : Mr le Pr F. Batteux

Rapporteur : Mme le Pr S. Chollet-Martin

Rapporteur : Mr le Pr J-D. Lelièvre

Examinateur : Mme le Dr A. Servettaz

Examinateur : Mr le Pr N. Dupin

Examinateur : Mr le Pr X. Mariette

Remerciements

A Mr le Pr Frédéric Batteux,

Qui m'a fait l'honneur de diriger mon travail de recherche au laboratoire au cours de ces 4 années, avec une énergie inépuisable et une disponibilité sans failles. Ses connaissances et son accessibilité sont exemplaires. Qu'il reçoive ici toute ma reconnaissance.

A Mme le Pr Marie-Christine Béné,

Qui m'a fait l'honneur de présider le jury de cette thèse. Qu'elle reçoive ici l'expression de ma sincère gratitude.

A Mme le Pr Sylvie Chollet-Martin,

Qui m'a fait l'honneur d'être rapporteur de ce travail. Qu'elle soit assurée de toute ma sincère reconnaissance.

A Mr le Pr Jean-Daniel Lelièvre,

Qui m'a fait l'honneur d'être rapporteur de ce travail. Qu'il reçoive ici l'expression de toute ma reconnaissance.

A Mr le Pr Nicolas Dupin,

Qui m'a fait l'honneur d'examiner ce travail. Qu'il soit assuré de l'expression de toute ma reconnaissance.

A Mr le Pr Xavier Mariette,

Qui m'a fait l'honneur d'examiner ce travail. Qu'il reçoive ici l'expression de ma sincère gratitude.

A Mme le Dr Amélie Servettaz,

Qui m'a fait l'honneur d'examiner ce travail. Ses travaux antérieurs sur la sclérodermie systémique m'ont ouvert des perspectives qui ont donné naissance à ce travail. Ses connaissances et sa gentillesse en font un modèle. Qu'elle sache que je lui suis infiniment reconnaissante.

A Mr Bernard Weill, qui m'a permis de découvrir l'immunologie alors que j'étais interne, qui m'a encouragée dans cette voie, et qui m'a ouvert les portes de son laboratoire. Je le remercie pour son accessibilité de tout instant, sa gentillesse, ses conseils linguistiques et orthographiques, et la note d'humour qu'il sait apporter à chaque moment. Je lui suis infiniment reconnaissante.

A Mme Christiane Chéreau, pour sa gentillesse, son soutien, ses conseils "cellulaires", son aide quotidienne qui ont permis à ce travail d'aboutir. Je lui suis infiniment reconnaissante.

A Mme Carole Nicco, pour son soutien à toute épreuve, ses précieux conseils et connaissances "murines" qui ont permis à ce travail d'être possible. Son énergie communicative, sa bonne humeur et ses talents en matière de gâteaux au chocolat ont été d'une grande aide tout au long de ce travail. Je lui suis infiniment reconnaissante.

A mes complices du laboratoire: Céline Mongaret, Andrew Wang, Audrey Thomas, Mathilde Bahuaud, Wioleta Marut, Philippe Guipain, qui m'ont accompagnés durant ces 4 années, partageant des bureaux plus ou moins bien rangés, des tasses de thé, de la musique, des arrivées à Paris, des départs en province et à l'étranger, des mariages, des naissances, et les mêmes succès, joies et doutes concernant les "manips" et les résultats de recherche.

A Mme Claire Goulvestre, pour son accueil à mon arrivée au laboratoire il y a plusieurs années, sa gentillesse et son soutien.

A tous les collaborateurs et collaboratrices du laboratoire EA 1833 et du Service d'Immunologie Biologique de l'Hôpital Cochin.

A Olivier, pour le bonheur qu'il m'apporte chaque jour et celui, plus grand encore, qui nous attend dans quelques mois.

A Elisabeth, Otared, Ava-djoon, Azadeh, Laurent, pour leur affection, leur soutien de chaque moment, les joies partagées passées et à venir, parisiennes et tourangelles.

Aux mathématiciens-informaticiens D. Knuth, H. Hagen et R. Koch qui ont inventé TeX, ConteXt et TeXshop, logiciels ayant permis à ce travail d'être mis en forme; et enfin particulièrement à O.K qui s'est rendu disponible quel que soit le fuseau horaire ou le lieu pour me donner des leçons techniques sur ces logiciels.

Table des matières

Abréviations	6
Liste des figures	7
Chapitre 1. Physiopathologie de la ScS	10
1.1 Présentation de la maladie	10
1.2 Dysfonctionnements fibroblastiques	11
1.2.1 Anomalies intrinsèques des fibroblastes	12
1.2.1.1 Activation du gène du procollagène via la signalisation des récepteurs du TGF- β	12
1.2.1.2 Le Connective Tissue Growth Factor (CTGF)	15
1.2.1.3 Early growth response factor-1(Egr-1)	16
1.2.1.4 Molécules impliquées dans la dégradation de la matrice extracellulaire	17
1.2.1.5 Synthèse accrue de radicaux libres	18
1.2.1.6 Synthèse de chimiokines et cytokines	18
1.2.1.7 La voie Wnt/ β -catenin	18
1.2.1.8 Sp1 et Sp3	19
1.2.1.9 c-Myb	19
1.2.1.10 c-Myc	19
1.2.1.11 Synthèse d'une matrice extra-cellulaire capable de résister à la dégradation des métalloprotéases	19
1.2.1.12 La voie Fas/Fas-ligand	20
1.2.1.13 Des anomalies de la voie des kinases Erk1/2	20
1.2.2 Eléments extrinsèques majorant le dysfonctionnement fibroblastique	20
1.2.2.1 La Sérotonine	20
1.2.2.2 Le Platelet Derived Growth Factor (PDGF)	21
1.2.2.3 L'interleukine-4 (IL-4)	22
1.2.2.4 L'interleukine-13 (IL-13)	23
1.2.2.5 L'interleukine-17 (IL-17)	23
1.2.2.6 L'endothéline-1	24
1.2.2.7 TGF- β	24
1.2.3 Nouvelles voies d'activation fibroblastique	25
1.2.3.1 La voie des récepteurs Notch	25
1.2.3.2 La voie des récepteurs aux cannabinoïdes	33
1.3 Anomalies endothéliales	35
1.3.1 Modifications morphologiques	35

1.3.2 Recrutement local de leucocytes	35
1.3.3 Déséquilibre de l'équilibre coagulation/fibrinolyse	37
1.3.4 Anomalies de régulation du tonus vasculaire	37
1.3.5 Défaut d'angiogénèse	38
1.4 Intervention du système immunitaire	39
1.4.1 Immunité innée	39
1.4.2 Immunité adaptative cellulaire	39
1.4.3 Immunité adaptative humorale	41
1.4.3.1 Eléments contribuant à l'activation des lymphocytes B	41
1.4.3.2 Auto-anticorps : origine, nature et rôle pathogène	43
1.4.3.3 Thérapeutique ciblée dirigée contre les lymphocytes B	47
1.5 Facteurs génétiques et environnementaux	48
1.5.1 Facteurs génétiques	48
1.5.2 Facteurs environnementaux : virus et toxiques	49
1.6 Modèles animaux	50
1.6.1 Modèles spontanés	50
1.6.2 Modèles induits	52
Chapitre 2. Rôle des Formes Réactives de l'Oxygène (FRO)	56
2.1 Définition des FRO	56
2.2 origine des FRO	56
2.3 Rôle et conséquences des FRO	60
2.3.1 Action sur les protéines	61
2.3.2 Action sur les lipides	61
2.3.3 Action sur l'ADN	61
2.3.4 Rôles et conséquences des FRO dans le métabolisme cellulaire	61
2.3.5 Systèmes antioxydants physiologiques	63
2.3.5.1 Exemples de systèmes antioxydants enzymatiques	63
2.3.5.2 Exemples de systèmes antioxydants non-enzymatiques physiologiques	64
2.4 stress oxydant et immunologie	64
2.4.1 Rôle des FRO dans l'immunité anti-infectieuse	65
2.4.1.1 Mécanisme microbicide dépendant de l'oxygène	65
2.4.2 Rôle des FRO dans le contrôle de la réponse immunitaire	67
2.4.2.1 FRO et présentation de l'antigène	67
2.4.2.2 Production de FRO au cours de l'activation lymphocytaire T ..	67
2.4.2.3 FRO et mort cellulaire	68
2.5 Rôle des FRO en Immunopathologie	69
2.5.1 Rôle des FRO dans la genèse d'épitopes pathogènes	69
2.5.2 FRO et Sclérodermie systémique	70

Chapitre 3. Travaux personnels	72
3.1 Article 1	74
3.2 Article 2	88
3.3 Article 3	101
3.4 Article 4	113
3.5 Article 5	126
3.6 Article 6	163
Chapitre 4. Discussion	173
Chapitre 5. Conclusion et Perspectives	196
Chapitre 6. Annexes	198
Bibliographie	231

Abréviations

<i>Ab</i>	Antibody	<i>LT</i>	Lymphocyte T
<i>Ac</i>	Anticorps	<i>MCP-1</i>	Monocyte Chemoattractant Protein-1
<i>ADAM</i>	A Disintegrin and Metalloprotease	<i>MMP</i>	Matrix Metalloproteinase
<i>Ag</i>	Antigène	<i>NICD</i>	Notch Intra-Cellulaire Domain
<i>AOPP</i>	Advanced Oxidation Protein Products	<i>NKT</i>	Natural Killer T Cells
<i>BAFF</i>	B cell Activator Factor of the TNF Family	<i>pDC</i>	plasmacytoid Dendritic Cell
<i>CB</i>	Cannabinoïdes	<i>PDGF</i>	Platelet Derived Growth Factor
<i>CD</i>	Cluster de Différenciation	<i>PDGFR</i>	Platelet Derived Growth Factor Receptor
<i>CE</i>	Cellule endothéliale	<i>PS</i>	Présénillines
<i>CK</i>	Cytokine	<i>RBP-J</i>	Recombination signal binding protein for Ig K J region
<i>CPA</i>	Cellule Présentatrice de l'Antigène	<i>SCID</i>	Severe Combined ImmunoDeficiency
<i>CSH</i>	Cellule Souche Hématopoïétique	<i>Scl-GVHD</i>	Sclérodermie associée à la GVHD
<i>CTGF</i>	Connective Tissue Growth Factor	<i>ScS</i>	Sclérodermie Systémique
<i>Dll</i>	Delta like	<i>SMA</i>	Smooth Muscle Actin
<i>Egr</i>	Early Growth Response Factor	<i>TACE</i>	TNF- α Converting Enzyme
<i>ET1</i>	Endothelin-1	<i>TGF</i>	Transforming Growth Factor
<i>FIZZ1</i>	Found in Inflammatory Zone-1	<i>Th1</i>	lymphocyte T helper 1
<i>FRO</i>	Formes Réactives de l'Oxygène	<i>Th2</i>	lymphocyte T helper 2
<i>GSH</i>	Glutathion	<i>TIMP</i>	Tissue Inhibitor of Metalloproteinase
<i>GSI</i>	Gamma-Secretase Inhibitor	<i>TKI</i>	Tyrosine Kinase Inhibitor
<i>GVHD</i>	Graft-versus-host Disease	<i>TLR</i>	Toll like Receptors
<i>HIF1</i>	Hypoxia-Induced Factor 1	<i>TNF</i>	Tumor Necrosis Factor
<i>IFN</i>	Interferon	<i>TSK</i>	Tight Skin
<i>Ig</i>	Immunoglobuline	<i>VEGF</i>	Vascular Endothelial Growth Factor
<i>IL</i>	Interleukine	<i>VEGFR</i>	Vascular Endothelial Growth Factor Receptor
<i>KO</i>	Knock-Out	<i>ZM</i>	Zone Marginale
<i>LAM</i>	Leucémie Aigue Myéloïde		
<i>LB</i>	Lymphocyte B		
<i>LPS</i>	Lipopolysaccharide		

Liste des figures

Figure 1.1	Lien entre les dysfonctionnements des fibroblastes, des cellules endothéliales, et des cellules immunitaires dans la sclérodermie systémique d'après Varga J, Journal of Clinical Investigation, 2007.	11
Figure 1.2	Signalisation du TGF- β dépendante des protéines Smad, d'après Varga J, Journal of Clinical Investigation, 2007.	13
Figure 1.3	Signalisation du TGF- β indépendante des protéines Smad, d'après Varga J, Journal of Clinical Investigations, 2007.	14
Figure 1.4	Régulation des signaux médiés par le TGF- β par Egr-1, d'après S. Bhattacharyya, Matrix Biology, 2011	16
Figure 1.5	Structure des récepteurs Notch et de leurs ligands d'après Osborne A. 2007. RAM: RBP-J Associated Molecule, ANK: Ankyrin, NLS: Nuclear Localisation Sequence, TAD: Transactivation Domain, PEST: Proline, Glutamate, Serine, Threonine-rich domain.	26
Figure 1.6	Etapes d'activation des récepteurs Notch d'après Osborne A. 2007	27
Figure 1.7	La voie Notch dans le développement hématopoïétique et dans le système immunitaire d'après Maillard I. HB: hemangioblast, HSC: hematopoietic stem cell, CLP: common lymphoid progenitor, ETP: arly T lineage progenitor, DN: CD4-CD8-double-negative thymocytes, Treg: CD4+CD25+ regulatory T cells, TrB: transitional B cells, FB: follicular B cell, MZB: marginal zone B cell, APC: antigen presenting cell.	29

Figure 1.8	Liens possibles entre les anomalies endothéliales et la fibrose dans la sclérodermie systémique d'après M. Trojanowska, <i>Nature Reviews Rheumatology</i> , 2010. La vasculopathie sclérodermique serait initiée par une première lésion ou par l'influx de cellules immunitaires. De forts taux de VEGF et d'autres médiateurs proangiogéniques sécrétés par les cellules immunitaires facilitent la prolifération des cellules endothéliales et des péricytes dans le but de réparer les vaisseaux lésés. Mais, un déséquilibre du statut des médiateurs proangiogéniques/antiangiogéniques, les propriétés intrinsèques des cellules endothéliales, et les facteurs antiangiogéniques sécrétés par les fibroblastes (dont MMP-12), empêchent la réparation d'être efficace et entraînent les anomalies morphologiques des vaisseaux. En présence de TGF- β et d'autres médiateurs, les cellules endothéliales acquièrent un phénotype migratoire via la transition endothélio-mésenchymateuse, et peuvent se différencier en cellules productrices de collagène. Les fibroblastes résidents activés et les fibrocytes qui entrent dans le tissu lésé via la circulation représentent des sources additionnelles de collagène contribuant ainsi à la fibrose dans les lésions sclérodermiques. EPCs: endothelial progenitor cells.	36
Figure 1.9	Lymphocytes B et environnement cytokinique dans la sclérodermie systémique, d'après S. Bosello, <i>Autoimmunity Reviews</i> , 2011	42
Figure 1.10	Modèles animaux de sclérodermie systémique spontanés et induits, d'après F. Batteux et al. <i>Current Opinion in Rheumatology</i> , 2011	51
Figure 2.1	Les formes réactives de l'oxygène et leur origine, d'après Temple et al., <i>Trends Cell Biol</i> , 2005	57
Figure 2.2	Formation d'anion superoxyde lors des phénomènes d'ischémie-reperfusion	59
Figure 2.3	Régulation de la prolifération des cellules tumorales par le stress oxydant, d'après A. Laurent, <i>Cancer Research</i> , 2005	62
Figure 4.1	Induction du phénotype sclérodermique chez la souris après injections quotidiennes intra-dermiques pendant 6 semaines de HOCl ou OH $^\bullet$. Batteux F. et al, <i>Curr. Op. Rheumatol</i> , 2011.	179

Figure 4.2

Voie d'activation de Notch dans la ScS selon notre modèle. Les FRO produites lors des phénomènes d'ischémie-reperfusion chez l'homme ou lors des injections d'*HOCl* activent ADAM17, qui est capable de libérer le domaine actif intra-cellulaire de Notch NICD. Ce dernier peut alors transloquer au noyau et activer la transcription de ses gènes cibles, ayant pour effets la prolifération fibroblastique et la fibrose, le développement d'une auto-immunité, et des lésions vacsulaires. 182

Chapitre 1

PHYSIOPATHOLOGIE DE LA ScS

1.1 PRÉSENTATION DE LA MALADIE

La sclérodermie (ScS) est une maladie systémique caractérisée par une fibrose cutanée et des anomalies microcirculatoires, notamment un phénomène de Raynaud très souvent inaugural [1]. C'est une maladie rare, qui appartient au groupe des maladies orphelines. Son incidence varie entre 2 et 16 cas par million de sujets par an, et sa prévalence de 3 à 30 pour 100 000 habitants. Elle est 4 fois plus fréquente chez la femme que chez l'homme, et débute le plus souvent entre 30 et 50 ans. L'expression clinique et la gravité de cette maladie sont très variables [2]. L'étendue de la fibrose cutanée peut se limiter à une atteinte des extrémités dans les formes cutanées limitées ou remonter au dessus des coudes et des genoux dans les formes diffuses. Elle peut se compliquer d'une fibrose pulmonaire, d'une hypertension artérielle pulmonaire, de crises rénales, d'une atteinte de la partie inférieure du tube digestif et/ou d'une atteinte cardiaque. Ces manifestations viscérales sont associées à une diminution de la survie. Il n'existe actuellement pas de traitement curatif pour cette maladie. Les atteintes rénales sont aujourd'hui plus rares grâce à l'utilisation d'inhibiteurs de l'enzyme de conversion de l'angiotensine. Les causes de décès sont aujourd'hui essentiellement cardio-pulmonaires, et l'espérance de vie globale est d'environ 70% à 5 ans.

L'hétérogénéité clinique se retrouve aussi au niveau des auto-anticorps détectés dans le sérum des patients et qui sont dirigés contre des cibles antigéniques différentes selon la forme de la maladie.

La ScS demeure une affection d'étiologie inconnue, et les facteurs à l'origine du dysfonctionnement des fibroblastes, des cellules endothéliales et des cellules du système immunitaire restent à préciser (voir figure 1.1). Parmi les facteurs environnementaux, certains virus, comme le cytomégalovirus [3] et certaines substances chimiques comme les solvants, la silice, ou les pesticides pourraient jouer un rôle dans le déclenchement de la maladie [4]. En outre, des facteurs intrinsèques comme les formes réactives de l'oxygène (FRO) [5] [6] [7] [8] [9] ou le TGF- β

[10] [11] ont été mis en cause dans l'amorçage et la progression de la maladie. Ces nouvelles pistes physiopathologiques ouvrent de nouvelles perspectives thérapeutiques dans cette maladie dont la progression est peu freinée par les traitements actuels.

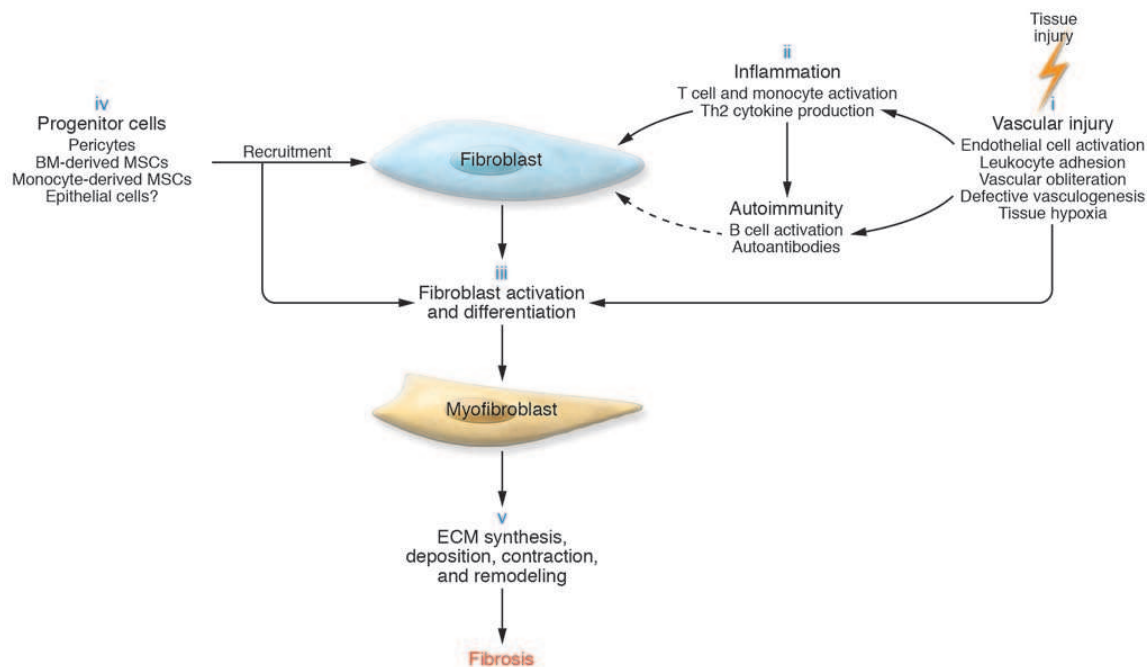


Figure 1.1 Lien entre les dysfonctionnements des fibroblastes, des cellules endothéliales, et des cellules immunitaires dans la sclérodermie systémique d'après Varga J, Journal of Clinical Investigation, 2007.

1.2 DYSFONCTIONNEMENTS FIBROBLASTIQUES

Les patients atteints de ScS présentent une accumulation de collagène dans le derme, et parfois dans les viscères. Les mécanismes conduisant à cette fibrose systémique ne sont pas encore complètement élucidés. Les fibroblastes de malades synthétisent *in vitro* des constituants de la matrice extracellulaire en excès (collagène de type IV, protéoglycans, fibronectine) et des protéines inhibant la dégradation de cette matrice (TIMP-3, inhibiteur tissulaire de la métalloprotéinase-3). Certains fibroblastes acquièrent un phénotype particulier de myofibroblastes et présentent des propriétés de cellules musculaires lisses. Ils deviennent hyperprolifératifs et expriment le marqueur α -SMA.

1.2.1 Anomalies intrinsèques des fibroblastes

1.2.1.1 Activation du gène du procollagène via la signalisation des récepteurs du TGF- β

La famille du transforming growth factor- β (TGF- β) inclut un grand nombre de protéines de signalisation, dont les isoformes du TGF- β , les "bone morphogenetic protéines" (BMPs), et différents facteurs de croissance. Ces protéines jouent un rôle important durant l'embryogenèse, mais sont également cruciales dans les organismes adultes, alors impliquées dans l'homéostasie. Le TGF- β , synthétisé par de nombreux types cellulaires, comporte trois isoformes codés par trois gènes différents (TGF- β 1,2 et 3). Le TGF- β 1 est synthétisé par les cellules endothéliales (CE), les cellules hématopoïétiques et les cellules du tissu conjonctif ; le TGF- β 2 est synthétisé par les cellules épithéliales et neuronales, TGF- β 3 est synthétisé par les cellules mésenchymateuses [12]. Toutes les isoformes sont libérées dans la matrice extracellulaire sous forme de propeptides, et sont liées, dans la matrice à une protéine, la "latent TGF- β binding protein" [12]. Leur libération, nécessaire à leur liaison à l'un de leurs récepteurs, est dépendante de la thrombospondine ou de la plasmine. Trois types de récepteurs du TGF- β (récepteur de type I, II et III) ont été décrits, et sont exprimés de manière ubiquitaire. Ces récepteurs avec une activité serine/thréonine kinase.

Deux types de voies sont possibles dans la signalisation du TGF- β :

- Signalisation dépendante des protéines Smad 2/3

La fixation du TGF- β sur ses récepteurs spécifiques induit une transduction de signal impliquant les protéines intracytoplasmiques Smad (voir figure 1.2). Smad 2 et smad 3 sont recrutées et phosphorylées par un hétérotrimère formé par l'association TGF- β -récepteur de type I-récepteur de type II (Figure 1.2). Smad 4 s'associe alors avec smad 2 et smad 3 et l'ensemble migre dans le noyau où il régule la transcription de certains gènes, en particulier du gène codant le procollagène. Les protéines Smad sont les plus puissants médiateurs de l'activation du promoteur du gène du procollagène COL1A2 dans les fibroblastes ScS. Une surexpression de Smad3 et Smad4, mais pas Smad1 et Smad2, entraîne l'activation en trans du promoteur de COL1A2 dans les fibroblastes normaux via l'interaction avec SBE (Smad Binding Element), et ainsi la transcription du gène COL1A2. D'autres protéines, outre les protéines Smad, participent également à la signalisation intracellulaire, incluant les GTPases

Ras et les mitogene-activated protein kinases (MAPKs) ERKs, p38 et c-Jun N-terminal kinases (JNKs) [13].

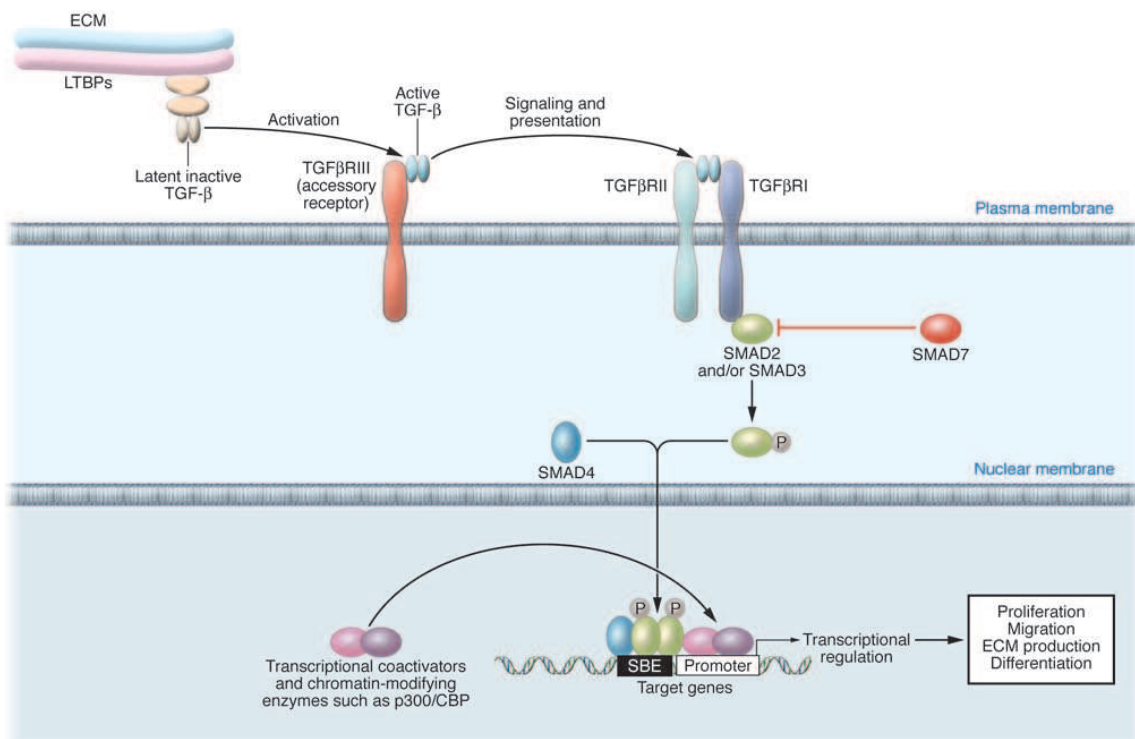


Figure 1.2 Signalisation du TGF- β dépendante des protéines Smad, d'après Varga J, Journal of Clinical Investigation, 2007.

Le TGF- β est un des plus puissants inducteurs de synthèse de matrice extra-cellulaire, et joue un rôle central dans les processus de fibrose observés dans la ScS et dans d'autres maladies s'accompagnant de fibrose. Comparativement aux fibroblastes de sujets sains, les fibroblastes de malades sclérodermiques sont le siège d'une accumulation nucléaire anormale et spontanée de molécules smad 3 phosphorylées en l'absence de stimulation par le TGF- β [14], ainsi qu'un défaut d'expression de smad 7, élément inhibiteur de cette cascade de signalisation [15]. Ce défaut de Smad7 contribue à maintenir une production anormale de collagène dans les fibroblastes ScS1.

- signalisation indépendante des protéines Smad 2/3

Les autres voies impliquées dans la signalisation du TGF- β , indépendamment de smad 2/3, semblent aussi anormalement activées dans les fibroblastes des patients sclérodermiques (voir figure 1.3). Ainsi, des dysfonctionnements d'une voie impliquant la tyrosine kinase c-abl, smad 1 et ERK-1/2 ont été mis en évidence [16]. Cette voie participe à l'excès de transcription du CTGF observée dans la ScS, et présente la particularité de pouvoir être inhibée par l'imatinib mesylate, contrairement à la voie impliquant smad 2/3 [16]. Par ailleurs, une boucle autocrine impliquant CCN2 et Smad-1 a été identifiée. Elle prolonge les signaux transmis par le TGF- β . En effet, une coopération avec CCN2 induite par le TGF- β est requise pour l'induction de la synthèse de collagène médiée par celui-ci [2].

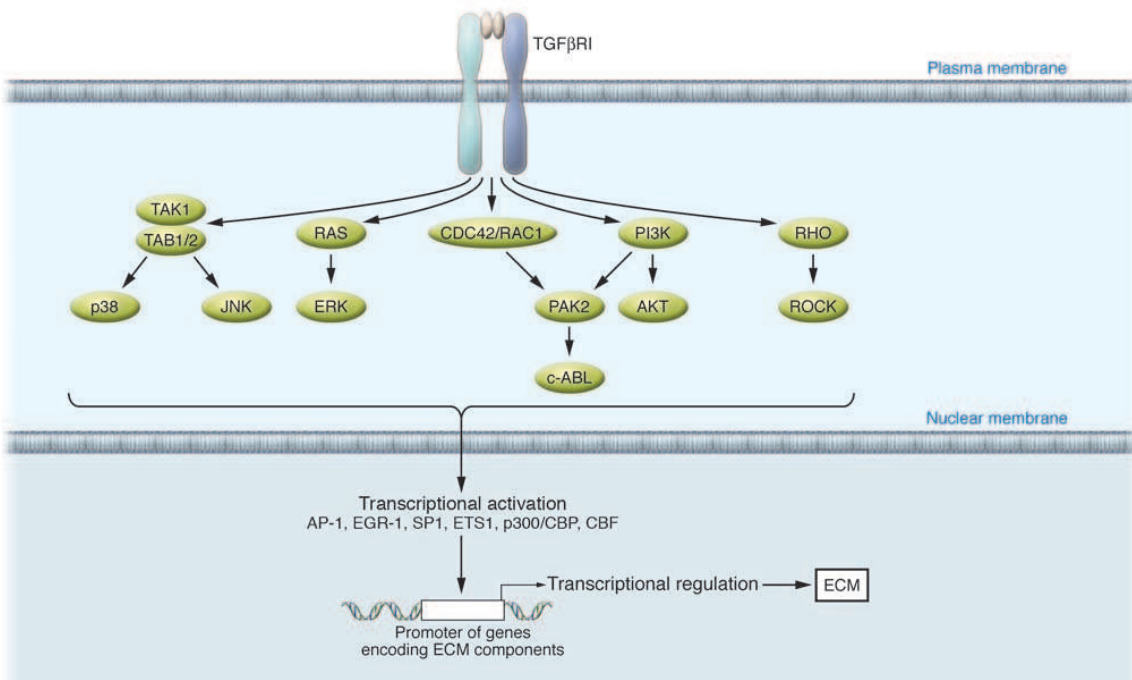


Figure 1.3 Signalisation du TGF- β indépendante des protéines Smad, d'après Varga J, Journal of Clinical Investigations, 2007.

Outre ces anomalies de la signalisation intracytoplasmique, plusieurs équipes ont mis en évidence une expression accrue des récepteurs de type I et de type II du TGF- β à la membrane des fibroblastes de patients sclérodermiques [17], [18]. Ces anomalies d'expression des récepteurs du TGF- β participent à l'activation excessive de la voie du TGF- β et à la fibrose, comme le suggèrent les résultats obtenus par Pannu et al [19]. Cette équipe a limité la traduction de TGF- β -RI en transfectant les fibroblastes de patients atteints de ScS avec des ARN interférents.

Ils ont montré une diminution de la synthèse de TGF- β RI mais aussi de collagène et de CTGF à un niveau transcriptionnel (analyse par quantitative RT-PCR). Néanmoins, la place exacte de ces anomalies et plus généralement le rôle exact du TGF- β reste difficile à préciser au cours de la maladie humaine, la majorité de ces études étant réalisées sur des fibroblastes en culture, et les fibroblastes utilisés n'étant pas toujours des fibroblastes obtenus à partir de peau de patients atteints.

1.2.1.2 Le Connective Tissue Growth Factor (CTGF)

Le gène du CTGF appartient à une famille de gènes récemment découverte: la famille connective tissue growth factor/cysteine-rich 61/nephroblastoma overexpressed (CCN: CTGF/CYR/NOV). Ces gènes et leurs produits sont impliqués dans des fonctions cellulaires essentielles, telles que le maintien de l'homéostasie, la réparation et le contrôle de la croissance cellulaire, ainsi que la régulation de l'angiogenèse. Ces gènes semblent également impliqués dans des processus pathologiques tels que la progression des cancers, l'athérosclérose et la fibrose [20]. La transcription du CTGF est normalement régulée par le TGF- β mais aussi par de nombreux autres facteurs (AMPc, angiotensine II, forces de cisaillement perçues par les cellules) [21]. Une expression augmentée du CTGF a été retrouvée dans de très nombreuses pathologies avec cicatrisation excessive et fibrose. Au cours de la ScS, les fibroblastes synthétisent de grandes quantités de CTGF, même en l'absence de stimulation par le TGF- β [22]. Cet excès de CTGF entraîne une dérégulation de la croissance des cellules endothéliales et des fibroblastes ainsi qu'un excès de synthèse de collagène et pourrait être impliqué dans l'entretien du processus de fibrose. Dans les modèles animaux de ScS comme le modèle Tsk1/+ et après injection de bléomycine, des niveaux élevés de CTGF sont associés au développement de la fibrose. Des travaux sont en cours pour préciser l'origine de la dérégulation de la voie du CTGF dans la ScS. Certains auteurs ont suggéré que le CTGF serait essentiel pour le maintien de la fibrose, après que celle-ci ait été induite par un signal médié par le TGF- β . Une autre hypothèse est qu'un facteur de transcription, SP1, pourrait entraîner une synthèse excessive de CTGF indépendamment de la voie du TGF- β [22]. Certains auteurs proposent d'utiliser le CTGF comme marqueur sérique dans la ScS puisque des taux élevés ont été retrouvés dans les sérum des patients sclérodermiques et seraient corrélés à la sévérité de l'atteinte viscérale, notamment pulmonaire.

1.2.1.3 Early growth response factor-1(Egr-1)

Egr-1 est un facteur de transcription de la voie du TGF- β identifié récemment. Une expression anormale d'Egr-1 a été retrouvée dans plusieurs modèles animaux de fibrose et chez l'homme dans la fibrose pulmonaire idiopathique et la sclérodermie (voir figure 1.4) [23] [24]. De plus, des niveaux élevés d'Egr-1 dans les cellules mononucléées périphériques des patients atteints de ScS est associée à une hypertension artérielle pulmonaire [25]. L'expression d'Egr-1 est très faible dans les cellules quiescentes, mais celle-ci peut être augmentée rapidement par divers stimuli. Le TGF- β peut notamment induire une augmentation de l'expresison d'Egr-1 dans les fibroblastes normaux, et entraîner son interaction avec le promoteur de COL1A2.

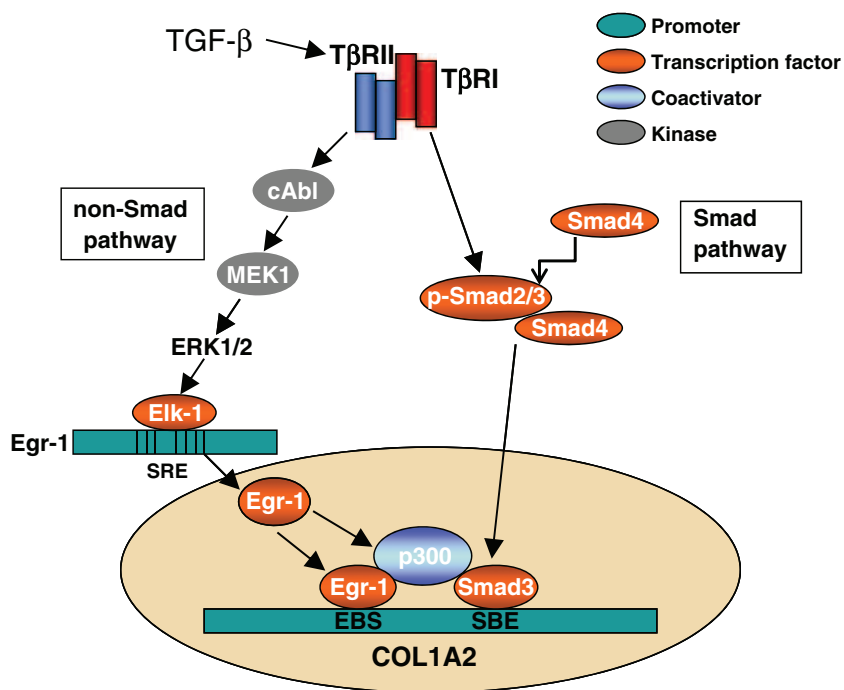


Figure 1.4 Régulation des signaux médiés par le TGF- β par Egr-1, d'après S. Bhattacharyya, Matrix Biology, 2011

Egr-1 régule l'expression des gènes de plusieurs facteurs pro-fibrosants : TGF- β , PDGF, CTGF, VEGF, fibronectin, TIMP-1. Dans les cellules Hep-G2, Egr-1 induit la transition epithélio-mesenchymale

(EMT) en augmentant l'expression de Snail. Dans les fibroblastes normaux de peau et de poumon, l'expression forcée d'Egr-1 est suffisante pour induire l'augmentation d'activité du promoteur du gène COL1A2. L'injection quotidienne de bléomycine à des souris entraîne une accumulation d'Egr-1 dans les fibroblastes cutanés. Les fibroblastes transgéniques Egr-1 expriment huit fois plus la NADPH-oxidase-4 (NOX-4), qui est impliquée dans la génération de FRO. Cette enzyme étant retrouvée à des taux élevés dans les situations d'hypoxie chronique via un mécanisme impliquant Egr-1, certains auteurs suggèrent que chez les patients atteints de ScS l'hypoxie et le TGF- β pourraient être responsables d'une surexpression d'Egr-1 résultant en une augmentation de l'activité de NOX-4 et entraînant ainsi la production de FRO qui aggrave encore la fibrose [1].

1.2.1.4 Molécules impliquées dans la dégradation de la matrice extracellulaire

La dégradation de la matrice extra-cellulaire par les métalloprotéases (MMP), et la régulation de celles-ci par les TIMP sont des éléments majeurs dans l'établissement de la fibrose en conditions normales et pathologiques. Les MMP sont une famille de protéases qui déclenchent une protéolyse par hydrolyse des ponts peptidiques. Elles sont synthétisées sous forme de précurseurs inactifs, peuvent être sécrétées ou transmembranaires à l'état de pro-enzymes nécessitant une activation pour dégrader la matrice [26]. Les MMP-1 à 8 sont les collagénases et jouent un rôle majeur dans la digestion du collagène de type 1. Les TIMP (Tissue Inhibitor of Metalloproteinases) sont les protéines inhibitrices principales des MMP en condition physiologique. Quatre membres de la famille TIMP ont été décrits : TIMP-1 à 4. Les MMP et les TIMP sont produites par les cellules mésenchymateuses (fibroblastes, myofibroblastes, cellules endothéliales), les cellules de l'immunité innée (macrophages, monocytes, neutrophiles) et les cellules cancéreuses métastatiques. Dans les fibroblastes ScS, l'expression de TIMP-1 est augmentée [27]. De même, les concentrations sériques de TIMP-1 sont élevées chez les patients sclérodermiques et corrélés à la sévérité de la maladie. Des auto-anticorps bloquants anti-MMP1 et -3 ont été retrouvés chez les patients sclérodermiques, et leurs concentrations sont corrélées avec l'étenue de la fibrose cutanée, pulmonaire et artériolaire rénale. Enfin, des souris invalidées pour MMP-1 développent une fibrose cutanée [28]. Toutes ces données suggèrent qu'un déséquilibre MMP/TIMP pourrait être à l'origine du développement de la fibrose dans la ScS.

1.2.1.5 Synthèse accrue de radicaux libres

Les fibroblastes de patients atteints de ScS synthétisent spontanément de grandes quantités de radicaux libres (anions superoxydes $O_2^{\bullet-}$ et de peroxyde d'hydrogène H_2O_2), molécules qui stimulent de manière autocrine la prolifération des fibroblastes et la synthèse de collagène [29]. Cette synthèse de FRO apparaît indépendante de l'IL4, du CTGF et du TGF- β et pourrait être en partie dépendante du platelet derived growth factor [30].

1.2.1.6 Synthèse de chimiokines et cytokines

Les fibroblastes participent au recrutement des leucocytes dans les tissus en secrétant chimiokines et cytokines (IL1- α , IL6, tumor necrosis factor- α (TNF- α), IL8, monocyte chemoattractant protein-1 (MCP-1) et PDGF notamment). Ils favorisent ainsi la migration des lymphocytes circulants à travers la barrière endothéliale et leur accumulation dans le derme [31] [32] [33].

Il semble également possible, d'après des données obtenues *in vitro*, que certaines cytokines sécrétées par les fibroblastes participent directement au dysfonctionnement des fibroblastes par une activation autocrine.

- L'interleukine-1 α Les fibroblastes de patients sclérodermiques synthétisent de manière aberrante de l' IL1 α sous une forme précurseur active (pro-IL1 α). Le blocage de la synthèse d'IL1 entraîne une réduction de la synthèse d'IL-6 et de collagène, et réduit la transcription du PDGF au sein de ces fibroblastes [34].
- MCP 1 Cette chimiokine semble aussi exercer un effet direct en stimulant la synthèse de collagène, d'après les données obtenues dans un modèle murin de fibrose induit par la bléomycine [31].

1.2.1.7 La voie Wnt/ β -catenin

On retrouve dans les biopsies de patients atteints de ScS diffuse une surexpression du récepteur Wnt Fzd2 et de la cible Wnt Lef1, et une sous-expression des antagonistes Wnt Dkk2 et wif1. Les composants de la voie Wnt ont un effet profibrotique, et jouent un rôle majeur dans

la physiopathologie de la fibrose et de la lipoatrophie dans la ScS. Un modèle de souris sclérodermiques transgéniques Wnt a d'ailleurs été récemment développé par l'équipe de J. Varga (voir 1.6 Modèles animaux).

1.2.1.8 Sp1 et Sp3

Les protéines Sp1 et Sp3 interagissent avec 3 régions du promoteur du gène COL1A2 et peuvent ainsi l'activer dans les fibroblastes normaux. Une phosphorylation augmentée, et donc une activation de Sp1 a été détectée dans les fibroblastes ScS par rapport aux fibroblastes normaux.

1.2.1.9 c-Myb

Les protéines de la famille Myb sont des facteurs de transcription de type « hélice-boucle-hélice leucine zipper » et interagissent avec des séquences spécifiques de l'ADN. C-Myb est surexprimé dans les fibroblastes de patients sclérodermiques, et peut augmenter l'activité des promoteurs COL1A1 et COL1A2 dans les fibroblastes normaux [35].

1.2.1.10 c-Myc

L'oncogène c-Myc appartient également à la famille des facteurs de transcription de type « hélice-boucle-hélice leucine zipper », et une surexpression de c-Myc a également été décrite dans les fibroblastes ScS [36].

1.2.1.11 Synthèse d'une matrice extra-cellulaire capable de résister à la dégradation des métalloprotéases

Une expression élevée du gène procollagene lysyl hydroxylase 2 (PLOD 2) est retrouvée dans les fibroblastes de patients sclérodermiques comparativement à des fibroblastes de sujets sains [37]. PLOD 2 code pour une lysyl-hydroxylase qui permet un assemblage particulier des fibres de collagène au sein de la matrice extracellulaire. Ceci entraîne la production d'une matrice capable de résister à l'action des métalloprotéinases.

1.2.1.12 La voie Fas/Fas-ligand

Un défaut d'apoptose médiée par la voie Fas-Fas ligand a été mis en évidence dans les fibroblastes sclérodermiques [38]. Ceci pourrait expliquer leur phénotype hyperprolifératif.

1.2.1.13 Des anomalies de la voie des kinases Erk1/2

Il existe dans les fibroblastes sclérodermiques une activation permanente de Erk1/2 accompagnée d'une production élevée de FRO via la NADPH oxydase.

1.2.2 Eléments extrinsèques majorant le dysfonctionnement fibroblastique

1.2.2.1 La Sérotonine

La sérotonine (5-Hydroxytryptamine, 5-HT) est relarguée par les plaquettes après activation. Elle joue un rôle vaso-actif bien démontré, mais semble également pourvue d'actions profibrosantes. Il est connu depuis plusieurs décennies que ses taux sont élevés dans le sang des patients sclérodermiques [39]. La sérotonine stimule la prolifération de fibroblastes isolés des artères pulmonaires de rats hypoxémiques [40]. De grandes quantités de récepteurs à la sérotonine de type 5-HT_{2B} sont exprimées au niveau pulmonaire chez les patients atteints de fibrose pulmonaire idiopathique et des récepteurs 5-HT_{2A} et B sont induits au niveau pulmonaire après instillation intratrachéale de bléomycine, molécule induisant une fibrose pulmonaire. L'inhibition de ces récepteurs diminue la fibrose induite par la bléomycine. L'inhibition du signal au niveau d'un des récepteurs de la sérotonine sur les fibroblastes humains, le récepteur 5-HT₃ diminuerait également la synthèse de collagène en inhibant une des voies dépendantes du TGF- β impliquant les protéines Smad.

En 2011, des auteurs ont démontré dans différents modèles murins de ScS que la sérotonine plaquettaire induisait la synthèse de matrice extra-cellulaire via l'activation des récepteurs 5-HT_{2B} par un mécanisme dépendant du TGF- β . Ils ont également retrouvé des taux élevés de 5-HT_{2B} dans la peau des patients sclérodermiques [41]. Ainsi, la sérotonine est un médiateur faisant le lien entre atteinte vasculaire, activation plaquettaire, et fibrose dans la ScS.

1.2.2.2 Le Platelet Derived Growth Factor (PDGF)

Le PDGF a été initialement étudié dans les phénomènes de cicatrisation, mais il est maintenant bien connu pour ses rôles dans l'hypertension artérielle pulmonaire, la fibrose pulmonaire et la sclérodermie. C'est un peptide dimérique sécrété par divers types cellulaires comme les plaquettes, les fibroblastes et les cellules musculaires lisses. C'est un puissant agent mitogène pour les cellules d'origine mésenchymateuse et neuroectodermiques. Le PDGF induit la migration, la différenciation et la transformation de divers types cellulaires et participe à la régulation de l'apoptose et de la génération de FRO. La transduction du signal médié par le PDGF se fait via deux récepteurs tyrosine kinases transmembranaires: le PDGFR α et le PDGFR β , qui diffèrent par les cascades de transduction du signal et par leurs effets biologiques.

L'activation des PDGFR induit la phosphorylation des MAP-kinases (Erk1/2, p38, JNK), l'activation de Ras, et l'expression de gènes comme Egr-1, c-fos, c-jun. Chez les souris, l'activation conditionnelle du PDGFR conduit à une fibrose progressive de la peau, du tracus gastro-intestinal et du cœur, ce qui suggère le rôle de cette voie de transduction dans le développement de la fibrose [42]. Dans la fibrose pulmonaire chez l'homme et chez l'animal, l'expression du PDGF est corrélée avec l'expansion des myofibroblastes qui contribuent à la synthèse de protéines de la matrice extra-cellulaire comme le collagène, la fibronectine ou les glycosaminoglycanes [43]. Il apparaît donc de plus en plus clairement que le PDGF joue un rôle dans la stimulation de l'expression de protéines de matrice par les myofibroblastes.

En 2006, il a été montré que des auto-anticorps stimulants dirigés contre le PDGFR étaient présents dans le sérum des patients sclérodermiques et que ces auto-anticorps pouvaient intervenir dans la physiopathologie de la maladie [44][45]. Ces anticorps se lient au PDGFR, l'activent et peuvent ainsi déclencher l'expression du gène du collagène de type I dans les fibroblastes. Nous détaillons le mécanisme d'action et les méthodes de détection utilisées par les auteurs dans le chapitre sur l'immunité humorale et les auto-anticorps dans la ScS (voir 1.4.3.2 Auto-anticorps). Ces anticorps stimulants ne sont pas spécifiques de la ScS puisque les auteurs en ont également détectés dans le sérum des patients atteints de maladie du greffon contre l'hôte, qui partage des manifestations cliniques avec la ScS [46]. Ces résultats doivent cependant aujourd'hui être nuancés puisqu'un article a infirmé en 2009 l'existence de ces Ac anti-PDGFR dans la ScS [47].

L'activation des PDGFR peut être inhibée par des molécules de synthèses « inhibitrices de tyrosine kinases » (TKI), dont l'imatinib, l'axitinib, le sunitinib, le dasatinib, la sorafenib et le nilotinib. Ces molécules ont été initialement développées pour le traitement de cancers comme les tumeurs gastro-intestinales et la leucémie myéloïde chronique, afin d'inhiber les signaux de prolifération via bcr/abl et c-kit. Ces molécules n'étant pas spécifiques, elles réagissent de façon croisée avec d'autres récepteurs de tyrosine kinases, ce qui a permis d'élargir leur spectre d'utilisation à d'autres cancers. L'imatinib a été testé avec succès dans un modèle murin d'hypertension pulmonaire [48]. Une autre équipe a montré que l'imatinib pouvait réduire la synthèse de collagène et de fibronectine par les fibroblastes humains du derme, et améliorer la fibrose dans le modèle murin de ScS induit par la bléomycine [49] [50]. L'article 4 de nos travaux personnels apporte de nouveaux éléments sur l'activation du PDGFR dans la ScS et sur l'efficacité de certaines molécules TKI pour lutter contre la fibrose, les anomalies vasculaires et l'activation du système immunitaire observées dans cette maladie.

1.2.2.3 L'interleukine-4 (IL-4)

Cette interleukine stimule la croissance des fibroblastes et augmente le dépôt de matrice extracellulaire au niveau des tissus. Les patients sclérodermiques ont des taux sériques élevés d'IL-4. De plus, l'IL-4 stimule la synthèse de cytokines pro-fibrosantes par les fibroblastes, comme le MCP-1, en particulier au niveau pulmonaire [51].

Chez l'animal, on observe que les fibroblastes de souris tight skin (TSK-1/+), souris développant spontanément une fibrose du derme, expriment le récepteur de l'IL-4 en grandes quantités et présentent une activation constitutive des voies de signalisation intra-cytoplasmique de l'IL-4 [52]. Dans ce modèle, un excès d'IL-4 semble avoir un rôle pathogène, puisqu'un traitement par Ac anti-IL-4 prévient le dépôt de collagène au niveau du derme [53]. Chez ces souris, ce sont surtout les lymphocytes T (LT) CD4+ qui sont à l'origine de la production accrue d'IL-4 [54]. Cependant, les souris résultant d'un croisement entre les Tsk-1/+ et les souris invalidées pour le gène RAG, qui n'ont ni de lymphocytes B ni de lymphocytes T, développent tout de même des lésions de sclérose cutanée, tandis que seules les souris Tsk1/+ invalidées pour le gène de l'IL-4 et du TGF- β ne développent pas de sclérose cutanée [55]. Ainsi les LT ne sont vraisemblablement pas les seules cellules à contribuer à cet excès de production d'IL-4 au cours de cette maladie. Enfin, dans ce modèle, la maladie peut être prévenue en rééquilibrant la balance Th1/Th2 via l'administration d'IL-12 plasmidique par voie intra-musculaire [56].

Chez les malades atteints de ScS comparativement à des sujets sains, des quantités accrues d'IL-4 et de son ARN messager (ARNm) ont été détectées dans le plasma [57], dans les cellules mononucléées du sang périphérique [58], dans les LT obtenus à partir d'un lavage broncho-alvéolaire [59], dans les fibroblastes [60]. Dans les pneumopathies infiltrantes diffuses de la ScS, l'alvélite lymphocytaire est constituée d'une majorité de LT CD8+ qui produisent des quantités augmentées d'ARNm codant l'IL-4 [59]. Dans la peau, l'infiltrat est composé majoritairement de LT CD4+, mais l'IL4 semble être synthétisée en excès par d'autres populations lymphocytaires minoritaires : des LT CD8+ et des LT doubles positifs CD4+CD8+ [61]. D'autre part, certains patients exprimeraient de fortes quantités d'un variant traductionnel de l'IL-4, (IL4delta2), qui aurait des propriétés accrues sur la stimulation de synthèse de collagène [62].

1.2.2.4 L'interleukine-13 (IL-13)

Les lymphocytes activés de type Th2 infiltrant la peau des patients sclérodermiques synthétisent de l'IL-13. Celle-ci peut, comme l'IL-4, induire l'expression du collagène de type 1 dans les fibroblastes cutanés [63]. Ainsi, les effets pro-fibrosants de l'IL-13 seraient dus à une activation fibroblastique irréversible directe ou médiée par le TGF- β . Les souris transgéniques pour l'IL-13 présentent une fibrose pulmonaire exacerbée avec de forts niveaux de TGF- β [64]. De plus, dans le modèle de ScS induit par la bléomycine les niveaux d'ARNm de l'IL-13 sont élevés dans la peau lésée et l'expression du récepteur de l'IL-13, IL-13R- α 2 est augmentée dans les cellules mononucléées et les macrophages infiltrant le derme. Enfin, les souris déficientes en IL-13 ne développent pas de sclérose cutanée après injection quotidienne de bléomycine, ce qui apporte un nouvel argument au rôle de médiateur de l'IL-13 dans le développement de la fibrose cutanée.

1.2.2.5 L'interleukine-17 (IL-17)

Cette cytokine est sécrétée par une population de lymphocytes T particulière, les Th17. L'IL-17A et l'IL-17F ont des similarités dans leur séquence d'amino-acides, et se lient toutes deux au même récepteur: l'IL-17R de type A. L'effet de l'IL-17 dans la ScS est encore mal élucidé.

Il a été très récemment montré que l'expression de l'IL-17A, mais pas de l'IL-17F était significativement augmentée dans la peau lésée et le sérum des patients atteints de ScS [65]. Au

contraire, le récepteur IL-17R de type A est sous-exprimé dans les fibroblastes ScS par rapport aux fibroblastes normaux. Ce phénomène est dû à une activation intrinsèque de la voie du TGF- β dans ces cellules. D'après l'équipe de Nakashima, l'IL-17A a une action anti-fibrosante puisqu'elle réduit l'expression du collagène de type I et du CTGF via la régulation de micro-RNAs. Ainsi, dans les fibroblastes ScS, la sous-expression du récepteur IL-17R de type A empêche la signalisation de l'IL-17A et son effet anti-fibrosant. Les taux élevés retrouvés dans la peau et le sérum des patients sont dus à un rétrocontrôle négatif. Selon l'équipe de Sato, au contraire, l'IL-17 est à un effet pro-fibrosant. Ces auteurs ont montré dans le modèle murin de ScS induite par la bléomycine, que les lymphocytes Th17 infiltrent le derme sous l'effet d'une expression augmentée de L-selectin et d'ICAM-1, et que leur présence est corrélée à une augmentation de la fibrose [66].

1.2.2.6 L'endothéline-1

L'endothéline-1 (ET-1) est un peptide vasoactif puissant, récemment impliqué dans la physiopathologie de la ScS. En effet, les concentrations sériques d'endothéline-1 sont augmentées chez les patients sclérodermiques [67], [68]. Outre ses effets vasoactifs, l'ET-1 peut induire la transformation des fibroblastes en myofibroblastes, ainsi que l'expression des collagènes de type I et III et l'inhibition de l'expression de la MMP-1 [69].

1.2.2.7 TGF- β

Il est intéressant enfin de rapporter que les fibroblastes de patients sclérodermiques ne synthétisent pas plus de TGF- β que des fibroblastes témoins [70] [71] [72]. Comme nous venons de le voir, le TGF- β en excès dans la peau permet l'activation de la transcription du gène du procollagène COL1A2, mais sa source paraît être extérieure aux fibroblastes eux-mêmes.

Les anomalies fibroblastiques mentionnées ci-dessus sont résumées dans le tableau suivant :

Anomalies intrinsèques	Anomalies extrinsèques
Activation du gène COL1A2 via Smad	PDGF
CTGF, c-Myc, c-Myb	TGF- β
Matrice résistante aux métalloprotéases	IL-4, IL-13
Défaut d'apoptose	Sérotonine
Formes réactives de l'oxygène	Endotheline-1
Chimiokines et cytokines	

Tableau 1.1

1.2.3 Nouvelles voies d'activation fibroblastique

1.2.3.1 La voie des récepteurs Notch

Les protéines Notch sont des récepteurs membranaires dont l'expression a été très conservée à travers les espèces au cours de l'évolution. Leur fonction principale est la régulation de nombreux processus développementaux, tels que la prolifération, la différenciation, et l'apoptose. La mutation Notch a été mise en évidence chez la drosophile au début du XXe siècle. Des mutations « perte de fonction partielles » avaient pour conséquence la formation d'encoches (« Notch » en anglais) à l'extrémité des ailes de mouches drosophiles. A la fin des années 30 Poulson a montré que la perte de fonctions totales de Notch entraînait un phénotype embryonnaire létal, caractérisé par une surproduction de neurones, appelé phénotype « neurogénique » [73]. Par la suite, quatre protéines Notch (Notch1 à 4) ont été décrites chez les mammifères. Elles ont des fonctions non-redondantes au cours de l'embryogénèse. En effet, l'inhibition de la signalisation de Notch1 et 2, entraîne la mort au stade embryonnaire, ce qui n'est pas le cas pour Notch3 et 4.

- Structure des récepteurs Notch et de leurs ligands

Les récepteurs Notch résident à la surface cellulaire, avec une portion extracellulaire et une portion intracellulaire liées de façon non-covalente, et constituent ainsi un hétérodimère (figure 1.5). La partie extracellulaire de Notch est caractérisée par de nombreux domaines

Epidermal Growth Factor (EGF)-like repeats. Notch1 et Notch2 sont de taille équivalente, et possèdent de grandes similarités structurelles (voir figure 1.5 ci-dessous):

- le domaine "RBP-J associated molecule" (RAM), au niveau membranaire, qui permet des interactions avec plusieurs protéines cytosoliques et nucléaires
- le domaine Ankyrin (ANK), également important pour des interactions protéine-protéine
- deux séquences de localisation nucléaire (NLS)
- un domaine carboxy-terminal de transactivation (TAD), permettant d'activer la transcription
- un domaine PEST (Proline, Glutamate, Serine, Threonine-rich domain) régulant sa dégradation

Notch3 et 4 sont de taille plus courte et ne possèdent pas le domaine TAD.

Les ligands de Notch sont codés par les gènes des familles Jagged (JAG1 et 2) et Delta-like (DLL1, 3, 4). Chacun des ligands contient des domaines EGF-like repeat et une séquence DSL « Delta/Serrate/Lag » conservée entre *Drosophila melanogaster*, *Caenorhabditis elegans* et les vertébrés. Jagged-1 et 2 ont également un domaine riche en cystéine.

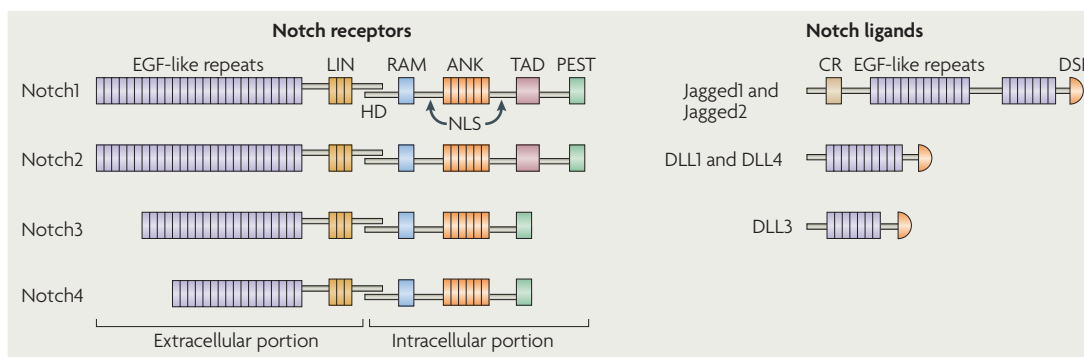


Figure 1.5 Structure des récepteurs Notch et de leurs ligands d'après Osborne A. 2007. RAM: RBP-J Associated Molecule, ANK: Ankyrin, NLS: Nuclear Localisation Sequence, TAD: Transactivation Domain, PEST: Proline, Glutamate, Serine, Threonine-rich domain.

- Modalités d'activation (figure 1.6)

La liaison du récepteur avec un de ses ligands déclenche un clivage extracellulaire assuré par la protéase TACE, une enzyme de type métalloprotéinase, membre de la famille ADAM (voir figure 1.6) [74].

Un second clivage est alors effectué par une γ -sécrétase [75]. Le clivage de Notch par le complexe γ -sécrétase permet la libération de la partie active de Notch, NIC. NIC est transporté dans le noyau, grâce à la présence de signaux de localisation nucléaire (NLS), où il régule l'expression de gènes cibles en s'associant avec d'autres facteurs nucléaires comme les membres de la famille CSL (C promoter binding factor/Suppressor of hairless/Lag-1 transcription factor) [76].

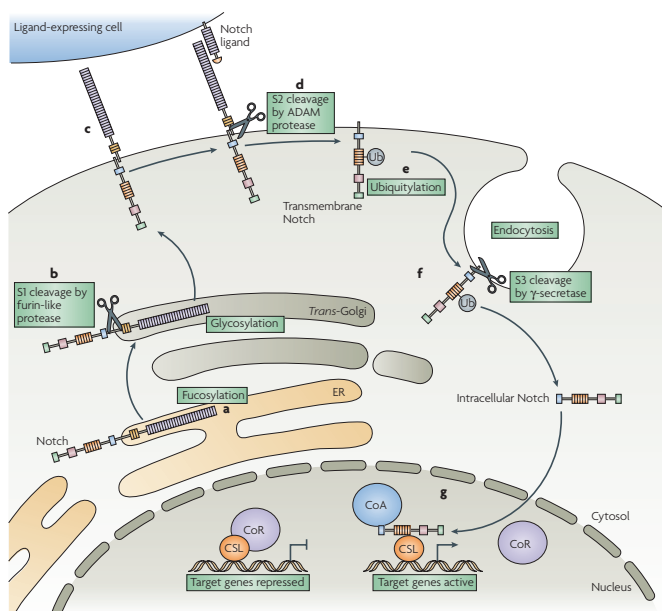


Figure 1.6 Etapes d'activation des récepteurs Notch
d'après Osborne A. 2007

- Expression cellulaire de Notch

Comme nous l'avons vu plus haut, Notch contrôle les processus de différenciation de différents types cellulaires durant la vie embryonnaire et adulte. Les récepteurs Notch sont exprimés dans des tissus et des organes très variés tels que le système nerveux, l'intestin, les follicules pileux, la glande mammaire, les cellules du système immunitaire (et donc la moelle osseuse et le thymus), le tissu cutané, le poumon, le système vasculaire. Nous détaillerons plus particulièrement l'expression de Notch dans ces quatre derniers tissus, puisqu'ils sont impliqués dans la physiopathologie de la ScS.

- Système immunitaire

Le rôle de Notch dans la lymphopoïèse a été très étudié. Les récepteurs Notch sont impliqués dans la formation des cellules souches hématopoïétiques (CSH), l'engagement des progéniteurs lymphoïdes vers la lignée T, le développement des lymphocytes T en périphérie, et celui des cellules B de la zone marginale (voir figure 1.7). Sa fonction la mieux caractérisée actuellement est son rôle dans les signaux d'engagement qui déterminent le devenir des progéniteurs lymphoïdes multipotents vers la lignée T ou B.

★ Notch et cellules souches hématopoïétiques

Plusieurs résultats suggèrent que Notch1 a un rôle crucial dans la génération de CSH. Les CSH sont générées au stade embryonnaire dans une région appelée Aorte-Gonade-Mésonéphros. Kumano a montré en 2003 grâce à des embryons Notch1 -/-, que Notch1 était essentiel pour la génération de CSH à partir de cellules endothéliales [77]. En outre, des expériences de « gain de fonction » ont montré que Notch pouvait entraîner le renouvellement des CSH chez l'adulte, chez la souris et chez l'homme [78]. Concernant les cellules capables d'activer la voie Notch dans la moelle osseuse, plusieurs hypothèses ont été formulées. Les cellules stromales de la moelle expriment Notch et pourraient donc remplir cette fonction. Les ostéoblastes sont étroitement associés aux CSH et pourraient également jouer un rôle. Il a été démontré qu'ils expriment Jagged-1, un ligand de Notch, sous certaines conditions [79].

★ Notch et le développement de la lignée T (figure 1.7)

Notch1 est requis au niveau des progéniteurs lymphoïdes dans les étapes précocees d'engagement vers la lignée T. Des mutations « perte de fonction » de Notch entraînent un thymus hypotrophique, sans cellules T et contenant un excès de cellules B. L'engagement T/B des progéniteurs dépend de Notch1, et est dépendant de CSL [80]. Les différentes études ayant permis la caractérisation de cette fonction de Notch1 ont été réalisées uniquement chez la souris.

L'expression des ligands de Notch dans le thymus est également un point important. Les protéines Jagged et Delta-like sont exprimées sur les cellules épithéliales thymiques, et sans doute également sur les thymocytes [81]. Les ligands de Notch sont également retrouvés au niveau des cellules dendritiques thymiques, mais celles-ci ne délivrent pas de signaux durant les étapes précocees du développement T. A côté de

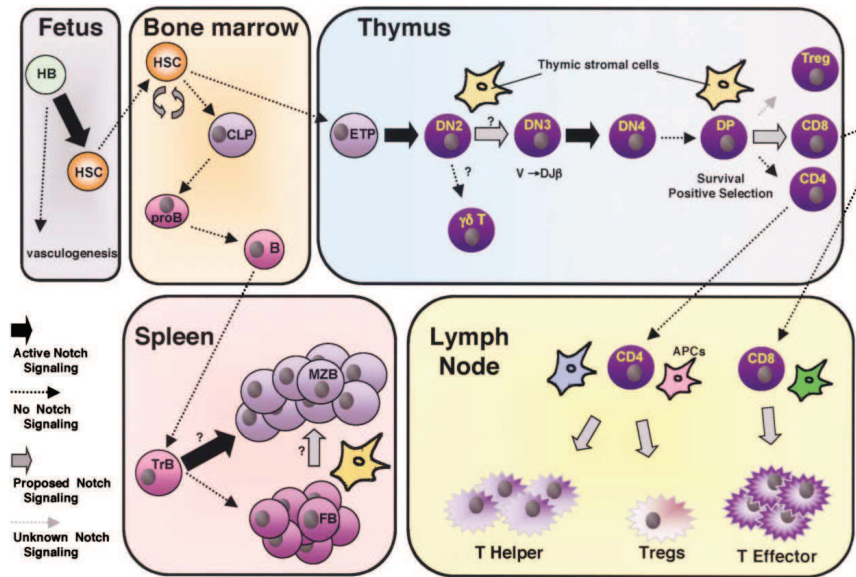


Figure 1.7 La voie Notch dans le développement hématopoïétique et dans le système immunitaire d'après Maillard I. HB: hemangioblast, HSC: hematopoietic stem cell, CLP: common lymphoid progenitor, ETP: early T lineage progenitor, DN: CD4-CD8- double-negative thymocytes, Treg: CD4+CD25+ regulatory T cells, TrB: transitional B cells, FB: follicular B cell, MZB: marginal zone B cell, APC: antigen presenting cell.

son rôle dans le choix de l'engagement vers la lignée T versus B, Notch intervient dans d'autres processus intra-thymiques, notamment la détermination du TCR $\alpha\beta$ versus $\gamma\delta$, et le choix du corécepteur CD4 versus CD8.

Notch1 a également un rôle essentiel dans la génération de lymphocytes intestinaux intraépithéliaux [82].

★ Notch et lymphocytes T périphériques

Plusieurs équipes ont confirmé le rôle de Notch dans l'activation, la prolifération et la production cytokinique des cellules T périphériques, mais la façon dont Notch est up-régulé dans les lymphocytes T activés reste à préciser. Les récepteurs Notch sont présents dans les lymphocytes T périphériques CD4+ et CD8+, et l'expression des 4 récepteurs est augmentée après activation des cellules T [83] [84].

Après l'activation des cellules T, Notch joue un rôle dans la différenciation des cellules T helper. L'activation de Notch résulte en l'activation de NF-KB, qui va déclencher l'expression des gènes associés aux lymphocytes Th1, tels que le gène de l'IFN- γ . Ceci suggère que Notch joue un rôle dans la différenciation des cellules T CD4+ vers le phénotype Th1. Notch interviendrait également dans la différenciation vers le phénotype Th2. Une étude indique que c'est la spécificité du ligand de Notch qui influencerait le destin des cellules T effectrices [85]. De plus, de récents résultats suggèrent que Notch1 serait impliqué dans les processus caractérisés par des réponses cytokiniques Th2 pathologiques, telles que la fibrose pulmonaire ou le remodelage tissulaire.

Il semblerait également que Notch ait un rôle dans le développement des lymphocytes T régulateurs. D'après les études sur des modèles animaux, Notch3 serait impliqué dans ce processus, et serait ainsi capable de réduire la susceptibilité au diabète auto-immun [86].

★ Notch et lymphocytes B

Notch2 est le récepteur Notch prédominant dans les cellules B, avec une expression allant du stade précurseur B aux différentes populations B périphériques [87]. L'expression de NIC1 dans plusieurs lignées B murines et humaines entraîne l'apoptose [88].

Des études très récentes ont mis en avant le rôle essentiel de Notch 2 dans le développement des cellules B de la zone marginale (BZM).

Par ailleurs, des études récentes suggèrent que Notch participe au développement des cellules B1, une population de cellules B non-conventionnelles [89].

– Tissus cutané et pulmonaire

Chez l'homme Notch1 est exprimé au niveau de toutes les couches épidermiques, et Notch2 uniquement dans la couche basale. Les ligands Jagged et Delta-like sont également exprimés dans l'épiderme. Notch1 induit la différenciation des kératinocytes par l'expression de marqueurs précoces de différenciation comme la keratine-1 et l'involucrine [90]. Chez l'homme, on retrouve une diminution d'expression de Notch1, Notch2

et Jagged1 dans le carcinome baso-cellulaire, ce qui suggère qu'une perte du signal induit par Notch pourrait entraîner le développement de cette pathologie. Notch1, Notch2, et Notch3 sont également exprimés dans le follicule pileux, et sont essentiels à la différenciation de ses cellules et à son homéostasie. En outre, la voie Notch contrôle certaines fonctions au sein des mélanocytes comme l'apoptose ou la différenciation. Enfin, des études *in vitro* suggèrent que cette voie de signalisation influencerait la différenciation des monocytes en cellules de Langerhans [91]. Notch1 est également présent au niveau fibroblastique, tant dans la peau que dans le poumon. Il est capable d'induire la transcription de l' α -SMA après activation par FIZZ1, entraînant alors la différenciation des fibroblastes en myofibroblastes [92]. Cette étude a été réalisée sur des fibroblastes pulmonaires, et il reste à confirmer ces résultats au niveau cutané.

– Système endothérial vasculaire

La voie Notch a récemment été impliquée dans les processus du développement vasculaire. En effet, des mutations de Notch ont été retrouvées dans deux pathologies humaines avec atteintes vasculaires : les syndromes d'Alagille et CADASIL (Cerebral Autosomal Dominant Arteriopathy with Subcortical Infarcts and Leucoencephalopathy). Plusieurs membres de la voie Notch sont exprimés au niveau de l'endothélium vasculaire [93] [94]: Notch1, Notch4, Dll-1, Dll-4, Jagged-1, Jagged-2, et les études réalisées sur des souris transgéniques ont révélé le rôle essentiel de Notch dans l'angiogénèse. Notch bloquerait la prolifération des CE et favoriserait leur survie. L'activation de Notch au niveau des CE les protégerait des agressions environnementales par activation de Bcl-2 [95].

L'équipe de Liaw a montré chez le rat que Jagged1, Jagged2 et Notch étaient constitutivement exprimés dans l'endothelium sain, et que leur expression est significativement augmentée dans les cellules vasculaires d'un endothélium lésé [96]. Les auteurs suggèrent que l'axe Jagged/Notch pourrait jouer un rôle décisif dans les contacts entre les cellules et dans les interactions cellule-matrice, et donc contrôlerait la migration cellulaire dans des situations de remodelages tissulaires.

Une autre équipe a travaillé sur les cellules endothéliales de la microcirculation cérébrale du rat, et montré que leur différenciation peut être favorisée par Notch4/Jagged1 [97].

En 2005, Sainson a utilisé un système *in vitro* en 3D pour montrer que Notch contrôlait la morphologie des vaisseaux et leurs ramifications. Notch interviendrait par deux mécanismes : en réduisant la prolifération des cellules endothéliales, limitant ainsi le diamètre des vaisseaux, et en inhibant la division des cellules des extrémités des vaisseaux [98].

Enfin, de nombreuses équipes s'intéressent au ligand Dll-4, et à l'utilisation de thérapeutiques anti-Dll4 en cancérologie. Le signal transmis par ce ligand de Notch pourrait en effet favoriser la croissance tumorale par la mise en place d'un réseau vasculaire hautement fonctionnel à proximité de la tumeur [95].

- Notch et maladies héréditaires

Chez l'homme, le lien avec des mutations de la voie Notch a été mis en évidence dans quatre maladies héréditaires :

- la tétralogie de Fallot
- le syndrome d'Alagille
- la spondylocostal dysostosis
- le syndrome CADASIL (Cerebral Autosomal Dominant Arteriopathy with Subcortical Infarcts and Leucoencephalopathy)

- Notch et cancers

Nous avons vu précédemment que la voie Notch participait à des processus fondamentaux du développement comme la prolifération, la différenciation et l'apoptose. Comme pour toutes les voies de signalisation impliquées dans ces processus, des mutations conduisant au dérèglement de la voie Notch peuvent entraîner la formation de cancers. En fait, Notch peut se comporter comme un oncogène ou comme un suppresseur de tumeur selon les types cellulaires [99].

Le lien entre dysfonctionnement de la voie Notch et cancer a été établi pour la première fois lorsqu'une translocation chromosomique conduisant à une forme tronquée et constitutivement active de Notch1, a été identifiée de façon récurrente dans plusieurs types de leucémies aigues lymphoblastiques T (LAL-T) [100].

1.2.3.2 La voie des récepteurs aux cannabinoïdes

Le système endocannabinoïde comprend deux récepteurs couplés à une protéine G : CB1 et CB2, leurs ligands lipidiques (endocannabinoïdes) et des enzymes impliquées dans leur synthèse et dégradation [101].

- Les récepteurs CB1 et CB2 :

- Le récepteur CB1 est le plus abondant récepteur couplé à une protéine G dans le cerveau, mais est aussi présent dans de nombreux tissus périphériques. CB1 est responsable des effets psychotropes des cannabinoïdes, mais peut également réguler des fonctions périphériques comme l'activité cardiovasculaire, ou les fonctions de reproduction.
- Le récepteur CB2, lui, est exprimé majoritairement en périphérie mais on en a récemment détecté de faible quantités dans le système nerveux central. CB2 est exprimé de façon prédominante sur les cellules immunitaires où il joue un rôle-clé dans la modulation de l'immunité innée dans des conditions variées telles que l'athérosclérose et les maladies inflammatoires de l'intestin. Les récepteurs CB2 ont également un rôle dans l'immunité anti-tumorale.

- Ligands exogènes et endogènes :

Les ligands de CB1 et CB2 sont les phytocannabinoïdes et les endocannabinoïdes, qui ont des effets autocrines et paracrines. Le Delta-9-tetrahydrocannabinol, issu de Cannabis sativa, se lie à CB1 et CB2 avec la même affinité [102]. Parmi les endocannabinoïdes, l'anandamide (AEA) et les 2-arachidonyl glycerol (2-AG) sont les plus étudiés [103] [101]. L'AEA est un agoniste partiel de CB1 et a une affinité faible pour CB2, alors que le 2-AG est un agoniste puissant de CB1 et CB2. Les endocannabinoïdes sont synthétisés localement et contribuent à l'activation endogène des récepteurs, même si CB1 et CB2 ont une activité de base constitutionnelle. L'AEA et le 2-AG sont synthétisés à partir de précurseurs phospholipidiques.

- Modulation pharmacologique des récepteurs aux cannabinoïdes :

- Modulation de CB1 :

Des antagonistes de CB1 ont été testés dans le traitement de l'obésité et du surpoids, mais des effets secondaires cardiaques se sont manifestés.

- Modulation de CB2 :

Des agonistes de CB2 sont actuellement testés de manière préclinique dans le diabète, l'athérosclérose, l'ostéoporose, et la fibrose hépatique [104] [105] [106] [107] [108] [109].

- Propriétés anti-fibrosantes des récepteurs CB2 :

Les propriétés anti-fibrosantes de CB2 ont été mises en évidence dans un modèle de fibrose hépatique induite par le tetrachlorure de carbone [110]. Dans ce modèle, les fibroblastes hépatiques de souris déficientes en CB2 ont une durée de vie une capacité de prolifération augmentées, ce qui résulte en une majoration de la fibrose [111]. Une seconde étude chez le rat a montré que l'administration de l'agoniste des récepteurs CB2 JWH-133 entraînait une amélioration de la fibrose hépatique et une réduction de l'infiltrat inflammatoire et de la densité des myofibroblastes hépatiques [112]. Les propriétés anti-fibrosantes des récepteurs ont été également évaluées dans un modèle de fibrose cardiaque, et plus récemment dans la sclérodermie systémique par nos travaux exposés dans l'article 3 qui ont été confirmés par les résultats d'autres équipes [113] [114] [115]. Dans ces différents articles, la preuve des propriétés anti-fibrosantes et anti-inflammatoires du récepteur CB2 dans la ScS est apportée par les arguments suivants :

- Dans le modèle de ScS induit par la bléomycine et par l'acide hypochloreux HOCl, l'utilisation d'un agoniste de CB2 limite la fibrose cutanée et pulmonaire ainsi que l'infiltrat inflammatoire dans ces deux organes [113].
- Les souris déficientes en CB2 développent un phénotype exacerbé de la maladie après injections quotidiennes d'HOCl pendant 6 semaines [113].
- Les fibroblastes de patients sclérodermiques présentent une surexpression des récepteurs CB1 et CB2 et l'exposition de ces cellules à des agonistes sélectifs de CB2 ou non sélectifs de CB1/CB2 réduit leur production de matrice extracellulaire et leur différenciation en myofibroblastes [114] [115].

1.3 ANOMALIES ENDOTHÉLIALES

Plus de 90% des patients sclérodermiques présentent un phénomène de Raynaud, ischémie transitoire et réversible au niveau digital. Il traduit un dysfonctionnement de la microvascularisation dermique. Il entraîne des modifications du métabolisme cellulaire et la génération des formes réactives de l'oxygène (FRO) par les mécanismes d'ischémie-reperfusion. Une apoptose précoce des cellules endothéliales est mise en évidence sur les biopsies cutanées de patients, entraînant une perte d'intégrité de la barrière endothéliale. Ce dysfonctionnement de l'endothélium a pour conséquences le recrutement de cellules inflammatoires, une modification de l'équilibre coagulation/fibrinolyse, et des anomalies du tonus vasculaire. De plus, les anomalies endothéliales peuvent contribuer au phénomène de fibrose de la ScS (figure 1.8).

1.3.1 Modifications morphologiques

Les anomalies vasculaires de la ScS prédominent au niveau de la microcirculation, particulièrement au niveau des capillaires et des artéries. Une dilatation des capillaires et une réduction de leur nombre sont observées en capillaroscopie. Une des modifications les plus précoces au niveau de l'endothélium consiste en un réarrangement du cytosquelette des cellules endothéliales, la formation de vésicules cytoplasmiques, et une augmentation de la perméabilité capillaire. Ces modifications capillaires sont présentes à la peau mais également au poumon, aux reins et d'autres viscères. Les patients développant une hypertension artérielle pulmonaire présentent des lésions vasculaires au niveau des petits et moyens vaisseaux du poumon. Ces lésions sont caractérisées par une prolifération de l'intima, une oblitération de la lumière, et la présence d'un infiltrat inflammatoire [116].

1.3.2 Recrutement local de leucocytes

Les CE de patients sclérodermiques sont capables, après activation *in vitro* de secréter MCP-1 et RANTES, deux chimiokines capables d'attirer les monocytes et les macrophages [117].

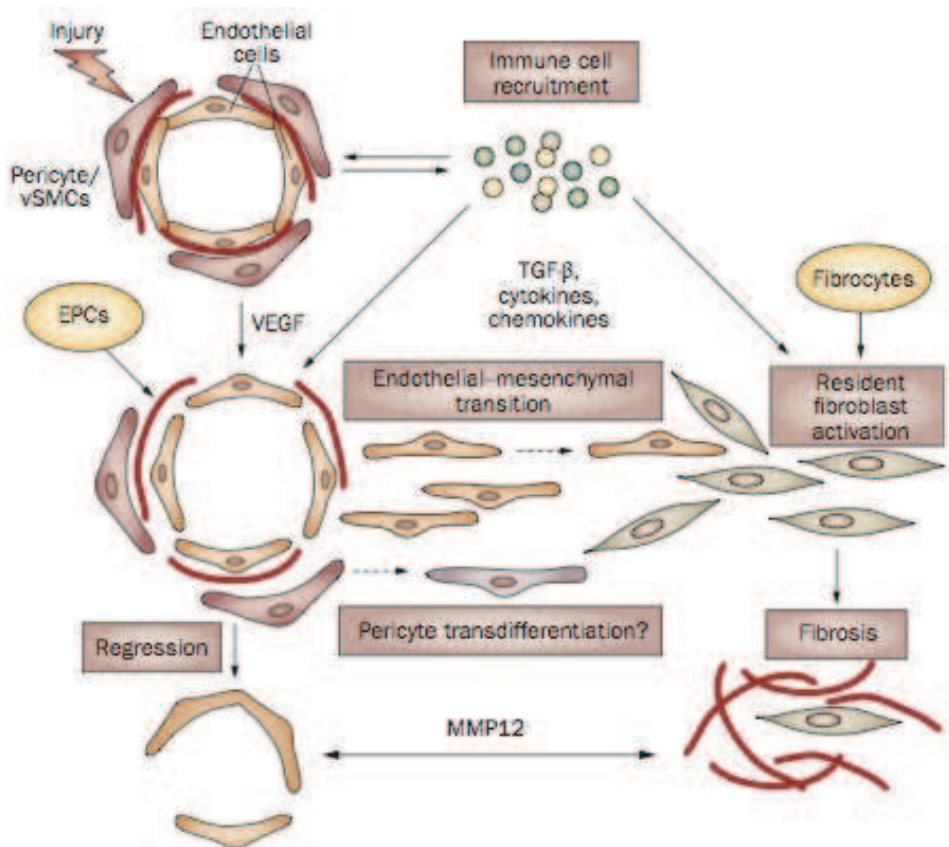


Figure 1.8 Liens possibles entre les anomalies endothéliales et la fibrose dans la sclérodermie systémique d'après M. Trojanowska, Nature Reviews Rheumatology, 2010. La vasculopathie sclérodermique serait initiée par une première lésion ou par l'influx de cellules immunitaires. De forts taux de VEGF et d'autres médiateurs proangiogéniques sécrétés par les cellules immunitaires facilitent la prolifération des cellules endothéliales et des péricytes dans le but de réparer les vaisseaux lésés. Mais, un déséquilibre du statut des médiateurs proangiogéniques/antiangiogéniques, les propriétés intrinsèques des cellules endothéliales, et les facteurs antiangiogéniques sécrétés par les fibroblastes (dont MMP-12), empêchent la réparation d'être efficace et entraînent les anomalies morphologiques des vaisseaux. En présence de TGF- β et d'autres médiateurs, les cellules endothéliales acquièrent un phénotype migratoire via la transition endothélio-mésenchymateuse, et peuvent se différencier en cellules productrices de collagène. Les fibroblastes résidents activés et les fibrocytes qui entrent dans le tissu lésé via la circulation représentent des sources additionnelles de collagène contribuant ainsi à la fibrose dans les lésions sclérodermiques. EPCs: endothelial progenitor cells.

1.3.3 Déséquilibre de l'équilibre coagulation/fibrinolyse

Une coagulabilité accrue est observée au cours de la ScS. De nombreux facteurs de la coagulation sont présents en excès au niveau plasmatique : dermatan-sulfate, thrombine, antithrombine, et vWF. L'excès de ce dernier reflète également la souffrance des CE qui le libèrent. Parallèlement, il existe un défaut relatif en D-dimères, suggérant un défaut de fibrinolyse chez ces patients [118].

1.3.4 Anomalies de régulation du tonus vasculaire

Deux facteurs de régulation sont importants à considérer:

- Le monoxyde d'azote (NO)

C'est une molécule douée de propriétés vasodilatatriques, et secrétée constitutivement par les CE. Le rôle du NO dans la pathogénie de la ScS demeure complexe. Les valeurs plasmatiques de NO mesurées chez les patients sont discordantes d'une étude à l'autre [119] [120]. Par son effet vasodilatateur le NO est capable de s'opposer à d'autres molécules vasoconstrictrices et ainsi d'apporter un effet bénéfique. Cependant son rôle est ambivalent puisqu'il peut interagir avec d'autres formes réactives de l'oxygène, entraînant ainsi la formation de peroxynitrites, responsables de lésions cellulaires irréversibles.

- L'endotheline-1

Il s'agit d'un peptide sécrété par l'endothélium vasculaire, ayant un effet vasoconstricteur puissant sur les cellules musculaires lisses. Les récepteurs de l'ET1 sont exprimés par différentes cellules, notamment les fibroblastes, les CE et les monocytes. Au cours de la ScS, les taux plasmatiques d'ET1 sont élevés, ce qui concourt au développement de phénomènes ischémiques distaux, et à l'apparition d'une hypertension pulmonaire [121]. Des inhibiteurs de la libération de l'ET1 ou de ses récepteurs sont actuellement utilisés dans le traitement de l'hypertension artérielle pulmonaire primitive ou associée à la ScS [122].

1.3.5 Défaut d'angiogénèse

La disparition des capillaires et petits vaisseaux chez les patients sclérodermiques suggère un défaut dans les processus d'angiogénèse chez ces patients, mais les mécanismes en sont inconnus à l'heure actuelle.

Déséquilibre entre les facteurs pro- et anti-angiogéniques:

- Les patients sclérodermiques présentent précocement des taux sériques élevés de VEGF, un facteur pro-angiogénique [123]. Le VEGF et ses récepteurs VEGFR-1 et VEGFR-2 sont également surexprimés dans la peau des patients sclérodermiques [124]. Cependant, le rôle du VEGF dans la physiopathologie de la ScS est inconnu bien que certains auteurs aient suggéré que l'hypoxie locale cutanée pouvait être un facteur contribuant à l'augmentation du VEGF chez certains patients [125]. D'autres médiateurs proangiogéniques ont également des taux plasmatiques élevés comparé aux sujets sains: le PDGF, le "Placental Growth Factor" (PIGF) et le "Fibroblast Growth Factor-2" (FGF-2).
- La concentration de certains facteurs anti-angiogéniques est également augmentée dans le serum de certains patients sclérodermiques: l'angiotensine, le CXCL4, la thrombospondine et l'IL-4 [126]. Ils pourraient contribuer au dysfonctionnement vasculaire mais il est peu probable qu'ils représentent un facteur déclenchant de la vasculopathie sclérodermique. Il reste donc à déterminer si la dérégulation de facteurs pro- ou anti-angiogéniques est cause ou conséquence de la maladie vasculaire au cours de la ScS.

Plusieurs études récentes ont concerné les cellules progénitrices endothéliales dans la ScS. Mais les résultats publiés sur la quantification et les propriétés de ces cellules sont contradictoires, probablement parce que les marqueurs de surface utilisés pour les sélectionner ne sont pas les mêmes d'une étude à l'autre. L'équipe de Del Papa montre ainsi que le taux de cellules progénitrices endothéliales CD45- CD133+ est significativement plus bas chez des patients atteints de ScS débutante que chez des sujets sains [127]. Ceci n'est pas retrouvé chez des patients ayant une ScS évoluant depuis plusieurs années. Cet article suggère que les cellules progénitrices endothéliales médullaires sont insuffisantes quantitativement et qualitativement dans la ScS pour compenser l'apoptose précoce des CE périphériques, phénomène précédant probablement de plusieurs années les signes cliniques de la ScS.

1.4 INTERVENTION DU SYSTÈME IMMUNITAIRE

L'immunité innée et l'immunité adaptative jouent toutes deux un rôle dans la physiopathologie de la ScS. Au début de la maladie, l'activation leucocytaire est visible dans le sang périphérique et dans les tissus lésés, où elle intervient directement dans l'induction des lésions tissulaires.

1.4.1 Immunité innée

Des monocytes et des macrophages ont été mis en évidence dans la peau de patients présentant une ScS débutante [128] [129]. Ces cellules ont également été observées dans un modèle murin de maladie de greffon contre l'hôte[130]. Elles expriment à leur surface de grandes quantités de molécules présentatrices d'antigènes et pourraient ainsi induire l'activation des LT. De nombreux mastocytes sont également observés dans la peau des malades dès le début de la maladie, au sein des lésions de sclérose mais également en peau saine [131]. Ces cellules libèrent en particulier de l'IL-4 et de l'histamine qui participent aux processus de fibrose. Dans des modèles murins de fibrose induite par la bléomycine, un déficit en mastocytes retarde en effet l'apparition de la fibrose cutanée [132].

1.4.2 Immunité adaptative cellulaire

Plusieurs arguments plaident en faveur d'un rôle des LT dans la pathogénie de la ScS, en particulier à la phase initiale de la maladie. Les infiltrats dermiques sont constitués principalement de lymphocytes T CD4+ activés [133]. L'importance de cet infiltrat cellulaire est corrélée avec une durée d'évolution courte et un score cutané élevé. En effet, les biopsies de peau réalisées à des phases tardives de la maladie, à un stade avancé de fibrose ne montrent plus qu'un infiltrat inflammatoire modéré [134]. L'infiltrat périvasculaire est composé de lymphocytes T CD4+ exprimant le marqueur HLA-DR et le récepteur à l'IL-2. Ces cellules peuvent secréter des cytokines et des chemokines pro-fibrosantes [135]. Les cellules T que l'on retrouve dans les tissus lésés ont des spécificités restreintes de TCR, ce qui suggère une expansion de type oligoclonal [136]. Cependant, on ne sait pas si ces clones sont activés de manière non spécifique par des cytokines ou chemokines ou de manière spécifique par des antigènes inconnus et restreints. Le recrutement des lymphocytes dans la peau se fait grâce à des molécules d'adhésion. En 2010,

l'équipe de Sato a étudié le rôle de différentes molécules d'adhésion dans ce processus dans le modèle murin de ScS induite par la bléomycine [66]. Grâce à diverses souches de souris K-O, ils ont pu montrer que la "L-selectin" et ICAM-1 régulaient l'accumulation des lymphocytes Th2 et Th17 dans la peau et le poumon, et que ces deux populations de lymphocytes avaient des propriétés pro-fibrosantes, contrairement à l'infiltrat Th1 qui semble être régulé par la "P-selectin", et PSGL-1 et qui aurait la propriété d'inhiber le développement de la fibrose dans ce modèle.

Le transfert de lymphocytes T CD4+ provenant de souris traitées par la bléomycine à des souris BALB/c nude non traitées par la bléomycine reproduit les mêmes effets cliniques, histologiques et biologiques que ceux observés dans le modèle expérimental [137]. Ce résultat conforte le rôle de la réaction immunitaire adaptative dans le développement ou l'entretien de la ScS induite par la bléomycine.

Des anomalies des LT circulants ont aussi été observées avec une diminution des LT CD8+ et une augmentation des LT CD4+ activés HLA-DR+ [138]. L'équilibre cytokinique Th1/Th2 est incertain dans la ScS, plusieurs études sur le sujet ayant donné des résultats discordants. Des taux élevés d'IL-4 ont, d'une part, été retrouvés dans le sérum de patients [58]. En outre, une analyse microarray du transcriptome des lymphocytes circulants des patients sclérodermiques réalisée en 2006 a montré des niveaux élevés de GATA-3, facteur impliqué dans la polarisation Th2. Enfin, l'analyse protéomique des lavages bronchoalvéolaires de patients confirme la pré-dominance de cytokines de type Th2 [139]. Mais d'autre part, les souris déficientes en T-bet, un facteur de transcription spécifique de l'activation des lymphocytes Th1 développent une fibrose exacerbée en réponse aux injections quotidiennes de bléomycine [140]. Et, un profil d'expression génique de type Th1 a été observé dans les cellules mononucléées du sang périphérique de patients [141].

ICOS, un membre de la famille du CD28 intervenant dans la coopération B-T a récemment été impliqué dans la physiopathologie de la ScS. En effet, le déficit en ICOS atténue la fibrose cutanée et pulmonaire induite par la bléomycine. Au contraire, le déficit en ICOS-ligand accentue le processus fibrotique, et des auteurs ont montré que la sévérité de la fibrose était corrélée avec les taux d'expression d'ICOS-ligand dans les lymphocytes B et les macrophages [142]. Ainsi, ICOS-ligand joue un rôle régulateur de l'activation des cellules présentatrices de l'antigène dans le développement de la fibrose induite par la bléomycine.

D'autres travaux soulignent également l'influence exercée par les LT sur les fibroblastes. Les LT circulants de patients sclérodermiques inhibent partiellement la synthèse de collagène par des fibroblastes de patients sclérodermiques [143]. Cet effet d'inhibition est médié par un contact direct entre LT et fibroblastes, et dépendant d'une activation préalable, *in vitro*, des LT du sang périphérique. La même équipe a montré plus récemment que les fibroblastes sclérodermiques sont résistants à l'effet des LT Th-2 extraits du derme de malades et activés *in vitro* [144]. Seuls les LT de type Th-1, activés par un anti-CD3, peuvent réduire la synthèse de collagène des fibroblastes de patients sclérodermiques. Ces deux derniers travaux, bien qu'étant réalisés uniquement sur des expériences *in vitro* montrent la complexité des interactions cellulaires dans cette maladie. De plus, ils suggèrent un rôle nouveau que pourraient avoir certains LT dans la maladie, celui de cellules régulatrices.

Le microchimérisme observé chez la mère après la grossesse place aussi l'immunité cellulaire au centre des hypothèses physiopathologiques envisagées la physiopathologie de la ScS [145]. La persistance de cellules foetales dans le sang maternel serait responsable d'une réaction allogénique comparable à une réaction du greffon contre l'hôte (GVH) chronique. Ces cellules foetales ont été retrouvées en quantité augmentée dans le sang des patientes sclérodermiques, et sont présentes dans les lésions cutanées de ces patientes [145]. En effet, on observe au cours de la GVH chronique chez l'homme et chez l'animal des manifestations proches de la sclérodermie. Certains modèles animaux de GVH sont d'ailleurs utilisés pour étudier les manifestations sclérodermiques cutanées et pulmonaires [146].

1.4.3 Immunité adaptative humorale

Les anomalies des lymphocytes B (LB) dans la ScS sont connues depuis plusieurs années et sont caractérisées par la production d'auto-anticorps, une hypergammaglobulinémie, et une hyper-réactivité des lymphocytes B. Plus récemment des anomalies touchant diverses populations B ont été identifiées.

1.4.3.1 Eléments contribuant à l'activation des lymphocytes B

Les LB des patients atteints de ScS semblent anormalement activés et surexpriment CD19 (voir figure 1.9) [147]. Or la surexpression de cette molécule de costimulation induit une synthèse

anormale d'immunoglobulines dans un modèle de souris transgénique pour le CD19. De plus, chez les souris TSK-1^{+/}, qui développe spontanément une fibrose cutanée, les voies de signalisation intra-cytoplasmiques dépendantes de CD19 sont constitutivement activées et le blocage de l'expression de cette molécule entraîne une diminution du titre des auto-Ac sériques et du degré de fibrose cutanée [148]. Chez les souris déficientes en CD19 et soumises au protocole d'induction de la ScS par la bléomycine, l'induction de la fibrose cutanée et pulmonaire, la production cytokinique, et la production d'auto-anticorps sont inhibées [149].

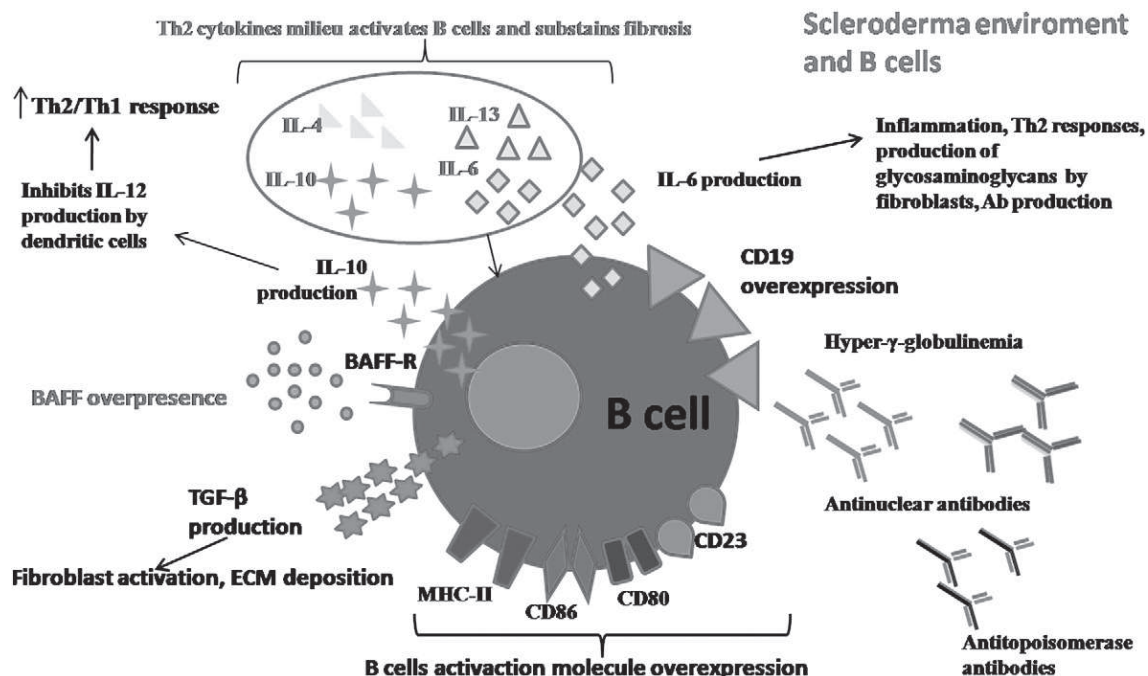


Figure 1.9 Lymphocytes B et environnement cytokinique dans la sclérodermie systémique, d'après S. Bosello, Autoimmunity Reviews, 2011

Une autre molécule, BAFF, aussi impliquée dans l'homéostasie des lymphocytes B (figure 1.9), est surexprimée dans le sang et la peau de patients atteints de ScS. En effet, comme les patients atteints de lupus érythémateux systémique ou souffrant d'un syndrome de Sjögren, les patients sclérodermiques, ont des taux sériques de BAFF plus élevés que des sujets sains [150] [151] [152]. De plus, ce taux sérique semble corrélé à la sévérité de l'atteinte cutanée et il existe une forte transcription de BAFF par les cellules inflammatoires de la peau dans les formes débutantes de ScS diffuse.

Les éléments indiquant une polarisation des lymphocytes T vers une réponse de type Th2 jouent un rôle dans le développement de la fibrose tissulaire. L'activation des LB et la réponse humorale sont ainsi facilités par cet environnement Th2 caractérisé par une surproduction d'IL-4, IL-5, IL-6, IL-10 et IL-13. Ces cytokines favorisent la production d'anticorps par les LB, et, comme nous l'avons vu précédemment stimulent la synthèse de collagène par les fibroblastes. Enfin, il est également possible que les LB influencent eux-mêmes la polarisation Th2 en régulant les fonctions des cellules dendritiques: l'IL-10 produite par les LB inhibe la production d'IL-12 par les cellules dendritiques, ce qui favorise la différenciation des LT en Th2. L'IL-6 produite par les LB peut induire la production de collagène et de glycosaminoglycane par les fibroblastes du derme. Dans plusieurs études, les niveaux élevés d'IL-6 dans la peau et le sérum des patients indiquent que cette cytokine joue un rôle dans le développement de la fibrose via son activité pro-inflammatoire [153]. Les fibroblastes de patients sclérodermiques produisent 4 fois plus d'IL-6 que les fibroblastes de sujets sains. Chez les souris Tsk1, les LB stimulés avec une Ig anti-IgM et une Ig anti-CD40 produisent des taux significativement plus élevés d'IL-6 que les LB provenant des souris contrôles [148]. Les LB activées secrèterait également du TGF- β , ce qui amplifierait la production excessive de matrice extra-cellulaire par les fibroblastes [154].

1.4.3.2 Auto-anticorps : origine, nature et rôle pathogène

La majorité des patients atteints de ScS ont des auto-Ac détectables dans le sérum. Les mécanismes contribuant à la rupture de tolérance vis-à-vis de certains antigènes demeurent inconnus dans la plupart des maladies accompagnées d'autoimmunité. Néanmoins, dans la ScS, plusieurs travaux ouvrent des pistes.

En effet, les antigènes cibles dominants et caractéristiques de la ScS, la protéine centromérique CENP B, l'ADN Topoisomérase-1, l'ARN polymérase, sont d'une part particulièrement sensibles à l'action de la protéase granzyme B des granules T cytotoxiques ; et d'autre part, l'ADN Topoisomérase-1 et l'ARN polymérase III peuvent être clivées sous l'effet d'une oxydation par la réaction de Fenton [155]. Les modifications ainsi subies par ces protéines changent leur conformation et augmentent leur antigénicité, favorisant une rupture de tolérance.

Une autre équipe a montré que les CE exposées au sérum de patients atteints de ScS synthétisaient des quantités aberrantes de fibrilline puis entraient en apoptose de manière accélérée

[156]. Cet excès de synthèse de fibrilline, favorisé également par l'apoptose accélérée des CE, pourrait également contribuer à l'apparition d'Ac notamment dirigés contre la fibrilline.

Une autre hypothèse est celle du mimétisme moléculaire puisqu'une homologie a été observée entre une protéine membranaire humaine exprimée par les CE et les fibroblastes normaux et une protéine virale du CMV [3].

Des associations particulières entre certains types d'auto-Ac et certaines manifestations cliniques sont bien établies [157], ce qui suggère une implication particulière des LB dans la ScS. Néanmoins, parmi les Ac dont les cibles sont identifiées, peu ont témoigné de manière reproductive d'un rôle pathogène. De plus un transfert de la maladie par auto-Ac n'a jamais été démontré au cours de grossesses ou dans des modèles animaux. Cependant, plusieurs équipes rapportent un effet direct des Ac anti-cellules endothéliales et Ac antifibroblaste sur leurs cellules cibles. Une équipe a, en 2006, mis en évidence dans les sérum de tous les malades testés des Ac anti-récepteur du PDGF capables d'induire chez des fibroblastes un phénotype de myofibroblastes [45]. La présence de ces auto-Ac a depuis été infirmée par une autre équipe [47].

Plusieurs Ac retrouvés dans le sérum de patients atteints de ScS sont rapportées ci-dessous, la liste des Ac abordés n'étant pas exhaustive.

- Ac anti-centromère

Les Ac anti-centromères sont détectés dans le sérum de 20 à 30% des patients sclérodermiques, la fréquence variant avec l'origine ethnique des patients. Ces Ac sont dirigés contre une ou plusieurs protéines centromériques nommées CENP-A, -B, -C, -D, -E, -F; CENP-B est constamment reconnu. La présence de ces Ac est corrélée avec certains signes cliniques : forme cutanée limitée de la maladie, calcinose, syndrome de Raynaud, mais aucun rôle pathogène pour ces Ac n'a été démontré.

- Ac anti-ADN Topoisomérase-1 (ou anti-Scl70)

Les Ac anti-ADN Topoisomérase-1 sont présents chez 15 à 20% des patients atteints de ScS, quelle que soit leur origine ethnique. Comme les Ac anti-centromère, leur présence est corrélée avec certains signes cliniques (fibrose pulmonaire) et retrouvés plus fréquemment

dans une forme particulière de la maladie (30% chez les patients atteints de la forme cutanée diffuse). Les Ac anti-centromère et anti-ADN Topoisomérase-1 sont mutuellement exclusifs (moins de 0,5% des sérum de patients contiennent les deux Ac), observation qui demeure inexpliquée à l'heure actuelle. Des travaux récents ont montré que des Ac anti-ADN Topoisomérase-1 étaient capables de se lier à la membrane des fibroblastes, et d'induire l'adhésion des monocytes aux fibroblastes puis leur activation [158]. L'ADN Topoisomérase-1 reconnue à la surface des fibroblastes est d'origine extra-fibroblastique, et se est adsorbée passivement à leur surface, avant d'être reconnue par des Ac [159].

- Ac anti-ARN polymérase III

Ces anticorps sont détectés chez environ 15% des patients sclérodermiques. Ils sont associés à la survenue de crise rénale chez les patients atteints de la forme diffuse de la maladie, et à un mauvais pronostic. Leur présence peut être associée à celle d'anticorps anti-ADN Topoisomérase-1. Ainsi, leur dosage dans le sérum des patients peut avoir un intérêt pronostique dans le cadre des crises rénales sclérodermiques. Leur pouvoir pathogène n'a pas été démontré.

- Ac anti-matrice metalloprotéase

Les métalloprotéases sont des endopeptidases dont la fonction est de dégrader la matrice extracellulaire. Il en existe plusieurs, chacune ayant des cibles particulières. Une équipe a identifié, chez des patients japonais atteints de ScS, des Ac dirigés contre deux métalloprotéinases, Matrix metalloproteinase 1 (MMP-1) et MMP-3 [160].

- Ac anti-cellules endothéliales

Comme au cours de nombreuses maladies, au premier rang desquelles les vascularites, des Ac anti-CE ont été détectés dans le sérum de malades atteints de ScS. Leur prévalence varie de 28 à 85% et dépend de la forme clinique mais aussi des techniques de détection utilisées [161] [162]. Ils sont plus fréquemment retrouvés chez les malades présentant une forme diffuse de ScS, des ulcères digitaux, un phénomène de Raynaud sévère, une fibrose pulmonaire et/ou une atteinte cardiaque. Leurs cibles antigéniques sont en cours d'identification. Plusieurs travaux ont montré un rôle pathogène de ces Ac. Chez les patients atteints de sclérodermie, des Ac anti-CE de malades atteints de ScS peuvent induire l'activation de

CE in vitro, entraînant l'expression de molécules d'adhésion et la libération de chimiokines et cytokines [163].

- Ac anti-fibroblastes

Les Ac anti-fibroblastes ont été identifiés dans le sérum de patients sclérodermiques dans les années 1980 [164]. Depuis, ces Ac ont été bien caractérisés. Ils peuvent être détectés par technique ELISA dans le sérum de 46 à 58% des patients atteints de ScS [165], semblent plus fréquents chez les patients atteints de forme diffuse. Ils ont aussi été détectés par immuno-fluorescence indirecte et par cytométrie en flux. Après fixation à leur ligand, certains de ces Ac sont internalisés. In vitro, ils induisent l'expression de molécules d'adhésion telles que ICAM-1, et de cytokines (IL1, IL6) par les fibroblastes [166]. La même équipe a montré ultérieurement que ces Ac n'induisaient pas de synthèse particulière de collagène au contact de fibroblastes, mais induisaient par contre une synthèse de métalloprotéinases. Ce résultat suggère que ces Ac ne seraient pas impliqués directement dans le processus de fibrose.

- Ac anti-fibrilline

La fibrilline est un constituant majeur des microfibrilles de la matrice extracellulaire. Un polymorphisme du gène de la fibrilline (gène fbn1) est associé au développement d'une ScS dans certaines populations. Des Ac anti-fibrilline peuvent être détectés chez des patients atteints de ScS ou de connectivité mixte [167]. La prévalence de ces Ac varie en effet selon l'origine ethnique des patients, puisqu'ils sont présents chez 94% des indiens Choctaw, chez 87% des patients japonais et seulement 4% des sujets d'origine afro-américaine. Dans un travail ultérieur, cette équipe a montré que des Ac antifibrilline purifiés induisaient une synthèse de collagène au niveau de fibroblastes [167].

- Ac anti-récepteur du PDGF (ou anti-PDGFR)

Ces Ac, dont la découverte est directement liée à leur pouvoir pathogène, semblent jouer un rôle plus central que tous les Ac précédemment cités [45]. Ils ont été retrouvés dans tous les sérums des patients testés par l'équipe les ayant identifiés, et leur effet pathogène concerne directement le fibroblaste. Leur détection est directement basé sur leur capacité d'induire des FRO. Ils induisent une phosphorylation des tyrosines intra-cytoplasmiques, une activation de la NADPH oxydase, une synthèse de FRO, une activation de ERK 1/2 et

une accumulation des GTPases Ha Ras. Une boucle autonome d'activation intracytoplasmique se forme, conduisant à la transcription de gènes, notamment du collagène. La même équipe a retrouvé, par la même technique, des Ac du même type chez les patients présentant une maladie du greffon contre l'hôte, maladie qui partage des similitudes cliniques avec la ScS [46]. Ces résultats apparaissent aujourd'hui nuancés puisqu'un article récent a infirmé l'existence des Ac anti-PDGFR dans la ScS [47]. Malgré l'utilisation de 4 méthodes différentes (étude de la phosphorylation du récepteur, de la signalisation par les MAP kinases, de la production de ROS, et de la prolifération cellulaire), les auteurs n'ont pu mettre en évidence l'activation spécifique des PDGFR α et PDGFR β par les IgG purifiées des sérum de leur cohorte de patients sclérodermiques.

1.4.3.3 Thérapeutique ciblée dirigée contre les lymphocytes B

Récemment, 4 essais cliniques et 4 études de cas suggèrent l'utilisation possible de l'anticorps chimérique monoclonal anti-CD20 (Rituximab) chez les patients sclérodermiques [168] [169] [170] [171]. Au total, 44 patients ont été inclus dans ces différentes études. Il s'agissait de patients atteints de la forme diffuse de la ScS et la plupart étaient positifs pour l'auto-anticorps anti-Scl70 (anti-DNA-Topoisomérase-1). Dans 3 des 4 essais cliniques, une amélioration significative du score de Rodnan et des modifications histologiques (réduction de l'infiltrat cellulaire B dans la peau, des myofibroblastes et du dépôt de collagène) et biologiques (concentration sérique d'IL-6 et de BAFF) a été rapportée. Les taux d'auto-anticorps n'étaient que modérément diminués. Les patients inclus dans ces essais cliniques avaient des formes cliniques relativement hétérogènes (durée de la maladie, sévérité, atteinte pulmonaire/cardiaque), avaient reçu différents traitements immunosuppresseurs par le passé, et les doses de Rituximab utilisées étaient très variables. De plus larges études comportant des groupes de patients plus homogènes doivent donc être réalisées afin de pouvoir tirer des conclusions sur l'efficacité de Rituximab dans la ScS.

1.5 FACTEURS GÉNÉTIQUES ET ENVIRONNEMENTAUX

1.5.1 Facteurs génétiques

La présence d'antécédents familiaux de ScS représente actuellement le plus important facteur de risque de développer la maladie [172]. Cependant une étude analysant la prévalence de la maladie chez des jumeaux mono et dizygotes montre une concordance faible et similaire dans les deux cas (4,7% en moyenne) [173]. S'il est clair que la ScS n'est pas une maladie uniquement déterminée par des facteurs génétiques, de nombreux gènes pourraient interagir pour favoriser son déclenchement et en influencer la présentation clinique et sérologique (forme diffuse ou cutanée limitée, vasculaire ou fibrosante, Ac anti-centromère ou anti-ADN Topoisomérase-1).

La fibrilline 1 fait partie des gènes candidats susceptibles de favoriser la fibrose. Des polymorphismes au niveau d'un nucléotide ont été mis en évidence dans ce gène dans la population d'indiens nord-Américains Choctaw, population dans laquelle la prévalence de la ScS est très élevée [174]. De plus, ce gène est dupliqué chez les souris TSK-1/+ qui développent spontanément une fibrose cutanée [175]. Cependant, un tel polymorphisme n'a pas été retrouvé dans d'autres populations.

Des mutations du gène codant le récepteur de type II des "bone morphogenetic proteins" (BMP) ont été mises en évidence au cours de formes familiales et sporadiques d'hypertension artérielle pulmonaire idiopathique, et des mutations du gène codant l'"activin-receptor-like kinase-1" (ALK-1) ont été mises en évidence au cours de l'hypertension artérielle pulmonaire associée à la maladie de Rendu-Osler [176]. Ces mutations n'ont jusqu'à présent pas été mises en évidence au cours de la ScS.

Il n'y a pas de gène du complexe majeur d'histocompatibilité (CMH) qui confère une prédisposition à la ScS. Cependant, de nombreux travaux soulignent des associations entre certains allèles de gènes du (CMH) et certains sous-groupes de patients sclérodermiques, porteurs d'un type d'auto-Ac particulier. En 2009, l'étude GENISOS (Genetic versus Environment In Scleroderma Outcome Study) a permis de démontrer que les allèles HLA DRB1*0802 et DQA1*0501 étaient des facteurs prédictifs de mortalité dans la ScS.

Un polymorphisme en position 945 du promoteur du gène du CTGF a récemment été mis en évidence dans deux groupes différents de patients atteints de ScS [177].

En 2010, la première étude de genome-wide scan dans la ScS a été réalisée par une équipe américaine, afin d'identifier les loci associés à une prédisposition à la ScS. Trois loci ont ainsi été mis en évidence: STAT4, CD247 et IRF5.

- STAT4 est un facteur de transcription majeur dans la signalisation et la différenciation lymphocytaire T. Il induit également la transcription des IFN de type I dans les monocytes activés. Son rôle de médiateur de l'inflammation dans la ScS a été confirmé par le développement d'une fibrose modérée après induction de la ScS par injections de bléomycine chez les souris STAT4-/-.
- CD247 code la sous-unité zeta du TCR, et une expression faible de CD247 peut entraîner un défaut de la réponse immunitaire [178].
- IRF5 appartient à la famille des facteurs de transcription de la voie des interférons de type I (IFN). L'allèle IRF5 rs4728142 est associé à une espérance de vie augmentée dans la ScS et à une atteinte interstitielle pulmonaire modérée [179].

1.5.2 Facteurs environnementaux : virus et toxiques

Le rôle potentiel de facteurs environnementaux, en particulier infectieux et toxiques dans la pathogénie de la ScS est aujourd'hui mieux connu.

Concernant le lien entre ScS et exposition à des substances chimiques, les études sont contradictoires mais un certain nombre d'arguments suggèrent le rôle de l'exposition à des particules de silice, aux polymères de chlorure de vinyle et à des solvants organiques [180].

Deux virus ont attiré particulièrement l'attention et fait l'objet de plusieurs travaux: le Parvovirus B19 et le CMV. De l'ADN de parvovirus B19 a en effet été détecté dans la peau et la moelle osseuse de patients atteints de ScS chez un nombre restreint de patients mais aucune protéine virale n'a été retrouvée [181]. Néanmoins ce virus reste un important candidat, en raison de sa capacité à activer les fibroblastes. D'autres arguments plus convaincants suggèrent une possible implication du CMV dans la ScS : il existe une homologie de structure entre la

protéine virale UL 94 et une protéine membranaire humaine exprimée par les CE et les fibroblastes normaux, NAG 2. Il a été montré que des Ac anti-UL94 étaient ainsi capables de se lier à des CE et à des fibroblastes et d'induire leur activation avec transcription de molécules d'adhésion, de cytokines, de TGF- β et de CTGF [182]. De plus ces Ac induisaient une apoptose des CE. Enfin, il existe une relation étroite entre ce virus et la maladie du greffon contre l'hôte, maladie présentant de nombreuses similitudes avec la ScS.

1.6 MODÈLES ANIMAUX

La figure 1.10 présentée à la page suivante reprend les caractéristiques des principaux modèles animaux spontanés et induits de sclérodermie systémique.

1.6.1 Modèles spontanés

- Poulets de l'University of California at Davis (UCD) lignée 200

Cette lignée présente des signes de nécrose au niveau de la crête et des pattes, des arthrites, et une fibrose cutanée [183]. Plus de la moitié des animaux décèdent avant 10 semaines. Ceux qui survivent développent une atteinte viscérale (oesophagienne et rénale), et des auto-Ac.

- Souris Tight skin (Tsk+)

Dans cette lignée de souris apparaît spontanément en quelques semaines un épaississement de la peau avec accumulation de collagène et de protéines de la matrice extra-cellulaire [175]. Elles présentent également des anomalies du parenchyme pulmonaire et une hypertrophie des oreillettes cardiaques. On détecte dans leur sérum des auto-Ac anti-nucléaires, anti-ADN, anti-ADN Topoisomérase 1. Ce modèle de fibrose partage des caractéristiques avec la ScS humaine mais il n'y a pas d'augmentation de taux d'apoptose des cellules endothéliales. Les mécanismes des anomalies de cette lignée restent à éclaircir, et sont probablement très différents de ceux de la ScS humaine.

Table 1 Genetic and induced-animal models of systemic sclerosis and their key physiopathologic features

	Fibrosis	Inflammation	Autoimmunity	Vasculopathy	Key mechanisms
Genetic models Tsk-1 mice	Skin	No	Autoantibodies	Endothelial dysfunction but no typical features of SSc vasculopathy	Spontaneous autosomal dominant mutation in the fibrillin gene <i>FBN1</i>
Tsk-2 mice	Lung: emphysema rather than fibrosis Skin	Inflammatory cellular infiltrate in the tissues Systemic inflammation	Autoantibodies	No	Unknown mechanism
Fra-2 mice	Skin	No		Loss of small blood vessels in the skin and lung Endothelial cell apoptosis	Transgenic construct with the ubiquitous promoter H2Kb and the <i>Fra-2</i> locus <i>Fra-2</i> is a member of the activator protein 1 family
UCD-200 chickens	Lung	Perivascular mononuclear cell infiltrates	Autoantibodies	Raynaud's like syndrome	Activation and apoptosis of endothelial cells
	Oesophagus			Necrotic and ischaemic lesions	
	Heart				
TGF β RII Δ k mice	Lung Kidney Skin (at 12 weeks)	Mild	No	Vascular remodelling in the lungs	Fibroblast-specific activation of TGF β signalling
Inducible models Bleomycin	Lung	Fibrotic cardiomyopathy			
	Skin	Inflammatory cellular infiltrates	Autoantibodies	Endothelial cell apoptosis	Production of reactive oxygen species
HOCl	Lung Skin	Inflammatory cells infiltrate in the lung High AOPP and nitrates serum concentration	Autoantibodies IL-4, IL-13	Endothelial cell damages (<i>svCAM1</i>)	Production of H_2O_2 by skin fibroblasts consequent to OH^{\bullet} generation in the skin Oxidation of DNA-Topoisomerase-1 leading to a break of tolerance and to the diffusion of the disease
ScI-GVHD	Kidney Skin	Tissue infiltration of T cells, monocytes, mast cells Alloreactive T-cells	Autoantibodies	Increase in splenic B cells number	
	Lung Kidney				

Figure 1.10 Modèles animaux de sclérodermie systémique spontanés et induits, d'après F. Batteux et al. Current Opinion in Rheumatology, 2011

1.6.2 Modèles induits

- Souris Tight skin (Tsk2/+)

Les souris Tsk2/+ ressemblent aux souris Tsk/+ car elles développent vers 10-15 jours un épaississement cutané [184]. Cet épaississement est lié à une accumulation de fibres de collagène dans le derme. Chez ces souris, la fibrose est génétiquement déterminée et se transmet sur un mode autosomique dominant. Contrairement aux souris Tsk/+, un important infiltrat inflammatoire est observé dans le derme et dans le tissu adipeux sous-cutané. Ces souris développent des Ac anti-nucléaires, des Ac anti-ADN Topoisomérase, des Ac anti-CENP-B, ainsi que des Ac anti-ADN.

- "Graft Versus Host (GVH)- induced systemic sclerosis"

Le transfert de splénocytes et de cellules de moelle-osseuse de souris B10.D2 (H-2d) à des souris BALB/c invalidées pour le gène RAG2 (H-2d) entraîne des incompatibilités HLA-mineures aboutissant à une réaction du greffon contre l'hôte [130]. Les souris présentent un épaississement de la peau en particulier des extrémités, maximal après 3 à 4 semaines [130]. L'analyse histologique de la peau montre d'abord un infiltrat inflammatoire constitué majoritairement de LT CD4+ puis une fibrose avec accumulation de matrice extracellulaire. Ces modifications ne se limitent pas à la peau mais sont également observées dans les reins et l'intestin. Outre une fibrose, on retrouve chez ces souris d'autres anomalies cliniques comme une vascularite, une alopecie et une diarrhée entraînant une perte de poids. Ces souris développent en plus des auto-Ac spécifiques de la ScS. Ce modèle repose sur une activation du système immunitaire et peut donc être utilisé pour étudier le rôle de l'activation immunitaire dans le développement de la fibrose, et pour tester de nouvelles approches thérapeutiques ciblant les lymphocytes T CD4+.

Un second modèle de ScS associée à la GVH a été établi en transférant des splénocytes et cellules de moelle-osseuse de souris B10.D2 à des souris BALB/c irradiées de manière sublétale à 7 Gray [185]. Ce modèle permet de s'affranchir de l'utilisation de souris BALB/c RAG, mais nécessite une étape d'irradiation. Les souris développent les mêmes anomalies que dans le modèle précédent.

- Souris exposées au Chlorure de Vinyl

Une équipe a accouplé des souris femelles BALB/c à des mâles C57BL/6J, puis a exposé ces souris femelles à du chlorure de vinyl, un solvant organique [186]. Ces femelles ont développé une fibrose cutanée et un infiltrat inflammatoire. L'exposition au chlorure de vinyle augmente quantitativement les cellules d'origine foetale circulantes chez ces souris femelles. Cette substance pourrait avoir un rôle dans l'activation de ces cellules d'origine foetale, qui à leur tour seraient impliquées dans le développement de la fibrose. Ce modèle est intéressant puisqu'il se base sur une cascade d'événements plausibles chez l'homme.

- Souris exposées à la bléomycine

La bléomycine induit une fibrose pulmonaire après instillation intra-trachéale. L'injection de cette molécule par voie sous-cutanée pendant 4 semaines tous les jours à des souris induit une fibrose cutanée et pulmonaire, ainsi que des Ac anti-fibroblastes et anti-ADN Topoisomérase-1 [132]. L'analyse histologique de la peau et des poumons de ces souris montre un infiltrat inflammatoire majoritairement composé de LT CD4+. Des mastocytes sont également présents. La matrice extracellulaire contient de grandes quantités de TGF β . Cette modification du derme se maintient au moins 6 semaines après la fin des injections. Selon leur fond génétique, certaines lignées murines semblent plus prédisposées que d'autres à développer une fibrose induite par la bléomycine. Les mécanismes impliqués dans la fibrose induite par la bléomycine apparaissent complexes et résultent probablement à la fois de la toxicité directe de la molécule et de l'effet de médiateurs secondaires. De plus, la bléomycine induit la synthèse de FRO, notamment d'anions superoxyde et de radicaux hydroxyl qui participent aussi à sa toxicité. En effet, des injections de SOD, enzyme qui transforme les anions superoxyde en H₂O₂, moins toxique, diminuent l'accumulation de collagène dans le derme si ces injections sont réalisées en même temps que les injections de bléomycine. Les souris exposées à la bléomycine sont donc un modèle intéressant à étudier. Néanmoins, cette molécule agit par des mécanismes complexes encore mal élucidés et probablement en partie différents -au moins pour la phase initiale - de ceux impliqués dans la ScS humaine, maladie indépendante de l'exposition à la bléomycine.

Le premier de nos articles présentés en annexe dans le chapitre 5 est une revue présentant les caractéristiques des modèles de ScS induits chimiquement, notamment le modèle de ScS induit par l'exposition à la bléomycine.

- Souris MRL/lpr déficientes en récepteur de l'IFN-gamma

Ces souris développent un érythème puis une fibrose avec accumulation de collagène dans la peau, les reins, le foie, les poumons et les glandes salivaires, ce que ne développent pas les souris exprimant le récepteur de IFN γ [187]. L'analyse histologique montre en outre une thrombose étendue des petits vaisseaux. Il n'y a en revanche pas de signes de glomé-rulonéphrite, contrairement aux souris MRL/lpr exprimant le récepteur de IFN γ .

- Souris transgéniques FRA-2

Une surexpression de FRA-2 a été observée dans la peau de patients sclérodermiques, suggérant que ce facteur de transcription exerçait un rôle important sur les anomalies vasculaires et la fibrose. Une équipe a mis au point un modèle basé sur la surexpression de ce facteur de transcription. Les souris FRA-2 (Fos-related antigen-2) présentent une microangiopathie et une fibrose cutanée progressive [188]. Ces événements sont précédés d'une apoptose des cellules endothéliales. FRA-2 est un facteur de transcription appartenant à la famille d'AP-1 (activation factor-1). L'expression de FRA-2 est indépendante du TGF- β et du PDGF.

- Souris Fli-1

Fli-1 ("Friend leukemia integration factor-1") joue un rôle inhibiteur dans l'expression de protéines de la matrice extra-cellulaire, et est impliqué dans le développement vasculaire. Les souris K-O conditionnelles pour Fli-1 ont une perméabilité vasculaire augmentée, similaire à celle observée chez les patients sclérodermiques, ainsi que des anomalies dans la formation des fibrilles de collagène [189].

- Souris Wnt-10b

Les protéines Wnt sont impliquées dans des phénomènes de remodelage tissulaire et de fibrose, et il a été montré que Wnt-10b jouait un rôle dans l'adipogénèse et l'ostéoblastogénèse. Un nouveau modèle de souris transgéniques Wnt-10b a récemment été décrit par l'équipe de J. Varga. Ces souris développent une perte progressive du tissu adipeux sous-cutané, avec une fibrose du derme, des dépôts importants de collagène, une activation des fibroblastes et une accumulation de myofibroblastes [190].

- Souris T- β -RII- δ -k-fib

L'expression sélective dans les fibroblastes de T- β -RII- δ -k, récepteur de type II au TGF- β déficient en kinase, a paradoxalement induit chez les souris transgéniques une activation de la voie du TGF- β avec développement d'une fibrose cutanée et pulmonaire. Les fibroblastes transgéniques sont hyperprolifératifs et synthétisent un excès de matrice extra-cellulaire [191].

- Souris exposées à l'acide hypochloreux HOCl

Le premier de nos articles présentés dans le chapitre 3 expose notre travail sur le rôle du stress oxydant dans la ScS. Ce travail a aboutit à la mise au point d'un nouveau modèle murin de ScS basé sur des injections d'HOCl. Ce modèle murin est aujourd'hui utilisé par d'autres équipes, notamment celle de J. Varga à Chicago et celle de R. Lafyatis à Boston.

Chapitre 2

RÔLE DES FORMES RÉACTIVES DE L'OXYGÈNE (FRO)

2.1 DÉFINITION DES FRO

Un radical libre est une espèce chimique contenant un électron non apparié. Cet état est transitoire puisqu'il y a ensuite soit acceptation d'un autre électron soit transfert de l'électron libre sur une autre molécule. Ces espèces chimiques sont d'une grande instabilité et donc d'une extrême réactivité chimique. L'appellation "Formes Réactives de l'Oxygène" inclut les radicaux libres de l'oxygène proprement dit (anion superoxyde $O_2^{\bullet-}$, radical hydroxyl OH^{\bullet} par exemple), mais aussi certains dérivés oxygénés réactifs non radicaillaires dont la toxicité est élevée (peroxyde d'hydrogène H_2O_2 , peroxynitrite $ONOO^-$). La figure 2.1 représente les différents FRO générées par les cellules.

2.2 ORIGINE DES FRO

- **L'anion superoxyde $O_2^{\bullet-}$**

L'anion superoxyde est formé par l'addition d'un électron à la molécule d'oxygène : $O_2 + e^- \rightarrow O_2^{\bullet-}$. Ce radical possède une demi-vie courte par dismutation spontanée ou accélérée par des superoxyde dismutases. Il est peu毒ique en lui-même mais peut réagir avec le peroxyde d'hydrogène ou le monoxyde d'azote et donner naissance à de puissants oxydants (radical hydroxyl et peroxynitrite). Quatre systèmes enzymatiques cellulaires peuvent aboutir à la formation d' $O_2^{\bullet-}$:

- **Chaîne respiratoire mitochondriale**

La chaîne respiratoire mitochondriale est formée de plusieurs enzymes groupées à l'intérieur de la membrane interne de la mitochondrie. Elle permet de réoxyder les co-enzymes NADH et FADH₂ réduites au cours des réactions du cycle de l'acide citrique

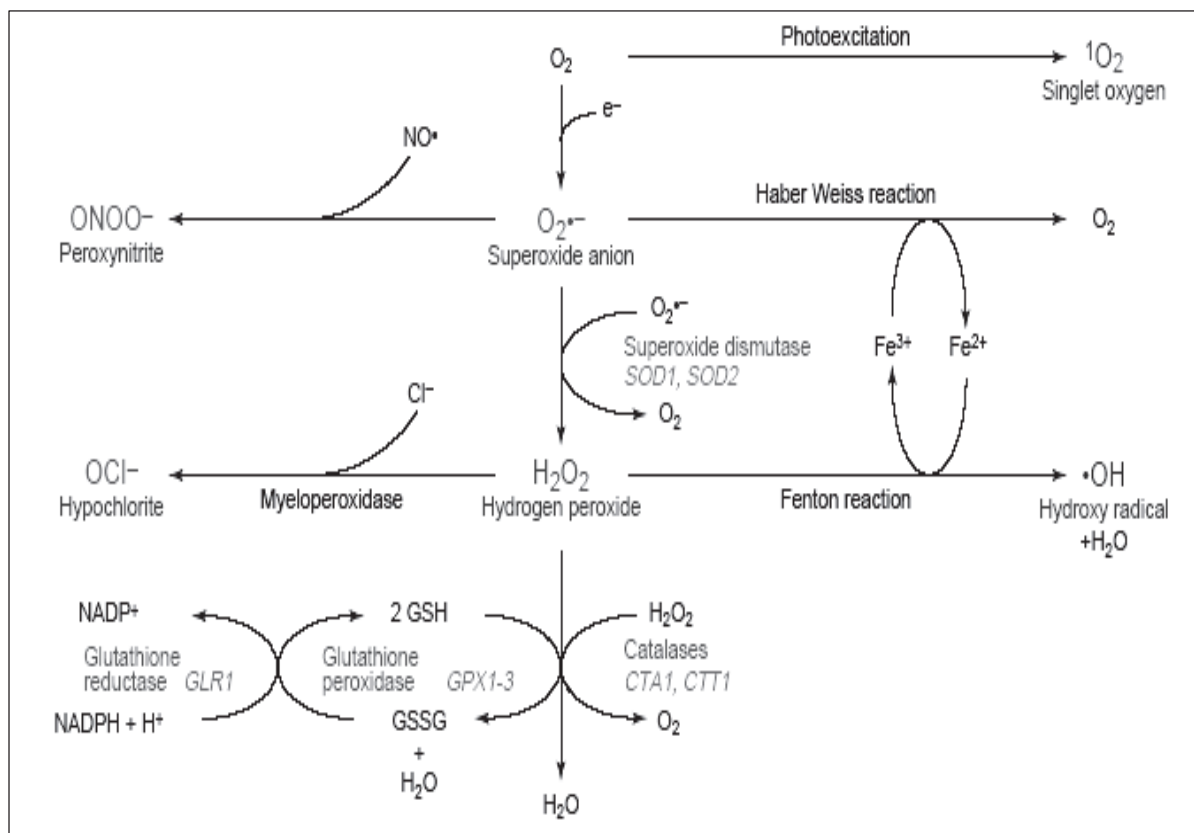


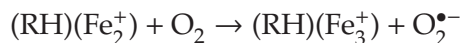
Figure 2.1 Les formes réactives de l'oxygène et leur origine, d'après Temple et al., Trends Cell Biol, 2005

ou cycle de Krebs. Dans cette chaîne respiratoire, des protons sont arrachés à leur substrat et traversent la membrane interne mitochondriale. Un gradient de potentiel transmembranaire est ainsi créé et le retour des protons à l'intérieur de la mitochondrie est couplé à la régénération d'ATP. Des électrons circulent dans les différents transporteurs et finissent par se fixer sur l'oxygène moléculaire. Cela aboutit à la formation d' H_2O : $O_2 + 2e^- + 2H^+ \rightarrow H_2O$. Cependant, il existe des fuites d'électron à chacune des étapes de transport et certaines molécules d' O_2 vont subir une réduction par un seul électron, aboutissant à la formation d'anion superoxyde $O_2^{\bullet-}$ [192] : $O_2 + 1e^- \rightarrow O_2^{\bullet-}$ Cette production d'anions superoxyde mitochondriale est continue et ubiquitaire.

- Complexe NADPH-Cytochrome P450

Les cytochromes P450 sont des hémoprotéines. Il en existe de nombreuses familles [193]. Certaines se localisent dans le réticulum endoplasmique (classe microsomiale des

cytochromes), et ont un rôle notamment dans le métabolisme des xénobiotiques ; d'autres sont situées dans les mitochondries (classe mitochondriale) et participent pour certaines au métabolisme des stéroïdes. Dans tous les cas, les cytochromes sont associés à des chaînes de transfert d'électrons et utilisent la NADPH comme source d'électrons. Au cours de ces réactions, il peut y avoir formation d'anions superoxyde $O_2^{\bullet-}$:



– Famille des NADPH oxydases

Cette famille est également nommée NOX family ("superoxide-producing NADPH oxydase"). Il en existe 7 membres : NOX 1 à NOX 5, DUOX1 et 2. Certaines enzymes sont ubiquitaires (NOX 4), d'autres seulement exprimées préférentiellement par certains types cellulaires comme les phagocytes (NOX 2) [194]. Ainsi, la NADPH oxydase phagocytaire est un complexe enzymatique composé de protéines transmembranaires (gp91phox (ou NOX2) et p22phox) et de protéines cytosoliques (p47 phox, p67 phox, p40 phox). Ces dernières doivent être phosphorylées et rejoindre la membrane cytoplasmique pour que le complexe soit actif. L'association de la protéine RAC, une petite protéine G, est également nécessaire. Ces événements surviennent lors de l'activation des phagocytes (monocytes, macrophages, polynucléaires neutrophiles et éosinophiles) et permettent finalement la réaction suivante (« explosion oxydative »), essentielle dans l'immunité innée :



– Xanthine oxydoréductase

Cette enzyme est la principale enzyme de dégradation des bases puriques et existe sous deux formes: xanthine déshydrogénase qui réduit le NAD+ et la xanthine oxydase qui réduit préférentiellement l'oxygène moléculaire et forme des anions superoxydes $O_2^{\bullet-}$. La xanthine déshydrogénase est convertie en oxydase par oxydation sulphydrylique notamment lors des phénomènes d'ischémie-reperfusion [6] (voir figure 2.2 ci-dessous).

• Le peroxyde d'hydrogène H_2O_2

Le peroxyde d'hydrogène peut résulter directement de la réduction de l'oxygène moléculaire, sous l'effet de différentes enzymes (glucose oxydase par exemple) :

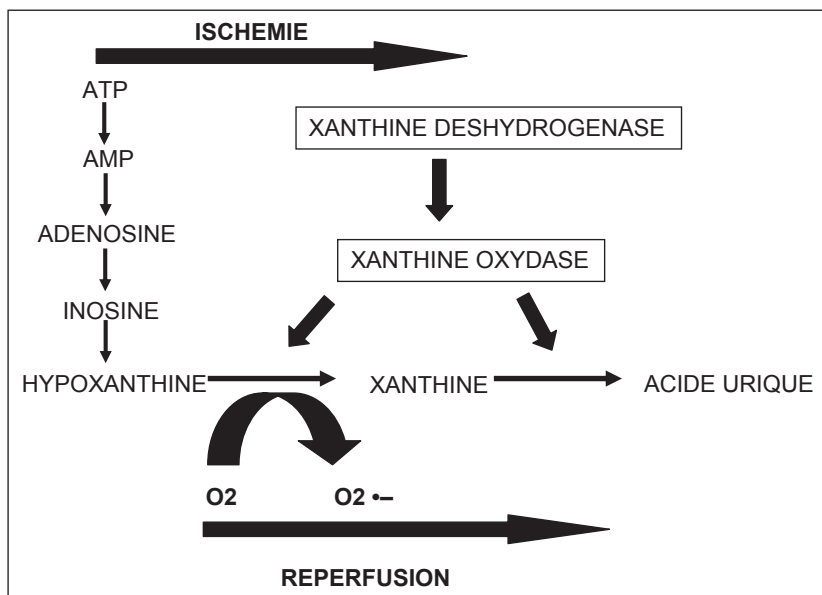
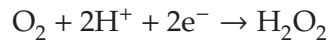


Figure 2.2 Formation d'anion superoxyde lors des phénomènes d'ischémie-reperfusion



Il peut aussi être formé à partir d' $\text{O}_2^{\bullet-}$ après dismutation spontanée ou accélérée par des superoxydes dismutases (SOD). Trois types de SOD ont été décrits dans les cellules eucaryotes [195]:

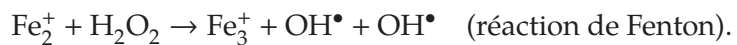
- SOD cytosolique, à cuivre et zinc
- SOD mitochondriale, à manganèse, essentiellement exprimée en réponse au stress oxydant
- SOD extracellulaire, à cuivre et zinc.

Ces enzymes catalysent la réaction suivante : $2\text{O}_2^{\bullet-} + 2\text{H}^+ \rightarrow \text{H}_2\text{O}_2 + \text{O}_2$.

Le peroxyde d'hydrogène est un dérivé toxique car il diffuse à travers les membranes et surtout peut interagir avec des ions métalliques et former le très réactif radical hydroxyle.

- **Le Radical hydroxyle OH^\bullet**

Il peut être formé par interaction d' H_2O_2 avec des cations métalliques, lors de lyses cellulaires par exemple (hémolyse, rhabdomyolyse) :



Des réactions entre différents types de FRO peuvent également entraîner sa formation :



Enfin, la myéloperoxydase, enzyme située dans les granules azurophiles des polynucléaires neutrophiles et des monocytes, catalyse une réaction aboutissant à la production d' OH^\bullet .

- **Le monoxyde d'azote NO^\bullet**

Le NO^\bullet est synthétisé à partir de L-arginine par la NO-synthase. Chez les mammifères, trois isoformes de cette enzyme existent :

- NO-synthase 1 ou neuronale
- NO-synthase 2 ou inducible
- NO-synthase 3 ou endothéliale

Contrairement aux deux autres isoformes, la NO-synthase 2 n'est pas exprimée constitutivement, mais est inducible par l'IFN- γ , le TNF- α , l'IL-1, l'IL-6, le LPS notamment. Diverses cellules ainsi activées peuvent alors l'exprimer, comme les CE, macrophages, lymphocytes, ou les fibroblastes. La production de NO^\bullet est physiologique et joue par exemple un rôle majeur dans le tonus vasculaire. Cependant, à forte concentration, le NO^\bullet devient délétère pour les cellules, notamment en réagissant avec un radical superoxyde ($O_2^\bullet-$) pour former un puissant oxydant, le peroxynitrite ($ONOO^-$). En outre, le peroxynitrite peut secondairement se décomposer en d'autres oxydants (NO_2 , OH^\bullet).

2.3 RÔLE ET CONSÉQUENCES DES FRO

Les dérivés réactifs de l'oxygène peuvent interagir entre eux, mais aussi avec tous les types de composants cellulaires : protéines, lipides, glucides, ADN. Ces effets dépendent de leur réactivité propre, de leur affinité préférentielle pour tel ou tel substrat, de leur quantité et de leur capacité de diffusion.

2.3.1 Action sur les protéines

Les formes radicalaires peuvent agir sur la chaîne principale de la protéine conduisant à une fragmentation ou à un pontage intra- ou inter-moléculaire. L'interaction peut aussi se situer sur la chaîne latérale avec des acides aminés aromatiques (tyrosine, tryptophane, phénylalanine) conduisant à la formation par exemple de dityrosine ou de nitrotyrosine. Les résidus soufrés méthionine et cystéine sont particulièrement sensibles. Les acides aminés aliphatiques sont moins sensibles et seuls les FRO puissants comme HOCl peuvent interagir avec la lysine ou l'arginine et aboutir dans ce cas à la formation de groupements carbonyls [196]. Ces modifications entraînent des modifications conformationnelles, des fragmentations ou des liaisons entre protéines et sont ainsi susceptibles de modifier l'activité des protéines.

2.3.2 Action sur les lipides

L'interaction des FRO avec les lipides conduit à la peroxydation lipidique. Les implications biologiques sont majeures puisque toutes les membranes cellulaires sont constituées de lipides. Ainsi, la peroxydation de la membrane mitochondriale peut aboutir à l'apoptose. La peroxydation lipidique entraîne en outre la formation de dérivés toxiques tels que le malone-dialdéhyde (MDA).

2.3.3 Action sur l'ADN

Les FRO entraînent l'oxydation de bases, avec pour conséquence une modification de bases (par exemple oxydation du carbone 8 de la guanine conduisant à la formation de 8-oxo-guanine) ou un site abasique, l'oxydation de sucre avec cassure d'une chaîne simple ou double brin. Les modifications peuvent également entraîner des liaisons ADN-lipides ou ADN-protéines.

2.3.4 Rôles et conséquences des FRO dans le métabolisme cellulaire

Les polynucléaires neutrophiles et les macrophages génèrent de grandes quantités de $\text{d}'\text{O}_2\bullet^-$ et $\text{d}'\text{H}_2\text{O}_2$ via l'activation du complexe NAPDH oxydase [197] [198]. Cette enzyme est une des

clés de l'arsenal antimicrobien. Le déficit en NAPDPH oxydase est responsable d'un déficit immunitaire chez l'homme, la granulomatose septique chronique. Les FRO, en particulier l' H_2O_2 , sont en outre impliquées dans la régulation du cycle cellulaire [199]. Ainsi, de faibles concentrations de FRO favorisent la prolifération cellulaire via l'activation du système ERK [200]. A un niveau de FRO supérieur, d'autres "mitogen-activated protein kinases" (MAP kinases) et les "stress activating protein kinases" (SAPK), sont activées et favorisent l'apoptose [201]. La prolifération des cellules tumorales est également régulée par l' H_2O_2 (voir figure 2.3 ci-dessous) [199].

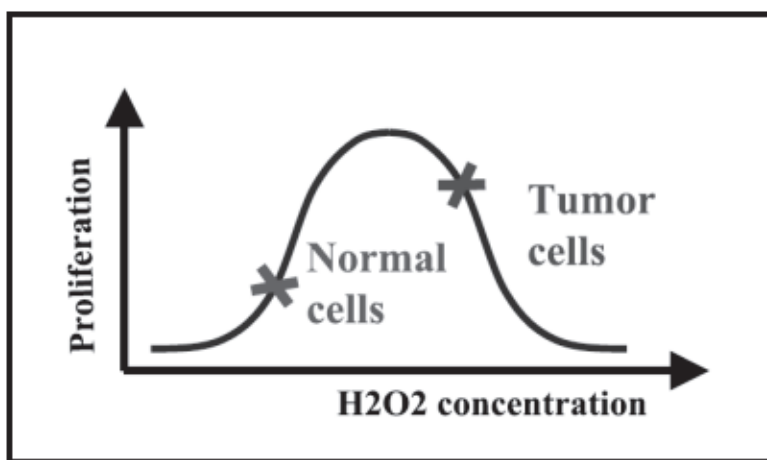


Figure 2.3 Régulation de la prolifération des cellules tumorales par le stress oxydant, d'après A. Laurent, Cancer Research, 2005

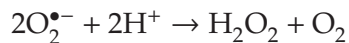
Il y a quelques années est né le concept de FRO comme messager du signal intracellulaire. Le NO peut en effet activer la guanylate cyclase et les modifications oxydatives des protéines intracellulaires (modification des tyrosines et des cystéines notamment) participent aussi à la transduction du signal. Les FRO peuvent également activer certains facteurs de transcription comme le nuclear factor- κ B (NF- κ B) et c-fos [202]. Les FRO sont aussi impliqués dans le processus d'angiogénèse dépendant du VEGF. La transduction du signal du VEGF dépend de la formation de FRO via la NADPH oxydase endothéliale [203]. Enfin, à côté des FRO classiques, le NO exerce des fonctions particulières au niveau des vaisseaux : vasodilatation, activité anti-thrombotique et cytoprotectrice [119].

2.3.5 Systèmes antioxydants physiologiques

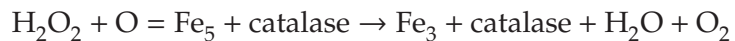
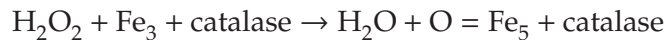
La production continue de FRO chez les organismes aérobies serait délétère en l'absence de puissants systèmes antioxydants. Bien que, même dans les conditions physiologiques, une fraction non négligeable de l' O_2 soit convertie en FRO, la concentration en $O_2^{\bullet-}$ dans les cellules n'excède pas 10^{10} – 10^{11} M, et celle d' H_2O_2 10^7 – 10^9 M.

2.3.5.1 Exemples de systèmes antioxydants enzymatiques

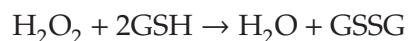
- Superoxyde dismutase (SOD), enzymes ubiquitaires qui catalysent la réaction suivante :



- Catalase, enzyme située surtout dans les peroxyzomes hépatiques et rénaux [204], et dont la synthèse est proportionnelle à la concentration en H_2O_2



- Glutathion peroxydase, enzyme dépendante qui catalyse la détoxication d' H_2O_2 et des hydroperoxydes lipidiques (ROOH). Elle utilise le glutathion (GSH) comme substrat.



Le système du GSH est un des plus puissants systèmes antioxydants des organismes aérobies. Le GSH est présent dans presque toutes les cellules eucaryotes. Il est synthétisé à partir du L-glutamate, de la L-cystéine et de la L-glycine par la γ -glutamylcystéine puis la GSH synthase [205]. Les fonctions anti-oxydantes du GSH sont liées à son groupement thiol (-SH) qui peut s'oxyder (GSSG). La GSH sert de cosubstrat à la glutathion peroxydase, mais aussi à la déhydroascorbat réductase qui régénère l'antioxydant ascorbate. Le GSH peut aussi détoxifier directement les FRO. Plus de 95% du GSH est sous forme réduite. Une modification du rapport GSH/GSSG peut induire de graves perturbations de l'homéostasie cellulaire. Le maintien du GSH sous forme réduite dépend de la glutathion réductase,

qui dépend elle-même d'un équilibre NADPH/NADP sous l'influence de la G6PD (glyco-6-phosphate deshydrogenase).

2.3.5.2 Exemples de systèmes antioxydants non-enzymatiques physiologiques

- Vitamine C et E

Les vitamines E au niveau de la membrane (lipophile) et les vitamines C majoritairement cytosoliques (hydrophile) éliminent les radicaux hydroxyl.

- Ubiquinone (coenzyme Q10)

Substance semblable à une vitamine, ayant un rôle significatif dans la production d'énergie au niveau de la chaîne respiratoire et un rôle antioxydant de protection des cellules contre les effets destructeurs des radicaux libres.

2.4 STRESS OXYDANT ET IMMUNOLOGIE

A l'échelle cellulaire, les FRO sont impliquées dans de nombreuses fonctions physiologiques. Leur production est localisée dans toutes les cellules au niveau de la membrane interne des mitochondries et la diffusion des FRO toxiques est contrôlée par différents systèmes anti-oxydants. Un déséquilibre important entre la production de FRO et leur élimination par les systèmes anti-oxydants définira le stress oxydant. Ce dernier est impliqué dans de nombreux phénomènes pathologiques comme l'athérosclérose, les désordres auto-immuns, la dégénération neuronale (Alzheimer notamment), la schizophrénie et le cancer. Les FRO représentent une voie finale commune à un grand nombre d'agressions. Ils exercent leur effet毒ique en provoquant un ensemble d'altérations des glycanes, des protéines et des acides nucléiques ainsi que la peroxydation des lipides. A cette toxicité directe s'ajoute un ensemble de mécanismes indirects qui amplifient la réaction inflammatoire et les lésions cellulaires : stimulation de la synthèse des médiateurs lipidiques (prostaglandines et leucotriènes), activation de certains facteurs de transcription (ex : NF κ B) et induction de la synthèse d'IL1 et de TNF- α [198]. Les FRO entraînent également la synthèse de dérivés toxiques formylés ou aldéhydés, tels que le malonyl-dialdéhyde qui forme des adduits avec différentes molécules et qui fonctionne comme un haptène.

2.4.1 Rôle des FRO dans l'immunité anti-infectieuse

2.4.1.1 Mécanisme microbicide dépendant de l'oxygène

Les mécanismes de lyse intracellulaire des bactéries sont très complexes et multiples. Ils peuvent être regroupés en deux grandes catégories, selon qu'ils dépendent ou non de l'oxygène. Les mécanismes de lyse dépendant de l'oxygène font appel à trois principaux systèmes enzymatiques : la NADPH oxydase (NOX) associée au cytochrome b558, la myéloperoxydase et la NO synthase.

- Rôle de la NADPH oxydase phagocytaire

L'étude des malades atteints de granulomatose septique chronique a permis d'élucider les mécanismes complexes qui permettent la production de FRO par les phagocytes. La NADPH oxydase est un complexe formé de sous-unités membranaires et cytoplasmiques dans le phagocyte au repos. Le cytochrome b comprend une sous-unité α (p22phox) et une sous-unité β (gp91phox) fortement glycosylée, avec un site de fixation du NADPH et un autre pour la flavine adénine dinucléotide (FAD). Les sous-unités cytoplasmiques sont p47phox, p67phox et p40phox assemblés sous forme de complexe et une petite protéine G, Rac-1 ou Rac-2.

L'activation des phagocytes par différents stimulus entraîne une phosphorylation des sous-unités cytosoliques et leur translocation vers la membrane où elles se lient aux composants gp91phox et p22phox. Simultanément Rac se dissocie de son inhibiteur et migre séparément vers la membrane se liant à la p67phox et au cytochrome p558. C'est le regroupement au niveau de la membrane de ces différentes sous-unités qui forme une enzyme biologiquement active. Cette activité NADPH oxydase permet le transfert d'électrons à partir du NADPH sur l'oxygène moléculaire donnant naissance à l' $O_2^{\bullet-}$, source des autres FRO.

La granulomatose septique est observée chez des sujets présentant des mutations sur l'une des quatre principales protéines constituant la NADPH oxydase.

- Rôle de la myéloperoxydase

Lorsqu'il y a fusion des phagosomes avec les lysosomes, la myéloperoxydase des granules azurophiles permet la production de dérivés toxiques de l'oxygène tels que l'acide hypochloreux (H^+OCl^-), en présence d'halogénures (iode, brome, chlore) qui diffusent du cytoplasme vers les phagosomes. L'interaction de OCl^- avec des amines endogènes (taurine par exemple) permet la formation de chloramine. Les macrophages tissulaires ne possèdent pas de myéloperoxydase et sont donc incapables de mettre en jeu les réactions dépendant de cette enzyme.

- Rôle de la NO synthase

La production de NO par les phagocytes est beaucoup plus importante chez la souris que chez l'homme. Une deuxième voie métabolique dépendant de l'oxygène joue probablement un rôle important dans la lyse des bactéries et des parasites intracellulaires par les macrophages : il s'agit de la formation de dérivés oxydés de l'azote aboutissant à la production de monoxyde d'azote (NO) qui est毒ique pour les bactéries et les cellules tumorales. Le NO est formé à partir de la L-arginine en présence d'une NO synthase qui utilise comme cofacteur indispensable la tétrahydrobioptérine. Cette voie est activée par l' $IFN\gamma$, le GM-CSF et de façon encore plus puissante par le $TNF-\alpha$. Trois isoformes de NO synthase ont été caractérisées : deux constitutives dans l'endothélium (eNOS) et le système nerveux (nNOS) et une inductible (iNOS) dont l'expression est prédominante dans les phagocytes, mais qui peut être induite par des cytokines ($IFN\gamma$) dans presque toutes les cellules nucléées. Le NO peut être transformé en différents dérivés très toxiques tels que le nitrosonium (NO^\bullet), les ions nitroxyl (NO^-), le dioxyde d'azote (NO_2), le peroxynitrite ($ONOO^-$) et les S-nitrosothiols.

La formation des dérivés toxiques de O_2 et de NO entraîne de multiples altérations des lipides, des protéines, des glycanes et des acides nucléiques. Les systèmes d'amplification de la production de FRO sont la réaction de Fenton (action du fer) ou la réaction de Haber-Weiss (action du cuivre). Les systèmes de défense anti-oxydants sont les vitamines E et C et le système du glutathion. La glutathion peroxydase oxyde le glutathion réduit (GSH) en glutathion oxyde (GSSG) et réduit le peroxyde d'hydrogène H_2O_2 . La détoxication par des superoxyde dismutases (SOD) nécessite ensuite l'action d'une catalase pour transformer H_2O_2 en H_2O .

2.4.2 Rôle des FRO dans le contrôle de la réponse immunitaire

2.4.2.1 FRO et présentation de l'antigène

La présentation croisée est le processus par lequel les cellules dendritiques phagocytent les agents pathogènes ou les fragments de cellules apoptotiques ou nécrotiques, et présentent, après protéolyse, les peptides dérivés de ces antigènes en association avec les molécules du Complexe Majeur d'Histocompatibilité (CMH) de classe I. Ce processus a pour résultat le déclenchement d'une réponse cytotoxique et est donc un mécanisme fondamental pour l'induction des réponses immunitaires anti-tumorale ou anti-infectieuse. Certaines voies de signalisation intracellulaires impliquant les FRO et permettant de relier les voies d'internalisation de l'antigène à leur apprêtement et leur chargement sur les molécules du CMH de classe I ont récemment été découvertes. Il a ainsi été démontré que les cellules dendritiques régulent la préparation des antigènes pour la présentation croisée à travers la modulation du pH et la dégradation protéique dans les phagosomes. La NADPH oxydase NOX2 est recrutée dans les phagosomes précoces et s'active à la membrane. Elle module alors durablement et à faible taux une production d'espèces réactives de l'oxygène, assurant une alcalinisation de la lumière du phagosome qui modifie son activité protéasique [206].

2.4.2.2 Production de FRO au cours de l'activation lymphocytaire T

En plus du rôle anti-microbien dans l'immunité innée, les FRO interviennent au cours de la réponse immunitaire adaptative comme des régulateurs de la transduction du signal médié par le TcR. Ainsi la stimulation des lymphocytes T par activation de leur TcR est oxydo-dépendante et induit une production rapide de FRO. Ces derniers représentent des seconds messagers régulant l'activation de protéines kinases, l'expression de gènes, la prolifération et la différentiation cellulaire. Il a ainsi été montré que les antioxydants inhibaient l'activation lymphocytaire induite par l'antigène. Les FRO impliqués dans l'activation des lymphocytes T sont le peroxyde d'hydrogène et l'anion superoxyde.

Le rôle protecteur des FRO au cours des maladies auto-immunes a été récemment décrit. En effet, certaines études suggèrent que les FRO produites par le complexe NOX2 pourraient

avoir des propriétés anti-inflammatoires et seraient capables de prévenir les réponses auto-immunes. Cet effet dépend du moment, du lieu et de la quantité et du type de molécules oxydantes produites [207]. Dans ce cas, et à l'opposé de leur action au cours de la destruction tissulaire et l'inflammation, les FRO joueraient le rôle de régulateurs de la réponse inflammatoire. Un tel phénomène a été décrit dans de nombreux systèmes. Notamment, les FRO produites par NOX2 peuvent avoir un effet bénéfique dans certains syndromes inflammatoires et auto-immuns comme la PR, la sclérose en plaques, le diabète de type 1 et la thyroïdite auto-immune.

2.4.2.3 FRO et mort cellulaire

Le maintien de l'homéostasie des cellules T est un processus complexe contrôlé par une balance entre production, prolifération et apoptose cellulaire. L'identification de facteurs moléculaires influençant ces processus est importante pour comprendre comment l'immunité est maintenue et comment l'auto-immunité est évitée. De plus, la capacité de manipuler la prolifération et/ou la survie des cellules T peut avoir un bénéfice thérapeutique direct soit en augmentant la survie des cellules T (par exemple au cours de stratégies vaccinales), soit en activant la mort cellulaire (par exemple au cours de phénomènes auto-immuns ou néoplasiques). Bien que les FRO jouent un rôle significatif dans la modulation de la prolifération des cellules T, et que de nombreuses études aient montré depuis longtemps le rôle des FRO au cours des processus de mort cellulaire, le rôle des FRO dans le contrôle de l'apoptose des lymphocytes T n'a été que récemment disséqué. Dans les cellules T activées, les FRO régulent la mort cellulaire en modifiant l'expression de deux gènes majeurs impliqués dans l'apoptose, Bcl-2 et FasL [208]. Les FRO contrôlent en effet l'apoptose extrinsèque des cellules T par action sur l'expression de FasL. Il a ainsi été montré que le peroxyde d'hydrogène produit au niveau mitochondrial activait NF- κ B et induisait l'expression de FasL. L'anion superoxyde peut aussi affecter l'expression de FasL, indépendamment de NF-AT et H₂O₂, par action sur les facteurs de transcription Egr 2 et Egr3. Les FRO contrôlent également l'apoptose intrinsèque des cellules T en inhibant l'expression de Bcl-2 dans les lymphocytes T activés. Le peroxyde d'hydrogène module ainsi l'expression de Bcl-2 par action sur la molécule CREB. L'ajout d'anti-oxydants peut prévenir l'induction de FasL et restaurer l'expression de Bcl-2. Enfin, des taux élevés de Bcl-2, ainsi que la molécule Bcl-3, préviennent l'apoptose médiée par la molécule pro-apoptotique Bim, molécule-clé de l'apoptose lymphocytaire. Le rôle des FRO dans l'apoptose des phagocytes (notamment les polynucléaires neutrophiles) peut aussi intervenir dans la physiopathologie des maladies

auto-immunes, au niveau de la dégradation des substances pathogènes, modifiant ainsi leur présentation aux cellules immunitaires adaptatives.

2.5 RÔLE DES FRO EN IMMUNOPATHOLOGIE

2.5.1 Rôle des FRO dans la genèse d'épitopes pathogènes

Un stress oxydant et nitrosatif est induit au cours de nombreux syndromes inflammatoires entraînant une modification des antigènes et par conséquent la genèse potentielle d'épitopes pathogènes. Ces modifications antigéniques peuvent impliquer trois types de molécules : les protéines qui peuvent subir une oxydation de certains acides aminés comme la méthionine, le tryptophane ou la transformation de l'asparatate en acide aspartique. Les lipides sont aussi impliqués et la peroxydation lipidique induit la modification des acides gras polyinsaturés avec apparition par exemple de LDL oxydés. Enfin, les acides nucléiques sont modifiés avec notamment la formation de 8-oxodéoxyguanine (8-oxodG) au sein des chaînes d'ADN.

Le stress oxydant a été impliqué dans la physiopathologie de différentes maladies comme l'athérosclérose [209], l'hépatite alcoolique [210], les glomérulonéphrites [211] et les maladies auto-immunes [212] [213] [214]. Le tableau ci-dessous présente les antigènes oxydés observés au cours de différentes maladies auto-immunes.

Maladies	Antigènes oxydés impliqués
Lupus érythémateux systémique	LDL oxydés, 8-oxodeoxyguanine
Polyarthrite rhumatoïde	IgG oxydées, pentosidine
Diabète insulino-dépendant	GAD oxydée
Maladie de Behcet	LDL oxydés

Tableau 2.1 Antigènes oxydés associés aux maladies auto-immunes (Free Radic. Biol. Med. 2006)

2.5.2 FRO et Sclérodermie systémique

Plusieurs facteurs plaident en faveur d'un rôle des FRO dans le développement de la ScS, au premier rang desquels le phénomène d'hyperactivité vasculaire responsable du phénomène de Raynaud. En effet, ce symptôme, présent chez plus de 90% des malades, précède en général de plusieurs années les autres signes de la maladie. Il peut être présent chez certains sujets sains (moins de 15%) mais est alors souvent familial et peu sévère, présent uniquement lors d'exposition au froid. Ce phénomène correspond à une ischémie suivie d'une reperfusion. Or la succession de ces deux conditions entraîne la formation d' $O_2^{\bullet-}$. Pendant la phase ischémique, la xanthine déshydrogénase se transforme en xanthine oxydase et l'ATP en hypoxanthine [215]. Lors de la reperfusion, l'oxygène est disponible localement et devient le substrat de la xanthine oxydase pour former des anions superoxydes toxiques [6].

Un deuxième argument est apporté par l'étude des différents toxiques qui pourraient déclencher ou favoriser la survenue d'une ScS. Nombre de ces toxiques exercent leurs effets en partie via un stress oxydant. C'est le cas de la silice qui induit directement la formation de FRO à sa surface, notamment par réaction de Fenton, et indirectement par le biais d'une activation des cellules phagocytaires [388]. De plus, chez la souris, plusieurs travaux soulignent le lien entre fibrose pulmonaire induite par l'inhalation de silice et stress oxydant [216] [217]. La bléomycine est responsable de fibrose pulmonaire chez l'homme et a été utilisée en injections sous-cutanées chez la souris pour induire une fibrose cutanée proche de la ScS [132]. L'étude de ce modèle murin a montré l'implication de FRO dans le développement de la fibrose cutanée entraînant des lésions proches des lésions observées chez l'homme [218]. Le syndrome des huiles toxiques, qui partage des similitudes avec la ScS, semble également médié par des radicaux libres [219]. Des études soulignent chez les sujets développant une ScS des différences dans les systèmes antioxydants par rapport aux sujets sains, suggérant un possible défaut d'élimination des radicaux libres chez les sujets enclins à développer une ScS [220] [9]. Ces observations renforcent l'hypothèse de l'implication du stress oxydant dans la ScS.

La DNA-Topoisomérase-1, antigène cible des anticorps anti-Scl70 présents chez les patients sclérodermiques, peut être clivée lors de réactions impliquant les FRO et un cation métallique [155]. L'auto-immunité observée dans la ScS pourrait donc être le reflet de cette fragmentation protéique provoquée par un stress oxydant exacerbé.

Au cours des dix dernières années, de nombreux travaux font état d'un stress oxydant accru chez les malades atteints de ScS. La grande majorité de ces travaux apporte en fait des preuves indirectes d'une implication des FRO en se focalisant non pas sur les FRO elles-mêmes mais sur leurs conséquences. L'un des problèmes des FRO est en effet leur grande labilité rendant leur dosage difficile. Il a ainsi été montré que les sérums des malades contenaient de plus grandes quantités de protéines oxydées (groupements carbonyls et advanced oxidation protein products (AOPP)) [221], et de marqueurs de peroxydation lipidique [5]. Cette oxydation lipidique a été directement observée au niveau des membranes d'érythrocytes de malades [222]. Ce phénomène diminue la plasticité des érythrocytes, et pourrait ainsi aggraver les anomalies micro-circulatoires. Il a aussi été montré que les protéines nucléolaires cibles des Ac de patients atteints de ScS sont des cibles privilégiées des FRO par rapport à des antigènes reconnus dans d'autres maladies, insensibles à l'oxydation. Ceci suggère que l'auto-immunité observée dans la ScS pourrait être la conséquence du stress oxydant [223].

Une équipe italienne a mis en évidence une synthèse en grande quantité de $O_2^{\bullet-}$ par des monocytes et des fibroblastes de patients sclérodermiques [7] [8]. Dans les deux types cellulaires, cette synthèse de FRO apparaît auto-entretenue et dépendante d'une NAPDH oxydase. Le travail de cette équipe suggère également que la synthèse de collagène des fibroblastes est dépendante de cette synthèse de FRO [44]. Concernant le NO, plusieurs études attestent de différences quantitatives dans le sérum entre patients et sujets sains, mais, comme il a été dit précédemment, les résultats de ces études sont parfois contradictoires. Une étude immunohistochimique à partir de peau de malades et de sujets sains a montré cependant un changement radical du métabolisme du NO dans les CE de patients sclérodermiques puisque la NO synthase endothéliale constitutive cesse d'être exprimée au profit de la NO synthase inducible [224]. Parallèlement à ce changement, le NO formé devient toxique, comme en témoigne dans les tissus lésés la présence de nitrotyrosine.

Chapitre 3

TRAVAUX PERSONNELS

Nous présentons dans ce chapitre les articles publiés sur le rôle des FRO dans la physiopathologie de la ScS, sur l'activation fibroblastique et sur les nouvelles approches thérapeutiques développées. Les travaux que nous présentons se sont déroulés en trois temps :

Dans un premier temps, nous avons étudié l'implication des FRO dans la physiopathologie de la ScS. Dans un travail précédemment mené au laboratoire une corrélation entre la production cellulaire de FRO induite par le sérum des patients sclérodermiques et les manifestations cliniques (complications fibrosantes ou vasculaires) présentes chez ces patients avait été mise en évidence [225]. Ceci représentait un argument fort en faveur d'un rôle central des FRO dans les mécanismes physiopathologiques de la ScS. Ainsi, en étudiant l'implication des FRO dans la physiopathologie de la ScS, nous avons mis au point un nouveau modèle animal de sclérodermie systémique induit par l'exposition chronique à certaines FRO (article 1).

Ce modèle nous a permis dans un deuxième temps d'étudier le rôle des formes réactives de l'oxygène dans les voies d'activation des fibroblastes dans la ScS. Comme chez l'homme, les fibroblastes cutanés issus du derme des souris sclérodermiques produisent de manière constitutive de grande quantités de FRO. Nous avons réalisé plusieurs études montrant l'implication de ce stress oxydant endogène dans la dérégulation de nombreuses voies métaboliques notamment celles contrôlées par les récepteurs Notch (article 2), les récepteurs aux cannabinoïdes (article 3) et les récepteurs au PDGF (article 4) dans les fibroblastes sclérodermiques.

L'implication de ces différentes voies dans le processus fibrotique nous a conduit à tester, dans un troisième temps, de nouvelles approches thérapeutiques dans la ScS. D'une part, la modulation des trois voies précédemment étudiées peut entraîner une amélioration clinique de la maladie et avoir des conséquences non seulement sur la composante fibreuse mais aussi sur les composantes vasculaires et immunologiques de la maladie (articles 2, 3, 4). D'autre part, ayant montré que les fibroblastes sclérodermiques produisaient de fortes quantités de FRO,

nous avons utilisé cette propriété pour induire leur apoptose sélective dans le derme des souris (article 5). En effet, le trioxyde d'arsenic, un agent cytotoxique utilisé en thérapeutique humaine, est capable d'augmenter la production de FRO des fibroblastes. Cette augmentation n'a pas d'effet sur les fibroblastes normaux mais tue les fibroblastes sclérodermique en induisant chez eux une explosion oxydative au-delà d'un seuil létal. Ce travail ayant donné des résultats prometteurs, nous avons étudié si cette molécule avait une efficacité similaire sur l'activation du système immunitaire observée dans la ScS en utilisant le modèle murin de ScS associée à la réaction de greffon contre l'hôte, où l'activation du système immunitaire est le premier événement responsable du développement des lésions observées (article 6).

Ainsi, grâce au développement d'un nouveau modèle animal de ScS basé sur l'exposition chronique à des FRO et présentant de très nombreuses similitudes, notamment au niveau fibroblastique, avec la maladie humaine, nous avons pu étudier les dysfonctionnements des fibroblastes sclérodermiques et les voies cellulaires dérégulées dans ces cellules. Ces travaux sur l'activation fibroblastique nous ont enfin conduits à développer de nouvelles approches thérapeutiques dans la ScS par la modulation de ces voies cellulaires, et selon une approche basée sur l'action cytotoxique des FRO induits par le trioxyde d'arsenic. Ces nouvelles stratégies thérapeutiques ouvrent des perspectives intéressantes dans le traitement de la ScS, où l'arsenal thérapeutique est actuellement encore limité.

3.1 ARTICLE 1

Une oxydation particulière de l'ADN Topoisomérase-1 induit une sclérodermie systémique chez la souris

Selective oxidation of DNA topoisomerase-1 induced systemic sclerosis in the mouse

Amélie Servettaz, Claire Gouvestre, Niloufar Kavian, Carole Nicco, Philippe Guelpain, Christiane Chéreau, Vincent Vuiblet, Loïc Guillevin, Luc Mouthon, Bernard Weill, Frédéric Batteux

Journal of Immunology, 2009

Dans un travail antérieur mené dans notre laboratoire, il avait été montré que les sérum de patients atteints de ScS contenaient des concentrations élevées de protéines oxydées AOPP [225]. Ces protéines oxydées étaient capables de déclencher in vitro une dysrégulation de la croissance des CE et des fibroblastes, deux cellules au cœur de la physiopathologie de la ScS. En outre, les sérum de patients ScS contenant ces AOPP pouvaient eux-même induire une production de formes réactives de l'oxygène par les fibroblastes et les cellules endothéliales. Ceci suggérait que le stress oxydant pouvait perdurer chez ces malades via une boucle d'entretien positive. Ainsi, la ScS, maladie systémique des fibroblastes, des cellules endothéliales et du système immunitaire, pourrait être causée par un premier dysfonctionnement local via l'oxydation. Afin de poursuivre notre hypothèse, nous avons étudié l'impact de l'exposition au stress oxydant dans l'article présenté ci-après. Nous avons ainsi exposé des souris BALB/c à diverses formes réactives de l'oxygène via des injections intra-dermiques. Nous avons utilisé plusieurs types d'agents pro-oxydants, mimant ainsi la majorité des stress oxydants physiologiques :

- Acide hypochloreux HOCl: produit au cours de l'explosion oxydative par les polynucléaires neutrophiles, et impliqué dans la formation des AOPP
- Anion hydroxyl OH[•]: provenant du peroxyde d'hydrogène H₂O₂ après réaction de Fenton dans les macrophages, et possiblement en cause dans les modifications antigéniques responsables de la production d'auto-anticorps anti-DNA-Topoisomérase d'après les expériences de Casciola-Rosen [155].

- Anion superoxyde $O_2^{\bullet-}$: principal FRO produite lors des phénomènes d'ischémie-reperfusion qui surviennent très précocément chez les malades ScS, avant l'apparition d'autres signes cliniques.
- Peroxynitrites $ONOO^-$: générés par la combinaison d' $O_2^{\bullet-}$ et de NO au cours de la reperfusion des tissus ischématisés et lors des phénomènes inflammatoires

Le groupe témoin positif a reçu des injections intra-dermiques de bléomycine, molécule induisant une fibrose cutanée et pulmonaire en quatre semaines. Le groupe témoin négatif a reçu des injections de PBS. Toutes les injections ont été réalisées quotidiennement pendant 6 semaines et les souris ont été sacrifiées à la septième semaine. Trois phénotypes différents ont été observés parmi les souris ayant été exposées aux 4 molécules capables de générer un stress oxydant :

- Les injections d'anion superoxyde $O_2^{\bullet-}$ n'ont induit aucun signe de fibrose locale ou systémique, et la recherche d'auto-anticorps anti-CENP-B et anti-ADN-Topoisomérase- 1 s'est révélée négative. Cependant, des niveaux élevés d'anticorps anti-ADN natif ont été détectés dans les sérum de ces souris.
- Les injections de peroxynitrites ont induit une fibrose cutanée. Cette fibrose était attestée par un épaississement local de la peau, des analyses histologiques et biochimiques avec une accumulation de collagène dans le derme.
- Les injections intra-dermiques de radicaux hydroxyl et d'acide hypochloreux HOCl ont induit, outre une fibrose cutanée, une fibrose pulmonaire, des anomalies rénales, c'est à dire toutes les manifestations cliniques caractéristiques de la sclérodermie cutanée diffuse. Cette forme de sclérodermie se distingue de la forme dite « cutanée limitée » dans laquelle l'atteinte cutanée se limite à la partie distale des membres, l'atteinte pulmonaire étant plus rare. Les auto-Ac détectés dans cette forme sont des Ac anti-centromère (dont la cible principale est la protéine centromérique CENP B) et non des Ac anti-ADN Topoisomérase-1.

Nous avons donc ensuite recherché la présence d'auto-Ac dans le sérum des souris qui avaient développé une fibrose soit limitée à la peau, soit systémique et atteignant le poumon. Nous avons mis en évidence des Ac anti-CENP B chez toutes les souris développant une fibrose cutanée (souris exposées à OH^{\bullet} , HOCl, $ONOO^-$, ou à la bléomycine). En revanche, seules les

souris exposées à OH[•], HOCl ou à la bléomycine et présentant une maladie fibrosante systémique ont développé des Ac anti-ADN Topoisomérase à un taux significatif. Aucun autre auto-Ac n'a été détecté chez ces souris, suggérant une baisse de la tolérance sélective vis-à-vis de certains antigènes chez ces souris. Nous avons alors comparé les propriétés des sérum des souris exposées à OH[•], HOCl, ou à la bléomycine et développant une maladie étendue, des souris exposées à ONOO⁻ et développant une maladie limitée, et des souris ne développant pas de maladie (souris exposées à O₂^{•-}). Les sérum des souris exposées à OH[•], HOCl et ONOO⁻ induisaient une synthèse de FRO par les cellules endothéliales, mais pas les sérum de souris exposées à O₂^{•-}, ni de celles exposées à la bléomycine. Ce dernier point suggérait que les mécanismes conduisant à la fibrose étaient différents pour les molécules pro-oxydantes et la bléomycine. Nous avons ensuite observé que les sérum des souris injectées avec OH[•], HOCl, mais pas des souris exposées à ONOO⁻ contenaient de grandes quantités d'AOPP, telles que nous les avions observées dans les sérum des patients atteints de ScS cutanée diffuse. Nous avions donc reproduit chez la souris, avec des injections de OH[•] et HOCl, les principales anomalies cliniques et biologiques caractéristiques de la ScS cutanée diffuse.

Notre hypothèse de départ était que les AOPP étaient directement impliqués dans le développement de la ScS. L'apparition d'une maladie proche de la ScS dans notre modèle murin était en faveur de notre hypothèse mais ne la prouvait pas. Nous avons alors réalisé deux types d'expériences. D'abord nous avons oxydé avec les quatre différentes solutions oxydantes diverses protéines *in vitro* et testé la capacité de ces « AOPP » de synthèse de reproduire les propriétés des sérum de patients et de souris (propriétés d'induire des FRO par les cellules endothéliales et d'induire une prolifération fibroblastique). Nous avons montré que ces « AOPP » de synthèse reproduisaient de manière très inégale les propriétés des sérum. C'est l'ADN Topoisomérase-1 oxydée par de l'HOCl qui avait les meilleures propriétés d'induction de FRO et de prolifération fibroblastique. Parallèlement, nous avons essayé de dépléter les AOPP des sérum de patients atteints de ScS et de souris exposées à OH[•], HOCl. Nous avons montré que le β-mercaptopropanoïde réduisait la concentration en AOPP dans les sérum, et diminuait ainsi leur propriétés d'une manière dose-dépendante. La déplétion des sérum en l'ADN-Topoisomérase 1 seule par un Ac spécifique diminuait leurs propriétés suggérant que, parmi l'ensemble des AOPP, l'ADN Topoisomérase-1 oxydée joue un rôle prépondérant dans la physiopathologie de la ScS et n'a pas simplement un rôle passif d'antigène.

Dans une dernière série d'expériences, le protocole d'injections intra-dermiques quotidiennes d'HOCl a été reproduit chez des souris immunodéficientes BALB/c SCID afin de déterminer

le rôle du système immunitaire dans l'induction des phénomènes de fibrose cutanée et pulmonaire observés dans ce modèle. L'exposition des souris BALB/c SCID à l'acide hypochloreux HOCl a entraîné une fibrose cutanée et pulmonaire, et une augmentation de la concentration sérique en AOPP. Cependant, l'étendue de la fibrose pulmonaire était plus faible chez ces souris que chez les BALB/c immunocompétentes, ce qui suggère un rôle du système immunitaire dans l'amplification systémique de la maladie.

Ce travail a permis de déterminer la nature des FRO impliquées dans le déclenchement de la maladie, ainsi que les mécanismes entraînant la propagation systémique de la maladie. Ce nouveau modèle animal apporte un argument supplémentaire pour le rôle des FRO dans l'induction de la ScS et montre que l'extension de la fibrose, la spécificité des anticorps produits, et la forme cutanée limitée ou diffuse de la maladie dépendant du type de FRO impliqué. C'est un nouvel outil pour mieux comprendre le rôle des FRO dans la physiopathologie de la ScS, et également pour l'étude des différentes voies d'activation fibroblastique, immunitaire, et endothéliale qui entrent en jeu dans cette maladie, pour finalement développer de nouvelles approches thérapeutiques.

Selective Oxidation of DNA Topoisomerase 1 Induces Systemic Sclerosis in the Mouse¹

Amélie Servettaz,^{2*}[‡] Claire Goulvestre,^{2*} Niloufar Kavian,^{*} Carole Nicco,^{*} Philippe Guilpain,^{*†} Christiane Chéreau,^{*} Vincent Vuillet,[§] Loïc Guillemin,[†] Luc Mouthon,^{*†} Bernard Weill,^{*} and Frédéric Batteux^{3*}

Systemic sclerosis (SSc) is a connective tissue disorder of great clinical heterogeneity. Its pathophysiology remains unclear. Our aim was to evaluate the relative roles of reactive oxygen species (ROS) and of the immune system using an original model of SSc. BALB/c and immunodeficient BALB/c SCID mice were injected s.c. with prooxidative agents (hydroxyl radicals, hypochlorous acid, peroxynitrites, superoxide anions), bleomycin, or PBS everyday for 6 wk. Skin and lung fibrosis were assessed by histological and biochemical methods. Autoantibodies were detected by ELISA. The effects of mouse sera on H₂O₂ production by endothelial cells and on fibroblast proliferation, and serum concentrations in advanced oxidation protein products (AOPP) were compared with sera from patients with limited or diffuse SSc. We observed that s.c. peroxynitrites induced skin fibrosis and serum anti-CENP-B Abs that characterize limited SSc, whereas hypochlorite or hydroxyl radicals induced cutaneous and lung fibrosis and anti-DNA topoisomerase 1 autoantibodies that characterize human diffuse SSc. Sera from hypochlorite- or hydroxyl radical-treated mice and of patients with diffuse SSc contained high levels of AOPP that triggered endothelial production of H₂O₂ and fibroblast hyperproliferation. Oxidized topoisomerase 1 recapitulated the effects of whole serum AOPP. SCID mice developed an attenuated form of SSc, demonstrating the synergistic role of the immune system with AOPP in disease propagation. We demonstrate a direct role for ROS in SSc and show that the nature of the ROS dictates the form of SSc. Moreover, this demonstration is the first that shows the specific oxidation of an autoantigen directly participates in the pathogenesis of an autoimmune disease. *The Journal of Immunology*, 2009, 182: 5855–5864.

Systemic sclerosis (SSc)⁴ is a connective tissue disorder of unknown etiology characterized by vascular hyperreactivity, fibrosis of skin and visceral organs, and immunological alterations, including a distinct pattern of autoantibodies in the sera (1). The mechanisms that determine the clinical manifestations of the disease remain unclear (2). Several reports have suggested that reactive oxygen species (ROS) are involved in the pathogenesis of SSc (3–9). Indeed, skin fibroblasts from SSc patients spontaneously produce large amounts of ROS that trigger collagen synthesis (7, 10). In addition, autoantibodies found in SSc

patients against the platelet-derived growth factor receptor expressed on fibroblasts also induce the production of ROS (11). Recently, we have demonstrated that sera from patients with SSc could induce not only the production of ROS by endothelial cells but also the hyperproliferation of fibroblasts (6).

However, no direct proof for the involvement of oxidative stress in SSc pathogenesis has been brought forth to date. Moreover, the origin and nature of the oxidative stress remain to be elucidated. Environmental factors, and in particular silica dust, may be involved, which generate hydroxyl radicals (OH[·]) (12). Iterative ischemia-reperfusion that occurs frequently in SSc patients before the development of fibrosis may also be a source of superoxide anions (O₂[·]) through the activation of the xanthine/xanthine oxidase pathway (5).

To better understand the role of ROS in the fibrotic, vascular, and autoimmune processes that characterize SSc, s.c. injections of various types of ROS-inducing agents were performed on the backs of normal and SCID mice. Four different types of ROS-generating substances were used to reproduce the vast majority of oxidative stresses that could occur in humans: hypochlorous acid (HOCl) produced during the neutrophil burst; OH[·] that mainly originate from hydrogen peroxide (H₂O₂) subsequent to the Fenton reaction in macrophages; O₂[·], the major ROS produced during ischemia-reperfusion injuries by endothelial cells; and peroxynitrites (ONOO[·]) generated by the combination of O₂[·] and NO during reperfusion of ischemic tissues and inflammatory process. This procedure allowed us to directly demonstrate the involvement of ROS in the induction of the disease, to precisely characterize the nature and origin of ROS involved in the induction of diffuse or limited SSc, to study the mechanism leading to local or systemic involvement, and to determine the role of the immune system in the disease process.

*Université Paris Descartes, Faculté de Médecine, EA1833, [†]Service de Médecine Interne, Centre National de Référence Sclérodermie-Vascularites, EA4058 Assistance Publique-Hôpitaux de Paris, Hôpital Cochin, Paris, France, [‡]Faculté de Médecine de Reims, Service de Médecine Interne et Maladies Infectieuses, Hôpital Robert Debré, and [§]Faculté de Médecine de Reims, Laboratoire d'anatomopathologie Pol Bouin, Hôpital Maison Blanche, Reims, France

Received for publication November 5, 2008. Accepted for publication February 25, 2009.

The costs of publication of this article were defrayed in part by the payment of page charges. This article must therefore be hereby marked *advertisement* in accordance with 18 U.S.C. Section 1734 solely to indicate this fact.

¹ This work was supported by a grant from “Fondation Philippe” (to F.B.), grants from Actelion and the “Association des Sclérodermiques de France” (to A.S.), and a grant from the “Fondation pour la Recherche Médicale” (to P.G. and N.K.).

² A.S. and C.G. contributed equally to this work.

³ Address correspondence and reprint requests to Dr. Frédéric Batteux, Faculté de Médecine, Laboratoire d’immunologie, EA 1833, Université Paris Descartes, Institut Féderatif de Recherche Alfred Jost, Assistance Publique-Hôpitaux de Paris, Hôpital Cochin, 75679 Paris cedex 14, France. E-mail address: frederic.batteux@ch.ap-hop-paris.fr

⁴ Abbreviations used in this paper: SSc, systemic sclerosis; AOPP, advanced oxidation protein product; NAC, *N*-acetylcysteine; O₂[·], superoxide anion; OH[·], hydroxyl radical; ONOO[·], peroxynitrite; ROS, reactive oxygen species; TLC, total lung capacity.

Copyright © 2009 by The American Association of Immunologists, Inc. 0022-1767/09/\$2.00

Materials and Methods

Animals, cells, and chemicals

Specific pathogen-free, 6-wk-old female BALB/c, DBA/1, (NZB x NZW)F₁, and BALB/c SCID mice were purchased from Harlan Sprague-Dawley and maintained with food and water ad libitum. All mice were housed in autoclaved cages with sterile food and water. They were given humane care according to the guidelines of our institution. HUVECs were obtained by digestion of umbilical cords with 0.1% collagenase. NIH 3T3 fibroblasts were obtained from American Type Culture Collection. HEp-2 cells were obtained from EuroBio. All cells were cultured as reported previously (13). All chemicals were from Sigma-Aldrich except H₂-DCFDA (2',7'-dichlorodihydrofluorescein diacetate; Molecular Probes), bleomycin (Bellon Laboratories), human IgG (IVIg, Tegeline; LFB), anti-DNA topoisomerase 1 Abs (Santa Cruz Biotechnology), and anti-B220-PE, anti-CD11b-FITC, anti-CD4-allophycocyanin Cy7, anti-CD8-PE Cy7 Abs, and anti-CD3 mAb (BD Pharmingen).

Patients and healthy controls

A total of 20 patients with SSc and 20 healthy controls were enrolled in the study. All participants gave written informed consent. SSc was defined according to LeRoy and Medsger criteria and the American Rheumatism Association (1, 14, 15). Among the 20 patients with SSc, 10 had limited cutaneous SSc with no interstitial fibrosis and 10 had diffuse cutaneous SSc with interstitial lung fibrosis and a total lung capacity (TLC) of lower than 75% of predicted values. Limited cutaneous SSc was defined by skin thickening only in areas distal to the elbows and knees, and diffuse cutaneous SSc was defined by the presence of proximal, as well as distal skin thickening, to the elbows and knees (15). Interstitial lung disease was assessed in all patients by chest high-resolution computed tomodensitometry and pulmonary function test values. After collection and centrifugation, serum aliquots of 1-ml serum were stored at -80°C until use.

ROS preparation and injections

The 6-wk-old female BALB/c, DBA/1, (NZB x NZW)F₁, and BALB/c SCID mice were randomly distributed into experimental and control groups ($n = 10$ per group). A total of 100 μ l of solution generating ROS (HOCl, O₂⁻, ONOO⁻, or OH) or bleomycin was injected s.c. into the shaved back of the mice, using a 27-gauge needle, everyday for 6 wk. All agents were prepared ex temporaneously. Control groups received injections of 100 μ l of sterilized PBS.

Generation of HOCl. HOCl was produced by adding 166 μ l of NaClO solution (2.6% as active chlorine) to 11.1 ml of KH₂PO₄ solution (100 mM (pH 7.2)) (16). HOCl concentration was determined by spectrophotometry at 292 nm (molar absorption coefficient = 350 M⁻¹ cm⁻¹).

Generation of O₂⁻. A total of 60 mg of 18-crown-6 ether were dissolved in 10 ml of dry DMSO, and 7 mg of KO₂ were added quickly to avoid contact with air humidity (17, 18). The mixture was stirred for 1 h to give a pale yellow solution of 10 mmol/L O₂⁻. The solution was stable at room temperature for 1 h.

Generation of ONOO⁻. A 0.6 M H₂O₂ solution was prepared by mixing 8.8 M H₂O₂ with 0.7 M HCl. Five milliliters of the solution obtained were mixed with 5 ml of NaNO₂ (0.6 M) on ice. Then 10 ml of 1.2 M NaOH were added. H₂O₂ in excess was removed by adding MnO₂. The concentration of ONOO⁻ in the solution was determined at 300 nm (molar absorption coefficient = 1670 M⁻¹ cm⁻¹) (19, 20).

Generation of OH⁻. Hydroxyl anions were generated by adding 20 mM H₂O₂ into 10 mM Fe(II)SO₄ (21, 22). The solution obtained was injected after dilution if 1/2 in H₂O.

Preparation of bleomycin. A solution of bleomycin (100 μ g/ml) was prepared in PBS.

Experimental procedure

Two weeks after the end of the injections, the animals were sacrificed by cervical dislocation. Serum samples were collected from each mouse and stored at -80°C until use. Lungs and kidneys were removed from each mouse and a skin biopsy was performed on the back region, involving the skin and the underlying muscle of the injected area. Samples were stored at -80°C for determination of collagen content or fixed in 10% neutral buffered formalin for histopathological analysis.

Treatment with N-acetylcysteine (NAC)

BALB/c mice were injected s.c. with a solution generating HOCl everyday for 6 wk, as described, and simultaneously i.p. treated with either NAC (150 mg/kg per injection diluted in PBS; Bristol-Myers Squibb) ($n = 10$)

or PBS ($n = 10$) three times per week for the same 6 wk. A control group ($n = 10$ mice) received both s.c. and i.p. injections of sterilized PBS. The experimental procedure described was applied.

Histopathologic analysis

Fixed lung, kidney, and skin samples were embedded in paraffin. A 5- μ m thick tissue section was prepared from the midportion of paraffin-embedded tissue and stained with H&E. Slides were examined by standard bright-field microscopy (Olympus BX60) by a pathologist who was blinded to the animal's group assignment. Dermal thickness was measured under a light microscope of stained sections.

Collagen content in skin and lung

Collagen content assay was based on the quantitative dye-binding Sircol method (Biocolor) (23). Skin taken from the site of injection and lung pieces from each mouse were diced using a sharp scalpel, put into aseptic tubes, thawed and mixed with pepsin (1:10 weight ratio) and 0.5 M acetic acid. Collagen extraction was performed overnight at room temperature under stirring. The solution was then centrifuged at 20,000 \times g for 20 min at 4°C and 50 μ l of each sample were added to 1.0 ml of Syrius red reagent. Tubes were rocked at room temperature for 30 min and centrifuged at 20,000 \times g for 20 min. The supernatants were discarded and 1.0 ml of the 0.5 M NaOH was added to the collagen-dye pellets. The concentration values were read at 540 nm on a microplate reader (Fusion; PerkinElmer) vs a standard range of bovine collagen type I concentrations (supplied as a sterile solution in 0.5 M acetic acid).

Isolation of fibroblasts from the skin of mice and proliferation assays

Skin fragments from the back of mice submitted to HOCl ($n = 7$), bleomycin ($n = 7$), or PBS ($n = 5$) injections for 6 wk were collected 1 wk after the last injection. Skin samples were digested with Liver Digest Medium (Invitrogen) for 1 h at 37°C. After three washes in complete medium, cells were seeded into sterile flasks. Isolated fibroblasts were cultured in DMEM/Glutamax-I supplemented with 10% heat-inactivated FCS and antibiotics at 37°C in humidified atmosphere with 5% CO₂. For proliferation assay, primary fibroblasts (2×10^3 per well) were seeded in 96-well plates and incubated with 150 μ l of culture medium with 10% FCS at 37°C in 5% CO₂ for 48 h. Cell proliferation was determined by pulsing the cells with [³H]thymidine (1 μ Ci/well) during the last 16 h of culture. Results were expressed as an absolute number of cells in cpm.

Immunohistochemistry of lung tissue section

Frozen lung tissue sections of 5- μ m thickness were fixed in acetone for 5 min at -20°C, washed with PBS, and blocked with 2% normal mouse serum for 30 min at room temperature. Slides were then stained for 1 h at room temperature with a 1/50 dilution of FITC-labeled rat anti-mouse B220 (clone RA3-6B2; BD Pharmingen), with a 1/50 dilution PE-labeled hamster anti-mouse CD3 (clone 145-2C11; BD Pharmingen), or with the respective FITC- and PE-labeled control isotype (BD Pharmingen). After extensive washing in PBS, slides were observed with an Olympus microscope equipped with an epifluorescence system and pictures taken at magnification $\times 400$ with a digital camera.

Serum autoantibodies detection

Levels of anti-DNA topoisomerase 1 IgG, anti-CENP-B IgG, anti-dsDNA IgG, anti-cardiolipin IgG Abs, anti-annexin V IgG Abs and of IgM rheumatoid factors were measured using standard ELISA in mouse serum diluted 1/50. Serum IgG reactivities were also analyzed by immunoblotting technique with whole cell HEp-2 and HUVEC protein extracts for mice and patients (serum diluted 1/50 in both cases). Levels of anti-DNA topoisomerase 1 IgG Abs were detected by ELISA using purified calf thymus DNA topoisomerase 1 bound to the wells of a polystyrene microwell plate (Inova Diagnostics). Levels of anti-CENP-B IgG Abs were measured by ELISA using microplates coated with full-length recombinant CENP-B (Pharmacia Diagnostics). Levels of anti-dsDNA IgG, anti-cardiolipin IgG Abs, anti-annexin V IgG Abs, and IgM rheumatoid factor were measured using standard ELISA (24). Calf thymus DNA (5 μ g/ml), cardiolipin (50 μ g/ml), annexin V (2 μ g/ml), or i.v. human IgG (10 μ g/ml, Tegeline; LFB) were coated onto ELISA plates (precoated with protamine sulfate when dsDNA was used as substrate) overnight at 4°C. All plates were blocked with PBS-1% BSA and washed, and 100 μ l of 1/50 mouse serum were added and allowed to react for 1 h at room temperature. After five washes, bound Abs were detected with alkaline phosphatase-conjugated goat anti-mouse IgG or IgM Abs, and the reaction was developed by adding *p*-nitrophenyl phosphate. Optical density was measured at 405 nm using a

Dynatech MR 5000 microplate reader (Dynex Technology) and the optical density in blank wells (no Ag coated) was subtracted.

HEP-2 cells and HUVEC were harvested in the presence of EDTA. Whole cell protein extracts were prepared in 125 mM Tris-HCl (pH 6.8) with 4% SDS, 1.45 M 2-ME, and 1 µg/ml each of aprotinin, pepstatin, and leupeptin on ice and sonicated four times during 30 s. Nuclear protein extracts were prepared as previously described (25). Briefly, cells were incubated in 10 mM HEPES, 1.5 mM MgCl₂, 0.5 mM DTT for 10 min on ice and lysed with 10 strokes of Dounce homogenizer. The homogenate was centrifuged for 20 min at 25,000 × g. The pellets of nuclei were resuspended in 3 ml of buffer with 20 mM HEPES, 25% glycerol, 0.42 M NaCl, 1.5 mM MgCl₂, 0.2 mM EDTA, 0.5 mM PMSF, 0.5 mM DTT and lysed with 10 strokes of Dounce homogenizer. The suspension was then centrifuged for 30 min at 25,000 × g, and the supernatant was dialyzed. The dialysate was finally centrifuged, and the supernatant used for quantification. Equal amounts of loading buffer with solubilized proteins (140 µl/gel) were subjected to 10% SDS-PAGE, transferred onto nitrocellulose membranes, and incubated for 4 h at room temperature with 1/50 mouse sera using a Cassette Miniblot System (Immunetics) (26). The membranes were then extensively washed and incubated with alkaline phosphatase-conjugated goat anti-mouse IgG Ab. Immunoreactivity was revealed with NBT/5-bromo-4-chloro-3-indolyl phosphate.

Flow cytometric analysis of spleen cell subsets

Spleen cell suspensions were prepared after hypotonic lysis of erythrocytes. Cells were incubated with the appropriate labeled Ab at 4°C for 45 min in PBS with 0.1% sodium azide and 5% normal rat serum to block nonspecific binding. Cell suspensions were then subjected to four-color analysis on a FACSCanto flow cytometer (BD Biosciences). The mAbs used in this study were anti-B220-PE, anti-CD11b-FITC, anti-CD4-allophycocyanin Cy7, and anti-CD8-PE Cy7 Abs.

In vitro spleen cell proliferation

Spleen cells were isolated by gentle disruption of spleens and erythrocytes lysed by hypotonic shock in potassium acetate solution. Spleen cells were cultured in RPMI 1640 supplemented with antibiotics, Glutamax (Invitrogen Life Technologies), and 10% heat-inactivated FCS (Invitrogen Life Technologies) as complete medium. The proliferation assay was conducted in 96-well flat-bottom plates. Briefly, spleen cell suspensions (2×10^5 cells) were cultured in complete medium for 48 h in the presence of 10 µg/ml LPS (Boehringer Mannheim) or with precoated anti-CD3 mAb (2.5 µg/ml). Cell proliferation was determined by pulsing the cells with [³H]thymidine (1 µCi/well) during the last 16 h of culture and measuring the radioactivity incorporated by liquid scintillation counting.

Total serum IgG and IgM Ab concentrations

Levels of total mouse IgG and IgM Abs were measured using standard ELISA.

H₂O₂ assay

Endothelial cells (8×10^3 per well) were seeded in 96-well plates (Costar; Corning) and incubated with their respective growth medium alone for 12 h at 37°C in 5% CO₂. Culture medium was removed after 12 h and cells were preincubated with 50 µl of H₂-DCFDA diluted 1/1000 in PBS to test cellular H₂O₂ production. After 30 min, 50 µl of mouse serum were added and H₂O₂ production was monitored spectrofluorimetrically for 6 h (Fusion; PerkinElmer). Results were expressed in arbitrary units per minute and per millions of cells.

Determination of advanced oxidation protein product (AOPP) concentrations in sera

AOPP concentration was measured by spectrophotometry as previously described (27). In test wells, 200 µl of serum diluted 1/20 in PBS were distributed onto a 96-well plate, and 20 µl of acetic acid was added. Next, 10 µl of 1.16 M potassium iodide were added. In standard wells, 10 µl of 1.16 M potassium iodide was added to 200 µl of chloramine-T solution followed by 20 µl of acetic acid. Calibration used chloramine-T within the range from 0 to 100 µmol/L. The absorbance was immediately read at 340 nm on a microplate reader (Fusion; PerkinElmer). AOPP concentration was expressed as 0–100 µmol/L of chloramine-T equivalents.

H₂O₂ production, fibroblast proliferation, and collagen synthesis induced by various types of oxidized proteins

DNA topoisomerase 1 (extracted from placenta (28)), human polyclonal IgG (IVIg, Tegeline; LFB) collagenase, pepsin, and BSA were oxidized

with 1 mM HOCl or 10 mM OH⁻ for 1 h at room temperature. Proteins were then dialyzed overnight against PBS and tested for AOPP content. For H₂O₂ production assay, endothelial cells (8×10^3 per well) were incubated with either oxidized or nonoxidized protein solutions (125 µg/ml) and the production of H₂O₂ was assessed spectrofluorometrically using H₂-DCFDA. For fibroblast proliferation assay, NIH 3T3 fibroblasts (4×10^3 per well) were seeded in 96-well plates (Costar) and incubated with 50 µl of one of the oxidized or nonoxidized protein preparations (500 µg/ml) and 150 µl of culture medium without FCS at 37°C in 5% CO₂ for 48 h. Cell proliferation was determined by pulsing the cells with [³H]thymidine (1 µCi/well) during the last 16 h of culture. Results were expressed as absolute number fibroblasts as cpm. For type I collagen mRNA synthesis assay, NIH 3T3 fibroblasts (10^6 per well in 4 ml of complete medium) were seeded in 6-well plates and incubated with 50 µl of one of the oxidized or nonoxidized protein preparations (500 µg/ml) for 24 h. After the incubation period, cells were washed three times with PBS, and total RNA was extracted from fibroblasts with TRIzol Reagent (Invitrogen). Type I collagen mRNA was then assayed by a standard two-step RT-PCR as previously described (29). The following PCR primers were used: for type I collagen (forward) 5'-TGTCGTGTTCTCAGGGTAG-3' and (reverse) 5'-TTGTCGTAGCAGGGTTCTTC-3'; and for β-actin (forward) 5'-TG GAATCTGTGGCATCCATGAAAC-3' and (reverse) 5'-TAAAACGC AGCTCAGTAACAGTCCG-3'. The PCR products were subjected to electrophoresis on a 2% agarose gel and detected by ethidium bromide staining. Amplicon intensity was quantified using a scanner densitometer (Vilber Lourmat). Results were expressed as densitometry units normalized for β-actin expression for collagen type I transcripts.

Determination of oxidized DNA topoisomerase 1 concentrations in the skin of mice exposed to ROS

DNA topoisomerase 1 was extracted from areas of skin injected with prooxidative agents, bleomycin, or PBS as previously described (28). AOPP was measured in the obtained extracts as described.

Determination of TGF-β1 in the skin of mice exposed to ROS

Skin samples taken from the site of injections from each mouse injected with HOCl, bleomycin, or PBS were diced using a sharp scalpel, put into aseptic tubes, thawed, and mixed with 500 µl of RIPA (50 mM Tris-HCl (pH 7.5), 150 mM NaCl, 1% Triton, 0.5% sodium desoxycholate, 0.5% SDS, 0.1% H₂O₂ antiproteases). Equal amounts of loading buffer with solubilized proteins (30 µg/well) were subjected to 15% SDS-PAGE, transferred onto PVDF membranes, and incubated for 1 h at room temperature with anti-TGF-β1 Abs (Promega) using a Cassette Miniblot System (Immunetics). The membranes were then extensively washed and incubated with an anti-Fc γ-chain-specific goat anti-rabbit IgG Abs coupled to HRP (DakoPatts). Immunoreactivity was revealed with ECL (Amersham Biosciences).

AOPP depletion assays

Sera from mice treated with HOCl ($n = 10$) or PBS ($n = 10$), or sera from patients with SSC ($n = 10$) or healthy controls ($n = 10$) were incubated for 5 min at 37°C with various amounts of 2-ME or PBS as indicated in the each experiment. Sera were then immediately tested for AOPP concentration and for the ability to induce H₂O₂ production by endothelial cells and fibroblast proliferation as described. Control experiments were performed with the same amount of 2-ME but without sera, to ensure that the results were not linked to a direct effect of 2-ME on H₂O₂ production by endothelial cells or on fibroblast proliferation. Endothelial cell viability was assessed by Hoechst method immediately after the measure of H₂O₂ production by spectrophotometry.

DNA topoisomerase 1 depletion assays

Sera from patients ($n = 5$) were diluted 1/2 in PBS, and 200 µl of the serum dilution was incubated with 5 µl of rabbit polyclonal anti-human DNA topoisomerase 1 Ab (Santa Cruz Biotechnology) or irrelevant sera as controls for 2 h at 4°C. Then, 50 µl of protein G (Sigma-Aldrich) was added and incubated with the serum dilution overnight at 4°C. After the incubation period, the suspensions were centrifuged 5 min at 10,000 × g to remove protein G, and the supernatants were tested for AOPP content and for their ability to induce H₂O₂ production by endothelial cells and to induce fibroblast proliferation.

Statistical analysis

All quantitative data were expressed as mean ± SEM. Data were compared using the Mann-Whitney nonparametric test or Student's *t* paired test. When analysis included more than two groups, one-way ANOVA was used. A value for *p* < 0.05 was considered significant.

Results

The s.c. injection of ROS-generating agents induced dermal fibrosis in mice

Histopathological analyses of skin biopsy samples showed an increase in the dermal thickness of BALB/c mice treated with solutions generating HOCl, ONOO⁻, OH[•], and bleomycin compared with sham-injected mice ($p = 0.006$, $p = 0.007$, $p = 0.011$, and $p = 0.002$, respectively, for dermal thickness) (Fig. 1a and b). These results were corroborated by the measure of the concentration of acid- and pepsin-soluble type I collagen content per milligram of skin directly exposed to agents generating ROS or bleomycin. The concentration of type I collagen was significantly higher in the skin of BALB/c mice directly exposed to agents generating HOCl, ONOO⁻, OH[•], and bleomycin than the concentration measured in skin of mice injected with PBS ($p = 0.002$, $p = 0.001$, $p = 0.008$, and $p = 0.008$, respectively) (Fig. 1c), whereas the solution generating O₂⁻ had no effect ($p = 0.27$ vs PBS). Identical results were observed in DBA/1 and in (NZB x NZW)F₁ mice injected (see Supplemental Fig. 1).⁵ In addition, fibroblasts isolated from the skin of mice submitted to treatment with agents generating HOCl displayed a higher proliferation rate than fibroblasts obtained from mice injected with PBS or bleomycin ($p = 0.01$ vs PBS and $p = 0.003$ vs bleomycin) (Fig. 1d). The concentration of collagen content in skin was significantly decreased in mice injected with agents producing HOCl and simultaneously treated with the antioxidative agent N-acetylcysteine (NAC), suggesting that the accumulation of collagen observed upon HOCl injection was associated with an oxidative stress ($p = 0.01$ vs mice exposed to HOCl and treated with PBS) (Fig. 1e).

The s.c. production of HOCl and OH[•] induced a systemic reaction with lung fibrosis and renal involvement

We next investigated whether s.c. production of ROS could trigger a systemic reaction as observed in the diffuse form of human SSc. Histopathological analysis of lung tissue from BALB/c mice injected with agents generating HOCl, OH[•], or bleomycin showed thickening of the pulmonary interalveolar septa accompanied by cell infiltrates, whereas mice treated with agents generating ONOO⁻, O₂⁻, or PBS showed no signs of fibrosis or inflammation (Fig. 2a). Moreover, in mice injected with agents generating HOCl, OH[•], and bleomycin, the concentration of type I collagen in the lung was higher than the concentration found in mice injected with PBS ($p = 0.0048$, $p = 0.024$, and $p = 0.024$, respectively) (Fig. 2b). By contrast, injection of agents generating ONOO⁻ or O₂⁻ did not increase the level of collagen synthesis in lung vs PBS ($p = 0.28$ for ONOO⁻, $p = 0.17$ for O₂⁻). As observed for the skin, the concentration of collagen content in lung was significantly decreased in mice injected with agents producing HOCl and simultaneously treated with NAC ($p = 0.0185$ vs mice exposed to HOCl and treated with PBS) (Fig. 1e). Immunohistochemistry analysis of lung tissue sections from BALB/c mice injected with agents generating HOCl or bleomycin were next performed to analyze the characteristics of the cell infiltrates observed in the lung of these mice. Staining with anti-mouse B220 or anti-mouse CD3 showed that most cells were consisting of T lymphocytes (Fig. 2d).

In addition, kidneys from mice injected with HOCl or OH[•]-producing agents displayed abnormal accumulation of collagen in the interstitium with some foci of inflammatory cells (see Supplemental Fig. 2).⁵ Intimal fibrosis with intima-media thickening and a decrease of lumen diameter were observed in small renal arteries of mice treated with either bleomycin or an HOCl- or OH[•]-producing agent.

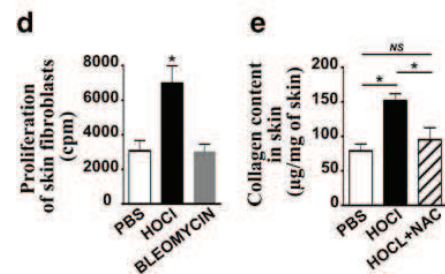
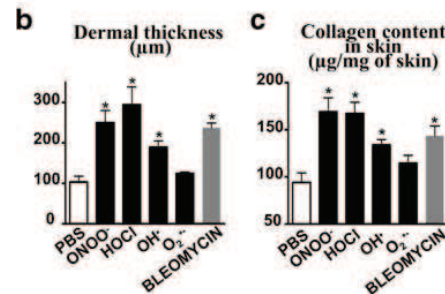
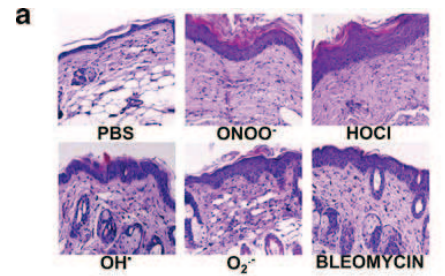


FIGURE 1. The s.c. injection of HOCl, OH[•], or ONOO⁻ induces a skin fibrosis in BALB/c mice. The s.c. injections of bleomycin or PBS, or of ROS-inducing substances (O₂⁻, HOCl, OH[•], and ONOO⁻) were performed daily for 6 wk in the back of BALB/c mice. *a*, Representative skin sections comparing dermal fibrosis in the injection areas from BALB/c mice. Tissue sections were stained with H&E. Magnification is $\times 50$ (Olympus DP70 Controller). *b*, Dermal thickness, as measured on skin sections in the injection areas of BALB/c mice. *, $p < 0.05$ vs mice injected with PBS. *c*, Results of the biochemical analysis of collagen content in skins from BALB/c mice ($n = 10$ per group) as measured by the quantitative dye-binding Sircol method. *, $p < 0.05$ vs mice injected with PBS. *d*, Results of proliferation assays of fibroblasts isolated from the skin of mice submitted to agents generating HOCl, bleomycin, and PBS by injection showing increased proliferation of fibroblasts taken from HOCl-exposed mice ($n = 10$ per group). *, $p < 0.05$ vs mice injected with PBS. *e*, Effect of NAC treatment on the collagen content in skin of BALB/c mice exposed to HOCl-inducing substances. Mice were s.c. injected with HOCl-inducing substances and simultaneously treated with NAC (150 mg/kg per i.p. injections, three times per week for 6 wk) or PBS. Collagen content was measured by the quantitative dye-binding Sircol method. *, $p < 0.05$. NS, Nonsignificant differences. Data are mean \pm SEM. Error bars represent SEM. Mean values were compared by using unpaired Mann-Whitney *U* tests.

By contrast, no signs of fibrosis or vascular damage were observed in kidneys from mice treated with an ONOO⁻- or O₂⁻-producing agent, or with PBS. In addition, kidneys from mice exposed to agents generating HOCl, OH[•], or ONOO⁻ displayed myocyte necrosis.

Exposition to an oxidative stress triggered a systemic autoimmune response

Because features of autoimmunity are observed in patients with SSc in addition to fibrosis, we investigated the presence of

⁵ The online version of this article contains supplemental material.

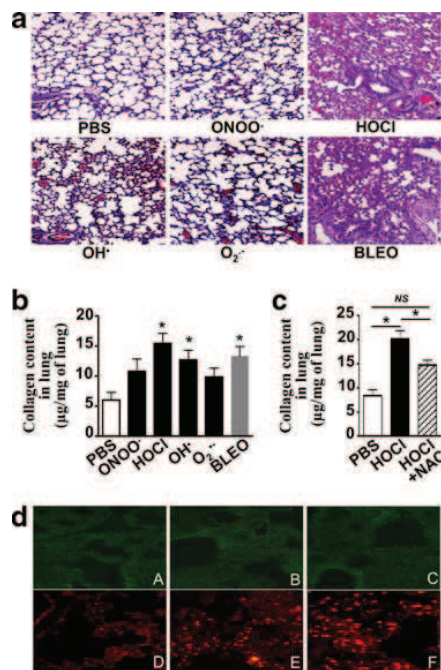


FIGURE 2. The s.c. injection of HOCl and OH⁻ but not of ONOO⁻ induces a systemic disease with lung fibrosis and inflammation in BALB/c mice. The s.c. injections of bleomycin or PBS, or of ROS-inducing substances (O₂⁻, HOCl, OH⁻, and ONOO⁻) were performed daily for 6 wk in the back of BALB/c mice. *a*, Representative lung sections from BALB/c mice. Tissue sections were stained with H&E. Magnification is $\times 50$ (Olympus DP70 Controller). *b*, Results of the biochemical analysis of collagen content in lungs from BALB/c mice ($n = 10$ per group) as measured by the quantitative dye-binding Sircol method. *, $p < 0.05$ vs mice injected with PBS. *c*, Effect of NAC treatment on the collagen content in lung of BALB/c mice exposed to HOCl-inducing substances. Mice were s.c. injected with HOCl-inducing substances and simultaneously treated with NAC (150 mg/kg per i.p. injections, three times per week for 6 wk) or PBS. Collagen content was measured in lung by the quantitative dye-binding Sircol method. *, $p < 0.05$. NS, Nonsignificant differences. Data are mean \pm SEM. Error bars represent SEM. Mean values were compared by using unpaired Mann-Whitney U tests. *d*, Immunohistochemistry of lung sections. Slides were stained with a 1/50 dilution of FITC-labeled rat anti-mouse B220, or with a 1/50 dilution PE-labeled hamster anti-mouse CD3 or with the respective FITC- and PE-labeled control isotype. *a* and *d*, PBS-treated mice. *b* and *e*, Bleomycin-treated mice (Bleo). *c* and *f*, HOCl-treated mice. Magnification is $\times 400$.

autoantibodies in the serum of mice injected with ROS-generating agents or bleomycin by immunoblotting experiments with whole cell protein extracts of HUVEC and HEp-2 cells. Serum Abs from mice submitted to the action of HOCl, OH⁻, ONOO⁻, or bleomycin but not O₂⁻ or PBS also bound to a 85-kDa protein band present in both endothelial and HEp-2 cell extracts. The same 85-kDa protein band was also recognized by the serum from a patient with limited cutaneous SSc and anti-centromere Abs (patient 1, Fig. 3*a*). Serum Abs from mice submitted to the action of HOCl, OH⁻, or bleomycin, but not other ROS or PBS, bound to several bands including two 100-kDa protein bands present in both endothelial (Fig. 3*a*) and HEp-2 cell extracts (data not shown). The same 100-kDa bands were recognized by the serum from a patient with diffuse cutaneous SSc and anti-DNA topoisomerase 1 IgG Abs (patient 2, Fig. 3*a*).

In addition to these immunoblotting experiments, we investigated the presence of autoantibodies by ELISA experiments with

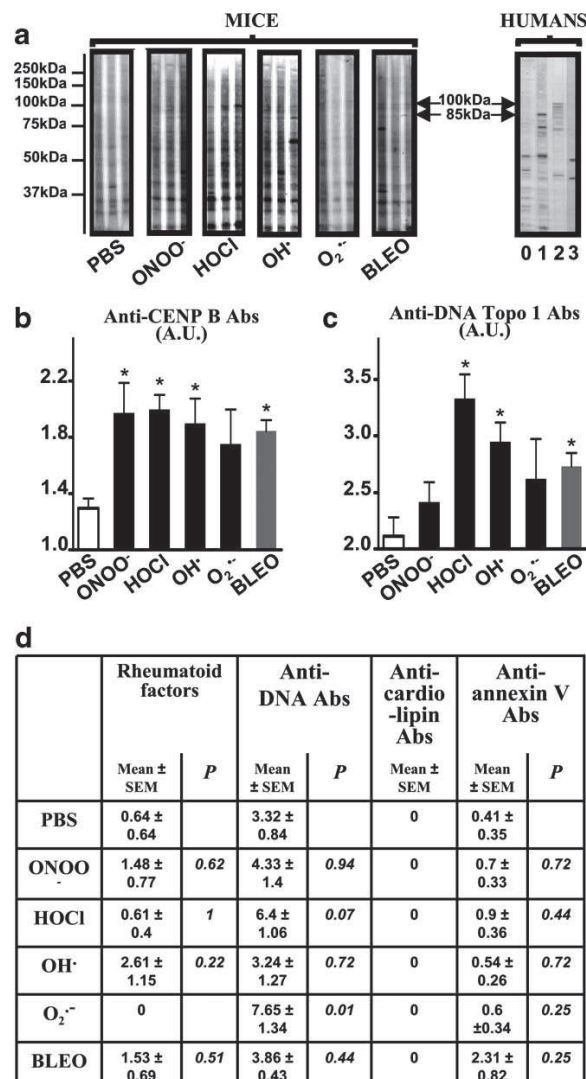


FIGURE 3. The s.c. injection of HOCl and OH⁻ trigger a selective immune activation leading to the production of high levels of anti-DNA topoisomerase 1 Abs. Injections of prooxidative agents, bleomycin, or PBS were performed daily for 6 wk in the back of BALB/c mice. *a*, Representative examples of Western blot analysis with whole cell protein extracts of HUVEC incubated with mice ($n = 10$ per group) or human sera. Serum in lane 0 was from a healthy individual, serum in lane 1 was from a patient with limited cutaneous SSc and contained anti-centromere Abs that bind to a 85-kDa band corresponding to CENP-B. Serum in lane 2 was from a patient with diffuse cutaneous SSc and contained anti-DNA topoisomerase 1 Abs that recognize two 100-kDa protein bands corresponding to different forms of DNA topoisomerase 1. Serum in lane 3 was from a patient with diffuse cutaneous SSc and contained no Abs characteristic of SSc. Serum from mice treated with HOCl, OH⁻, or bleomycin bound to several Abs including two 100-kDa proteins as IgG from patient with sera in lane 2. Serum from mice treated with HOCl, OH⁻, ONOO⁻, or bleomycin but not O₂⁻ or PBS bound to a 85-kDa protein as the patient with serum from lane 1. *b*, Anti-CENP-B IgG Abs titers detected by ELISA. *c*, Anti-DNA topoisomerase 1 IgG Abs titers measured by ELISA. *d*, Levels of IgG Abs (rheumatoid factors), and of anti-dsDNA, anti-cardiolipin, and anti-annexin V IgG Abs. Data are mean \pm SEM of data gained from all mice in the experimental or control group. Mean values were compared using unpaired Mann-Whitney U tests. *, $p < 0.05$ vs mice injected with PBS.

recombinant DNA topoisomerase 1, the major target of autoantibodies in patients with diffuse cutaneous SSc and recombinant CENP-B, the main centromeric Ag targeted by autoantibodies in patients with limited cutaneous SSc. We detected higher levels of anti-CENP-B Ab in the sera of mice exposed to ROS (except O_2^-) and bleomycin compared with mice injected with PBS ($p = 0.004$ for ONOO^- , $p = 0.001$ for HOCl, $p = 0.004$ for OH^- , and $p = 0.001$ for bleomycin) (Fig. 3b). Sera from mice exposed to agents generating HOCl, OH^- , and bleomycin contained a significant level of anti-DNA topoisomerase 1 Abs ($p = 0.001$, $p = 0.006$, and $p = 0.006$ vs mice treated with PBS, respectively) (Fig. 3c). Consequently, both immunoblotting and ELISA experiments detected the presence of anti-CENP-B Ab in the sera of mice injected with agents generating HOCl, OH^- , ONOO^- , or bleomycin and confirmed the presence of significant levels of anti-DNA topoisomerase 1 Abs in the sera of mice injected with agents generating HOCl, OH^- , or bleomycin, but not ONOO^- .

We next tried to detect the presence of autoantibodies usually found in other connective tissue diseases but not in SSc in the sera of experimental mice (Fig. 3d). We detected no significant levels of rheumatoid factors, anti-annexin V, or anti-cardiolipin Abs, regardless of the prooxidative product injected. Anti-DNA IgG Abs were detected in the sera from mice exposed to agents generating O_2^- but in no other group of mice ($p = 0.017$ as compared with mice receiving PBS). Therefore, all the prooxidative agents tested induced an autoimmune response, but only the exposition to agents generating HOCl, OH^- , and ONOO^- elicited an immune response characteristic of the SSc phenotype.

We then analyzed the spleen cell subpopulations in mice exposed to HOCl ($n = 7$), PBS ($n = 5$), or bleomycin ($n = 7$) for 6 wk. The s.c. injections of HOCl increased the number of total spleen cells and of spleen B cells when compared with PBS-injected mice ($p = 0.039$ for total spleen cells and $p = 0.019$ for spleen B cells) (see Supplemental Fig. 3, a and b).⁵ By contrast, no significant difference was observed in the number of CD11b⁺, CD4⁺, or CD8⁺ spleen cells between the animals exposed to HOCl or PBS (see Supplemental Fig. 3b).⁵ We next investigated the rate of proliferation of splenocytes after stimulation with an anti-CD3 mAb or with LPS. When stimulated by an anti-CD3 mAb, splenocytes isolated from mice submitted to HOCl displayed a higher proliferation rate than splenocytes obtained from mice injected with PBS ($p = 0.032$) (see Supplemental Fig. 3c).⁵ LPS exerted a higher pro-proliferative effect on splenocytes from mice injected with HOCl than on splenocytes from mice injected with PBS ($p = 0.041$) (see Supplemental Fig. 3c).⁵

We finally measured total serum IgM and IgG Ab concentrations in these mice. No significant difference was observed in total serum IgG Ab concentrations between mice treated with HOCl or PBS (see Supplemental Fig. 3d),⁵ whereas mice exposed to HOCl displayed higher serum IgM Ab concentrations than mice exposed to PBS ($p = 0.005$) (see Supplemental Fig. 3d).⁵

Taken together, our results confirm that HOCl injections induce an immune activation involving both B and T lymphocytes in BALB/c mice. This immune activation leads to T cell infiltration of the lung and to the production of autoantibodies, especially of anti-DNA topoisomerase I Abs.

Sera from mice and patients with SSc induced H_2O_2 production by endothelial cells

Because some mice s.c. injected with prooxidative agents developed not only a local reaction with skin sclerosis, but also systemic involvement with lung fibrosis and autoimmunity, we hypothesized that soluble factors generated at the site of ROS production and subsequently carried by the peripheral blood could mediate distal fibrotic

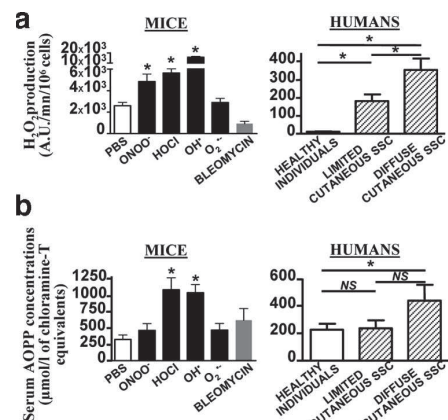


FIGURE 4. Sera from mice exposed to s.c. injection of HOCl and OH^- contain high amounts of AOPP and trigger the production of H_2O_2 by endothelial cells, as the sera from patients with a diffuse form of SSc. *a*, H_2O_2 production by endothelial cells induced by sera from mice injected with prooxidative agents, bleomycin, or PBS ($n = 10$ per group) and from SSc patients and 20 healthy controls. Ten patients had limited cutaneous SSc (with TLC >75%) and 10 patients had diffuse cutaneous SSc (with TLC <75%). *, $p < 0.05$ vs mice injected with PBS or healthy subjects. NS, Nonsignificant differences. *b*, Concentrations of AOPP in the sera from mice s.c. injected with ROS-inducing substances, bleomycin, or PBS and in the sera from patients with limited cutaneous SSc (with TLC >75%) ($n = 10$), patients with diffuse cutaneous SSc (with TLC <75%) ($n = 10$), and healthy subjects ($n = 20$). *, $p < 0.05$ vs mice injected with PBS or healthy controls. NS, Nonsignificant differences. Data are mean \pm SEM. Mean values were compared using unpaired Mann-Whitney *U* test in arbitrary units (A.U.).

processes. We thus tested the ability of the sera of these mice to induce the production of H_2O_2 by endothelial cells in vitro. The sera of mice exposed to agents generating HOCl, OH^- , and to a lesser extent, ONOO^- induced a higher production of H_2O_2 by endothelial cells than the sera of mice treated with PBS ($p = 0.015$, $p = 0.004$, and $p = 0.032$) (Fig. 4*a*).

We tested sera from 20 patients with SSc and from 20 healthy individuals for their ability to mediate endothelial cell activation and H_2O_2 production. There were 10 patients who had limited cutaneous SSc and no lung involvement, 10 patients suffered from diffuse cutaneous SSc with pulmonary fibrosis (with TLC <75%). All the sera from patients with limited and diffuse SSc induced a higher production of H_2O_2 by endothelial cells than sera from healthy subjects ($p < 0.0001$ in each case) (Fig. 4*a*). Nevertheless, the sera from patients with diffuse SSc and lung involvement induced a higher release of H_2O_2 by endothelial cells than the sera from patients with limited SSc and no lung fibrosis ($p = 0.03$) (Fig. 4*a*). Thus, s.c. generation of ROS resulted in the production of some serum-soluble factors capable of activating endothelial cells and inducing the production of other ROS types.

Sera containing AOPP

We then investigated which circulating factors were involved in the propagation of the oxidative stress from skin to lung. We hypothesized that the soluble factors possibly related to the systemic oxidative stress could be proteins oxidized in the skin subsequently carried by the peripheral blood to the lung where they could induce the fibrotic process. Consistent with this hypothesis, we observed that sera from mice exposed to agents generating HOCl or OH^- and sera from patients with diffuse cutaneous SSc and lung fibrosis SSc contained AOPP. The sera from mice injected with agents generating HOCl and OH^- contained higher amounts of AOPP than the sera from mice

treated with PBS ($p = 0.024$ and $p = 0.006$, respectively) (Fig. 4b). In contrast, the sera from mice exposed to other types of ROS or bleomycin did not contain higher levels of AOPP than those from mice injected with PBS. Sera from patients with diffuse SSc and lung fibrosis (with TLC <75%) also contained higher amounts of AOPP than sera from healthy subjects ($p = 0.04$) (Fig. 4b), whereas serum AOPP concentrations in patients with limited cutaneous SSc and no lung fibrosis did not differ from concentrations observed in healthy individuals ($p = 0.88$) (Fig. 4b).

Oxidized DNA topoisomerase 1 induced ROS production, fibroblast proliferation, and type I collagen synthesis

To further characterize the nature of AOPP associated with the systemic oxidative stress observed in mice exposed to agents generating HOCl or OH⁻, we tested the ability of a variety of in vitro-synthesized AOPP to reproduce fibroblast proliferation and H₂O₂ production by endothelial cells and type I collagen synthesis. We tested albumin and IgG, given their high concentration in serum, and unrelated proteins like collagenase and pepsin for their ability to trigger H₂O₂ production by endothelial cells, fibroblast proliferation, and collagen synthesis. In addition, we also tested DNA topoisomerase 1 because this protein is a specific autoantigen in SSc and is able to be cleaved in an oxidation reaction (30). We observed that the properties of these in vitro-synthesized AOPP were dependent on the nature of the protein used. Indeed, AOPP generated from DNA topoisomerase 1 oxidized by HOCl or OH⁻ induced a higher production of H₂O₂ by endothelial cells than AOPP derived from IgG, collagenase, albumin, or pepsin oxidized by HOCl or OH⁻ ($p < 0.0001$ in all cases) (Fig. 5a). Moreover, AOPP resulting from the oxidation of DNA topoisomerase 1 oxidized by HOCl or OH⁻ induced the highest rate of fibroblast proliferation ($p < 0.0001$ in all cases) (Fig. 5b) and the highest rate of type I collagen mRNA synthesis in vitro ($p < 0.05$ in all cases) (Fig. 5c).

The s.c. injections of HOCl- and OH⁻-generating agents induced local formation of DNA topoisomerase 1-derived AOPP but not of TGF- β 1

We then hypothesized that oxidized DNA topoisomerase 1 was formed in the skin areas where ROS were generated and was subsequently responsible for the development of the distal fibrotic lesions observed that may not be depending on cytokines such as TGF- β . To test this hypothesis, we performed selective DNA topoisomerase 1 extraction from the dorsal skin of mice exposed to HOCl or OH⁻ because those two types of ROS induced the highest concentrations of AOPP in serum (Fig. 5a). Oxidized DNA topoisomerase 1, as assayed by the measure of AOPP concentration in the DNA topoisomerase extract, was found in skin of mice treated with agents producing HOCl and OH⁻, but not in the skin of mice injected with bleomycin or PBS (Fig. 5d). By contrast, the skin extracts from mice treated with bleomycin, but not those from mice injected with HOCl, contained TGF- β 1 (Fig. 5e).

Reduction of serum AOPP and DNA topoisomerase 1 decreased the production of H₂O₂ by endothelial cells and fibroblast proliferation

To directly investigate the involvement of AOPP and oxidized DNA topoisomerase 1 in the spreading of systemic fibrosis in this model, we reduced serum AOPP by using the reducing agent 2-ME. By adding 5 μ M 2-ME to sera from mice exposed to agents producing HOCl, we obtained a significant decrease in AOPP concentrations ($p = 0.033$ vs similar sera without 2-ME) (Fig. 6a). Conversely, no significant decrease of AOPP concentrations was

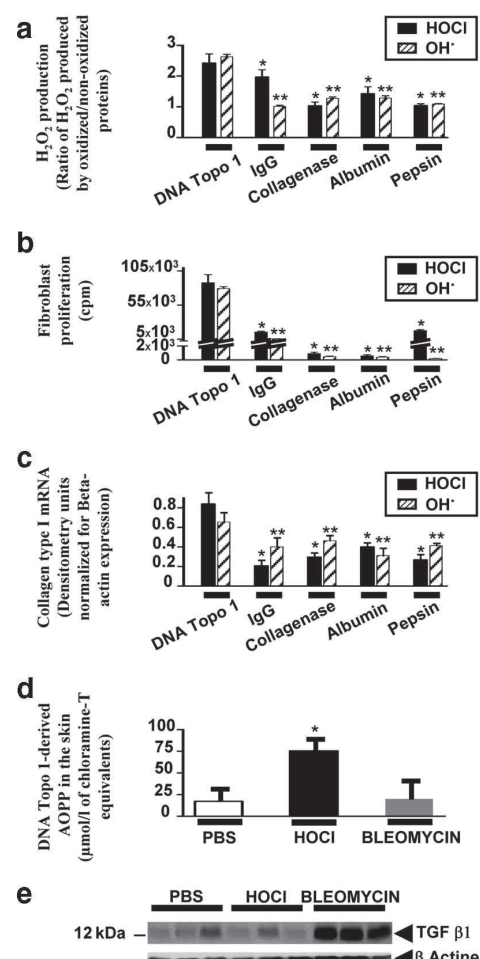


FIGURE 5. DNA topoisomerase 1 oxidized by HOCl or OH⁻ reproduces the effects of serum AOPP from HOCl- or OH⁻-treated mice. DNA topoisomerase 1 (DNA Topo 1), IgG, collagenase, albumin, and pepsin were submitted to oxidation by HOCl or OH⁻ in vitro. *a*, The ability of the oxidized proteins to induce H₂O₂ production by endothelial cells and proliferation of fibroblasts is shown. For each protein tested, data shown represent the ratio of H₂O₂ produced by endothelial cells exposed to oxidized proteins to H₂O₂ production following exposition to nonoxidized proteins. Data are mean \pm SEM. *, $p < 0.05$ vs DNA topoisomerase 1 submitted to oxidation by HOCl; **, $p < 0.05$ vs DNA topoisomerase 1 submitted to oxidation by OH⁻. *b*, Proliferation rate of NIH 3T3 fibroblasts upon incubation with the various oxidized proteins tested. Data are mean \pm SEM. *, $p < 0.05$ vs DNA topoisomerase 1 submitted to oxidation by HOCl; **, $p < 0.05$ vs DNA topoisomerase 1 submitted to oxidation by OH⁻. *c*, Type I collagen mRNA synthesis in NIH 3T3 fibroblasts upon incubation with the various oxidized proteins tested. Amplicon intensity was quantified using a scanner densitometer. Results are expressed as densitometry units normalized for β -actin expression for collagen type I transcripts. Data are mean \pm SEM. *, $p < 0.05$ vs DNA topoisomerase 1 submitted to oxidation by HOCl; **, $p < 0.05$ vs DNA topoisomerase 1 submitted to oxidation by OH⁻. *d*, Concentrations of oxidized DNA topoisomerase 1 in the skin areas of BALB/c mice exposed to HOCl, bleomycin, or PBS for 2 wk. DNA topoisomerase 1 was selectively extracted from the skin in the areas of injections. Data are mean \pm SEM. *, $p < 0.05$ vs mice injected with PBS. *e*, TGF- β 1 expression in skin of BALB/c mice exposed to HOCl, bleomycin, or PBS ($n = 3$ mice per group). Results are one representative experiment of three completed.

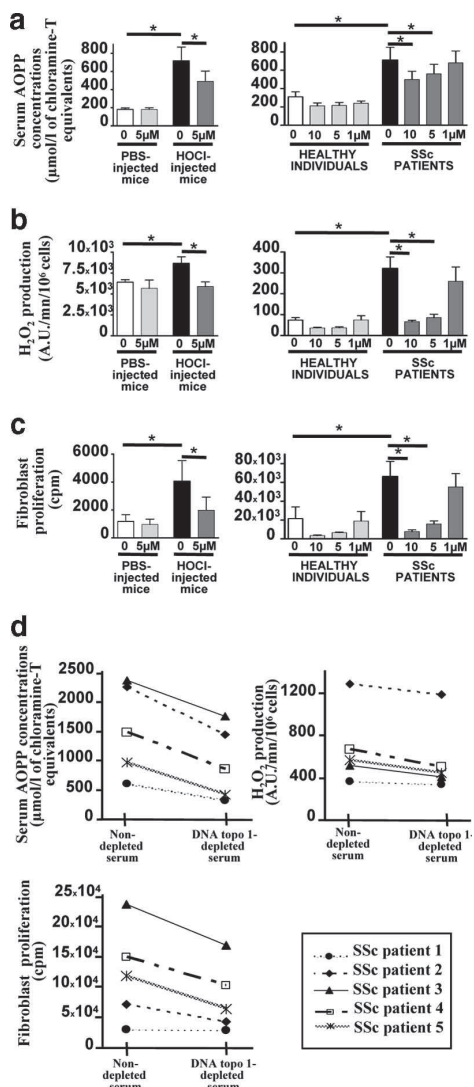


FIGURE 6. Reduction of serum AOPP, especially of oxidized DNA topoisomerase 1, decreases endothelial H₂O₂ production and fibroblast proliferation. Serum AOPP was reduced by adding 2-ME to sera from mice exposed to PBS or HOCl and to sera from healthy individuals or SSc patients sera. *a*, Serum AOPP concentrations measured in sera from mice exposed to HOCl or PBS after incubation with 5 μM 2-ME or PBS in vitro (*left*). Serum AOPP concentrations in sera from SSc patients or healthy individuals after incubation with 1, 5, or 10 μM 2-ME or PBS (*n* = 10 per group) (*right*). *b*, Endothelial H₂O₂ production in arbitrary units (A.U.) induced by sera from HOCl- or PBS-treated mice previously incubated with 5 μM 2-ME or PBS (*left*). Endothelial H₂O₂ generation induced by sera from SSc patients or healthy individuals after incubation with 1, 5, or 10 μM 2-ME or PBS (*n* = 10 per group) (*right*). *c*, Rate of NIH 3T3 fibroblast proliferation induced by sera from HOCl- or PBS-treated mice previously incubated with 5 μM 2-ME or PBS (*left*). Rate of NIH 3T3 fibroblast proliferation induced by sera from SSc patients or healthy individuals after incubation with 1, 5, or 10 μM 2-ME or PBS (*n* = 10 per group) (*right*). 2-ME alone did not change endothelial cell viability, endothelial H₂O₂ production, or fibroblast proliferation. *d*, Effects of DNA topoisomerase 1 (DNA topo 1) depletion from the sera of patients with SSc (*n* = 5) on H₂O₂ production by endothelial cells and fibroblast proliferation. H₂O₂ production measured in arbitrary units (A.U.). Data are mean ± SEM. *, *p* < 0.05.

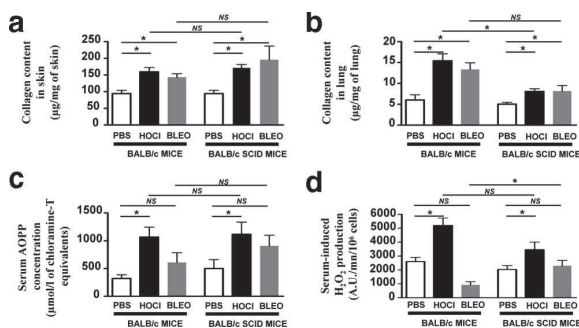


FIGURE 7. HOCl-induced pulmonary fibrosis is less extensive in BALB/c SCID mice than in BALB/c mice. BALB/c and BALB/c SCID mice were injected daily for 6 wk with an HOCl-generating agent, or bleomycin (BLEO) or PBS (*n* = 10 per group). Skin, lungs, and sera from those mice were collected at the time of sacrifice. Collagen content in skin (*a*) and lung (*b*) was measured by the quantitative dye-binding Sircol method. *c*, Serum AOPP concentrations in BALB/c and BALB/c SCID mice. *d*, Serum-induced H₂O₂ production by endothelial cells measured in arbitrary units (A.U.). Data are mean ± SEM gained from all mice in the experimental or control group. Mean values were compared using unpaired Mann-Whitney *U* tests. *, *p* < 0.05. NS, Nonsignificant differences.

observed in the sera from PBS-treated mice (*p* = 0.99 vs similar sera without 2-ME) (Fig. 6*a*).

We next tested the sera depleted of AOPP for the ability to induce endothelial H₂O₂ production as compared with homologous nondepleted sera. AOPP depletion decreased H₂O₂ production in mice treated with a solution inducing HOCl (*p* = 0.001 vs similar sera without 2-ME) (Fig. 6*b*). Control experiments performed with 2-ME alone showed no changes in endothelial cell viability and in H₂O₂ production (data not shown).

Finally, we tested the effects of all depleted and nondepleted sera on the proliferation of fibroblasts. Sera from mice treated with HOCl tended to exert a higher pro-proliferative effect on NIH 3T3 fibroblasts than sera from mice receiving PBS (*p* = 0.05 vs serum from PBS-treated mice) (Fig. 6*c*). After AOPP depletion, sera from mice treated with HOCl lost their higher ability to stimulate fibroblast proliferation (*p* = 0.037 vs similar sera without 2-ME) (Fig. 6*c*). 2-ME alone did not modify fibroblast proliferation (data not shown).

Similar results were observed with sera from SSc patients after addition of 5 μM 2-ME ex vivo (Fig. 6, *a–c*). In addition, because higher volumes of serum were available from patients than from mice, we performed additional experiments with human sera and mixed the sera with 1 and 10 μM 2-ME, respectively. AOPP concentrations and serum properties (induction of H₂O₂ production and of fibroblast proliferation) were related to the dose of 2-ME used, in a dose-dependent fashion.

Previous experiments showed that oxidized DNA topoisomerase 1 exerted higher effects than other AOPP. To assess the involvement of this protein in the spreading of the disease, we depleted DNA topoisomerase 1 protein from human sera by immunoprecipitation using an anti-human DNA topoisomerase 1 Ab. The SSc sera depleted of DNA topoisomerase 1 (*n* = 5) showed a decrease in whole AOPP concentration, in the production of H₂O₂ by endothelial cells, and in the proliferation of fibroblasts (Fig. 6*d*).

Role of the immune system in the development of SSc in mice

We next investigated whether skin and lung fibrosis observed in BALB/c mice exposed to HOCl was dependent on a simultaneous activation of the immune system. For that purpose, immunodeficient SCID mice were injected s.c. with a solution generating

HOCl. As observed in normal mice, immunodeficient SCID mice developed more skin and lung fibrosis than SCID mice exposed to PBS as assessed by collagen content ($p = 0.001$ and $p = 0.029$ for skin and lung, respectively) (Fig. 7, *a* and *b*). These results indicate that the immune system was not required for the initiation of SSc in mice. However, SCID mice exposed to a solution generating HOCl showed significantly lower pulmonary fibrosis than wild-type BALB/c, with no differences in the extent of skin fibrosis ($p = 0.428$ and $p = 0.0158$ for skin and lung collagen content respectively) (Fig. 7, *a* and *b*). This decrease in lung fibrosis was related to the immune system and not to differences in serum AOPP levels (Fig. 7*c*) or endothelial H₂O₂ production potentials (Fig. 7*d*) between the strains. Taken together, these results suggest that the immune system is not required for the development of skin fibrosis, but rather for the full development of lung fibrosis through synergistic interactions with the direct toxicity of oxidized proteins.

Discussion

In this study, we produced and described original animal models of SSc for both the limited and diffuse forms of SSc that support the direct role of ROS in both forms of the disease (3). These tools offer new opportunities for studying this chronic and fatal human disease of unknown etiology.

We observed three different phenotypes in mice submitted to s.c. oxidative stress, depending on the type of ROS injected. The s.c. injections of agents generating O₂⁻ did not induce any feature of SSc. By contrast, s.c. injections of agents generating OH⁻ or HOCl induced cutaneous and lung fibrosis and kidney involvement along with the production of serum anti-DNA topoisomerase 1 Abs; all features that characterize diffuse cutaneous SSc in humans. The injections of agents generating ONOO⁻, conversely, induced limited cutaneous fibrosis and the production of anti-CENP-B Abs in the absence of either lung involvement or the presence of serum anti-DNA topoisomerase 1 Abs. This disease shares numerous similarities to the limited cutaneous form of SSc. To our knowledge, this experimental demonstration is the first to show the two different clinical forms of human SSc in mice.

Using these animal models, we discovered a new mechanism involving AOPP, which accounts for the systemic propagation of the disease. AOPP were first described as new markers of oxidative stress in patients with uremia (27). Recently, these oxidized protein products have been shown to act as true inflammatory mediators. They are able to trigger the oxidative burst of neutrophils and monocytes and to stimulate dendritic cells *in vitro* (31, 32). In addition, they promote renal fibrosis in a remnant kidney model (33).

Our experiments suggest that AOPP, generated in high amounts after exposition of the skin to agents generating hypochlorite or hydroxyl anions, are directly involved in the spreading of the fibrosis from the skin into visceral organs via the systemic circulation, thus leading to the development of the diffuse form of SSc and anti-DNA topoisomerase 1 Abs. These observations are consistent with previous studies, which demonstrate a direct link between the concentration of AOPP in the serum of SSc patients and the development of lung fibrosis (6). Nevertheless, future research is necessary to fully understand the exact molecular mechanisms of the damages induced by AOPP.

Our study also demonstrated a new role for the protein DNA topoisomerase 1 in SSc. This protein is known to be the selective target of the immune response in patients with diffuse cutaneous SSc (34). Such anti-DNA topoisomerase 1 Abs are neither detected in patients with limited cutaneous SSc nor in those with other connective tissue disorders. Interestingly, Casciola-Rosen et al. (30) have shown that OH⁻, generated by the Fenton reaction, can

cleave DNA topoisomerase 1. It was postulated that this modification could increase DNA topoisomerase 1 antigenicity and thus may be required for the development of anti-DNA topoisomerase 1 Abs. Our observations corroborate the findings of Casciola-Rosen et al. (30). In our animal model, we found that exposition to HOCl or OH⁻, generated via the Fenton reaction from H₂O₂, induced high amounts of oxidized DNA topoisomerase in the skin along with concomitantly high serum levels of anti-DNA topoisomerase 1 Abs. However, in addition to this known antigenic property, we found a direct pathogenic role for oxidized DNA topoisomerase 1 in SSc. Indeed, high amounts of oxidized DNA topoisomerase 1 were detected in the skin of mice after exposition to HOCl. We showed *in vitro* that oxidized DNA topoisomerase 1 was capable of triggering H₂O₂ production by endothelial cells and fibroblast proliferation, fully recapitulating the effects of whole AOPP contained in the sera of HOCl-treated mice and of patients with diffuse cutaneous SSc. These results were not reproduced with other oxidized proteins, suggesting that the observed phenotypes were solely due to the toxic properties of oxidized DNA topoisomerase 1. As expected, when we depleted DNA topoisomerase 1 in SSc sera, ROS production and fibroblast proliferation decreased close to baseline levels. Taken together, these results suggest that DNA topoisomerase 1, exposed to a specific oxidation, is not only the target of the immune response in SSc but is a crucial factor responsible for the diffusion of the oxidative stress and the induction of tissular damages in this mouse model and in SSc patients.

The pathogenic role of oxidized DNA topoisomerase 1 per se was confirmed by the development of SSc in SCID mice exposed to HOCl. These results obtained in mice with no operational immune system suggest that B and T lymphocytes are not required for the development of the disease (35–37). However, the extent of the HOCl-induced pulmonary fibrosis was lower in SCID mice than in immunocompetent mice, indicating that the immune system synergizes with the direct effects of oxidized proteins for the full development of the systemic disease (see Supplemental Fig. 4).⁵ This conclusion is consistent with the fact that, in mice exposed to HOCl, the lung fibrosis is associated with a T cell infiltrate, similar to that observed in human SSc (38).

Thus far, the classical model available to study SSc has been the bleomycin model. Bleomycin is a well known profibrotic agent that causes pulmonary fibrosis after tracheal instillation (39) and skin and lung fibrosis following s.c. injections (40). However, there are many features of bleomycin treatment that are not consistent with human SSc. First, whereas bleomycin treatment does not modify the phenotype of fibroblasts, fibroblasts obtained from SSc patients display a high rate of spontaneous proliferation. Our animal models reproduce this latter phenotype following treatment with agents generating HOCl. Second, in the bleomycin-induced SSc, systemic fibrosis is caused by the intrinsic chemical properties of the drug and involves the generation of cytokines such as TGF- β (41, 42). This cytokine, able to stimulate fibroblasts to produce matrix proteins *in vitro*, is not involved in our models and seems not to be involved in human SSc. Although the data regarding the presence of this cytokine in the skin of SSc patients are contradictory (43, 44), it has been clearly shown that fibroblasts from patients with SSc do not secrete more TGF- β than normal cells (45). Thus, we believe that we have created a more representative model of human SSc than the bleomycin model.

In conclusion, we provide new animal models recapitulating the different clinical forms of human SSc. Using these models, we demonstrate a novel, direct role for ROS in the induction of SSc. We show that the nature of the ROS involved determines the extent of fibrosis and the specificity of the autoantibodies produced,

thus dictating the form of the resulting SSc. In addition, we demonstrate for the first time that specific oxidation of an autoantigen, in this case DNA topoisomerase 1, can participate in the pathogenesis of an autoimmune disease by not only inducing a breach in tolerance, but also by exerting a direct toxic effect ultimately responsible for the initiation and systemic propagation of the disease.

Acknowledgments

We are indebted to Dr. Andrew Wang for reviewing the manuscript and to Agnes Colle for typing the manuscript.

Disclosures

The authors have no financial conflict of interest.

References

- LeRoy, E. C., and T. A. J. Medsger. 2001. Criteria for the classification of early systemic sclerosis. *J. Rheumatol.* 28: 1573–1576.
- Herrick, A. L., and A. Worthington. 2002. Genetic epidemiology: systemic sclerosis. *Arthritis Res.* 4: 165–168.
- Gabrielli, A., S. Svegliati, G. Moroncini, M. Santillo, and E. Avvedimento. 2008. Oxidative stress and the pathogenesis of scleroderma: the Murrell's hypothesis revisited. *Semin. Immunopathol.* 30: 329–337.
- Simonini, G., M. Matucci Cerinic, S. Generini, M. Zoppi, M. Anichini, C. Cesaretti, A. Pignone, F. Falcnici, T. Lotti, and M. Cagnoni. 1999. Oxidative stress in Systemic Sclerosis. *Mol. Cell Biochem.* 196: 85–91.
- Herrick, A. L., and M. Matucci Cerinic. 2001. The emerging problem of oxidative stress and the role of antioxidants in systemic sclerosis. *Clin. Exp. Rheumatol.* 19: 4–8.
- Servettaz, A., P. Guelpain, C. Goulvestre, C. Chéreau, C. Hercend, C. Nicco, L. Guillemin, B. Weill, L. Mouthon, and F. Batteux. 2007. Radical oxygen species production induced by advanced oxidation protein products predicts clinical evolution and response to treatment in systemic sclerosis. *Ann. Rheum. Dis.* 66: 1202–1209.
- Sambo, P., S. S. Baroni, M. Luchetti, P. Paroncini, S. Dusi, G. Orlandini, and A. Gabrielli. 2001. Oxidative stress in scleroderma: maintenance of scleroderma fibroblast phenotype by the constitutive up-regulation of reactive oxygen species generation through the NADPH oxidase complex pathway. *Arthritis Rheum.* 44: 2653–2664.
- Ogawa, F., K. Shimizu, E. Muroi, T. Hara, M. Hasegawa, K. Takehara, and S. Sato. 2006. Serum levels of 8-isoprostane, a marker of oxidative stress, are elevated in patients with systemic sclerosis. *Rheumatology* 45: 815–818.
- Allanore, Y., D. Borderie, H. Lemarchal, O. G. Ekindjian, and A. Kahan. 2004. Acute and sustained effects of dihydropyridine-type calcium channel antagonists on oxidative stress in systemic sclerosis. *Am. J. Med.* 116: 595–600.
- Sambo, P., L. Janmino, M. Candela, A. Salvi, M. Donini, S. Dusi, M. M. Luchetti, and A. Gabrielli. 1999. Monocytes of patients with systemic sclerosis (scleroderma) spontaneously release in vitro increased amounts of superoxide anion. *J. Invest. Dermatol.* 112: 78–59.
- Baroni, S. S., M. Santillo, F. Bevilacqua, M. Luchetti, T. Spadoni, M. Mancini, P. Fraticelli, P. Sambo, A. Funaro, A. Kazlauskas, et al. 2006. Stimulatory autoantibodies to the PDGF receptor in systemic sclerosis. *N. Engl. J. Med.* 354: 2667–2676.
- Black, C., S. Pereira, A. McWhirter, K. Welsh, and R. Laurent. 1986. Genetic susceptibility to scleroderma-like syndrome in symptomatic and asymptomatic workers exposed to vinyl chloride. *J. Rheumatol.* 13: 1059–1062.
- Tamby, M. C., M. Humbert, P. Guelpain, A. Servettaz, N. Dupin, J. J. Christner, G. Simonneau, J. Fermanian, B. Weill, L. Guillemin, and L. Mouthon. 2006. Antibodies to fibroblasts in idiopathic and scleroderma-associated pulmonary hypertension. *Eur. Respir. J.* 28: 799–807.
- Masi, A. T., G. P. Rodnan, T. A. Medsger, R. D. Altman, W. A. D'Angelo, and J. F. Fries. 1980. Preliminary criteria for the classification of systemic sclerosis (scleroderma): Subcommittee for scleroderma criteria of the American Rheumatism Association Diagnostic and Therapeutic Criteria Committee. *Arthritis Rheum.* 23: 581–590.
- LeRoy, E. C., C. Black, R. Fleischmajer, S. Jablonska, T. Krieg, T. A. J. Medsger, N. Rowell, and F. Wollheim. 1988. Scleroderma (systemic sclerosis): classification, subsets and pathogenesis. *J. Rheumatol.* 15: 205–2025.
- Dalle-Donne, I., R. Rossi, D. Giustarini, N. Gagliano, L. Lusini, A. Milzani, P. Di Simplicio, and R. Colombo. 2001. Actin carbonylation: from a simple marker of protein oxidation to relevant signs of severe functional impairment. *Free Radic. Biol. Med.* 1: 1075–1083.
- Kuo, C. F., and I. Fridovic. 1986. Free-radical chain oxidation of 2-nitropropane initiated and propagated by superoxide. *Biochem. J.* 237: 505–510.
- Sakai, T., T. Ishizaki, T. Nakai, S. Miyabo, S. Matsukawa, M. Hayakawa, and T. Ozawa. 1996. Role of nitric oxide and superoxide anion in leukotoxin-9,10-epoxy-12-octadecenoate-induced mitochondrial dysfunction. *Free Radic. Biol. Med.* 20: 607–612.
- Beckman, J. S., T. W. Beckman, J. Chen, P. A. Marshall, and B. A. Freeman. 1990. Apparent hydroxyl radical production by peroxynitrite: Implications for endothelial injury from nitric oxide and superoxide. *Proc. Natl. Acad. Sci. USA* 87: 1620–1624.
- Hughes, M. N., and H. G. Nicklin. 1968. The chemistry of pernitrite: Part 1. Kinetics of decomposition of pernitrous acid. *J. Am. Chem. Soc.* 2: 450–452.
- Walling, C. 1982. The nature of the primary oxidants in oxidations mediated by metal ions. In *Oxidases and Related Redox Systems*. T. E. King, H. S. Mason, and M. Morrison, eds. Pergamon Press, Oxford, U.K., p. 85–97.
- Norisue, M., K. Todoki, and E. Okabe. 1997. Inhibition by hydroxyl radicals of calcitonin gene-related peptide-mediated neurogenic vasorelaxation in isolated canine lingual artery. *J. Pharmacol. Exp. Ther.* 280: 492–500.
- Burdick, M. D., L. A. Murray, M. P. Keane, Y. Y. Xue, D. A. Zisman, J. A. Belperio, and R. M. Strieter. 2005. CXCL11 attenuates bleomycin-induced pulmonary fibrosis via inhibition of vascular remodeling. *Am. J. Respir. Crit. Care Med.* 171: 261–268.
- Preud'homme, J. L., E. Rochard, D. Gouet, F. Danon, M. Alcalay, G. Touchard, and P. Autourtuer. 1988. Isotypic distribution of anti-double-stranded DNA antibodies: a diagnostic evaluation by enzyme-linked immunosorbent assay. *Diagn. Clin. Immunol.* 5: 256–261.
- Dignam, J. D., R. M. Lebowitz, and R. G. Roeder. 1983. Accurate transcription initiation by RNA polymerase II in a soluble extract from isolated mammalian nuclei. *Nucleic Acids Res.* 11: 1475–1489.
- Nobreza, A., M. Haury, A. Grandien, E. Malanchere, A. Sundblad, and A. Coutinho. 1993. Global analysis of antibody repertoires. II. Evidence for specificity, self-selection and the immunological "homunculus" of antibodies in normal serum. *Eur. J. Immunol.* 23: 2851–2859.
- Witko-Sarsat, V., M. Friedlander, C. Capeillere-Blandin, T. Nguyen-Khoa, A. T. Nguyen, J. Zingraff, P. Jungers, and B. Descamps-Latscha. 1996. Advanced oxidation protein products as a novel marker of oxidative stress in uremia. *Kidney Int.* 49: 1304–1313.
- Holden, J. A., D. H. Rolfsen, and R. H. Low. 1990. DNA topoisomerase I from placenta. *Biochim. Biophys. Acta* 1049: 303–310.
- Min, L. J., T. X. Cui, Y. Yahata, K. Yamasaki, T. Shiuchi, H. W. Liu, R. Chen, J. M. Li, M. Okumura, T. Jinno, et al. 2004. Regulation of collagen synthesis in mouse skin fibroblasts by distinct angiotensin II receptor subtypes. *Endocrinology* 145: 253–260.
- Casciola-Rosen, L., F. Wigley, and A. Rosen. 1997. Scleroderma autoantigens are uniquely fragmented by metal-catalyzed oxidation reactions: implications for pathogenesis. *J. Exp. Med.* 185: 71–79.
- Witko-Sarsat, V., M. Friedlander, T. Nguyen Khoa, C. Capeillere-Blandin, A. T. Nguyen, S. Canteloup, J. M. Dayer, P. Jungers, T. Drueke, and B. Descamps-Latscha. 1998. Advanced oxidation protein products as novel mediators of inflammation and monocyte activation in chronic renal failure. *J. Immunol.* 161: 2524–2532.
- Alderman, C. J., S. Shah, J. C. Foreman, B. M. Chain, and D. R. Katz. 2002. The role of advanced oxidation protein products in regulation of dendritic cell function. *Free Radic. Biol. Med.* 1: 377–385.
- Li, H. Y., F. F. Hou, X. Zhang, P. Y. Chen, S. X. Liu, J. X. Feng, Z. Q. Liu, Y. X. Shan, G. B. Wang, Z. M. Zhou, et al. 2007. Advanced oxidation protein products accelerate renal fibrosis in a remnant kidney model. *J. Am. Soc. Nephrol.* 18: 528–538.
- Ho, K. T., and J. D. Reveille. 2003. The clinical relevance of autoantibodies in scleroderma. *Arthritis Res. Ther.* 5: 80–93.
- Kahaleh, M. B., and E. C. LeRoy. 1999. Autoimmunity and vascular involvement in systemic sclerosis (SSc). *Autoimmunity* 31: 195–214.
- Chizzolini, C., Y. Parec, C. De Luca, A. Tyndall, A. Akesson, A. Scheja, and J. Dayer. 2003. Systemic sclerosis Th2 cells inhibit collagen production by dermal fibroblasts via membrane-associated-tumor necrosis factor α . *Arthritis Rheum.* 48: 2593–2604.
- Matsushita, T., M. Hasegawa, K. Yanaba, M. Kodera, K. Takehara, and S. Sato. 2005. Elevated serum BAFF levels in patients with systemic sclerosis: enhanced BAFF signaling in systemic sclerosis B lymphocytes. *Arthritis Rheum.* 54: 192–201.
- Luzina, I. G., S. P. Atamas, R. Wise, F. M. Wigley, J. Choi, H. Q. Xiao, and B. White. 2003. Occurrence of an activated, profibrotic pattern of gene expression in lung CD3 $^{+}$ T cells from scleroderma patients. *Arthritis Rheum.* 48: 2262–2274.
- Snider, G. L., J. A. Hayes, and A. L. Kothy. 1978. Chronic interstitial pulmonary fibrosis produced in hamsters by endotracheal bleomycin: pathology and stereology. *Am. Rev. Respir. Dis.* 117: 1099–1108.
- Yamamoto, T., S. Takagawa, I. Katayama, K. Yamazaki, Y. Hamazaki, H. Shinkai, and K. Nishioka. 1999. Animal model of sclerotic skin: local injections of bleomycin induce sclerotic skin mimicking scleroderma. *J. Invest. Dermatol.* 112: 456–462.
- Yoshizaki, A., Y. Iwata, K. Komura, F. Ogawa, T. Hara, E. Muroi, M. Takenaka, K. Shimizu, M. Hasegawa, M. Fujimoto, T. Tedder, and S. Sato. 2008. CD19 regulates skin and lung fibrosis via Toll-like receptor signaling in a model of bleomycin-induced scleroderma. *Am. J. Pathol.* 172: 1650–1663.
- Oi, M., T. Yamamoto, and K. Nishioka. 2004. Increased expression of TGF- β 1 in the sclerotic skin in bleomycin-susceptible mouse strains. *J. Med. Dent. Sci.* 51: 7–17.
- Cotton, S. A., A. L. Herrick, M. I. Jayson, and A. J. Freemont. 1998. TGF β : a role in systemic sclerosis? *J. Pathol.* 184: 4–6.
- Querfeld, C., B. Eckes, C. Huerkamp, T. Krieg, and S. Sollberg. 1999. Expression of TGF- β 1, - β 2 and - β 3 in localized and systemic scleroderma. *J. Dermatol. Sci.* 21: 13–22.
- Needleman, B. W., J. Choi, A. Burrows-Mezu, and J. A. Fontana. 1990. Secretion and binding of transforming growth factor β by scleroderma and normal dermal fibroblasts. *Arthritis Rheum.* 33: 650–656.

3.2 ARTICLE 2

L'inhibition de la voie ADAM-17/Notch bloque le développement de la Sclérodermie systémique chez la souris

Targeting ADAM-17/Notch signaling abrogates the development of systemic sclerosis in a murine model

*Niloufar Kavian, Amélie Servettaz, Céline Mongaret, Andrew Wang,
Carole Nicco, Christiane Chéreau, Philippe Grange, Vincent Vuiblet, Philippe
Birembaut, Marie-Danièle Diebold, Bernard Weill, Nicolas Dupin, Frédéric Batteux*

Arthritis and Rheumatism, 2010

Ce travail a été réalisé afin d'évaluer le rôle de Notch dans la physiopathologie de la ScS. Nous avons tout d'abord étudié l'expression de la forme active de Notch, Notch Intra Cellular Domain (NICD), dans différents tissus de souris sclérodermiques et témoins, et aussi chez des patients sclérodermiques et sujets sains. Les Western-BLOTS ont révélé de forts taux de Notch IC dans la peau, les poumons, et les splénocytes de souris développant une sclérodermie, et dans la peau des patients ScS.

Afin d'analyser l'effet de l'inhibition de Notch dans la sclérodermie, nous avons ensuite soumis des souris à notre protocole d'induction de la maladie (injections quotidiennes d'HOCl), et nous les avons traitées de façon concomitante avec un inhibiteur de Notch : le GSI (Gamma Secretase Inhibitor). Nous avons observé que le traitement par le GSI diminuait significativement l'accumulation de collagène dans la peau et les poumons induite par les injections intra-dermiques d'HOCl. Nous avons alors analysé l'effet du GSI sur les fibroblastes afin de déterminer le mécanisme de cette amélioration clinique de la fibrose. Les sérum de souris HOCl traitées par le GSI entraînent une moindre prolifération des fibroblastes NIH-3T3 que les sérum de souris HOCl non traitées. De même, les fibroblastes cutanés extraits des peaux de ces souris ont des taux de prolifération réduits par rapport aux souris HOCl non traitées. De plus, nous avons confirmé l'effet anti-prolifératif du GSI en traitant *in vitro* les fibroblastes NIH-3T3 et les fibroblastes cutanés extraits des peaux de souris HOCl.

Le traitement *in vivo* par le GSI a aussi eu un impact positif sur les propriétés pro-oxydatives des sérum de souris ScS que nous avions mises en évidence lors de la mise au point du modèle murin. En effet, les sérum de souris HOCl traitées par le GSI avaient une diminution des taux sériques d'AOPP, et induisaient une production d' H_2O_2 par les cellules endothéliales HUVEC réduite par rapport aux sérum de souris HOCl non traitées. Nous avons pu montrer que le GSI pouvait directement bloquer la production d' H_2O_2 des cellules endothéliales HUVEC de manière dose-dépendante.

Nous avons ensuite exploré l'effet du GSI sur l'activation du système immunitaire au cours de la ScS. Nous avons observé une diminution du nombre et de l'activation des cellules B spléniques chez les souris HOCl traitées par GSI, ainsi qu'une réduction des taux d'IgM totales et d'auto-anticorps anti-DNA Topoisomérase-1.

Enfin, dans une dernière série d'expériences, nous avons exploré la voie ADAM17 dans notre modèle murin de ScS et chez les patients. En effet, les protéines ADAM sont une famille de protéines transmembranaires et secrétées impliquées dans diverses voies de signalisation. ADAM17 peut déclencher la libération de l'ecto-domaine de Notch, étape nécessaire à son activation. Comme ADAM17 est impliquée dans l'activation de Notch, et que de récentes données ont montré qu'elle pouvait être induite par le stress oxydant, il semblait pertinent de l'étudier dans ce travail. Nous avons observé une augmentation de l'activité d'ADAM17 dans la peau des souris HOCl, corrélée avec l'augmentation de l'activation de Notch observée dans la première partie de ce travail. Chez les patients atteints de sclérodermie diffuse, nous avons aussi mis en évidence par western-blot et par immunofluorescence directe une forte expression d'ADAM17 corrélée avec l'augmentation de l'activation de Notch.

Grâce à ce protocole, nous avons pu mettre en évidence le rôle de Notch dans les processus fibrosants de la sclérodermie systémique chez l'animal, et aussi pour la première fois chez l'homme. Ce travail montre l'existence d'un lien entre stress oxydant, induction d'ADAM17 et activation de Notch, et nos données mettent en avant le rôle central de la voie Notch dans le développement de la sclérodermie, et son effet direct sur les fibroblastes, les cellules endothéliales et l'activation lymphocytaire B. L'inhibition de Notch par l'utilisation d'inhibiteurs de gamma-secrétase semble être efficace pour lutter contre le développement des anomalies clinico-biologiques de la ScS.

Nos résultats ont depuis été confirmés par d'autres équipes [226] [227].

Targeting ADAM-17/Notch Signaling Abrogates the Development of Systemic Sclerosis in a Murine Model

Niloufar Kavian,¹ Amélie Servettaz,² Céline Mongaret,¹ Andrew Wang,³ Carole Nicco,¹ Christiane Chéreau,¹ Philippe Grange,¹ Vincent Vuiblet,⁴ Philippe Birembaut,⁴ Marie-Danièle Diebold,⁵ Bernard Weill,¹ Nicolas Dupin,¹ and Frédéric Batteux¹

Objective. Systemic sclerosis (SSc) is characterized by the fibrosis of various organs, vascular hyperreactivity, and immunologic dysregulation. Since Notch signaling is known to affect fibroblast homeostasis, angiogenesis, and lymphocyte development, we undertook this study to investigate the role of the Notch pathway in human and murine SSc.

Methods. SSc was induced in BALB/c mice by subcutaneous injections of HOCl every day for 6 weeks. Notch activation was analyzed in tissues from mice with SSc and from patients with scleroderma. Mice with SSc were either treated or not treated with the γ -secretase inhibitor DAPT, a specific inhibitor of the Notch pathway, and the severity of the disease was evaluated.

Results. As previously described, mice exposed to HOCl developed a diffuse cutaneous SSc with pulmonary fibrosis and anti-DNA topoisomerase I antibodies. The Notch pathway was hyperactivated in the skin, lung, fibroblasts, and splenocytes of diseased mice and in skin biopsy samples from patients with scleroderma. ADAM-17, a proteinase involved in Notch activation, was over-

expressed in the skin of mice and patients in response to the local production of reactive oxygen species. In HOCl-injected mice, DAPT significantly reduced the development of skin and lung fibrosis, decreased skin fibroblast proliferation and ex vivo serum-induced endothelial H₂O₂ production, and abrogated the production of anti-DNA topoisomerase I antibodies.

Conclusion. Our results show the pivotal role of the ADAM-17/Notch pathway in SSc following activation by reactive oxygen species. The inhibition of this pathway may represent a new treatment of this life-threatening disease.

In mammals, the Notch family consists of 4 transmembrane receptors (Notch-1 through Notch-4) and 5 ligands (Jagged1, Jagged2, Delta1, Delta3, and Delta4) (1,2). The binding of the ligand to its cognate receptor initiates metalloproteinase-mediated and γ -secretase-mediated proteolysis of the receptor. The Notch intracellular domain (NICD) is then cleaved from the plasma membrane and translocates into the nucleus where it associates with transcription factors RBP-Jn/CSL and mastermind-like-1 to form a heteromeric complex. Notch signaling, initially known to be critical for organism development, has recently been implicated in the regulation of tissue homeostasis in adults (3).

Systemic sclerosis (SSc) is a connective tissue disorder characterized by vascular hyperreactivity, fibrosis of skin and visceral organs, and immunologic dysregulation associated with autoantibodies (4). To date, the mechanisms that determine the clinical manifestations remain unclear (5–7). Although it is not known whether Notch plays a role in SSc, Notch signaling has been reported to affect the behavior of endothelial cells (angiogenesis) (8) and fibroblasts (9,10), 2 cell types that play important roles in SSc. In addition, Notch participates in humoral and cellular immune responses that are both dysregulated in SSc. Those observations have

Dr. Kavian's work was supported by a grant from the Fondation pour la Recherche Médicale. Dr. Servettaz's work was supported by grants from Actelion and the Association des Sclérodermiques de France.

¹Niloufar Kavian, MD, Céline Mongaret, MD, Carole Nicco, PhD, Christiane Chéreau, PharmD, Philippe Grange, PhD, Bernard Weill, MD, PhD, Nicolas Dupin, MD, PhD, Frédéric Batteux, MD, PhD: Université Paris Descartes and Hôpital Cochin, Assistance Publique Hôpitaux de Paris, Paris, France; ²Amélie Servettaz, MD, PhD: Université Paris Descartes and Hôpital Cochin, Assistance Publique Hôpitaux de Paris, Paris and Hôpital Robert Debré, Reims, France; ³Andrew Wang, PhD: University of Texas Southwestern Medical Center, Dallas; ⁴Vincent Vuiblet, MD, Philippe Birembaut, MD: INSERM UMR-S 903, IFR 53, Centre Hospitalier Universitaire de Reims, Reims, France; ⁵Marie-Danièle Diebold, MD: Centre Hospitalier Universitaire de Reims, Reims, France.

Drs. Kavian and Servettaz contributed equally to this work.

Address correspondence and reprint requests to Frédéric Batteux, MD, PhD, Laboratoire d'Immunologie, Faculté de Médecine Paris Descartes, 27 Rue du Faubourg St. Jacques, 75679 Paris Cedex 14, France. E-mail: frederic.batteux@cch.aphp.fr.

Submitted for publication April 28, 2009; accepted in revised form June 17, 2010.

prompted us to investigate the role of the Notch pathway in a recently designed animal model of SSc that recapitulates the main features of the diffuse cutaneous form of the human disease (11), as well as in human patients with either diffuse or localized SSc.

Our results show that Notch signaling is activated in humans and mice with SSc. In mice with experimental SSc, the inhibition of Notch signaling by the γ -secretase inhibitor DAPT (N-S-phenyl-glycine-t-butyl ester) limits both fibrosis and autoimmune activation. These findings suggest that the Notch pathway could be a novel therapeutic target for the treatment of SSc.

MATERIALS AND METHODS

Animals, cells, and chemicals. Six-week-old female BALB/c mice were purchased from Harlan. Human umbilical vein endothelial cells were obtained by digestion of umbilical cords as described in a previous report on endothelial cells (12) and according to the method described by Jaffe et al (13) (further information is available at <https://sites.google.com/site/notchssc/>). NIH3T3 fibroblasts were obtained from American Type Culture Collection. All cells were cultured as previously reported (14,15). All chemicals were from Sigma, except for anti-Cleaved Notch1 (Val 1744) Antibody (Cell Signaling Technology), horseradish peroxidase (HRP)-conjugated anti-IgG antibody (Santa Cruz Biotechnology), ECL reagent (Amersham), and fluorogenic peptide substrate III and anti-human ADAM-17 antibody (R&D Systems).

Experimental procedure. Induction of SSc by subcutaneous injections. Mice were randomly distributed into experimental and control groups ($n = 14$ per group). One hundred microliters of substances generating HOCl were injected subcutaneously into the back of the mice every day for 6 weeks, as previously described (11). Control groups received injections of 100 μ l sterilized phosphate buffered saline (PBS).

DAPT or vehicle treatment. Each mouse receiving subcutaneous injections was randomized to treatment with DAPT (Sigma) or vehicle control by gavage for 6 weeks. DAPT was given 5 days a week at a dose of 5 mg/kg per day in corn oil.

Two weeks after the end of injections and treatment, the animals were killed by cervical dislocation. Lungs were collected and skin biopsies were performed on the back region with a 6-mm diameter punch. Samples were stored at -80°C for determination of collagen content or fixed in 10% formalin for histopathologic analysis.

Western blot analysis of activated Notch proteins in the skin, lungs, fibroblasts, splenocytes, and splenic B cells from mice and in the skin of SSc patients. Skin, lung, and spleen cell suspensions were mixed in radioimmunoprecipitation assay lysis buffer. Fibroblasts were isolated from skin biopsy samples taken in diseased areas of mice as described below. B cells were isolated from splenocytes by magnetic cell sorting using the B cell isolation kit (Miltenyi Biotec) according to the manufacturer's recommendations. For human samples, diseased skin was obtained from 3 patients with localized scleroderma (morphoea) and from 4 patients with diffuse cutaneous SSc. Five normal skin samples served as controls.

Proteins (30 μ g per well) were subjected to 15% poly-

acrylamide gel electrophoresis, transferred onto nitrocellulose membranes, blocked with 5% nonfat dry milk in Tris buffered saline-Tween, then incubated overnight at 4°C with anti-Cleaved Notch1 (Val 1744) Antibody. The membranes were then washed and incubated with an HRP-conjugated secondary antibody for 1 hour at room temperature. Immunoreactivities were revealed with ECL reagent. Optical densities were measured using Multi-gauge Software (Fujifilm).

Immunofluorescence analysis of skin sections from SSc patients and controls. Diseased skin was obtained from 4 patients with early diffuse cutaneous SSc (different from the patients whose skin had been used for Western blotting). Four patients without SSc served as controls. Formalin-fixed paraffin-embedded skin sections were dewaxed, and an enzymatic (Notch staining) or heat-mediated (ADAM-17 staining) antigen retrieval technique was used to overcome antigen masking. Slides were washed with sodium borohydride (NaBH_4) to avoid spontaneous autofluorescence and then blocked with mouse serum for 1 hour at room temperature. Slides were stained with 1:200 anti-Cleaved Notch1 (Val 1744) Antibody or anti-ADAM-17 antibody or isotype control antibody overnight at 4°C. A secondary fluorescein isothiocyanate-labeled antibody was then applied on the slides, and after washing in PBS, slides were observed with an Olympus microscope equipped with an epifluorescence system, and pictures were taken at 400 \times magnification with a digital camera. Immunostaining of skin sections was analyzed using ImageJ 1.36 b software (National Institutes of Health; <http://rsb.info.nih.gov/ij>) for a quantitative assessment of fluorescence intensity as described by Noursadeghi et al (16).

Dermal thickness assessment and histopathologic analysis. One day before mice were killed, skin thickness of the shaved back of mice was measured with a caliper and expressed in millimeters. A 5 μm -thick tissue section was prepared from the midportion of paraffin-embedded lung and skin pieces and stained with hematoxylin and eosin. Slides were examined using standard brightfield microscopy (Olympus BX60) by a pathologist who was blinded to the animal's group assignment. Pictures were taken using the Olympus DP70 Controller Software.

Collagen content in skin and lung. Skin and lung pieces were diced using a sharp scalpel, then mixed with pepsin (1:10 weight ratio) and 0.5M acetic acid overnight at room temperature under stirring. Collagen content assay was based on the quantitative dye-binding Sircol method (Biocolor) (17). Hydroxyproline content was measured as recommended by Woessner (18).

Fibroblast assays. NIH3T3 fibroblasts (4×10^3 per well) were incubated in 96-well plates (Costar) with 20 μ l of mouse serum and 180 μ l of culture medium without fetal calf serum at 37°C for 48 hours. Cell proliferation was determined by pulsing the cells with ^3H -thymidine (1 $\mu\text{Ci}/\text{well}$) during the last 16 hours of culture. Results were expressed as absolute numbers of counts per minute.

Skin samples were digested with "Liver Digest Medium" (Invitrogen) for 1 hour at 37°C. After 3 washes in complete medium, skin fibroblasts were cultured in Dulbecco's modified Eagle's medium/GlutaMAX-I (Invitrogen) supplemented with 10% heat-inactivated fetal calf serum and antibiotics at 37°C. Primary fibroblasts (2×10^3 per well) were seeded in 96-well plates and incubated with 150 μ l of culture medium for 48 hours. Cell proliferation was determined as described above.

Analysis of α -smooth muscle actin (α -SMA) expression and production of H_2O_2 . The expression of α -SMA in mouse skin was analyzed using Western blotting as described above with an anti-mouse α -SMA antibody (clone 1A4; Sigma). Endothelial cells (8×10^3 per well) were incubated in 96-well plates with medium alone for 12 hours at 37°C. Culture media were removed after 12 hours, and cells were preincubated with 50 μ l 2',7'-dichlorodihydrofluorescein diacetate diluted 1:1,000 in PBS to test cellular H_2O_2 production. After 30 minutes, 50 μ l of mouse serum was added, and H_2O_2 production was monitored spectrofluorimetrically for 6 hours (Fusion; PerkinElmer). Results were expressed in arbitrary units (AU) per minute and per million cells.

Assessment of the effects of various concentrations of DAPT on H_2O_2 production by endothelial cells and on NIH3T3 fibroblast proliferation in vitro. Endothelial cells (2×10^4 per well) were incubated in 96-well plates with medium alone or with 10, 20, or 40 μ M DAPT for 12 hours at 37°C. Cellular H_2O_2 production was performed as described above. NIH3T3 fibroblasts (4×10^3 per well) were incubated in 96-well plates with 50 μ l of 10, 20, or 40 μ M DAPT and 50 μ l of culture medium supplemented with 1% fetal calf serum at 37°C for 48 hours. Cell proliferation was determined as previously described.

Assessment of the effects of DAPT on the production of type I collagen messenger RNA by human fibroblasts in vitro. Human primary fibroblasts were seeded in 6-well plates and incubated with complete medium either with 40 μ M of DAPT or with 100 μ M of DAPT for 24 hours. Type I collagen and 28S ribosomal RNA complementary DNA (cDNA) were quantified by real-time polymerase chain reaction (PCR) on a Light-Cycler using the LightCycler-FastStart DNA Master SYBR Green I kit (Roche Diagnostics).

Determination of advanced oxidation protein product concentrations in sera. Advanced oxidation protein products were measured by spectrophotometry as previously described (19).

In vitro modulation of the expression of activated Notch protein by N-acetylcysteine (NAC) and H_2O_2 treatments. Fibroblasts isolated from skin biopsy samples from diseased mice were cultured in complete medium alone for 24 hours or with 5 mM of NAC added for 24 hours. Western blots of activated cleaved Notch-1 protein were performed as previously described. Primary human fibroblasts were cultured in 6-well plates and incubated with 100 μ M H_2O_2 in complete medium for 24 hours. Western blots of activated cleaved Notch-1 protein were performed as previously described.

Detection of serum antibodies. Anti-DNA topoisomerase I IgG antibodies were detected using coated enzyme-linked immunosorbent assay (ELISA) microplates (Immunovision). Levels of total mouse IgG and IgM antibodies, anti-double-stranded DNA (anti-dsDNA) IgG antibodies, anticardiolipin IgG antibodies, and IgM rheumatoid factors were measured using standard ELISAs as previously described (20). A 1:50 serum dilution was used for the determination of all autoantibodies.

Metalloproteinase activity of ADAM-17 protein in mouse skin extracts and Western blot analysis of ADAM-17 in skin biopsy samples from patients. Skin extracts were prepared as previously described. Fluorogenic peptide substrate III (25 μ l) was directly added to 25 μ l of skin extracts for 1 hour at 37°C. Fluorescence was recorded after 60 minutes on a spectrofluorimeter (Fusion; Packard) at 320 nm and 405 nm

as excitation and emission wavelengths, respectively. Diseased skin was obtained from 3 patients with localized scleroderma and from 4 patients with diffuse cutaneous SSc. Five normal skin samples served as controls. Skin extracts were prepared as described for Western blot analysis of Notch. Membranes were incubated with an anti-human ADAM-17 antibody.

Analysis of Notch ligand and Notch member expression in mouse skin fibroblasts using real-time PCR. RNA was extracted with TRIzol reagent (Invitrogen) from skin fibroblasts isolated from 5 PBS-treated mice and 5 HOCl-treated mice. Notch ligand and Notch family member cDNA were quantified using real-time PCR (further information is available at <https://sites.google.com/site/notchssc/>).

Statistical analysis. All quantitative data are expressed as the mean \pm SEM. Data were compared using the Mann-Whitney nonparametric test or Student's paired *t*-test. When analysis included more than 2 groups, one-way analysis of variance was used. *P* values less than 0.05 were considered significant.

RESULTS

Notch is hyperactivated in skin, lungs, and fibroblasts and in splenic B cells of mice with HOCl-induced SSc, and this activation is abrogated in the skin by the γ -secretase inhibitor. First, we compared the activation of Notch signaling in tissues from mice with HOCl-induced SSc and in tissues from control animals. The activation of the Notch receptor is followed by 2 subsequent cleavages of the activated receptor. High amounts of the cleaved form of Notch-1 (NICD) were found in the skin from mice with HOCl-induced SSc compared with the skin from control mice (mean \pm SEM 14.16 \pm 1.64 AU versus 4.43 \pm 2.17 AU; *P* < 0.001). High amounts of NICD were also found in lungs and spleen cells as well as in purified skin fibroblasts and splenic B cells from diseased mice (Figure 1A). In vivo treatment of mice with the γ -secretase inhibitor DAPT downregulated Notch-1 activation (Figure 1B).

Notch is activated in the skin of patients with localized scleroderma or diffuse cutaneous SSc. We next investigated whether the activation of the Notch pathway observed in our mouse model of SSc was relevant to the human disease. As observed in mice, high amounts of activated forms of Notch-1 were found by Western blot analysis in the skin of patients with diffuse cutaneous SSc ($n = 4$) or with localized scleroderma ($n = 3$) as compared with normal skin ($n = 5$) (Figure 1C). Quantitative determination of NICD showed a significant increase in NICD proteins in the skin biopsy samples from patients with diffuse cutaneous SSc (mean \pm SEM 0.75 \pm 0.07 AU) (*P* = 0.008 versus controls) and from patients with localized scleroderma (mean \pm SEM 0.68 \pm 0.08 AU) (*P* = 0.047 versus controls). The difference between diffuse cutaneous SSc and localized

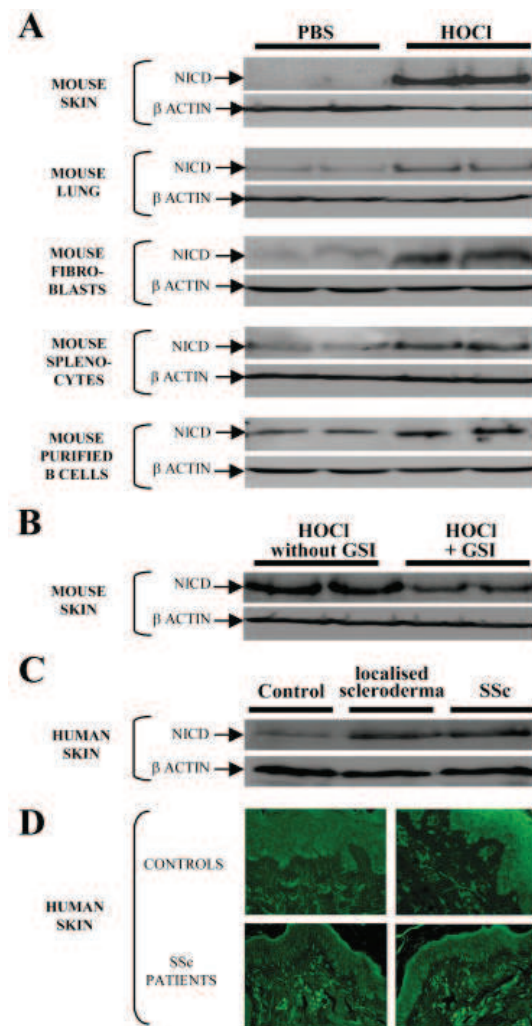


Figure 1. Activation of Notch pathway in the skin, lung, and splenocytes of mice developing HOCl-induced systemic sclerosis (SSc) and in the skin of patients with localized or diffuse cutaneous SSc. This activation is down-regulated by treatment with γ -secretase inhibitor (GSI). Notch intracellular domain (NICD) was determined by Western blotting in protein extracts from mice exposed to HOCl or phosphate buffered saline (PBS) with or without γ -secretase inhibitor treatment ($n = 7$ per group) as well as in protein extracts from human skin (7 SSc patients and 5 controls). **A**, Immunoblot of NICD in skin, lung, skin fibroblast, splenocyte, and purified B cell extracts from HOCl- or PBS-injected mice (2 mice per group, representative of 7). **B**, Determination of NICD by Western blotting in the skin of HOCl-injected mice with or without γ -secretase inhibitor treatment (2 mice per group, representative of 7). **C**, Representative immunoblots of NICD in skin extracts from 1 patient with localized scleroderma, 1 patient with diffuse cutaneous SSc, and 1 control patient. The internal control was β -actin. **D**, Representative immunohistochemistry of skin sections obtained from 2 controls and 2 patients with SSc. Slides were stained with anti-NICD antibodies (original magnification $\times 400$).

scleroderma was not significant ($P = 0.28$). In addition, high amounts of NICD were also detected by immunohistochemistry in skin sections obtained from 4 other

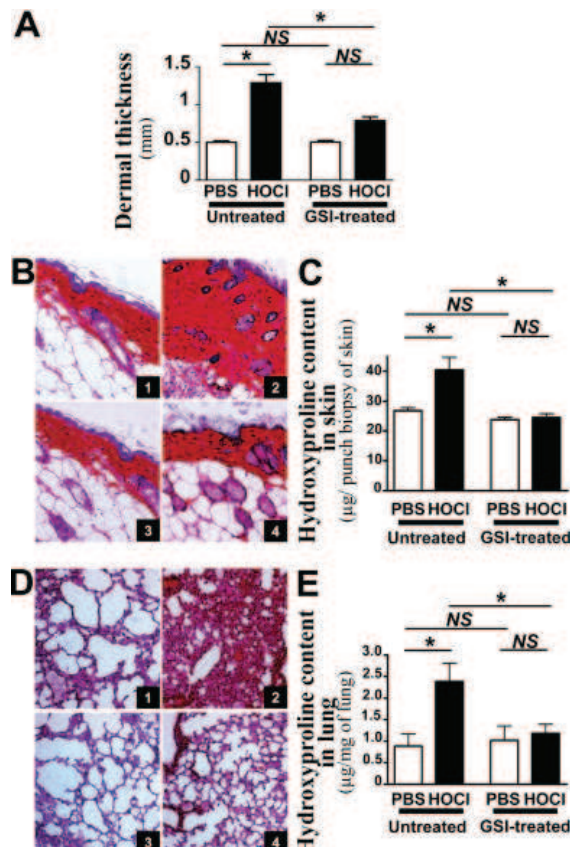


Figure 2. Effect of γ -secretase inhibitor on skin and lung collagen contents after subcutaneous injections of HOCl-generating agents or PBS in BALB/c mice. BALB/c mice were injected daily for 6 weeks with either HOCl-generating agents or PBS ($n = 7$ per group) and simultaneously treated with γ -secretase inhibitor or vehicle control by gavage. Skin and lungs were collected at the time the mice were killed. **A**, Dermal thickness, as measured on skin sections in the injected areas of BALB/c mice. **B**, Representative skin sections taken from the injected areas in BALB/c mice. Fibrosis in HOCl-injected mice is abrogated by treatment with γ -secretase inhibitor. Skin sections were treated with 1, PBS; 2, HOCl; 3, PBS and γ -secretase inhibitor; 4, HOCl and γ -secretase inhibitor. Tissue sections were stained with hematoxylin and eosin (original magnification $\times 20$). **C**, Hydroxyproline content in 6-mm punch biopsy sample of skin. **D**, Representative lung sections from BALB/c mice. Lung sections were treated with 1, PBS; 2, HOCl; 3, PBS and γ -secretase inhibitor; 4, HOCl and γ -secretase inhibitor. Tissue sections were stained with hematoxylin and eosin (original magnification $\times 10$). **E**, Hydroxyproline content in lung. Values in **A**, **C**, and **E** are the mean and SEM from all mice in the experimental or control group. * = $P < 0.05$ by Mann-Whitney unpaired U test. NS = not significant (see Figure 1 for other definitions).

patients with SSc as compared with skin sections from 4 normal controls (mean \pm SEM mean fluorescence intensity 7.7 ± 1.77 AU versus 4.04 ± 1.98 AU; $P = 0.03$) (Figure 1D).

Notch inhibition decreases both skin and lung fibrosis in mice with SSc. Subcutaneous injections of HOCl induced significant dermal thickness in mice compared with PBS injections ($P = 0.002$) (Figure 2A). Histopathologic analysis revealed dermal fibrosis (Figure 2B). The concentration of collagen evaluated through the concentration of hydroxyproline and by the Sircol method in the skin extracts of HOCl-injected mice was higher than in PBS-injected mice ($P = 0.004$) (Figure 2C) (further information is available at <https://sites.google.com/site/notchssc/>). Notch inhibition by the γ -secretase inhibitor reduced the dermal thickness and the accumulation of collagen induced by HOCl in the skin ($P = 0.005$ for dermal thickness and $P = 0.001$ for hydroxyproline concentration in the skin, versus untreated mice) (Figures 2A and C) (further information is available at <https://sites.google.com/site/notchssc/>). These results were confirmed by histopathologic analysis of skin, which showed a decrease in dermal thickness in HOCl-injected BALB/c mice that were simultaneously treated with γ -secretase inhibitor (Figure 2B).

In addition to skin fibrosis, HOCl-treated BALB/c mice developed lung fibrosis, as shown by histopathologic analysis (Figure 2D) and by the concentration of collagen in the lungs of these mice, which was higher than that in mice treated with PBS ($P = 0.017$) (Figure 2E) (further information is available at <https://sites.google.com/site/notchssc/>). Treatment with γ -secretase inhibitor reduced the concentration of collagen in lungs of HOCl-exposed mice compared with HOCl-exposed mice treated with vehicle alone ($P = 0.018$) (Figures 2D and E) (further information is available at <https://sites.google.com/site/notchssc/>). Evaluation of the antifibrotic role of γ -secretase inhibitor in the model of systemic fibrosis induced by subcutaneous injections of bleomycin confirmed the results gained in the HOCl model (further information is available at <https://sites.google.com/site/notchssc/>).

Notch inhibition reduces the proproliferative effect exerted by the sera from HOCl-injected mice ex vivo, normalizes the rate of dermal fibroblast proliferation, decreases type I collagen production, and decreases α -SMA expression in the skin of mice with HOCl-induced SSc. Sera from mice exposed to HOCl exerted a proproliferative effect on NIH3T3 fibroblasts in vitro compared with sera from PBS-injected mice ($P = 0.032$) (Figure 3A). Treatment with γ -secretase inhibitor abolished the proproliferative effect exerted by

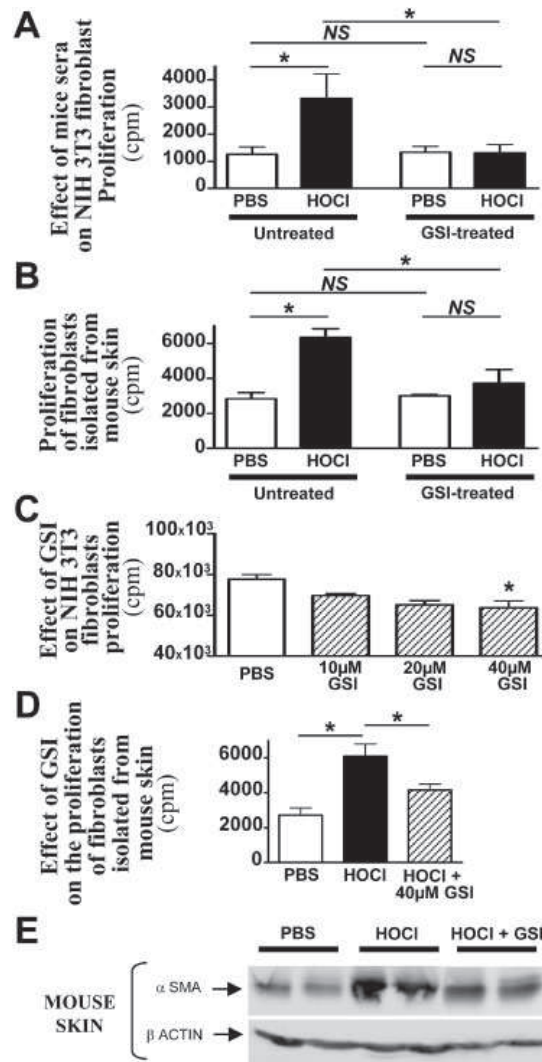


Figure 3. Effect of γ -secretase inhibitor on fibroblast proliferation and on α -smooth muscle actin (α -SMA) expression in mouse skin. **A**, Effect of mouse sera on NIH3T3 fibroblast proliferation in vitro. Sera were incubated with NIH3T3 fibroblasts for 48 hours ($n = 7$ per group). **B**, Spontaneous proliferation of fibroblasts isolated from the skin of mice. **C**, Effect of γ -secretase inhibitor on NIH3T3 fibroblast proliferation in vitro. NIH3T3 fibroblasts were incubated with γ -secretase inhibitor or PBS for 48 hours. **D**, Effect of γ -secretase inhibitor on the proliferation of fibroblasts isolated from the skin of PBS- or HOCl-treated mice in the areas of injections. Fibroblasts were incubated with γ -secretase inhibitor or PBS for 48 hours. Results are expressed as absolute cpm. **E**, Increased expression of α -SMA in protein extracts from mouse skin after exposure to HOCl, as determined on Western blot. This expression is down-regulated by treatment with γ -secretase inhibitor. Values in **A–D** are the mean and SEM. * = $P < 0.05$ (versus PBS in **C**) by Mann-Whitney unpaired U test. NS = not significant (see Figure 1 for other definitions).

the sera of HOCl-injected mice compared with sera from PBS-injected mice ($P = 0.798$) (Figure 3A).

We next investigated whether γ -secretase inhibitor administered to mice modified the growth of fibroblasts isolated from fibrotic skin areas injected with HOCl. Skin fibroblasts isolated from HOCl-injected mice not treated with γ -secretase inhibitor displayed a higher proliferation rate than fibroblasts obtained from mice injected with PBS ($P < 0.0001$) (Figure 3B). Treatment with γ -secretase inhibitor significantly decreased the proliferation rate of fibroblasts isolated from HOCl-injected mice ($P = 0.026$ versus HOCl-injected mice not treated with γ -secretase inhibitor) (Figure 3B). Additional experiments were performed to assess whether γ -secretase inhibitor by itself can influence the rate of fibroblast proliferation in vitro. Consistent with a direct role of γ -secretase inhibitor, we observed that γ -secretase inhibitor reduced the proliferation rate of NIH3T3 fibroblasts in vitro in a dose-dependent manner (Figure 3C). Fibroblasts isolated from fibrotic skin of HOCl-treated mice and incubated with 40 μM γ -secretase inhibitor displayed a lower proliferation rate than the same fibroblasts incubated without γ -secretase inhibitor ($P = 0.032$) (Figure 3D). In addition, Notch pathway inhibition by either 40 or 100 μM γ -secretase inhibitor significantly abrogated the production of type I collagen by normal human fibroblasts, as compared with fibroblasts exposed to medium alone ($P < 0.05$ and $P < 0.01$, respectively, for 40 or 100 μM γ -secretase inhibitor) (further information is available at <https://sites.google.com/site/notchssc/>).

Since α -SMA is overexpressed in SSc fibroblasts in both human and animal models (21,22), we investigated whether a modulation of the Notch pathway could have consequences for α -SMA expression in our SSc model. We found that α -SMA was overexpressed in the skin and in the fibroblasts from mice with HOCl-induced fibrosis (Figure 3E and data not shown). The in vivo treatment of mice with γ -secretase inhibitor downregulated the expression of α -SMA in fibrotic skin.

Notch inhibition reduces serum concentrations of advanced oxidation protein products, decreases endothelial H₂O₂ production induced by sera from mice exposed to HOCl, and directly reduces the production of H₂O₂ by endothelial cells in vitro. The sera from mice injected with HOCl contained higher amounts of advanced oxidation protein products than the sera from mice treated with PBS ($P = 0.009$) (Figure 4A). Treatment with γ -secretase inhibitor reduced the concentration of advanced oxidation protein products in the sera of mice exposed to HOCl ($P = 0.01$) (Figure 4A). The sera of mice exposed to HOCl induced a higher produc-

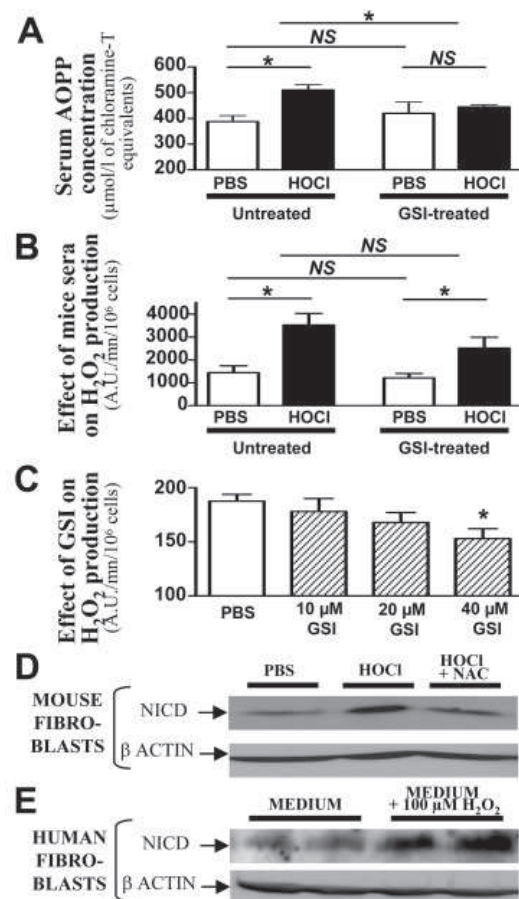


Figure 4. Effect of γ -secretase inhibitor on advanced oxidation protein product (AOPP) concentrations and H₂O₂ production by endothelial cells. BALB/c mice were injected daily for 6 weeks with either HOCl-generating agents or PBS ($n = 7$ per group) and simultaneously treated with γ -secretase inhibitor or vehicle. Sera were collected at the time the mice were killed. **A**, Concentrations of advanced oxidation protein products. **B**, Effect of mouse sera on H₂O₂ production by endothelial cells. Endothelial cells were incubated with 50 μ l of mouse sera. H₂O₂ production was monitored spectrophotometrically for 6 hours. Results are expressed in arbitrary units (AU) per minute (mn) and per million cells. **C**, Effect of γ -secretase inhibitor on H₂O₂ production by endothelial cells. Endothelial cells were incubated with γ -secretase inhibitor or PBS. H₂O₂ production was monitored spectrophotometrically for 6 hours. **D**, Down-regulated overexpression of Notch (represented by NICD) by SSc mouse skin fibroblasts exposed to *N*-acetylcysteine (NAC) in vitro. Fibroblasts were isolated from skin biopsy samples from mice treated with HOCl or PBS. Fibroblasts were cultured in complete medium alone for 24 hours or with 5 mM of NAC added for 24 hours, and Western blots of NICD were performed. **E**, Activation of Notch on normal human fibroblasts by exogenous addition of H₂O₂. Values in A–C are the mean and SEM. * = $P < 0.05$ (versus PBS in C) by Mann-Whitney unpaired U test. NS = not significant (see Figure 1 for other definitions).

Table 1. Effects of Notch inhibition on spleen cell count and on serum IgM, IgG, and autoantibody levels*

	Spleen cells, × 10 ⁶	Serum IgM concentration, mg/ml	Serum IgG concentration, mg/ml	Anti-DNA		Anticardiolipin IgG antibodies, AU	IgM rheumatoid factor, AU
				topoisomerase I IgG antibodies, AU	Anti-dsDNA IgG antibodies, AU		
Untreated mice							
PBS-injected	70.18	0.93	3.08	0.39 ± 0.02	0.32 ± 0.01	0.01 ± 0.01	0.28 ± 0.05
HOCl-injected	87.54	1.69	3.47	1.18 ± 0.75	0.33 ± 0.01	0.0 ± 0.07	0.37 ± 0.31
<i>P</i> , PBS-injected vs. HOCl-injected	0.016	0.005	0.788	0.003	0.792	0.343	0.792
Mice treated with γ-secretase inhibitor							
PBS-injected	74.18	1.15	2.72	0.54 ± 0.12	0.30 ± 0.01	0.06 ± 0.06	0.20 ± 0.05
HOCl-injected	90.92	1.19	3.03	0.65 ± 0.24	0.28 ± 0.03	0.02 ± 0.01	0.031 ± 0.13
<i>P</i> , PBS-injected vs. HOCl-injected	0.026	0.534	0.383	0.535	0.259	0.535	0.073

* Values are the mean or mean ± SEM. AU = arbitrary units; anti-dsDNA = anti-double-stranded DNA; PBS = phosphate buffered saline.

tion of H₂O₂ by endothelial cells than the sera of mice treated with PBS ($P = 0.002$) (Figure 4B). The inhibition of Notch by γ-secretase inhibitor tended to decrease the effect of mouse sera on H₂O₂ production by endothelial cells, but the decrease was not statistically significant ($P = 0.23$) (Figure 4B).

We next investigated whether γ-secretase inhibitor could by itself modify the production of H₂O₂ by endothelial cells. Adding increasing amounts of γ-secretase inhibitor to endothelial cells incubated with sera from HOCl-treated mice dose dependently reduced the levels of H₂O₂ released by endothelial cells (Figure 4C).

In vitro treatment with NAC decreases Notch activation in skin fibroblasts from mice with HOCl-induced SSc, while exogenous H₂O₂ activates Notch in normal fibroblasts. NAC, an antioxidant molecule, was used to assess the link between oxidative stress and the activation of Notch. SSc mouse skin fibroblasts exposed to NAC in vitro down-regulated Notch cleavage (Figure 4D). In contrast, addition of exogenous H₂O₂ to normal human fibroblasts favored Notch cleavage (Figure 4E).

Notch inhibition decreases the autoimmune response induced by HOCl. Subcutaneous injections of HOCl increased the total numbers of splenocytes as compared with PBS injection ($P = 0.016$) (Table 1). We then assayed the total serum IgM and IgG antibody concentrations in control and HOCl-treated mice. Mice exposed to HOCl displayed higher serum IgM antibody levels than PBS-exposed mice ($P = 0.005$) (Table 1). Treatment with γ-secretase inhibitor reduced serum IgM antibody concentrations in those mice ($P = 0.026$). No significant differences were observed in total serum IgG antibody concentrations between HOCl- and PBS-injected mice treated or not with γ-secretase inhibitor (Table 1). We next tested the effects of Notch inhibition

on the specific autoimmune response that characterized the SSc phenotype. Mice exposed to HOCl developed anti-DNA topoisomerase I IgG antibodies ($P = 0.003$ versus mice exposed to PBS) (Table 1). In contrast, no significant differences in levels of anti-dsDNA IgG antibodies, anticardiolipin IgG antibodies, or IgM rheumatoid factors were detected in the sera of these mice regardless of the product injected (Table 1). Mice treated with γ-secretase inhibitor did not develop significantly more anti-DNA topoisomerase I IgG antibodies following exposure to HOCl compared with untreated control mice ($P = 0.535$) (Table 1).

The ADAM-17 proteinase that activates Notch signaling is up-regulated in the skin from mice and patients with SSc. The initiation of Notch signaling requires the cleavage of Notch by proteinases of the ADAM family, particularly ADAM-17. Thus, we analyzed ADAM-17 activity and expression in the skin from mice and patients with scleroderma. The activity of this metalloproteinase was higher in the skin of mice with HOCl-induced SSc than in that of PBS-injected control mice ($P = 0.004$) (Figure 5A). Immunoblotting and immunohistochemistry experiments were performed on extracts of skin obtained from 9 control patients and from diseased areas in 8 patients with diffuse cutaneous SSc and from the 3 patients with localized scleroderma. ADAM-17 expression was higher in the skin obtained from the 8 patients with diffuse cutaneous SSc and from the 3 patients with localized scleroderma than in the skin obtained from the 9 control patients (by immunohistochemistry, mean ± SEM mean fluorescence intensity 3.77 ± 0.18 AU versus 1.61 ± 0.03 AU; $P = 0.006$) (Figures 5B and C). In contrast, no significant difference in the expression of the Notch ligands (Jagged1, Jagged2, Delta1, Delta3, and Delta4) and of the differ-

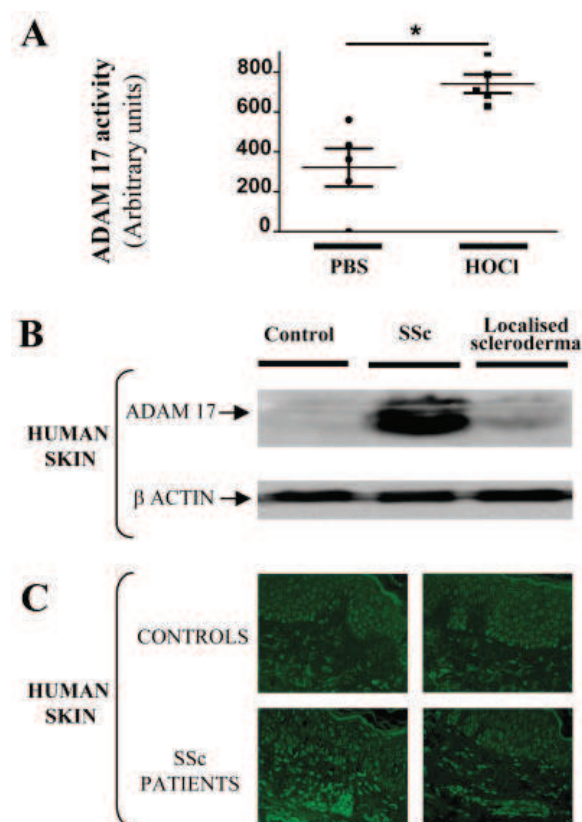


Figure 5. ADAM-17 is activated in the skin of mice developing HOCl-induced SSc and is found in high amounts in the skin of patients with SSc. **A**, Determination of the metalloproteinase activity of ADAM-17 in skin extracts from the back of mice that had received HOCl or PBS for 6 weeks. Fluorescence was recorded on a spectrofluorimeter at 320 nm and 405 nm as excitation and emission wavelengths, respectively. Bars show the mean \pm SEM. * = P = 0.004 by Mann-Whitney unpaired U test. **B**, Representative immunoblot of ADAM-17 in skin extracts from 1 patient with localized scleroderma, 1 patient with diffuse cutaneous SSc, and 1 control patient. The internal control was β -actin. **C**, Immunohistochemistry of skin sections obtained from 2 controls and 2 patients with SSc representative of 4 controls and 4 patients with SSc. Slides were stained with anti-ADAM-17 antibodies (original magnification \times 400). See Figure 1 for definitions.

ent members of the Notch family was found in skin fibroblasts between mice exposed to HOCl and those exposed to PBS (further information is available at <https://sites.google.com/site/notchssc/>).

DISCUSSION

In this study, we demonstrate for the first time the activation of the Notch pathway in the skin, lung, and

splenocytes of mice with HOCl-induced SSc and in the skin of patients with systemic and localized scleroderma. Moreover, we show that the inhibition of the Notch pathway can represent an effective treatment that abrogates the fibrotic process and the autoimmune activation that characterize SSc, even though the number of patients studied is limited.

Notch signaling controls a variety of processes, involving cell fate specification, differentiation, proliferation, and survival (23). In our study, Notch inhibition by the γ -secretase inhibitor DAPT decreased skin and lung fibrosis induced by HOCl and normalized the rate of proliferation of dermal fibroblasts. A hyperproliferative phenotype of fibroblasts has been observed both in mice and in humans with SSc (24,25). This phenotype and the increased production of extracellular matrix proteins such as type I collagen are both hallmarks of scleroderma (25,26).

The role of Notch in the control of cell proliferation has led to some contradictory conclusions. Indeed, Notch can function as a tumor promoter or a suppressor depending on its cellular target and context. In the skin, Notch signaling induces the arrest of cell growth and differentiation of keratinocytes (27,28), suggesting a role for Notch-1 as a tumor suppressor (29). However, several studies have highlighted the activation of the Notch pathway as a novel mechanism of melanocytic transformation (30). Moreover, in fibroblasts, oncogenic Ras activates Notch-1 signaling, which is required to maintain the neoplastic phenotype in Ras-transformed human fibroblasts (31). Interestingly, the hyperproliferative phenotype of SSc fibroblasts has been associated with abnormalities in the Ras pathway, since high amounts of Ha-Ras and Ki-Ras are found in fibroblasts isolated from skin of SSc patients and from skin of mice with HOCl-induced SSc (data not shown) (32). In addition, the increase in fibroblast proliferation during wound healing is correlated with Notch activation and can be abrogated both in vitro and in vivo by γ -secretase treatment (33), which is consistent with our results.

In the present work, the inhibition of the Notch pathway reduces fibroblast proliferation through at least 2 mechanisms. First, Notch inhibition directly reduces the rate of proliferation of SSc fibroblasts. Second, γ -secretase inhibitor reduces the production of reactive oxygen species, particularly H_2O_2 , by endothelial cells. Consequently, Notch inhibition reduces the amount of advanced oxidation protein products in the serum. Since we have previously shown in our murine model of SSc that advanced oxidation protein products stimulate the proliferation of fibroblasts, this effect of Notch inhibition may also participate in the reduction of fibroblast proliferation. Little is known about the role of Notch in the control of oxidative stress. We had previously

shown that sera from patients and mice with SSc triggered the production of high amounts of H₂O₂ on human umbilical vein macrovascular endothelial cells, even if SSc mostly involves microvascular endothelial cells. Here, we show that Notch inhibition reduces this endothelial production of H₂O₂. Our data are in accordance with a previous study showing that Notch inhibition significantly reduces the production of reactive oxygen species such as nitric oxide by macrophages (34). Taken together, our data allow us to identify 2 causes of hyperproliferation of fibroblasts: high amounts of serum oxidized protein (and especially of oxidized DNA topoisomerase I) and activation of the Notch pathway in SSc fibroblasts.

The skin and the lungs of SSc patients contain myofibroblasts, a cellular population that produces high amounts of collagen and expresses α -SMA (22,25). This cell subset is also observed in our mouse model of SSc induced by HOCl. Interestingly, Notch/CSL activation induces α -SMA expression during epithelial-to-mesenchymal transformation, and Notch activation is required for the expression of α -SMA in vascular smooth muscle cells (35,36). Moreover, Notch-1 signaling in response to FIZZ1 plays a significant role in myofibroblast differentiation during lung fibrosis (37). Therefore, the down-regulation of myofibroblast differentiation by the γ -secretase inhibitor DAPT can also participate in the beneficial effects of Notch inhibition in SSc.

However, abundant evidence exists for activation of humoral and cellular immune mechanisms in SSc that probably lead to vascular damage and fibrosis. In our model, exposure to HOCl increased splenic B cell numbers and activation by lipopolysaccharide (not shown). In addition, exposure to HOCl increased total IgM antibody levels in the serum and led to the production of anti-DNA topoisomerase I autoantibodies, which are a hallmark of SSc. Notch is known to play a key role in lymphocyte development, since Notch-1 is crucial for the T versus B lymphoid cell fate decision (38,39). Notch-2 activation drives the development of splenic marginal zone B cells (40). However, Notch inhibition did not prevent the increase of splenic B cell number induced by HOCl exposure, and no significant difference was observed in marginal zone B cells between treated and untreated mice (data not shown). This observation may be explained by the age of the mice used in the experiments and by the short course of the treatment. In mice exposed to HOCl and treated with the Notch inhibitor, total IgM antibodies and anti-DNA topoisomerase I autoantibody serum levels were reduced. This effect of Notch on B cell activation has been recently reported (41,42), and its inhibition by DAPT

treatment could participate in the benefits obtained by the treatment with DAPT in our model.

ADAM-17, an activator of the Notch pathway (43), is overexpressed in the skin of mice with HOCl-induced SSc and in the skin of patients with both systemic and localized scleroderma. The initiation of Notch signaling requires the binding of a ligand to the Notch ectodomain, triggering the shedding of that domain by the ADAM-10 or the ADAM-17 proteinase (44). Importantly, no increase among the different Notch ligands was found in the skin of mice exposed to HOCl, in contrast to the effect of ADAM-17. ADAM-17 has been found to be overexpressed in a variety of diseases, including cancers and autoimmune and inflammatory diseases (45,46). Recently, ADAM-17 synthesis has been shown to be induced by oxidative stress (47,48). Therefore, our results unravel a new mechanism through which oxidative stress can activate the ADAM-17/Notch pathway. While we consider reactive oxygen species-induced ADAM-17 to be a major factor activating the Notch pathway, other factors such as hypoxia or proinflammatory cytokines like transforming growth factor β can also amplify Notch activation in SSc (49,50).

In conclusion, we demonstrate for the first time a direct link between oxidative stress, the induction of ADAM-17, and the activation of the Notch pathway in SSc development in a mouse model of the disease (further information is available at <https://sites.google.com/site/notchssc/>) and in the skin of SSc patients. The central role of this new pathway in the development of human SSc could be confirmed by the study of a larger cohort of patients. In addition, we demonstrate that Notch inhibition by γ -secretase inhibitor is effective and safe in our animal model of SSc. Several γ -secretase inhibitors have gone through clinical trials, and results of these trials may provide a basis for future clinical trials of other γ -secretase inhibitors in patients at an early stage of SSc.

ACKNOWLEDGMENT

The authors are indebted to Ms Agnes Colle for typing the manuscript.

AUTHOR CONTRIBUTIONS

All authors were involved in drafting the article or revising it critically for important intellectual content, and all authors approved the final version to be published. Dr. Batteux had full access to all of the data in the study and takes responsibility for the integrity of the data and the accuracy of the data analysis.

Study conception and design. Kavian, Servettaz, Batteux.
Acquisition of data. Kavian, Servettaz, Mongaret, Wang, Nicco, Chéreau, Grange, Vuillet, Batteux.

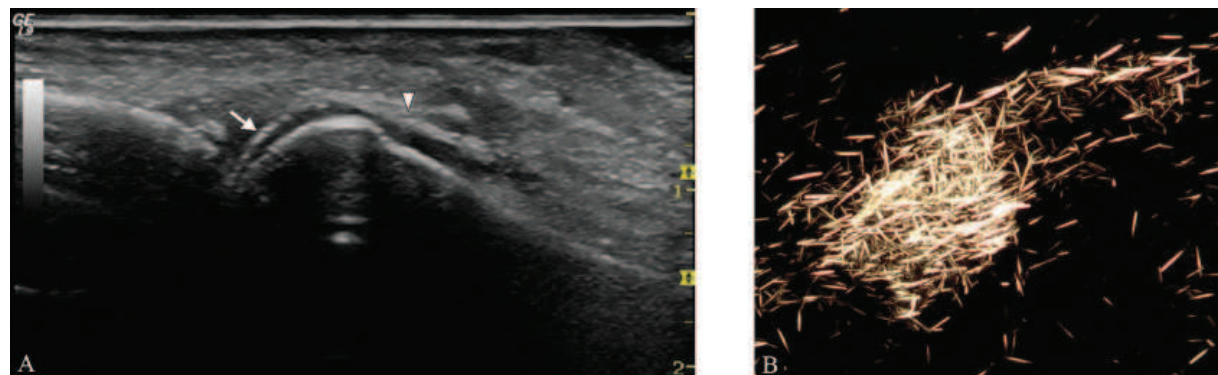
Analysis and interpretation of data. Kavian, Servettaz, Birembaut, Diebold, Weill, Dupin, Batteux.

REFERENCES

- Iso T, Hamamori Y, Kedes L. Notch signaling in vascular development. *Arterioscler Thromb Vasc Biol* 2003;23:543–53.
- Shi S, Stanley P. Evolutionary origins of Notch signaling in early development. *Cell Cycle* 2006;5:274–8.
- Kared H, Adle-Biassette H, Fois E, Masson A, Bach JF, Chatenoud L, et al. Jagged2-expressing hematopoietic progenitors promote regulatory T cell expansion in the periphery through Notch signaling. *Immunity* 2006;25:823–34.
- LeRoy EC, Medsger TA Jr. Criteria for the classification of early systemic sclerosis. *J Rheumatol* 2001;28:1573–6.
- Gabrielli A, Avvedimento EV, Krieg T. Scleroderma. *N Engl J Med* 2009;360:1989–2003.
- Yamamoto T. Scleroderma-pathophysiology. *Eur J Dermatol* 2009;19:14–24.
- Gabrielli A, Svegliati S, Moroncini G, Pomponio G, Santillo M, Avvedimento EV. Oxidative stress and the pathogenesis of scleroderma: the Murrell's hypothesis revisited. *Semin Immunopathol* 2008;30:329–37.
- Uyttendaele H, Closson V, Wu G, Roux F, Weinmaster G, Kitajewski J. Notch4 and Jagged-1 induce microvessel differentiation of rat brain endothelial cells. *Microvasc Res* 2000;60:91–103.
- Dorsch M, Zheng G, Yowe D, Rao P, Wang Y, Shen Q, et al. Ectopic expression of Delta4 impairs hematopoietic development and leads to lymphoproliferative disease. *Blood* 2002;100:2046–55.
- Savill NJ, Sherratt JA. Control of epidermal stem cell clusters by Notch-mediated lateral induction. *Dev Biol* 2003;258:141–53.
- Servettaz A, Gouvestre C, Kavian N, Nicco C, Guilpain P, Chereau C, et al. Selective oxidation of DNA topoisomerase 1 induces systemic sclerosis in the mouse. *J Immunol* 2009;182:5855–64.
- Servettaz A, Guilpain P, Camoin L, Mayeux P, Broussard C, Tamby M, et al. Identification of target antigens of anti-endothelial cell antibodies in healthy individuals: a proteomic approach. *Proteomics* 2008;8:1000–8.
- Jaffe E, Nachman R, Becker C, Minick CR. Culture of human endothelial cells derived from umbilical veins: identification by morphologic and immunological criteria. *J Clin Invest* 1973;52:2745–56.
- Servettaz A, Tamby MC, Guilpain P, Reinbolt J, Garcia de la Peña-Lefebvre P, Allanore Y, et al. Anti-endothelial cell antibodies from patients with limited cutaneous systemic sclerosis bind to centromeric protein B (CENP-B). *Clin Immunol* 2006;120:212–9.
- Tamby MC, Humbert M, Guilpain P, Servettaz A, Dupin N, Christner JJ, et al. Antibodies to fibroblasts in idiopathic and scleroderma-associated pulmonary hypertension. *Eur Respir J* 2006;28:799–807.
- Noursadeghi M, Tsang J, Haustein T, Miller RF, Chain BM, Katz DR. Quantitative imaging assay for NF-κB nuclear translocation in primary human macrophages. *J Immunol Methods* 2008;329:194–200.
- Burdick MD, Murray LA, Keane MP, Xue YY, Zisman DA, Belperio JA, et al. CXCL11 attenuates bleomycin-induced pulmonary fibrosis via inhibition of vascular remodeling. *Am J Respir Crit Care Med* 2005;171:261–8.
- Woessener JF. The determination of hydroxyproline in tissue and protein samples containing small proportions of this amino acid. *Arch Biochem Biophys* 1961;93:440–7.
- Witko-Sarsat V, Friedlander M, Capeillere-Blandin C, Nguyen-Khoa T, Nguyen AT, Zingraff J, et al. Advanced oxidation protein products as a novel marker of oxidative stress in uremia. *Kidney Int* 1996;49:1304–13.
- Preud'homme JL, Rochard E, Gouet D, Danon F, Alcalay M, Touchard G, et al. Isotypic distribution of anti-double-stranded DNA antibodies: a diagnostic evaluation by enzyme-linked immunosorbent assay. *Diagn Clin Immunol* 1988;5:256–61.
- Sappino AP, Masouye I, Saurat JH, Gabiani G. Smooth muscle differentiation in scleroderma fibroblastic cells. *Am J Pathol* 1990;137:585–91.
- Rajkumar VS, Howell K, Csiszar K, Denton CP, Black CM, Abraham DJ. Shared expression of phenotypic markers in systemic sclerosis indicates a convergence of pericytes and fibroblasts to a myofibroblast lineage in fibrosis. *Arthritis Res Ther* 2005;7:R113–23.
- Artavanis-Tsakonas S, Rand MD, Lake RJ. Notch signaling: cell fate, control, and signal integration in development. *Science* 1999;284:770–6.
- Yamamoto T, Nishioka K. Animal model of sclerotic skin. V: Increased expression of α-smooth muscle actin in fibroblastic cells in bleomycin-induced scleroderma. *Clin Immunol* 2002;102:77–83.
- Kirk TZ, Mark ME, Chua CC, Chua BH, Mayes MD. Myofibroblasts from scleroderma skin synthesize elevated levels of collagen and tissue inhibitor of metalloproteinase (TIMP-1) with two forms of TIMP-1. *J Biol Chem* 1995;270:3423–8.
- Jimenez SO, Derk CT. Following the molecular pathways toward an understanding of the pathogenesis of systemic sclerosis. *Ann Intern Med* 2004;140:37–50.
- Rangarajan A, Talora C, Okuyama R, Nicolas M, Mammucari C, Oh H, et al. Notch signaling is a direct determinant of keratinocyte growth arrest and entry into differentiation. *EMBO J* 2001;20:3427–36.
- Lowell S, Jones P, Le Roux I, Dunne J, Watt FM. Stimulation of human epidermal differentiation by Delta-Notch signalling at the boundaries of stem-cell clusters. *Curr Biol* 2000;10:491–500.
- Nicolas M, Wolfer A, Raj K, Kummer JA, Mill P, van Noort M, et al. Notch 1 functions as a tumor suppressor in mouse skin. *Nat Genet* 2003;33:416–21.
- Hoek K, Rimm DL, Williams KR, Zhao H, Ariyan S, Lin A, et al. Expression profiling reveals novel pathways in the transformation of melanocytes to melanomas. *Cancer Res* 2004;64:5270–82.
- Weijzen S, Rizzo P, Braid M, Vaishnav R, Jonkheer SM, Zlobin A, et al. Activation of Notch-1 signaling maintains the neoplastic phenotype in human Ras-transformed cells. *Nat Med* 2002;8:979–86.
- Svegliati S, Cancello R, Sambo P, Luchetti M, Paroncini P, Orlandini G, et al. Platelet-derived growth factor and reactive oxygen species (ROS) regulate Ras protein levels in primary human fibroblasts via ERK1/2. *J Biol Chem* 2005;280:36474–82.
- Chigurupati S, Arumugam TV, Son TG, Lathia JD, Jameel S, Mughal MR, et al. Involvement of Notch signaling in wound healing. *PLoS One* 2007;2:e1167.
- Palaga T, Buranaruk C, Rengpipat S, Fauq AH, Golde TE, Kaufmann SH, et al. Notch signaling is activated by TLR stimulation and regulates macrophage functions. *Eur J Immunol* 2008;38:174–83.
- Noseda M, McLean G, Niessen K, Chang L, Pollet I, Montpetit R, et al. Notch activation results in phenotypic and functional changes consistent with endothelial-to-mesenchymal transformation. *Circ Res* 2004;94:910–7.
- Noseda M, Fu Y, Niessen K, Wong F, Chang L, McLean G, et al. Smooth muscle α-actin is a direct target of Notch/CSL. *Circ Res* 2006;98:1468–70.
- Liu T, Hu B, Choi YY, Chung M, Ullenbruch M, Yu H, et al. Notch1 signaling in FIZZ1 induction of myofibroblast differentiation. *Am J Pathol* 2009;174:1745–55.
- Pui JC, Allman D, Xu L, DeRocco S, Karnell FG, Bakkour S, et al. Notch1 expression in early lymphopoiesis influences B versus T lineage determination. *Immunity* 1999;11:299–308.
- Radtke F, Wilson A, Stark G, Bauer M, van Meerwijk J, MacDonald HR, et al. Deficient T cell fate specification in mice with an induced inactivation of Notch1. *Immunity* 1999;10:547–58.

40. Maillard I, Adler SH, Pear WS. Notch and the immune system. *Immunity* 2003;19:781–91.
41. Santos MA, Sarmento LM, Rebelo M, Doce AA, Maillard I, Dumortier A, et al. Notch1 engagement by Delta-like-1 promotes differentiation of B lymphocytes to antibody-secreting cells. *Proc Natl Acad Sci U S A* 2007;104:15454–9.
42. Thomas M, Calamito M, Srivastava B, Maillard I, Pear WS, Allman D. Notch activity synergizes with B-cell–receptor and CD40 signaling to enhance B-cell activation. *Blood* 2007;109:3342–50.
43. Edward DR, Handsley MM, Pennington CJ. The ADAM metalloproteinases. *Mol Aspects Med* 2008;29:258–89.
44. Brou C, Logeat F, Gupta N, Bessia C, LeBail O, Doedens JR, et al. A novel proteolytic cleavage involved in Notch signaling: the role of the disintegrin-metalloprotease TACE. *Mol Cell* 2000;5:207–16.
45. Charbonneau M, Harper K, Grondin F, Pelmus M, McDonald PP, Dubois CM. Hypoxia-inducible factor mediates hypoxic and tumor necrosis factor α -induced increases in tumor necrosis factor α converting enzyme/ADAM 17 expression by synovial cells. *J Biol Chem* 2007;282:33714–24.
46. McGowan PM, Ryan BM, Hill AD, McDermott E, O'Higgins N, Duffy MJ. ADAM17 overexpression in breast cancer correlates with variables of tumor progression. *Clin Cancer Res* 2007;13: 2335–43.
47. Shao MX, Nadel JA. Dual oxidase 1-dependent MUC5AC mucin expression in cultured human airway epithelial cells. *Proc Natl Acad Sci U S A* 2005;102:767–72.
48. Zhang Z, Oliver P, Lancaster JR Jr, Schwarzenberger OO, Joshi MS, Cork J, et al. Reactive oxygen species mediate tumor necrosis factor α -converting, enzyme dependent ectodomain shedding induced by phorbol myristate acetate. *FASEB J* 2001;15:303–5.
49. Bedogni B, Warneke JA, Nickoloff BJ, Giaccia AJ, Broome Powell M. Notch1 is an effector of Akt and hypoxia in melanoma development. *J Clin Invest* 2008;118:3660–70.
50. Morrissey J, Guo G, Moridaira K, Fitzgerald M, McCracken R, Tolley T, et al. Transforming growth factor- β induces renal epithelial jagged-1 expression in fibrotic disease. *J Am Soc Nephrol* 2002;13:1499–508.

DOI 10.1002/art.27646

Clinical Images: Ultrasonographic signs of gout in symmetric polyarthritis

The patient, a 66-year-old woman, was referred to our outpatient clinic after experiencing 6 months of persistent pain and stiffness in both hands. She had symmetric polyarthritis with swelling and tenderness of the metacarpophalangeal (MCP) joints and proximal interphalangeal joints of both hands, in addition to swollen ankle joints and tender knee joints. The patient had a history of hypertension and type 2 diabetes mellitus. For >10 years, she had experienced self-limited episodes of arthritis in her feet. The clinical examination was supplemented with ultrasound examination of the hands (representative findings from the second MCP joint, shown in A). In several MCP joints, a double contour sign (**arrow**) and hyperechoic soft-tissue areas (**arrowhead**), indicative of urate deposits on the cartilaginous surface and in the synovial membrane, were seen. Arthrocentesis of the second left MCP joint was performed with an injection of 0.5 ml isotonic saline. Under polarized light microscopy, the aspirated joint showed characteristic needle-shaped crystals (**B**) that were seen to be negatively birefringent on compensated double-phase polarized light microscopy. The patient was diagnosed as having polyarticular gout and started treatment with low-dose colchicine, which yielded positive effects. Laboratory tests showed a serum urate level of 0.81 mmoles/liter (13.5 mg/dl), and treatment with allopurinol was subsequently initiated. Ultrasonography is becoming increasingly recognized as a useful investigational tool in locating urate deposits in patients with suspected gout; these deposits can be aspirated and examined in order to properly diagnose gout (Perez-Ruiz F, Dalbeth N, Urresola A, de Miguel E, Schlesinger N. Imaging of gout: findings and utility. *Arthritis Res Ther* 2009;11:232).

Ole Slot, MD
Lene Terslev, MD, PhD
Glostrup Hospital
Glostrup, Denmark

3.3 ARTICLE 3

L'activation de la voie des récepteurs aux cannabinoïdes CB2 limite le développement de la fibrose et de l'auto-immunité dans un modèle murin de Sclérodermie systémique

Targeting the cannabinoid pathway limits the development of fibrosis and auto-immunity in a mouse model of systemic sclerosis

*Amélie Servettaz, Niloufar Kavian, Carole Nicco, Vanessa Deveaux, Christiane Chéreau,
Andrew Wang, Andreas Zimmer, Sophie Lotersztajn, Bernard Weill, Frédéric Batteux*

American Journal of Pathology, 2010

Les cannabinoïdes endogènes sont des molécules lipidiques produites par le système nerveux central et divers tissus. L'Anandamide et le 2-arachidonoylglycerol sont les deux molécules cannabinoïdes endogènes les plus étudiées. Il existe deux types de récepteurs aux cannabinoïdes : CB1, exprimé par les cellules du système nerveux central, et CB2 exprimé par les fibroblastes, les cellules endothéliales, et les cellules hématopoïétiques. De récentes données suggèrent que le système des cannabinoïdes endogènes pourrait être impliqué dans des phénomènes de fibrose, notamment hépatique, et que la modulation de cette voie pourrait limiter l'étendue de la fibrose. L'objectif de ce travail était d'évaluer les rôles de la voie des canabinoïdes dans les phénomènes d'induction et de propagation de la maladie dans la Sclérodermie systémique.

Nous avons utilisé le modèle murin de sclérodermie induite par l'acide hypochloreux, mis au point dans notre laboratoire. Dans un premier temps, les souris BALB/c ont été traitées de façon concomitante à l'induction de la maladie par des injections intra-péritonéales de WIN-55212, un agoniste non-sélectif des récepteurs aux cannabinoïdes CB1 et CB2, ou par des injections intra-péritonéales de JWH-133, un agoniste sélectif des récepteurs CB2. Les souris contrôles ont reçu des injections de PBS. Dans un deuxième temps, nous avons appliqué le protocole d'induction de la sclérodermie par l'acide hypochloreux à des souris déficientes en récepteurs CB2 (*Cnr2 -/-*). Nous avons évalué la fibrose cutanée et pulmonaire par histopathologie et par mesure des concentrations en collagène de type I dans ces organes. Les fibroblastes cutanés ont été

extraits des peaux de souris, et nous avons déterminé leur taux de prolifération par incorporation de thymidine tritiée. Les titres des auto-anticorps ont été mesurés par technique ELISA. Les populations de splénocytes ont été analysées par cytométrie de flux. Nous avons aussi réalisé des études *in vitro* pour évaluer les propriétés anti-prolifératives du WIN-55212 et du JWH-133.

Le traitement des souris ScS par le WIN-55212 et le JWH-133 a permis de réduire le développement de la fibrose cutanée et pulmonaire, les taux de prolifération des fibroblastes cutanés, ainsi que les taux d'auto-anticorps anti-ADN Topoisomérase-1. Les expériences réalisées chez les souris déficientes en CB2 nous ont permis de confirmer le rôle de ces récepteurs dans le développement de la fibrose et de l'auto-immunité puisque les souris Cnr2^{-/-} soumises au protocole d'induction de la ScS par HOCl ont présenté un phénotype exacerbé de la maladie, avec notamment une fibrose significativement plus importante au niveau cutané et pulmonaire que les souris Wild-Type.

Ce travail nous a permis de démontrer le rôle des récepteurs CB2 dans les phénomènes fibrotiques et auto-immuns observés dans la ScS. Les cannabinoïdes peuvent réguler les mécanismes de fibrose directement en agissant au niveau de l'activation et de la prolifération fibroblastique mais aussi indirectement en contrôlant l'activation des lymphocytes B et la réponse inflammatoire. La modulation de la voie des cannabinoïdes endogènes semble donc être une nouvelle approche thérapeutique pour la ScS, via la prolifération fibroblastique, l'activation du système immunitaire, et des interactions avec les cellules endothéliales.

Nos résultats ont depuis été confirmés par d'autres équipes [228] [115].

Matrix Pathobiology

Targeting the Cannabinoid Pathway Limits the Development of Fibrosis and Autoimmunity in a Mouse Model of Systemic Sclerosis

Amélie Servettaz,^{*†} Niloufar Kavian,^{*} Carole Nicco,^{*} Vanessa Deveaux,[‡] Christiane Chéreau,^{*§} Andrew Wang,[¶] Andreas Zimmer,^{||} Sophie Lotersztajn,[‡] Bernard Weill,^{*} and Frédéric Batteux^{*§}

From the Laboratoire d'Immunologie Biologique et EA 1833,^{*} Faculté de Médecine, AP-HP Hôpital Cochin, Université Paris Descartes, Paris, France; the Service de Médecine Interne, Maladies Infectieuses, Immunologie Clinique,[†] Faculté de Médecine de Reims, Hôpital Robert Debré, Reims, France; INSERM, Unité 955,[‡] Institut Mondor de Recherche Biomédicale Crétel, Université Paris 12, Faculté de Médecine, UMR-S955, Crétel, France; ERTI,[§] Faculté de Médecine, Université Paris Descartes, Paris, France; the Department of Immunology,[¶] University of Texas Southwestern Medical Center, Dallas, Texas; and the Department of Molecular Psychiatry,^{||} University of Bonn, Bonn, Germany

Our aim was to evaluate the roles of the cannabinoid pathway in the induction and propagation of systemic sclerosis (SSc) in a mouse model of diffuse SSc induced by hypochlorite injections. BALB/c mice injected subcutaneously every day for 6 weeks with PBS or hypochlorite were treated intraperitoneally with either WIN-55,212, an agonist of the cannabinoid receptors 1 (CB1) and receptors 2 (CB2), with JWH-133, a selective agonist of CB2, or with PBS. Skin and lung fibrosis were then assessed by histological and biochemical methods, and the proliferation of fibroblasts purified from diseased skin was assessed by thymidine incorporation. Autoantibodies were detected by ELISA, and spleen cell populations were analyzed by flow cytometry. Experiments were also performed in mice deficient for CB2 receptors (*Cnr2*^{-/-}). Injections of hypochlorite induced cutaneous and lung fibrosis as well as increased the proliferation rate of fibroblasts isolated from fibrotic skin, splenic B cell counts, and levels of anti-DNA topoisomerase-1 autoantibodies. Treatment with WIN-55,212 or with the selective CB2 agonist JWH-133 prevented the development of skin and lung fibrosis as well as reduced fibroblast proliferation and the development of autoantibodies. Experi-

ments performed in CB2-deficient mice confirmed the influence of CB2 in the development of systemic fibrosis and autoimmunity. Therefore, we demonstrate that the CB2 receptor is a potential target for the treatment of SSc because it controls both skin fibroblast proliferation and the autoimmune reaction. (Am J Pathol 2010; 177:187–196; DOI: 10.2353/ajpath.2010.090763)

Systemic sclerosis (SSc) is a connective tissue disorder characterized by vascular alterations, extensive fibrosis, and immunological dysregulations associated with specific autoantibodies (AAbs).¹ The involvement of visceral organs determines the prognosis of the disease, which can be life threatening. Despite progresses in the treatment of some visceral complications, no treatment has been designed to date that can cure SSc, in part because the mechanisms underlying the disease remain unclear.^{2,3}

Endogenous cannabinoids are lipid molecules produced by most cell types in the brain and various peripheral tissues. They exert a broad range of biological effects that are reproduced by Δ9-tetra-hydroxycannabinol, the main constituent of marijuana. Anandamide and 2-arachidonoylglycerol are the two most widely studied endocannabinoids. They exert their effects through the binding to two protein G-coupled specific receptors: cannabinoid receptors 1 (CB1) and receptors 2 (CB2).^{4,5} The CB1 receptor, predominantly expressed in brain, is present to a lesser extent in endothelium and liver. The CB2 receptor has been initially detected in hematopoietic and immune cells, but recent studies have identified this receptor in fibroblasts, endothelial cells, liver cells, and myocytes.^{6–13} Moreover, the ex-

Supported by a grant from the "Fondation pour la Recherche Médicale (FRM)" (N.K.).

A.S. and N.K. contributed equally to this work.

Accepted for publication March 15, 2010.

Supplemental material for this article can be found on <http://ajp.amjpathol.org>.

Address reprint requests to Dr. Frédéric Batteux, Université Paris Descartes, Faculté de Médecine, Laboratoire d'immunologie, EA 1833, IFR Alfred Jost, 75679 Paris cedex 14, France. E-mail: frederic.batteux@cch.ap-hop-paris.fr.

pression of the CB2 receptor can be influenced by various pathological conditions such as inflammation.

In addition to their well-characterized psychoactive effects, cannabinoids modulate various key functions, especially cardiovascular and endothelial functions. The endocannabinoid pathway abrogates the activation of endothelial cells isolated from sinusoidal vessels of human liver and from human coronary arteries and prevents ischemia/reperfusion damages in the liver,^{13–15} the heart, and the brain.^{16,17} This role is assumed by CB2 agonists that act as modulators of endothelial cell activation and endothelial/inflammatory cell interaction and down-regulate adhesion molecules such as intracellular cell adhesion molecule 1 and vascular cell adhesion molecule 1.¹⁸ Moreover, natural or synthetic cannabinoids display immunomodulatory effects on the proliferation and apoptosis of T and B lymphocytes, the activation of macrophage, and the production of cytokines and chemokines.^{19–21} Most of these effects are CB2 receptor-dependent. In addition, recent data have shown that CB2 receptor agonists counteract liver fibrogenesis.^{12,22} CB2 receptors are also present in the skin,²³ and their activation prevents bleomycin-induced dermal fibrosis in the mouse.²⁴

Because endothelial cells, fibroblasts, and immune cells are dysregulated in SSc and are also the targets of cannabinoids, we were prompted to investigate the role of these molecules in SSc. To this end, we used a recently described murine model of SSc that recapitulates the main features of the cutaneous diffuse form of the human disease.²⁵

Materials and Methods

Animals, Cells, and Chemicals

Specific pathogen-free 6-week-old female BALB/c and C57BL/6 CB2^{+/+} mice were purchased from Harlan (Gannat, France) and maintained with food and water *ad libitum*. To obtain single mutant mice with a targeted mutation of the *Cnr2* gene on an inbred congenic genetic background, heterozygous *Cnr2*^{+/−} mice were back-crossed with wild-type C57BL/6J animals (The Jackson Laboratory, Bar Harbor, ME) over 10 generations. Heterozygous mice from the N10 generation were intercrossed to homozygous *Cnr2*^{−/−} animals (CB2^{−/−} mice).²⁶ All mice were housed in autoclaved cages with free access to food and water. They were given humane care according to the guidelines of our institution. All cells were cultured as previously reported.^{27,28} All chemicals, except for monoclonal antibodies, were from Sigma (Saint-Quentin Fallavier, France) except JWH-133 (Tocris Bioscience, Ellisville, MO).

Induction of SSc by Subcutaneous Injections of a HOCl-Generating Solution to BALB/c Mice

Six week-old BALB/c mice were randomly distributed into experimental and control groups ($n = 21$ per group). One hundred microliters of a solution generating HOCl were injected subcutaneously into the shaved back of the mice, using a 27-gauge needle, every day for 6 weeks, as previously described (HOCl mice).²⁵ Control

groups received injections of 100 μ l sterilized PBS (PBS mice). All agents were prepared extemporaneously. HOCl was produced by adding 166 μ l NaClO solution (2.6% as active chlorine) to 11.1 ml KH₂PO₄ solution (100 mmol/L, pH 7.2).²⁹ HOCl concentration was determined by spectrophotometry at 292 nm (molar absorption coefficient = 350 M^{−1} cm^{−1}).

Treatment by Cannabinoid Agonists

HOCl and PBS BALB/c mice were randomized and treated simultaneously by intraperitoneal injections either with WIN-55,212, a nonselective CB1 and CB2 agonist, or JWH-133, a selective CB2 agonist, or vehicle alone for 6 weeks ($n = 14$ per group). Cannabinoid agonists were given 5 days a week from Monday to Friday. The doses increased each week: WIN-55,212 was started at 0.5 mg/kg per day the first week, and then 1, 2, 3, 4, and 5 mg/kg per day the following weeks; JWH-133 was started at 1 mg/kg per day, and then 1.5, 2, 2.5, 3, and 4 mg/kg per day. WIN-55,212 and JWH-133 were reconstituted with DMSO, aliquoted, and stored as stock solutions at a concentration of 1 mg/ml at −20°C. Each day, the stock solutions were diluted in PBS. One week after the end of the subcutaneous and peritoneal injections, the animals were killed by cervical dislocation. Serum samples were collected and stored at −80°C until use. Lungs were removed from each mouse. One lung was stored at −80°C for collagen assay. The remaining lung was reinflated by injection of 10% phosphate buffered formalin fixative for 24 hours and then washed and stored in 70% ethanol fixative. A skin biopsy was performed on the back region with a punch (6 mm of diameter), involving the skin and the underlying muscle of the injected area. Samples were stored at −80°C for determination of collagen content or fixed in 10% neutral buffered formalin for histopathological analysis. All tissues were examined by a pathologist blind with respect to the experimental groups.

Induction of SSc by Subcutaneous Injections of a HOCl-Generating Solution to C57BL/6 CB2^{−/−} Mice

Ten-week-old C57BL/6 CB2^{−/−} and CB2^{+/+} mice were randomly distributed into experimental and control groups ($n = 5$ per group). The experimental procedure was similar to that applied to BALB/c mice, except that C57BL/6 CB2^{+/+} and CB2^{−/−} mice were killed after three weeks of subcutaneous injections.

Assessment of Dermal Thickness

Skin thickness of the shaved back of mice was measured one day before sacrifice with a caliper and expressed in millimeters.

Histopathological Analysis

Fixed lung and skin pieces were embedded in paraffin. A 5- μ m-thick tissue section was prepared from the midpor-

tion of paraffin-embedded tissue and stained either with hematoxylin eosin and safran or with picro-sirius red. Slides were examined by standard brightfield microscopy (Olympus BX60, Tokyo, Japan) by a pathologist who was blinded to the assignment of the animal group.

Collagen Content in Skin and Lung

Skin taken from the site of injection and lung pieces were diced using a sharp scalpel, put into aseptic tubes, thawed, and mixed with pepsin (1:10 weight ratio) and 0.5 M acetic acid overnight at room temperature under stirring. Collagen content assay was based on the quantitative dye-binding Sircol method (Biocolor, Belfast, N. Ireland).³⁰

Isolation of Fibroblasts from the Skin of Mice and Proliferation Assays

Skin fragments from the back of mice were collected at the time of sacrifice. Skin samples were digested with "Liver Digest Medium" (Invitrogen) for 1 hour at 37°C. After three washes in complete medium, cells were seeded into sterile flasks and isolated fibroblasts were cultured in DMEM/Glutamax-I supplemented with 10% heat-inactivated fetal calf serum and antibiotics at 37°C in humidified atmosphere with 5% CO₂. For proliferation assays, primary fibroblasts (2×10^3 per well) were seeded in 96-well plates and incubated with 150 µl of culture medium with 10% fetal calf serum at 37°C in 5% CO₂ for 48 hours. Cell proliferation was determined by pulsing the cells with [³H]thymidine (1 µCi per well) during the last 16 hours of culture. Results were expressed as absolute numbers of counts per minute.

Effect of Various Concentrations of WIN-55,212 and JWH-133 on the in Vitro Proliferation of Skin Fibroblasts

Fibroblasts isolated from the skin of HOCl BALB/c mice were seeded in 96-well plates (4×10^3 per well) and incubated with 10, 20, or 40 µmol/L WIN-55,212 or JWH-133 in culture medium supplemented with 10% fetal calf serum at 37°C in 5% CO₂ for 48 hours. Cell proliferation was determined as previously described.

Flow Cytometric Analysis of Spleen Cell Subsets

Cell suspensions from spleens were prepared after hypotonic lysis of erythrocytes. Cells were incubated with the appropriately labeled antibody (Ab) at 4°C for 45 minutes in PBS with 0.1% sodium azide and 5% normal rat serum to block nonspecific binding. Cell suspensions were then subjected to four-color analysis on a FACS Canto flow cytometer (BD Biosciences, San Jose, CA). The monoclonal Abs used in this study were as follows: anti-B220-PE mAb, anti-CD11b-FITC mAb, anti-CD4-APC-Cy7 mAb, and anti-CD8-PE-Cy7 mAb (BD Pharmingen, Franklin, NJ).

Assays of Serum Immunoglobulins and AAbs

Serum samples were frozen at the time of sacrifice, and all samples were analyzed at the same time. Levels of anti-DNA topoisomerase 1 IgG Abs were detected by ELISA on microtiter plates (Immunovision, Springdale, AR) coated with Scl 70 antigen. Levels of total mouse IgG and IgM Abs, of anti-dsDNA IgG Abs, of anti-cardiolipin IgG Abs, and of IgM rheumatoid factors were measured using standard ELISA as previously described.³¹ A 1:50 serum dilution was used for the determination of all AAbs.

Statistical Analysis

All quantitative data are expressed as means ± SEM. Data were compared using the Mann-Whitney nonparametric test or the Student paired *t* test. When analysis included more than two groups, one way analysis of variance was used. A *P* value <0.05 was considered significant.

Results

Activation of the Cannabinoid Receptors Prevents the Development of Skin Fibrosis in HOCl mice

As previously observed, subcutaneous injections of HOCl in BALB/c mice induced an increase in dermal thickness and in the concentration of acid- and pepsin-soluble type I collagen in the skin versus injections of PBS (*P* < 0.0001 in both cases; Figure 1, A and B). Histopathological analysis confirmed the dermal fibrosis (Figure 1A).

To evaluate whether the activation of cannabinoid receptors affects the development of dermal fibrosis in this model of SSc, mice exposed to HOCl were simultaneously treated with WIN-55,212, an agonist of both CB1 and CB2 receptors. WIN-55,212 reduced the dermal thickness and the accumulation of collagen induced by HOCl (*P* = 0.0007 for dermal thickness and *P* = 0.0006 for collagen concentration in the skin, versus untreated mice exposed to HOCl; Figure 1, A and B). Those results were confirmed by histopathological analysis of skin biopsies stained with hematoxylin and eosin (Figure 1C) and with picro-sirius red staining (Figure 2A), which showed a decrease in dermal thickness in HOCl-BALB/c mice treated with WIN-55,212.

We next investigated the effect JWH-133, a selective agonist of CB2, on the development of dermal fibrosis induced by HOCl. JWH-133 significantly reduced the dermal thickness and the accumulation of collagen in the skin of HOCl mice (*P* = 0.0004 for dermal thickness and *P* = 0.005 for collagen concentration in the skin, versus untreated HOCl mice; Figure 1, A and B). These results, confirmed by histopathological analysis (Figures 1C and 2A), show that the selective activation of CB2 is sufficient to reduce the fibrotic process triggered by HOCl.

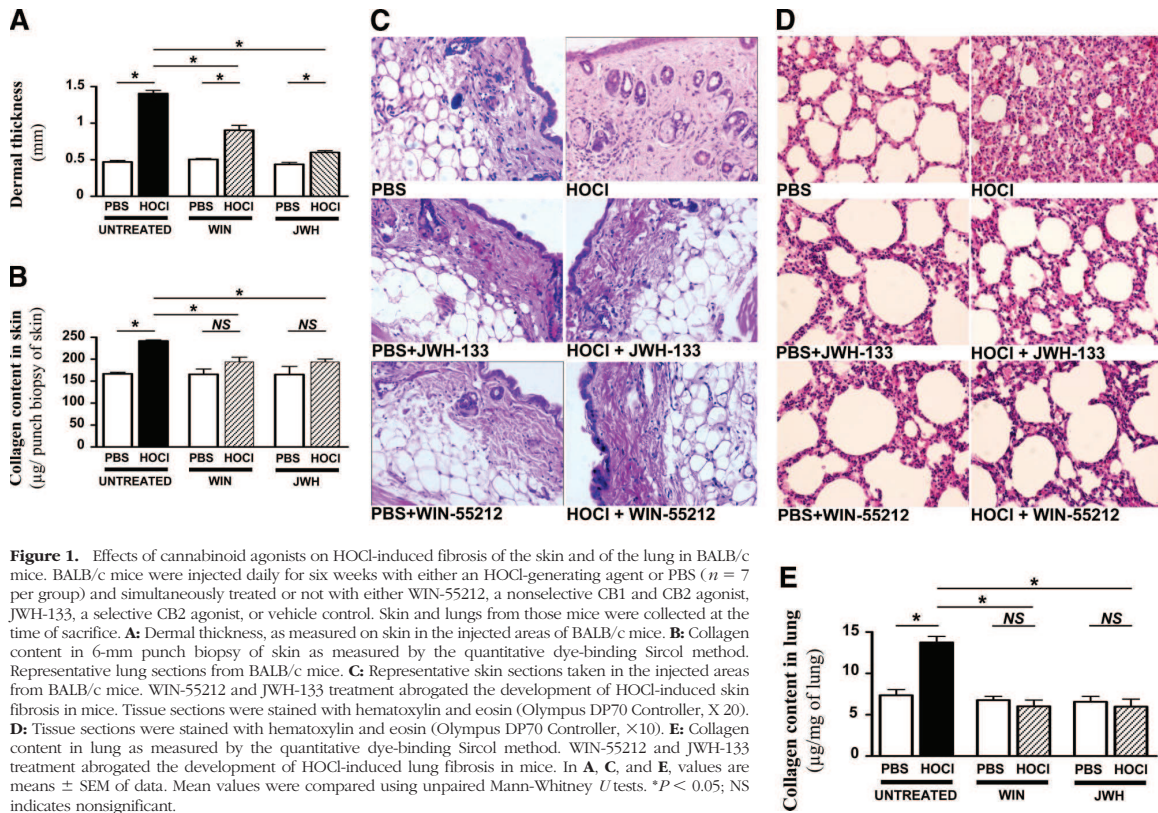


Figure 1. Effects of cannabinoid agonists on HOCl-induced fibrosis of the skin and of the lung in BALB/c mice. BALB/c mice were injected daily for six weeks with either an HOCl-generating agent or PBS ($n = 7$ per group) and simultaneously treated or not with either WIN-55212, a nonselective CB1 and CB2 agonist, JWH-133, a selective CB2 agonist, or vehicle control. Skin and lungs from those mice were collected at the time of sacrifice. **A:** Dermal thickness, as measured on skin in the injected areas of BALB/c mice. **B:** Collagen content in 6-mm punch biopsy of skin as measured by the quantitative dye-binding Sircol method. Representative lung sections from BALB/c mice. **C:** Representative skin sections taken in the injected areas from BALB/c mice. WIN-55212 and JWH-133 treatment abrogated the development of HOCl-induced skin fibrosis in mice. Tissue sections were stained with hematoxylin and eosin (Olympus DP70 Controller, X20). **D:** Tissue sections were stained with hematoxylin and eosin (Olympus DP70 Controller, X10). **E:** Collagen content in lung as measured by the quantitative dye-binding Sircol method. WIN-55212 and JWH-133 treatment abrogated the development of HOCl-induced lung fibrosis in mice. In **A**, **C**, and **E**, values are means \pm SEM of data. Mean values were compared using unpaired Mann-Whitney *U* tests. * $P < 0.05$; NS indicates nonsignificant.

Activation of the Cannabinoid Receptors Prevents the Development of Lung Fibrosis in HOCl Mice

In addition to skin fibrosis, HOCl-treated BALB/c mice developed lung fibrosis, as shown by histopathological analysis (Figure 1D) and by the higher concentration of type I collagen in the lungs of HOCl mice as compared with mice treated with PBS ($P = 0.0002$; Figure 1E). WIN-55,212 abrogated the development of lung fibrosis induced by HOCl, as shown by histopathological analysis and by the weaker accumulation of type I collagen in lungs ($P = 0.0002$ for WIN-treated versus untreated HOCl mice; Figures 1, D and E, and 2B).

The selective agonist of CB2, JWH-133, also reduced the concentration of type I collagen in the lungs compared with untreated HOCl mice ($P = 0.002$ for JWH-treated versus untreated HOCl mice; Figure 1E). Those data were confirmed by the histopathological analysis of lung biopsies stained with hematoxylin and eosin (Figure 1D) and with picro-sirius red staining (Figure 2B), which showed a decreased fibrosis in BALB/c mice submitted to HOCl injections and simultaneously treated with JWH-133.

Immunohistochemistry analysis of lung tissue sections from BALB/c mice injected with HOCl evidenced an inflammatory infiltrate mostly consisting of T lymphocytes. WIN-55,212 and JWH-133 reduced the pulmonary T cell infiltrate triggered by HOCl (see supplemental Figure S1 at <http://ajp.amjpathol.org>).

Activation of Cannabinoid Receptors Normalized the Rate of Dermal Fibroblast Proliferation in Vivo and in Vitro

We next investigated whether the activation of the cannabinoid signaling pathway modified the growth of fibroblasts isolated from fibrotic skin. Skin fibroblasts isolated from HOCl mice displayed a higher proliferation rate than fibroblasts obtained from mice injected with PBS ($P = 0.0004$; Figure 3A). By contrast, the rate of proliferation of fibroblasts isolated from HOCl mice treated with WIN-55,212 was lower than that of fibroblasts isolated from mice injected with PBS ($P = 0.02$ for HOCl mice treated with WIN-55,212 versus HOCl mice not treated with WIN-55,212; $P = 0.71$ for HOCl mice treated with WIN-55,212 versus PBS mice treated with WIN-55,212; Figure 3A).

The rate of proliferation of skin fibroblasts was also reduced when HOCl mice were treated with the selective CB2 agonist JWH-133, compared with that of fibroblasts isolated from HOCl mice without any treatment ($P = 0.02$ for HOCl mice treated with JWH-133 versus HOCl mice and untreated with JWH-133 and $P = 0.13$ for HOCl mice treated with JWH-133 versus PBS mice treated with JWH-133; Figure 3A).

Because fibroblasts from HOCl mice displayed an abnormal phenotype with an excessive rate of proliferation, additional experiments were performed to assess

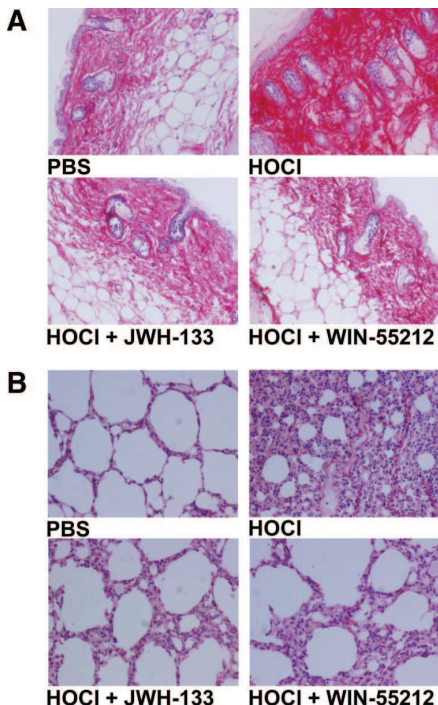


Figure 2. Effects of cannabinoid agonists on HOCl-induced fibrosis of the skin and of the lung in BALB/c mice; representative sections of skin and lung stained with picro-sirius red. BALB/c mice were injected daily for six weeks with either an HOCl-generating agent or PBS ($n = 7$ per group) and simultaneously treated or not with either WIN-55212, a nonselective CB1 and CB2 agonist, or JWH-133, a selective CB2 agonist, or vehicle control. Skin and lungs from those mice were collected at the time of sacrifice. **A:** Representative skin sections from BALB/c mice WIN-55212 and JWH-133 treatment abrogated the development of HOCl-induced skin fibrosis in mice. Tissue sections were stained with picro-sirius red (Olympus DP70 Controller, $\times 20$). **B:** Representative lung sections from BALB/c mice. Tissue sections were stained with picro-sirius red (Olympus DP70 Controller, $\times 10$).

whether WIN-55,212 and JWH-133 could directly decrease the rate of fibroblast proliferation *in vitro*. Skin fibroblasts from HOCl mice were incubated with 10, 20, or 40 $\mu\text{mol/L}$ WIN-55,212, or JWH-133 or PBS. WIN-55,212 reduced the proliferation rate of fibroblasts *in vitro* in a dose-dependent manner ($P = 0.022$ for each concentration of WIN-55,212 tested versus PBS; Figure 3B). For JWH-133, the doses of 10 and 20 $\mu\text{mol/L}$ did not reverse the proproliferative of HOCl treatment, but at a dose of 40 $\mu\text{mol/L}$ JWH-133 significantly abrogated the rate of proliferation of fibroblasts from HOCl mice ($P = 0.914$, $P = 0.171$, and $P = 0.032$ for the respective concentrations of 10, 20, and 40 $\mu\text{mol/L}$ of JWH-133 versus PBS; Figure 3B). Thus, cannabinoid agonists counteracted the proproliferative effect of HOCl on fibroblasts both *in vivo* and *in vitro* and prevented skin and lung fibrosis.

Activation of CB2 Receptors Decreases the Expansion of Splenic B-Cells in HOCl Mice

We next investigated the effects of the activation of cannabinoid receptors on the immune system because both

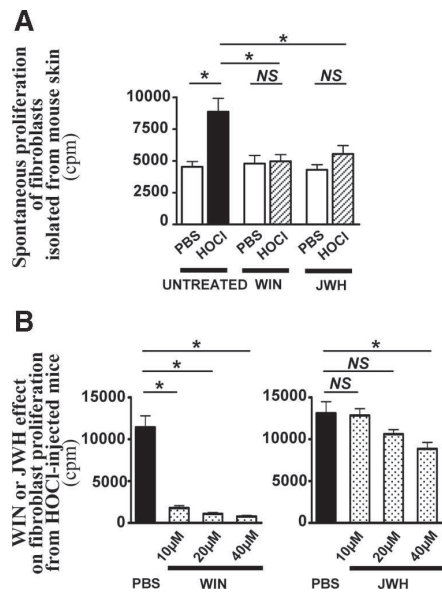


Figure 3. Effect of cannabinoid agonists on fibroblast proliferation. BALB/c mice were injected daily for 6 weeks with either an HOCl-generating agent or PBS ($n = 7$ per group) and simultaneously treated or not with either WIN-55212, a nonselective CB1 and CB2 agonist, or JWH-133, a selective CB2 agonist, or vehicle control. Skin biopsies from the injected areas were collected at the time of sacrifice. Fibroblasts were isolated by collagenase digestion of the skin then cultured in complete medium. Cell proliferation was determined by pulsing the cells with [^3H]thymidine (1 $\mu\text{Ci}/\text{well}$) during the last 16 hours of culture. **A:** Spontaneous rate of proliferation of fibroblasts isolated from fibrotic skin of mice submitted to HOCl or PBS injections and simultaneously treated *in vivo* with WIN-55212, JWH-133, or vehicle alone. **B:** Direct *in vitro* effect of WIN-55212 (10, 20, or 40 $\mu\text{mol/L}$) and JWH-133 (10, 20, or 40 $\mu\text{mol/L}$) on the growth of fibroblasts isolated from the skin of mice submitted to HOCl injections for six weeks. Results are expressed as absolute counts per minute (cpm). Values are means \pm SEM of data. Mean values were compared using unpaired Mann-Whitney *U* tests. * $P < 0.05$; NS indicates nonsignificant.

in humans and mice, diffuse SSc is characterized by B cell activation and the production of AAbs. As previously reported, exposure to HOCl for six weeks increased the total numbers of splenic B220 $^{+}$ B cells compared with PBS-injected mice ($P = 0.011$; Figure 4A). No significant difference was observed in the numbers of CD11b $^{+}$, CD4 $^{+}$, or CD8 $^{+}$ spleen cells between HOCl and PBS-injected mice (data not shown).

Activation of the cannabinoid pathway by WIN-55,212 or by the selective CB2 agonist JWH-133 prevented the increase in splenic B cell numbers in HOCl mice ($P = 0.003$ for HOCl mice treated by WIN-55,212 versus HOCl mice; $P = 0.003$ for HOCl mice treated by JWH-133 versus HOCl mice; Figure 4A).

Activation of CB2 Receptors Decreases the Serum Levels of Anti-DNA-Topoisomerase 1 AAbs Induced by HOCl

We next tested the effects of WIN-55,212 and JWH-133 on the specific autoimmune response to DNA-topoisomerase 1 that characterizes the cutaneous diffuse SSc phenotype. As previously observed, mice exposed to

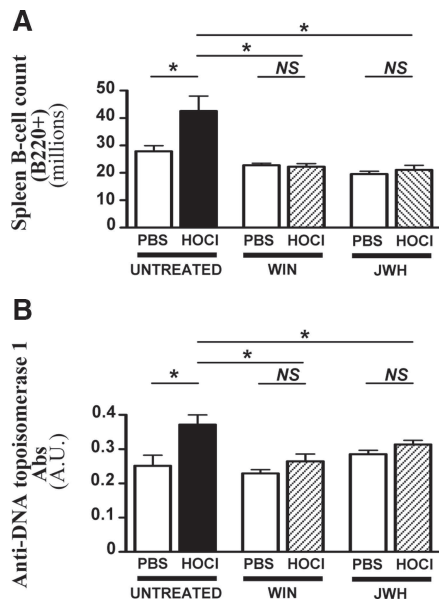


Figure 4. Activation of the cannabinoid pathway abrogated splenic B220⁺ cell expansion and anti-DNA-topoisomerase Ab production in HOCl mice. BALB/c mice were injected daily for six weeks with either an HOCl-generating agent or PBS ($n = 7$ per group) and simultaneously treated with WIN-55212, JWH-133, or vehicle control. Spleen and serum from those mice were collected at the time of sacrifice. **A:** Absolute numbers of splenic B220 positive B cells as assessed by flow cytometry. **B:** Levels of serum anti-DNA-topoisomerase1 AAbs as detected by ELISA. Values are means \pm SEM of data gained from all mice. Mean values were compared using unpaired Mann-Whitney *U* tests. * $P < 0.05$; NS indicates nonsignificant.

HOCl developed anti-DNA topoisomerase 1 IgG Abs ($P = 0.002$ versus PBS; Figure 4B). No significant levels of anti-DNA IgG Abs, anticardiolipine IgG Abs or rheumatoid factors were detected in the sera of these mice (data not shown).

Mice treated with WIN-55,212 or JWH-133 did not develop anti-DNA topoisomerase1 IgG Abs after exposure to HOCl compared with untreated mice ($P = 0.002$ for HOCl mice treated by WIN-55,212 versus HOCl mice; $P = 0.03$ for HOCl mice treated by JWH-133 versus HOCl mice; Figure 4B).

Thus, the nonselective cannabinoid agonist WIN-55,212 and the selective CB2 agonist JWH-133 counteracted the proliferative effects of HOCl on B cells and prevented the selective autoimmune response to DNA-topoisomerase 1.

CB2^{-/-} Mice Develop an Enhanced Cutaneous Fibrosis Compared with CB2^{+/+} Mice

To further evaluate the role of CB2 receptors in the development of SSc, we performed subcutaneous injections of a HOCl-generating solution or PBS in CB2^{-/-} mice and compared the extension of the induced fibrosis to that observed in CB2^{+/+} mice submitted to the same regimen. Because of the rapid establishment of the disease in CB2^{-/-} mice, all animals were killed after 3 weeks of treatment to maximize the differences. Subcutaneous injections of HOCl every day

for three weeks induced a significant dermal thickness compared with PBS-injected mice both in CB2^{-/-} and CB2^{+/+} mice ($P < 0.0001$ for CB2^{-/-} mice and $P = 0.0002$ for CB2^{+/+} mice; Figure 5A). The dermis was thicker in CB2^{-/-} mice than in CB2^{+/+} mice ($P = 0.029$; Figure 5A). Those results were confirmed by histopathological analysis of skin biopsies, which showed more skin fibrosis in CB2^{-/-} mice than in CB2^{+/+} mice submitted to HOCl injections (Figure 5B). The concentration of acid- and pepsin-soluble type I collagen in the skin extracts of both CB2^{-/-} mice and CB2^{+/+} mice was higher than in their respective controls injected with PBS ($P = 0.029$ for CB2^{-/-} mice and $P = 0.016$ for CB2^{+/+} mice versus their respective controls; Figure 5C). The accumulation of collagen in the skin was higher in CB2^{-/-} mice than in CB2^{+/+} mice ($P = 0.029$; Figure 5C).

CB2^{-/-} Mice Develop an Earlier and Enhanced Lung Fibrosis Compared With CB2^{+/+} Mice

In addition to skin fibrosis, CB2^{-/-} mice exposed to HOCl subcutaneously for three weeks developed a lung fibrosis, as shown by the higher concentration of type I collagen in the lungs compared with PBS-injected CB2^{-/-} mice ($P = 0.016$; Figure 5D) and by histopathological analysis (Figure 5E). CB2^{+/+} mice displayed a slight lung fibrosis as shown by few foci of fibrosis on histological analysis (Figure 5E) and by a 32% increase in type I collagen content of the lung. However, after three weeks of treatment, this increase did not yet reach significance ($P = 0.413$ versus PBS-injected CB2^{+/+} mice; Figure 5, D and E).

The Rate of Skin Fibroblast Proliferation Is Higher in HOCl-CB2^{-/-} Mice Than in HOCl-CB2^{+/+} Mice

We next investigated whether CB2 modulated the growth of fibroblasts isolated from fibrotic skin areas of mice. Skin fibroblasts isolated from HOCl-CB2^{-/-} mice displayed a higher proliferation rate than fibroblasts obtained from CB2^{-/-} mice injected with PBS ($P = 0.032$; Figure 5F). Moreover, the rate of proliferation of fibroblasts isolated from HOCl-CB2^{-/-} mice was higher than that of fibroblasts from HOCl-CB2^{+/+} mice ($P = 0.032$; Figure 5F).

HOCl Injections Induced a Rapid and High Increase in Splenic B Cells in CB2^{-/-} Mice

The consequences of CB2 gene silencing on the activation of the immune system in this model of SSc were then evaluated. Subcutaneous injections of HOCl induced a significant increase in the total numbers of splenic B220⁺ B cells in CB2^{-/-} mice compared with PBS-injected CB2^{-/-} mice ($P = 0.016$; Figure 6A), but no significant difference was observed in the numbers of splenic B cells in HOCl-CB2^{+/+} mice compared with PBS-injected CB2^{+/+} controls ($P = 0.86$; Figure 6A) after only three weeks of HOCl injections.

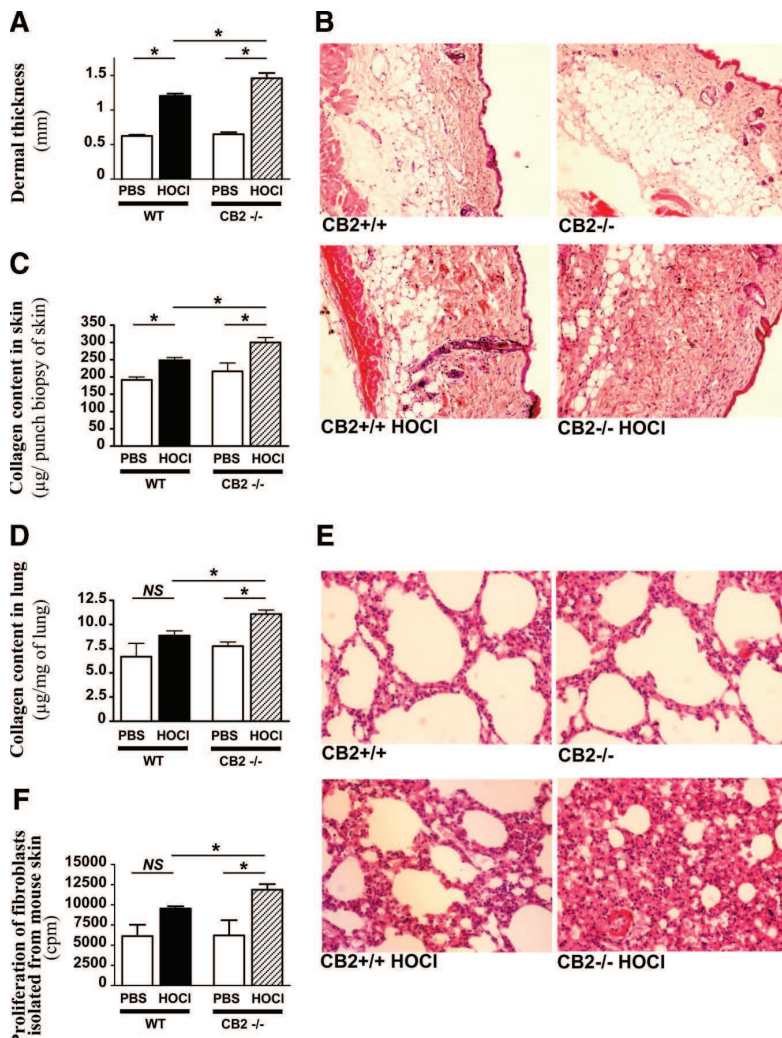


Figure 5. Effect of CB2 silencing on HOCl-induced skin and lung fibrosis. CB2^{+/+} and CB2^{-/-} C57BL/6 mice were injected daily for 3 weeks with either an HOCl-generating agent or PBS ($n = 7$ per group). Skin and lungs from those mice were collected at the time of sacrifice. **A:** Dermal thickness, as measured on skin in the injected areas of CB2^{+/+} and CB2^{-/-} C57BL/6 mice treated or not with HOCl. **B:** Representative skin sections taken in the injected areas from CB2^{+/+} and CB2^{-/-} C57BL/6 mice treated or not with HOCl. Tissue sections were stained with hematoxylin and eosin (Olympus DP70 Controller, $\times 10$). Skin fibrosis was increased in CB2^{-/-} mice. **C:** Collagen content in 6-mm punch biopsies of skin as measured by the quantitative dye-binding Sircol method. **D:** Collagen content in lung as measured by the quantitative dye-binding Sircol method. **E:** Representative lung sections from CB2^{+/+} and CB2^{-/-} C57BL/6 mice treated or not with HOCl. Tissue sections were stained with hematoxylin and eosin (Olympus DP70 Controller, $\times 10$). CB2^{-/-} mice displayed earlier and more extensive lung damages compared with CB2^{+/+} mice after HOCl exposure. **F:** Spontaneous rate of proliferation of fibroblasts isolated from fibrotic skin of CB2^{+/+} and CB2^{-/-} C57BL/6 mice submitted to HOCl or PBS injections. Skin biopsies from the injected areas were collected at the time of sacrifice. Fibroblasts were isolated by collagenase digestion of the skin, then cultured in complete medium. Fibroblast proliferation was determined by pulsing the cells with [³H]thymidine (1 μCi per well) during the last 16 hours of culture. Results are expressed as absolute counts per minute (cpm). In **A**, **C**, **D**, and **F**, values are means \pm SEM of data. Mean values were compared using unpaired Mann-Whitney *U* tests. * $P < 0.05$; NS indicates nonsignificant.

CB2^{-/-} Mice Exposed to HOCl Display a Strong and Selective Autoimmune Response Directed Toward DNA-Topoisomerase 1

Finally, we tested the effect of the inhibition of CB2 signaling on the specific autoimmune response that characterizes the cutaneous diffuse form of SSc. As previously observed in BALB/c mice, no significant levels of anti-DNA IgG Abs, anticardiolipine IgG Abs, or rheumatoid factors were detected in the sera of CB2^{+/+} or CB2^{-/-} C57BL/6 mice after three weeks' HOCl exposure, whereas both CB2^{+/+} and CB2^{-/-} mice developed anti-DNA topoisomerase 1 IgG AAbs ($P = 0.032$ for CB2^{+/+} mice and $P = 0.016$ for CB2^{-/-} mice versus the respective PBS-injected control mice; Figure 6B and data not shown). In addition, the level of anti-DNA topoisomerase 1 IgG Abs was higher in HOCl-CB2^{-/-} mice than in HOCl-CB2^{+/+} mice ($P = 0.032$; Figure 6B).

Discussion

In this article, we have shown that the cannabinoid pathway is involved in the control of skin and lung fibrosis and of autoimmunity in SSc. Consequently, we suggest that cannabinoid agonists could represent a new treatment in this life-threatening disease.

In addition to their well-characterized psychoactive effects, cannabinoids display a broad range of properties, through the binding to their receptors CB1 and CB2. These receptors control several central and peripheral functions including neuronal transmission, cardiovascular functions, inflammation, and autoimmunity. They can also modulate cell motility, proliferation, and apoptosis.⁴ In our hands, both nonselective CB1/CB2 and selective CB2 agonists prevent systemic fibrosis in a recently described murine model of SSc mimicking the human disease. The disease, induced by chronic subcutaneous

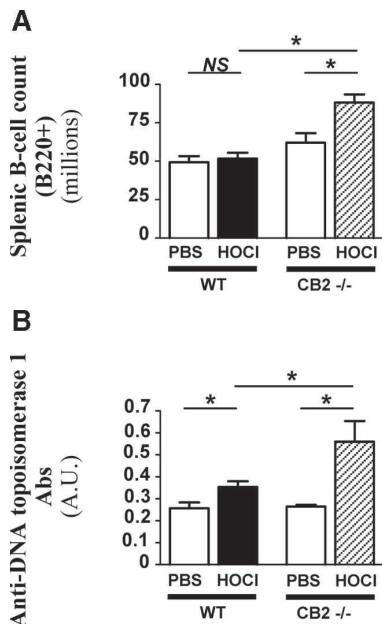


Figure 6. CB2 silencing increased splenic B220⁺ B cell count and anti-DNA-topoisomerase 1 AAb production in HOCl-C57BL/6 mice. CB2^{+/+} and CB2^{-/-} C57BL/6 mice were injected daily for 3 weeks with either an HOCl-generating agent or PBS ($n = 7$ per group). Spleen and sera from those mice were collected at the time of sacrifice. **A:** Absolute numbers of splenic B220-positive B cells as assessed by flow cytometry. **B:** Levels of serum anti-DNA-topoisomerase 1 AAbs as detected by ELISA. Values are means \pm SEM of data gained from all mice. Mean values were compared using unpaired Mann-Whitney *U* tests. * $P < 0.05$; NS indicates nonsignificant.

injections of agents generating hypochlorous acid (HOCl),²⁵ includes cutaneous and lung fibrosis, kidney involvement, and the production of serum anti-DNA topoisomerase 1 AAbs—all features that characterize diffuse cutaneous SSc in humans. Moreover, in these mice, the lung fibrosis is associated with a T cell infiltrate, similar to that observed in human SSc. Experiments performed in SCID mice suggest that B and T lymphocytes are not required for the development of the disease in this new model of SSc. However, the extent of the HOCl-induced pulmonary fibrosis was lower in SCID mice than in immunocompetent mice, indicating that the immune system synergizes with the direct effects of oxidative molecules for the full development of the systemic disease.²⁵ In this model, cannabinoid agonists can counteract the profibrogenic effect of HOCl on skin and lung. Conversely, mice lacking the CB2 receptor are more susceptible to HOCl and develop enhanced and accelerated skin and lung fibrosis. If CB2 receptor agonists have been found to inhibit LPS-induced pulmonary inflammation,³² this is the first report showing the role of the cannabinoid pathway in lung fibrosis. On the other hand, several studies have previously shown the antifibrogenic role of cannabinoid agonists in dermal, cardiac, and liver fibrosis. In a recent work by Akhmetshina et al,²⁴ treating mice by the CB2 agonist JWH-133 prevented the profibrotic effect of bleomycin in the skin. In the same model, inhibiting of CB2 signaling increased bleomycin-induced dermal fibrosis. CB2 stimulation by JWH-133 has been shown to protect

murine hearts against fibrosis after myocardial infarction, whereas hearts from CB2^{-/-} mice displayed fibrosis, myocyte hypertrophy, and cardiac dysfunction four weeks after ischemia/reperfusion injury.¹³ In addition, evidence has been reported for the involvement of the cannabinoid pathway in liver fibrosis. Thus, the expression of CB1 and CB2 receptors is up-regulated in cirrhotic liver,¹¹ but CB1 and CB2 stimulations exert opposite effects. Indeed, whereas CB1 is profibrogenic, CB2 activation abrogates the fibrotic process by arresting growth and triggering the apoptosis of myofibroblasts in human cirrhotic liver *in vitro*.¹² In line with this result, mice lacking CB2 receptors develop enhanced liver fibrosis after chronic carbon tetrachloride treatment.¹² Furthermore, CB2 activation not only limits the development of fibrosis but can induce the regression of pre-existing fibrosis, as demonstrated in cirrhotic rats. In those animals, JWH-133 decreases the inflammatory infiltrate in the liver, the number of activated stellate cells and the extension of the fibrosis and increases the expression of the matrix metalloproteinase MMP-2.²² We also observed a tendency of pre-existing skin fibrosis to decrease in our mouse model of systemic fibrosis with the cannabinoid agonist WIN-55212 (see supplemental Figure S2 at <http://ajp.amjpathol.org>). Those results showing a protective role of cannabinoid agonists, especially CB2 agonists, are concordant with those previous results obtained in other fibrotic diseases.

Beside skin and visceral fibrosis, SSc is characterized by B and T cell activation and by the production of AAbs, whose targets differ in the cutaneous limited and in the cutaneous diffuse subtype of SSc. As observed in the cutaneous diffuse form of the human disease, BALB/c and C57BL/6 mice exposed to HOCl develop AAbs that selectively target DNA topoisomerase 1. In our hands, the use of agonists of cannabinoid receptors and of mice with silenced CB2 genes as well, has shown the involvement of the cannabinoid pathway to abrogate B cell proliferation and the production of anti-DNA topoisomerase 1 AAbs. The part played by the cannabinoid pathway in immune cell development and activation has been well established. Cannabinoid receptors are expressed in virtually all human peripheral blood immune cells, especially on B cells. However, both human and mouse immune cells express CB2 at higher levels than CB1.^{33,34} The best studied vegetal cannabinoid, Δ9-tetrahydrocannabinol, is immunosuppressive both *in vivo* and *in vitro*, and a reduction in B cell proliferation and in antibody production has been observed on treatment with cannabinoid agonists.^{20,35} Our results in a mouse model of SSc are in agreement with those observations and with the beneficial effects of cannabinoid agonists in other mouse models of inflammatory autoimmune diseases, such as collagen-induced arthritis³⁶ and experimental autoimmune encephalitis.³⁷

Altogether, the effects of cannabinoid agonists on fibrogenesis, on the immune system, and on endothelial activation can associate to abrogate the development of SSc. However, the mechanisms through which the cannabinoid pathway controls fibrosis are not fully understood and may be different according to the topography

of the phenomenon and to its etiology. In our hands, cannabinoid agonists significantly decrease *in vitro* and *in vivo* the proliferation rates of dermal fibroblasts. These data argue for a direct role of the cannabinoid pathway on fibroblasts to limit the fibrotic process. It is in agreement with the demonstration that, in hepatic myofibroblasts derived from human cirrhotic liver, CB2 agonists induce both growth arrest and apoptosis through COX-2 activation and reactive oxygen species production, respectively.¹² Importantly, in our experiments, the nonselective CB1 and CB2 agonist WIN-55,212 dramatically reduces the proliferation rate of fibroblasts *in vitro*, whereas JWH-133, a selective CB2 agonist, exerts a more moderate inhibitory effect on the proliferation of fibroblasts. Nevertheless, JWH-133 limits the development of skin and lung fibrosis as efficiently as WIN-55,212 in mice exposed to HOCl. Thus, the cannabinoid system might affect the outcome of fibrosis not only by reducing fibroblast proliferation but also indirectly by controlling B cell activation. Consistent with this hypothesis, we observed a decrease in B cell proliferation and in the production of anti-DNA topoisomerase 1 AAbs in mice treated with agonists of cannabinoid receptors and in CB2^{-/-} mice. Other reports are consistent with this hypothesis, suggesting that the cannabinoid pathway limits the fibrotic process by controlling the inflammatory response.^{14,18} In mice exposed to bleomycin, CB2 mediates its antifibrogenic properties by inhibiting leukocyte infiltration in the skin.²⁴ In this model of fibrosis, the increased susceptibility of CB2^{-/-} mice to experimental fibrosis was fully replicated by transplantation of CB2-deficient bone marrow cells into CB2^{+/+} mice.²⁴ In cardiac remodeling after ischemia/reperfusion injuries, CB2 activation prevents fibroblast activation and limits macrophage infiltration and TGF- β production.¹³ In addition, the cannabinoid system has been shown to activate the synthesis of matrix metalloproteinases that control collagen deposition.^{22,38}

In conclusion, modulation of the endocannabinoid system is a novel approach for the treatment of various inflammatory diseases. SSc appears as a privileged condition because the cannabinoid pathway modulates fibroblast proliferation, immune cell activation, and the interaction between endothelial cells and immune cells, all targets that determine the tissular damages in SSc. In this report, we demonstrate for the first time the highly protective role of cannabinoid agonists in SSc. Because these agonists are available and well-tolerated under clinical conditions, our data offer a new therapeutic opportunity in this life-threatening disease.

References

- LeRoy EC, Medsger TAJ: Criteria for the classification of early systemic sclerosis. *J Rheumatol* 2001; 28:1573–1576
- Herrick AL, Matucci Cerinic M: The emerging problem of oxidative stress and the role of antioxidants in systemic sclerosis. *Clin Exp Rheumatol* 2001; 19:4–8
- Lunardi C, Bason C, Navone R, Millo E, Damonte G, Corrocher R, Puccetti A: Systemic sclerosis immunoglobulin G autoantibodies bind the human cytomegalovirus late protein UL94 and induce apoptosis in human endothelial cells. *Nat Med* 2000; 6:1183–1186
- De Petrocellis L, Di Marzo V: An introduction to the endocannabinoid system: from the early to the latest concepts. *Best Pract Res Clin Endocrinol Metab* 2009; 23:1–15
- Caraceni P, Domenicali M, Giannone F, Bernardi M: The role of the endocannabinoid system in liver diseases. *Best Pract Res Clin Endocrinol Metab* 2009; 23:65–77
- Springs AE, Karmaus PW, Crawford RB, Kaplan BL, Kaminski NE: Effects of targeted deletion of cannabinoid receptors CB1 and CB2 on immune competence and sensitivity to immune modulation by Delta9-tetrahydrocannabinol. *J Leukoc Biol* 2008; 84:1574–1584
- Croxford JL, Yamamura T: Cannabinoids and the immune system: potential for the treatment of inflammatory diseases? *J Neuroimmunol* 2005; 166:3–18
- McPartland JM: Expression of the endocannabinoid system in fibroblasts and myofascial tissues. *J Bodyw Mov Ther* 2008; 12:169–182
- Waldeck-Weiermair M, Zoratti C, Osibow K, Balenga N, Goessnitzer E, Waldhoer M, Malli R, Graier WF: Integrin clustering enables anandamide-induced Ca²⁺ signaling in endothelial cells via GPR55 by protection against CB1-receptor-triggered repression. *J Cell Sci* 2008; 121:1704–1717
- Lépicié P, Lagreux C, Sirois MG, Lamontagne D: Endothelial CB1-receptors limit infarct size through NO formation in rat isolated hearts. *Life Sci* 2007; 81:1373–1380
- Teixeira-Clerc F, Julien B, Grenard P, Tran Van Nhieu J, Deveaux V, Li L, Serriere-Lanneau V, Ledent C, Mallat A, Lotersztajn S: CB1 cannabinoid receptor antagonism: a new strategy for the treatment of liver fibrosis. *Nat Med* 2006; 12:671–676
- Julien B, Grenard P, Teixeira-Clerc F, Tran Van Nhieu J, Li L, Karsak M, Zimmer A, Mallat A, Lotersztajn S: Antifibrogenic role of the cannabinoid receptor CB2 in the Liver. *Gastroenterology* 2005; 128:742–755
- Defer N, Wan J, Soukhanian R, Escoubet B, Perier M, Caramelle P, Manin S, Deveaux V, Bourin MC, Zimmer A, Lotersztajn S, Pecker F, Pavoine C: The cannabinoid receptor type 2 promotes cardiac myocyte and fibroblast survival and protects against ischemia/reperfusion-induced cardiomyopathy. *FASEB J* 2009; 23:2120–2130
- Batkai S, Osei-Hyiaman D, Pan H, El-Assal O, Rajesh M, Mukhopadhyay P, Hong F, Harvey-White J, Jafri A, Hasko G, Huffman JW, Gao B, Kunos G, Pacher P: Cannabinoid-2 receptor mediates protection against hepatic ischemia-reperfusion injury. *FASEB J* 2007; 21:1781–2000
- Montecucco F, Lenglet S, Brauner-Sreuther V, Burger F, Pelli G, Bertolotto M, Mach F, Steffens S: CB2 cannabinoid receptor activation is cardioprotective in a mouse model of ischemia/reperfusion. *J Mol Cell Cardiol* 2009; 46:612–620
- Pacher P, Hasko G: Endocannabinoids and cannabinoid receptors in ischaemia-reperfusion injury and preconditioning. *Br J Pharmacol* 2008; 153:252–262
- Zhang M, Adler MW, Abood ME, Ganea D, Jallo J, Tuma RF: CB2 receptor activation attenuates microcirculatory dysfunction during cerebral ischemic/reperfusion injury. *Microvasc Res* 2009; 78:86–94
- Rajesh M, Mukhopadhyay P, Batkai S, Hasko G, Liaudet L, Huffman JW, Csizsar A, Ungvari Z, Mackie K, Chatterjee S, Pacher P: CB2-receptor stimulation attenuates TNF-alpha-induced human endothelial cell activation, transendothelial migration of monocytes, and monocyte-endothelial adhesion. *Am J Physiol Heart Circ Physiol* 2007; 293:2210–2218
- Klein TW, Newton CA, Widen R, Friedman H: The effect of delta-9-tetrahydrocannabinol and 11-hydroxy-delta-9-tetrahydrocannabinol on T-lymphocyte and B-lymphocyte mitogen responses. *J Immunopharmacol* 1985; 7:451–466
- Klein TW, Newton C, Friedman H: Cannabinoid receptors and immunity. *Immunol Today* 1998; 19:373–381
- Klein TW, Lane B, Newton CA, Friedman H: The cannabinoid system and cytokine network. *Proc Soc Exp Biol Med* 2000; 225:1–8
- Munoz-Luque J, Ros J, Fernandez-Varo G, Tugues S, Morales-Ruiz M, Alvarez CE, Friedman SL, Arroyo V, Jimenez W: Regression of fibrosis after chronic stimulation of cannabinoid CB2 receptor in cirrhotic rats. *J Pharmacol Exp Ther* 2008; 324:475–483
- Karsak M, Gaffal E, Date R, Wang-Eckhardt L, Rehneit J, Petrosino S, Starowicz K, Steuder R, Schlicker E, Cravatt B, Mechoulam R, Buettner R, Werner S, Di Marzo V, Tütting T, Zimmer A: Attenuation of alaergic

- contact dermatitis through the endocannabinoid system. *Science* 2007; 316:1494–1497
24. Akhmetshina A, Dees C, Busch N, Beer J, Sarter K, Zwerina J, Zimmer A, Distler O, Schett G, Distler JHW: The cannabinoid receptor CB2 exerts antifibrotic effects in experimental dermal fibrosis. *Arthritis Rheum* 2009; 60:1129–1136
 25. Servettaz A, Gouvestre C, Kavian N, Nicco C, Guipain P, Chéreau C, Vuiblet V, Guillevin L, Mouton L, Weill B, Batteux F: Selective oxidation of DNA topoisomerase 1 induced systemic sclerosis in the mouse. *J Immunol* 2009; 182:5855–5864
 26. Buckley NE, McCoy KL, Mezey E, Bonner T, Zimmer A, Felder CC, Glass M, Zimmer A: Immunomodulation by cannabinoids is absent in mice deficient for the cannabinoid CB(2) receptor. *Eur J Pharmacol* 2000; 396:141–149
 27. Servettaz A, Tamby MC, Guipain P, Reimbold J, Garcia De La Pena-Lefebvre P, Allaire Y, Kahan A, Meyer O, Guillevin L, Mouton L: Anti-endothelial cell antibodies from patients with limited cutaneous systemic sclerosis bind to centromeric protein B (CENP-B). *Clin Immunol* 2006; 120:212–219
 28. Tamby MC, Humbert M, Guipain P, Servettaz A, Dupin N, Christner JJ, Simonneau G, Fermanian J, Weill B, Guillevin L, Mouton L: Antibodies to fibroblasts in idiopathic and scleroderma-associated pulmonary hypertension. *Eur Respir J* 2006; 28:799–807
 29. Dalle Donne I, Rossi R, Giustarini D, Gagliano N, Lusini L, Milzani A, Di Simplicio P, Colombo R: Actin carbonylation: from a simple marker of protein oxidation to relevant signs of severe functional impairment. *Free Radic Biol Med* 2001; 1:1075–1083
 30. Burdick MD, Murray LA, Keane MP, Xue YY, Zisman DA, Belperio JA, Strieter RM: CXCL11 attenuates bleomycin-induced pulmonary fibrosis via inhibition of vascular remodeling. *Am J Respir Crit Care Med* 2005; 171:261–268
 31. Preud'homme JL, Rochard E, Gouet D, Danon F, Alcalay M, Touchard G, Aucouturier P: Isotypic distribution of anti-double-stranded DNA antibodies: a diagnostic evaluation by enzyme-linked immunosorbent assay. *Diagn Clin Immunol* 1988; 5:256–261
 32. Berdyshev E, Boichot E, Corbel M, Germain N, Lagente V: Effects of cannabinoid receptor ligands on LPS-induced pulmonary inflammation in mice. *Life Sci* 1998; 63:125–129
 33. Schatz AR, Lee M, Condie RB, Pulaski JT, Kaminski NE: Cannabinoid receptors CB1 and CB2: a characterization of expression and adenylyl cyclase modulation within the immune system. *Toxicol Appl Pharmacol* 1997; 142:278–287
 34. Gallegue S, Mary S, Marchand J, Dussossoy D, Carriere D, Carayon P, Bouaboula M, Shire D, Le Fur G, Casellas P: Expression of central and peripheral cannabinoid receptors in human immune tissues and leukocyte subpopulations. *Eur J Biochem* 1995; 232:54–61
 35. Klein TW, Newton C, Zhu W, Daaka Y, Friedman H: Delta 9-Tetrahydrocannabinol, cytokines, and immunity to *Legionella pneumophila*. *Proc Soc Exp Biol Med* 1995; 209:205–212
 36. Malfait AM, Galily R, Sumariwalla PF, Malik AS, Andreakos E, Mechoulam R, Feldmann M: The nonpsychoactive cannabis constituent cannabidiol is an oral anti-arthritis therapeutic in murine collagen-induced arthritis. *Proc Natl Acad Sci U S A* 2000; 97:9561–9566
 37. Arevalo-Martin A, Vela JM, Molina-Holgado E, Borrell J, Guaza C: Therapeutic action of cannabinoids in a murine model of multiple sclerosis. *J Neurosci* 2003; 23:2511–2516
 38. Ramer R, Hinz B: Inhibition of cancer cell invasion by cannabinoids via increased expression of tissue inhibitor of matrix metalloproteinases-1. *J Natl Cancer Inst* 2008; 100:59–69

3.4 ARTICLE 4

Le sunitinib inhibe la phosphorylation du PDGF-récepteur β dans la peau des souris sclérodermiques et prévient le développement de la maladie.

Sunitinib inhibits the phosphorylation of PDGF-receptor β in the skin of mice with scleroderma-like features and prevents the development of the disease.

Niloufar Kavian, Amélie Servettaz, Wioleta Marut, Carole Nicco, Christiane Chéreau, Bernard Weill, Frédéric Batteux

Arthritis and Rheumatism, 2011

Les membres de la famille du "Platelet-derived growth factor" (PDGF) jouent un rôle majeur dans l'homéostasie des tissus conjonctifs chez l'adulte. On retrouve des niveaux élevés de PDGF et des récepteurs au PDGF (PDGFR) dans les biopsies de peau et de poumons de patients sclérodermiques. Des auto-anticorps activateurs anti-PDGFR sont également présents dans le sérum des patients ScS et peuvent induire dans les fibroblastes la production de FRO et l'activation des MAP kinases, conduisant à la prolifération de ces cellules. Le VEGF ("Vascular endothelial growth factor") récepteur (VEGFR) a aussi été impliqué dans la physiopathologie de la ScS. On retrouve notamment des taux élevés de VEGF-A et de VEGFR dans la peau des patients ScS, et plusieurs données suggèrent une dérégulation de cette voie dans la ScS, avec pour conséquence la microangiopathie observée chez les patients. Nous avons étudié dans ce travail les effets de deux molécules inhibitrices de tyrosine-kinase ciblant le PDGFR, le sunitinib et le sorafenib, sur le développement de la ScS. Nous avons induit la maladie chez des souris BALB/c grâce au protocole d'induction par HOCl mis au point au laboratoire, et les souris ont été traitées de manière concomitante par gavage avec le sunitinib, le sorafenib ou le placebo (PBS). Après 6 semaines, nous avons mesuré par western-blot les taux de PDGFR phosphorylé et de VEGFR phosphorylé dans les fibroblastes extraits des peaux des souris. Nous avons également évalué l'étendue de la fibrose cutanée et pulmonaire, et l'activation immunitaire par détection des auto-anticorps et analyse des populations spléniques. Nous avons observé dans les fibroblastes de peaux des souris atteintes de sclérodermie induite par HOCl une augmentation de la phosphorylation du PDGFR et du VEGFR par rapport aux fibroblastes extraits de peaux de souris témoins. Le traitement *in vivo* par le sunitinib et le sorafenib des

souris ScS a entraîné une diminution de la phosphorylation, et donc de l'activation du PDGFR et dans une moindre mesure du VEGFR. Cliniquement, les souris traitées par le sunitinib ont développé un phénotype modéré de ScS par rapport aux souris non traitées avec une fibrose cutanée et pulmonaire réduites. Cette amélioration clinique était corrélée au taux de prolifération spontanée des fibroblastes cutanés, qui était réduit chez les souris traitées par rapport aux souris non traitées. Des expériences *in vitro* nous ont montré que le sunitinib et le sorafenib avaient une action anti-proliférative sur les fibroblastes cutanés des souris ScS. Cependant le sunitinib avait une CI50 (Concentration Inhibant 50% de la prolifération) inférieure à celle du sorafenib, démontrant la supériorité de l'activité anti-proliférative du sunitinib par rapport au sorafenib. Les deux inhibiteurs de tyrosine kinase ont permis *in vivo* de réduire la production d'auto-anticorps anti-ADN Topoisomérase-1, d'IL-6 et de TGF- β par les lymphocytes B. Notre travail est ainsi le premier à décrire un effet du sunitinib sur l'activation du système immunitaire, et il est possible que cet effet mette en jeu la voie du VEGF qui joue un rôle important dans l'inflammation. Enfin, nous avons mesuré les taux sériques de VCAM soluble, un marqueur de l'atteinte endothéiale chez les souris. Ce marqueur est augmenté chez les souris ScS non traitées par rapport aux souris témoins saines, attestant l'atteinte vasculaire dans notre modèle de ScS. Le traitement *in vivo* par sunitinib et sorafenib a permis une réduction des taux de VCAM soluble relargué dans la circulation, et ainsi une amélioration de l'atteinte endothéiale.

Notre travail souligne l'activation du PDGF-R β dans les fibroblastes sclérodermiques, et le rôle central de l'axe PDGF/PDGFR β dans l'induction de la fibrose, de l'auto-immunité, et des anomalies vasculaires de la ScS. Nos résultats dans ce modèle *in vivo* suggèrent également qu'une activation de l'axe VEGF/VEGFR est délétère et directement impliquée dans la microangiopathie de la ScS. Finalement, nous suggérons que certains inhibiteurs de tyrosine kinases ciblant le PDGF-R et le VEGF-R pourraient être testés comme nouveaux outils thérapeutiques dans la ScS, agissant sur la fibrose, l'activation immunitaire et les anomalies vasculaires.

AQ:1

Sunitinib Inhibits the Phosphorylation of Platelet-Derived Growth Factor Receptor β in the Skin of Mice With Scleroderma-like Features and Prevents the Development of the Disease

Niloufar Kavian,¹ Amélie Servettaz,² Wioleta Marut,¹ Carole Nicco,¹ Christiane Chéreau,³ Bernard Weill,¹ and Frédéric Batteux³

Objective. Systemic sclerosis (SSc) is characterized by fibrosis of the skin and visceral organs, vascular dysfunction, and immunologic dysregulation. Platelet-derived growth factors (PDGFs) have been implicated in the development of fibrosis and dysregulation of vascular function. We investigated the effects of sunitinib and sorafenib, two tyrosine kinase inhibitors that interfere with PDGF signaling, in a mouse model of diffuse SSc.

Methods. SSc was induced in BALB/c mice by subcutaneous injections of HOCl daily for 6 weeks. Mice were randomized to treatment with sunitinib, sorafenib, or vehicle. The levels of native and phosphorylated PDGF receptor β (PDGFR β) and vascular endothelial growth factor receptor (VEGFR) in the skin were assessed by Western blot and immunohistochemical analyses. Skin and lung fibrosis were evaluated by histologic and biochemical methods. Autoantibodies were

detected by enzyme-linked immunosorbent assay, and spleen cell populations were analyzed by flow cytometry.

Results. Phosphorylation of PDGFR β and VEGFR was higher in fibrotic skin from HOCl-injected mice with SSc than from PBS-injected mice. Injections of HOCl induced cutaneous and lung fibrosis, increased the proliferation rate of fibroblasts in areas of fibrotic skin, increased splenic B cell and T cell counts, and increased anti-DNA topoisomerase I autoantibody levels in BALB/c mice. All of these features were reduced by sunitinib but not by sorafenib. Sunitinib significantly reduced the phosphorylation of both PDGF and VEGF receptors.

Conclusion. Inhibition of the hyperactivated PDGF and VEGF pathways by sunitinib prevented the development of fibrosis in HOCl-induced murine SSc and may represent a new SSc treatment for testing in clinical trials.

Supported by the European Union Seventh Framework Programme (FP7/2007-2013 grant 215009) and University Paris-Descartes. Dr. Kavian's work was supported by a grant from the Fondation pour la Recherche Médicale. Dr. Servettaz' work was supported by grants from Actelion and the Association des Sclérodermiques de France.

AQ:2

¹Niloufar Kavian, MD, PharmD, Wioleta Marut, •••, Carole Nicco, PhD, Bernard Weill, MD, PhD: Université Paris Descartes, EA1833, Hôpital Cochin, AP-HP, Paris, France; ²Amélie Servettaz, MD, PhD: Université Paris Descartes, EA1833, Hôpital Cochin, AP-HP, Paris, France, and Centre Hospitalier Universitaire de Reims and Hôpital Robert Debré, Reims, France; ³Christiane Chéreau, PharmD, Frédéric Batteux, MD, PhD: Université Paris Descartes, EA1833, ERTi, Hôpital Cochin, AP-HP, Paris, France, and Centre Hospitalier Universitaire de Reims and Hôpital Robert Debré, Reims, France.

Drs. Kavian and Servettaz contributed equally to this work.
Address correspondence to Frédéric Batteux, MD, PhD, Laboratoire d'Immunologie, Faculté de Médecine Paris Descartes, 27 Rue du Faubourg St. Jacques, 75679 Paris Cedex 14, France. E-mail: frederic.batteux@cch.aphp.fr.

Submitted for publication February 7, 2011; accepted in revised form December 15, 2011.

Systemic sclerosis (SSc) is a connective tissue disorder characterized by fibrosis of the skin and visceral organs, vascular dysfunction, and immunologic dysregulation associated with autoantibodies (1). To date, the mechanisms that determine the clinical manifestations of the disease remain unclear (2–4).

Platelet-derived growth factors (PDGFs) are potent mitogens and chemoattractants for cells of mesenchymal and neuroectodermal origin (5). Members of the PDGF family play a major role during embryonic development and contribute to the maintenance of connective tissue in adults (6). Increased levels of PDGF and PDGF receptors (PDGFRs) have been found in skin and lung biopsy samples from patients with scleroderma (7–9). Moreover, sera from patients with SSc may contain autoantibodies directed toward PDGFRs (10). These

AQ:2

antibodies can induce the production of reactive oxygen species that activate the MAP kinase/ERK-1/2 pathway and lead to fibroblast proliferation (11). Transforming growth factor β (TGF β) and interleukin-1 α (IL-1 α) can also trigger PDGFR signaling through increasing either PDGFR levels or PDGF synthesis by fibroblasts (12). Thus, SSc skin and lung fibroblasts are more sensitive to mitogenic stimulation by PDGF than normal fibroblasts are. The functional significance of the activation of PDGF signaling in fibroblasts has not been fully evaluated in scleroderma, but it may contribute to their enhanced proliferative, migratory, and contractile potential both in vitro and in vitro (13).

AQ:4 Protein tyrosine kinase inhibitors (TKIs) are a new class of therapeutic agents that were initially developed for the treatment of cancers (14,15). They can inhibit proliferative signals via the blockade of the tyrosine kinases Bcr-Abl or c-Kit. Sunitinib and sorafenib also block the tyrosine kinase activity of PDGFRs, as well as the VEGF/VEGFR pathway, which plays a role in the pathogenesis of SSc (16). The aim of this study was to investigate the effects of sunitinib and sorafenib in the HOCl-induced mouse model of SSc (17). We found that these TKIs prevent fibrosis development, immune activation, and endothelial dysfunction in SSc, and thus appear to be attractive therapeutic tools for this disease.

MATERIALS AND METHODS

AQ:5 **Animals, cells, and chemicals.** Six-week-old female BALB/c mice were purchased from Harlan and were given humane care according to our institutional guidelines. The project was approved by the Regional Ethics Committee on Animal Experimentation. All chemicals were obtained from Sigma, except for sunitinib, which was from Pfizer, and sorafenib, which was from Bayer Health Care.

Experimental procedure. Induction of SSc. Mice were randomly distributed into experimental and control groups ($n = 14$ per group). A total of 200 μ L of substances that generate HOCl was injected intradermally into the back of the mice everyday for 6 weeks, as previously described (17). Control groups received injections of 200 μ L of sterilized phosphate buffered saline (PBS).

Treatment with TKIs. Each mouse receiving subcutaneous injections was randomized to receive 6 weeks of oral treatment (by gavage) with sunitinib (50 mg/kg/day), sorafenib (50 mg/kg/day), or vehicle alone. The dosage of 50 mg/kg/day was chosen as being consistent with the report from the European Medicines Agency on sunitinib malate and sorafenib tosylate.

One week after the end of the injections and treatment, the animals were euthanized by cervical dislocation. Lungs were collected, and biopsies of the skin of the back were performed with a punch (6 mm in diameter). Samples for determination of collagen content were stored at -80°C.

Samples for histopathologic analysis were fixed in 10% formalin.

Immunofluorescence analysis of skin sections. Diseased skin was taken from each mouse in each treated and untreated group. Formalin-fixed paraffin-embedded skin sections were dewaxed, and an enzymatic antigen retrieval method was used to overcome antigen masking. Slides were washed for 1 hour at room temperature with sodium borohydride and then blocked with mouse serum. Slides were stained overnight at 4°C with a 1:200 dilution of anti-PDGFR β , anti-phosphorylated PDGFR β , anti-VEGFR, or anti-phosphorylated VEGFR monoclonal antibodies or with isotype control (all from Santa Cruz Biotechnology). A secondary fluorescein isothiocyanate (FITC)-labeled antibody was then applied, and after washing in PBS, slides were examined using an Olympus microscope equipped with an epifluorescence system. Photographs were captured with an Olympus DP70 **AQ:6** camera and analyzed with accompanying controller software as previously described (18).

Western blot experiments. Proteins for pPDGFR/PDGFR analysis were extracted from purified primary skin fibroblasts; those for pVEGFR/VEGFR analysis were extracted from the skin. Proteins (30 μ g per sample) were subjected to immunoprecipitation with PDGFR β antibodies and VEGFR antibodies, respectively, using a protein G immunoprecipitation kit (Sigma-Aldrich). Samples were then subjected to 10% polyacrylamide gel electrophoresis, transferred onto nitrocellulose membranes, blocked for 2 hours with 5% dry milk in Tris buffered saline-Tween (TBST), and then incubated overnight at 4°C with anti-PDGFR β antibody, anti-phosphorylated PDGFR β antibody Tyr¹⁰²¹, anti-VEGFR (fetal liver kinase 1) antibody, or anti-phosphorylated VEGFR antibody Tyr⁹⁹⁶. The membranes were then washed and incubated for 1 hour at room temperature with a horseradish peroxidase-conjugated secondary antibody (all from Santa Cruz Biotechnology).

For α -smooth muscle actin (α -SMA) Western blots, primary skin fibroblasts were treated with several doses of sorafenib or sunitinib. Cell pellets were then thawed and mixed in radioimmunoprecipitation assay buffer and stored at -80°C. Proteins were then subjected to 10% polyacrylamide gel electrophoresis, transferred onto nitrocellulose membranes, blocked for 1 hour with 5% dry milk in TBST, and then incubated overnight at 4°C with an anti- α -SMA antibodies diluted 1:2,000 (clone 1A4; Sigma-Aldrich). As an internal control, we used β -actin.

Assessment of dermal thickness. The thickness of the skin of the shaved back of each mouse was measured with calipers, and the results were expressed in millimeters. Measurements were performed every week and on the day of euthanization by the same operator. Two sides on the back of each mouse were measured, and the mean was calculated and recorded.

Histopathologic analysis. A 5- μ m-thick tissue section was prepared from the midportion of paraffin-embedded lung and skin pieces and stained with hematoxylin and eosin. Slides were examined under standard brightfield microscopy (Olympus BX60 microscope) by a pathologist who was blinded to the group assignment of the animal.

Measurement of collagen content in skin and lung tissues. Skin and lung pieces were diced using a sharp scalpel and were mixed with pepsin (1:10 weight ratio) and 0.5M acetic

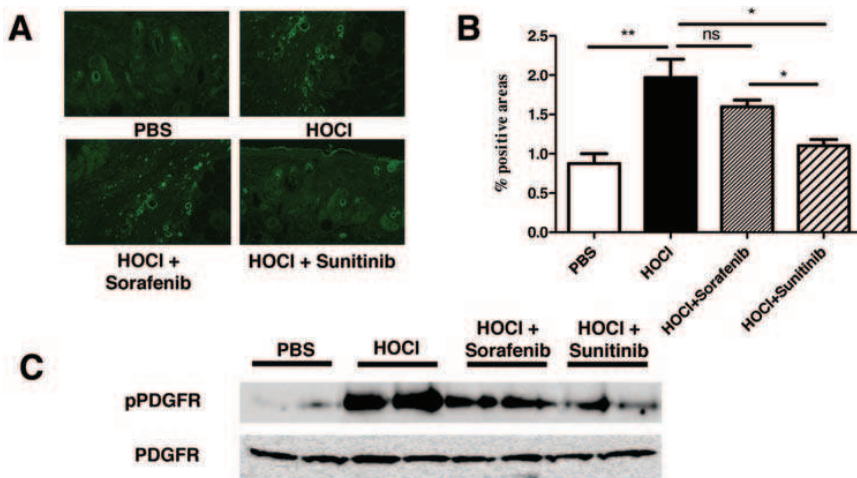


Figure 1. Effects of sunitinib and sorafenib on the levels of platelet-derived growth factor receptor (PDGFR) and phosphorylated PDGFR in the skin of mice exposed to HOCl. **A**, Detection of pPDGFRs by immunofluorescence in skin sections from a representative mouse from each of the 4 experimental groups ($n = 7$ per group): phosphate buffered saline (PBS) injected, HOCl injected, HOCl injected and sorafenib treated, and HOCl injected and sunitinib treated. Original magnification $\times 200$. **B**, Quantification of pPDGFR staining in skin sections, as determined using ImageJ software. Values are the mean \pm SEM of 7 mice per group. * = $P < 0.05$; ** = $P < 0.001$ by Mann-Whitney unpaired U test. NS = not significant. **C**, Levels of native and phosphorylated PDGFR, as determined by Western blotting of protein extracts from purified fibroblasts isolated from mouse skin. β -actin was used as an internal control. Levels of pPDGFR were increased in skin fibroblasts from HOCl-injected mice. Sunitinib down-regulated the phosphorylation of PDGFR. Results are from 2 representative mice ($n = 7$ per group).

acid overnight at room temperature, with constant stirring. The collagen content assay was based on the quantitative dye-binding Sircol method (Biocolor) (19).

Isolation of skin fibroblasts and proliferation assays. Skin fibroblasts were extracted as previously described. Primary fibroblasts (2×10^3 /well) were seeded in 96-well plates and incubated for 48 hours with 150 μ l of culture medium or a solution of sorafenib (0.75–100 mg/ml) or sunitinib (0.16–25 mg/ml). Cell proliferation was determined by pulsing the cells with 3 H-thymidine (1 μ Ci/well) during the last 16 hours of culture. Results were expressed as absolute counts per minute or as the ratio of the absolute counts per minute with sorafenib or with sunitinib to the absolute counts per minute with medium alone.

Detection of serum antibodies. Levels of anti-DNA topoisomerase I IgG (anti-topo I IgG) antibodies were detected using DNA topo I-coated enzyme-linked immunosorbent assay (ELISA) microplates (ImmunoVision). A 1:50 serum dilution was used for the determination of anti-topo I IgG antibodies.

Flow cytometric analysis of spleen cell subsets. Cell suspensions from spleens were prepared after hypotonic lysis of erythrocytes. Cells were incubated with the appropriate labeled antibodies for 45 minutes at 4°C in PBS with 0.1% sodium azide and 5% normal rat serum. Cells were then analyzed with a FACSCanto flow cytometer (BD Biosciences). The antibodies used in this study were FITC-conjugated anti-CD11b, phycoerythrin (PE)-conjugated anti-B220, allophycocyanin (APC)-Cy7-conjugated anti-CD4, PE-Cy7-conjugated anti-CD8, PerCP-Cy-conjugated anti-CD3, PE-

conjugated anti-CD11b, and FITC-conjugated anti-B7.1 monoclonal antibodies (BD PharMingen).

ELISA determination of IL-6 and TGF β production by B cells. B cells were isolated from splenocytes with CD45R (B220) microbeads and MS columns according to the manufacturer's instructions (Miltenyi Biotec). B cell suspensions were then seeded (1×10^6 cells) in 96-well flat-bottomed plates and cultured for 48 hours in complete medium in the presence of 10 μ g/ml of lipopolysaccharide (Sigma-Aldrich). Supernatants were collected, and IL-6 and TGF β concentrations determined by ELISA (eBioscience). Results are expressed in nanograms per milliliter.

ELISA determination of soluble vascular cell adhesion molecule (sVCAM) in serum. Levels of sVCAM in mouse serum were measured by ELISA. A 1:800 serum dilution and a mouse sVCAM/CD106 DuoSet kit were used according to the manufacturer's instructions (R&D Systems).

Statistical analysis. All quantitative data were expressed as the mean \pm SEM. Data were compared using a nonparametric Mann-Whitney test or Student's paired *t*-test. When the analysis included more than 2 groups, one-way analysis of variance was used. P values less than 0.05 were considered significant.

RESULTS

High levels of phosphorylated PDGFR β in skin fibroblasts from mice with HOCl-induced fibrosis. Higher amounts of phosphorylated PDGFR β were

RESEARCH

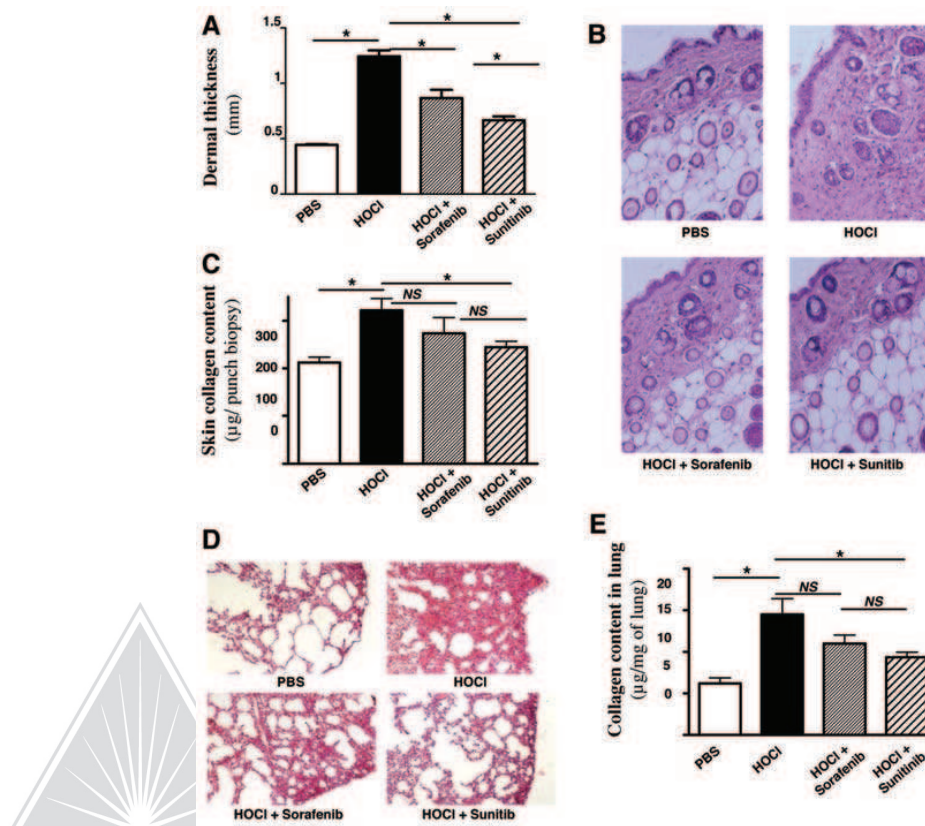


Figure 2. Effects of sunitinib and sorafenib on skin and lung collagen contents following subcutaneous injections of an HOCl-generating agent or phosphate buffered saline (PBS) in BALB/c mice ($n = 7$ per group). Skin and lungs were collected at the time of euthanization. **A**, Dermal thickness in the injected areas of skin from the 4 experimental groups of BALB/c mice. **B**, Representative sections of injected skin from BALB/c mice. Fibrosis was inhibited by sunitinib more than by sorafenib. Hematoxylin and eosin stained; original magnification $\times 20$. **C**, Collagen content in skin samples obtained with a 6-mm punch biopsy, as measured by the quantitative dye-binding Sircol method. **D**, Representative sections of lung from BALB/c mice. Lung fibrosis was inhibited by sunitinib more than by sorafenib. Hematoxylin and eosin stained; original magnification $\times 20$. **E**, Collagen content in the lung, as measured by the quantitative dye-binding Sircol method. Sunitinib inhibited both skin and lung fibrosis. Values in **A**, **C**, and **E** are the mean \pm SEM of 7 mice per group. * = $P < 0.05$ by Mann-Whitney unpaired U test. NS = not significant.

found in fibrotic areas of skin from HOCl-injected mice than in skin from PBS-injected mice, as demonstrated by immunohistochemistry (Figures 1A and B) and by Western blotting using protein extracts from fibroblasts (Figure 1C). Treatment of mice with HOCl-induced SSc with the TKI sunitinib abrogated the phosphorylation of PDGFR β in skin fibroblasts, whereas phosphorylated PDGFRs could still be detected in the skin of mice with SSc treated with sorafenib (Figures 1A–C). No significant difference in the expression of nonphosphorylated PDGFRs in mice exposed to HOCl versus control mice exposed to PBS was observed (Figures 1B and C).

Better prevention of skin fibrosis in HOCl-injected mice by sunitinib than by sorafenib. As previously observed, subcutaneous injections of HOCl in BALB/c mice increased dermal thickness and the concentration of acid- and pepsin-soluble type I collagen in the skin as compared with injections of PBS ($P < 0.001$ for dermal thickness and $P = 0.003$ for collagen concentration in the skin) (Figures 2A and C). Histopathologic analysis confirmed the presence of dermal fibrosis (Figure 2B).

To evaluate whether the inhibition of tyrosine kinases affects the development of dermal fibrosis in this

model of SSc, mice exposed to HOCl were simultaneously treated with sorafenib or sunitinib, two different TKIs that interfere with the PDGF pathway.

Sorafenib moderately reduced the dermal thickness ($P = 0.001$) and the accumulation of collagen ($P = 0.529$) induced by HOCl as compared with untreated mice exposed to HOCl (Figures 2A and C). These results were confirmed by histopathologic analysis of skin biopsy samples stained with hematoxylin and eosin (Figure 2B), which showed a moderate decrease in dermal thickness in HOCl-injected BALB/c mice treated with sorafenib.

In contrast, sunitinib significantly reduced dermal thickness and accumulation of collagen in the skin of HOCl-injected mice ($P = 0.0003$ and $P = 0.039$, respectively, versus untreated HOCl-injected mice) (Figures 2A and C). These results were confirmed by histopathologic analysis (Figure 2B).

Better prevention of lung fibrosis in HOCl-injected mice by sunitinib than by sorafenib. In addition to skin fibrosis, HOCl-injected mice developed lung fibrosis, as shown by histopathologic analysis (Figure 2D) and by the higher concentration of type I collagen in the lungs of HOCl-injected mice than in PBS-injected mice ($P < 0.001$) (Figure 2E). Sorafenib did not abrogate the development of lung fibrosis induced by HOCl, as shown by histopathologic analysis and by the accumulation of type I collagen in lungs ($P = 0.139$ versus untreated HOCl-injected mice) (Figures 2D and E).

In contrast, sunitinib significantly reduced the concentration of type I collagen in the lungs as compared with untreated HOCl-injected mice ($P = 0.012$) (Figure 2E). These findings were confirmed by histopathologic analysis of lung biopsy sections stained with hematoxylin and eosin (Figure 2D), which showed a more marked decrease in lung fibrosis in BALB/c mice treated with sunitinib than in untreated HOCl-injected mice.

Analysis of bronchoalveolar lavage fluid from 4 mice showed a significant increase in the numbers of total leukocytes ($P = 0.029$), neutrophils ($P = 0.028$), monocytes ($P = 0.036$), and lymphocytes ($P = 0.032$) in HOCl-injected mice, which were decreased with sunitinib ($P = 0.079$, $P = 0.88$, and $P = 0.048$, respectively) (data not shown).

Normalization of the rate of dermal fibroblast proliferation by sunitinib and sorafenib treatment. We next investigated whether treatment with various TKIs modified the growth of fibroblasts isolated from the fibrotic skin of mice with SSc. As previously reported, skin fibroblasts isolated from HOCl-injected mice dis-

played a higher rate of proliferation than did fibroblasts from mice injected with PBS ($P = 0.007$) (Figure 3A). The rate of proliferation of fibroblasts isolated from HOCl-injected mice treated with sorafenib or sunitinib was lower than that of fibroblasts isolated from HOCl-injected mice treated with PBS ($P = 0.028$ for sorafenib and $P < 0.001$ for sunitinib) (Figure 3A). Sunitinib was more efficient than sorafenib in reducing the rate of dermal fibroblast proliferation ($P = 0.019$) (Figure 3A).

We then analyzed the in vitro effects of both TKIs on fibroblast proliferation. At low doses (0.16–0.75 mg/ml), sunitinib had no effect, whereas at 3.125 mg/ml, the proliferation rate was reduced by 75% (Figure 3C). In vitro treatment with sorafenib also had major effects on fibroblast proliferation, but effective doses were 4 times higher than the effective doses of sunitinib (Figure 3D). Indeed, the 50% inhibition concentration (IC_{50}) of sunitinib was 2.75 mg/ml, whereas for sorafenib, the IC_{50} was 9.75 mg/ml ($P = 0.029$). These results were confirmed by Western blotting showing α -SMA expression in fibroblasts after in vitro exposure to different doses of sorafenib or sunitinib (Figure 3B).

Decreased serum levels of HOCl-induced anti-topo I autoantibodies by sunitinib and sorafenib treatment. We next tested the effects of the two TKIs on the specific autoimmune response to DNA topo I that characterizes the diffuse cutaneous SSc phenotype. IgG antibodies directed toward DNA topo I were found, as usual, in the sera of mice exposed to HOCl for 6 weeks ($P < 0.001$ versus PBS-injected mice) (Figure 4C). As previously observed, no significant levels of other autoantibodies, such as anti-DNA IgG antibodies, anti-cardiolipin IgG antibodies, or rheumatoid factors, could be detected in the sera of HOCl-injected mice (data not shown).

Both sunitinib and sorafenib prevented the development of anti-topo I IgG antibodies in mice exposed to HOCl ($P < 0.001$ for comparison of each TKI versus untreated mice) (Figure 4C).

Decreased expansion of splenic B cells in HOCl-injected mice by sunitinib, but not sorafenib, treatment. We next investigated the effects of the 2 TKIs on the different spleen cell populations. Daily subcutaneous exposure to HOCl for 6 weeks increased the numbers of splenic B220+ B cells and CD4+ T cells in the HOCl-injected mice as compared to PBS-injected mice ($P < 0.001$ for each comparison) (Figures 4A and B). Sunitinib prevented the increase in splenic B cell and CD4+ T cell numbers in mice exposed to HOCl ($P = 0.002$ and $P = 0.004$, respectively, versus untreated mice) (Figures 4A and B). Moreover, treatment with sunitinib

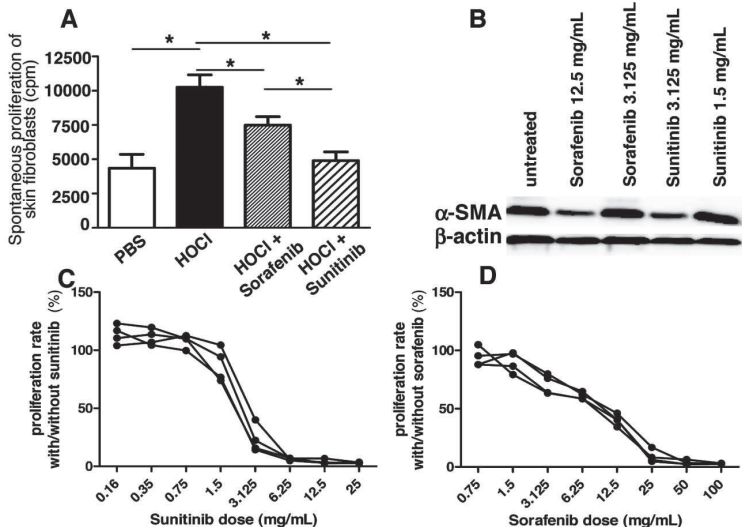


Figure 3. Proliferative properties of skin fibroblasts. **A**, Fibroblasts were isolated from injected areas of skin of the 4 experimental groups obtained at the time of euthanization, and cell proliferation was determined by measurement of ^3H -thymidine ($1 \mu\text{Ci}/\text{well}$) incorporation during the last 16 hours of culture. Fibroblasts from HOCl-injected mice treated with sunitinib showed a lower proliferation rate than those from HOCl-injected mice treated with vehicle alone. Values are the mean \pm SEM. * = $P < 0.05$ by Mann-Whitney unpaired U test. NS = not significant; PBS = phosphate buffered saline. **B–D**, Fibroblasts from HOCl-injected mice were isolated and treated in vitro with various doses of sunitinib or sorafenib. Western blotting for the expression of α -smooth muscle actin (α -SMA) was performed in untreated cells and in cells treated with 2 different concentrations of sorafenib or sunitinib (**B**). β -actin was used as an internal control. The fibroblast proliferation rate was measured after exposure to increasing concentrations of sunitinib (**C**) or sorafenib (**D**). Results in **C** and **D** are expressed as the ratio of proliferation with sunitinib or sorafenib, respectively, to the proliferation with medium alone.

AQ: 20

AQ: 12

AQ: 13

reduced the expression of B7.1 on splenic B cells ($P = 0.0089$). Sorafenib tended to decrease B cell and CD4+ T cell numbers and B7.1 expression on B cells, but these results didn't achieve significance ($P = 0.095$, $P = 0.48$, and $P = 0.21$, respectively) (Figures 4A, B, and D).

Reduced production of IL-6 and TGF β by B cells in HOCl-injected mice by sunitinib, but not sorafenib, treatment. Since sunitinib and sorafenib exerted beneficial effects on autoantibody production and B cell activation, we tested their actions on the production of profibrotic cytokines by B cells. Both sorafenib and sunitinib decreased the production of IL-6 ($P = 0.032$ and $P = 0.029$, respectively) and TGF β ($P = 0.097$ and $P = 0.010$, respectively) (Figures 4E and F).

Significant reduction of phosphorylated VEGFR concentrations in the skin of mice with HOCl-induced fibrosis by sunitinib treatment. Since VEGF signaling has been found to be abnormal in SSc patients, we investigated the level of phosphorylation of VEGF receptors in the fibrotic skin of HOCl-injected mice and the effect of the two TKIs on this pathway. Higher levels of phosphorylated VEGFRs were detected in the dis-

• TREATMENT • RESEARCH

eased areas of skin from HOCl-injected mice than in skin from control mice (Figure 5). Sunitinib prevented the phosphorylation of this receptor, since no phosphorylated VEGFRs were found in the diseased areas of skin from HOCl-injected mice treated with sunitinib, as assessed by immunohistochemistry and Western blotting (Figure 5). In contrast, sorafenib had only a weak effect (Figure 5).

Prevention of increased serum levels of VCAM by sunitinib and sorafenib treatment. Elevated serum levels of markers of endothelial cell damage such as sVCAM are observed in SSc. This was confirmed in mice exposed to HOCl as compared with those exposed to PBS ($P = 0.037$) (Figure 6). Sunitinib and sorafenib prevented the increase in sVCAM in mice exposed to HOCl ($P = 0.015$ for sunitinib versus vehicle alone and $P = 0.010$ for sorafenib versus vehicle alone) (Figure 6).

DISCUSSION

In the present study, we describe the hyperactivation of PDGFR β and VEGFR in areas of fibrotic skin

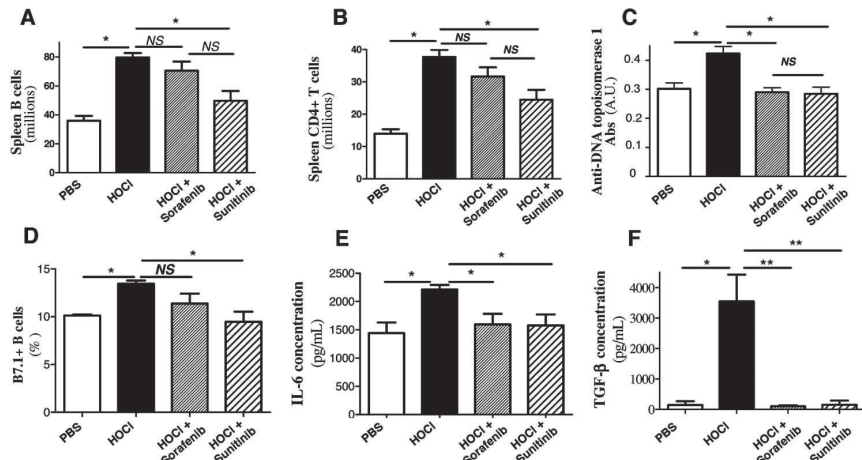


Figure 4. Effects of sunitinib and sorafenib on spleen cells, anti-DNA topoisomerase I (anti-topo I) autoantibody production, and interleukin-6 (IL-6) and transforming growth factor β (TGF β) production. BALB/c mice were injected daily for 6 weeks with either an HOCl-generating agent or phosphate buffered saline (PBS) and treated with sunitinib, sorafenib, or vehicle alone. Spleens and sera were collected at the time of euthanization, and cells were enumerated by flow cytometry. **A**, Total numbers of B220+ cells in the spleen. **B**, Total numbers of CD4+ T cells in the spleen. **C**, Levels of anti-topo I antibodies (Abs), as determined by enzyme-linked immunosorbent assay (ELISA) in sera, expressed in arbitrary units (AU). **D**, Percentages of B7.1+ B cells in the spleen. **E**, Concentrations of IL-6 in supernatants from B cells stimulated for 48 hours with lipopolysaccharide (LPS). **F**, Concentrations of TGF β in supernatants from B cells stimulated for 48 hours with LPS. Sunitinib treatment decreased splenic B cell and CD4+ T cell numbers, the concentration of anti-topo I antibodies, and the level of activation of B cells. Values are the mean \pm SEM of 7 mice per group. * = $P < 0.05$; ** = $P < 0.01$ by Mann-Whitney unpaired U test. NS = not significant.

AQ: 21

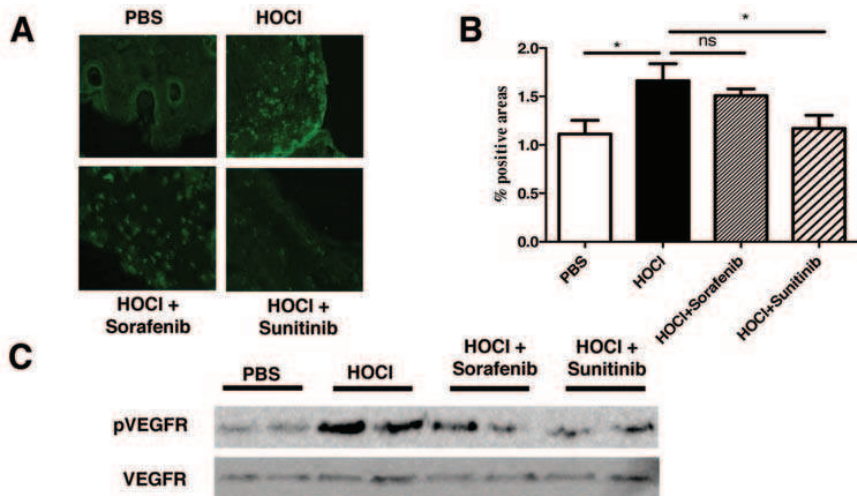
obtained from mice with HOCl-induced SSc. In addition, we show that TKIs targeting the PDGF and VEGF pathways can represent effective treatments in SSc by abrogating the fibrotic process, endothelial damage, and autoimmune activation that characterize the disease.

PDGFs and their receptors are physiologically involved in the embryogenesis of many organs and in the formation of blood vessels (6). They are also implicated in various diseases. Autocrine or paracrine activation of PDGF signaling pathways has been demonstrated in certain type of cancers and has been shown to affect tumor growth, angiogenesis, invasion, and metastasis. PDGFs and their receptors also play a role in vascular disorders, such as atherosclerosis and pulmonary hypertension, as well as in fibrotic diseases, including pulmonary fibrosis, liver cirrhosis, and cardiac fibrosis.

We first assessed the presence of high levels of PDGFR β and its phosphorylation in the fibrotic skin of HOCl-injected mice. The elevated rate of phosphorylation, which reflects receptor hyperactivation, is consistent with the role played by PDGF in several fibrotic diseases. For example, high levels of phosphorylated PDGFRs have been reported in a histologic study of 2 patients with SSc (20). In other studies in which the phosphorylation levels were not investigated, elevated

expression of PDGFs or PDGFRs in various tissues obtained from SSc patients have been reported. In contrast, PDGF is almost undetectable in healthy skin or lung (7,8). Similarly, elevated levels of PDGF-A and PDGF-B have been found in bronchoalveolar lavage fluid from scleroderma patients (9). PDGFRs and their signaling pathway may be activated not only by the binding of PDGF, but also by the autoantibodies found in SSc patients (10). Another possible mechanism, which has been observed in SSc fibroblasts, is that TGF β released by platelets or infiltrating mononuclear cells increases the expression of PDGFRs and enhances the mitogenic effect of PDGF-A (21). Taken together, those data strongly suggest a crucial role of the PDGF signaling pathway in the pathogenesis of SSc.

We therefore undertook an investigation of the potential inhibiting effects of 2 TKIs that interfere with the PDGF signaling pathway: sunitinib and sorafenib. Sunitinib was more effective than the same dosage of sorafenib in preventing skin and lung fibrosis in the HOCl-induced SSc model. The higher capacity of sunitinib over sorafenib to prevent fibrosis was associated with a stronger reduction of the phosphorylation rates of PDGFR β and VEGFRs. Sorafenib can in fact reduce some features of autoimmunity and abrogate



AQ: 22

Figure 5. Effects of sunitinib and sorafenib on the levels of phosphorylated vascular endothelial growth factor receptor (pVEGFR) in the skin of mice injected with HOCl. **A,** Immunohistochemistry of skin sections obtained from a representative mouse from each of the 4 experimental groups ($n = 7$ per group). Slides were stained with anti-pVEGFR monoclonal antibody. Original magnification $\times 200$. PBS = phosphate buffered saline. **B,** Quantification of pVEGFR staining in skin sections, as determined using ImageJ software. Values are the mean \pm SEM of 7 mice per group. * = $P < 0.05$ by Mann-Whitney unpaired U test. NS = not significant. **C,** Levels of native and phosphorylated VEGFR, as determined by Western blotting of protein extracts from the skin. Sunitinib reduced the levels of pVEGFR in the skin of HOCl-injected mice. Results are from 2 representative mice ($n = 7$ per group).

endothelial cell damage, but because of its low capacity to prevent fibrosis, the drug, when administered at a dosage of 50 mg/kg/day, is not able to prevent the development of disease; in contrast, sunitinib acts simul-

taneously on the vascular, immune, and fibrotic features of the disease.

Many differences between sorafenib and sunitinib can account for the superiority of the latter drug in our experiments. First, sorafenib has a shorter half-life (22), being 30–40 hours, whereas the half-life of sunitinib is 80–100 hours. Second, sunitinib is metabolized as the active metabolite SU012662, increasing the duration of the effects of the molecule. SU012662 is 2-fold less potent than sunitinib, but it inhibits PDGF and VEGF receptors and contributes to the pharmacologic activity of sunitinib. Third, sorafenib and sunitinib do not have identical activity on their target receptors (23). With regard to PDGFR β , for example, the IC_{50} of sorafenib is 1129 nM, whereas it is 75 nM for sunitinib (i.e., >15-fold less). Moreover, the two TKIs do not have identical kinase selectivity, as they both are multikinase inhibitors. Sunitinib has a wider spectrum of inhibition than sorafenib and could inhibit additional receptors, possibly affecting the development of scleroderma in our model (23). Despite these differences, however, it is possible that sorafenib would have been more potent in SSc at higher doses, and further studies are needed to confirm the effects of sorafenib on fibrosis and vascular dysfunctions.

The reduction of dermal fibrosis induced by the

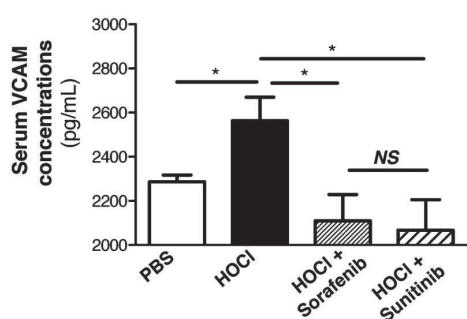


Figure 6. Effects of sunitinib and sorafenib on serum concentrations of soluble vascular cell adhesion molecule (sVCAM). BALB/c mice were injected daily for 6 weeks with either an HOCl-generating agent or phosphate buffered saline (PBS) and treated with sunitinib, sorafenib, or vehicle alone. Sera were collected at the time of euthanization, and concentrations of sVCAM were determined by enzyme-linked immunosorbent assay. Soluble VCAM concentrations were lower in sera from HOCl-injected mice treated with sunitinib than in those from HOCl-injected mice treated with vehicle alone. Values are the mean \pm SEM of 7 mice per group. * = $P < 0.05$ by Mann-Whitney unpaired U test. NS = not significant.

profibrotic drug bleomycin has been observed in studies using other TKIs that target PDGFRs, such as imatinib, dasatinib, and nilotinib (24,25). However, the effects on lung fibrosis have not yet been studied. Sorafenib, in contrast, has been shown to attenuate intrahepatic fibrogenesis, hydroxyproline accumulation, and collagen deposition in 2 rat models of liver fibrosis (26). Our study is the first to show clearcut effectiveness of sunitinib on the development of lung fibrosis in experimental SSc. A study of 5 SSc patients with lung fibrosis treated with a combination of imatinib and cyclophosphamide reported variable results among the patients (27). However, the small number of patients and the absence of a control group render the interpretation of these data difficult (27).

The skin and lungs of patients with SSc contain myofibroblasts, a cell population that produces high amounts of collagen, expresses α -SMA, and displays an excessive rate of proliferation (28–30). The same observation has been made in the mouse model of HOCl-induced SSc (18). The reduction of fibroblast proliferation by sunitinib and sorafenib in fibrotic areas of the skin of mice exposed to HOCl is consistent with the inhibitory role of other TKIs: imatinib has been shown to inhibit the proliferation of normal and scleroderma-tous human fibroblasts in the presence or absence of PDGF or TGF β *in vitro* (8,20). Moreover, treatment with dasatinib and nilotinib was shown to strongly decrease the number of myofibroblasts in bleomycin-induced dermal fibrosis (25).

In addition to the inhibition of fibroblast proliferation and myofibroblast differentiation, we suggest that 2 other mechanisms can also lead to the reduction of skin fibrosis by sunitinib and, to a lesser extent, sorafenib in our SSc model. First, by inhibiting the phosphorylation of PDGFRs, sunitinib and sorafenib may directly decrease collagen production by fibroblasts. This phenomenon has been observed in 2 models of liver fibrosis in which sorafenib treatment directly reduced collagen production by hepatic stellate cells *in vitro* (26). Dasatinib and nilotinib, 2 other TKIs that interfere with the PDGF pathway, have been shown to decrease collagen synthesis in dermal fibroblasts from bleomycin-treated mice or from scleroderma patients (25). Alternatively, sunitinib and sorafenib can indirectly mediate a reduction in collagen deposition by decreasing the expression of tissue inhibitor of metalloproteinases 1 (TIMP-1), thereby potentially enhancing extracellular matrix degradation. Such a phenomenon, which is caused by an alteration in the balance between matrix metalloproteinase 13 and TIMP-1, has been observed in

hepatic stellate cells treated with sorafenib and in dermal fibroblasts exposed to dasatinib or nilotinib (26).

As in patients with diffuse cutaneous SSc, the mice with HOCl-induced SSc develop anti-topo I auto-antibodies, and increased numbers of B cells and CD4+ T cells are found in the spleens of these mice. Both sunitinib and sorafenib prevent the development of these autoantibodies as well as the B cell production of IL-6 and TGF β . However, only sunitinib significantly limits the expansion of B cells and CD4+ T cells in the spleen and B cell activation through down-regulation of B7.1. To our knowledge, the effects of sunitinib on the immune system have not previously been reported.

Imatinib may induce a reversible dose-dependent lymphopenia and hypogammaglobulinemia, inhibit the development of dendritic cells derived from human CD34+ progenitor cells, and inhibit the expansion of memory cytotoxic T lymphocytes without affecting primary T cell or B cell responses (31,32). These effects of imatinib may be linked to the inhibition of the Abl protein tyrosine kinase, but the exact mechanism remains unclear. Sunitinib only slightly interferes with Abl, but it strongly inhibits the VEGF receptor. VEGFs play a key role in activating naïve T cells (33). VEGFR-1, which is expressed in monocyte/macrophages at both the messenger RNA and protein levels, is involved in the migration of these cells and in chronic inflammation (34,35). Mice lacking VEGFR-1 do not develop type II collagen arthritis because they display a decreased inflammatory response of monocyte/macrophages and hematopoietic proliferation (35).

Based on these findings, we hypothesize that the effects of sunitinib on the immune cells observed in our SSc model may be dependent on the inhibition of the phosphorylation of VEGFR. Moreover, sunitinib strongly inhibits B7.1 expression on B cells. The effects of B7.1 downstream signaling on B cell/T cell cooperation may also explain why sunitinib is more effective than sorafenib in preventing disease progression. Indeed, experiments using SCID mice have clearly demonstrated that the immune system is required for the systemic spreading of the disease in the HOCl model of SSc (17).

In addition to fibroblast hyperproliferation and collagen hyperproduction, SSc is characterized by vascular abnormalities. High levels of soluble VCAM, a marker of damage to the endothelium, are found in the sera of SSc patients (36) and in sera from mice with HOCl-induced SSc. Sunitinib and, to a lesser extent, sorafenib prevent the elevation of VCAM in the sera of these mice. Little is known about the events that initiate vascular injury, prevent its repair, and lead to loss of

angiogenesis (37). Early stages of SSc are characterized by an exaggerated angiogenic response, which is later followed by fibrosis (38,39). One of the predominant growth factors associated with vascular endothelial proliferation, migration, and survival is VEGF (40). VEGF binds to 2 major receptors, VEGFR-1 and VEGFR-2. The VEGF-A/VEGFR-2 signaling pathway promotes the proliferation, survival, adhesion, and migration of endothelial cells. Several groups of investigators have reported the up-regulation of VEGF-A and its receptors VEGFRs in sclerodermatos skin (41–43), consistent with the data reported herein.

Taken together, all of these studies indicate a dysregulation of the VEGF/VEGFR axis in SSc. This dysregulation varies with the stage of the disease but is undisputable. A chronic and uncontrolled activation of VEGF-A/VEGFR-2 signaling may play a role in the microangiopathy of SSc (41). In addition, a prolonged exposure to VEGF and uncontrolled activation of VEGFRs can induce the formation of irregularly abnormal vessels with reduced blood flow in vitro (44). Both sunitinib and sorafenib block the kinase activity associated with VEGFRs. The beneficial effects following the use of these 2 drugs on the markers of endothelium damage emphasize the above hypothesis that excessive activation of the VEGFR signaling pathway may trigger the endothelial dysfunction in SSc.

In conclusion, the findings of this study emphasize the pivotal role of the PDGF/PDGFR β signaling pathway in SSc by showing a steady phosphorylated state of PDGFR β in the fibrotic skin of a mouse model of SSc. In addition, the results of this work strengthen the hypothesis that the uncontrolled activation of the VEGF/VEGFR pathway could be deleterious in this disease and could be directly involved in the microangiopathy of SSc. Our findings also suggest that some TKIs that target both PDGFRs and VEGFRs could be a new and attractive therapeutic tool for use in SSc by acting on the fibrotic, immune, and vascular components of the disease.

ACKNOWLEDGMENT

The authors are indebted to Ms Agnes Colle for typing the manuscript.

AUTHOR CONTRIBUTIONS

All authors were involved in drafting the article or revising it critically for important intellectual content, and all authors approved the final version to be published. Dr. Batteux had full access to all of

the data in the study and takes responsibility for the integrity of the data and the accuracy of the data analysis.

Study conception and design. Kavian, Servettaz, Weill, Batteux.

Acquisition of data. Kavian, Marut, Nicco, Chéreau.

Analysis and interpretation of data. Kavian, Servettaz, Marut, Nicco, Chéreau, Batteux.

REFERENCES

1. Gabrielli A, Avvedimento EV, Krieg T. Scleroderma. *N Engl J Med* 2009;360:1989–2003.
2. Mukerjee D, St George D, Coleiro B, Knight C, Denton CP, Davar J, et al. Prevalence and outcome in systemic sclerosis associated pulmonary arterial hypertension: application of a registry approach. *Ann Rheum Dis* 2003;62:1088–93.
3. Mautucci-Cerinic M, Denton CP, Furst DE, Mayes MD, Hsu VM, Carpentier P, et al. Bosentan treatment of digital ulcers related to systemic sclerosis: results from the RAPIDS-2 randomised, double-blind, placebo-controlled trial. *Ann Rheum Dis* 2011;70: 32–8.
4. Launay D, Sitbon O, Le Pavec J, Savale L, Tcherakian C, Yaici A, et al. Long-term outcome of systemic sclerosis-associated pulmonary arterial hypertension treated with bosentan as first-line monotherapy followed or not by the addition of prostacyclins or sildenafil. *Rheumatology (Oxford)* 2010;49:490–500.
5. Fredriksson L, Li H, Eriksson U. The PDGF family: four gene products form five dimeric isoforms. *Cytokine Growth Factor Rev* 2004;15:197–204.
6. Andrae J, Gallini R, Betsholtz C. Role of platelet-derived growth factors in physiology and medicine. *Genes Dev* 2008;22:1276–312.
7. Gay S, Jones JR, Huang GQ, Gay R. Immunohistologic demonstration of platelet-derived growth factor (PDGF) and sis oncogene expression in scleroderma. *J Invest Dermatol* 1989;92: 301–3.
8. Soria A, Cario-Andre M, Lepreux S, Rezvani HR, Pasquet JM, Pain C, et al. The effect of imatinib (Glivec) on scleroderma and normal dermal fibroblasts: a preclinical study. *Dermatology* 2008; 216:109–17.
9. Ludwicka A, Olba T, Trojanowska M, Yamakage A, Strange C, Smith EA, et al. Elevated levels of platelet derived growth factor and transforming growth factor- β 1 in bronchoalveolar lavage fluid from patients with scleroderma. *J Rheumatol* 1995;22:1876–83.
10. Svegliati Baroni S, Santillo M, Bevilacqua F, Luchetti M, Spadoni T, Mancini M, et al. Stimulatory autoantibodies to the PDGF receptor in systemic sclerosis. *N Engl J Med* 2006;354:2667–76.
11. Svegliati S, Cancello R, Sambo P, Luchetti M, Paroncini P, Orlandini G, et al. Platelet-derived growth factor and reactive oxygen species (ROS) regulate Ras protein levels in primary human fibroblasts via ERK1/2. *J Biol Chem* 2005;280:36474–82.
12. Trojanowska M. Role of PDGF in fibrotic diseases and systemic sclerosis. *Rheumatology (Oxford)* 2008;47:2–4.
13. Tingstrom A, Hedin CH, Rubin K. Regulation of fibroblast-mediated collagen gel contraction by platelet-derived growth factor, interleukin-1 α and transforming growth factor- β 1. *J Cell Sci* 1992;102:315–22.
14. Virgili A, Koptyra M, Dasgupta Y, Glodkowska-Mrowka E, Stoklosa T, Nacheva EP, et al. Imatinib sensitivity in BCR-ABL1-positive chronic myeloid leukemia cells is regulated by the remaining normal ABL1 allele. *Cancer Res* 2011;71:5381–6.
15. Mahmood ST, Agresta S, Vigil C, Zhao X, Han G, D'Amato G, et al. Phase II study of sunitinib malate, a multitargeted tyrosine kinase inhibitor in patients with relapsed or refractory soft tissue sarcomas: focus on 3 prevalent histologies: leiomyosarcoma, liposarcoma, and malignant fibrous histiocytoma. *Int J Cancer* 2011; 129:1963–9.
16. Pendergrass SA, Hayes E, Farina G, Lemaire R, Farber HW,

- Whitfield ML, et al. Limited systemic sclerosis patients with pulmonary arterial hypertension show biomarkers of inflammation and vascular injury. *PLoS One* 2010;5:e12106.
17. Servettaz A, Gouvestre C, Kavian N, Nicco C, Guilpain P, Chereau C, et al. Selective oxidation of DNA topoisomerase I induced systemic sclerosis in the mouse. *J Immunol* 2009;182:5855–64.
 18. Kavian N, Servettaz A, Mongaret C, Wang A, Nicco C, Chereau C, et al. Targeting ADAM-17/Notch signaling abrogates the development of systemic sclerosis in a murine model. *Arthritis Rheum* 2010;62:3477–87.
 19. Burdick MD, Murray LA, Keane MP, Xue YY, Zisman DA, Belperio JA, et al. CXCL11 attenuates bleomycin-induced pulmonary fibrosis via inhibition of vascular remodeling. *Am J Respir Crit Care Med* 2005;171:261–8.
 20. Chung L, Fiorentino DF, BenBarak MJ, Adler AS, Mariano MM, Paniagua RT, et al. Molecular framework for response to imatinib mesylate in systemic sclerosis. *Arthritis Rheum* 2009;60:584–91.
 21. Yamakage A, Kikuchi K, Smith EA, LeRoy EC, Trojanowska M. Selective upregulation of platelet-derived growth factor α receptors by transforming growth factor β in scleroderma fibroblasts. *J Exp Med* 1992;175:1227–34.
 22. Clark JW, Eder JP, Ryan D, Lathia C, Lenz HJ. Safety and pharmacokinetics of the dual action Raf kinase and vascular endothelial growth factor receptor inhibitor, BAY 43-9006, in patients with advanced, refractory solid tumors. *Clin Cancer Res* 2005;11:5472–80.
 23. Kumar R, Crouthamel MC, Rominger DH, Gontarek RR, Tummolo PJ, Levin RA, et al. Myelosuppression and kinase selectivity of multikinase angiogenesis inhibitors. *Br J Cancer* 2009;101:1717–23.
 24. Akhmetshina A, Venalis P, Dees C, Busch N, Zwerina J, Schett G, et al. Treatment with imatinib prevents fibrosis in different preclinical models of systemic sclerosis and induces regression of established fibrosis. *Arthritis Rheum* 2009;60:219–24.
 25. Akhmetshina A, Dees C, Pileckyte M, Maurer B, Axmann R, Jungel A, et al. Dual inhibition of c-abl and PDGF receptor signaling by dasatinib and nilotinib for the treatment of dermal fibrosis. *FASEB J* 2008;22:2214–22.
 26. Wang Y, Gao J, Zhang D, Zhang J, Ma J, Jiang H. New insights into the antifibrotic effects of sorafenib on hepatic stellate cells and liver fibrosis. *J Hepatol* 2010;53:132–44.
 27. Sabnani I, Zucker MJ, Rosenstein ED, Baran DA, Arroyo LH, Tsang P, et al. A novel therapeutic approach to the treatment of scleroderma-associated pulmonary complications: safety and efficacy of combination therapy with imatinib and cyclophosphamide. *Rheumatology (Oxford)* 2009;48:49–52.
 28. Rajkumar VS, Howell K, Csizsar K, Denton CP, Black CM, Abraham DJ. Shared expression of phenotypic markers in systemic sclerosis indicates a convergence of pericytes and fibroblasts to a myofibroblast lineage in fibrosis. *Arthritis Res Ther* 2005;7:R1113–23.
 29. Kirk TZ, Mark ME, Chua CC, Chua BH, Mayes MD. Myofibroblasts from scleroderma skin synthesize elevated levels of collagen and tissue inhibitor of metalloproteinase (TIMP-1) with two forms of TIMP-1. *J Biol Chem* 1995;270:3423–8.
 30. Yamamoto T, Nishioka K. Animal model of sclerotic skin. V: increased expression of a smooth muscle actin in fibroblastic cells in bleomycin-induced scleroderma. *Clin Immunol* 2002;102:77–83.
 31. Appel S, Boehm AM, Grunebach F, Muller MR, Rupf A, Weck MM, et al. Imatinib mesylate affects the development and function of dendritic cells generated from CD34 $^{+}$ peripheral blood progenitor cells. *Blood* 2004;103:538–44.
 32. Mumprecht S, Matter M, Pavelic V, Ochsenbein AF. Imatinib mesylate selectively impairs expansion of memory cytotoxic T cells without affecting the control of primary viral infections. *Blood* 2006;108:3406–13.
 33. Kim YS, Hong SW, Choi JP, Shin TS, Moon HG, Choi EJ, et al. Vascular endothelial growth factor is a key mediator in the development of T cell priming and its polarization to type 1 and type 17 T helper cells in the airways. *J Immunol* 2009;183:5113–20.
 34. Barleon B, Sozzani S, Zhou D, Weich HA, Mantovani A, Marme D. Migration of human monocytes in response to vascular endothelial growth factor (VEGF) is mediated via the VEGF receptor flt-1. *Blood* 1996;87:3336–43.
 35. Murakami M, Iwai S, Hiratsuka S, Yamauchi M, Nakamura K, Iwakura Y, et al. Signaling of vascular endothelial growth factor receptor-1 tyrosine kinase promotes rheumatoid arthritis through activation of monocytes/macrophages. *Blood* 2006;108:1849–56.
 36. Kuryliszyn-Moskal A, Klimiuk PA, Sierakowski S. Soluble adhesion molecules (sVCAM-1, sE-selectin), vascular endothelial growth factor (VEGF) and endothelin-1 in patients with systemic sclerosis: relationship to organ systemic involvement. *Clin Rheumatol* 2005;24:111–6.
 37. Kontinen YT, Mackiewicz Z, Ruuttila P, Ceponis A, Sukura A, Povilenaite D, et al. Vascular damage and lack of angiogenesis in systemic sclerosis skin. *Clin Rheumatol* 2003;22:196–202.
 38. Distler O, Del Rosso A, Giacomelli R, Cipriani P, Conforti ML, Guiducci S, et al. Angiogenic and angiostatic factors in systemic sclerosis: increased levels of vascular endothelial growth factor are a feature of the earliest disease stages and are associated with the absence of fingertip ulcers. *Arthritis Res* 2002;4:R11.
 39. Guiducci S, Distler O, Distler JH, Matucci-Cerinic M. Mechanisms of vascular damage in SSc—implications for vascular treatment strategies. *Rheumatology (Oxford)* 2008;47:v18–20.
 40. Ferrara N. The role of VEGF in the regulation of physiological and pathological angiogenesis. *EXS* 2005;94:209–31.
 41. Jinnin M, Makino T, Kajihara I, Honda N, Makino K, Ogata A, et al. Serum levels of soluble vascular endothelial growth factor receptor-2 in patients with systemic sclerosis. *Br J Dermatol* 2010;162:751–8.
 42. Distler O, Distler JH, Scheid A, Acker T, Hirth A, Rethage J, et al. Uncontrolled expression of vascular endothelial growth factor and its receptors leads to insufficient skin angiogenesis in patients with systemic sclerosis. *Circ Res* 2004;95:109–16.
 43. Davies CD, Jeziorska M, Freemont AJ, Herrick AL. The differential expression of VEGF, VEGFR-2, and GLUT-1 proteins in disease subtypes of systemic sclerosis. *Hum Pathol* 2006;37:190–7.
 44. Dor Y, Djonov V, Abramovitch R, Itin A, Fishman GI, Carmeliet P, et al. Conditional switching of VEGF provides new insights into adult neovascularization and pro-angiogenic therapy. *EMBO J* 2002;21:1939–47.

3.5 ARTICLE 5

L'action ciblée du trioxyde d'arsenic sur les fibroblastes sclérodermiques via les FRO prévient le développement de la fibrose dans un modèle murin de sclérodermie systémique .

Ros mediated killing of activated fibroblasts ameliorates fibrosis in a murine model of systemic sclerosis

*Niloufar Kavian, Wioleta Marut, Amélie Servettaz, Carole Nicco, Christiane Chéreau,
Hervé Lemaréchal, Didier Borderie Nicolas Dupin, Bernard Weill, Frédéric Batteux*

Accepté dans Arthritis and Rheumatism, 2012

Comme nous l'avons vu dans les travaux précédents, les fibroblastes de la peau des souris sclérodermiques HOCl ont un phénotype activé, et produisent des FRO qui stimulent leur prolifération et la synthèse de collagène. Par analogie avec les cellules tumorales qui entrent en apoptose sous l'action de molécules qui augmentent le niveau de FRO au dessus d'un seuil létal, nous avons testé dans un premier volet de ce travail l'efficacité du trioxyde d'arsenic (As_2O_3), un agent cytotoxique utilisé en thérapeutique humaine notamment dans la leucémie aigue promyélocyttaire, sur les fibroblastes activés sclérodermiques dans notre modèle murin de ScS. In vitro, le trioxyde d'arsenic cible de façon sélective les fibroblastes activés extraits de peaux de souris ScS par rapport aux fibroblastes normaux extraits de peaux de souris témoins, comme le montre l'expression du marqueur d'apoptose Yopro dans ces cellules traitées avec l'arsenic. Sous l'action de l'arsenic, les fibroblastes ScS produisent un excès d' H_2O_2 qui ne peut pas être contre-balancé par leur faible concentration en glutathion (GSH). Cet excès d' H_2O_2 entraîne l'apoptose et la mort des fibroblastes ScS.

Dans un deuxième volet de ce travail, nous avons utilisé le trioxyde d'arsenic *in vivo* dans notre modèle murin de ScS. En traitant les souris ScS avec le trioxyde d'arsenic pendant 6 semaines, nous avons observé une amélioration de la fibrose cutanée et pulmonaire comme en témoignent les analyses histopathologiques de peaux et de poumons chez les souris traitées par rapport aux souris contrôles, ainsi que la concentration en collagène dans ces deux organes. De

plus, le traitement *in vivo* par le trioxyde d'arsenic a entraîné une réduction des anomalies vasculaires (notamment du marqueur VCAM-1), et de l'activation lymphocytaire avec diminution de la production d'auto-anticorps et modification du profil cytokinique des lymphocytes T de la rate (IL-4, IL-13).

Ces résultats apportent des arguments pour l'évaluation du trioxyde d'arsenic dans le traitement de la ScS. Ils nous ont poussé à continuer notre étude par l'évaluation de l'effet du trioxyde d'arsenic dans un autre modèle de ScS : le modèle de ScS associée à la réaction du greffon contre l'hôte.

**ROS-mediated Killing of Activated Fibroblasts by Arsenic Trioxide
Ameliorates Fibrosis in a Murine Model of SSc**

Niloufar Kavian^{1,2,*}, Wioleta Marut^{1,*}, Amélie Servettaz^{1,3}, Carole Nicco¹, Christiane Chéreau¹, Hervé Lemaréchal⁴, Didier Borderie⁴, Nicolas Dupin^{1,5}, Bernard Weill^{1,2}, and Frédéric Batteux^{1,2}

¹ EA 1833, Faculté de Médecine, Université Paris Descartes, Sorbonne Paris-Cité,

² Service d'Immunologie Biologique, Hôpital Cochin, Paris, AP-HP

³ Faculté de Médecine de Reims, Service de Médecine Interne, Maladies Infectieuses, Immunologie Clinique, Hôpital Robert Debré, Reims, France

⁴ Laboratoire de Biochimie A, Hôpital Cochin, Paris, APHP

⁵ Service de Dermatologie, Hôpital Cochin, Paris, APHP

* Both authors contributed equally to this work

This work was supported by grants from Université Paris-Descartes and Cephalon. Niloufar Kavian was on a grant from Assistance Publique-Hôpitaux de Paris.

Address correspondence to: Frédéric Batteux, Laboratoire d'Immunologie EA1833, Faculté de Médecine Paris Descartes, 75679 Paris cedex 14, France. Phone 33-1-58-41-20-09; fax 33-1-58-41-20-08; frederic.batteux@cch.aphp.fr

Non standard abbreviations used: AAbs, Autoantibodies; As₂O₃, arsenic trioxide; Aminotriazole, 3-amino-1,2,4-triazole; BSO, DL-buthionine-(S,R)-sulfoximine; DDC,

diethyldithio-carbamate, GSH, Glutathione; HOCl-mice, HOCl-injected mice;; NAC, N-acetylcysteine; ROS, reactive oxygen species; SOD, Superoxide Dismutase ; SSc, systemic sclerosis.

ABSTRACT

Objective: In systemic sclerosis, activated fibroblasts produce reactive oxygen species that stimulate their proliferation and collagen synthesis. By analogy with tumor cells that undergo apoptosis upon cytotoxic treatment that increases reactive oxygen species levels beyond a lethal threshold, we tested whether activated fibroblasts could be selectively killed by the cytotoxic molecule arsenic trioxide (As_2O_3) in a murine model of systemic sclerosis.

Methods: Systemic sclerosis was induced in BALB/c mice by daily intradermal injections of hypochlorous acid. Mice were simultaneously treated with daily intraperitoneal injections of As_2O_3 .

Results: As_2O_3 limited dermal thickness and inhibited collagen deposition as assessed by histological examination and measurement of skin and lung collagen contents. As_2O_3 abrogated vascular damages as shown by determination of serum VCAM-1, and inhibited the productions of auto-antibodies, IL-4 and IL-13 produced by activated T cells. Those beneficial effects were mediated through reactive oxygen species generation that selectively killed activated fibroblasts, that contained low levels of glutathione. **Conclusions:** The dramatic improvement of skin and lung fibrosis provides a rationale for the evaluation of As_2O_3 in patients affected by systemic sclerosis.

INTRODUCTION

Disruption of the oxidant/antioxidant balance is a crucial step in the initiation and the development of most systemic fibrotic diseases, particularly of liver, pancreatic, renal, and lung fibrosis (1-5). Systemic sclerosis (SSc) is a prototypic systemic fibrotic disease involving skin and visceral organs. The first stage of the disease associates inflammation and vascular abnormalities followed by the spreading of fibrosis. During this early stage, reactive oxygen species (ROS) overproduced by fibroblasts from the skin and internal organs trigger the proliferation of fibroblasts and the synthesis of type I collagen (4). The role of ROS in the initiation of SSc has been recently highlighted by a new murine model based on intradermal injections of HOCl-generating agents that induce skin and visceral fibrosis, vascular disease and autoimmunity, all features characterizing SSc (6). On the other hand, the involvement of the immune system is reflected by the production of various autoantibodies (AAbs). The AAbs to the platelet-derived growth factor receptor activate fibroblasts to produce ROS (7) and establish a loop that perpetuates the disease.

The early inflammatory process and the development of fibrosis caused by fibroblast proliferation and collagen production are stimulated by endogenous ROS up to a certain level of concentration beyond which ROS induce cell apoptosis. This ambivalent effect of ROS has been clearly shown in cancer cells, since chronic exposure to low levels of ROS induce carcinogenesis and tumor progression, whereas the oxidative burst induced by cytotoxic drugs leads to the apoptosis of tumor cells (8).

Since SSc is associated with the activation of fibroblasts that overproduce ROS, we tested the therapeutic effect of the cytotoxic agent arsenic trioxide (As_2O_3) that raises the intracellular level of ROS (9). As_2O_3 is an inorganic trivalent salt that exhibits potent antitumor effects *in*

vitro and *in vivo* (10, 11) especially in the treatment of haematological malignancies (12). It can affect many cellular functions such as proliferation, apoptosis, differentiation, and angiogenesis in various cell lines. Transformed keratinocytes (13) or activated autoimmune lymphocytes (14) can also be killed by ROS-mediated apoptosis triggered by As₂O₃.

In this study, we have evaluated the effects of As₂O₃ on the fibrotic, vascular and immune dysregulations of the disease, in HOCl-induced SSc, an inflammatory model of SSc characterized by an early activation of fibroblasts by ROS.

METHODS

Isolation of fibroblasts from the skin of mice

Fragments of diseased skin were collected from the back of mice at the time of sacrifice. Skin samples (from control- or HOCl-induced-SSc-mice) were digested with “Liver-Digest-Medium” (Invitrogen) for 1h at 37°C. After three washes, cells were seeded into sterile flasks and isolated fibroblasts (control- or SSc-fibroblasts) were seeded in 96-well plates (Costar, Corning, USA), then cultured in DMEM/Glutamax-I supplemented with 10% heat-inactivated fetal calf serum and antibiotics.

Measurement of intracellular levels of GSH and H₂O₂ and O₂^{•-} released by fibroblasts in response to *in vitro* treatment with As₂O₃

Fibroblasts were coated in triplicate in 96-well microplates (8×10^3 cells/well) and incubated with complete medium for 24h at 37°C, and various doses of As₂O₃ (0 to 40 µM) were added in the last 6 hours of culture. Levels of H₂O₂, O₂^{•-}, and GSH were assessed by spectrofluorometry (Fusion, PerkinElmer, Wellesley, MA) using 2',7'-dichlorodihydrofluorescein diacetate (H₂DCFDA), dihydroethidium (DHE,), or monochlorobimane respectively (Molecular-Probes, Netherlands). Cells were incubated with 200 µM H₂DCFDA, DHE, or 50 µM monochlorobimane in PBS for 30 minutes at 37 °C. Fluorescence intensity was read every hour for 6 hours. Results are expressed as arbitrary units of fluorescence intensity per million of viable cells.

***In vitro* assay of As₂O₃ cytotoxicity on mouse fibroblasts**

Fibroblasts coated in triplicate (8×10^3 cells/well), and incubated with complete medium alone or 10 μM As₂O₃ for 48h at 37°C. The numbers of viable cells were evaluated by cristal violet assay. Results are expressed as percentages of viability among cells exposed to As₂O₃ or not.

Modulation of ROS metabolism in control- and SSc-fibroblasts

Isolated normal or SSc fibroblasts (2×10^4 cells/well) were seeded in 96-well plates and incubated for 24 hours in complete medium alone or with the following molecules: 3.2 mM N-acetylcysteine (NAC), 1.6 mM BSO, 20 U PEG-catalase, 400 μM AT, or 8 μM DDC. As₂O₃ (10 μM) was added in the last 6 hours. Cells were then washed three times with PBS and incubated with 100 μl per wells of 200 μM H₂DCFDA or 50 μM monochlorobimane for 30 min. H₂O₂ and GSH levels were expressed as described above.

HOCl-induced SSc

Induction of SSc by intra-dermal injections of HOCl-generating solution to BALB/c mice

Six week-old female BALB/c mice were purchased from Harlan (Gannat, France) and maintained with food and water *ad libitum*. They were given humane care according to the guidelines of our institution. Mice were randomly distributed into experimental and control groups ($n = 21$ per group). SSc was induced according the protocol of Servettaz *et al* with minor modifications as described herein (6). Four hundred microliters (two injections of 200 μL) of a solution generating HOCl were prepared extemporaneously and injected intra-dermally into the shaved back of the mice, using a 27 gauge needle, everyday for 6 weeks (HOCl-mice). HOCl was produced by adding NaClO solution (9.6 % as active chlorine) to KH₂PO₄ solution (100 mM, pH 6.2) (15). HOCl concentration was determined by measuring the optical density of the solution at 292 nm, and then adjusted to obtain an O.D between 0.7 and 0.9. Control groups received injections of 400 μl sterilized PBS (PBS-mice).

Treatment of HOCl-mice with As₂O₃

Mice were randomized and treated simultaneously by HOCl-generating solution or PBS and by intra-peritoneal injections of As₂O₃ or vehicle alone for 6 weeks ($n = 14$ per group). A stock solution was prepared extemporaneously by dissolving As₂O₃ powder (Sigma Aldrich) in 1M NaOH, and diluted 1:200 in PBS. As₂O₃ was given intraperitoneally 5 days a week at a dose of 5 µg/g body weight., Bobé P *et al* tested several doses of As₂O₃ in mice and the dose of 5 µg/g seemed to be optimal(14). Control mice received intraperitoneal PBS added with NaOH (1:200) 5 days a week.

Three days after the end of the injections, animals were sacrificed by cervical dislocation. Serum samples were collected and stored at -80°C. Lungs were removed from each mouse and a skin biopsy was performed on the back region with a punch (4 mm of diameter), involving the skin and the underlying muscle of the injected area. Spleens were also collected and splenocyte suspensions were prepared after hypotonic lysis of erythrocytes in potassium acetate solution.

Assessment of collagen accumulation

Skin thickness

Skin thickness of the shaved back of mice was measured one day before sacrifice with a caliper and expressed in millimeters.

Histopathological analysis

Fixed lung and skin pieces were embedded in paraffin. A 5-µm-thick tissue section was prepared stained with hematoxylin eosin or with picro-sirius red. Slides were examined by standard brightfield microscopy (Olympus BX60, Japan) by a pathologist who was blinded to the assignment of the animal group.

Collagen content in skin and lung

Skin and lung pieces were diced using a scalpel, put into tubes, thawed and mixed with pepsin (1:10 weight ratio) and 0.5 M acetic acid overnight at room temperature under stirring. The assay of collagen content was based on the quantitative dye-binding Sircol method (Biocolor, Ireland).

Immunohistochemistry of phospho-Smad2/3 on diseased skin of mice

Sections of diseased skin were deparaffinized and antigen retrieval was performed by incubating the slides with proteinase-K (Dako, France) for 20 min. Slides were then incubated with 3% H₂O₂ for 10 min, then with 5% bovine serum albumin and 1% rabbit serum to block non-specific binding. Slides were immunostained with a monoclonal mouse antibody directed to Phospho-Smad2/3 (Cell Signalling Technology, USA) for one h. After washing in Tris-Buffer-Solution-Tween, slides were incubated with alkaline-phosphatase-labeled secondary rabbit anti-mouse antibody (Rockland, USA) for 1 hour. Staining was visualized with Diaminobenzidine solution kit (Sigma, France). Irrelevant isotype-matched-antibodies were used as negative controls. All slides were analyzed by two independent pathologists blinded with regard to the groups. Pictures were taken with a digital camera on a BX60 microscope (Olympus, France), using DP Manager software, at a magnification of x100, and analyzed using ImageJ Software (1.36 version).

Western-Blot analysis of α-SMA protein in mouse fibroblasts

Fibroblasts were isolated from skin biopsies as described above. Proteins (30 µg per well) were subjected to 10% polyacrylamide gel electrophoresis, transferred onto nitrocellulose membranes, blocked with 5% nonfat dry milk in Tris Buffer Solution-Tween, then incubated

overnight at 4°C with an α -SMA antibody (Clone 1A4, Sigma, France). The membranes were then washed and incubated with a HRP-conjugated secondary antibody (Santa-Cruz, France) for one hour. Immunoreactivities were revealed with ECL (Amersham).

Measurement of oxidized derivatives in sera

Advanced oxidation protein products (AOPP) concentration

AOPP were measured by spectrophotometry as previously described(16). The assay was calibrated using Chloramine-T.

Nitrate levels

Nitrate levels were measured by spectrophotometry using oxidation catalysed by cadmium metal (Oxis, Bioxytech, USA), which converts nitrates into nitrites. The detection limit for nitrites was 0.1 μ mol/l.

Measurement of intracellular glutathione (GSH) levels in fibroblasts from treated mice

Fibroblasts were isolated from the skin of mice (10 per group) and seeded as described above. The levels of GSH were assessed by spectrofluorometry using monochlorobimane staining, as described above. The number of viable cells was evaluated by the cristal violet assay.

Determination of sVCAM-1 concentrations in the sera. Levels of sVCAM-1 in sera were measured by ELISA using a 1:800 dilution of sera and the Mouse VCAM-1/CD106 DuoSet kit (R&D-Systems, USA) following the manufacturer's instructions.

Flow cytometric analysis of spleen cell subsets

Cell suspensions from spleens were prepared after hypotonic lysis of erythrocytes in potassium acetate solution. Cells were incubated with the appropriate labelled Ab at 4°C for 30 min in PBS with 0.1% sodium azide and 5% normal rat serum. Flow cytometry was performed on FACS Canto flow cytometer (BD-biosciences, USA) according to standard techniques. The monoclonal Abs used in this study were: anti-B220-PE-Cy7, anti-CD11b-Biotin, anti-CD4-PERCP, and anti-CD8-PE-Cy7, monoclonal Abs (BD-biosciences). Data were analyzed with Flow-Jo software (Tree Star, Ashland, USA).

Assays of serum immunoglobulins and autoantibodies

Levels of anti-DNA topoisomerase 1 IgG Abs were detected by ELISA on microtiter plates (Immunovision, Springdale, AR, USA). Levels of total mouse IgG and IgM Abs were measured using standard ELISA as previously described.(17) A 1:50 serum dilution was used for the determination of all antibodies.

Determination of IL-4, IL-13, IFN- γ production by splenocytes by ELISA

Spleen cells were cultured in RPMI-1640 supplemented with antibiotics, Glutamax (Invitrogen Life Technologies), and 10% heat-inactivated FCS (Invitrogen Life Technologies) (complete medium). Spleen cell suspensions were seeded in 96-well flat-bottom plates and cultured (2×10^5 cells) in complete medium for 48h in the presence of 5 μ g/mL concanavalin A. Supernatants were collected and cytokine concentrations determined by ELISA (for IL-4, IL-13 and IFN- γ : Ebioscience, San Diego, USA). Results are expressed in ng/mL.

Analysis of IL-13 expression in mouse skin fibroblasts by RT-PCR

RNA was extracted with Trizol reagent (Invitrogen) from skin fibroblasts isolated from mice (7 mice per group). IL-13 cDNAs were quantified by semi-quantitative RT-PCR, using the

following primers: F 5'-CCTGGCTCTTGCTTGCCTT-3' and R 5'-GGTCTTGTGTGATGTTGCTCA-3'. IL-13 cDNA levels were normalized to the level of expression of β -actin, using the following primers: F 5'-GTGGGCCGCTCTAGGCACCAA-3' and R 5'-CTCTTGATGTCACGCACGATTTC-3'.

Statistical Analysis

All the quantitative data are expressed as means \pm SEM and have been analyzed by Prism Version 5 (GraphPad) with one-way ANOVA as appropriate. A *P* value < 0.05 was considered statistically significant.

RESULTS

As₂O₃ exerted cytotoxic and pro-oxidative effects on SSc fibroblasts *in vitro*

Fibroblasts from control- and SSc-mice were exposed *in vitro* to increasing concentrations of As₂O₃ from 0 to 40 µM.

The basal production (without arsenic) of H₂O₂ was increased by 34 % in SSc-fibroblasts compared to normal fibroblasts (p=0.035, figure 1A). Incubation of control-fibroblasts with low doses (2.5 to 10 µM) of As₂O₃ didn't affect significantly their production of H₂O₂. Only high doses of As₂O₃ (20 to 40 µM) were able to increase significantly H₂O₂ production in those cells. In contrast, HOCl-SSc-fibroblasts were hyper-sensitive to the prooxidative effects of As₂O₃. At 2.5 and 5 µM, As₂O₃ raised the production of H₂O₂ by HOCl-SSc-fibroblasts by 34 % and 64 % (p=0.06 and p=0.004 vs untreated-HOCl-SSc-fibroblasts respectively, figure 1A), and from 10 to 40 µM the production of H₂O₂ was increased by 85 % and more (p=0.025 for HOCl-SSc-fibroblasts with 10 µM arsenic vs untreated-HOCl-SSc-fibroblasts, figure 1A).

The basal level of GSH, an essential cofactor of H₂O₂ catabolism, was decreased by 51 % in SSc fibroblasts compared to normal fibroblasts (p=0.0007, figure 1B). As₂O₃ dose-dependently induced a drop in the glutathione (GSH) content in control- and HOCl-SSc-fibroblasts. In control-fibroblasts, As₂O₃ had this effect only at high concentrations (from 10 to 40 µM), whereas in HOCl-SSc-fibroblasts the molecule was able to reduce significantly the intracellular GSH content from 5 µM (p=0.042, figure 1B).

We also investigated the effects of As₂O₃ on O₂^{•-} production. The basal production of O₂^{•-} didn't differ between control-fibroblasts and HOCl-SSc-fibroblasts (data not shown). The addition of arsenic in the culture medium didn't affect the production of O₂^{•-} by control- or HOCl-SSc-fibroblasts, even at high concentrations (data not shown).

As₂O₃ had a powerful cytotoxic effect on HOCl-SSc-fibroblasts compared to PBS-fibroblasts. Indeed, the rate of viability of fibroblasts from control mice was affected only slightly by in

vitro treatment with arsenic as it varied from 98 % with 2.5 μM As_2O_3 to 78 % with 20 μM As_2O_3 (figure 1C). Inversely, the viability rate of HOCl-SSc-fibroblasts in the presence of As_2O_3 was 85 % with 2.5 μM ($p=0.059$ vs untreated HOCl-SSc-fibroblasts), 68 % with 5 μM ($p = 0.006$ vs untreated HOCl-SSc-fibroblasts), 50 % with 10 μM ($p = 0.003$ vs untreated HOCl-fibroblasts), 38 % with 20 μM ($p=0.003$ vs untreated SSc- fibroblasts, and 27% with 40 μM ($p=0.002$, figure 1C).

Finally, after these dose-effects experiments, the dose of 10 μM was chosen for further experiments of modulation of ROS metabolism by As_2O_3 .

Modulation of H_2O_2 metabolism by arsenic

Using specific modulators of enzymatic and non-enzymatic systems involved in H_2O_2 metabolism, we investigated the mechanism of action of As_2O_3 . Control- and HOCl-SSc-fibroblasts were incubated with or without 10 μM As_2O_3 in association with N-acetylcysteine (NAC), buthionin sulfoximine (BSO), catalase, diethyldithio-carbamate (DDC) or Aminotriazole (AT).

NAC, a precursor of GSH, decreased significantly the production of H_2O_2 and increased the intracellular levels of GSH in untreated control- and HOCl-SSc-fibroblasts. Co-incubation of As_2O_3 with NAC decreased by more than 70 % the production of H_2O_2 in both control- and HOCl-SSc-fibroblasts ($p=0.003$ for both cell types, figure 1D) and increased by 180 % the intracellular levels of GSH in control-fibroblasts and by 800% in HOCl-SSc-fibroblasts ($p<0.001$ for both cell types figure 1E). In addition, incubation with BSO, a molecule that blocks the synthesis of GSH by selectively inhibiting gamma-glutamylcysteine synthetase, increased significantly the production of H_2O_2 by HOCl-SSc-fibroblasts ($p=0.002$ versus cells without BSO, figure 1D) and inversely significantly decreased the concentration of GSH in those cells ($p=0.003$, figure 1E). Moreover, HOCl-SSc-fibroblasts co-incubated with As_2O_3

and BSO displayed an H₂O₂ production of 7522.9±206.9 A.U versus 6078±207.3 A.U when incubated with BSO alone, showing the additive effect of Arsenic and BSO (p=0.0048). We observed the same additive effect concerning intracellular levels of GSH in HOCl-SSc-fibroblasts (mean of 3797.1±429.3.7 A.U for HOCl-SSc-fibroblasts with BSO alone, and 528.3±118.1 A.U for HOCl-SSc-fibroblasts with BSO and As₂O₃, p=0.0042). Increasing the cellular levels of catalase, an enzyme that converts hydrogen peroxide into H₂O, by adding PEG-catalase to medium culture with arsenic had no effects on H₂O₂ cell production or GSH intracellular levels in both types of fibroblasts (p=0.127 for and p=0.245 respectively, figure 1D and 1E). In addition, blocking catalase with aminotriazole or adding DDC didn't affect the production of H₂O₂ and GSH content in control- or HOCl-SSc-fibroblasts (p=0.262 and p=0.312 respectively, figure 1D and 1E). Moreover, adding DDC, an inhibitor of SOD, has no effects on both parameters, confirming the non involvement of O₂^{•-} in As₂O₃ cytotoxicity. Altogether, these results indicate that As₂O₃ targets selectively HOCl-SSc-fibroblasts by depleting GSH and increasing H₂O₂ production.

As₂O₃ reduced skin and lung fibrosis in HOCl-mice

A significant increase in dermal thickness was observed in mice injected with HOCl compared to PBS (p<0.001, figure 2A). Dermal fibrosis was also significantly increased in HOCl- mice *versus* controls as demonstrated by the histopathological analysis of the skins (Figure 2B) and by measurement of type-I collagen concentration in the skin extracts (p<0.001, figure 2C). *In vivo* treatment with As₂O₃ reduced the dermal thickness, histological signs of fibrosis and the accumulation of type-I collagen in the skin of HOCl-mice (p=0.023, figure 2A, 2B, 2C). The myofibroblast marker α-Smooth-Muscle-Actin (α-SMA) was overexpressed in the skin of HOCl-treated mice compared to PBS-mice and was significantly

reduced by As₂O₃ treatment (Figure 2E). Additionally, the expression of Phospho-Smad2/3, a key intracellular mediator of fibrosis, was strongly increased in the skins from HOCl-mice compared to unaffected skins from control mice (6.7 ± 2.3 versus 23.2 ± 2.9 , p=0.0021, figure 2D). As₂O₃ treatment of HOCl-mice significantly reduced the expression of Phospho-Smad2/3 in the skins (10.7 ± 2.5 , p=0.0042 versus untreated HOCl-mice, figure 2D).

As in some patients with SSc, lung fibrosis developed in HOCl-mice. Figures 2F and 2G show the hematoxylin-eosin staining of lung biopsies and the significant increase in type-I collagen concentrations in lungs of HOCl-treated mice compared to control mice (p=0.037). As₂O₃ abrogated the development of lung fibrosis induced by HOCl, as shown by the weaker accumulation of type-I collagen in the lungs of those mice (p=0.006, figure 2E).

The anti-fibrotic effects of arsenic trioxide were confirmed in the model of bleomycin-induced scleroderma. Indeed, skin thickness as well as skin and lung collagen contents were significantly reduced in mice receiving bleomycin and concomitantly treated with As₂O₃ compared to mice receiving bleomycin alone (for skin thickness: p<0.0001, for skin collagen content: p=0.0127, for lung collagen content: p=0.0079, supplemental figure 1). The histopathological analysis of skin and lung sections confirmed those results (supplemental figure 1 B and 1D).

In vivo treatment with As₂O₃ reduced local and systemic oxidative stress and prevented endothelial injuries

Because ROS are major mediators implicated in the development of SSc and particularly in HOCl-induced SSc, we investigated the *in vivo* effects of As₂O₃ on systemic oxidative stress markers at the local and systemic levels. We measured the intracellular levels of GSH, a major antioxidant involved in the cellular defense against ROS, in skin fibroblasts isolated from normal or diseased mice. HOCl-mice displayed lower levels of GSH in their skin

fibroblasts than PBS-mice ($p=0.0049$, figure 3A). *In vivo* treatment of HOCl-mice with As₂O₃ prevented this drop in GSH concentration, since skin fibroblasts displayed GSH levels similar to those observed in control-mice ($p=0.003$, figure 3A). In addition, fibroblasts isolated from HOCl-SSc-mice treated with As₂O₃ displayed lower levels of H₂O₂ than fibroblasts isolated from untreated HOCl-SSc-mice (mean of 2535 ± 131 for fibroblasts from As₂O₃-treated HOCl-SSc-mice versus 3652 ± 114 for fibroblasts from PBS-treated SSc-mice, $p=0.079$, figure 3B). The sera from HOCl-mice contained higher amounts of AOPP, a major marker of the systemic oxidative stress in SSc, than the sera from mice treated with PBS ($p=0.048$, figure 3C). As₂O₃ reduced by 40 % the serum concentrations of AOPP in mice exposed to HOCl ($p=0.029$, figure 3C). The concentration of nitrates, a marker of the nitrosative stress, reached $0.37 \mu\text{mol/g}$ of protein in the sera of HOCl-mice *versus* $0.21 \mu\text{mol/g}$ of protein in control mice ($p=0.04$, figure 3D). *In vivo* treatment of HOCl-mice with As₂O₃ decreased the concentration of nitrates to $0.20 \mu\text{mol/g}$ of protein ($p=0.042$, figure 3C). HOCl-mice displayed higher levels of sVCAM-1 in their sera than PBS-mice ($1249\pm74 \text{ pg/mL}$ *versus* $969\pm61 \text{ pg/mL}$ for HOCl- and PBS-mice, respectively, $p=0.026$, figure 3E). As₂O₃ reduced sVCAM-1 levels in the sera of treated-HOCl-mice ($p=0.024$, figure 3E).

Arsenic down-regulated the expansion of splenic B cells and decreased the serum levels of anti-DNA–Topoisomerase 1 autoantibodies in HOCl-mice.

We next tested the effects of As₂O₃ on splenic cell populations. HOCl-mice showed an increase in total splenocytes ($p=0.039$, figure 4A), B ($p=0.035$, figure 4B), CD4+ ($p=0.048$, figure 5A), and CD8+ T cells ($p=0.006$, figure 5B) compared to PBS-mice. As₂O₃ inhibited the increase in splenic B ($p=0.043$, figure 4B), CD4+ ($p<0.001$, figure 5A) and CD8+ ($p<0.001$, figure 5B) T cell numbers in HOCl-mice and treated by As₂O₃ *versus* untreated HOCl-mice.

Levels of total IgG were elevated in the sera from HOCl-mice ($p=0.0048$ versus PBS-mice, figure 4C), and treatment with As_2O_3 allowed a decrease of that parameter ($p=0.001$ for HOCl-mice treated with As_2O_3 versus HOCl-non treated-mice, figure 4C). IgG Abs directed to DNA-Topoisomerase-1 were found in the sera from mice after 6 weeks of HOCl injections ($p=0.043$, figure 4D) but not in the sera from HOCl-mice treated with As_2O_3 ($p=0.05$ versus HOCl-non treated-mice).

In vivo administration of arsenic reduced the *ex vivo* production of IL-4 and IL-13 by spleen cells of HOCl-mice.

The supernatants of splenocytes from HOCl-mice contained higher concentrations of IL-4 and IL-13 than supernatants from normal mice (0.10 ± 0.03 versus 0.07 ± 0.01 ng/mL for IL-4 and 0.30 ± 0.07 versus 0.22 ± 0.06 ng/mL for IL-13, $p=0.044$ and $p=0.045$ respectively,, figure 5C and 5E). As_2O_3 reduced the concentrations of both cytokines by 30% ($p=0.011$ and $p=0.05$ respectively, figure 5C and 5E). The IFN- γ production was modified neither by HOCl-injections nor by As_2O_3 treatment (Figure 5D). Moreover, As_2O_3 abrogated the local production of IL-13 in the skin of HOCl-mice, as shown by the measurement of IL-13 mRNA levels in fibroblasts (Figure 5F).

DISCUSSION

In the present study, we report that As₂O₃, a common chemotherapeutic drug used to treat hematological malignancies, can inhibit the development of systemic fibrosis in a chemically-induced murine model of SSc.

We first investigated the mechanisms through which As₂O₃ can exert this therapeutic effect. Among the factors that determine the cellular susceptibility to As₂O₃, the balance between ROS generation and detoxification plays a major role (18). We observed that HOCl-SSc-fibroblasts from HOCl-mice are more prone to As₂O₃-induced apoptosis than normal fibroblasts. This difference in arsenic-susceptibility between SSc- and normal-fibroblasts correlates with different oxidant/antioxidant status in the two cell types. Indeed, skin fibroblasts isolated from HOCl-mice show a higher intracellular concentration of H₂O₂ and a lower level of GSH than skin fibroblasts from control mice. Moreover, NAC, a GSH precursor, has a protective effect against As₂O₃-induced apoptosis in HOCl-SSc-fibroblasts, while BSO, that depletes intracellular GSH, increases arsenic-cytotoxicity. Our data on fibroblasts are in agreement with previous reports on other cell types. In NB4 cells, GSH depletion increases the apoptosis triggered by arsenic (19), and hydrogen-peroxide-resistant CHO cells are less susceptible to As₂O₃ (20). In addition, GSH can bind to arsenic and protect its target through the formation of a transient As(GS)₃ complex, thus explaining the enhanced susceptibility of HOCl-SSc-fibroblasts to As₂O₃ (21).

In vivo, diseased skin fibroblasts are selectively killed by arsenic, while normal fibroblasts survive and grow in place of the latter. Thus, fibroblasts isolated from As₂O₃-treated-SSc-mice display levels of GSH approaching those of fibroblasts from PBS-mice. Therefore,

despite its prooxidative activity, As₂O₃ paradoxically improves the antioxidant status of the SSc-skin.

This effect of As₂O₃ is also observed at the systemic level. AOPP are oxidized proteins generated by fibroblasts in the skin of SSc-mice. AOPP are responsible of the spreading of the disease from skin to visceral organs via the systemic circulation (6). Levels of AOPP are decreased in As₂O₃-treated-SSc-mice compared to untreated SSc-mice. Since AOPP are released by HOCl-SSc-fibroblasts, the selective killing of those cells early in the course of the disease explains the decrease of serum AOPP levels in SSc-mice treated with As₂O₃.

In HOCl-induced SSc, AOPP can elicit the apoptosis of endothelial cells and cause vascular damages (6). In vivo treatment of SSc-mice with As₂O₃ reduces the levels of AOPP and consequently the concentration of nitrates and sVCAM1, markers of vascular activation and injury in murine and human SSc (22, 23), reflecting the beneficial effect of arsenic on the vascular component of the disease.

Another major beneficial effect of As₂O₃ in SSc-mice consists in an inhibition of skin and lung fibrosis. Smad2 and Smad3 are transcription factors constitutively upregulated in human SSc fibroblasts, that activate the promoter COL1A2 in SSc fibroblasts and the synthesis of collagen (24, 25). The expression of phosphor-Smad2/3 is downregulated in the skin of SSc-mice treated with As₂O₃ compared to untreated SSc-mice, in agreement with recent data showing that As₂O₃ alters the phosphorylation of Smad2/3 in fibroblasts (24). Moreover, TGF-β-induced Smad2/3 phosphorylation is inhibited by NAC, glutathione and L-cysteine, a thiol antioxidant, emphasizing the role of ROS in the activation of the Smad2/3 pathway (26). Thus, in our model, the decreased phosphorylation of Smad2/3 is consecutive to the reduced oxidative damages observed in SSc-skin following the selective killing of diseased-fibroblasts

by arsenic. Globally, the decreased phosphorylation of Smad2/3 contributes to inhibit an excessive deposition of collagen leading to fibrosis.

The breach of natural tolerance and the development of an auto-immune reaction is a key feature of SSc in both humans and rodents. As₂O₃ exerts an immuno-regulating effect in SSc-mice, reflected by the reduction in B, CD4 and CD8 T cell numbers in the spleens of treated mice, and in the decrease in serum anti-DNA-topoisomerase-1Ab levels. The beneficial effect of As₂O₃ on the immune system also results in the decrease in spleen production of IL-4 and IL-13, two closely linked cytokines that trigger the synthesis of collagen in human skin fibroblasts, and whose concentrations are elevated in the serum and the affected skin of SSc patients (27-29). By deleting HOCl-SSc-fibroblasts, As₂O₃ abrogates the chronic production of ROS and the consequent oxidation of proteins (especially of DNA-topoisomerase-1). Oxidized DNA-topoisomerase-1 is particularly immunogen and implicated in the breach of immune tolerance in SSc. Therefore, in vivo treatment with As₂O₃ could inhibit the induction of the auto-immune reaction by limiting the production and the spreading of the auto antigen. However, a direct effect of arsenic on activated T cells leading to an abrogation of the auto immune response cannot be ruled out. Indeed, previous reports have shown that the elevated concentration of H₂O₂ in acute promyelocytic leukemia cells renders them extremely susceptible to the pro-apoptotic effects of As₂O₃. The same effects have been observed in other cell lines, and particularly in lymphocytes during systemic autoimmunity (14, 30-32).

In conclusion, we propose that the selective cytotoxic action of As₂O₃ on activated fibroblasts that produce high amounts of H₂O₂ could be used in the treatment of systemic sclerosis in addition to hematological or solid malignancies.

ACKNOWLEDGMENTS

The authors are indebted to Ms Agnès Colle for typing the manuscript.

REFERENCES

1. Masamune A, Shimosegawa T. Signal transduction in pancreatic stellate cells. *J Gastroenterol*. 2009;44:249-60.
2. Pongnimitprasert N, El-Benna J, Foglietti MJ, Gougerot-Pocidalo MA, Bernard M, Braut-Boucher F. Potential role of the "NADPH oxidases" (NOX/DUOX) family in cystic fibrosis. *Ann Biol Clin (Paris)*. 2008;66:621-9.
3. Urtasun R, Conde de la Rosa L, Nieto N. Oxidative and Nitrosative Stress and Fibrogenic Response. *Clin Liver Dis*. 2008;12:769-90.
4. Sambo P, Baroni SS, Luchetti M, Paroncini P, Dusi S, Orlandini G, et al. Oxidative stress in scleroderma: maintenance of scleroderma fibroblast phenotype by the constitutive up-regulation of reactive oxygen species generation through the NADPH oxidase complex pathway. *Arthritis Rheum* 2001;44(11):2653-64.
5. Ziegler TR, Panoskaltsus-Mortari A, Gu LH, Jonas CR, Farrell CL, Lacey DL, et al. Regulation of glutathione redox status in lung and liver by conditioning regimens and keratinocyte growth factor in murine allogeneic bone marrow transplantation. *Transplantation* 2001;72:1354-62.
6. Servettaz A, Goulvestre C, Kavian N, Nicco C, Guilpain P, Chéreau C, et al. Selective oxidation of DNA topoisomerase 1 induced systemic sclerosis in the mouse. *J Immunol* 2009;182(9):5855-5864.
7. Svegliati Baroni S, Santillo M, Bevilacqua F, Luchetti M, Spadoni T, Mancini M, et al. Stimulatory autoantibodies to the PDGF receptor in systemic sclerosis. *N Engl J Med* 2006;354:2667-2676.
8. Laurent A, Nicco C, Chereau C, Goulvestre C, Alexandre J, Alves A, et al. Controlling tumor growth by modulating endogenous production of reactive oxygen species. *Cancer Res* 2005;65(3):948-56.
9. Miller WHJ, Schipper HM, Lee JS, Singer J, Waxman S. Mechanisms of action of arsenic trioxide. *Cancer Res*. 2002;62:3893-903.
10. Tallman MS, Nabhan C, Feusner JH, Rowe JM. Acute promyelocytic leukemia: evolving therapeutic strategies. *Blood*. 2002;99:759-67.
11. Sanz MA, Grimwade D, Tallman MS, Lowenberg B, Fenaux P, Estey EH, et al. Management of acute promyelocytic leukemia: recommendations from an expert panel on behalf of the European LeukemiaNet. *Blood* 2009;113:1875-91.
12. Chen GQ, Zhu J, Shi XG, Ni JH, Zhong HJ, Si GY, et al. In vitro studies on cellular and molecular mechanisms of arsenic trioxide (As₂O₃) in the treatment of acute promyelocytic leukemia: As₂O₃ induces NB4 cell apoptosis with downregulation of Bcl-2 expression and modulation of PML-RAR alpha/PML proteins. *Blood*. 1996;88:1052-61.
13. Tse WP, Cheng CH, Che CT, Lin ZX. Arsenic trioxide, arsenic pentoxide, and arsenic iodide inhibit human keratinocyte proliferation through the induction of apoptosis. *J Pharmacol Exp Ther*. 2008;326:388-94.
14. Bobé P, Bonardelle D, Benihoud K, Opolon P, Chelbi-Alix MK. Arsenic trioxide: A promising novel therapeutic agent for lymphoproliferative and autoimmune syndromes in MRL/lpr mice. *Blood* 2006;108:3967-75.
15. Dalle-Donne I, Rossi R, Giustarini D, Gagliano N, Lusini L, Milzani A, et al. Actin carbonylation: from a simple marker of protein oxidation to relevant signs of severe functional impairment. *Free Radic Biol Med* 2001;1:1075-1083.
16. Servettaz A, Guilpain P, Goulvestre C, Chereau C, Hercend C, Nicco C, et al. Radical oxygen species production induced by advanced oxidation protein products predicts clinical

- evolution and response to treatment in systemic sclerosis. *Ann Rheum Dis.* 2007;66(9):1202-1209.
17. Preud'homme JL, Rochard E, Gouet D, Danon F, Alcalay M, Touchard G, et al. Isotypic distribution of anti-double-stranded DNA antibodies: a diagnostic evaluation by enzyme-linked immunosorbent assay. *Diagn Clin Immunol.* 1988;5(5):256-61.
 18. Chou WC, Jie C, Kenedy AA, Jones RJ, Trush MA, Dang CV. Role of NADPH oxidase in arsenic-induced reactive oxygen species formation and cytotoxicity in myeloid leukemia cells. *Proc Natl Acad Sci U S A.* 2004;101:4578-83.
 19. Davison K, Côté S, Mader S, Miller WH. Glutathione depletion overcomes resistance to arsenic trioxide in arsenic-resistant cell lines. *Leukemia.* 2003;17:931-40.
 20. Wang TS, Kuo CF, Jan KY, Huang H. Arsenite induces apoptosis in Chinese hamster ovary cells by generation of reactive oxygen species. *J Cell Physiol.* 1996;169:256-68.
 21. Scott N, Hatlelid KM, MacKenzie NE, Carter DE. Reactions of arsenic(III) and arsenic(V) species with glutathione. *Chem Res Toxicol.* 1993;6:102-6.
 22. Kavian N, Servettaz A, Marut W, Nicco C, Chéreau C, Weill B, et al. Sunitinib inhibits the phosphorylation of platelet-derived growth factor receptors in the skin and abrogates the development of HOCl-induced systemic sclerosis in mice. Submitted 2011.
 23. Pendergrass SA, Hayes E, Farina G, Lemaire R, Farber HW, Whitfield ML, et al. Limited systemic sclerosis patients with pulmonary arterial hypertension show biomarkers of inflammation and vascular injury. *PLoS One* 2010;5(8):e12106.
 24. Smith DM, Patel S, Raffoul F, Haller E, Mills GB, Nanjundan M. Arsenic trioxide induces a beclin-1-independent autophagic pathway via modulation of SnoN/SkiL expression in ovarian carcinoma cells. *Cell Death Differ.* 2010;17:1867-81.
 25. Asano Y, Ihn H, Yamane K, Kubo M, Tamaki K. Impaired Smad7-Smurf-mediated negative regulation of TGF-beta signaling in scleroderma fibroblasts. *J Clin Invest.* 2004;113:253-64.
 26. Li WQ, Qureshi HY, Liacini A, Dehnade F, Zafarullah M. Transforming growth factor Beta1 induction of tissue inhibitor of metalloproteinases 3 in articular chondrocytes is mediated by reactive oxygen species. *Free Radic Biol Med* 2004;37(2):196-207.
 27. Hasegawa M, Fujimoto M, Kikuchi K, Takehara K. Elevated serum levels of interleukin 4 (IL-4), IL-10, and IL-13 in patients with systemic sclerosis. *J Rheumatol* 1997;24(2):328-32.
 28. Needleman BW, Wigley FM, Stair RW. Interleukin-1, interleukin-2, interleukin-4, interleukin-6, tumor necrosis factor alpha, and interferon-gamma levels in sera from patients with scleroderma. *Arthritis Rheum* 1992;35(1):67-72.
 29. Jinnin M, Ihn H, Yamane K, Tamaki K. Interleukin-13 stimulates the transcription of the human alpha2(I) collagen gene in human dermal fibroblasts. *J Biol Chem* 2004;279:41783-41791.
 30. Dai J, Weinberg RS, Waxman S, Jing Y. Malignant cells can be sensitized to undergo growth inhibition and apoptosis by arsenic trioxide through modulation of the glutathione redox system. *Blood.* 1999;93:268-77.
 31. Li YM, Broome JD. Cancer Res. Arsenic targets tubulins to induce apoptosis in myeloid leukemia cells. 1999;59:776-80.
 32. Biswas S, Zhao X, Mone AP, Mo X, Vargo M, Jarjoura D, et al. Arsenic trioxide and ascorbic acid demonstrate promising activity against primary human CLL cells in vitro. *Leuk Res.* 2010;34:925-31.

FIGURE LEGENDS

Figure 1. Dose-response effect and modulation of ROS metabolism in fibroblasts treated with arsenic trioxide. A, B, C, Control- and HOCl-SSc-fibroblasts were seeded in a 96-wells plate in triplicate and exposed to various doses of As₂O₃ ranging from 2.5 to 40 µmol/l or medium alone for 6 hours (8.103 cells/well). Production of H₂O₂ (A), intracellular levels of GSH (B), and viability (C) were measured on a spectrofluorometer. * p<0.05 , SSc- versus control-fibroblasts, p<0.05 f SSc- or control-fibroblasts in vitro treated with arsenic versus untreated SSc- or control-fibroblasts, respectively. D, E, F, Fibroblasts from control- or SSc-mice (3 mice per group) were seeded in a 96-well plate in triplicate (8.103/well) with various chemical and enzymatic modulators (NAC, BSO, Catalase, DDC, Aminotriazole) for 24 hours and exposed to As₂O₃ for the last 6 hours of culture. Production of H₂O₂ (D), intracellular levels of GSH (E), and viability (F) were measured on a spectrofluorometer. * p<0.05, SSc- or control-fibroblasts untreated or treated with 10 µmol/l arsenic with ROS modulator versus without ROS modulator.

Figure 2. Arsenic trioxide reduced skin and lung fibrosis in HOCl-induced SSc mice. BALB/c mice received daily intradermal injections of HOCl or PBS and were concomitantly treated with As₂O₃ 5 µg/g or vehicle alone for 6 weeks (n=10 per group). A. Dermal thickness, in the injected skin areas of BALB/c mice, expressed in millimeters. B. Representative skin sections taken in the injected skin areas from BALB/c mice and stained with hematoxylin-eosin. (Olympus DP70 Controller, X 20). C. Collagen content in 6 mm punch biopsies of skin as measured by the quantitative dye-binding Sircol method. D. Phospho-Smad2/3 expression in skin by immunohistochemistry. Skin sections taken in the injected areas from BALB/c mice were stained with an anti-phospho-Smad2/3 antibody and

revealed with DAB. E. α -SMA western-blot in skin extracts (3 mice representative of 10) F. Collagen content in lungs as measured by the quantitative dye-binding Sircol method. G. Representative lung sections from BALB/c mice stained with hematoxylin-eosin. Values are means \pm SEM of data gained from all mice in the experimental or control group. Mean values were compared using paired Mann Whitney U- tests. * $P < 0.05$; NS: non significant differences.

Figure 3. In vivo treatment with arsenic trioxide exerted beneficial effects on the local and systemic oxidative stress and abrogated endothelial injuries. BALB/c mice received daily intradermal injections of HOCl or PBS and were concomitantly treated with As₂O₃ 5 μ g/g or vehicle alone for 6 weeks (n=10 per group). A. Intracellular GSH levels in skin fibroblasts from mice. Fibroblasts were isolated at the time of sacrifice from skin areas injected with HOCl, and GSH levels were determined by spectrofluorimetry. Results are expressed as optical density (O.D) per viable cells. B. Levels of H₂O₂ production by skin fibroblasts from mice, determined by spectrofluorimetry. C. Serum AOPP levels (μ mol/l of chloramin T equivalents). D. Serum nitrate levels (μ mol/g of proteins). E. Serum VCAM-1 concentrations (pg/mL). Values are means \pm SEM of data. Mean values were compared using paired U-tests.

* $p < 0.05$.

Figure 4. In vivo treatment with arsenic trioxide inhibits the production of autoantibodies in HOCl-induced SSc. SSc was induced in BALB/c mice by daily injections of an HOCl-generating solution. As₂O₃ was administered simultaneously by intra-peritoneal injections at a dose of 5 μ g/g. A. Total splenocyte numbers on the day of sacrifice (millions of cells). B. Splenic B cell numbers, as assessed by flow cytometry (millions of cells). C. Total serum IgG Ab levels measured by ELISA (ng/mL). D. Serum anti-topoisomerase-1 Ab levels measured

by ELISA (A.U). Values are means \pm SEM of data gained from all mice in the experimental or control groups. Mean values were compared using paired Mann Whitney U- tests. * $P < 0.05$.

Figure 5. *In vivo* administration of arsenic trioxide reduced the numbers of T splenocytes and the production of IL-4 and IL-13 by splenocytes from HOCl-mice. SSc was induced in BALB/c mice by daily injections of an HOCl-generating solution. As₂O₃ was administered simultaneously by intra-peritoneal injections at a dose of 5 µg/g. A. Splenic CD4 T cell numbers (millions). B. Splenic CD8 T cell numbers (millions). C. IL-4 concentrations in spleen cell supernatants (ng/mL). D. IFN-γ concentrations in spleen cell supernatants (ng/mL). E. IL-13 concentrations in spleen cell supernatants (ng/mL). F. IL-13 mRNA levels in the skin (O.D). Values are means \pm SEM of data gained from all mice in the experimental or control groups. Mean values were compared using paired Mann Whitney U- tests. * $P < 0.05$.

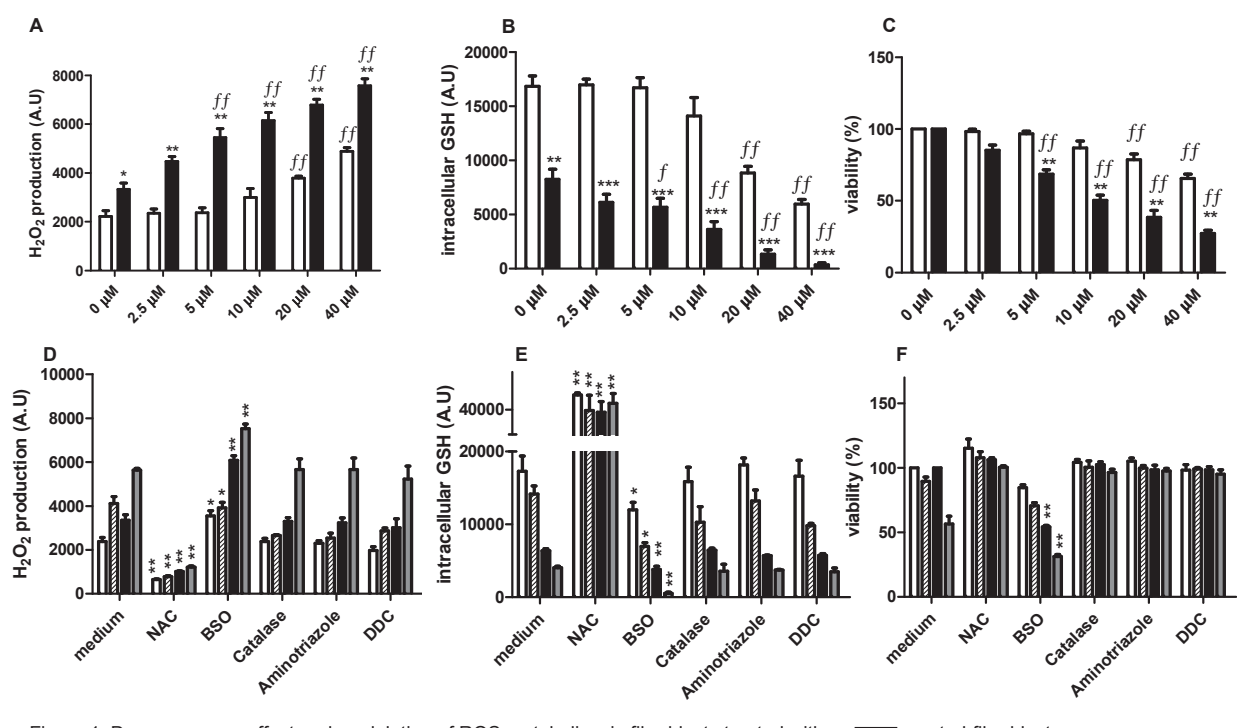


Figure 1. Dose-response effect and modulation of ROS metabolism in fibroblasts treated with arsenic trioxide. A, B, C, Control- and HOCl-SSc-fibroblasts were seeded in a 96-wells plate in triplicate and exposed to various doses of arsenic trioxide ranging from 2.5 to 40 $\mu\text{mol/l}$ or medium alone for 6 hours ($8 \cdot 10^3$ cells/well). Production of H₂O₂ (A), intracellular levels of GSH (B), and viability (C) were measured on a spectrofluorometer. * p<0.05 , HOCl-SSc- versus control-fibroblasts, p<0.05 f HOCl-SSc- or control-fibroblasts in vitro treated with arsenic versus untreated HOCl-SSc- or control-fibroblasts, respectively. D, E, F, Fibroblasts from control- or SSc-mice (3 mice per group) were seeded in a 96-well plate in triplicate ($8 \cdot 10^3$ /well) with various chemical and enzymatic modulators (NAC, BSO, Catalase, CDD, Aminotriazole) for 24 hours and exposed to As₂O₃ for the last 6 hours of culture. Production of H₂O₂ (D), intracellular levels of GSH (E), and viability (F) were measured on a spectrofluorometer. * p<0.05, HOCl-SSc- or control-fibroblasts untreated or treated with 10 $\mu\text{mol/l}$ arsenic with ROS modulator versus without ROS modulator.

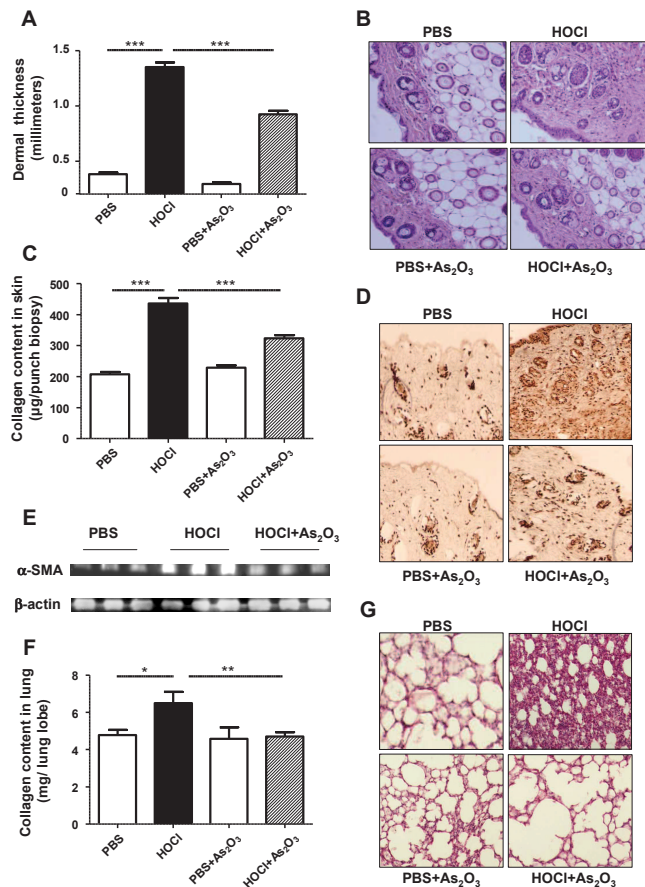


Figure 2. Arsenic trioxide reduced skin and lung fibrosis in HOCl-induced SSc mice. BALB/c mice received daily intradermal injections of HOCl or PBS and were concomitantly treated with As₂O₃ 5 µg/g or vehicle alone for 6 weeks (n=10 per group). A. Dermal thickness, in the injected skin areas of BALB/c mice, expressed in millimeters. B. Representative skin sections taken in the injected skin areas from BALB/c mice and stained with hematoxylin-eosin. (Olympus DP70 Controller, X 20). C. Collagen content in 6 mm punch biopsies of skin as measured by the quantitative dye-binding Sircol method. D. Phospho-Smad2/3 expression in skin by immunohistochemistry. Skin sections taken in the injected areas from BALB/c mice were stained with an anti-phospho-Smad2/3 antibody and revealed with DAB. E. α-SMA western-blots in skin extracts (3 mice representative of 10) F. Collagen content in lungs as measured by the quantitative dye-binding Sircol method. G. Representative lung sections from BALB/c mice stained with hematoxylin-eosin. Values are means ± SEM of data gained from all mice in the experimental or control group. Mean values were compared using paired Mann Whitney U-tests. * P < 0.05; NS: non significant differences.

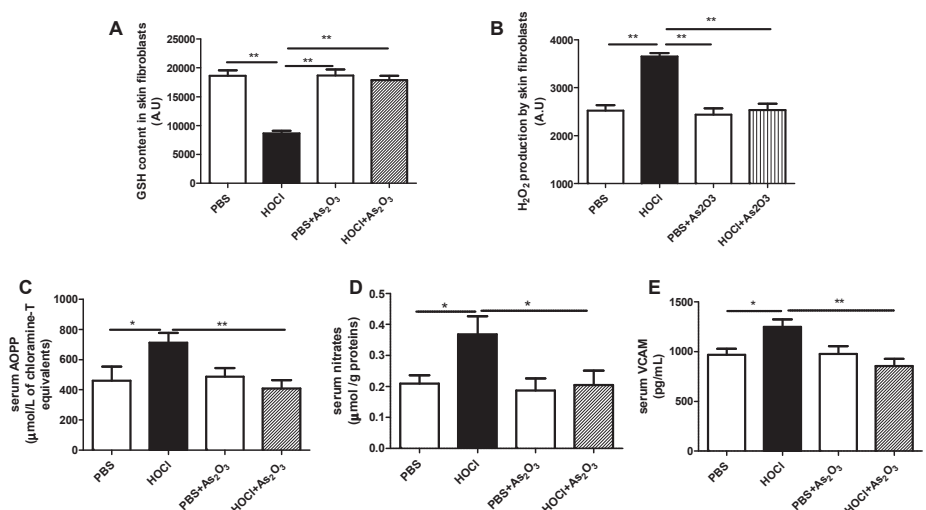


Figure 3. *In vivo* treatment with arsenic trioxide exerted beneficial effects on the local and systemic oxidative stress and abrogated endothelial injuries. BALB/c mice received daily intradermal injections of HOCl or PBS and were concomitantly treated with As₂O₃ 5 µg/g or vehicle alone for 6 weeks (n=10 per group). A. Intracellular GSH levels in skin fibroblasts from mice. Fibroblasts were isolated at the time of sacrifice from skin areas injected with HOCl, and GSH levels were determined by spectrofluorimetry. Results are expressed as optical density (O.D) per viable cells. B. Levels of H₂O₂ production by skin fibroblasts from mice, determined by spectrofluorimetry. C. Serum AOPP levels (µmol/l of chloramine T equivalents). D. Serum nitrate levels (µmol/g of proteins). E. Serum VCAM-1 concentrations (pg/mL). Values are means ± SEM of data. Mean values were compared using paired U-tests. * p<0.05.

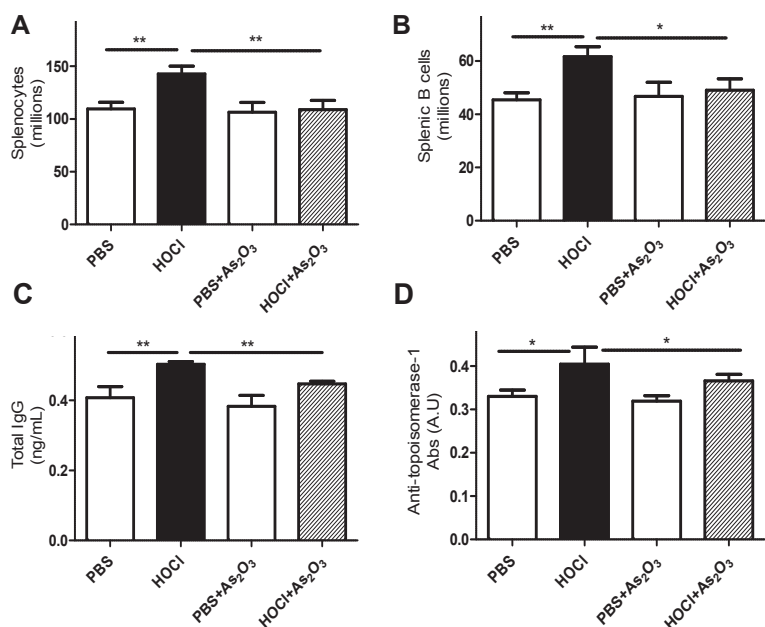


Figure 4. In vivo treatment with arsenic trioxide inhibits the production of autoantibodies in HOCl-induced SSc. SSc was induced in BALB/c mice by daily injections of an HOCl-generating solution. As₂O₃ was administered simultaneously by intra-peritoneal injections at a dose of 5 µg/g. A. Total splenocyte numbers on the day of sacrifice (millions of cells). B. Splenic B cell numbers, as assessed by flow cytometry (millions of cells). C. Total serum IgG Ab levels measured by ELISA (ng/mL). D. Serum anti-topoisomerase-1 Ab levels measured by ELISA (A.U.). Values are means ± SEM of data gained from all mice in the experimental or control groups. Mean values were compared using paired Mann Whitney U- tests. * P < 0.05.

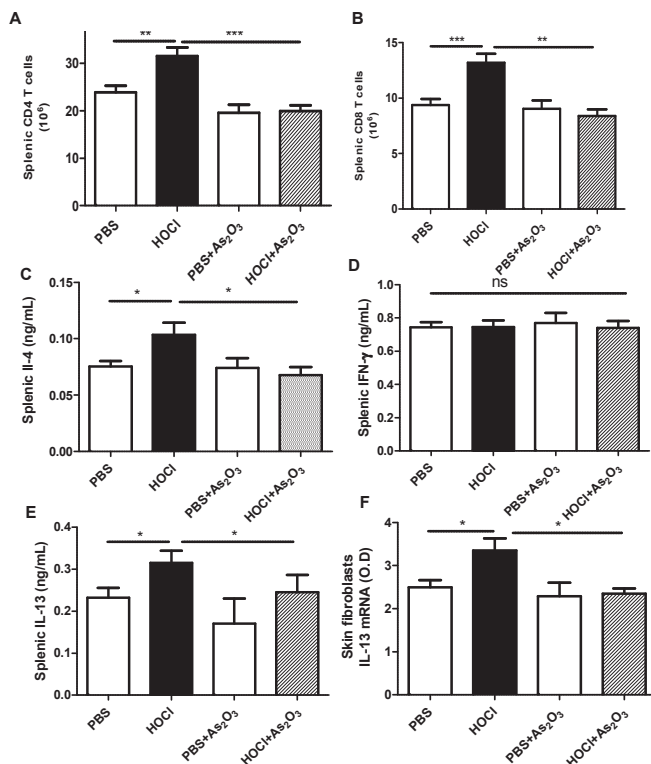
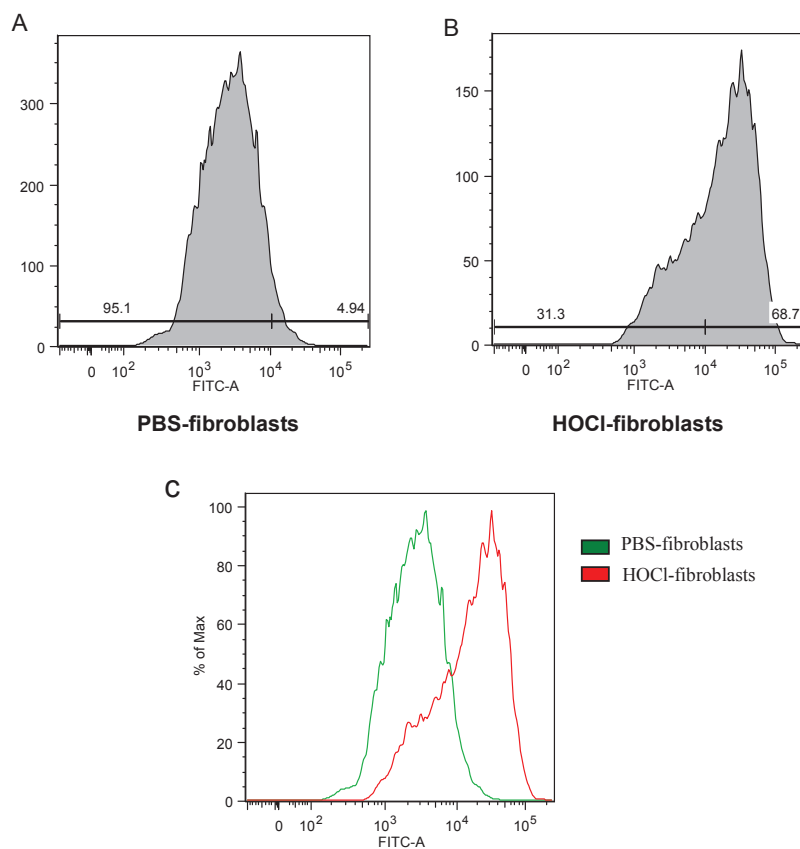
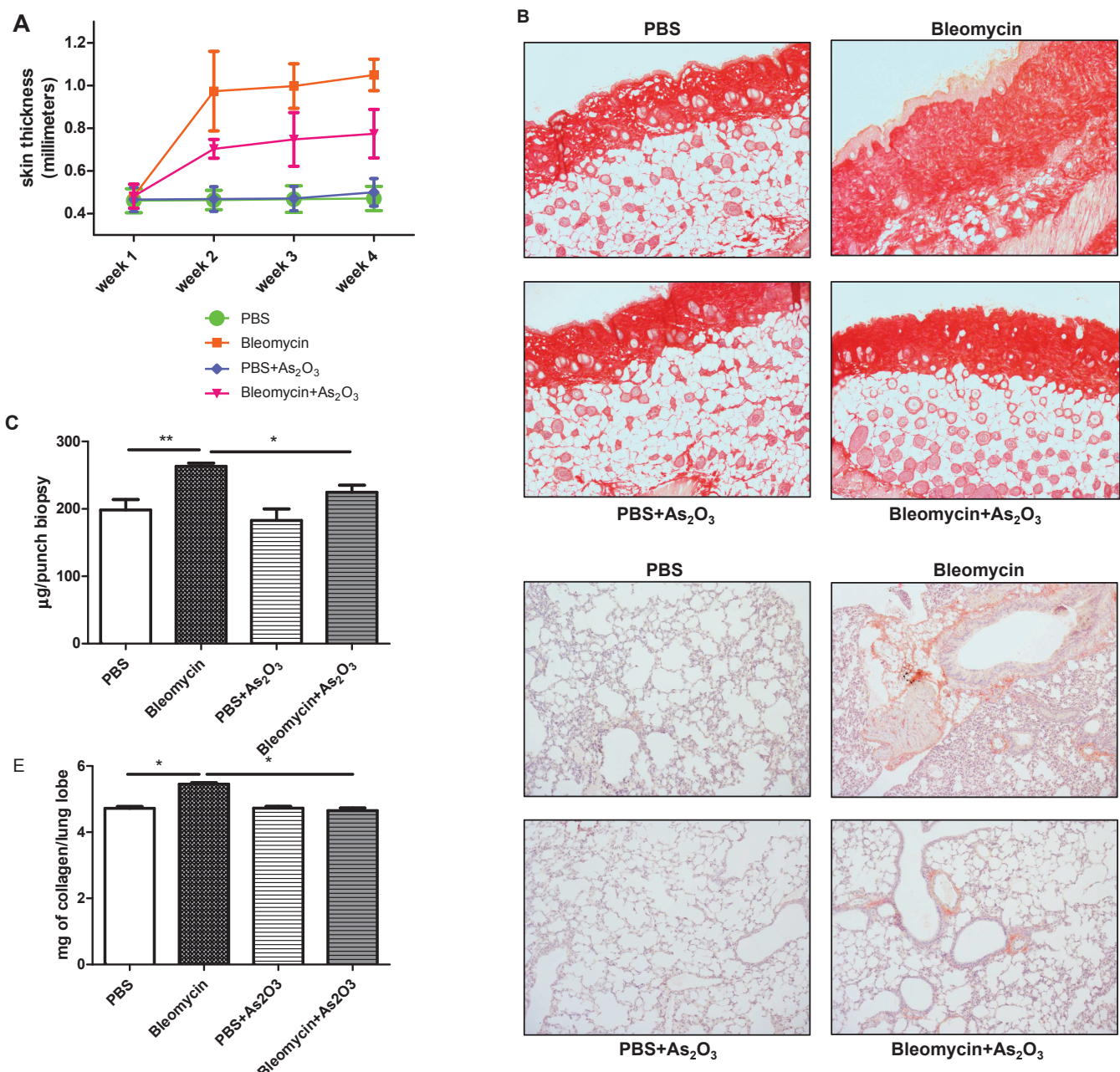


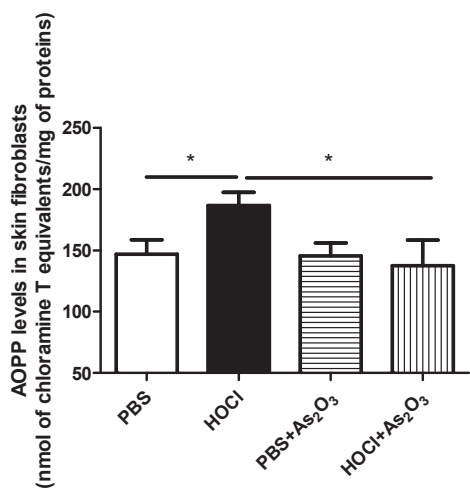
Figure 5. *In vivo* administration of arsenic trioxide reduced the numbers of T splenocytes and the production of IL-4 and IL-13 by splenocytes from HOCl-mice. SSc was induced in BALB/c mice by daily injections of an HOCl-generating solution. As2O3 was administered simultaneously by intraperitoneal injections at a dose of 5 µg/g. A. Splenic CD4 T cell numbers (millions). B. Splenic CD8 T cell numbers (millions). C. IL-4 concentrations in spleen cell supernatants (ng/mL). D. IFN- γ concentrations in spleen cell supernatants (ng/mL). E. IL-13 concentrations in spleen cell supernatants (ng/mL). F. IL-13 mRNA levels in the skin (O.D.). Values are means \pm SEM of data gained from all mice in the experimental or control groups. Mean values were compared using paired Mann Whitney U-tests. * $P < 0.05$.



Supplemental figure 1. FACS analysis of α -SMA (α -smooth muscle actin) expression in skin fibroblasts extracted from PBS- and HOCl-mice. Fibroblasts were extracted from the skin of PBS- or HOCl-mice ($n = 4$ per group). Cells were cultured and then harvested for α -SMA labelling using an anti- α -SMA-FITC antibody. A. α -SMA expression in PBS-fibroblasts. B. α -SMA expression in HOCl-SSc-fibroblasts. C. overlay of α -SMA expression in PBS- and HOCl-SSc-fibroblasts. Data are representative of 4 mice per group.



Supplemental figure 2. Arsenic trioxide reduced skin and lung fibrosis in mice with bleomycin-induced-SSc. BALB/c mice received daily subcutaneous injections of bleomycin (100 µg/mL) or PBS and were concomitantly treated with As₂O₃ 5 µg/g or vehicle alone for 5 weeks (n=7 per group). Pictures were taken with the Nikon Eclipse 80I microscope and the Nikon Digital Sight DS-U3 camera A. Dermal thickness, in the injected skin areas of BALB/c mice, expressed in millimeters. B. Representative skin sections taken in the injected skin areas from BALB/c mice and stained with picro-sirius red. (x10). C. Collagen content in 6 mm punch biopsies of skin as measured by the quantitative dye-binding Sircol method. D. Representative lung sections stained with picro-sirius red. (x10). E. Collagen content in lungs as measured by the quantitative dye-binding Sircol method, expressed in mg of collagen per lung lobe. Values are means ± SEM of data gained from all mice in the experimental or control group. Mean values were compared using paired Mann Whitney U-tests. * P < 0.05; NS: non significant differences.



Supplemental figure 3. Levels of AOPP in skin fibroblasts isolated from mice. Fibroblasts were isolated at the time of sacrifice from skin areas injected with HOCl or PBS and AOPP levels were measured as described in the Materials and Methods section. Results are expressed in $\mu\text{mol/l}$ of chloramin T equivalents per mg of proteins. Values are means \pm SEM of data gained from all mice in the experimental or control group. Mean values were compared using paired Mann Whitney U- tests. * $P < 0.05$; NS: non significant differences.

3.6 ARTICLE 6

Le trioxyde d'arsenic prévient le développement de la sclérodermie associée à la réaction du greffon contre l'hôte

Arsenic trioxide prevents murine sclerodermatous-graft-versus-host disease

Niloufar Kavian, Wioleta Marut, Amélie Servettaz, Hélène Laude,
Carole Nicco, Christiane Chéreau, Bernard Weill, Frédéric Batteux

Journal of Immunology, 2012

Dans le précédent travail, nous avons montré que le trioxyde d'arsenic pouvait causer l'apoptose sélective des fibroblastes cutanés sclérodermiques via l'induction d'une production de peroxyde d'hydrogène H_2O_2 dépassant le seuil létal pour ces cellules déficientes en glutathion. En traitant les souris ScS *in vivo* par le trioxyde d'arsenic, nous avons observé une amélioration clinique significative de la maladie. Nous avons voulu poursuivre ce travail en testant cette molécule dans un autre modèle murin de ScS: le modèle de ScS associée à la réaction du greffon contre l'hôte. Dans ce modèle, l'activation du système immunitaire s'accompagne d'une fibrose cutanée et viscérale. Ces phénomènes résultent d'incompatibilités mineures au niveau du Complexe Majeur d'Histocompatibilité entre donneur du greffon et receveur entraînant l'activation de lymphocytes T alloréactifs.

Nous avons induit la maladie en greffant des cellules hématopoïétiques de rate (2.10^6 cellules) et de moelle osseuse (1.10^6 cellules) de souris B10.D2 ($H2^d$) à des souris BALB/c ($H2^d$) irradiées de manière sublétale (7 Grays). Des souris contrôles BALB/c ont reçu un greffon syngénique provenant de souris BALB/c. Les souris ont commencé à recevoir le traitement par injections intra-péritonéales de trioxyde d'arsenic à 5 mg/kg à J7 post-greffe, et ont été sacrifiées à J28 post-greffe.

Les souris greffées et traitées par l'arsenic ont présenté une réduction significative des symptômes de la GVH : diarrhées, alopecie, vascularite, fibrose de la peau et des poumons. Ces effets bénéfiques étaient associés à une déplétion en lymphocytes T CD4 $^+$ de phénotype mémoire activé (CD62L $^-$ CD44 $^+$) et en cellules dendritiques plasmacytoides (pDCs). In vitro, l'arsenic a

également entraîné l'apoptose de ces cellules par une déplétion en glutathion et une surproduction en H₂O₂ dépassant le seuil cytotoxique. Cette action de l'arsenic était sélective envers les cellules T CD4+ B10.D2 activées par les cellules BALB/c irradiées et les pDCs activées.

Ce travail souligne les effets bénéfiques du trioxyde d'arsenic dans la GVHD chronique et ses manifestations associées partageant des similitudes avec la ScS (fibrose cutanée et systémique, activation du système immunitaire, anomalies endothéliales). De plus, ils renforcent les données obtenues dans l'article 5 dans notre modèle murin de ScS induite par HOCl. Ainsi, nous suggérons que le trioxyde d'arsenic, molécule utilisée chez l'homme dans le traitement d'hémopathies lymphoïdes et bien tolérée, pourrait être testée dans le traitement de la GVHD chronique.

Arsenic Trioxide Prevents Murine Sclerodermatous Graft-versus-Host Disease

Niloufar Kavian,^{*,†,1} Wioleta Marut,^{*,1} Amélie Servettaz,^{*,‡} Hélène Laude,^{*,§}
Carole Nicco,^{*} Christiane Chéreau,^{*} Bernard Weill,^{*,†} and Frédéric Batteux^{*,†}

Chronic graft-versus-host disease (GVHD) follows allogeneic hematopoietic stem cell transplantation. It results from alloreactive processes induced by minor MHC incompatibilities triggered by activated APCs, such as plasmacytoid dendritic cells (pDCs), and leading to the activation of CD4⁺ T cells. Therefore, we tested whether CD4⁺ and pDCs, activated cells that produce high levels of reactive oxygen species, could be killed by arsenic trioxide (As_2O_3), a chemotherapeutic drug used in the treatment of acute promyelocytic leukemia. Indeed, As_2O_3 exerts its cytotoxic effects by inducing a powerful oxidative stress that exceeds the lethal threshold. Sclerodermatous GVHD was induced in BALB/c mice by body irradiation, followed by B10.D2 bone marrow and spleen cell transplantation. Mice were simultaneously treated with daily i.p. injections of As_2O_3 . Transplanted mice displayed severe clinical symptoms, including diarrhea, alopecia, vasculitis, and fibrosis of the skin and visceral organs. The symptoms were dramatically abrogated in mice treated with As_2O_3 . These beneficial effects were mediated through the depletion of glutathione and the overproduction of H_2O_2 that killed activated CD4⁺ T cells and pDCs. The dramatic improvement provided by As_2O_3 in the model of sclerodermatous GVHD that associates fibrosis with immune activation provides a rationale for the evaluation of As_2O_3 in the management of patients affected by chronic GVHD. *The Journal of Immunology*, 2012, 188: 000–000.

Chronic graft-versus-host disease (GVHD) is a major factor of morbidity following allogeneic hematopoietic stem cell transplantation, with variable clinical presentations (1, 2). Chronic GVHD emerges from alloreactive processes between donor-derived immune cells and host cell populations induced by minor MHC incompatibilities between donor and recipient. Its pathophysiology is poorly understood in contrast to that of acute GVHD (1, 3). Donor CD4⁺ T cells are involved in the induction of chronic GVHD, but the effector mechanisms through which they mediate tissue inflammation are unclear; the recognition of MHC class II alloantigens on host dendritic cells (DCs) is sufficient to prime donor CD4⁺ T cells and induce GVHD (3–5). Moreover, among APCs, plasmacytoid DCs (pDCs) were shown to be pathogenic in GVHD. In the absence of other APCs, pDCs alone can stimulate donor T cells to trigger GVHD, and total-body irradiation is crucial for their maturation and the subsequent priming of alloreactive CD4⁺ T cells (6).

Chronic GVHD often mimics autoimmune diseases (7). Sclerodermatous-GVHD (Scl-GVHD) makes up 10–15% of cases of chronic GVHD (8). This clinical form of GVHD resembles systemic sclerosis, because it includes fibrotic changes and chronic inflammation of the skin, lung, and gastrointestinal tract. Several animal models have been developed to help define the pathophysiology of chronic GVHD. One of them is based on the transfer of donor immune cells into sublethally irradiated host mice with mismatched minor MHC histocompatibility Ags, resulting in full donor lymphoid chimerism (9). This model recapitulates the clinical features of Scl-GVHD, with fibrosis of the skin and visceral organs 14 d following the graft.

Activated T cells with a high rate of production of reactive oxygen species (ROS) play a pivotal role in the development of Scl-GVHD. Therefore, we investigated whether a cytotoxic molecule that acts by enhancing ROS production beyond a lethal threshold could be of any help in treating chronic GVHD.

Arsenic trioxide (As_2O_3) is an inorganic trivalent salt that exhibits potent antitumor effects in vitro and in vivo, especially in the treatment of hematological malignancies, such as acute promyelocytic leukemia refractory to all-trans retinoic acid (10). Several reports suggested that As_2O_3 can affect many cellular functions, such as proliferation, apoptosis, differentiation, and angiogenesis, in various cell lines. An important cellular event occurring after As_2O_3 treatment is the elevation of intracellular ROS levels (11). This ROS generation appears to be regulated through several pathways, including NADPH oxidase, mitochondrial electron transport chain, and inhibition of antioxidant enzymes (12–14). The ROS-mediated apoptosis triggered by As_2O_3 can impact hematological tumor cells; under certain circumstances, it can also affect nontumor cells, such as keratinocytes, fibroblasts, or activated autoimmune lymphocytes (15–17).

In this study, we tested the therapeutic effects of As_2O_3 in a murine model of Scl-GVHD generated by grafting B10.D2 ($H-2^d$) bone marrow and spleen cells into sublethally irradiated BALB/c mice ($H-2^d$). We show that As_2O_3 limits both the acti-

*Laboratoire EA 1833, Faculté de Médecine, Sorbonne Paris Cité, Université Paris Descartes, 75679 Paris Cedex 14, France; †Laboratoire d'Immunologie Biologique, Hôpital Cochin, Assistance Publique Hôpitaux de Paris, 75014 Paris, France; [‡]Faculté de Médecine de Reims, Service de Médecine Interne, Maladies Infectieuses, Immunologie Clinique, Hôpital Robert Debré, 51092 Reims Cedex, France; and [§]Laboratoire de Virologie, Hôpital Cochin, Assistance Publique Hôpitaux de Paris, 75014 Paris, France

¹N.K. and W.M. contributed equally to this work.

Received for publication December 12, 2011. Accepted for publication March 9, 2012.

This work was supported by grants from Assistance Publique Hôpitaux de Paris (to N.K.) and Redcat (to W.M.).

Address correspondence and reprint requests to Prof. Frédéric Batteux, Laboratoire d'Immunologie EA 1833, Faculté de Médecine Paris Descartes, 75679 Paris Cedex 14, France. E-mail address: frederic.batteux@chc.aphp.fr

Abbreviations used in this article: As_2O_3 , arsenic trioxide; BMT, bone marrow transplantation; cDC, conventional dendritic cell; DC, dendritic cell; GSH, glutathione; GVHD, graft-versus-host disease; MFI, mean fluorescence intensity; NAC, *N*-acetyl-cysteine; pDC, plasmacytoid dendritic cell; ROS, reactive oxygen species; Scl-GVHD, sclerodermatous graft-versus-host disease.

Copyright © 2012 by The American Association of Immunologists, Inc. 0022-1767/12/\$16.00

vation of the immune system and fibrosis in mice with Scl-GVHD. As₂O₃ induces apoptosis in alloreactive CD4⁺ T cells and activated pDCs, thus limiting the development of GVHD reaction in mice.

Materials and Methods

Animals, cells, and chemicals

Specific pathogen-free, 6-wk-old female BALB/c and male B10.D2 mice were purchased from Harlan (Gannat, France) and maintained with food and water ad libitum. They were given humane care, according to the guidelines of our institution (Université Paris Descartes). All cells were cultured as previously reported (18). All chemicals were from Sigma-Aldrich (Saint-Quentin Fallavier, France).

Experimental procedure in Scl-GVHD mice

Induction of GVHD in BALB/c mice. GVHD following bone marrow transplantation (BMT) was induced in BALB/c mice (H-2^d; Janvier Laboratory, Le Genest Saint Isle, France) by grafting cells from 7–8-week-old female B10.D2 mice (H-2^d; Janvier Laboratory), as previously described by Jaffee and Claman (19). Briefly, recipient mice were lethally irradiated with 750 cGy from a Gammacel [¹³⁷Cs] source. Three hours later, they were injected i.v. with donor spleen cells (2×10^7 /mouse) and bone marrow cells (1×10^6 /mouse) suspended in RPMI 1640. A control group of BALB/c recipient mice received BALB/c spleen and bone marrow cells (syngeneic BMT, referred to as control animals). Transplanted animals were maintained in sterile microisolator cages (Lab Products, Langenselbold, Germany) and supplied with autoclaved food and sterile water. Animals were sacrificed by cervical dislocation 4 wk after BMT.

Treatment of Scl-GVHD mice with As₂O₃. Scl-GVHD and control mice were randomized and treated for 3 wk with i.p. injections of either As₂O₃ or vehicle alone beginning on day 7 post-BMT (10 mice/group). A stock solution was prepared ex temporaneously, as described above. As₂O₃ was given 5 d/wk at a dose of 5 µg/g body weight, as described by Bobé et al. (17). Control mice received i.p. injections of PBS 5 d/wk. Four weeks after BMT, the animals were sacrificed by cervical dislocation.

Assessment of collagen accumulation

Skin thickness. Skin thickness of the shaved back of mice was measured 1 d before sacrifice with a caliper and expressed in millimeters.

Histopathological analysis. Fixed lung and skin pieces were embedded in paraffin. A 5-µm-thick tissue section was stained with H&E or Picosirius Red. Slides were examined by standard bright-field microscopy (Olympus BX60, Rungis, France) by a pathologist who was blinded to the assignment of the animal group.

Collagen content in skin and lung. Skin and lung pieces were diced using a scalpel, put into tubes, thawed, and mixed with pepsin (1:10 weight ratio) and 0.5 M acetic acid overnight at room temperature under stirring. The assay of collagen content was based on the quantitative dye-binding Sircol method (Biocolor, Belfast, Ireland).

Disease severity score

To determine the incidence and severity of disease, we assigned a score to each mouse using the following criteria: 0: no external sign; 1: piloerection on back and underside, 1: hunched posture or lethargy; 1: weight loss >10%; 0.5: alopecia <1 cm²; 1: alopecia >1 cm²; 1: vasculitis (one or more purpuric lesions); and 1: eyelid sclerosis (blepharophymosis). The severity score is the sum of these values and ranges from 0 (unaffected) to a maximum of 6. The incidence and severity score was recorded every week by two blinded scientists.

Flow cytometric analysis of spleen cell subsets

Cell suspensions from spleens were prepared after hypotonic lysis of erythrocytes in potassium acetate solution. Cells were incubated with the appropriate labeled Ab at 4°C for 30 min in PBS with 0.1% sodium azide and 5% normal rat serum. Flow cytometry was performed using a FACS-Canto flow cytometer (BD Biosciences, San Jose, CA), according to standard techniques. The mAbs used in this study were anti-B220-PE-Cy7, anti-CD11b-biotin, anti-CD11c-FITC, anti-CD4-PerCP, and anti-CD8-PE-Cy7 (BD Biosciences). Data were analyzed with FlowJo software (Tree Star, Ashland, OR).

Determination of IL-4 and IL-17 production by splenocytes

Spleen cells were isolated by gentle disruption of the tissues, and the erythrocytes were lysed by hypotonic shock in potassium acetate solution.

Spleen cells were cultured in RPMI 1640 supplemented with antibiotics, GlutaMAX (Invitrogen Life Technologies), and 10% heat-inactivated FCS (Invitrogen Life Technologies) (complete medium). CD4 T cells were isolated from spleen cell suspensions by positive selection using CD4 microbeads and LS columns (Miltenyi Biotec, Paris, France), according to the manufacturer's instructions. CD4 T cell suspensions were then seeded in 96-well flat-bottom plates and cultured (2×10^5 cells) in complete medium for 48 h in the presence of 5 µg/ml Con A. Supernatants were collected, and cytokine concentrations were determined by ELISA (for IL-4: eBioscience, San Diego, CA; for IL-17: DuoSet; R&D Systems). Results are expressed in ng/ml.

Assays of serum anti-DNA topoisomerase I autoantibodies

Levels of anti-DNA topoisomerase I IgG Abs were detected by ELISA on microtiter plates (ImmunoVision, Springdale, AR). A 1:50 serum dilution was used for the ELISA.

Effects of As₂O₃ on B10.D2 CD4 T cells *in vitro*

Suspensions of spleen cells from a male B10.D2 mouse and a female BALB/c mouse were prepared after hypotonic lysis of erythrocytes. The BALB/c cell suspension was irradiated at 30 Gy. A B10.D2 cell suspension was also prepared and irradiated at 30 Gy for syngeneic control.

B10.D2 cells were labeled with PKH26 dye, according to the manufacturer's instructions (Sigma-Aldrich).

Measurement of H₂O₂ concentration in CD4 T cells. B10.D2 cells labeled with PKH26 were incubated with irradiated BALB/c cells and complete medium for 24 h. After this incubation period, cells were washed without serum and incubated with 5 µM CM-H₂DCFDA (Sigma-Aldrich) at 37°C for 20 min. After washing, cells were incubated with 10 µM As₂O₃, with or without 4 mM N-acetylcysteine (NAC), for 5 h at 37°C. Cells were then washed and labeled with anti-CD4 mAb.

Measurement of glutathione concentration in CD4 T cells. B10.D2 cells labeled with PKH26 were incubated with or without irradiated BALB/c cells and complete medium, with or without 10 µM As₂O₃ and with or without 4 mM NAC, for 24 h. Cells were washed and labeled with 100 µM monochlorobimane at 37°C for 20 min, followed by labeling with anti-CD4 mAb for 20 min.

Determination of apoptosis in CD4 T cells. B10.D2 cells labeled with PKH26 were incubated with or without irradiated BALB/c spleen cells and complete medium alone, with 10 µM As₂O₃ alone, or with 4 mM NAC for 24 h. Cells were then washed and stained with anti-CD4 mAb (eBioscience) at 4°C for 20 min and Yopro-1 (Sigma-Aldrich) at room temperature for 10 min.

Effects of As₂O₃ on B10.D2 pDCs *in vitro*

A suspension of spleen cells from a male B10.D2 mouse was prepared after hypotonic lysis of erythrocytes.

Measurement of H₂O₂ concentration in pDCs. B10.D2 cells were incubated in complete medium, washed without serum, and incubated with 5 µM CM-H₂DCFDA (Sigma-Aldrich) at 37°C for 20 min. After washing, cells were incubated with 10 µM As₂O₃, with or without 4 mM NAC, for 5 h at 37°C. Cells were then washed and labeled with anti-B220, anti-CD11b, and anti-CD11c mAb (BD, Le Pont de Claix, France).

Measurement of glutathione concentration in pDCs. B10.D2 cells were incubated with complete medium with or without 10 µM As₂O₃ and with or without 4 mM NAC for 24 h. Cells were then washed and labeled with 100 µM monochlorobimane at 37°C for 20 min, followed by labeling with anti-B220, anti-CD11b, and anti-CD11c mAb (BD) for 20 min.

Determination of apoptosis in pDCs. B10.D2 cells were incubated with complete medium alone, with 10 µM As₂O₃ alone, or with 10 µM As₂O₃ and 4 mM NAC for 24 h. Cells were then washed and stained with anti-B220, anti-CD11b, and anti-CD11c mAb (BD) at 4°C for 20 min and Yopro-1 (Sigma-Aldrich) at room temperature for 10 min.

For all flow cytometry analyses, pDCs were defined as B220⁺CD11c^{int} CD11b^{low}. Data were acquired on a FACSCanto II flow cytometer (BD Biosciences) and analyzed with FlowJo software (Tree Star).

Measurement of *in vitro* IFN- α production by pDCs

pDCs were isolated from the spleen of a BALB/c mouse using the pDC isolation kit and MS columns (Miltenyi Biotec). pDCs were then coated in six-well plates and incubated with 10 µg/ml Gardiquimod (InvivoGen, Toulouse, France) and increasing doses of As₂O₃ (from 0 to 25 µM) or with medium alone for 24 h. Supernatants were harvested, and IFN- α was assayed as described by Dubois et al. (20). Briefly, L929 cells (5×10^4 /well; kindly provided by P. Lebon, Laboratoire de Virologie, Hôpital

Cochin, Paris, France) were coated in 96-well plates and cultured in RPMI 1640 at 37°C with 5% CO₂ until confluence. Culture media were discarded, and plates were incubated for an additional 24 h with 50 µl 2-fold serial dilutions (from 1:2 to 1:256 in RPMI 1640) of supernatant samples or with serial dilutions of a standard solution of murine IFN- α . Thereafter, vesicular stomatitis virus was added; the final concentration was 1:400 of a stock solution previously shown to cause complete lysis of L929 cells at a dilution of 1:2000. We considered the dilution that destroyed half of the cell layer at 24 h, and IFN- α units were determined by comparison with cells incubated with 2-fold serial dilutions of mouse IFN- α (kindly provided by P. Lebon).

Statistical analysis

All of the quantitative data are expressed as mean \pm SEM and were analyzed with Prism 5 (GraphPad), using one-way ANOVA or the Student *t* test, as appropriate. A *p* value <0.05 was considered statistically significant.

Results

As₂O₃ prevented clinical symptoms of systemic sclerosis induced by GVHD

We investigated the effects of As₂O₃ on the development of Scl-GVHD, a fibrotic variant of GVHD. As₂O₃ was administered daily from day 7 following BMT, and mice were sacrificed 21 d later. Lethally irradiated BALB/c mice transplanted with bone marrow and spleen cells from B10.D2 mice developed skin fibrosis, as shown by the measurement of ear skin thickening in Fig. 1A. Control BALB/c animals with syngeneic grafts did not develop skin fibrosis or GVHD (Fig. 2). In addition to skin thickening, the engrafted animals displayed alopecia (100% of mice), vasculitis (>80% of mice), or diarrhea (100% of mice). On day 21, the disease severity score of Scl-GVHD mice was ≥ 5 , whereas that of control animals (syngeneic graft) was 0 (Fig. 2B). As₂O₃ effectively prevented severe GVHD; the mean severity score of treated mice at day 14 was 2.5 ± 0.2 versus 5 ± 0.4 in untreated Scl-GVHD mice (*p* < 0.001, Fig. 2B). Scl-GVHD mice treated with As₂O₃ displayed a reduction in skin thickness >40% compared with untreated Scl-GVHD mice (*p* = 0.007, Fig. 1B). Moreover, type 1 collagen content in the skin of Scl-GVHD mice treated

with As₂O₃ was 45% lower than in untreated Scl-GVHD mice (*p* = 0.002, Fig. 1C). Picosirius Red staining of ear sections showed important collagen deposits in the ears from Scl-GVHD mice but not in those of Scl-GVHD mice treated with As₂O₃ (Fig. 1A). Also, type 1 collagen concentration was higher in the lungs of Scl-GVHD mice than in Scl-GVHD mice treated with As₂O₃ (data not shown). Altogether, these results show that As₂O₃ limits the deposition of collagen and prevents the development of alopecia, vasculitis, and diarrhea in Scl-GVHD mice.

As₂O₃ altered spleen cell subsets in Scl-GVHD mice

GVHD is caused by a donor T cell antihost reaction. We investigated whether the clinical improvement observed in Scl-GVHD mice treated with As₂O₃ correlated with quantitative or qualitative alterations in spleen cell subsets. Flow cytometric analysis of splenocytes showed that As₂O₃ decreased the percentage of CD4⁺ T cells (*p* = 0.049 versus untreated Scl-GVHD mice). This reduction involved the CD44⁺CD62L⁻ effector memory CD4 subset, because the ratio of CD4⁺CD44^{high}CD62L^{low}/CD4⁺CD44^{low} CD62L^{high} cells was 15.7 ± 4.6 in Scl-GVH mice versus 3.6 ± 0.7 in Scl-GVHD mice treated with arsenic (*p* = 0.001, Fig. 3A-C). Furthermore, the percentage of splenic pDCs, defined as B220⁺CD11c⁺CD11b^{low}, was three times lower in arsenic-treated Scl-GVHD mice compared with untreated Scl-GVHD mice (*p* = 0.021, Fig. 3D).

As₂O₃ modified the splenic production of cytokines and the serum levels of autoantibodies in Scl-GVHD mice

In addition, we explored the splenic production of IL-4 and IL-17, two cytokines implicated in the development of GVHD in mice (21). Scl-GVHD mice produced more IL-4 and IL-17 than did control mice (IL-4: 0.24 ± 0.023 for Scl-GVHD mice and 0.12 ± 0.021 for control mice, *p* = 0.011; IL-17: 0.64 ± 0.083 for Scl-GVHD mice and 0.37 ± 0.088 for control mice, *p* = 0.042; Fig. 3E, 3F). As₂O₃ significantly reduced the production of the two cytokines (*p* = 0.043 and *p* = 0.022 for IL-4 and IL-17, respectively, versus nontreated mice, Fig. 3E, 3F). We then investigated

FIGURE 1. As₂O₃ reduces the fibrotic changes in mice with Scl-GVHD. GVHD was induced by allogeneic transplant of B10.D2 bone marrow and spleen cells into irradiated BALB/c mice. Control mice received syngeneic transplants. As₂O₃ was administered from day 7 post-BMT at a dose of 5 µg/g. Mice were sacrificed on day 28. Data from two independent experiments were pooled (*n* = 10/group). (A) Representative Picosirius Red staining of the skin (objective $\times 10$). (B) Skin thickness measured with a caliper and expressed in millimeters. (C) Collagen content in skin of mice expressed in µg/punch biopsy. Values are mean \pm SEM of data from all mice in the experimental or control groups. **p* < 0.05, paired Mann-Whitney *U* test.

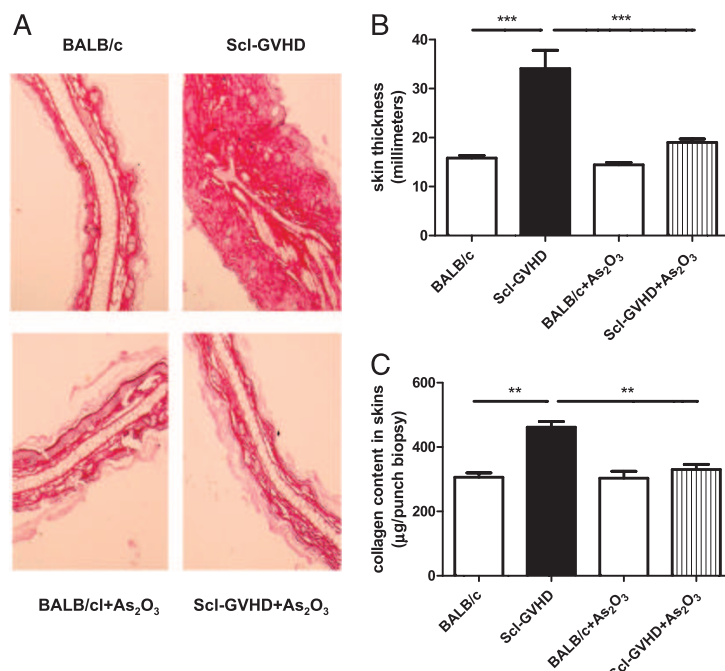
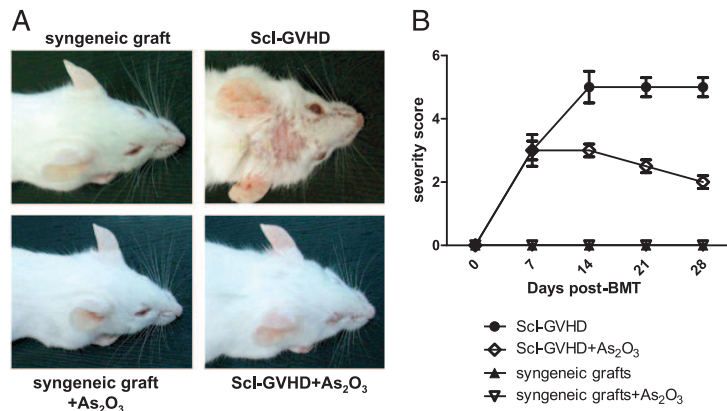


FIGURE 2. As₂O₃ improves the clinical symptoms of Scl-GVHD in mice. GVHD was induced by allogeneic transplant of B10.D2 bone marrow and spleen cells into irradiated BALB/c mice. Control mice received syngeneic transplants. As₂O₃ was administered from day 7 post-BMT at a dose of 5 µg/g. Mice were sacrificed on day 28. Data from two independent experiments were pooled. (A) Representative photographs of mice on day 28 post-BMT ($n = 10/\text{group}$). (B) Disease severity scores (mean \pm SEM).



the presence of anti-DNA topoisomerase 1 Abs, a hallmark of the Scl-GVHD model, which are generally detected 3–9 wk following the onset of disease (9). On the day of sacrifice, 80% of Scl-GVHD mice and only 20% of Scl-GVHD mice treated with As₂O₃ were positive for anti-DNA-topoisomerase 1 Abs ($p = 0.048$, Fig. 3G).

As₂O₃ triggered apoptosis of activated B10.D2 CD4⁺ T cells by enhancing ROS production

In vitro, ROS production was higher in B10.D2 CD4⁺ T cells stimulated with BALB/c splenocytes than in B10.D2 CD4⁺ T cells stimulated with B10.D2 splenocytes (syngeneic controls) (mean fluorescence intensity [MFI] = 1721 \pm 40 versus 1186 \pm 92, $p = 0.032$). Treatment of stimulated B10.D2 CD4⁺ T cells with As₂O₃ further increased their production of H₂O₂ that reached an

MFI of 2172 \pm 103 ($p = 0.031$ versus stimulated B10.D2 CD4⁺ T cells without As₂O₃, Fig. 4A). The enhancement of ROS production was abrogated by incubation with 4 mM NAC (MFI: 1636 \pm 87, $p = 0.021$ versus As₂O₃ alone, Fig. 4A). The level of glutathione (GSH) in B10.D2 CD4⁺ T cells was in accordance with those results. Syngeneic stimulated cells displayed elevated levels of GSH (mean of 45 \pm 2% of GSH⁺ cells), whereas allogeneic stimulated cells had a slight decrease in their GSH content (mean 31 \pm 2.5% of positive cells) ($p = 0.041$, Fig. 4B). Incubation with 10 µM As₂O₃ dramatically decreased the GSH content in stimulated B10.D2 CD4⁺ T cells (Fig. 4B). In addition, Yopro-1 staining of activated B10.D2 CD4⁺ T cells indicated that arsenic dramatically triggered apoptosis in those cells. Apoptosis correlated with ROS production measured by flow cytometry and was downregulated by incubation with 4 mM NAC ($p = 0.0009$, Fig. 4C).

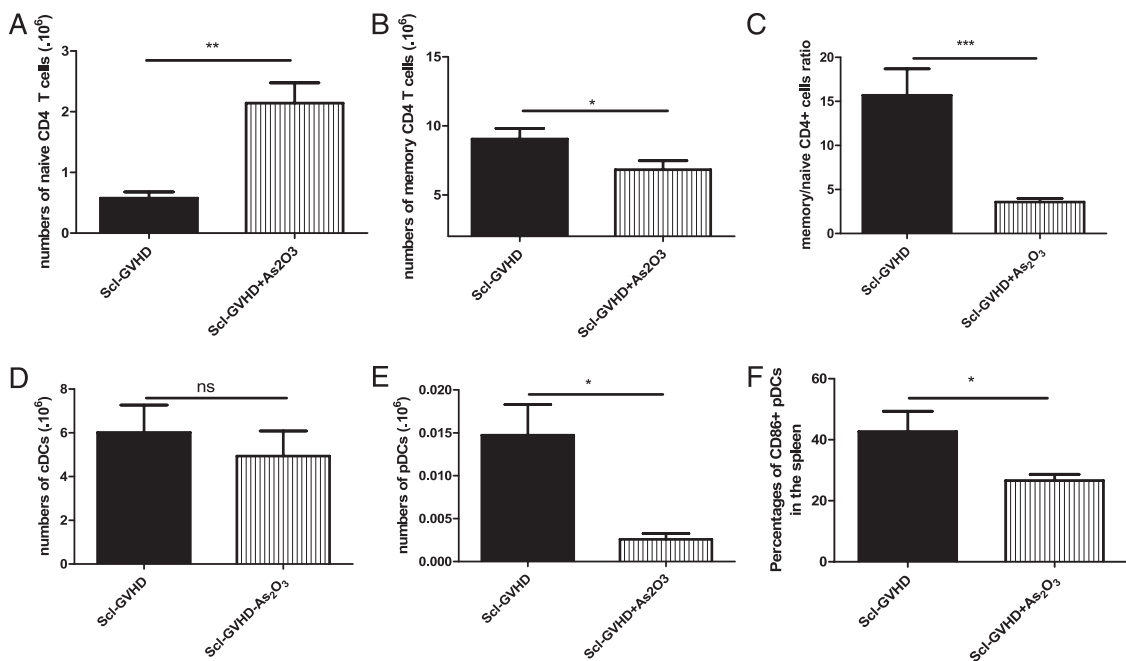


FIGURE 3. Treatment of Scl-GVHD mice with As₂O₃ altered the balance between memory and naive CD4⁺ T cells and decreased numbers of splenic pDCs. Mice were treated with As₂O₃ from day 7 post-BMT at a dose of 5 µg/g ($n = 10/\text{group}$). Spleen cells were harvested on day 28 post-BMT. (A) Numbers of CD4⁺ naive T cells in untreated and treated Scl-GVHD mice. (B) Numbers of CD4⁺ effector memory T cells. (C) Effector memory/naive CD4⁺ T cell ratio. (D) Numbers of splenic pDCs in untreated and treated Scl-GVHD mice. (E) Numbers of splenic cDCs in untreated and treated Scl-GVHD mice. (F) Percentages of CD86⁺ pDCs in untreated and treated Scl-GVHD mice. Values are mean \pm SEM of data from all mice in the experimental or control groups. * $p < 0.05$, ** $p < 0.01$, *** $p < 0.001$, paired Mann-Whitney *U* test.

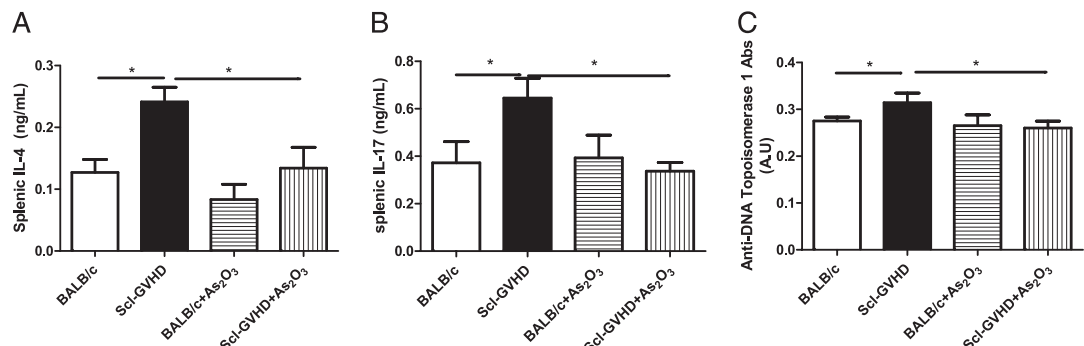


FIGURE 4. In vivo treatment with As₂O₃ reduced the production of IL-4, IL-17, and autoantibodies in Scl-GVHD mice. Mice were treated with As₂O₃ from day 7 post-BMT at a dose of 5 µg/g ($n = 10$ /group). Spleen cells were harvested on day 28 post-BMT, and CD4 T cells were purified as described in *Materials and Methods*. (A) IL-4 secretion measured in supernatants of CD4 T cells by ELISA (ng/ml). (B) IL-17 secretion measured in supernatants of CD4 T cells by ELISA (ng/ml). (C) Anti-DNA-topoisomerase 1 autoantibody concentrations in the sera (A.U.). Values are mean ± SEM of data from all mice in the experimental or control groups. * $p < 0.05$, paired Mann-Whitney *U* test.

As₂O₃ also triggered apoptosis of pDCs by enhancing H₂O₂ production

We observed the same effects on ROS production and apoptosis in B10.D2 pDCs incubated with 10 µM As₂O₃. Indeed, the basal detection MFI of CM-H₂DCFDA by flow cytometry was 5405 ± 12 for B10.D2 pDCs and 6527 ± 25 when treated with As₂O₃. Adding NAC reduced H₂O₂ production by pDCs, as shown by the CM-H₂DCFDA MFI of 3675 ± 15 (Fig. 5). Monochlorobimane staining was also reduced in pDCs treated with arsenic compared with untreated pDCs (MFI = 707 ± 10 versus 1583 ± 80), whereas coaddition of NAC and As₂O₃ increased the intracellular content of GSH (MFI = 1541 ± 8). The effects of As₂O₃ were also studied on conventional DCs (cDCs). There was a tendency toward an increase in H₂O₂ production and a decrease in GSH content in cDCs upon treatment with arsenic, but those results did not reach significance (for H₂O₂ levels: MFI = 1,118 ± 90 for cDCs alone, 1,445 ± 86 for cDCs + As₂O₃, 1,325 ± 76 for cDCs + As₂O₃ + NAC; $p = 0.08$ for cDCs versus cDCs + As₂O₃, $p = 0.09$ for cDCs + As₂O₃ + NAC versus cDCs + As₂O₃; for GSH levels: MFI = 24,308 ± 395 for cDCs alone, 21,719 ± 384 for cDCs + As₂O₃, 23,000 ± 376 for cDCs + As₂O₃ + NAC; $p = 0.089$ for cDCs versus cDCs + As₂O₃, $p = 0.10$ for cDCs + As₂O₃ + NAC versus cDCs + As₂O₃).

As₂O₃ blocked IFN-α production of B10.D2 pDCs

To assess the specificity of As₂O₃ against pDCs, we investigated its effect on the production of IFN-α by splenic pDCs, with and without activation by the TLR7 agonist Gardiquimod. Fig. 6 shows that, in the absence of stimulation of pDCs, As₂O₃ has a significant effect on the production of IFN-α only at the highest concentrations tested (10 and 25 µM). In contrast, after stimulation of TLR7 and incubation with 10 and 25 µM As₂O₃, the levels of IFN-α in cell supernatants were strongly decreased ($p = 0.002$ for 10 µM As₂O₃). Incubation with 5 µM As₂O₃ decreased the concentration of IFN-α in the supernatants >2-fold, whereas lower doses of As₂O₃ had no effect on IFN-α production (Fig. 7).

Discussion

This study shows that As₂O₃ selectively deletes activated CD4⁺ T cells and pDCs that have low levels of GSH and overproduce H₂O₂ and, thus, ameliorates Scl-GVHD in mice.

We tested the effects of As₂O₃, a chemotherapeutic drug used in hematological malignancies, on the development of Scl-GVHD in mice. This model of chronic GVHD shares typical features with

systemic sclerosis, including skin and visceral fibrosis and autoimmune manifestations (22). As₂O₃ dramatically improved the clinical outcome of sublethally irradiated BALB/c mice transplanted with B10.D2 hematopoietic cells; weight loss, fibrosis, vasculitis, and alopecia were markedly reduced in treated versus untreated mice.

The percentages of effector memory CD4⁺ T cells (CD4⁺ CD44^{high}CD62L^{low}) decreased in mice with Scl-GVHD that were treated with arsenic. The pathophysiology of chronic GVHD remains poorly understood, although a large amount of evidence suggests that, in contrast to acute GVHD, which is dependent on CD8⁺ T cells, the manifestations observed in chronic GVHD are dependent on the activation of minor histocompatibility Ag-specific donor CD4⁺ T cells (4, 23–26). After transplantation of B10.D2 lymphoid cells into irradiated BALB/c mice, naive donor CD4⁺ T cells initiate the disease. As a result, donor CD4⁺ T cells infiltrate the skin, recruit macrophages and monocytes, and induce fibrosis and destructive changes. Because activated CD4⁺ T cells play a pivotal role in the induction of the disease and are decreased by in vivo treatment with arsenic, we investigated the mechanism of action of arsenic on those cells. We show that B10.D2 CD4⁺ T cells stimulated with irradiated BALB/c spleen cells display lower GSH contents and produce higher levels of H₂O₂ than do unstimulated CD4⁺ T cells. These results are in agreement with previous studies showing that, upon activation, T cells overproduce ROS (23, 24). Then, we showed that the high levels of ROS production by activated CD4⁺ T cells make them hypersensitive to arsenic-induced apoptosis. Indeed, in vitro treatment with arsenic induced an important decrease in GSH content and a subsequent increase in H₂O₂ levels beyond a lethal threshold, inducing cell apoptosis. These data confirm the role of the oxidant/antioxidant balance as a crucial factor that determines cell susceptibility to arsenic (25). Several studies demonstrated that GSH can bind arsenic from attacking its target by formation of a transient As(GS)₃ complex and that GSH depletion in acute promyelocytic leukemia cells synergizes with As₂O₃ in the induction of apoptosis (27).

We next investigated whether an alteration in the profile of cytokine production by splenocytes from mice with Scl-GVHD and treated with As₂O₃ could reflect changes in splenic T cell populations. Splenic IL-17 production was lower in arsenic-treated Scl-GVHD mice than in untreated mice. These data are consistent with a large number of recent studies conducted in mice that concluded that Th17 cells are implicated in GVHD development

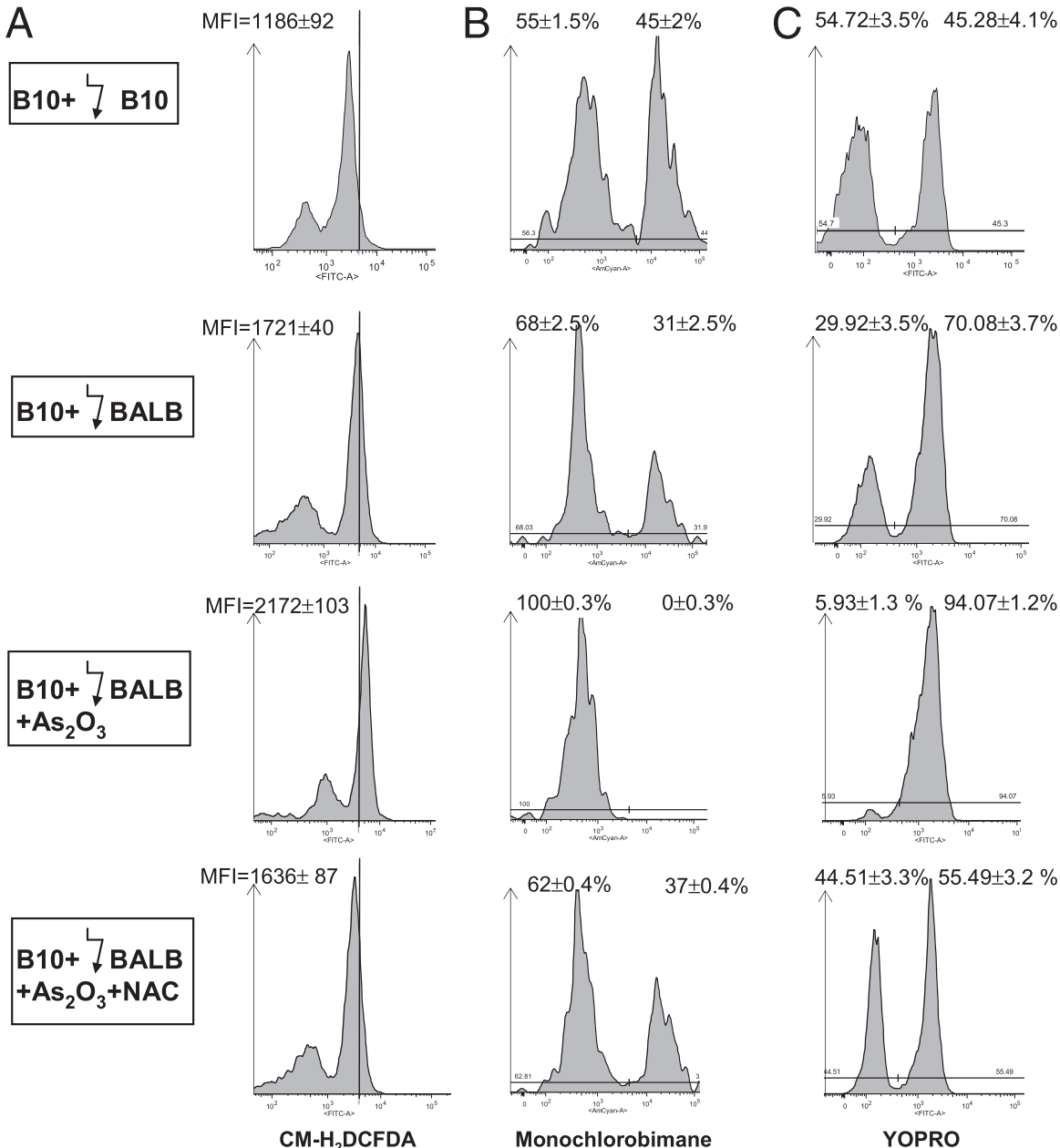


FIGURE 5. As₂O₃ induced apoptosis of activated B10.D2 CD4⁺ T cells in culture through ROS production. B10D2 spleen cells were incubated with irradiated B10.D2 splenocytes (↓B10, syngeneic control) or BALB splenocytes (↓BALB) and treated or not with 10 μM As₂O₃ with or without NAC. Flow cytometry analysis was gated on CD4⁺ T cells. Results are representative of four experiments carried out in duplicates. Data were analyzed with FlowJo software. (A) Increase in H₂O₂ generation by As₂O₃, measured by flow cytometry using CM-H₂DCFDA. (B) GSH content in B10.D2 CD4 T cells, measured by flow cytometry using monochlorobimane staining. (C) Induction of apoptosis by As₂O₃, measured by flow cytometry using Yopro staining. Mean values were compared using paired Mann-Whitney *U* tests.

in mice. Among them, a study reported that amplification of IL-17 production by the use of the stem cell mobilization factor G-CSF leads to a cutaneous fibrosis occurring late after the graft, as in Scl-GVHD (21). Consistent with those data, another recent article stated that the use of an anti-IL-17 mAb can ameliorate skin symptoms in chronic GVHD (20, 26). Moreover, Nishimori et al. (28) recently showed the beneficial effects of the synthetic retinoid

Am80, which belongs to the same family as all-*trans* retinoic acid, on chronic GVHD. These effects are mediated through the downregulation of Th17 cells. Because other synthetic retinoids, such as N-(4-hydroxyphenyl)retinamide, can induce apoptosis through increased production of ROS, it is possible that Am80 also acts on Th17 cells through the induction of ROS, because As₂O₃ does in our model (29).

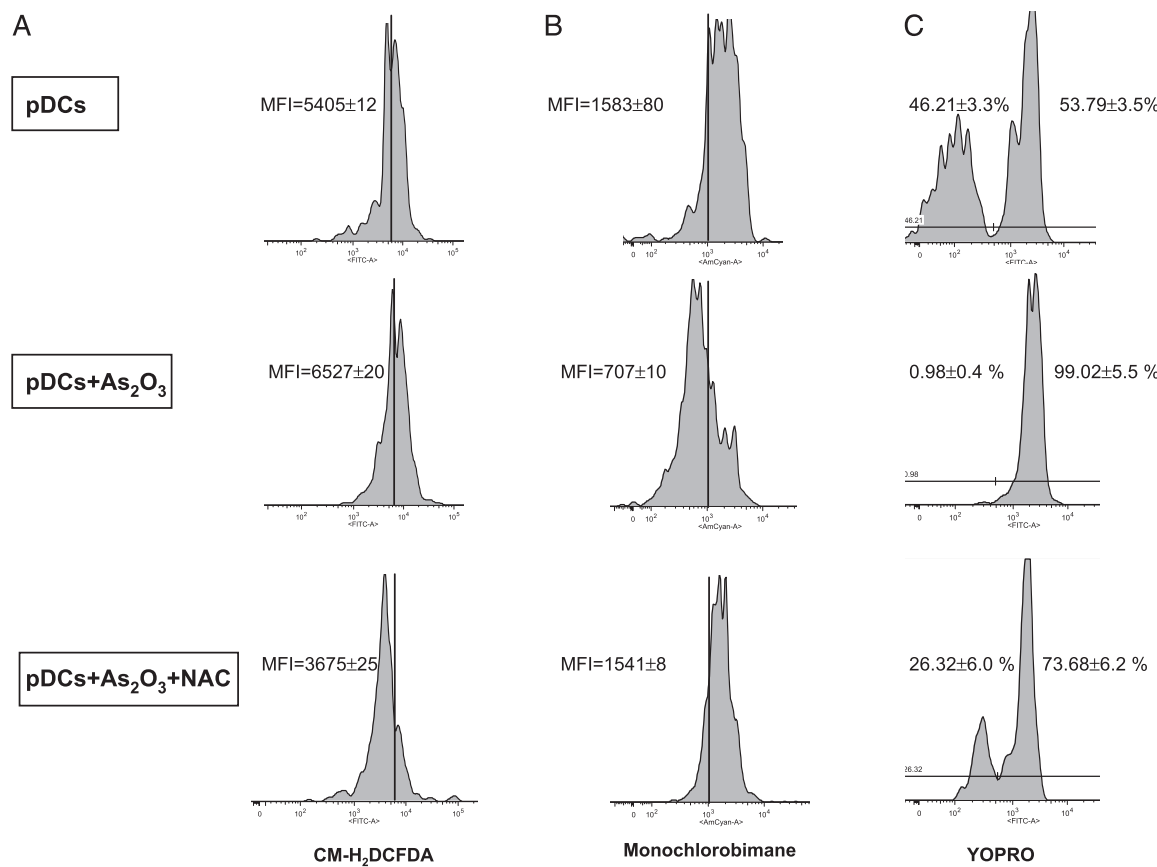


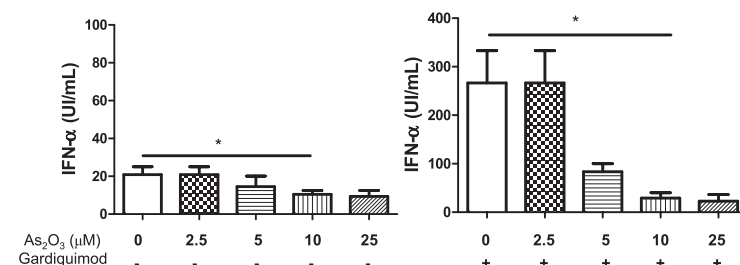
FIGURE 6. Effects of in vitro treatment with As_2O_3 on B10.D2 pDCs. B10.D2 spleen cells were incubated with $10 \mu\text{M}$ As_2O_3 with or without NAC for 24 h. Flow cytometry analysis was gated on pDCs subsets defined as $\text{B}220^+$ $\text{CD}11\text{c}^{\text{int}}$ $\text{CD}11\text{b}^{\text{low}}$. Results are representative of four experiments carried out in duplicates. Data were analyzed with FlowJo software. **(A)** Induction of ROS formation by As_2O_3 , measured by flow cytometry using $\text{CM-H}_2\text{DCFDA}$. **(B)** Arsenic induces a decrease in the GSH content in pDCs, measured by flow cytometry using monochlorobimane staining. **(C)** Induction of apoptosis in pDCs by As_2O_3 , measured by flow cytometry using Yopro staining.

The decrease in splenic $\text{CD}4^+$ effector memory cells in Scl-GVHD mice treated with As_2O_3 also correlates with a reduction in the Th2 cytokine IL-4 produced in vitro by activated splenocytes. Following the graft of B10.D2 spleen and bone marrow cells into sublethally irradiated BALB/c mice, Zhou et al. (30) observed an increase in the expression of type 2 cytokines in the skin of Scl-GVHD mice compared with syngeneic grafts. Moreover, in other chronic GVHD models, type 2 polarized immune responses are required for the induction of skin GVHD in mice and the development of fibrosis in the skin and visceral organs (31). Thus, the decreased production of IL-4 observed in our study probably contributes to the improvement of skin fibrosis.

As a whole, the alterations in splenic production of cytokines in our model are consecutive to a reduced immune activation after treatment with arsenic and, thus, contribute to the amelioration of Scl-GVHD symptoms.

Chronic GVHD is associated with other autoimmune manifestations, such as the production of autoantibodies in relation to the production of Th2 cytokines. As described by others, we observed the production of anti-DNA-topoisomerase 1 Abs in mice with Scl-GVHD. The levels of these autoantibodies were decreased by As_2O_3 in our model. Similar effects of As_2O_3 were reported in a lupus mouse model (MRL/lpr mice), with a decrease in the production of autoantibodies (anti-dsDNA and rheumatoid factors) (17). Consistent with these data, we conclude that As_2O_3

FIGURE 7. As_2O_3 targets pDCs and blocks IFN- α production by those cells. pDCs were seeded in six-well plates and coincubated with $10 \mu\text{g}/\text{ml}$ Gardiquimod and/or increasing doses (0 – $25 \mu\text{M}$) of As_2O_3 . * $p < 0.05$.



prevents the development of an autoimmune reaction in Scl-GVHD mice by specifically targeting CD4⁺ T cells.

In contrast, the role of APCs in chronic GVHD was recently emphasized by the observation that costimulation of donor T cells through CD80 or CD86 on either host or donor APCs is necessary to induce chronic GVHD (32). pDCs are especially involved in the physiopathology of GVHD because the adoptive transfer of mature pDCs exacerbates GVHD, and they can stimulate donor T cells to trigger GVHD in the absence of other APCs (6, 33). Yet, the state of maturation of pDCs seems to be crucial in their ability to trigger GVHD. On the one hand, total-body irradiation induces inflammation and maturation of pDCs, which can subsequently activate T cells (6). On the other hand, Banovic et al. (34) showed that precursors of pDCs, but not mature pDCs, can attenuate the symptoms of GVHD, emphasizing the differential functions of pDCs depending on the environment and the model of GVHD. In our hands, the pDC subset was decreased in treated mice compared with untreated mice. As observed for CD4⁺ T cells, the increased levels of H₂O₂ production, along with the decreased GSH content, render pDCs sensitive to As₂O₃-induced apoptosis. The action of arsenic on pDCs was confirmed in vitro by the decrease in IFN- α production following stimulation of pDCs by a TLR-7 agonist. This selective effect of arsenic on pDCs could also lead to interesting insights about IFN- α -related diseases, such as systemic lupus erythematosus. Indeed, Bobé et al. (17) showed the beneficial effects of As₂O₃ in MRL/lpr lupus-prone mice. In accordance with our results, they reported a cytotoxic effect of As₂O₃ on activated CD4⁺ T cells through the reduction in GSH levels, but the beneficial effects observed in their model could also be mediated through regulation of IFN- α production by pDCs.

In summary, our work highlights the beneficial effects of As₂O₃ in chronic GVHD. As₂O₃ could be a therapeutic tool in hematologic and solid malignancies, as well as in chronic GVHD (10).

Acknowledgments

We thank P. Lebon for kindly providing L229 cells and IFN- α standard solution and A. Colle for typing the manuscript.

Disclosures

The authors have no financial conflicts of interest.

References

- Lee, S. J., J. P. Klein, A. J. Barrett, O. Ringden, J. H. Antin, J. Y. Cahn, M. H. Carabasi, R. P. Gale, S. Giralt, G. A. Hale, et al. 2002. Severity of chronic graft-versus-host disease: association with treatment-related mortality and relapse. *Blood* 100: 406–414.
- Baird, K., and S. Z. Pavletic. 2006. Chronic graft versus host disease. *Curr. Opin. Hematol.* 13: 426–435.
- Coghill, J. M., S. Sarantopoulos, T. P. Moran, W. J. Murphy, B. R. Blazar, and J. S. Serody. 2011. Effector CD4⁺ T cells, the cytokines they generate, and GVHD: something old and something new. *Blood* 117: 3268–3276.
- Korngold, R., and J. Sprent. 1978. Lethal graft-versus-host disease after bone marrow transplantation across minor histocompatibility barriers in mice. Prevention by removing mature T cells from marrow. *J. Exp. Med.* 148: 1687–1698.
- Duffner, U. A., Y. Maeda, K. R. Cooke, P. Reddy, R. Ordemann, C. Liu, J. L. Ferrara, and T. Teshima. 2004. Host dendritic cells alone are sufficient to initiate acute graft-versus-host disease. *J. Immunol.* 172: 7393–7398.
- Koyama, M., D. Hashimoto, K. Aoyama, K. Matsuoka, K. Karube, H. Niilo, M. Harada, M. Tanimoto, K. Akashi, and T. Teshima. 2009. Plasmacytoid dendritic cells prime alloreactive T cells to mediate graft-versus-host disease as antigen-presenting cells. *Blood* 113: 2088–2095.
- Filipovich, A. H., D. Weisdorf, S. Pavletic, G. Socie, J. R. Wingard, S. J. Lee, P. Martin, J. Chien, D. Przepiorka, D. Couriel, et al. 2005. National Institutes of Health consensus development project on criteria for clinical trials in chronic graft-versus-host disease: I. Diagnosis and staging working group report. *Biol. Blood Marrow Transplant.* 11: 945–956.
- Vogelsang, G. B., L. Lee, and D. M. Bensen-Kennedy. 2003. Pathogenesis and treatment of graft-versus-host disease after bone marrow transplant. *Annu. Rev. Med.* 54: 29–52.
- Ruzek, M. C., S. Jha, S. Ledbetter, S. M. Richards, and R. D. Garman. 2004. A modified model of graft-versus-host-induced systemic sclerosis (scleroderma) exhibits all major aspects of the human disease. *Arthritis Rheum.* 50: 1319–1331.
- Sanz, M. A., D. Grimwade, M. S. Tallman, B. Lowenberg, P. Fenoux, E. H. Estey, T. Naoe, E. Lengfelder, T. Büchner, H. Döhner, et al. 2009. Management of acute promyelocytic leukemia: recommendations from an expert panel on behalf of the European LeukemiaNet. *Blood* 113: 1875–1891.
- Miller, W. H., Jr., H. M. Schipper, J. S. Lee, J. Singer, and S. Waxman. 2002. Mechanisms of action of arsenic trioxide. *Cancer Res.* 62: 3893–3903.
- Lynn, S., J. R. Guru, H. T. Lai, and K. Y. Jan. 2000. NADH oxidase activation is involved in arsenite-induced oxidative DNA damage in human vascular smooth muscle cells. *Circ. Res.* 86: 514–519.
- Smith, K. R., L. R. Klei, and A. Barchowsky. 2001. Arsenite stimulates plasma membrane NADPH oxidase in vascular endothelial cells. *Am. J. Physiol. Lung Cell. Mol. Physiol.* 280: L442–L449.
- Pelican, H., L. Feng, Y. Zhou, J. S. Carew, E. O. Hileman, W. Plunkett, M. J. Keating, and P. Huang. 2003. Inhibition of mitochondrial respiration: a novel strategy to enhance drug-induced apoptosis in human leukemia cells by a reactive oxygen species-mediated mechanism. *J. Biol. Chem.* 278: 37832–37839.
- Tse, W. P., C. H. Cheng, C. T. Che, and Z. X. Lin. 2008. Arsenic trioxide, arsenic pentoxide, and arsenic iodide inhibit human keratinocyte proliferation through the induction of apoptosis. *J. Pharmacol. Exp. Ther.* 326: 388–394.
- Chen, Y. C., S. Y. Lin-Shiau, and J. K. Lin. 1998. Involvement of reactive oxygen species and caspase 3 activation in arsenite-induced apoptosis. *J. Cell. Physiol.* 177: 324–333.
- Bobé, P., D. Bonardelle, K. Benihoud, P. Opolon, and M. K. Chelbi-Alix. 2006. Arsenic trioxide: A promising novel therapeutic agent for lymphoproliferative and autoimmune syndromes in MRL/lpr mice. *Blood* 108: 3967–3975.
- Kavian, N., A. Servettaz, C. Mongaret, A. Wang, C. Nicco, C. Chéreau, P. Grange, V. Vuiblet, P. Birembaut, M. D. Diebold, et al. 2010. Targeting ADAM-17/notch signaling abrogates the development of systemic sclerosis in a murine model. *Arthritis Rheum.* 62: 3477–3487.
- Jaffee, B. D., and H. N. Claman. 1983. Chronic graft-versus-host disease (GVHD) as a model for scleroderma. I. Description of model systems. *Cell. Immunol.* 77: 1–12.
- Dubois, M. F., V. Mezger, M. Morange, C. Ferrieux, P. Lebon, and O. Bensaude. 1988. Regulation of the heat-shock response by interferon in mouse L cells. *J. Cell. Physiol.* 137: 102–109.
- Hill, G. R., S. D. Olver, R. D. Kuns, A. Varelias, N. C. Raffelt, A. L. Don, K. A. Markey, Y. A. Wilson, M. J. Smyth, Y. Iwakura, et al. 2010. Stem cell mobilization with G-CSF induces type 17 differentiation and promotes scleroderma. *Blood* 116: 819–828.
- McCormick, L. L., Y. Zhang, E. Tootell, and A. C. Gilliam. 1999. Anti-TGF- β treatment prevents skin and lung fibrosis in murine sclerodermatous graft-versus-host disease: a model for human scleroderma. *J. Immunol.* 163: 5693–5699.
- Chu, Y. W., and R. E. Gress. 2008. Murine models of chronic graft-versus-host disease: insights and unresolved issues. *Biol. Blood Marrow Transplant.* 14: 365–378.
- Shlomchik, W. D. 2007. Graft-versus-host disease. *Nat. Rev. Immunol.* 7: 340–352.
- Kappel, L. W., G. L. Goldberg, C. G. King, D. Y. Suh, O. M. Smith, C. Ligh, A. M. Holland, J. Grubin, N. M. Mark, C. Liu, et al. 2009. IL-17 contributes to CD4⁺mediated graft-versus-host disease. *Blood* 113: 945–952.
- Kansu, E. 2004. The pathophysiology of chronic graft-versus-host disease. *Int. J. Hematol.* 79: 209–215.
- Davison, K., S. Côté, S. Mader, and W. H. Miller. 2003. Glutathione depletion overcomes resistance to arsenic trioxide in arsenic-resistant cell lines. *Leukemia* 17: 931–940.
- Nishimori, H., Y. Maeda, T. Teshima, H. Sugiyama, K. Kobayashi, Y. Yamasaji, S. Kadobisa, H. Uryu, K. Takeuchi, T. Tanaka, et al. 2012. Synthetic retinoid Am80 ameliorates chronic graft-versus-host disease by down-regulating Th1 and Th17. *Blood* 119: 285–295.
- Asuendi, A., M. C. Morales, A. Alvarez, J. Aréchaga, and G. Pérez-Yarza. 2002. Implication of mitochondria-derived ROS and cardiolipin peroxidation in N-(4-hydroxyphenyl)retinamide-induced apoptosis. *Br. J. Cancer* 86: 1951–1956.
- Zhou, L., D. Askew, C. Wu, and A. C. Gilliam. 2007. Cutaneous gene expression by DNA microarray in murine sclerodermatous graft-versus-host disease, a model for human scleroderma. *J. Invest. Dermatol.* 127: 281–292.
- Wynn, T. A. 2004. Fibrotic disease and the T(H)1/T(H)2 paradigm. *Nat. Rev. Immunol.* 4: 583–594.
- Anderson, B. E., J. M. McNiff, D. Jain, B. R. Blazar, W. D. Shlomchik, and M. J. Shlomchik. 2005. Distinct roles for donor- and host-derived antigen-presenting cells and costimulatory molecules in murine chronic graft-versus-host disease: requirements depend on target organ. *Blood* 105: 2227–2234.
- MacDonald, K. P., V. Rowe, C. Filippich, R. Thomas, A. D. Clouston, J. K. Welby, D. N. Hart, J. L. Ferrara, and G. R. Hill. 2003. Donor pretreatment with progenyopoietin-1 is superior to granulocyte colony-stimulating factor in preventing graft-versus-host disease after allogeneic stem cell transplantation. *Blood* 101: 2033–2042.
- Banovic, T., K. A. Markey, R. D. Kuns, S. D. Olver, N. C. Raffelt, A. L. Don, M. A. Degli-Esposti, C. R. Engwerda, K. P. MacDonald, and G. R. Hill. 2009. Graft-versus-host disease prevents the maturation of plasmacytoid dendritic cells. *J. Immunol.* 182: 912–920.

Chapitre 4

DISCUSSION

En 2012, la ScS reste une maladie à la physiopathologie obscure malgré de nombreux travaux de recherche dans de multiples directions. Cette obscurité est probablement liée à la complexité des facteurs conjointement impliqués dans la physiopathologie de la maladie, mais aussi à sa grande hétérogénéité d'expression clinique. En effet, on peut penser que les différentes formes cliniques de la maladie et ses différentes complications résultent de mécanismes plus ou moins distincts, ce qui rend difficile la compréhension des mécanismes. Pourtant on discerne dans toutes les formes de la maladie un dysfonctionnement des fibroblastes et des cellules endothéliales, une activation du système immunitaire, une synthèse de cytokines et d'auto-Ac et des facteurs environnementaux, notamment de toxiques. Il apparaît cependant difficile de déterminer si ces différents facteurs agissent en synergie ou s'ils sont chacun en cause à une phase précise de la maladie.

Le stress oxydant paraît jouer un rôle majeur dans la ScS car il est capable de modifier la structure et l'antigénicité des protéines. Plusieurs arguments, cliniques, épidémiologiques et biologiques, plaident en effet en faveur de l'imputabilité d'un stress oxydant au début de la ScS. Sur le plan clinique d'abord, il est remarquable que plus de 90% des sujets présentent des phénomènes digitaux répétés d'ischémie - reperfusion au cours des années qui précèdent le développement d'une ScS (ces phénomènes surviennent six ans en moyenne avant le développement d'une ScS cutanée limitée, et deux ans et demi en moyenne avant le développement d'un ScS cutanée diffuse). Or ce phénomène génère une grande quantité de FRO, notamment d' $O_2^{\bullet-}$ et d' $ONOO^-$. Sur le plan épidémiologique, plusieurs toxiques impliqués dans le déclenchement de ScS ou d'entités proches exercent leur action via la génération de FRO. C'est le cas de la silice qui induit directement la formation de FRO à sa surface par réaction de Fenton, et indirectement par l'activation de cellules phagocytaires. Le syndrome des huiles toxiques, qui partage des similitudes avec la ScS, semble aussi faire intervenir des radicaux libres. Enfin, sur un plan biologique, il a été montré que les monocytes et des fibroblastes de patients sclérodermiques produisaient de grandes quantités d' $O_2^{\bullet-}$. Dans une première partie du travail réalisé sur la ScS, nous avons donc essayé d'évaluer l'importance, la nature et les conséquences du

stress oxydant dans la ScS. Un premier travail a été réalisé en exposant des souris directement à des FRO et a permis la création d'un nouveau modèle murin de ScS. Plusieurs autres travaux ont découlé de celui-ci pour l'étude des dysfonctionnements fibroblastiques et la recherche de nouvelles approches thérapeutiques.

Dans un précédent travail mené au laboratoire, il a été observé que les sérum de patients atteints de ScS sont capables d'induire un stress oxydant [225]. Ce stress est véhiculé par des produits protéiques oxydés sériques (AOPP) et induit des effets opposés sur les fibroblastes (stimulation de la prolifération) et les CE (inhibition de la prolifération). Néanmoins, d'importantes différences existaient parmi les patients sclérodermiques étudiés. Ainsi, les sérum des patients présentant une maladie fibrosante pulmonaire induisent une plus grande prolifération des fibroblastes et une plus grande synthèse d' H_2O_2 que les patients avec ScS sans atteinte pulmonaire. Les sérum des patients avec des complications vasculaires graves induisent une libération de NO par les CE, et inhibent fortement leur croissance. Contrairement aux sérum des patients atteints de fibrose pulmonaire, ils ne stimulent pas la croissance des fibroblastes.

L'observation d'une corrélation entre la production de FRO induite par le sérum (quantitativement et qualitativement) et les complications cliniques présentes chez les patients est un argument fort en faveur d'un rôle des FRO dans la physiopathologie de la ScS. Nous avons donc souhaité confirmer cette hypothèse et avons réalisé le travail de l'article 1 qui présente un nouveau modèle murin de ScS induite par certaines FRO.

Nous avons injecté dans le tissu sous-cutané dorsal de souris BALB/c des solutions capables de générer différents types de stress oxydant. Parmi les solutions injectées, celles qui génèrent OH[•] ou HOCl induisent chez ces souris une maladie systémique proche de la forme dite «cutanée diffuse» de la ScS humaine caractérisée par une fibrose cutanée et pulmonaire, et la présence d'Ac anti-ADN Topoisomérase-1. Les injections de solutions contenant ONOO⁻ induisent une fibrose cutanée, mais pas pulmonaire et des Ac anti-CENP B, mais pas d'Ac anti-ADN Topoisomérase 1. Cette maladie se rapproche de la forme, dite «cutanée limitée» de la ScS humaine.

De plus, comme chez les patients, il existe dans ce modèle murin une corrélation entre les propriétés des sérum des souris et la forme de la maladie développée. En effet, les sérum des souris injectées avec OH[•] ou HOCl et qui développent une fibrose pulmonaire, contiennent de plus grandes quantités d'AOPP que les sérum de souris exposées à ONOO⁻, souris qui ne développent pas de fibrose pulmonaire. Ces résultats montrent que la simple exposition à un

stress oxydant de manière répétée peut induire des lésions systémiques très proches de celles observées dans la ScS et confirment donc que certains FRO peuvent être des acteurs majeurs dans la genèse de la maladie humaine.

Ce travail ouvre également de nouvelles pistes dans la compréhension des différentes étapes conduisant d'une anomalie cutanée à la véritable maladie systémique qu'est la ScS. En effet, nous montrons que le sérum des souris présentant une maladie proche de la ScS, comme celui des patients, véhicule un stress oxydant. Nous faisons l'hypothèse que le stress oxydant progresse via la circulation systémique, de la peau vers les autres organes (notamment vers les poumons et les reins), entraînant des lésions à distance de l'atteinte initiale.

De plus, nos travaux suggèrent que les AOPP ne sont pas seulement un marqueur du stress oxydant, mais en sont également la forme de diffusion et la forme active. En effet, nous avons montré que des AOPP oxydés *in vitro* induisent sur les CE et les fibroblastes les mêmes effets que le sérum total de patients et de souris, c'est-à-dire génèrent une production de FRO par les CE et stimulent la prolifération des fibroblastes. Inversement, la déplétion des sérum de patients en AOPP par le β -mercaptopropanoïde réduit les effets de ces séums sur les CE et les fibroblastes.

Ce rôle directement pathogène des AOPP a été récemment rapporté par d'autres équipes. Il a été montré que ces produits, que l'on croyait être jusqu'ici le seul reflet du stress oxydant, sont capables de stimuler l'explosion oxydative au niveau des monocytes et des neutrophiles [229]. En effet, les AOPP issus de sérum de patients insuffisants rénaux hémodialysés, comme des AOPP issus de l'oxydation *in vitro* par HOCl de l'albumine activent la NADPH oxydase et la myéloperoxydase des neutrophiles [230]. Ces produits peuvent également activer les cellules dendritiques *in vitro* [231], [84]. *In vivo*, dans un modèle d'insuffisance rénale par néphrectomie subtotale chez le rat, l'injection d'AOPP par voie intraveineuse (albumine oxydée *in vitro* par HOCl) aggrave les lésions rénales avec apparition de signes de fibrose précoce [232], démontrant un rôle pathogène des AOPP dans ce modèle. Nos résultats, obtenus dans un modèle très différent après exposition par voie sous-cutanée aux AOPP, suggèrent aussi un rôle pathogène, profibrosant, des AOPP, qui pourrait être crucial dans les lésions de ScS.

Néanmoins, nos travaux suggèrent que ce pouvoir pathogène des AOPP n'est pas généralisable à tous les AOPP. En effet, dans nos expériences, les propriétés des AOPP de synthèse étaient très variables et dépendaient de la protéine utilisée et du type d'oxydation appliquée.

Nous avons obtenu la meilleure reproduction des effets des sérums de patients sclérodermiques avec de l'ADN Topoisomérase 1 oxydée par de l'HOCl. D'autres protéines (albumine,...) oxydées par HOCl entraînaient des effets moindres ; et inversement, l'ADN Topoisomérase-1 non oxydée, ou oxydée avec d'autres FRO avait beaucoup moins d'effet sur les CE et les fibroblastes. Il a d'ailleurs été rapporté récemment que des injections de protéines ADN Topoisomérase-1 humaines recombinantes non oxydées n'induisaient pas de sclérodermie dans diverses souches de souris et n'aggravaient pas les lésions histologiques des souris Tsk/+ . Néanmoins, certaines souches de souris exposées à de grandes quantités d'ADN Topoisomérase-1 développaient des Ac dirigés contre cette molécule [233].

Les facteurs conduisant à la baisse du seuil de tolérance vis-à-vis de différentes protéines dans la ScS sont inconnus. Néanmoins, dans la ScS, plusieurs hypothèses ont été avancées, étayées ou non sur un plan expérimental : hypothèse d'une libération massive d'antigènes par les CE apoptotiques [156] ; hypothèse d'une stimulation du système immunitaire par un agent infectieux tel que le CMV, dont la protéine UL70 présente une homologie avec l'ADN Topoisomérase 1 [234] ; hypothèse biochimique, basée sur les propriétés physico-chimiques des protéines devenant antigéniques. En effet, une équipe a montré que CENP B et l'ADN Topoisomérase 1 étaient particulièrement sensibles à l'action de la protéase granzyme B des granules T cytotoxiques [235]. De plus, l'ADN Topoisomérase-1 et l'ARN polymérase III (un autre antigène cible chez certains patients atteints de ScS) peuvent être clivées sous l'effet de l'oxydation par la réaction de Fenton [155]. Les modifications ainsi subies par ces protéines modifient leur conformation et favorisent vraisemblablement une rupture de tolérance. Dans nos expériences, nous avons mis en évidence des Ac anti-CENP B chez les souris exposées à OH[•] ou HOCl ou ONOO⁻. En revanche, seules les souris exposées à OH[•] ou HOCl développent des Ac anti-ADN Topoisomérase-1 à un taux significatif. Nous faisons l'hypothèse que ces molécules sont devenues antigéniques en raison de leur oxydation qui a modifié leur conformation, fait apparaître des épitopes cryptiques, et facilité leur reconnaissance et internalisation par des cellules présentatrices d'antigènes. Dans cette hypothèse, la baisse de tolérance serait initialement limitée aux épitopes oxydés, puis pourrait s'étendre à d'autres régions de la protéine (ou lipide). Un mécanisme similaire de déclenchement de l'auto-immunité est envisageable dans d'autres maladies humaines, en dehors de la ScS, notamment dans le lupus érythémateux systémique et le diabète de type 1. Dans le lupus érythémateux systémique, plusieurs marqueurs évoquent un stress oxydant important, comme une élévation des protéines oxydées dans le sérum et un

défaut d'activité des enzymes anti-oxydantes superoxyde-dismutases (SOD) [236]. Certains patients développent des Ac dirigés contre des molécules de LDL cholestérol oxydées, Ac dont la présence est corrélée avec celle d'Ac dirigés contre les phospholipides [237]. De plus, l'injection de Ro oxydé, une ribonucléoprotéine de 60 kDa antigène cible fréquemment reconnu par les autoAc de patients atteints de lupus, sous une forme oxydée accélère sa reconnaissance par le système immunitaire et le développement d'une maladie proche du lupus chez le lapin, par rapport à l'injection de la même protéine Ro non oxydée [238]. Ces résultats suggèrent dans ce modèle de lupus, comme dans notre modèle de ScS, un rôle déterminant de l'oxydation d'antigènes dans le déclenchement de la réponse immunitaire auto-immune.

La réponse immunitaire associée à la présence d'auto-Ac chez les souris HOCl qui développent une maladie proche de la ScS, relance la question du rôle du système immunitaire dans notre modèle et dans la ScS en général. Aucun rôle pathogène direct n'a été démontré pour les Ac anti-centromère chez l'homme. Les Ac anti-ADN Topoisomérase-1 peuvent exercer un certain rôle pathogène en facilitant l'adhérence des monocytes aux fibroblastes puis l'activation des fibroblastes [159], [158]. Néanmoins, il est difficile de tirer des conclusions globales à partir de ces expériences réalisées *in vitro*. Pour tenter de répondre à cette question *in vivo*, nous avons exposé des souris BALB/c SCID à des solutions contenant des oxydants dans les mêmes conditions que les souris BALB/c non SCID. Chez les souris immunodéprimées, nous avons observé une fibrose systémique, mais le dépôt de collagène au niveau pulmonaire était moindre que chez les souris avec un système immunitaire fonctionnel. Ce résultat suggère que, dans ce modèle de ScS induit par des FRO, le système immunitaire est peu impliqué dans le déclenchement des lésions de fibrose mais exerce un rôle amplificateur en stimulant la synthèse de matrice extracellulaire par les fibroblastes.

Finalement, nous proposons un double mécanisme physiopathologique : un mécanisme toxique, impliquant un excès de FRO particulières (HOCl et OH[•] conduisant plutôt à une forme diffuse de ScS, ONOO⁻ déclenchant une forme cutanée limitée) et un mécanisme immunologique. Nous suggérons que ces deux mécanismes ne s'opposent pas mais au contraire entrent en synergie, du moins en ce qui concerne la forme cutanée diffuse de la maladie.

Dans cette hypothèse pathologique, le facteur déclenchant initial correspond à une exposition à de grandes quantités de FRO au niveau cutané. Ces FRO entraînent localement une activation des fibroblastes, une apoptose des CE et une oxydation de certaines protéines aboutissant à l'apparition de nouveaux épitopes reconnus par les cellules présentatrices d'antigènes

locales. Rapidement, ces cellules recrutent des lymphocytes T dans le derme, lymphocytes T oligoclonaux reconnaissant spécifiquement les auto-antigènes oxydés. Les lymphocytes B également spécifiques des premiers antigènes oxydés sont aussi activés, entraînant rapidement l'apparition d'auto-Ac (Ac anti-ADN Topoisomérase 1 en cas d'exposition initiale à HOCl ou OH[•], Ac anti-centromère après exposition à ONOO⁻).

Les premiers signes cliniques de la maladie apparaissent localement. En cas d'exposition à HOCl ou OH[•], de grandes quantités d'AOPP sont formées et diffuseraient dans tout l'organisme via la circulation systémique. Ces molécules seraient responsables de la diffusion du stress oxydant et la progression des lésions à distance, dans la peau, les poumons et les reins, aboutissant à une forme cutanée diffuse de ScS. La figure 4.1 ci-dessous montre l'effet de l'exposition cutanée à HOCl ou OH[•] sur les fibroblastes et leur activation puis au niveau systémique. En cas d'oxydation initiale par ONOO⁻, un stress oxydant quantitativement et qualitativement différent serait généré, responsable de lésions cutanées plus limitées et de l'absence d'atteinte pulmonaire interstitielle. Cette hypothèse physiopathologique fait du stress oxydant un élément-clé du développement de la ScS. Se pose donc, dans cette hypothèse, la question de l'origine des FRO. Il est possible que les FRO soient initialement d'origine environnementale, l'exposition pouvant alors être professionnelle (cas des patients développant une ScS après exposition à la silice) ou domestique. Néanmoins, il est probable que ces sources de FRO exogènes ne suffisent pas à entretenir l'ensemble des processus conduisant à une ScS. Des FRO d'origine endogène peuvent expliquer l'entretien des mécanismes pathologiques. Les travaux de l'équipe de Gabrielli ont mis à jour en 2006 plusieurs mécanismes conduisant à une synthèse accrue de FRO endogènes chez les patients atteints de ScS. Les monocytes et les fibroblastes de patients sclérodermiques produisent en effet une grande quantité de O₂^{•-} [8], [7]. Cette synthèse est dépendante d'auto-Ac présents dans le sérum des patients. Ils reconnaissent le récepteur du PDGF à la surface des fibroblastes et forment une boucle d'activation dans ces cellules aboutissant à une synthèse permanente de FRO [44], [46]. Cette synthèse endogène de FRO observée chez les patients atteints de ScS à une phase d'état de la maladie pourrait donc prendre le relais d'une source de FRO initialement exogène. A ce stade, les mécanismes pathologiques deviennent indépendants de facteurs extrinsèques et deviennent peu sensibles aux thérapeutiques actuellement disponibles. La présence de ces auto-Ac anti-PDGF chez les patients sclérodermiques est aujourd'hui discutée par d'autres équipes, mais nombre d'arguments prouvent que les FRO sont synthétisées de manière endogène chez les patients sclérodermiques.

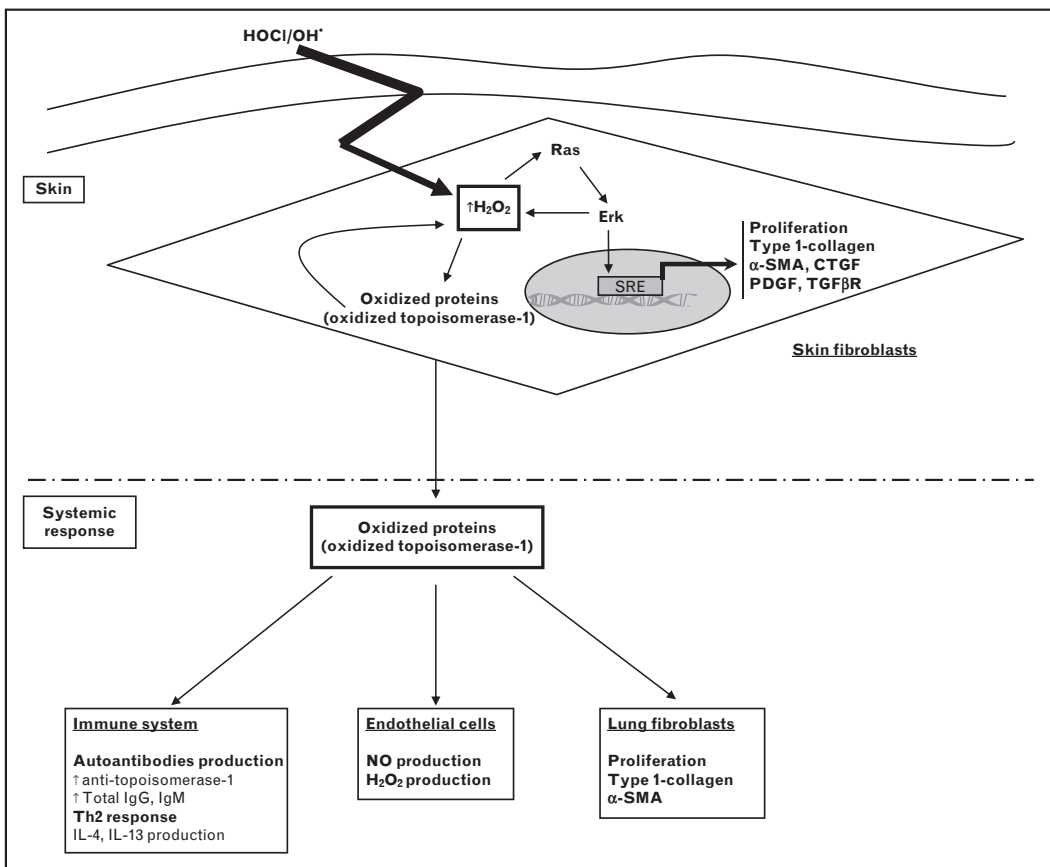


Figure 4.1 Induction du phénotype sclérodermique chez la souris après injections quotidiennes intra-dermiques pendant 6 semaines de HOCl ou OH[•]. Batteux F. et al, Curr. Op. Rheumatol, 2011.

Dans la seconde partie de notre travail, nous présentons nos résultats sur les nouvelles voies d'activation fibroblastique et les approches thérapeutiques qui pourraient en découler.

Dans le travail présenté dans l'article 2, nous avons mis en évidence pour la première fois l'activation de Notch dans la peau, les poumons et les splénocytes des souris sclérodermiques. Nous avons aussi observé cette activation dans la peau de patients atteints de sclérodermie localisée de type morphée et de ScS. Plusieurs hypothèses peuvent expliquer l'activation de Notch dans la ScS. Tout d'abord, la faible concentration en oxygène dans la peau saine fait augmenter les taux d'ARNm de Notch 1 grâce au facteur HIF-1 α . Dans la ScS, l'ischémie tissulaire, due au défaut d'angiogénèse, peut activer HIF-1 α et celui-ci peut induire l'expression de gènes de la matrice extra-cellulaire dans les fibroblastes du derme. De plus, dans un modèle d'ischémie-reperfusion du rein chez le rat, les ARNm de Delta-1 (ligand de Notch), Notch 2, et Hes-1 (cible

de Notch) sont fortement exprimés et régulent la régénération et la prolifération des tubules rénaux. Enfin, le TGF- β , cytokine clairement impliquée dans la physiopathologie de la ScS, est capable d'induire fortement l'expression du ligand de Notch Jagged-1, contribuant ainsi au développement de la fibrose dans un modèle murin de fibrose rénale [239].

Le traitement *in vivo* par un inhibiteur de gamma-secrétase (GSI) réduit de façon significative la fibrose cutanée et pulmonaire chez nos souris sclérodermiques, et réduit le taux de prolifération aberrant des fibroblastes dermiques. Grâce à un test *in vitro* nous avons également pu montrer que le GSI pouvait directement normaliser la prolifération des fibroblastes extraits de peau sclérodermique. Dans la ScS, le phénotype hyperprolifératif des fibroblastes a été démontré chez la souris et chez l'homme, et est, avec la surproduction de protéines de matrice extracellulaire, un des signes biologiques caractéristiques de la ScS [30]. La diminution de la prolifération des fibroblastes *ex vivo* sous l'effet du GSI suivie de l'inhibition de l'accumulation de collagène dans la peau et les poumons expliquent les effets bénéfiques de l'inhibition de Notch dans notre modèle.

Le rôle de Notch dans le cycle cellulaire apparaît très complexe. Il peut induire l'apoptose ou la prolifération selon les types cellulaires et le contexte [240]. Dans les fibroblastes, l'oncogène Ras peut activer la voie Notch, ce qui permet de maintenir le phénotype néoplasique des fibroblastes transformés [241]. Dans un modèle de plaie-cicatrisation, l'augmentation de la prolifération fibroblastique est corrélée à l'activation de Notch et peut être annulée par un traitement *in vitro* et *in vivo* par le GSI [242]. D'autre part, une étude récente révèle une réduction de la fibrose hépatique chez les patients atteints du syndrome d'Alagille (dû à des mutations affectant les signaux transmis par Jagged1) [243]. Ces données démontrent le rôle pro-prolifératif de Notch dans les fibroblastes concordant avec notre modèle et expliquent le bénéfice obtenu chez les souris sclérodermiques avec le traitement par le GSI.

Dans notre étude, l'inhibition de Notch réduit les concentrations sériques en AOPP et diminue la production endothéliale d' H_2O_2 induite par les sérum de souris sclérodermiques. De plus, nous avons montré que l'incubation *in vitro* du GSI avec des cellules endothéliales réduisait le niveau d' H_2O_2 relargué par ces cellules proportionnellement à la concentration de GSI utilisée. Nous disposons de peu de données sur le rôle de Notch dans la régulation du stress oxydant. Cependant, un article récent met en évidence le rôle de Notch dans la transcription de certains gènes dans les macrophages : les agonistes des Toll-like récepteurs induisent une surexpression de Notch 1 et de ses gènes cibles. L'inhibition de Notch entraîne une baisse du

TNF alpha, de l'IL-6, et du NO libérés par les macrophages [244]. Ces données, ainsi que les nôtres, indiquent que l'inhibition de Notch favorise une réponse anti-inflammatoire.

Les anomalies vasculaires sont un des signes majeurs de la ScS. Les sérum des souris exposées à HOCl contiennent de grandes quantités de substances oxydées telles que les AOPP, capables de générer à leur tour la production d' H_2O_2 par les cellules endothéliales, et donc de participer à la formation de lésions vasculaires. Les altérations vasculaires entraînent secondairement des perturbations du flux vasculaire aboutissant à l'hypoxie tissulaire, l'inflammation et la fibrose. L'inhibition de Notch par le GSI a pu abolir ce phénomène, confirmant ainsi le rôle majeur de la voie Notch dans le contrôle du développement et de la physiologie vasculaire.

Comme nous l'avons décrit dans le chapitre 1, il existe une activation de l'immunité cellulaire et humorale dans la ScS. Les mécanismes immunitaires et inflammatoires jouent certainement un rôle dans les lésions vasculaires et l'activation de voies conduisant à la fibrose. Dans notre modèle, l'exposition des souris à HOCl entraîne une hausse du nombre de cellules B spléniques et de leur activation par le LPS. De plus, on note chez ces souris une augmentation des IgM et IgG sériques totales et des taux d'anticorps anti-ADN Topoisomérase 1, caractéristiques de la ScS. L'inhibition de Notch par le traitement au GSI fait baisser le nombre de cellules B spléniques, leur activation, et les niveaux d'IgG, IgM, et d'anti-ADN Topoisomérase-1. Le rôle de Notch dans le développement lymphocytaire a été très étudié et est aujourd'hui bien connu. Notch 1 est un médiateur-clé dans le développement lymphoïde T [245]. Notch 2, lui, est requis dans les lymphocytes B destinés à devenir des lymphocytes de la zone marginale (ZM). Ainsi, les souris présentant une délétion conditionnelle de Notch 2 n'ont pas de lymphocytes B de la ZM [246]. Les lymphocytes de la ZM sont des cellules non circulantes, à longue durée de vie, qui répondent à des Ag T-dépendants ou T-indépendants, et qui se différencient rapidement en plasmocytes. Le rôle de ces cellules dans la ScS n'est pas bien connu, mais on sait qu'il existe parmi elles un grand nombre de clones auto-réactifs et elles ont été incriminées dans plusieurs modèles d'auto-immunité. En effet, l'amplification de ces cellules a été décrite dans un modèle murin de lupus [247]. De même, la surexpression de BAFF associée au phénotype lupique chez la souris entraîne l'augmentation du compartiment des lymphocytes B de la ZM. Il apparaît clairement aujourd'hui que la réponse B joue un rôle important dans la pathogénie de la ScS. Un modèle de ScS induit par la bléomycine chez des souris KO pour le CD19 montre une réduction de la fibrose et de la production d'Ac [149]. En outre, chez l'homme, des niveaux élevés de BAFF sont détectés chez des patients sclérodermiques, et corrèlent avec l'étendue de la fibrose

cutanée [150]. Il est ainsi possible que les cellules B de la ZM soient impliquées dans la pathogénie de la ScS. Le traitement par le GSI pourrait entraîner la diminution de cette population via l'inhibition de Notch 2, et ainsi réduire les mécanismes immunitaires pathogéniques impliqués dans la ScS.

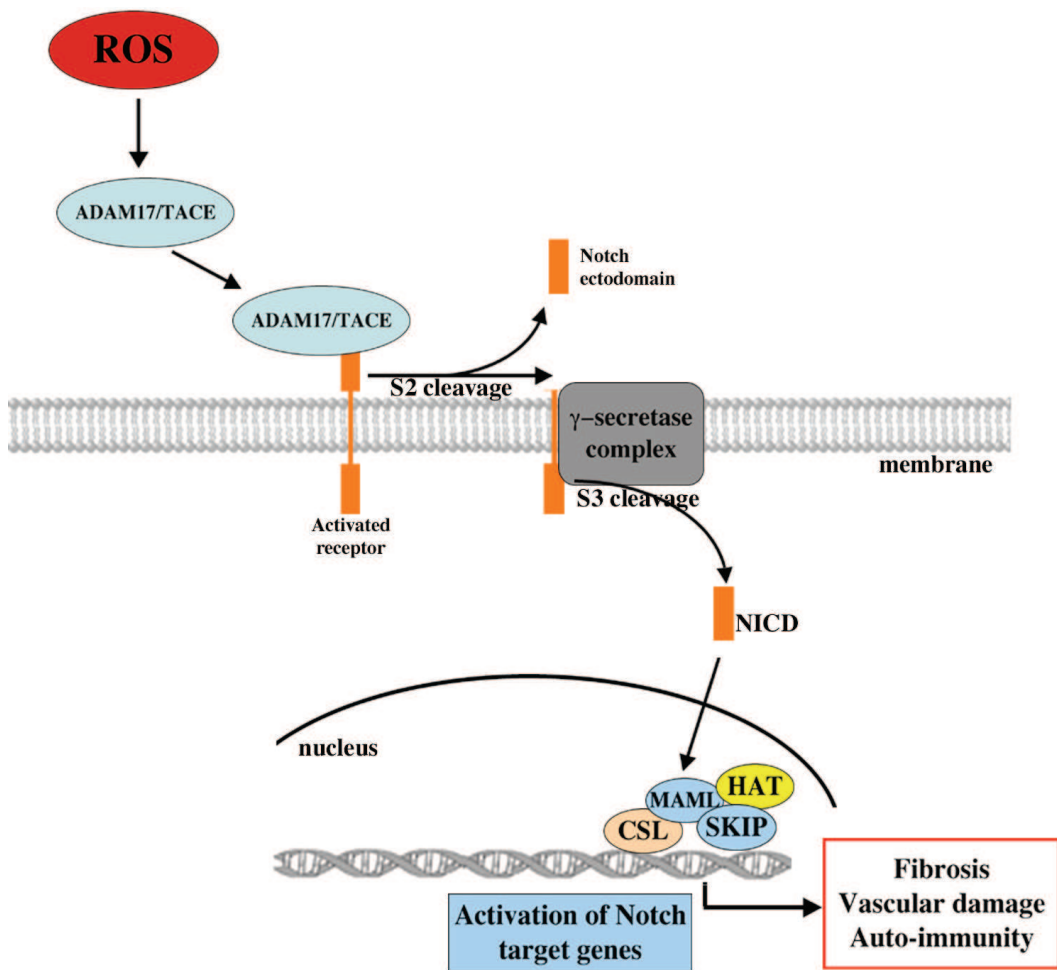


Figure 4.2 Voie d'activation de Notch dans la ScS selon notre modèle. Les FRO produites lors des phénomènes d'ischémie-reperfusion chez l'homme ou lors des injections d'HOCl activent ADAM17, qui est capable de libérer le domaine actif intra-cellulaire de Notch NICD. Ce dernier peut alors transloquer au noyau et activer la transcription de ses gènes cibles, ayant pour effets la prolifération fibroblastique et la fibrose, le développement d'une auto-immunité, et des lésions vasculaires.

Plusieurs hypothèses peuvent expliquer l'activation de Notch observée dans la ScS chez l'homme et chez la souris. Nous avons retrouvé une surexpression d'ADAM dans la peau des souris exposées à HOCl et dans celle des patients atteints de sclérodermie systémique et morphée. Les protéines ADAM sont une famille de protéines transmembranaires et secrétées qui sont impliquées dans plusieurs voies de signalisation. ADAM17 est impliquée dans l'activation de la voie Notch. Le déclenchement du signal Notch requiert la fixation d'un ligand à l'ecto-domaine de Notch, déclenchant la libération de ce domaine par la protéase ADAM17 [74]. ADAM17 est sur-exprimée dans un grand nombre de maladies, comme les cancers mais aussi certaines maladies auto-immunes et inflammatoires. Une étude a récemment montré que la synthèse d'ADAM17 pouvait être induite par le stress oxydant [248]. Nos résultats soulignent le fait qu'ADAM17, et également Notch, peuvent être activés par le stress oxydant. La figure 4.2 représente l'activation possible de Notch dans notre modèle. Il ne faut cependant pas négliger l'importance d'autres facteurs capables d'activer la voie Notch, tels que l'hypoxie et les cytokines pro-inflammatoires comme le TNF- α [249].

Dans la suite de notre travail sur l'activation fibroblastique et les nouvelles approches thérapeutiques dans la ScS, nous avons évalué le rôle d'une autre voie possible d'activation des fibroblastes : la voie des cannabinoïdes. Nous avons ainsi mis en évidence que cette voie était impliquée dans le contrôle de la fibrose cutanée et pulmonaire et dans le développement de la réponse immunitaire dans la ScS. Outre leurs effets psychoactifs, les cannabinoïdes peuvent jouer un rôle dans de nombreux autres processus tels que l'inflammation et l'auto-immunité. Ils peuvent aussi moduler la motilité cellulaire, la prolifération et l'apoptose. Dans ce travail, nous avons démontré que les agonistes non-sélectifs de CB1/CB2 (WIN-55212) et sélectifs de CB2 (JWH-133) étaient efficaces dans la prévention de la fibrose systémique dans le modèle murin de ScS que nous avions récemment décrit. Ainsi, les agonistes des cannabinoïdes peuvent bloquer les effets profibrosants de l'acide hypochloreux HOCl dans la peau et le poumon. De plus, nous avons montré que les souris déficientes en récepteur CB2 étaient plus sensibles à l'induction de la maladie par HOCl et qu'elles développaient un phénotype exacerbé de fibrose cutanée et pulmonaire. Les agonistes des récepteurs CB2 sont capables d'inhiber l'inflammation pulmonaire induite par le LPS dans un modèle murin, et nos résultats ont apporté de nouvelles données concernant leur rôle dans la fibrose pulmonaire. D'autres études avaient déjà rapporté leurs propriétés anti-fibrosantes dans des modèles de fibrose cutanée, cardiaque et hépatique [106], [114], [111]. Une autre équipe a d'ailleurs publié des résultats intéressants concernant l'activité

anti-fibrosante du JWH-133 dans le modèle de ScS induite par la bléomycine de manière concomitante avec la publication de nos travaux [114]. Dans le cœur, il a été montré que la stimulation des récepteurs CB2 par le JWH-133 protégeait de la fibrose post-infarctus, et que les cœurs des souris CB2-/- présentaient des signes histologiques de fibrose et une hypertrophie des myocytes 4 semaines après l'induction de lésions d'ischémie-reperfusion. Dans le foie, l'expression des récepteurs CB1 et CB2 est augmentée au cours de la cirrhose, et CB1 et CB2 exercent des effets opposés. CB1 aurait ainsi des propriétés pro-fibrosantes, alors que l'activation de CB2 permettrait d'abroger le processus fibrosant en inhibant la survie des myofibroblastes et en déclenchant leur apoptose [250], [111]. De plus, les souris CB2-/- développent une fibrose hépatique exacerbée après exposition chronique au tetrachlorure de carbone [110]. L'activation du récepteur CB2 peut non seulement limiter le développement de la fibrose de manière préventive, mais peut aussi permettre la régression d'une fibrose pré-existante via l'augmentation de l'expression de la métalloprotéase MMP-2 [112]. Nous avons également pu démontrer l'action des récepteurs CB2 sur la fibrose pré-existante en débutant le traitement par WIN-55212 quatre semaines après induction de la ScS par injections d'HOCl.

Comme nous l'avons vu dans la première partie de ce travail, la forme diffuse de la ScS est caractérisée par une activation lymphocytaire T et B et par la production d'auto-Ac. L'utilisation des agonistes des cannabinoïdes et des souris déficientes en CB2 nous a permis de montrer que cette voie jouait un rôle dans l'activation immunitaire de la ScS. En effet, le traitement *in vivo* des souris ScS par le WIN-55212 et le JWH-133 a permis une réduction de la prolifération lymphocytaire B et de la production d'auto-Ac anti-ADN Topoisomérase-1. CB2 est exprimé par les cellules immunitaires, et de façon particulièrement élevée par les lymphocytes B. D'autres études ont montré dans différents modèles infectieux que le traitement par agoniste des CB pouvait diminuer l'activation des lymphocytes B et ainsi la production d'Ac [251], [252]. Dans des modèles de maladies auto-immunes inflammatoires telles que l'arthrite induite au collagène et l'encéphalite auto-immune expérimentale, les agonistes des CB ont également fait preuve d'efficacité [253].

Nos résultats suggèrent que les effets des récepteurs aux cannabinoïdes sur les fibroblastes, les cellules immunitaires, et les cellules endothéliales s'associent pour inhiber le développement de la maladie. Nous avons réalisé des expériences *in vitro* afin d'évaluer les propriétés du JWH-133 et du WIN-55212 sur les fibroblastes ScS. En effet, comme nous l'avons montré dans le travail précédent, les fibroblastes des souris ScS exposées à HOCl ont un phénotype hyperprolifératif, caractéristique biologique également observée chez l'homme. Les expériences

réalisées *in vitro* ont montré que les deux agonistes étaient capables d'inhiber la prolifération des fibroblastes extraits de peaux de souris ScS. Ces résultats sont en faveur d'une action directe de la voie des cannabinoïdes sur les fibroblastes. Ils concordent avec ceux obtenus dans la cirrhose hépatique humaine, où le JWH-133 est également capable d'induire l'arrêt de croissance et l'apoptose des myofibroblastes. Nos résultats montrent, de façon surprenante, que l'agoniste non-sélectif WIN-55212 réduit plus fortement la prolifération des fibroblastes ScS que l'agoniste sélectif de CB2 JWH-133, alors que les deux molécules témoignent d'une efficacité semblable sur la fibrose dans nos expériences *in-vivo*. Il est ainsi possible que l'activation du récepteur CB2 réduise la fibrose non seulement par une action directe sur les fibroblastes ScS mais aussi par une action indirecte sur l'activation lymphocytaire B. Plusieurs de nos résultats confortent cette hypothèse : la réduction de la prolifération cellulaire B chez les souris ScS traitées par WIN-55212 et JWH-133, et la diminution de la production d'auto-Ac anti-ADN Topoisomérase-1 chez les souris ScS traitées par les deux agonistes. D'autres équipes ont également rapporté que la voie des cannabinoïdes pouvait moduler la réponse inflammatoire [254], [255]. Dans le modèle de ScS induit par la bléomycine, l'activation du récepteur CB2 inhibe l'infiltrat inflammatoire dans la peau, et ainsi réduit la fibrose cutanée. Après des lésions d'ischémie-reperfusion, l'activation des récepteurs CB2 empêche l'activation des fibroblastes mais limite également l'infiltrat macrophagique et la production de TGF- β .

L'activation des récepteurs CB2 apparaît donc comme une nouvelle approche thérapeutique possible dans la ScS, compte-tenu de ses effets sur la prolifération fibroblastique et l'activation immunitaire.

Compte-tenu des hypothèses concernant le rôle de la voie des récepteurs au PDGF dans le développement de la ScS, il convenait d'étudier son implication dans notre modèle. Les composants de la voie du PDGF sont impliqués dans de multiples processus physiologiques et pathologiques tels que la croissance tumorale et l'angiogénèse, l'athérosclérose, l'hypertension artérielle pulmonaire et la fibrose pulmonaire, hépatique et cardiaque. Notamment, dans la fibrose cutanée et pulmonaire chez l'homme, l'expression du PDGF est corrélée avec l'expansion de myofibroblastes contribuant à la synthèse de collagène [43]. Nous avons donc cherché à savoir si la sclérodermie que nous avions réussi à reproduire chez la souris grâce à des injections d' HOCl partageait cette caractéristique biologique avec l'homme. Pour cela, nous avons réalisé des western-blots dans les fibroblastes cutanés de souris ScS et de souris contrôles pour quantifier l'expression du PDGFR dans sa forme phosphorylée et activée (p-PDGFR) ou non-phosphorylée (PDGFR) dans ces cellules. Ces premiers résultats montraient une augmentation

de la phosphorylation du PDGFR, et donc de son activation, dans les fibroblastes des souris ScS par rapport aux fibroblastes des souris contrôles. Ce résultat rapprochait donc encore notre modèle murin de la maladie humaine puisqu'une étude immunohistochimique rapportait que les patients sclérodermiques présentaient des taux élevés de pPDGFR dans la peau lésée, alors qu'ils étaient indétectables dans la peau de patients contrôles [256]. D'autres études ont rapporté une augmentation des ligands du PDGFR: PDGF-A et PDGF-B dans les lavages bronchoalvéolaires des patients sclérodermiques, suggérant qu'ils pouvaient induire une activation des récepteurs dans les poumons et ainsi être responsables de la fibrose. Il est aussi possible que d'autres facteurs activent le PDGFR. Ainsi, comme nous l'avons vu précédemment, des auto-Ac activateurs anti-PDGFR ont été décrits chez les patients sclérodermiques [45]. Aussi, le TGF- β libéré par les cellules mononucléées infiltrantes est capable d'augmenter l'expression du PDGFR et d'accroître les effets du PDGF-A [257].

Comme l'activation du PDGFR semblait cruciale dans l'activation fibroblastique de la ScS dans notre modèle murin mais aussi chez l'homme, nous avons entrepris de tester l'effet d'une inhibition de cette voie dans notre modèle murin. En effet, plusieurs molécules inhibitrices de tyrosine kinases capables de cibler le PDGFR étaient disponibles et utilisées en thérapeutique humaine en oncologie. Nous avons choisi de tester le sunitinib et le sorafenib car parmi les molécules inhibitrices de tyrosine kinases ces deux molécules ont la plus forte affinité pour le PDGFR. Les souris ScS ont été traitées avec la même dose de sunitinib ou sorafenib. Pourtant le sunitinib a montré une efficacité supérieure au sorafenib dans la prévention du développement de la fibrose cutanée et pulmonaire de notre modèle murin de ScS induite par l' HOCl . Le sunitinib réduisait également de manière plus importante la phosphorylation du PDGFR dans les fibroblastes des souris ScS traitées, que le sorafenib. L'étude de l'effet des deux molécules sur les différents paramètres biologiques de fibrose, d'activation immunitaire et de lésions endothéliales montre que le sorafenib n'est pas efficace à 50 mg/kg/jour pour prévenir le développement de la ScS, contrairement au sunitinib. Plusieurs différences entre les 2 molécules peuvent expliquer ce phénomène. Tout d'abord, le sorafenib a une demi-vie plus courte que le sunitinib (30-40 heures versus 80-100 heures). De plus, le sunitinib possède un métabolite actif: le SU012662, qui permet d'augmenter sa durée d'action, ce qui n'est pas le cas du sorafenib. Le métabolite actif SU012662, bien que deux fois moins puissant que le sunitinib, a également la propriété d'inhiber le PDGFR et le VEGFR, et contribue ainsi à l'activité du sunitinib. Enfin, le sorafenib et le sunitinib n'ont pas la même activité vis à vis du PDGFR: la concentration inhibant 50% de l'activité du PDGFR (CI50) est de 1129 nM pour le sorafenib alors qu'elle est de 75

nM pour le sunitinib, c'est à dire 15 fois inférieure. Il faut, de plus, considérer que ces molécules inhibitrices de tyrosine kinase ne sont pas sélectives vis à vis d'un récepteur mais au contraire ciblent de multiples récepteurs. Ainsi, le sunitinib a un spectre d'inhibition de récepteurs plus large que le sorafenib et pourrait donc avoir une action bénéfique sur d'autres récepteurs impliqués dans l'activation fibroblastique et le développement de la ScS dans notre modèle. D'autres expériences seraient nécessaires pour clarifier ce point.

Comme nous l'avons vu dans les premiers articles sur l'activation fibroblastique, la peau de nos souris ScS contient, comme celle des patients sclérodermiques, une population particulière de fibroblastes: les myofibroblastes. Ils expriment l' α -SMA, produisent de fortes quantités de collagène et de FRO, et sont hyperprolifératifs. Afin de mieux caractériser l'effet des 2 molécules inhibitrices de tyrosine kinases sur la fibrose, nous avons réalisé plusieurs expériences *in vitro*. Tout d'abord, nous avons réalisé un test de prolifération spontanée des fibroblastes extraits des peaux de souris contrôles (PBS), de souris HOCl, de souris HOCl+sorafenib, de souris HOCl+sunitinib. Les fibroblastes des souris ScS traitées *in vivo* par le sorafenib et le sunitinib ont une capacité de prolifération réduite par rapport à ceux extraits des peaux de souris ScS non traitées. Les deux molécules étaient capables d'inhiber de façon proportionnelle à leur concentration la prolifération fibroblastique, mais à la même dose le sunitinib avait une capacité d'inhibition plus importante que le sorafenib. Cette expérience nous a apporté la preuve directe des propriétés anti-prolifératives des deux molécules sur les fibroblastes ScS. Afin de confirmer ce résultat, nous avons évalué l'expression de l' α -SMA dans les fibroblastes ScS traités *in vitro* ou non avec différentes doses de sunitinib et de sorafenib. Le traitement par l'une ou l'autre molécule permettait une diminution de l'expression de l' α -SMA, suggérant une diminution du nombre de myofibroblastes en culture au profit des fibroblastes normaux.

Outre l'effet d'inhibition de la prolifération fibroblastique et de la différenciation myofibroblastique, il est possible que le sunitinib, et dans une moindre mesure le sorafenib, inhibent directement la synthèse de collagène par les fibroblastes. C'est en tout cas ce que suggèrent les résultats obtenus dans deux modèles de fibrose hépatique où le sorafenib est capable de réduire *in vitro* directement la production de collagène par les hépatocytes [258]. Deux autres TKI, le dasatinib et le nilotinib ont montré des résultats similaires sur les fibroblastes du derme de souris ScS induite par la bléomycine et de patients sclérodermiques. De plus, le sunitinib et le sorafenib pourraient également réduire les dépôts de collagène via une action inhibitrice sur TIMP-1, ce qui améliorerait l'action des métalloprotéases et donc la dégradation de la matrice

extra-cellulaire. Là-encore, ce phénomène a été observé dans un modèle de fibrose hépatique où le sorafenib altère l'équilibre entre MMP-13 et TIMP-1 en agissant en défaveur de TIMP-1.

Le rôle du système immunitaire dans la ScS et dans notre modèle a été abordé dans l'article 1 grâce à nos expériences sur souris SCID qui démontrent que le système immunitaire joue un rôle dans l'amplification systémique de la maladie. Ainsi, dans les différents travaux réalisés *in vivo* sur l'activation fibroblastique, nous avons toujours observé une activation du système immunitaire. Dans le travail de l'article 4 sur le PDGFR et les inhibiteurs de tyrosine kinases dans la ScS, nous avons aussi observé cette activation du système immunitaire chez les souris ScS avec augmentation des populations spléniques B et T CD4+ ainsi que la production d'auto-Ac. Le traitement par sunitinib et sorafenib a permis de réduire la production d'auto-Ac. Ce phénomène était corrélé à une diminution de la production d'IL-6 et de TGF- β par les lymphocytes B spléniques en culture. Le sunitinib était également capable de réduire l'expansion splénique des lymphocytes B, et leur activation puisque les cellules positives pour l'expression du marqueur B7.1, impliqué dans la coopération B-T, était diminuée sur les cellules B des souris ScS traitées par sunitinib comparé au souris ScS non traités. Les effets du sunitinib sur le système immunitaire n'ont jamais été rapportés auparavant. Cependant, il est connu que l'imatinib, un autre TKI, peut induire une lymphopénie et une hypogammaglobulinémie chez l'homme, et affecter l'expansion des lymphocytes T cytotoxiques mémoires [259]. Le mécanisme de ces effets de l'imatinib restent obscurs. Concernant les effets du sunitinib sur le système immunitaire observés dans notre modèle, il ne faut pas négliger que cette molécule interagit également avec le VEGFR. La voie du VEGF joue un rôle important dans l'activation des lymphocytes T naïfs [260]. Le VEGFR-1 est exprimé par les monocytes/macrophages et est impliqué dans leur migration et dans l'inflammation chronique [261], [262]. Ainsi, les souris déficientes en VEGFR-1 ne développent pas d'arthrite induite au collagène car elles ont une réponse moindre des monocytes/macrophages dans un contexte inflammatoire [262]. Il est donc possible, dans notre modèle, que le sunitinib ait une action anti-inflammatoire et réduise l'activation immunitaire dans ce contexte d'activation fibroblastique induite par le stress oxydant via une inhibition du VEGFR.

En plus des anomalies fibrosantes et immunitaires, la ScS est caractérisée par des anomalies vasculaires et endothéliales qui ont été présentées dans le chapitre 1. Grâce à la mise au point du modèle murin, nous avons montré que les protéines oxydées (AOPP) générées dans la peau peuvent migrer dans la circulation systémique, activer les cellules endothéliales et favoriser leur production de FRO, entraînant à nouveau la formation d'AOPP capables de provoquer

des lésions de l'endothélium. Dans notre travail sur le PDGF et les TKI dans la ScS, nous avons mis en évidence une augmentation des taux de VCAM sériques chez les souris ScS, qui était réduite par le traitement *in vivo* par le sunitinib. Le VCAM est un marqueur de souffrance endothéliale qui est également élevé chez les patients sclérodermiques. Le VEGF est un des facteurs majeurs associés à la prolifération des cellules endothéliales vasculaires, à leur migration et à leur survie. Il peut se lier à deux récepteurs, le VEGFR-1 et le VEGFR-2. Les signaux médiés par le VEGFR-2 favorisent la prolifération, la survie, la migration et l'adhésion des cellules endothéliales. Plusieurs équipes ont décrit une activation de cette voie dans la peau des patients sclérodermiques. Nos résultats apportent également la preuve de l'activation du VEGFR (via une augmentation de sa phosphorylation) dans la peau des souris de notre modèle murin, ce qui concorde avec les observations réalisées chez l'homme. L'activation chronique de la voie du VEGFR2 pourrait être impliquée dans la microangiopathie sclérodermique, comme le suggère l'équipe de Jinnin [263]. L'activation incontrôlée du VEGFR ou l'exposition prolongée au VEGF peut induire la formation de néo-vaisseaux anormaux. Comme le sunitinib et le sorafenib sont tous deux capables d'inhiber le VEGFR, nos résultats apportent des arguments supplémentaires en faveur du rôle d'une hyper-activation de la voie du VEGFR dans le déclenchement des anomalies endothéliales dans la ScS.

Nos résultats apportent de nouvelles pistes concernant le rôle de la voie du PDGFR dans l'activation fibroblastique et celui de la voie du VEGFR dans la microangiopathie de la ScS. Les inhibiteurs de tyrosine kinases ciblant le PDGFR et le VEGFR constituent ainsi une nouvelle piste thérapeutique dans la ScS puisque ces molécules sont déjà utilisées chez l'homme en oncologie et qu'elles ont témoigné d'une efficacité certaine sur les composants fibrotiques, immuns et vasculaires dans notre modèle murin de ScS.

Dans l'article 5 de nos travaux personnels, nous avons exploré le statut oxydo-réducteur des fibroblastes cutanés des souris de notre modèle de ScS, et les avons exploitées afin de tester les propriétés du trioxyde d'arsenic sur ces cellules. Comme nous l'avons vu précédemment, les FRO jouent un rôle certain dans la physiopathologie de la ScS et l'équilibre des systèmes oxydants versus anti-oxydants est crucial dans le développement des maladies fibrosantes telles que la ScS. Ainsi, les FRO peuvent stimuler la croissance et la prolifération des fibroblastes jusqu'à un certain seuil, au-delà duquel elles vont induire l'apoptose cellulaire (voir chapitre 2). Cette propriété ambivalente des FRO est d'ailleurs bien connue dans le cas des cellules cancéreuses où des faibles niveaux de FRO entraînent la prolifération des cellules tumorales alors que des concentrations élevées de FRO induites par les molécules anticancéreuses entraînent leur

apoptose [199]. Il est connu que les fibroblastes des patients sclérodermiques surproduisent des FRO et nous avons confirmé cette propriété dans notre modèle murin. Nous avons donc testé l'effet thérapeutique du trioxyde d'arsenic (As_2O_3), molécule cytotoxique utilisée en oncologie dans la leucémie aiguë promyélocyttaire (LAM3) notamment, dans la ScS puisque cette molécule est capable d'augmenter les taux intracellulaires de FRO dans les cellules de LAM3.

Nous avons tout d'abord exploré les propriétés du trioxyde d'arsenic sur les fibroblastes. La sensibilité cellulaire à l'arsenic est déterminée par l'équilibre entre la génération de FRO et leur détoxicification. En exposant *in vitro* à des doses croissantes d'arsenic des fibroblastes extraits de peaux de souris HOCl et de témoins, nous avons mesuré la production d' H_2O_2 , le contenu intracellulaire en glutathion (GSH), et la viabilité des cellules. Nous avons ainsi observé des différences de sensibilité vis à vis de l'arsenic entre les 2 types cellulaires: il faut 8 fois moins de trioxyde d'arsenic pour induire l'apoptose de fibroblastes HOCl que pour induire l'apoptose de fibroblastes normaux. Cette apoptose met en jeu une explosion oxydative caractérisée par une surproduction importante d' H_2O_2 et un déficit en GSH. En effet, les fibroblastes ScS ont une production basale d' H_2O_2 importante et corrélée avec de faibles réserves intracellulaires en GSH. Ces cellules ont donc un statut oxydant/anti-oxydant déséquilibré qui les rend particulièrement sensibles à l'action de l' As_2O_3 , ce qui n'est pas le cas des fibroblastes normaux. Suite à ces résultats, nous avons modulé le métabolisme des FRO dans les fibroblastes avec divers agents chimiques. La N-acteylcysteine (NAC), un précurseur du GSH, a eu un effet protecteur vis à vis de l'apoptose induite par l'arsenic dans les fibroblastes ScS. Au contraire, la BSO, un agent qui déplete les taux intracellulaires de GSH, a intensifié la cytotoxicité de l'arsenic. Nos résultats concordent ainsi avec ceux obtenus sur les cellules NB4 de LAM3 où la déplétion en GSH augmente la sensibilité de ces cellules à l'apoptose induite par l'arsenic [264]. De plus, le GSH peut se lier à l'arsenic et protéger ainsi la cellule de l'apoptose [265]. Ces différentes données expliquent donc la sensibilité accrue des fibroblastes ScS déficients en GSH et surproduisant de l' H_2O_2 au trioxyde d'arsenic.

Suite à ces premiers résultats *in vitro*, nous avons entrepris de tester les propriétés thérapeutiques de l'arsenic *in vivo* dans notre modèle de ScS. Les fibroblastes des souris ScS traitées par As_2O_3 présentent des niveaux de GSH comparables à ceux des souris contrôles (PBS) et supérieurs à ceux des souris ScS (HOCl). Ce résultat indique que les myofibroblastes "malades" présents dans la peau des souris ScS sont sélectivement tués par l'arsenic et remplacés par les fibroblastes normaux qui survivent et croissent. En effet, comme chez l'homme, la peau des souris ScS contient une population mixte de myofibroblastes "malades" majoritaires (environ

70%) et de fibroblastes normaux minoritaires (environ 30%). Ici, avec le traitement par l'arsenic, ce sont les myofibroblastes surproduisant de l' H_2O_2 et déficitaires en GSH qui entrent en apoptose et les fibroblastes normaux ayant un contenu suffisant en GSH qui survivent. C'est pour cette raison que malgré ses effets pro-oxydants, l'arsenic exerce paradoxalement *in vivo* une activité globale anti-oxydante dans la peau des souris ScS.

Nous avons aussi observé cet effet anti-oxydant également au niveau systémique puisque les niveaux d'AOPP sériques étaient diminués chez les souris traitées par l'arsenic par rapport aux souris ScS non traitées. Comme nous l'avons vu dans l'article 1, les AOPP sont générés au niveau cutané par les fibroblastes ScS qui surproduisent des FRO, et sont acheminés ensuite par la circulation dans les tissus. Ici, les fibroblastes ScS étant sélectivement tués par l'arsenic, la source des AOPP est éliminée, ce qui explique la baisse de leurs taux sériques.

Le traitement par le trioxyde d'arsenic a aussi eu un impact bénéfique sur le composant vasculaire de la maladie. Dans notre modèle de ScS, les AOPP sont les médiateurs du stress oxydant et de la maladie et peuvent ainsi induire l'apoptose des cellules endothéliales et les lésions vasculaires. La diminution des taux d'AOPP sériques chez les souris ScS traitées permet donc de réduire les lésions endothéliales, ce qui explique la normalisation des taux sériques de VCAM1 chez ces souris.

La fibrose cutanée et pulmonaire est réduite chez les souris ScS traitées par l'arsenic. Ce résultat est corrélé avec la diminution de la phosphorylation du facteur de transcription Smad2/3 dans la peau des souris ScS traitées par rapport aux souris ScS non traitées. Smad2/3, qui est augmenté dans la peau des patients sclérodermiques [266], est capable d'activer le promoteur du gène du procollagène COL1A2 induisant ainsi la synthèse de collagène. Le trioxyde d'arsenic est capable d'altérer la phosphorylation de Smad2/3 et ainsi de réduire son activation et ses effets. La phosphorylation de Smad2/3 peut également être induite par le TGF- β et inhibée par des agents anti-oxydants *in vitro* tels que la NAC, le glutathion et la L-cystéine, ce qui souligne le rôle des FRO dans l'activation de la voie Smad2/3. Ainsi, dans notre modèle, la diminution de phosphorylation de Smad2/3 est consécutive à la réduction des anomalies oxydatives observées dans la peau des souris ScS traitées par arsenic puisque celui-ci a un effet pro-apoptotique sur les fibroblastes ScS. Cette diminution d'activation de Smad2/3 contribue à inhiber l'excès de dépôt de collagène conduisant à la fibrose.

Comme avec les précédents traitements in-vivo administrés aux souris, nous avons observé que le trioxyde d'arsenic exerçait des effets immuno-régulateurs chez les souris ScS. En effet, les souris ScS traitées par l' As_2O_3 présentent une diminution du nombre de lymphocytes B, et T CD4+ spléniques et des concentrations d'auto-Ac sériques. De plus, cet effet immuno-modulateur est aussi observé au niveau cytokinique avec une baisse de la production splénique d'IL-4 et d'IL-13, deux cytokines capables de déclencher la synthèse de collagène par les fibroblastes (voir chapitre 1). Les concentrations de ces cytokines sont d'ailleurs augmentées dans le sérum et la peau des patients sclérodermiques [57], [267], [63]. En délestant de manière sélective les fibroblastes "malades", l' As_2O_3 abroge la production chronique de FRO et l'oxydation consécutive de protéines (en particulier d'ADN Topoisomérase-1). Comme nous l'avons vu dans l'article 1 sur la mise au point du modèle murin, l'ADN Topoisomérase-1 oxydée est particulièrement immunogène et est responsable de la rupture de tolérance immunologique dans la ScS. Ainsi, l'arsenic, en inhibant l'oxydation protéique, empêche l'induction d'une réaction auto-immune en limitant la production de l'auto-antigène. Cependant, il n'est pas exclu que le trioxyde d'arsenic ait également un effet direct sur les cellules T activées pour inhiber le développement de la réponse auto-immune. En effet, il a été montré dans différents modèles cellulaires et animaux que les lymphocytes activés pouvaient surproduire de l' H_2O_2 et devenir hyper-sensibles à l'effet pro-apoptotique de l'arsenic. Nous avons donc souhaité tester cette hypothèse dans le travail présenté dans l'article 6 en utilisant un autre modèle de ScS basé sur l'activation lymphocytaire dans un contexte d'histo-incompatibilités mineures.

A la suite des résultats obtenus dans l'article 5 concernant la régulation de la réaction auto-immune, nous avons voulu savoir si l'arsenic pouvait avoir un effet sur les lymphocytes activés. En effet, l' As_2O_3 a une efficacité démontrée sur les cellules hématopoïétiques malignes puisqu'il est utilisé en thérapeutique chez l'homme depuis quelques années pour traiter certaines hémapathies malignes comme la LAM3 [268], ([269]. En outre, un article de 2010 a montré qu'en plus de son activité sur les cellules malignes, l'arsenic pouvait induire l'apoptose de lymphocytes auto-immuns dans un modèle de lupus murin via un mécanisme mettant en jeu le stress oxydant [270]. L'activation immunitaire joue un rôle indéniable dans l'entretien de la maladie dans la ScS (voir chapitre 1.3 et article 1). D'ailleurs, la forme chronique de réaction du greffon contre l'hôte (GVHD) qui est causée par des phénomènes alloréactifs entre cellules immunitaires du donneur et du receveur, est souvent comparée à la sclérodermie sur le plan clinique. En effet, dans 15% des cas de GVHD chronique, on parle de réaction du greffon contré l'hôte

"sclérodermiforme". Des modèles animaux de sclérodermie basés sur la transplantation de cellules hématopoïétiques chez un hôte irradié, avec des incompatibilités HLA mineures entre donneur et receveur ont d'ailleurs été mis au point (chapitre 1 voir 1.6). Afin d'étudier l'impact du trioxyde d'arsenic *in vivo* sur les lymphocytes activés, nous avons utilisé un modèle animal de sclérodermie associée à la GVHD (Scl-GVHD), et avons traité les souris avec l' As_2O_3 sept jours après la transplantation. Dans le modèle utilisé, des souris BALB/c irradiées ont été transplantées avec des cellules de moelle-osseuse et de rate de souris B10.D2.

Quatre semaines après la transplantation, les souris non traitées ont développé une fibrose cutanée et viscérale et diverses manifestations cliniques proches de celles observées chez l'homme. Les souris traitées par l' As_2O_3 ont présenté une amélioration clinique manifeste avec un score clinique global à J28 de 2 versus 5 pour les souris Scl-GVHD non traitées.

Le traitement *in vivo* par l'arsenic a entraîné une diminution du nombre des lymphocytes T CD4+ activés mémoires ($\text{CD4+ CD44}^{\text{high}} \text{CD62L}^{\text{low}}$). Les manifestations observées dans la GVHD chronique dépendent de l'activation de cellules CD4+ du donneur spécifiques pour certains antigènes HLA mineurs, alors que la GVHD aiguë serait plutôt dépendante des lymphocytes T CD8+ [271] [272] [273] [274] [275]. A la suite de la transplantation des cellules B10.D2 aux souris BALB/c irradiées, les lymphocytes T CD4+ naïfs du donneur vont s'activer et déclencher la maladie en infiltrant la peau, en y recrutant des macrophages et des monocytes, et en induisant une fibrose.

Puisque les T CD4+ activées sont les cellules initiatrices de la maladie et que le traitement par l'arsenic entraîne une réduction de cette population chez les souris, nous avons étudié le mécanisme d'action de l'arsenic sur ces cellules. Nous avons ainsi pu montrer par des expériences *in vitro* que les lymphocytes T CD4+ B10.D2 stimulés par les splénocytes de BALB/c irradiés contenaient de faibles concentrations de GSH et produisaient de fortes quantités d' H_2O_2 par rapport aux T CD4+ B10.D2 stimulés par des splénocytes de B10.D2 irradiés. De précédentes études avaient également rapporté une surproduction de FRO par les lymphocytes T dans certaines conditions d'activation [272]. Nous avons ensuite montré que les forts taux d' H_2O_2 produits par les T CD4+ activés rendaient ces cellules particulièrement sensibles à l'action de l'arsenic et à l'apoptose induite par l'arsenic. Ainsi, dans nos expériences *in vitro*, l'arsenic induit une chute des taux de GSH intra-cellulaires associée à une augmentation de la production d' H_2O_2 au-delà du seuil létal pour la cellule, induisant son apoptose. Nos résultats confirment donc

le rôle joué par le statut oxydant/anti-oxydant du lymphocytes dans sa sensibilité à l'arsenic comme nous l'avons observé pour les fibroblastes.

Dans ce modèle de ScS basé sur l'activation immunitaire, nous avons ensuite exploré les altérations du profil cytokinique des splénocytes induites par l'arsenic, pensant qu'elles pourraient refléter les modifications des populations spléniques que nous avions observées. La production splénique d'IL-17 était réduite chez les souris Scl-GVHD traitées par rapport aux souris Scl-GVHD non traitées. L'IL-17 semble jouer un rôle important dans le développement de la GVHD. Ainsi, une étude a rapporté que l'amplification de la production d'IL-17 via l'utilisation du G-CSF dans un modèle de GVHD chronique conduisait à l'apparition d'une fibrose cutanée exacerbée [276]. Une autre équipe a utilisé un anticorps monoclonal dirigé contre l'IL-17 dans la GVHD et a montré que ce traitement pouvait améliorer la fibrose cutanée [274][275]. Très récemment, l'équipe de Nishimori a montré que l'acide rétinoïque de synthèse Am80 (appartenant à la famille de l'acide-tout-trans-rétinoïque ATRA) avait un effet bénéfique sur la GVHD chronique via un effet régulateur sur les lymphocytes Th17 sécrétateurs d'IL-17 [277]. Puisque les acides rétinoïques de synthèse augmentent la production cellulaire de FRO, il est possible qu'ils aient une action toxique pro-oxydante vis-à-vis des LT Th17, comme l'arsenic dans notre modèle. Outre la réduction de la production d'IL-17, nous avons observé une diminution des taux d'IL-4 produits par les lymphocytes T spléniques activés des souris Scl-GVHD traitées par rapport aux souris Scl non traitées. L'équipe de Zhou a observé dans le même modèle de sclérodermie associée à la GVHD une augmentation des taux des cytokines Th2 dans la peau des souris Scl-GVHD par rapport aux souris greffées de manière syngénique [278]. Dans d'autres modèles murins de GVHD chroniques, la réponse Th2 est requise pour le développement de la fibrose cutanée et viscérale [154]. Ainsi, la diminution de la production d'IL-4 que nous avons observée chez les souris Scl-GVHD traitées par l'arsenic contribue probablement à l'amélioration de la fibrose. Globalement, les modifications des productions spléniques de cytokines dans notre modèle sont consécutives à une réduction de l'activation immunitaire après traitement par le trioxyde d'arsenic, et contribuent à l'amélioration des symptômes cliniques.

Les concentrations d'anticorps anti-ADN Topoisomérase-1 étaient diminuées chez les souris Scl-GVHD traitées par l'arsenic par rapport aux souris Scl-GVHD non traitées. Le trioxyde d'arsenic a eu le même effet sur la production d'auto-anticorps (anti-DNA et facteurs rhumatoïdes) chez les souris lupiques MRL/lpr [12]. Il est possible que dans ce modèle comme dans le nôtre, l'arsenic prévienne le développement de la réaction auto-immune en ciblant spécifiquement les LT CD4+.

Le rôle des cellules présentatrices de l'antigène (CPA) dans la GVHD chronique a récemment été mis en avant. En effet, la co-stimulation des LT du donneur via l'expression de CD80 ou CD86 par les CPA de l'hôte ou du donneur est nécessaire pour induire une GVHD chronique [279]. Les pDCs sont tout particulièrement impliquées dans la physiopathologie de la GVHD. Ainsi, le transfert adoptif de pDCs matures chez le receveur entraîne l'exacerbation de la réaction de GVHD [280]. De plus, elles peuvent stimuler les cellules du donneur et induire une réaction de GVHD en l'absence d'autres sous-populations de CPA [281]. L'irradiation du receveur induit une inflammation et la maturation des pDCs, qui pourront ensuite activer les LT [280]. Cependant, il a été récemment montré que les cellules précurseurs des pDCs pouvaient atténuer les symptômes de la GVHD [282]. Ces derniers résultats soulignent les différentes fonctions des pDCs selon l'environnement et le modèle de GVHD étudié [282]. Dans notre cas, la population des pDCs spléniques était réduite chez les souris Scl-GVHD traitées par l'arsenic par rapport aux souris non traitées. Nous avons observé dans cette population une production élevée d' H_2O_2 et un contenu intra-cellulaire réduit en GSH, comme pour les LT CD4+ alloréactifs, rendant ces cellules sensibles à l'apoptose induite par l'arsenic. Nous avons confirmé l'action cytotoxique de l'arsenic sur les pDCs *in vitro* par la diminution de la production d'IFN- α après stimulation des pDCs par un agoniste du TLR-7. Cet effet sélectif de l'arsenic sur les pDCs pourrait apporter des éléments intéressants concernant le lupus érythémateux systémique puisque l'IFN-alpha a un rôle central dans la physiopathogénie de cette maladie [283], [284]. Ainsi, l'équipe de Bobé a montré les effets bénéfiques de l'arsenic dans le modèle de souris lupique MRL/lpr [270]. Comme nous, ils ont rapporté un effet cytotoxique de l'arsenic sur les LT CD4+ activés via une réduction du GSH intra-cellulaire dans ces cellules, mais les effets bénéfiques observés dans leur modèle pourraient aussi être médiés via une régulation de la production d'IFN-alpha par les pDCs.

Les travaux que nous avons conduits sur les effets de l'utilisation du trioxyde d'arsenic dans deux modèles animaux de ScS (induite par l'HOCl et associée à la GVHD) suggèrent que cette molécule déjà utilisée en hématologie clinique pourrait être utilisée dans le traitement des différentes formes de cette maladie.

Chapitre 5

CONCLUSION ET PERSPECTIVES

Notre travail montre que le stress oxydant est au centre de la physiopathologie de la ScS. Ainsi, grâce au modèle murin mis au point au laboratoire et aux différents travaux d'étude de ses voies d'activation, nous avons établi que les FRO étaient impliquées dans l'induction de la maladie. Le stress oxydant contribue directement à la dérégulation de diverses voies de signalisation aboutissant au phénotype hyperprolifératif des fibroblastes. Ceux-ci apparaissent comme un phénomène-clé dans l'initiation de la maladie. L'activation du système immunitaire semble, elle, être secondaire à l'oxydation de protéines telles que l'ADN Topoisomérase-1 qui provoque l'apparition de néo-épitopes et la rupture de tolérance du système immunitaire. Les cellules immunitaires activées participent alors aux mécanismes lésionnels en association avec les FRO.

Les données présentées ici ouvrent plusieurs perspectives.

Tout d'abord, tenter d'identifier l'origine du stress oxydant initial chez les malades. En effet, les FRO impliquées peuvent être d'origine endogène dès le début de la maladie, mais également d'origine environnementale chez certains malades. Une étude épidémiologique permettant d'identifier les substances susceptibles de générer des FRO pourrait être conduite afin de renforcer les mesures préventives vis à vis de ces substances et de diminuer l'incidence de la maladie ou au moins retarder son apparition.

La dérégulation de nouvelles voies de signalisation fibroblastique telles que la voie Notch, celle des récepteurs aux cannabinoïdes, ainsi que les voies du PDGF et du VEGF, a été mise en évidence dans ce travail. Nos résultats mettent en avant le lien entre stress oxydant et dysfonctionnement fibroblastique via la dérégulation de ces différentes voies de signalisation. Elles représentent ainsi de nouvelles cibles thérapeutiques et ouvrent de nouvelles perspectives pour le traitement de la sclérodermie systémique, alors même que les cliniciens disposent de peu de ressources thérapeutiques efficaces pour les patients. Plusieurs molécules agissant sur les voies de signalisation étudiées sont actuellement testées en phase I ou II dans d'autres maladies, et ont fait preuve de leur inocuité chez l'homme. Nos résultats apportent des arguments pour de

futurs essais cliniques avec certaines de ces molécules, ainsi qu'avec l'arsenic trioxide, chez les patients en phase précoce de développement de la sclérodermie systémique.

Chapitre 6

ANNEXES

Nous présentons dans ce chapitre nos autres travaux réalisés sur la sclérodermie systémique.

New insights on chemically induced animal models of systemic sclerosis

Frédéric Batteux^a, Niloufar Kavian^a and Amélie Servettaz^{a,b}

^aLaboratoire d'Immunologie, EA 1833, Université Paris Descartes, Faculté de Médecine, Hôpital Cochin, Assistance Publique-Hôpitaux de Paris (AP-HP), Paris and ^bFaculté de Médecine de Reims, Service de Médecine Interne, Maladies Infectieuses, Immunologie Clinique, Hôpital Robert Debré, Reims Cedex, France

Correspondence to Dr Frédéric Batteux, Laboratoire d'Immunologie, UPRES EA 1833, 24 rue du faubourg St Jacques, 75679 Paris Cedex 14, France
Tel: +33 1 58 41 21 41; fax: +33 1 58 41 20 08;
e-mail: frederic.batteux@cch.aphp.fr

Current Opinion in Rheumatology 2011,
23:511–518

Purpose of review

To discuss the most recent published studies on chemical-induced animal models of systemic sclerosis (SSc) and to precise the important signalling pathways that lead to the initiation and progression of the disease in these models.

Recent findings

Environmental factors undoubtedly contribute to the initiation and the development of SSc. Among those factors, bleomycin has been identified as a possible SSc-inducing substance in mice. The bleomycin model mimics the inflammatory changes observed in the early phase of the disease. This model has been extensively studied and has allowed identification of several key pathways activated in the human disease. More recently, a new chemical-induced model of scleroderma has been developed in mice using daily intradermal injections of a solution generating hypochlorous acid (HOCl)-model. This HOCl-model recapitulates the whole spectrum of the human disease, as fibrosis, inflammation, autoimmunity and vasculopathy can be observed in mice and brought new arguments for a major role of reactive oxygen species in the induction of local and systemic fibrosis.

Summary

Chemically induced models truly develop a SSc-like disease and argue for a crucial role of ROS in SSc.

Keywords

animal models, bleomycin, reactive oxygen species, systemic sclerosis

Curr Opin Rheumatol 23:511–518
© 2011 Wolters Kluwer Health | Lippincott Williams & Wilkins
1040-8711

Introduction

Despite growing efforts in the field of scleroderma research, the pathogenesis of this possible life-threatening disease remains mysterious. More importantly, no treatment has allowed full recovery from this disorder to date. Therefore, animal models are needed to help clarify the mechanisms involved in the development of this condition and open new therapeutic avenues. Systemic sclerosis (SSc) is a complex multifaceted disease characterized by fibroblast dysfunction leading to skin and sometimes systemic fibrosis, early endothelium damages and production of specific autoantibodies (AAbs) targeting nuclear proteins. Several animal models, mostly murine, have been proposed to study one or several of the aspects of the disease [1–3]. Their main features are given in Table 1. Avian models have been helpful in assessing endothelial apoptosis [4,5]. Significant physiopathological and clinical differences are observed between these models of SSc (Table 1). In some of them, the animals develop an organ-specific disease with a limited fibrosis, whereas in other models, the animals display a more systemic disease including

extensive fibrosis and vascular abnormalities. In addition, features of autoimmunity can be observed. In this review, we will focus on the chemically induced models that recapitulate the systemic pattern of the disease. We will detail their main clinical features and update some pathophysiological mechanisms that have been recently unravelled.

Bleomycin-induced fibrosis

The model of bleomycin-induced skin fibrosis is widely used in the research on SSc. Yamamoto *et al.* [6] have established this murine model of skin fibrosis using daily subcutaneous injections of bleomycin over a 4-week period.

Overall features of bleomycin-induced fibrosis in mice

In this model, histopathological examination reveals dermal sclerosis with cellular infiltrates that mimics the histological features of human scleroderma (Table 1). Hydroxyproline and type-I collagen contents are significantly higher in bleomycin-treated skin than in normal skin [6,7]. Alpha-smooth muscle actin (α -SMA)-positive

myofibroblasts differentiate progressively in the dermis of bleomycin-treated mice and their count parallels the development of dermal sclerosis [8]. The fibrosis is not isolated, but is infiltrated by T cells, monocytes/macrophages and mast cells that are not pivotal in the induction of fibrosis as the lesions can be induced in immunodeficient and in mast cell-deficient mice [9–11]. The cutaneous changes are localized to the area surrounding the injected site and persist at least 6 weeks after the end of the treatment. In addition, lung fibrosis with cellular infiltrates and damaged lung architecture can appear following the administration of very high doses of subcutaneous bleomycin [12]. Antinuclear AAbs, such as anti-Scl-70, anti-U1-RNP, and antihistone antibodies also reflect the development of a systemic immune reaction [13]. The severity of the disease varies with the murine strain [7].

Role of the inflammatory process in bleomycin-induced systemic sclerosis

The model of bleomycin-induced skin fibrosis mimics early inflammatory changes in SSc. Indeed, bleomycin triggers the production of reactive oxygen species (ROS) that damage the surrounding cells, in particular endothelial cells, and upregulate the expression of adhesion molecules [14]. This sequence of events leads to the attraction of leukocytes and the activation of resident fibroblasts [6]. Activated fibroblasts produce and release large amounts of extracellular matrix (ECM) proteins that lead to skin fibrosis. In addition, activated fibroblasts produce TGF β [8,15,16] that plays a key role in the pathogenesis of fibrosis through synthesis of type-I and type-III collagens or fibronectin.

In the bleomycin model, TGF β is produced by fibroblasts and infiltrating cells that predominantly comprise macrophages at the sclerotic stage. Lesional skin not only shows upregulated TGF β production, but also increased phosphorylated Smad2/3 [16], coactivators of the TGF β /Smad pathway, such as histone acetyltransferase p300 [17], and CTGF [18] but decreased the expression of Smad7. The role of the Smad3 pathway is confirmed by the scarce fibrosis observed in Smad3-null mice [19] and by the beneficial effect of novel inhibitor of Smad-dependent transcriptional activation, HSc025, on bleomycin-induced dermal and lung fibrosis [20*]. However, in this model, TGF β -stimulated collagen production is also upregulated via Smad-independent signals with chronic upregulation of the early growth response factor (Egr)-1 [21]. Mice with targeted deletion of Nab2, a factor blocking Egr-1-dependent transcriptional responses, display collagen accumulation in the dermis [22].

Bleomycin-induced skin fibrosis is widely used to mimic the inflammatory stage of SSc and evaluate the potential role of individual proinflammatory genes that could play a role in the early phase of SSc. For instance, the mPGES-1

Key points

- Chemically induced models develop a systemic disease with skin and lung fibrosis, autoimmunity and some signs of vasculopathy that mimics the human disease.
- In these models, particularly in the case of the HOCl-model, the immune system does not seem crucial for the initiation of the disease, but is involved in the spreading of the damages.
- Both bleomycin and HOCl-models emphasize the role of reactive oxygen species in the pathogenesis of systemic sclerosis.

isoenzyme (microsomal prostaglandin E2 synthase), an enzyme that catalyzes the conversion of PGH2 to PGE2 [23] in response to inflammation [24], is elevated in SSc fibroblasts from both patients, and bleomycin-treated mice and mPGES-1-null mice are resistant to bleomycin-induced inflammation and fibrosis [25*].

Chemokines are also proinflammatory molecules that play a pivotal role in SSc. Proinflammatory cytokines and ROS are potent stimulators of CCL2 in skin fibroblasts [26]. CCL2 and its receptor CCR2 are upregulated in dermal fibroblasts and inflammatory cells from SSc patients and from bleomycin-treated mice [27]. CCL2 upregulates TGF β gene expression and subsequently the expression of type I collagen in fibroblasts [28]. Bleomycin administration to CCL2 knockout mice reduces early inflammatory infiltrates and fibrosis [29]. The role of the inflammatory processes in the bleomycin model has been further emphasized by the observation that stat4^{-/-} mice are protected. The signal transducer and activator of transcription-4 (STAT4) is a central mediator of inflammation [30], and STAT4 variants have been established as genes of susceptibility for SSc [31]. Consistent with a primary role of STAT4 in inflammation, STAT4 deficiency is not associated with a decrease in fibrosis in tsk-1 mice [32].

The role of cannabinoid agonists as anti-inflammatory and antifibrotic agents has been demonstrated in several inflammatory and fibrotic diseases. In bleomycin-induced and HOCl-induced SSc, CB2 agonists limit leukocyte infiltration and fibrosis, whereas CB2(−/−) mice display a more severe disease in chemically induced models of SSc [33,34*]. In fibroblasts from patients with SSc, both CB1 and CB2 receptors are increased and their exposure to CB2 agonist or CB2/CB1 agonists reduces the deposition of extracellular matrix and the differentiation into myofibroblasts [35]. The role of the CB1 receptor in controlling the inflammatory and fibrotic process in SSc is less clear, but CB1(−/−) mice display mild dermal infiltrates of leukocytes and fibrosis following bleomycin injections [34*,36].

Table 1 Genetic and induced-animal models of systemic sclerosis and their key physiopathologic features

	Fibrosis	Inflammation		Vasculopathy	Key mechanisms
Genetic models					
Tsk-1 mice	Skin	No	Autoantibodies	Endothelial dysfunction but no typical features of SSc vasculopathy	Spontaneous autosomal dominant mutation in the fibrillin gene FBN1
Tsk-2 mice	Lung: emphysema rather than fibrosis Skin	Inflammatory cellular infiltrate in the tissues Systemic inflammation	Autoantibodies	No	Unknown mechanism
Fra-2 mice	Skin		No	Loss of small blood vessels Endothelial cell apoptosis	Transgenic construct with the ubiquitous promoter H2Kb and the Fra-2 locus Fra-2 is a member of the activator protein 1 family
UCD-200 chickens	Lung Oesophagus	Perivascular mononuclear cell infiltrates	Autoantibodies	Raynaud's like syndrome	Activation and apoptosis of endothelial cells
TGF β R1 Δ k mice	Heart Lung Kidney Skin (at 12 weeks)	Mild	No	Vascular remodelling in the lungs	Fibroblast-specific activation of TGF β signalling
Inducible models					
Bleomycin	Lung	Inflammatory cellular infiltrates	Autoantibodies	Endothelial cell apoptosis	Production of reactive oxygen species
HOCl	Skin	Inflammatory cells infiltrate in the lung High AOPP and nitrates serum concentration	Autoantibodies IL-4, IL-13	Endothelial cell damages (\cdot svCAM1)	Production of H_2O_2 by skin fibroblasts consequent to OH^{\bullet} generation in the skin Oxidation of DNA-Topoisomerase-1 leading to a breach of tolerance and to the diffusion of the disease
ScI-GVHD	Kidney Skin	Tissue infiltration of T cells, monocytes, mast cells Alloreactive T-cells	Autoantibodies		
	Lung			Increase in splenic B cells number	
	Kidney				

Human systemic sclerosis (SSc) is characterized by fibrosis, inflammation, autoimmunity and vasculopathy. ScI-GVHD, sclerodermatous graft versus host disease.

Serotonin, also known as 5-hydroxytryptamine (5-HT), is released upon platelet activation. Platelets from SSc patients are hyperactivated and serum levels of 5-HT are elevated [37]. Serotonin is a key mediator between microvascular injury and tissue fibrosis in SSc and injection of bleomycin in 5-HT_{2B}^{-/-} mice induces only minor dermal fibrosis [38*].

Immunological alterations in mice with bleomycin-induced systemic sclerosis

The role of the various T helper subsets has been extensively studied in SSc. Fibrosis has been associated with a T-helper (Th)-2 immune response, partly consecutive to the downregulation of the antifibrotic Th1 cytokine interferon (IFN)- γ . IL-4 is produced by activated memory Th-2 cells and mast cells and promotes fibroblast proliferation and synthesis of ECM proteins [39,40]. IL-4 upregulates TGF β production in eosinophils and T cells [41]. Increased IL-4 levels are detected in the sera or in diseased skin from patients with SSc [42] and from bleomycin-treated mice [43,44]. Mice deficient for T-bet, a Th1 initiating factor, show increased and faster development of fibrosis with an exaggerated immune response and a constitutive elevation of IL-13 [45,46]. IL-13 is a potent stimulator of fibroblast proliferation and of collagen production [47,48] either directly [49] or indirectly through TGF β [50]. In the bleomycin model, IL-13 synthesis is increased in the lesional skin, and IL-13 receptor (IL-13R- α 2) expression is increased in the mononuclear cells and macrophages of the skin infiltrate [44]. Furthermore, IL-13-deficient mice fail to develop skin sclerosis following bleomycin treatment [46], confirming the role of IL-13 in bleomycin-induced scleroderma.

As in scleroderma, autoantibodies have been detected in the bleomycin model. The transfer of CD4(+) T-cells from bleomycin mice into untreated BALB/c nude mice reproduce the clinical, histological and biological changes of the conventional model, supporting the immunological basis of the experimental disease [13]. On the other hand, activated peripheral B cells also play a major role in SSc through antibody or cytokine production [51]. In CD19-deficient mice, induction of dermal and lung fibrosis, cytokine expression and autoantibody production are inhibited [12].

Consistent with the implication of B and T cells in the pathophysiology of SSc, a deficiency in ICOS, a member of the CD28 family involved in the B-T cell cooperation, also attenuates lung and skin fibrosis in bleomycin-induced SSc [52*].

Signalling through adhesion molecules is activated in fibroblasts from SSc patients and believed to be a key step in the formation of fibrosis. Indeed, the deletion of

β 1 integrin results in resistance to bleomycin-induced fibrosis [53]. Moreover, L-selectin and ICAM-1 regulate Th2 and Th17 cell accumulation in skin and lung, leading to the development of fibrosis, and P-selectin, E-selectin, and PSGL-1 regulate Th1 cell infiltration, resulting in the inhibition of fibrosis [54**].

In terms of pharmacological treatment, if rapamycin, an immunosuppressive drug with mTOR inhibitory properties, inhibits fibrosis and immunological abnormalities by decreasing the production of profibrotic cytokines such as IL4, IL6, IL17 and TGF β in bleomycin-injected animals [55*], methotrexate fails to exert any antifibrotic or any anti-inflammatory effect in this model [56].

Reactive oxygen species-mediated animal models of systemic sclerosis

The role of ROS in the pathophysiology of SSc has been stressed by several observations in human and in murine models [57–63]. Indeed, skin fibroblasts from SSc patients spontaneously produce large amounts of ROS that trigger collagen synthesis [61,64]. Moreover, in SSc patients, AAbs to the platelet-derived growth factor (PDGF) receptor expressed on fibroblasts also induce the production of ROS [65]. In addition, sera from patients with SSc can induce the production of ROS by endothelial cells, and also the proliferation of fibroblast [60].

Implication of reactive oxygen species in the pathogenesis of systemic sclerosis

The release of ROS by fibroblasts and endothelial cells can activate several pathological processes triggering the development of SSc. Thus, ROS can oxidize DNA-topoisomerase-1 and induce the breach of tolerance to this nuclear autoantigen [66,67]. The autoimmune phenomenon can be amplified by the inflammatory reaction that results from the overproduction of ROS. The fibrotic process can also be stimulated by the disequilibrium in the redox status. Indeed, ROS elicit the differentiation of fibroblasts into myofibroblasts either directly or through the activation of the ADAM17/NOTCH pathway [68*] or through the release of TGF- β from activated cells [69]. Finally, ROS can also stimulate the growth of dermal fibroblasts through the activation of the Ras pathway and thus explain the proliferative capabilities of SSc fibroblasts extracted from diseased SSc skin [70].

Phenotype of hypochlorous acid-induced systemic sclerosis

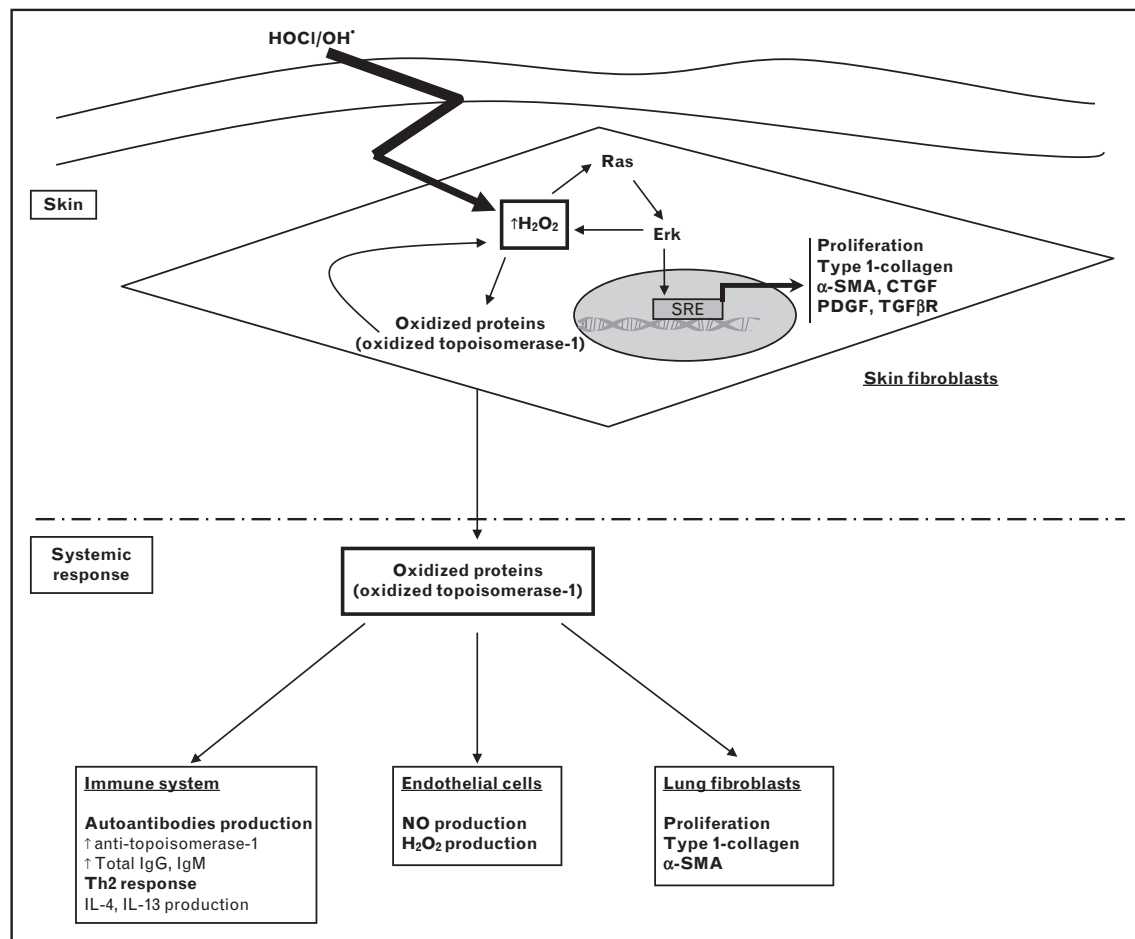
Recently, limited and diffuse forms of SSc have been reproduced in mice by repeated intradermal injections of agents generating various types of ROS [67]. Those experiments not only provide an additional

demonstration of the implication of ROS in the development of SSc, but also provide new animal models of SSc mimicking limited or diffuse SSc. The intradermal injections of agents generating peroxynitrite anions (ONOO^-) into the skin of BALB/c mice induce limited cutaneous fibrosis and the production of anti-CENP-B antibodies in the absence of lung involvement. This disease shares numerous features with the limited cutaneous form of SSc in human. On the other hand, intradermal injections of agents generating hydroxyl radicals (OH^\bullet) or hypochlorous acid (HOCl) to BALB/c mice induce cutaneous and lung fibrosis, characteristic kidney damages along with the production of serum anti-DNA-topoisomerase-1 antibodies, all features that characterize diffuse cutaneous SSc in humans (Fig. 1 and Table 1).

The phenotype of mice exposed to HOCl injections has been further investigated. These mice develop an

extensive skin and lung fibrosis after 6 weeks of daily intradermal HOCl injections. As in the bleomycin-model, cutaneous changes are localized in the area surrounding the injected site. However, skin fibrosis persists at least 10 weeks after the end of HOCl administration. HOCl-induced SSc can be induced in various strains of mice including BALB/c, C57BL6, DBA/1 or NZB mice. The skin of mice exposed to HOCl contains myofibroblasts that produce high amounts of collagen, express α -SMA and display a high proliferation rate. HOCl injection increases B-cell and CD4^+ T-cell numbers in the spleens and total serum IgG and IgM Ab levels, with the production of anti-DNA topoisomerase-1 AAbs, which are a hallmark of SSc. In the lungs, immunohistochemical analysis evidences inflammatory infiltrates that mostly comprise T lymphocytes. In this model, endothelial cell damages occur early as suggested by the high amounts of endothelial microparticles and of

Figure 1 Injections of an HOCl solution generating hydroxyl radicals (OH^\bullet) intradermally for 6 weeks induces a systemic sclerosis phenotype in mice



sVCAM-1 and sE-selectin found in the bloodstream of HOCl mice.

Pathophysiology of hypochlorous acid-induced systemic sclerosis

The pathophysiological mechanisms of the HOCl-model are not fully understood but HOCl injections produce inflammatory changes as in the early phase of SSc. ROS play a direct role in the induction of local and systemic fibrosis, in the autoimmune process and in the vascular damages. Intradermal HOCl stimulates fibroblasts to produce ROS that increase the phosphorylation of ERK1/2, activate the Ras pathway and confer a hyperproliferative phenotype to diseased fibroblasts. As in humans, this phenomenon becomes autonomous, because fibroblasts extracted from diseased skin and cultured in the absence of HOCl still display a hyperproliferative rate and an overproduction of ROS after several passages. The production of ROS induces the differentiation into α -SMA-expressing myofibroblasts, stimulate the production of type-I collagen and leads to skin fibrosis. In addition, ROS decreases the intracellular pool of reduced glutathione and allows the production of oxidized intracellular proteins, especially of oxidized DNA-topoisomerase-1. Remarkably, the sera of both HOCl-mice and SSc patients contain high amounts of oxidized proteins that reflect the severity of the disease and whose release into the bloodstream participates in the spreading of the disease. Indeed, the serum of HOCl-mice and of SSc patients triggers the in-vitro production of high amounts of H_2O_2 when applied to fibroblasts or endothelial cells. The oxidized proteins contained in those sera are necessary and sufficient to reproduce the whole pro-oxidative properties of the sera. Among them, oxidized DNA-topoisomerase-1 is especially involved in the progression of the disease. Oxidized DNA-topoisomerase-1 activates fibroblasts to produce ROS, to proliferate and to synthesize type I collagen. Oxidized DNA-topoisomerase-1 is a modified autoantigen probably responsible for the breach of tolerance to native DNA-topoisomerase-1. Indeed, AAbs to DNA-topoisomerase-1 show a higher avidity to the oxidized than to the native protein. The role of the immune system in this model has been extensively studied. In addition to AAbs, HOCl-mice have higher numbers of T and B cells than normal mice. Moreover, activated T cells overproduce the two Th2 profibrotic cytokines IL-13 and IL-4. The immune reaction essentially affects lung fibrosis which is abrogated in SCID mice, whereas skin fibrosis is the same as in immunocompetent mice. Thus, the autoimmune process is essential for the systemic spreading of the disease in the HOCl-model. Several pathways are involved in the induction of the disease by HOCl: less TGF β is found in the skin of HOCl-mice than in the bleomycin-model but the same increase in phosphorylated Smad2/3 is found in the skin

of both models. This discrepancy can be explained by the increased catabolism of skin TGF β because of HOCl injections. In patients as in both HOCl and bleomycin models, the activation of the Notch pathway plays a central role in the development of fibrosis and autoimmunity. Moreover, Notch inhibition by a γ -secretase inhibitor effectively abrogates the development of the disease [68*,71]. In the HOCl-model, the overproduction of ROS activates ADAM 17, a protease involved in NOTCH cleavage [68*]. As in patients [72–74], the diseased skin of HOCl-mice contains high levels of activated phosphorylated PDGFRs and vascular endothelial growth factors (VEGFRs). The PDGF/PDGFRs signalling pathway could induce fibrosis as suggested in the human disease, whereas the uncontrolled activation of the VEGF/VEGFRs pathway could be responsible for the microangiopathy. In HOCl-mice, the simultaneous inhibition of the phosphorylation of VEGFR and PDGFR by the tyrosine kinase inhibitor sunitinib prevents the development of skin and lung fibrosis (N. Kavian *et al.*, unpublished observation).

Conclusion

Among the numerous models that may help researchers in the field of scleroderma, chemically induced models are easy to handle and reproducible. These models can be induced in several different strains of mice. More importantly, these models truly develop a systemic disease with skin and lung fibrosis, autoimmunity and some signs of vasculopathy. If the mechanisms of both bleomycin-induced and HOCl-induced models are not fully understood to date, both models argue for a crucial role of ROS in SSc, data that are confirmed in human SSc.

Nevertheless, there is no doubt that none of these models can fully encompass all the features of SSc, which is all the more true given the heterogeneity of the human disease. Consequently, the most important point to keep in mind may be to know the limits of each model, and to test, as soon as possible, the hypothesis drawn from animal experiments in SSc patients.

Acknowledgements

The authors are indebted to Ms Agnes Colle for typing the manuscript.

Conflicts of interest

There are no conflicts of interest.

References and recommended reading

Papers of particular interest, published within the annual period of review, have been highlighted as:

- of special interest
- of outstanding interest

Additional references related to this topic can also be found in the Current World Literature section in this issue (p. 620).

- 1 Abraham DJ, Varga J. Scleroderma: from cell and molecular mechanisms to disease models. *Trends Immunol* 2005; 26:587–595.

- 2** Beyer C, Schett G, Distler O, et al. Animal models of systemic sclerosis: prospects and limitations. *Arthritis Rheum* 2010; 62:2831–2844.
- 3** Wei J, Melichian D, Komura K, et al. Canonical Wnt signaling induces skin fibrosis and subcutaneous lipodystrophy: a novel mouse model for scleroderma? *Arthritis Rheum* 2011; 63:1707–1717.
- 4** Sgong R, Gruschwitz MS, Dietrich H, et al. Endothelial cell apoptosis is a primary pathogenetic event underlying skin lesions in avian and human scleroderma. *J Clin Invest* 1996; 98:785–792.
- 5** Worda M, Sgong R, Dietrich H, et al. In vivo analysis of the apoptosis-inducing effect of antiendothelial cell antibodies in systemic sclerosis by the chorionallantoic membrane assay. *Arthritis Rheum* 2003; 48:2605–2614.
- 6** Yamamoto T, Takagawa S, Katayama I, et al. Animal model of sclerotic skin. I: Local injections of bleomycin induce sclerotic skin mimicking scleroderma. *J Invest Dermatol* 1999; 112:456–462.
- 7** Yamamoto T, Kuroda M, Nishioka K. Animal model of sclerotic skin. III: Histopathological comparison of bleomycin-induced scleroderma in various mice strains. *Arch Dermatol Res* 2000; 292:535–541.
- 8** Yamamoto T, Nishioka K. Animal model of sclerotic skin. V: Increased expression of a-smooth muscle actin in fibroblastic cells in bleomycin-induced scleroderma. *Clin Immunol* 2002; 102:77–83.
- 9** Yamamoto T, Takahashi Y, Takagawa S, et al. Animal model of sclerotic skin. II: Bleomycin induced scleroderma in genetically mast cell deficient WBB6F1-W/W(V) mice. *J Rheumatol* 1999; 26:2628–2634.
- 10** Yamamoto T, Nishioka K. Animal model of sclerotic skin. IV: Induction of dermal sclerosis by bleomycin is T cell independent. *J Invest Dermatol* 2001; 117:999–1001.
- 11** Yamamoto T, Nishioka K. Animal model of sclerotic skin. VI: Evaluation of bleomycin-induced skin sclerosis in nude mice. *Arch Dermatol Res* 2004; 295:453–456.
- 12** Yoshizaki A, Iwata Y, Komura K, et al. CD19 regulates skin and lung fibrosis via toll-like receptor signaling in a model of bleomycin-induced scleroderma. *Am J Pathol* 2008; 172:1650–1663.
- 13** Ishikawa H, Takeda K, Okamoto A, et al. Induction of autoimmunity in a bleomycin-induced murine model of experimental systemic sclerosis: an important role for CD4⁺ T cells. *J Invest Dermatol* 2009; 129:1688–1695.
- 14** Yamamoto T, Nishioka K. Cellular and molecular mechanisms of bleomycin-induced murine scleroderma: current update and future perspective. *Exp Dermatol* 2005; 14:81–95.
- 15** Oi M, Yamamoto T, Nishioka K. Increased expression of TGF-beta1 in the sclerotic skin in bleomycin-'susceptible' mouse strains. *J Med Dent Sci* 2004; 51:7–17.
- 16** Takagawa S, Lakos G, Mori Y, et al. Sustained activation of fibroblast transforming growth factor-beta/Smad signaling in a murine model of scleroderma. *J Invest Dermatol* 2003; 121:41–50.
- 17** Bhattacharyya S, Ghosh AK, Pannu J, et al. Fibroblast expression of the coactivator p300 governs the intensity of profibrotic response to transforming growth factor beta. *Arthritis Rheum* 2005; 52:1248–1258.
- 18** Mori Y, Hinchliff M, Wu M, et al. Connective tissue growth factor/CCN2-null mouse embryonic fibroblasts retain intact transforming growth factor-beta responsiveness. *Exp Cell Res* 2008; 314:1094–1104.
- 19** Lakos G, Takagawa S, Chen SJ, et al. Targeted disruption of TGF-beta/Smad3 signaling modulates skin fibrosis in a mouse model of scleroderma. *Am J Pathol* 2004; 168:203–217.
- 20** Hasegawa M, Matsushita Y, Horikawa M, et al. A novel inhibitor of Smad-dependent transcriptional activation suppresses tissue fibrosis in mouse models of systemic sclerosis. *Arthritis Rheum* 2009; 60:3465–3475.
- In this article, the authors use Hsc025, a compound that antagonizes TGF β /Smad signalling, to reduce collagen accumulation in the skin and lung from Tsk-1 mice and bleomycin-treated mice.
- 21** Chen SJ, Ning H, Ishida W, et al. The early-immediate gene EGR-1 is induced by transforming growth factor-beta and mediates stimulation of collagen gene expression. *J Biol Chem* 2006; 281:21183–21197.
- 22** Bhattacharyya S, Wei J, Melichian DS, et al. The transcriptional cofactor Nab2 is induced by TGF-Beta and suppresses fibroblast activation: physiological roles and impaired expression in scleroderma. *PLoS One* 2009; 4:e7620.
- 23** Jakobsson PJ, Thoren S, Morgenstern R, et al. Identification of human prostaglandin E synthase: a microsomal, glutathione-dependent, inducible enzyme, constituting a potential novel drug target. *Proc Natl Acad Sci U S A* 1999; 96:7220–7225.
- 24** Stichtenoth DO, Thoren S, Bian H, et al. Microsomal prostaglandin E synthase is regulated by proinflammatory cytokines and glucocorticoids in primary rheumatoid synovial cells. *J Immunol* 2001; 167:469–474.
- 25** McCann MR, Monemdjou R, Ghassemi-Kakroodi P, et al. mPGES-1 null mice are resistant to bleomycin-induced skin fibrosis. *Arthritis Res Ther* 2011; 13:R6.
- In this research study, the authors show that the expression of mPGES-1 (microsomal prostaglandin E2 synthase-1), an inducible enzyme acting downstream of COX, is required for bleomycin-induced skin fibrogenesis.
- 26** Galindo M, Santiago B, Alcami J, et al. Hypoxia induces expression of the chemokines monocyte chemoattractant protein-1 (MCP-1) and IL-8 in human dermal fibroblasts. *Clin Exp Immunol* 2001; 123:36–41.
- 27** Yamamoto T, Nishioka K. Role of monocyte chemoattractant protein-1 and its receptor, CCR-2, in the pathogenesis of bleomycin-induced scleroderma. *J Invest Dermatol* 2003; 121:510–516.
- 28** Gharaei-Kermani M, Denholm EM, Phan SH. Costimulation of fibroblast collagen and transforming growth factor b1 gene expression by monocyte chemoattractant protein-1 via specific receptors. *J Biol Chem* 1996; 271:17779–17784.
- 29** Ferreira AM, Takagawa S, Fresco R, et al. Diminished induction of skin fibrosis in mice with MCP-1 deficiency. *J Invest Dermatol* 2006; 126:1900–1908.
- 30** Kaplan MH. STAT4: a critical regulator of inflammation in vivo. *Immunol Res* 2005; 31:231–242.
- 31** Dieudé P, Guedj M, Wipff J, et al. STAT4 is a genetic risk factor for systemic sclerosis having additive effects with IRF5 on disease susceptibility and related pulmonary fibrosis. *Arthritis Rheum* 2009; 60:2472–2479.
- 32** Avouac J, Fürnrohr BG, Tomcik M, et al. Inactivation of the transcription factor STAT-4 prevents inflammation-driven fibrosis in animal models of systemic sclerosis. *Arthritis Rheum* 2011; 63:800–809.
- 33** Akhmetshina A, Dees C, Busch N, et al. The cannabinoid receptor CB2 exerts antifibrotic effects in experimental dermal fibrosis. *Arthritis Rheum* 2009; 60:1129–1136.
- 34** Servettsaz A, Kavian N, Nicco C, et al. Targeting the cannabinoid pathway limits the development of fibrosis and autoimmunity in a mouse model of systemic sclerosis. *Am J Pathol* 2010; 177:187–196.
- Using CB1/CB2 nonselective and CB2 selective agonists in the mouse, and CB2 KO-mice, the authors emphasize the role of cannabinoid receptors in the development of systemic fibrosis and autoimmunity.
- 35** Balistreri E, García-Gonzalez E, Selvi E, et al. The cannabinoid WIN55, 212-2 abrogates dermal fibrosis in scleroderma bleomycin model. *Ann Rheum Dis* 2011; 70:695–699.
- 36** Marquart S, Zerr P, Akhmetshina A, et al. Inactivation of the cannabinoid receptor CB1 prevents leukocyte infiltration and experimental fibrosis. *Arthritis Rheum* 2010; 62:3467–3476.
- 37** Postlethwaite AE, Chiang TM. Platelet contributions to the pathogenesis of systemic sclerosis. *Curr Opin Rheumatol* 2007; 19:574–579.
- 38** Dees C, Akhmetshina A, Zerr P, et al. Platelet-derived serotonin links vascular disease and tissue fibrosis. *J Exp Med* 2011; 208:961–972.
- The results from this study suggest that serotonin from platelets induces collagen synthesis by fibroblasts via 5HT(2B) receptors, and that this signalling pathway links vascular damage to tissue remodelling.
- 39** Makhluf HA, Stepienakowska J, Hoffman S, et al. IL-4 upregulates tenascin synthesis in scleroderma and healthy skin fibroblasts. *J Invest Dermatol* 1996; 107:856–859.
- 40** Postlethwaite AE, Holness MA, Katai H, et al. Human fibroblasts synthesize elevated levels of extracellular matrix proteins in response to interleukin 4. *J Clin Invest* 1992; 90:1479–1485.
- 41** Seder RA, Marth T, Sieve MC, et al. Factors involved in the differentiation of TGF-beta-producing cells from naive CD4⁺ T cells: IL-4 and IFN-gamma have opposing effects, while TGF-beta positively regulates its own production. *J Immunol* 1998; 160:5719–5728.
- 42** Needlemann BW, Wigley FM, Stair RW. Interleukin-1, interleukin-2, interleukin-4, interleukin-6, tumor necrosis factor α , and interferon- γ levels in sera from patients with scleroderma. *Arthritis Rheum* 1985; 28:775–780.
- 43** Yamamoto T, Takagawa S, Katayama I, et al. Antisclerotic effect of anti-transforming growth factor β antibody in bleomycin-induced scleroderma. *Clin Immunol* 1999; 92:6–13.
- 44** Matsushita M, Yamamoto T, Nishioka K. Upregulation of interleukin-13 and its receptor in a murine model of bleomycin-induced scleroderma. *Int Arch Allergy Immunol* 2004; 135:348–356.
- 45** Lakos G, Melichian D, Wu M, et al. Increased bleomycin-induced skin fibrosis in mice lacking the Th1-specific transcription factor T-bet. *Pathobiology* 2006; 73:224–237.

- 46** Aliprantis AO, Wang J, Fathman JW, et al. Transcription factor T-bet regulates skin sclerosis through its function in innate immunity and via IL-13. *Proc Natl Acad Sci U S A* 2007; 104:2827–2930.
- 47** Doucet C, Brouty-Boye D, Pottin-Clemeau C, et al. Interleukin (IL) 4 and IL-13 act on human lung fibroblasts. Implication in asthma. *J Clin Invest* 1998; 101:2129–2139.
- 48** Jinnin M, Ihn H, Yamane K, et al. Interleukin-13 stimulates the transcription of the human alpha2(I) collagen gene in human dermal fibroblasts. *J Biol Chem* 2004; 279:41783–41791.
- 49** Doucet C, Brouty-Boye D, Pottin-Clemeau C, et al. IL-4 and IL-13 specifically increase adhesion molecule and inflammatory cytokine expression in human lung fibroblasts. *Int Immunol* 1998; 10:1421–1433.
- 50** Lee CG, Homer RJ, Zhu Z, et al. Interleukin-13 induces tissue fibrosis by selectively stimulating and activating transforming growth factor b1. *J Exp Med* 2001; 194:809–821.
- 51** Sato S, Fujimoto M, Hasegawa M, et al. Altered blood B lymphocyte homeostasis in systemic sclerosis. Expanded naive B cells and diminished but activated memory B cells. *Arthritis Rheum* 2001; 50:918–927.
- 52** Tanaka C, Fujimoto M, Hamaguchi Y, et al. Inducible costimulator ligand • regulates bleomycin-induced lung and skin fibrosis in a mouse model independently of the inducible costimulator/inducible costimulator ligand pathway. *Arthritis Rheum* 2010; 62:1723–1732.
- This study highlights the regulatory role of the ICOS ligand, ICOSL, during the development of bleomycin-induced fibrosis, independently of the ICOS/ICOSL pathway.
- 53** Liu S, Kapoor M, Denton CP, et al. Loss of beta1 integrin in mouse fibroblasts results in resistance to skin scleroderma in a mouse model. *Arthritis Rheum* 2009; 60:2817–2821.
- 54** Yoshizaki A, Yanaba K, Iwata Y, et al. Cell adhesion molecules regulate fibrotic process via Th1/Th2/Th17 cell balance in a bleomycin-induced scleroderma model. *J Immunol* 2010; 185:2502–2515.
- The authors assessed the role of the adhesion molecules L-selectin and ICAM-1 in bleomycin-induced SSc using mice lacking these molecules. Their results show that L-selectin and ICAM-1 regulate Th2 and Th17 cell accumulation in the skin and lung, and the development of fibrosis.
- 55** Yoshizaki A, Yanaba K, Yoshizaki A, et al. Treatment with rapamycin prevents • fibrosis in tight-skin and bleomycin-induced mouse models of systemic sclerosis. *Arthritis Rheum* 2010; 62:2476–2487.
- This study shows that rapamycin, an immunosuppressive drug used for posttransplant immunosuppression and autoimmune diseases, has inhibitory effects on fibrosis in Tsk-induced and bleomycin-induced SSc.
- 56** Ozgen M, Koca SS, Isik A, et al. Methotrexate has no antifibrotic effect in bleomycin-induced experimental scleroderma. *J Rheumatol* 2010; 37:678–679.
- 57** Allanore Y, Borderie D, Lemarechal H, et al. Acute and sustained effects of dihydropyridine-type calcium channel antagonists on oxidative stress in systemic sclerosis. *Am J Med* 2004; 116:595–600.
- 58** Simonini G, Matucci Cerinic M, Generini S, et al. Oxidative stress in systemic sclerosis. *Mol Cell Biochem* 1999; 196:85–91.
- 59** Herrick AL, Matucci Cerinic M. The emerging problem of oxidative stress and the role of antioxidants in systemic sclerosis. *Clin Exp Rheumatol* 2001; 19:4–8.
- 60** Servettaz A, Guilpain P, Gouvestre C, et al. Radical oxygen species production induced by advanced oxidation protein products predicts clinical evolution and response to treatment in systemic sclerosis. *Ann Rheum Dis* 2007; 66:1202–1209.
- 61** Sambo P, Baroni SS, Luchetti M, et al. Oxidative stress in scleroderma: maintenance of scleroderma fibroblast phenotype by the constitutive up-regulation of reactive oxygen species generation through the NADPH oxidase complex pathway. *Arthritis Rheum* 2001; 44:2653–2664.
- 62** Ogawa F, Shimizu K, Muroi E, et al. Serum levels of 8-isoprostane, a marker of oxidative stress, are elevated in patients with systemic sclerosis. *Rheumatology (Oxford)* 2006; 45:815–818.
- 63** Herrick AL, Rieley F, Schofield D, et al. Micronutrient antioxidant status in patients with primary Raynaud's phenomenon and systemic sclerosis. *J Rheumatol* 1994; 21:1477–1483.
- 64** Sambo P, Jannino L, Candela M, et al. Monocytes of patients with systemic sclerosis (scleroderma) spontaneously release in vitro increased amounts of superoxide anion. *J Invest Dermatol* 1999; 112:78–84.
- 65** Svegliati Baroni S, Santillo M, Bevilacqua F, et al. Stimulatory autoantibodies to the PDGF receptor in systemic sclerosis. *N Engl J Med* 2006; 354:2667–2676.
- 66** Casciola-Rosen L, Wigley F, Rosen A. Scleroderma autoantigens are uniquely fragmented by metal-catalyzed oxidation reactions: implications for pathogenesis. *J Exp Med* 1997; 185:71–79.
- 67** Servettaz A, Gouvestre C, Kavian N, et al. Selective oxidation of DNA topoisomerase 1 induced systemic sclerosis in the mouse. *J Immunol* 2009; 182:5855–5864.
- 68** Kavian N, Servettaz A, Mongaret C, et al. Targeting ADAM-17/notch signaling • abrogates the development of systemic sclerosis in a murine model. *Arthritis Rheum* 2010; 62:3477–3487.
- The results of this study show that the Notch pathway is hyperactivated in the skin and lungs from HOCl-induced SSc mice and from SSc patients, and that targeting this signalling pathway could be an effective treatment in the human disease.
- 69** Bellocq A, Azoulay E, Marullo S, et al. Reactive oxygen and nitrogen intermediates increase transforming growth factor-beta1 release from human epithelial alveolar cells through two different mechanisms. *Am J Respir Cell Mol Biol* 1999; 21:128–136.
- 70** Svegliati S, Cancello R, Sambo P, et al. Platelet-derived growth factor and reactive oxygen species (ROS) regulate Ras protein levels in primary human fibroblasts via ERK1/2. *J Biol Chem* 2005; 280:36474–36482.
- 71** Dees C, Zerr P, Tomcik M, et al. Inhibition of Notch signaling prevents experimental fibrosis and induces regression of established fibrosis. *Arthritis Rheum* 2011; 63:1396–1404.
- 72** Davies CD, Jezierska M, Freemont AJ, et al. The differential expression of VEGF, VEGFR-2, and GLUT-1 proteins in disease subtypes of systemic sclerosis. *Hum Pathol* 2006; 37:190–197.
- 73** Distler O, Del Rosso A, Giacomelli R, et al. Angiogenic and angiostatic factors in systemic sclerosis: increased levels of vascular endothelial growth factor are a feature of the earliest disease stages and are associated with the absence of fingertip ulcers. *Arthritis Res* 2002; 4:R11.
- 74** Gay S, Jones JRE, Huang GQ, et al. Immunohistologic demonstration of platelet-derived growth factor (PDGF) and sis-oncogene expression in scleroderma. *J Invest Dermatol* 1989; 92:301–303.

Fibrose et activation de Notch : revue des données récentes

New insights into the mechanism of Notch signalling in fibrosis

Niloufar Kavian¹, Amélie Servettaz², Bernard Weill¹, Frédéric Batteux¹

Article accepté dans The Open Rheumatology Journal

¹ Laboratoire d'immunologie, EA 1833, Université Paris Descartes, Sorbonne Paris-Cité,
Faculté de Médecine, Hôpital Cochin, Assistance Publique-Hôpitaux de Paris (AP-HP).

² Service de Médecine Interne, Maladies Infectieuses, Immunologie Clinique, Faculté de
Médecine de Reims, Hôpital Robert Debré, 51092 Reims cedex, France

Address correspondence to: Dr. Frédéric Batteux, Laboratoire d'Immunologie, UPRES
EA1833, 24, rue du faubourg St Jacques 75679 Paris cedex 14, France. Tel: +33 (0) 1 58 41
21 41; Fax: +33 (0) 1 58 41 20 08; e-mail: frederic.batteux@cch.aphp.fr

Key words: Notch, fibrosis, systemic sclerosis, scleroderma, fibroblasts, epithelial cells,
epithelial-mesenchymal transition, reactive oxygen species

Abbreviations: NICD, Notch Intra-Cellular Domain; EGF, Epidermal Growth Factor; SSc,
systemic sclerosis; ROS,reactive oxygen species; ECM: extracellular matrix; EMT: epithelial-
to-mesenchymal transition; FIZZ-1, found in inflammatory zone

ABSTRACT

The Notch pathway is an evolutionary conserved signalling mechanism that regulates cellular fate and development in various types of cells. The full spectrum of Notch effects has been well studied over the last decade in the fields of development and embryogenesis. But only recently several studies emphasized the involvement of the Notch signalling pathway in fibrosis. This review summarizes the structure and activation of the Notch family members, and focuses on recent findings regarding the role of Notch in organ fibrogenesis, in humans and in animal models.

INTRODUCTION

The treatment of tissue fibrosis is a challenge for the medical community. Indeed, 40 % of the developed world mortality is caused by fibrotic diseases and, to date, no efficient therapy is available. Over the past two years, an increasing number of papers have reported the involvement of new mediators in fibrogenesis, including the Notch-signalling pathway. In the present review, we will first present the Notch family members, their functions and structures. Then, we will focus on the implication of Notch-signalling in fibrosis and develop its role in the development of fibrotic diseases affecting various organs especially in the context of rheumatic diseases.

STRUCTURE, ACTIVATION AND FUNCTIONS OF NOTCH RECEPTORS AND LIGANDS

Notch proteins are single-pass transmembrane receptors with a conserved expression among animal species during evolution. Their principal function is the regulation of many developmental processes, including proliferation, differentiation and apoptosis [1]. Four Notch proteins have been described in mammals (Notch 1 to 4), and they have non-redundant functions during embryogenesis [2].

Structure of Notch receptors and ligands

Notch receptors are located at the cell surface with extracellular and intracellular portions linked in a non-covalent manner (figure 1). The binding of the extracellular portion to its ligand triggers two successive proteolytic cleavages in the receptor. The second cleavage leads to the release of the intracellular portion of the receptor in the cytoplasm and its translocation to the nucleus. The Notch extracellular domain is characterized by numerous EGF-like repeat domains (29 to 36) that are critical for the binding of the ligand [3]. EGF-like repeats are followed by three cystein-rich domains (LIN) that prevent signalling in the

absence of ligation [4]. The intracellular portion of Notch receptors (NICD, Notch Intracellular Domain) contains regions which mediate signal transduction: a RBP-J-associated-molecule (RAM) domain, ankyrin repeats (ANK) which interact with downstream proteins, a transactivation domain (TAD) and a C-terminal PEST (Prolin, Glutamic acid, Serin, Threonin) domain that is pivotal for the stability of the protein. Vertebrates and mammals have four different Notch receptors, that differ mainly in the number of EGF-like repeats and C-terminal sequences located between the ANK and PEST domains.

Notch ligands are transmembrane proteins with a large extracellular portion. They are encoded by genes of the Jagged (JAG1 and JAG2) and Delta-like (DLL1, 3 and 4) families [4]. Each ligand contains EGF-like domains and a “Delta-Serrate-Lag” (DSL) sequence, conserved among *Drosophila melanogaster*, *Caenorhabditis elegans* and vertebrates (figure 1). Depending on the context, the ligand can be produced by a cell from the same lineage as the cell expressing Notch receptor or from a distinct population [5]. Also, ligands can interact with Notch within the same cell (*cis*-interactions), and inhibit Notch signalling [6]. The mechanisms leading to the expression of an active ligand on the cell surface are still not clear, and further molecular studies are needed.

Activation of Notch receptors

The activation of the Notch-signalling pathway requires cell to cell contact. The binding of Notch to one of its ligands triggers an extracellular cleavage by the ADAM17 metalloprotease (also named TACE, for Tumor-necrosis-factor Alpha Converting Enzyme), thus leading to the formation of a membrane-tethered cleaved form of Notch (called NEXT), which is not the active form of the receptor [7]. This first step is followed by a second cleavage achieved by a γ -secretase complex [8]. The Notch cleavage by the γ -secretase enzymatic complex allows the release of the intracellular domain of Notch (NICD), the active form of Notch proteins [9].

The γ -secretase complex is the target of DAPT, a pharmacological inhibitor of the Notch pathway used in several preclinical studies mentioned below. NICD translocates to the nucleus where it induces target genes, that belong mainly to the Hes and Hey family [1, 2]. The release of the intracellular portion of Notch receptors is a key-step in the activation of the Notch pathway because NICD is directly involved in the transcriptional regulation of nuclear target genes, without relying on second messengers or phosphorylation cascades [5]. Not only is the activity of Notch receptors regulated by ligand binding and proteolytic cleavages, it is also regulated through post-transcriptional mechanisms such as glycosylation, endocytosis, , endosomal trafficking and recycling, and ubiquitination [3, 5].

Functions of Notch receptors

Notch-signalling controls the developmental fate and differentiation of cells. Thus, mutations of Notch receptors and ligands in mice lead to dysfunctions in many tissues, including the vascular system and the immune system. In humans, mutations of genes coding for different members of the Notch pathway have been linked to hereditary diseases, including the Alagille syndrome, CADASIL syndrome (Cerebral Autosomal Dominant Arteriopathy with Subcortical Infarcts and Leucoencephalopathy), tetralogy of Fallot, and spondylocostal dysostosis [10, 11]. Moreover, deregulation of Notch signalling can lead to cancer [12]. The involvement of Notch in the development of haematological malignancies, such as T-acute lymphoid leukemia, is now established, and recent studies have reported a role for Notch in solid tumours [11]. Indeed, depending on the cell type and context, Notch can act as a tumor promoter or suppressor [12].

NOTCH AND EPITHELIAL-MESENCHYMAL TRANSITION (EMT)

Epithelial-mesenchymal transition is a process, initially described in early embryogenesis, through which epithelial cells acquire a mesenchymal-like phenotype [13]. Epithelial cells lose their epithelial characteristics, including E-cadherin expression and apical-basal polarity, and reorganize their cytoskeleton to acquire a motile behaviour and the phenotype of myofibroblasts. This dynamic process has been well studied in the embryonic development, but also plays a key role in the genesis of new fibroblasts during the development of organ fibrosis in adult tissues. Indeed, in mature tissues, epithelium can undergo EMT following epithelial stress such as inflammation or wounding, leading to fibroblast proliferation and fibrogenesis [14]. Thus, epithelia contribute to fibrosis by creating new fibroblasts that coexist with resident fibroblasts to produce extracellular matrix in excess.

A large bulk of evidence suggests that EMT is associated with fibrotic diseases such as progressive chronic kidney disease, lung fibrosis and, possibly, liver fibrosis [14, 15]. Recently, several studies have shown that the Notch pathway is involved in the EMT induction process [16, 17]. In 9.5 days old mouse embryos Timmerman and colleagues demonstrated that Notch is critical for the promotion of EMT in the developing heart. In this study, mice with a targeted deletion of Notch1 receptor or its effector RBP-JK-CSL exhibited abnormal maintenance of intracellular endocardial adhesion complexes and abortive endocardial EMT *in vivo* and *in vitro*. In another recent study [17], Aoyagi-Ikeda and colleagues have shown in RLE-6TN cells (rat alveolar epithelial cells) that the activation of the Notch pathway by ectopic expression of NICD or by co-culture of RLE-6TN cells with Jagged-1, induces the expression of α -SMA, a marker of myofibroblasts, type-1 collagen and vimentin. They showed that the Jagged1/Notch signalling pathway induces epithelial-to-mesenchymal transition by interactions with the TGF- β pathway. Indeed, Notch induces the production of TGF- β 1 and the phosphorylation of Smad3 that favours the expression of α -

SMA and leads to EMT. Thus, overexpression of Notch family members can induce EMT and fibrogenesis in various organs.

NOTCH AND FIBROTIC DISEASES

Recently, several papers have suggested that overexpression of Notch signalling may have fibrogenic effects in a wide spectrum of diseases, including scleroderma [18, 19], idiopathic pulmonary fibrosis [20], kidney fibrosis [21], and cardiac fibrosis [22].

Skin fibrosis and systemic sclerosis

In humans, Notch1 is expressed in all epidermal layers. Notch ligands Jagged and Delta-like are also expressed in the epidermis. Notch1 induces the differentiation of keratinocytes through the expression of early markers such as keratin1 and involucrin [23]. Notch1, 2, and 3 are also expressed in the hair follicle and are essential for its homeostasis.

Interestingly, Notch1 is also expressed in skin fibroblasts, and is able to induce the transcription and expression of α -SMA through the activation of FIZZ1 (also known as resistin-like molecule- α , RELM- α , or hypoxia-mediated inducible factor), thus triggering the differentiation of fibroblasts into myofibroblasts.

Systemic sclerosis (SSc) is a connective tissue disease characterized by vascular dysfunction, fibrosis of skin and visceral organs, and immunologic dysregulation associated with the presence of autoantibodies [24]. Although environmental and genetic factors have been incriminated, the mechanisms that are directly implicated in the pathogenesis of the disease are still unclear [25]. Some advances have been made to treat vascular complications, but no

treatment has shown convincing effectiveness to reduce skin and visceral fibrosis. An increasing amount of evidence suggests that the Notch pathway is implicated in the development of the fibrosis that characterizes SSc in both rodent and human [18, 26, 27]. Indeed, Notch1 is activated in the lesional skin of SSc patients and in their fibroblasts [18, 26]. Mice with ROS-induced SSc, bleomycin-induced SSc and Tsk1-mice also display elevated levels of NICD in skin and lungs. This accumulation of NICD is associated with the overactivation of ADAM17 (TACE), a proteinase involved in Notch activation through the first cleavage of the Notch receptor [18]. Moreover, treating mice with DAPT, a γ -secretase inhibitor that blocks the release of NICD, can reduce the collagen content in skin and lungs and the production of autoantibodies, thus preventing the development of SSc in the different mouse models [18, 26, 27]. Similarly, treating SSc-mice with Notch siRNA prevented dermal thickening and fibrosis [27].

The activation of the Notch cascade has major implications on the activation of fibroblasts in SSc. Indeed, the stimulation of SSc fibroblasts with a recombinant Jag-1-Fc chimera results in their differentiation into myofibroblasts expressing high levels of α -SMA and producing high amounts of collagen and ECM [26]. The pharmacological blockade of Notch-signalling with DAPT can also normalize the proliferation rate of dermal fibroblasts extracted from lesional skin. In a wound-healing mouse model, the increase in fibroblast proliferation has been correlated with the activation of the Notch pathway and can be blocked by the treatment of mice with DAPT, showing that Notch-signalling plays important roles in the proliferative properties of fibroblasts [28].

These data emphasize the role of Notch in the fibrotic process observed in SSc in humans and in several animal models.

Several hypotheses can explain the overactivation of Notch1 in SSc. First, reactive oxygen species (ROS) could activate Notch in SSc-fibroblasts. Indeed, the involvement of ROS in the

pathophysiology of SSc [29-33] has been emphasized in a large number of studies, and we have developed a model of murine SSc induced by ROS [34]. In this model, skin fibrosis is induced by intradermal generation of HOCl that oxidizes skin proteins. Among those proteins, oxidized DNA topoisomerase-1 itself can generate an oxidative stress. This stress leads to the stimulation and proliferation of fibroblasts and to the overproduction of collagen and fibrosis. It also involves endothelial cells and is, at least partly, responsible for a vasculopathy. The development of fibrosis is not limited to the skin, because DNA topoisomerase-1 and other oxidized proteins can circulate and determine a systemic fibrosis. Figure 2 describes the hypothetical mechanisms of activation of Notch receptors in ROS-mediated SSc during this process. Intradermal ROS can also induce the synthesis of the metalloprotease ADAM17 [18, 35, 36]. ADAM17 that triggers the first step of Notch activation, that is the shedding of the ectodomain of the receptor. ROS-induced ADAM17 could be a major factor of activation of the Notch pathway in SSc. In addition, the ischemia-reperfusion process can activate HIF-1 α and lead to an increase in Notch1 mRNA levels. In Ras-transformed human fibroblasts, oncogenic Ras activates Notch1-signalling, which is required to maintain the neoplastic phenotype of these cells [37]. In SSc, the hyperproliferative phenotype of fibroblasts has been associated with elevated levels of Ha-Ras and Ki-Ras [38]. Ha-Ras and Ki-Ras could activate the Notch pathway and thus trigger their differentiation into myofibroblasts with elevated proliferative capacities.

Altogether, the data obtained in skin fibroblasts both in vitro and in vivo, demonstrate a pivotal role for Notch-signalling in the development of skin fibrosis especially in patients with SSc.

Pulmonary fibrosis

Progressive primary idiopathic or secondary pulmonary fibrosis as observed in SSc, is a rapidly progressive illness whose pathophysiology remains poorly understood. The histological lesions show fibroblast foci where mesenchymal cells proliferate and produce aberrant levels of ECM. Some studies suggest that TGF- β is involved in the recruitment of the fibroblasts [39]. Active pulmonary fibrosis is characterized by fibroblast proliferation, emergence of myofibroblasts, ECM deposition and tissue remodelling. A recent study on the abnormal differentiation of respiratory epithelial cells in idiopathic pulmonary fibrosis has reported the activation of the Notch pathway in the lung. Hes-1, a Notch target gene, was highly expressed in lung mucus cells from patients with chronic obstructive pulmonary disease, idiopathic pulmonary arterial hypertension and idiopathic pulmonary fibrosis [20]. FIZZ-1 is expressed by airway epithelial cells and alveolar epithelial cells and is endowed with fibrogenic properties [40]. In the lung, TGF- β and FIZZ-1 can induce myofibroblast differentiation and stimulate α -SMA expression in fibroblasts [41]. A study published by Liu and colleagues has shown that the Jagged1/Notch-signalling pathway is upregulated in response to FIZZ-1 and is crucial for the myofibroblast differentiation of lung fibroblasts [42]. Using FX-ko mice that exhibit deficient Notch-signalling in the absence of exogenous fucose supplementation, they showed that Notch is required for the upregulation of α -SMA induced by FIZZ-1. They used the model of bleomycin-induced pulmonary fibrosis to confirm that FIZZ-1 induces and promotes myofibroblast differentiation *in vivo* through Notch-signalling. Pulmonary fibrosis is associated with a TH2 cytokine response modulated in part by Jagged 1/Notch 1 signalling that regulates TH2 differentiation and the transcription of the gene of IL-4 (33). Interestingly, the induction of pro-inflammatory and pro-fibrotic factors (MCP-1, TNF- α , IL-4, TGF- β) was impaired in Notch-deficient mice.

Chronic kidney disease

Renal fibrosis is characterized by the increased deposition of collagen and extracellular matrix, proliferation of myofibroblasts, migration of leukocytes, dysfunctions of epithelial cells and loss of capillaries. During kidney injury, fibroblasts can originate from various sources. Recent experiments have suggested that 15 % of fibroblasts originate from bone-marrow, 35 % from local EMT involving tubular epithelial cells under inflammatory conditions, and the rest results from local proliferation [14]. Several pathways have been implicated in the development of renal fibrosis, and a growing number of data indicate that Notch-signalling plays a key role in its pathogenesis.

During kidney development, Notch1 and Notch2 are expressed but do not play redundant roles [43]. Both receptors are required for proximal tubule and podocyte developments. In mature human and rodent developed kidneys, Notch activity is not detected, indicating that the pathway is mostly silenced once kidney development is complete [44]. The reactivation of this pathway is implicated in various renal disorders in humans and in animal models. Murea and colleagues have shown that elevated levels of Notch ligands and receptors are detected in several glomerular diseases, such as membranous nephropathy, lupus nephritis, crescentic glomerulonephritis and tubulointerstitial fibrosis [44, 45]. A correlation was found between the severity of the tubulointerstitial fibrosis and the expression of cleaved Notch1 in the tubulointerstitium. Concomitantly, another study showed that Notch plays a key role in the development of tubulointerstitial fibrosis in patients and in mouse models [21]. Using pharmacologic and genetic *in vivo* and *in vitro* experiments, the authors demonstrated that the expression of Notch in renal tubular epithelial cells is necessary and sufficient for the development of tubulointerstitial fibrosis. Moreover, genetic deletion of the Notch pathway in these cells reduced renal fibrosis. A previous report had shown that transgenic mice with elevated expression of Notch1 in podocytes develop albuminuria and sclerosis of the glomerule and die by the age of 3 weeks [46].

Taken together, all these data indicate that the Notch pathway plays a key role in kidney fibrosis. Pharmacological inhibition of the Notch pathway could be an important therapeutic strategy for chronic kidney diseases and further studies are needed to determine the effectiveness of such treatments.

Cardiac repair

Notch-signalling plays a central role in heart development. In humans, the Alagille syndrome, an autosomal dominant disorder characterized by congenital heart deficiency with pulmonary artery stenosis, enlarged right ventricle and atrial and ventricular septation defects, is linked to Jag1 and Notch2 mutations [47]. In mice, null mutants for Jag1, Notch1, Notch2 and RBPJK display multiple cardiac defects leading to early embryonic mortality [48]. In the mammalian adult heart, Notch-signalling is downregulated [49]. The mammalian adult heart responds to injury with fibrosis, and recent findings suggest that Notch-signalling is critical for cardiac repair. Increasing Notch1 signalling in mesenchymal-stem cells leads to decreased infarction size and improved cardiac function after myocardial infarction [50]. Furthermore, Russell and colleagues showed that the Notch pathway is activated in epicardial-derived cells and drives their transdifferentiation into fibroblasts after injury, through an EMT process [22]. Finally, these data provide new evidence for a role for Notch in cardiac repair.

CONCLUSION

The Notch pathway, first described for its major role in the development of organisms, is also a key mediator in fibrogenesis as demonstrated by recent studies on skin, lung, kidney and cardiac fibrosis. Further studies are needed, especially *in vivo* and in patients, to determine

whether the inhibition of Notch ligands, receptors or downstream target genes could be effective curative strategies to treat established fibrosis.

REFERENCES

- [1] Artavanis-Tsakonas S, Rand MD, Lake RJ. Notch signaling: cell fate control and signal integration in development. *Science* (New York, NY). 1999 Apr 30;284(5415):770-6.
- [2] Egan SE, St-Pierre B, Leow CC. Notch receptors, partners and regulators: from conserved domains to powerful functions. *Curr Top Microbiol Immunol*. 1998;228:273-324.
- [3] Bray SJ. Notch signalling: a simple pathway becomes complex. *Nature reviews*. 2006 Sep;7(9):678-89.
- [4] Osborne B, Miele L. Notch and the immune system. *Immunity*. 1999 Dec;11(6):653-63.
- [5] Fortini ME. Notch signaling: the core pathway and its posttranslational regulation. *Developmental cell*. 2009 May;16(5):633-47.
- [6] D'Souza B, Miyamoto A, Weinmaster G. The many facets of Notch ligands. *Oncogene*. 2008 Sep 1;27(38):5148-67.
- [7] Brou C, Logeat F, Gupta N, Bessia C, LeBail O, Doedens JR, et al. A novel proteolytic cleavage involved in Notch signaling: the role of the disintegrin-metalloprotease TACE. *Mol Cell*. 2000 Feb;5(2):207-16.
- [8] Okochi M, Steiner H, Fukumori A, Tanii H, Tomita T, Tanaka T, et al. Presenilins mediate a dual intramembranous gamma-secretase cleavage of Notch-1. *Embo J*. 2002 Oct 15;21(20):5408-16.
- [9] Fortini ME. Gamma-secretase-mediated proteolysis in cell-surface-receptor signalling. *Nature reviews*. 2002 Sep;3(9):673-84.
- [10] Gridley T. Notch signaling in vascular development and physiology. *Development*. 2007 Aug;134(15):2709-18.
- [11] Ranganathan P, Weaver KL, Capobianco AJ. Notch signalling in solid tumours: a little bit of everything but not all the time. *Nat Rev Cancer*. 2011 May;11(5):338-51.
- [12] Lobry C, Oh P, Aifantis I. Oncogenic and tumor suppressor functions of Notch in cancer: it's NOTCH what you think. *The Journal of experimental medicine*. 2011 Sep 26;208(10):1931-5.
- [13] Kalluri R, Neilson EG. Epithelial-mesenchymal transition and its implications for fibrosis. *The Journal of clinical investigation*. 2003 Dec;112(12):1776-84.
- [14] Iwano M, Plieth D, Danoff TM, Xue C, Okada H, Neilson EG. Evidence that fibroblasts derive from epithelium during tissue fibrosis. *The Journal of clinical investigation*. 2002 Aug;110(3):341-50.
- [15] Chilosì M, Poletti V, Zamo A, Lestani M, Montagna L, Piccoli P, et al. Aberrant Wnt/beta-catenin pathway activation in idiopathic pulmonary fibrosis. *Am J Pathol*. 2003 May;162(5):1495-502.
- [16] Timmerman LA, Grego-Bessa J, Raya A, Bertran E, Perez-Pomares JM, Diez J, et al. Notch promotes epithelial-mesenchymal transition during cardiac development and oncogenic transformation. *Genes Dev*. 2004 Jan 1;18(1):99-115.
- [17] Aoyagi-Ikeda K, Maeno T, Matsui H, Ueno M, Hara K, Aoki Y, et al. Notch Induces Myofibroblast Differentiation of Alveolar Epithelial Cells via Transforming Growth Factor- β -Smad3 Pathway. *Am J Respir Cell Mol Biol*. 2011 Jul;45(1):136-44.
- [18] Kavian N, Servettaz A, Mongaret C, Wang A, Nicco C, Chéreau C, et al. Targeting ADAM-17/notch signaling abrogates the development of systemic sclerosis in a murine model. *Arthritis and rheumatism*. 2010;62(11):3477-87.
- [19] de Bandt M, Meyer O, Ribard P, Kahn M. Rhumatisme fibroblastique. Une nouvelle observation. *Rev Rhum Mal Osteoartic*. 1992;59:369.

- [20] Plantier L, Crestani B, Wert SE, Dehoux M, Zwey tick B, Guenther A, et al. Ectopic respiratory epithelial cell differentiation in bronchiolised distal airspaces in idiopathic pulmonary fibrosis. *Thorax*. 2011 Aug;66(8):651-7.
- [21] Bielesz B, Sirin Y, Si H, Niranjan T, Gruenwald A, Ahn S, et al. Epithelial Notch signaling regulates interstitial fibrosis development in the kidneys of mice and humans. *The Journal of clinical investigation*. 2010 Nov 1;120(11):4040-54.
- [22] Russell JL, Goetsch SC, Gaiano NR, Hill JA, Olson EN, Schneider JW. A dynamic notch injury response activates epicardium and contributes to fibrosis repair. *Circulation research*. Jan 7;108(1):51-9.
- [23] Okuyama R, Tagami H, Aiba S. Notch signaling: its role in epidermal homeostasis and in the pathogenesis of skin diseases. *Journal of dermatological science*. 2008 Mar;49(3):187-94.
- [24] LeRoy EC, Medsger TAJ. Criteria for the classification of early systemic sclerosis. *J Rheumatol*. 2001 Aug;28(7):1573-6.
- [25] Gabrielli A, Avvedimento EV, Krieg T. Scleroderma. *N Engl J Med*. 2009;360:1989-2003.
- [26] Dees C, Tomcik M, Zerr P, Akhmetshina A, Horn A, Palumbo K, et al. Notch signalling regulates fibroblast activation and collagen release in systemic sclerosis. *Ann Rheum Dis*. 2011 Jul;70(7):1304-10.
- [27] Dees C, Zerr P, Tomcik M, Beyer C, Horn A, Akhmetshina A, et al. Inhibition of Notch signaling prevents experimental fibrosis and induces regression of established fibrosis. *Arthritis Rheum*. 2011;63:1396-404.
- [28] Chigurupati S, Arumugam TV, Gen Son T, Lathia JD, Jameel S, Mughal MR, et al. Involvement of Notch Signaling in Wound Healing. *PLoS ONE*. 2007;2(11):e1167.
- [29] Allanore Y, Borderie D, Lemarechal H, Ekindjian OG, Kahan A. Acute and sustained effects of dihydropyridine-type calcium channel antagonists on oxidative stress in systemic sclerosis. *Am J Med*. 2004 May 1;116(9):595-600.
- [30] Herrick AL, Matucci Cerinic M. The emerging problem of oxidative stress and the role of antioxidants in systemic sclerosis. *Clin Exp Rheumatol*. 2001 Jan-Feb;19(1):4-8.
- [31] Servettaz A, Guilpain P, Goulvestre C, Chereau C, Hercend C, Nicco C, et al. Radical oxygen species production induced by advanced oxidation protein products predicts clinical evolution and response to treatment in systemic sclerosis. *Ann Rheum Dis*. 2007;66(9):1202-9.
- [32] Sambo P, Baroni SS, Luchetti M, Paroncini P, Dusi S, Orlandini G, et al. Oxidative stress in scleroderma: maintenance of scleroderma fibroblast phenotype by the constitutive up-regulation of reactive oxygen species generation through the NADPH oxidase complex pathway. *Arthritis and rheumatism*. 2001 Nov;44(11):2653-64.
- [33] Ogawa F, Shimizu K, Muroi E, Hara T, Hasegawa M, Takehara K, et al. Serum levels of 8-isoprostan e, a marker of oxidative stress, are elevated in patients with systemic sclerosis. *Rheumatology (Oxford)*. 2006;45(7):815-8.
- [34] Servettaz A, Goulvestre C, Kavian N, Nicco C, Guilpain P, Chéreau C, et al. Selective oxidation of DNA topoisomerase 1 induced systemic sclerosis in the mouse. *J Immunol*. 2009;182(9):5855-64.
- [35] Zhang Z, Oliver P, Lancaster JJ, Schwarzenberber OO, Joshi MS, Cork J, et al. Reactive oxygen species mediate tumor necrosis factor alpha-converting, enzyme dependent ectodomain shedding induced by phorbol myristate acetate. *Faseb J*. 2001;15(2):303-5.

- [36] Shao MX, Nadel JA. Dual oxidase 1-dependent MUC5AC mucin expression in cultured human airway epithelial cells. *Proceedings of the National Academy of Sciences of the United States of America*. 2005 Jan 18;102(3):767-72.
- [37] Weijzen S, Rizzo P, Braid M, Vaishnav R, Jonkheer SM, Zlobin A, et al. Activation of Notch-1 signaling maintains the neoplastic phenotype in human Ras-transformed cells. *Nat Med*. 2002 Sep;8(9):979-86.
- [38] Svegliati S, Cancello R, Sambo P, Luchetti M, Paroncini P, Orlandini G, et al. Platelet-derived growth factor and reactive oxygen species (ROS) regulate Ras protein levels in primary human fibroblasts via ERK1/2. *J Biol Chem*. 2005;280:36474-82.
- [39] Gross TJ, Hunninghake GW. Idiopathic pulmonary fibrosis. *The New England journal of medicine*. 2001 Aug 16;345(7):517-25.
- [40] Holcomb IN, Kabakoff RC, Chan B, Baker TW, Gurney A, Henzel W, et al. FIZZ1, a novel cysteine-rich secreted protein associated with pulmonary inflammation, defines a new gene family. *Embo J*. 2000 Aug 1;19(15):4046-55.
- [41] Liu T, Dhanasekaran SM, Jin H, Hu B, Tomlins SA, Chinnaiyan AM, et al. FIZZ1 stimulation of myofibroblast differentiation. *Am J Pathol*. 2004 Apr;164(4):1315-26.
- [42] Liu T, Hu B, Choi YY, Chung M, Ullenhag M, Yu H, et al. Notch1 signaling in FIZZ1 induction of myofibroblast differentiation. *Am J Pathol*. 2009;174:1745-55.
- [43] Sharma S, Sirin Y, Susztak K. The story of Notch and chronic kidney disease. *Curr Opin Nephrol Hypertens*. 2011 Jan;20(1):56-61.
- [44] Niranjan T, Bielez B, Gruenwald A, Ponda MP, Kopp JB, Thomas DB, et al. The Notch pathway in podocytes plays a role in the development of glomerular disease. *Nat Med*. 2008 Mar;14(3):290-8.
- [45] Murea M, Park JK, Sharma S, Kato H, Gruenwald A, Niranjan T, et al. Expression of Notch pathway proteins correlates with albuminuria, glomerulosclerosis, and renal function. *Kidney international*. Sep;78(5):514-22.
- [46] Waters AM, Wu MY, Onay T, Scutaru J, Liu J, Lobe CG, et al. Ectopic notch activation in developing podocytes causes glomerulosclerosis. *J Am Soc Nephrol*. 2008 Jun;19(6):1139-57.
- [47] High FA, Epstein JA. The multifaceted role of Notch in cardiac development and disease. *Nature reviews*. 2008 Jan;9(1):49-61.
- [48] Grego-Bessa J, Luna-Zurita L, del Monte G, Bolos V, Melgar P, Arandilla A, et al. Notch signaling is essential for ventricular chamber development. *Developmental cell*. 2007 Mar;12(3):415-29.
- [49] Colles C, Zentilin L, Sinagra G, Giacca M. Notch1 signaling stimulates proliferation of immature cardiomyocytes. *The Journal of cell biology*. 2008 Oct 6;183(1):117-28.
- [50] Li Y, Hiroi Y, Ngoy S, Okamoto R, Noma K, Wang CY, et al. Notch1 in bone marrow-derived cells mediates cardiac repair after myocardial infarction. *Circulation*. Mar 1;123(8):866-76.

The Organotelluride Catalyst (PHTe)₂NQ Prevents HOCl-Induced Systemic Sclerosis in Mouse

Wioleta K. Marut^{1,4}, Niloufar Kavian^{1,4}, Amélie Servettaz^{1,2}, Carole Nicco¹, Lalla A. Ba³, Mandy Doering³, Christiane Chéreau¹, Claus Jacob³, Bernard Weill¹ and Frédéric Batteux¹

Systemic sclerosis (SSc) is a connective tissue disorder characterized by skin and visceral fibrosis, microvascular damage, and autoimmunity. HOCl-induced mouse SSc is a murine model that mimics the main features of the human disease, especially the activation and hyperproliferation rate of skin fibroblasts. We demonstrate here the efficiency of a tellurium-based catalyst 2,3-bis(phenyltellanyl)naphthoquinone ((PHTe)₂NQ) in the treatment of murine SSc, through its selective cytotoxic effects on activated SSc skin fibroblasts. SSc mice treated with (PHTe)₂NQ displayed a significant decrease in lung and skin fibrosis and in alpha-smooth muscle actin (α -SMA) expression in the skin compared with untreated mouse SSc animals. Serum concentrations of advanced oxidation protein products, nitrate, and anti-DNA topoisomerase I autoantibodies were increased in SSc mice, but were significantly reduced in SSc mice treated with (PHTe)₂NQ. To assess the mechanism of action of (PHTe)₂NQ, the cytotoxic effect of (PHTe)₂NQ was compared in normal fibroblasts and in mouse SSc skin fibroblasts. ROS production is higher in mouse SSc fibroblasts than in normal fibroblasts, and was still increased by (PHTe)₂NQ to reach a lethal threshold and kill mouse SSc fibroblasts. Therefore, the effectiveness of (PHTe)₂NQ in the treatment of mouse SSc seems to be linked to the selective pro-oxidative and cytotoxic effects of (PHTe)₂NQ on hyperproliferative fibroblasts.

Journal of Investigative Dermatology advance online publication, 26 January 2012; doi:10.1038/jid.2011.455

INTRODUCTION

Systemic sclerosis (SSc) is an autoimmune disease of unknown etiology, characterized by fibrosis of the skin and internal organs, vascular dysfunction, and impaired immunity (LeRoy and Medsger, 2001). However, the mechanisms that underlie the clinical manifestations of the disease remain unclear (Gabrielli *et al.*, 2009). Several reports have shown that reactive oxygen species (ROS) are involved in the pathogenesis of SSc (Simonini *et al.*, 1999; Sambo *et al.*, 2001; Allanore *et al.*, 2004; Ogawa *et al.*, 2006; Servettaz *et al.*, 2007; Avouac *et al.*, 2010). Indeed, skin fibroblasts in SSc patients spontaneously produce large amounts of ROS that trigger collagen synthesis (Sambo *et al.*, 1999, 2001). Intradermal injection of specific ROS-generating substances

can reproduce the main features of local and systemic mouse SSc, depending on the type of ROS generated (Servettaz *et al.*, 2009). In addition, anti-PDGFR (Platelet-Derived Growth Factor Receptor) autoantibodies found in SSc patients trigger the production of ROS (Svegliati Baroni *et al.*, 2006). Recently, we have reported that sera from patients with SSc can induce the production of ROS not only by endothelial cells but also by the proliferation of fibroblasts (Servettaz *et al.*, 2007). The release of ROS by fibroblasts and endothelial cells can activate several processes that trigger the development of SSc. In fact, ROS can oxidize specific SSc antigens such as DNA topoisomerase 1 and lead to this autoantigen's breach of tolerance (Casciola-Rosen *et al.*, 1997; Servettaz *et al.*, 2009). The autoimmune phenomenon can be amplified by the inflammatory reaction that results from the overproduction of ROS. This fibrotic process may also be related to the imbalance of the oxidant/antioxidant status in SSc. For instance, *in vitro* studies have shown that ROS triggers the differentiation of fibroblasts into myofibroblasts, either directly or through the activation of the ADAM17/NOTCH pathway (Kavian *et al.*, 2010), and also through the release of transforming growth factor- β from activated cells (Bellocq *et al.*, 1999). Finally, ROS can stimulate the growth of dermal fibroblasts through the activation of the RAS pathway, which explains the hyperproliferative properties of SSc skin fibroblasts (Svegliati *et al.*, 2005). However, if intracellular ROS can stimulate cell growth, they can also induce cell death beyond a certain threshold, as seen in tumor cells (Laurent *et al.*, 2005; Morgan

¹Université Paris Descartes, Sorbonne-Paris-Cité, Faculté de Médecine, EA 1833 et Laboratoire d'Immunologie Biologique, Hôpital Cochin AP-HP, Paris, France; ²Faculté de Médecine de Reims, Service de Médecine Interne, Maladies Infectieuses, Immunologie Clinique, Hôpital Robert Debré, Reims, France and ³Division of Bioorganic Chemistry, School of Pharmacy, Saarland University, Saarbrücken, Germany

⁴These authors contributed equally to this work.

Correspondence: Frédéric Batteux, Laboratoire d'Immunologie, UPRES EA 1833, 8 Rue Méchain 75679 Paris Cedex 14, France.
E-mail: frederic.batteux@cch.aphp.fr

Abbreviations: BSO, buthionine sulfoximine; GSH, glutathione; NO, nitric oxide; (PHTe)₂NQ, 2,3-bis(phenyltellanyl)naphthoquinone; ROS, reactive oxygen species; SSc, systemic sclerosis

Received 20 February 2011; revised 27 October 2011; accepted 29 October 2011

and Liu, 2010; Coriat et al., 2011; Lonkar and Dedon, 2011). Interestingly, some catalytic agents called “sensor/effect” multifunctional redox catalysts can modulate the intracellular redox balance by generating more reactive oxidants or by targeting cysteine residues in proteins. These molecules seem to be particularly effective and selective (Fry and Jacob, 2006). Among the “sensor/effect” multifunctional redox catalyst agents, quinone- and chalcogen (selenium, tellurium)-containing agents have shown an *in vitro* cytotoxic activity against various types of tumor cells (Doering et al., 2010; Coriat et al., 2011; Lilienthal et al., 2011). These observations have prompted us to try these new cytotoxic organotelluride catalysts in the treatment of mouse SSc.

The organotelluride catalyst, 2,3-bis(phenyltellanyl)-naphthoquinone ((PHTe)₂NQ), is a prototypical member of this newly described family (Fry and Jacob, 2006; Shabaan et al., 2009; Ba et al., 2010; Jamier et al., 2010). Within this family of compounds, (PHTe)₂NQ has been the most widely studied compound *in vitro* on tumor cells (Doering et al., 2010; Jamier et al., 2010), and it has also been the only one used *in vivo* on mice (Coriat et al., 2011). Intracellular oxygen radicals and H₂O₂ associate with the quinone moiety of the (PHTe)₂NQ and strongly oxidize cellular thiols in a reaction catalyzed by the tellurium part of the molecule. This reaction significantly increases the intracellular level of ROS. Therefore, cells already overproducing H₂O₂, which are treated with (PHTe)₂NQ, are likely to significantly increase their intracellular concentration of ROS over its cytotoxic level, to ultimately get pushed over a critical “life and death (redox) threshold” (Fry and Jacob, 2006; Mecklenburg et al., 2009). As mouse SSc fibroblasts produce high amounts of H₂O₂, as opposed to normal fibroblasts, we hypothesize that (PHTe)₂NQ could selectively kill disease fibroblasts in murine HOCl-induced SSc (Servettaz et al., 2009) and inhibit the development of the disease.

RESULTS

(PHTe)₂NQ exerted cytotoxic effects on normal and SSc fibroblasts *in vitro*

Fibroblasts from normal mice and from HOCl mice were exposed *in vitro* to increasing amounts of (PHTe)₂NQ (Supplementary data, Supplementary Figure 7 online) to assess the cytotoxic properties of this “sensor/effect” multifunctional redox catalyst agent on those different types of fibroblasts. In the presence of 1 μM (PHTe)₂NQ, the rate of viability of normal fibroblasts was 72% ($P=0.0001$ vs. untreated fibroblasts) and 68% with 4 μM (PHTe)₂NQ ($P=0.0001$ vs. untreated fibroblasts; Figure 1a). (PHTe)₂NQ had a more powerful cytotoxic effect on diseased SSc fibroblasts than on normal fibroblasts. In the presence of 1 μM (PHTe)₂NQ, the rate of viability of SSc fibroblast was 45% ($P=0.0001$ vs. untreated fibroblasts and vs. normal fibroblasts) and 30% with 4 μM (PHTe)₂NQ ($P=0.0001$ vs. untreated fibroblasts and vs. normal fibroblasts; Figure 1a).

(PHTe)₂NQ exerted pro-oxidative effects *in vitro*

The basal production of H₂O₂ was increased by 56% in SSc fibroblasts compared with normal fibroblasts ($P=0.001$).

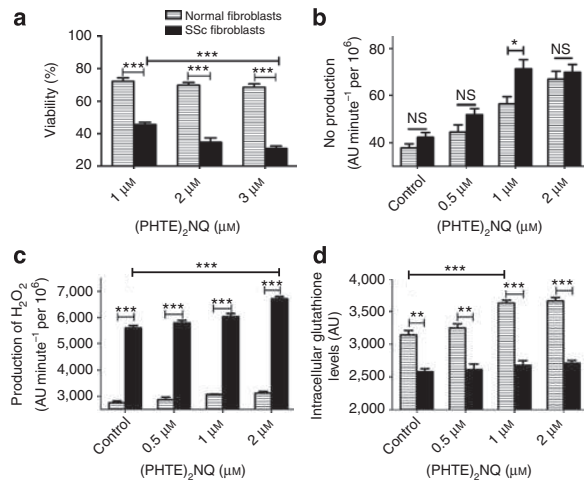


Figure 1. Effects of 2,3-bis(phenyltellanyl)naphthoquinone ((PHTe)₂NQ) on normal and diseased systemic sclerosis (SSc) fibroblasts *in vitro*. Primary skin fibroblasts extracted from three different normal skins (normal fibroblasts) or three different diseased skins (SSc fibroblasts) were tested. (a) Cytotoxic effects of (PHTe)₂NQ on normal and diseased SSc fibroblasts *in vitro*. Cytotoxicity was assayed using the crystal violet method. Results are expressed as the percentage of viable treated cells compared with untreated cells. (b) Production of hydrogen peroxide by fibroblasts incubated with increasing concentrations of (PHTe)₂NQ. H₂O₂ levels were analyzed spectrofluorimetrically using 2',7'-dichlorodihydrofluorescein diacetate (H₂DCFDA). (c) Production of nitric oxide (NO) by fibroblasts incubated with increasing concentrations of (PHTe)₂NQ. NO levels were analyzed spectrofluorimetrically using diaminofluorescein-2 diacetate (DAF-2DA). (d) Intracellular glutathione levels in fibroblasts treated with various concentrations of (PHTe)₂NQ. Glutathione (GSH) levels were analyzed spectrofluorimetrically using monochlorobimane. * $P<0.05$, ** $P<0.01$, and *** $P<0.001$. AU, arbitrary units; NS, not significant.

Production of nitric oxide (NO) was also higher in SSc fibroblasts than in normal fibroblasts ($P=0.01$). Incubation of normal fibroblasts and SSc fibroblasts with increasing amounts of (PHTe)₂NQ dose-dependently increased the production of H₂O₂ ($P=0.009$ and $P=0.001$, respectively) and NO ($P=0.018$ in both cases; Figure 1b and c).

Imbalance of glutathione (GSH) metabolism in fibroblasts

GSH is an essential cofactor of H₂O₂ catabolism. The basal level of GSH was decreased by 22% in SSc fibroblasts compared with normal fibroblasts ($P=0.0032$). The level of intracellular glutathione was higher ($P=0.0001$) in normal fibroblasts following exposure to 1 μM (PHTe)₂NQ than in untreated normal fibroblasts. By contrast, the treatment of diseased SSc fibroblasts with (PHTe)₂NQ failed to increase the level of intracellular glutathione (Figure 1d).

Modulations of H₂O₂ metabolism in SSc fibroblasts

We next investigated the mechanism of action of (PHTe)₂NQ using specific modulators of the enzymatic and nonenzymatic systems involved in H₂O₂ catabolism. Hydrogen peroxide is converted into H₂O by two sets of enzymes, catalase and the GSH/GPx system. The latter uses reduced glutathione as the cofactor. Depleting GSH with buthionine

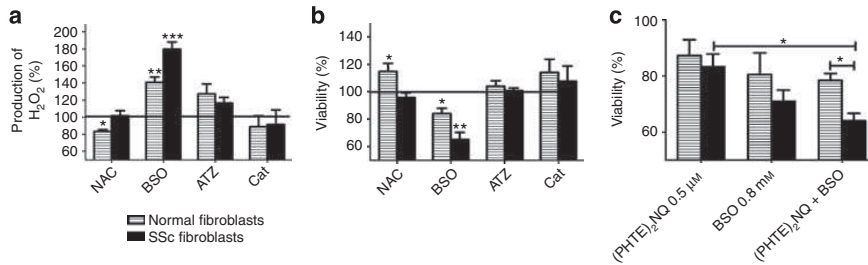


Figure 2. Modulation of H₂O₂ metabolism by 2,3-bis(phenyltellanyl)naphthoquinone ((PHTE)₂NQ) in systemic sclerosis (SSc) fibroblasts. (a) Percentage of H₂O₂ production by treated fibroblasts compared with untreated fibroblasts in the presence of specific modulators of the enzymatic systems involved in reactive oxygen species (ROS) metabolism. The concentrations used were as follows: 3.2 mM N-acetylcysteine (NAC), 0.8 mM buthionine sulfoximine (BSO), 400 μM aminotriazol (ATZ), and 20 U catalase (Cat). (b) Viability of normal and SSc fibroblasts in the presence of 3.2 mM NAC, 0.8 mM BSO, 400 μM ATZ, and 20 U catalase. (c) Cytotoxic effects of (PHTE)₂NQ on normal and diseased SSc fibroblasts *in vitro*. Cytotoxicity was assayed using the crystal violet method. Results are expressed as percentage of viable treated cells compared with untreated cells. *P<0.05, **P<0.01, and ***P<0.0001.

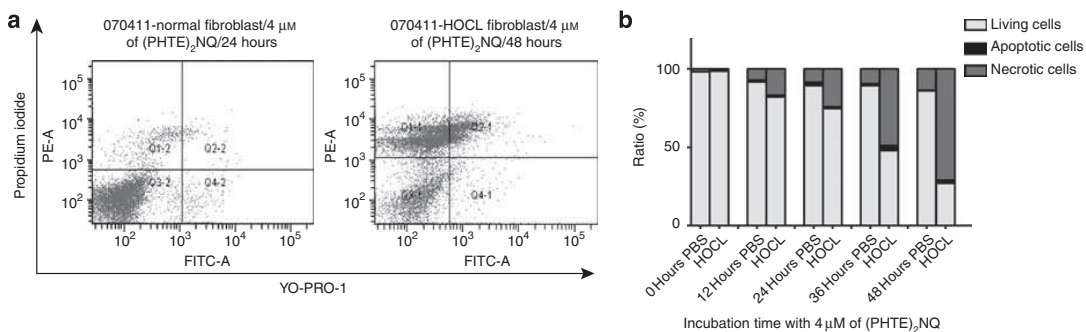


Figure 3. Analysis of cell death by fluorescence-activated cell sorting. Apoptosis/necrosis was analyzed by flow cytometry using the Membrane Permeability/Dead Cell Apoptosis Kit with YO-PRO-1 and propidium iodide (PI) on isolated normal and systemic sclerosis (SSc) fibroblasts treated with 4 μM of 2,3-bis(phenyltellanyl)naphthoquinone ((PHTE)₂NQ) for 48 hours (a). Necrotic cells are PI-positive and YO-PRO-1 positive or negative. Apoptotic cells are PI negative and YO-PRO-1 positive. Viable cells are negative for both dyes. Analysis of cell death is presented over 48 hours (b).

sulfoximine (BSO) significantly increased H₂O₂ production in SSc fibroblasts ($P=0.0007$) and normal fibroblasts ($P=0.0029$; Figure 2a). Moreover, incubation with (PHTE)₂NQ in association with BSO increased H₂O₂ production by 10.9% in normal fibroblasts and by 22% in SSc fibroblasts compared with BSO alone ($P=0.001$, data not shown). By contrast, adding N-acetylcysteine, a precursor of GSH, decreased H₂O₂ production in normal fibroblasts ($P=0.04$) but had no effect on SSc fibroblasts (Figure 2a). On the other hand, specific inhibition of catalase by aminotriazol, or addition of exogenous catalase, had no effect on the levels of H₂O₂ in normal and SSc fibroblasts (Figure 2a). Depleting GSH with BSO significantly decreased the viability of SSc fibroblasts ($P=0.0026$) and normal fibroblasts ($P=0.017$). By contrast, specific inhibition of catalase by aminotriazol had no effect on the viability of normal and SSc fibroblasts (Figure 2b). Moreover, suboptimal doses of BSO and (PHTE)₂NQ worked jointly to kill SSc fibroblasts more efficiently than (PHTE)₂NQ alone ($P=0.0168$) (Figure 2c).

Determination of cell death pathway in normal and SSc fibroblasts

Fibroblasts from normal and HOCl mice were incubated with 1, 2, and 4 μM of (PHTE)₂NQ for 12, 24, 36, or 48 hours. The

highest cytotoxic effect of (PHTE)₂NQ was observed at a concentration of 4 μM. At this concentration, the viability was decreased by 73% for SSc fibroblasts and only by 14.2% for normal fibroblasts ($P=0.001$). A kinetic analysis of cell death between 12 and 48 hours indicated that the (PHTE)₂NQ effects are mainly mediated through a necrotic process (Figure 3).

(PHTE)₂NQ decreased both skin and lung fibrosis in mice with SSc

Clinically, HOCl-induced SSc in mice (HOCl-mice) is associated with an increase in dermal thickness that is significantly reduced by (PHTE)₂NQ ($P=0.0001$ vs. untreated SSc mice; Figure 4a). Histopathological analysis of skin (Figure 4c) and lung (Figure 5a) biopsies stained with hematoxylin and eosin, and lung biopsy stained with Sirius Red (Figure 5c), confirmed the dermal thickness reduction and evidenced a decrease in fibrosis in both tissues (Figures 4c, and 5a, c). (PHTE)₂NQ reduced the accumulation of type I collagen induced by HOCl in the skin compared with untreated mice (Figure 4b). We also investigated the effects of (PHTE)₂NQ in the bleomycin model and found the data to yield results similar to those obtained by the HOCl model in terms of skin fibrosis. However, no lung fibrosis was

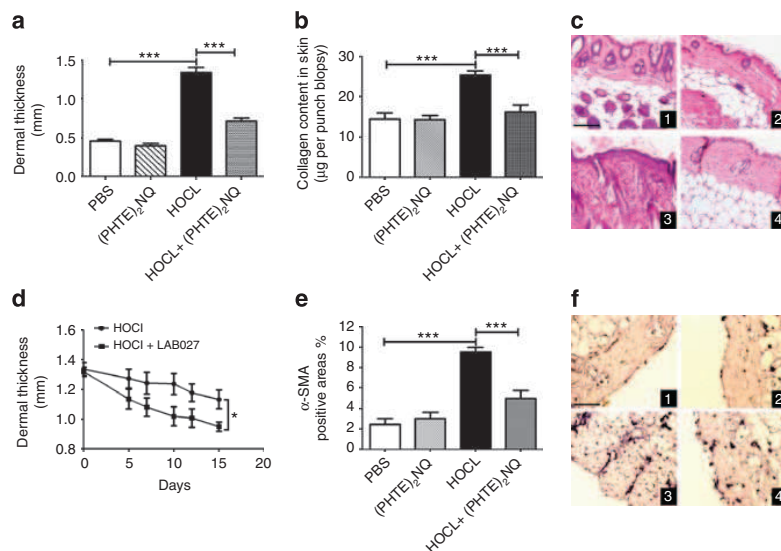


Figure 4. Effect of 2,3-bis(phenyltellanyl)naphthoquinone ((PHTe)₂NQ) on skin fibrosis induced by HOCl in BALB/c mice. Subcutaneous injections of HOCl or phosphate-buffered saline (PBS) were administered every day for 6 weeks in the back of mice, and intravenous injections of (PHTe)₂NQ (10 mg kg⁻¹) were administered once a week for 6 weeks ($n=7$ –10 mice per group as described in the materials and methods section). (a) Dermal thickness, as measured on skin sections in the injected areas of BALB/c mice. (b) Collagen content in 4-mm punch biopsy of skin as assayed by the Sircol method. (c) Representative skin sections comparing dermal fibrosis in the injected areas from BALB/c mice. 1, PBS; 2, (PHTe)₂NQ; 3, HOCl; 4, HOCl+(PHTe)₂NQ. Tissue sections were stained with hematoxylin and eosin. Bar = 100 μm (Olympus DP70 Controller). (d) Curative treatment of SSc mice with (PHTe)₂NQ. (e) Percentage of positive areas for alpha-smooth muscle actin (α-SMA). (f) α-SMA expression in mouse skin by immunohistochemistry. * $P<0.05$ and *** $P<0.001$.

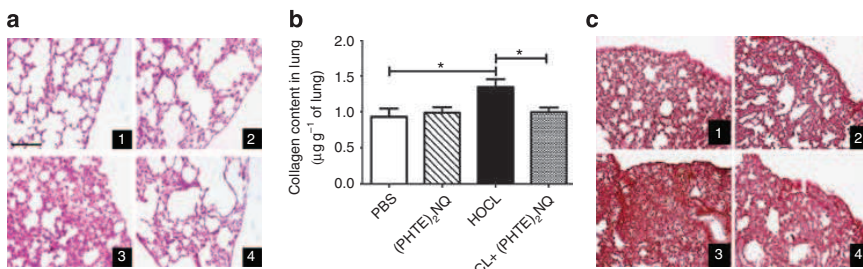


Figure 5. Effect of 2,3-bis(phenyltellanyl)naphthoquinone ((PHTe)₂NQ) on lung fibrosis induced by HOCl in BALB/c mice. Subcutaneous injections of HOCl or phosphate-buffered saline (PBS) were administered every day for 6 weeks in the back of mice, and intravenous injections of (PHTe)₂NQ (10 mg kg⁻¹) were administered once a week for 6 weeks ($n=7$ –10 mice per group as described in the materials and methods section). (a) Representative lung sections from BALB/c mice. 1, PBS; 2, (PHTe)₂NQ; 3, HOCl; 4, HOCl+(PHTe)₂NQ. Tissue sections were stained with H&E. Bar = 100 μm (Olympus DP70 Controller). (b) Collagen content in lung as assayed by the Sircol method. (c) Sirius Red staining for lung sections, 1, PBS; 2, (PHTe)₂NQ; 3, HOCl; 4, HOCl+(PHTe)₂NQ. * $P<0.05$.

observed after 5 weeks of bleomycin injections (Supplementary data, Supplementary Figure 8 online).

Furthermore, alpha-smooth muscle actin (α-SMA) staining in skin sections showed that HOCl-treated SSc animals displayed increased numbers of myofibroblasts ($9.53\% \pm 0.483$ of positive area) compared with phosphate-buffered saline (PBS)-injected mice ($2.46\% \pm 0.555$ of positive area, $P=0.0001$; Figure 4e and f). The number of myofibroblasts was reduced by 47.6% after treating HOCl-mice with (PHTe)₂NQ ($P=0.0005$). (PHTe)₂NQ also reduced the concentration of type I collagen in the lungs of HOCl-mice by 26.7% ($P=0.0106$; Figure 5a and b).

Decrease of dermal thickness in SSc mice through (PHTe)₂NQ curative treatment

(PHTe)₂NQ decreased dermal thickness when administered as a curative treatment. Mice with SSc were treated with (PHTe)₂NQ (10 mg kg⁻¹ of (PHTe)₂NQ), which was administered intravenously once a week for 2 weeks. After 2 weeks, the dermal thickness in treated mice was significantly less than that in the untreated group ($P=0.0151$; Figure 4d).

(PHTe)₂NQ reduced the concentration of serum AOPP and nitrite production

Advanced oxidation protein products (AOPP), a marker of systemic oxidative stress, increased in the sera of HOCl-mice

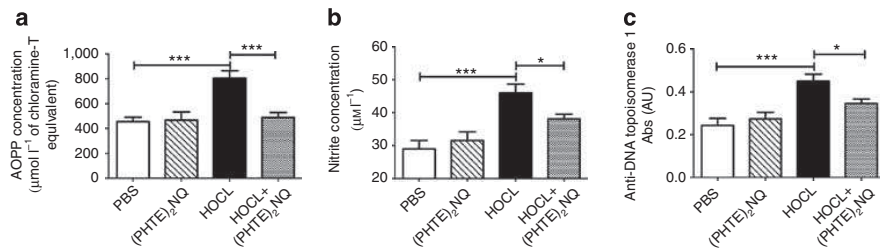


Figure 6. Effect of the organotellurium compound 2,3-bis(phenyltellanyl)naphthoquinone ((PHTe)₂NQ) on advanced oxidation protein products (AOPP) nitrite concentration, and anti-DNA topoisomerase 1 antibodies (Abs) in mice sera. HOCl or PBS was injected subcutaneously every day for 6 weeks in the back of mice. (PHTe)₂NQ (10 mg kg⁻¹) was similarly injected once a week for 6 weeks ($n=7$ –10 mice per group as described in the Materials and Methods section). Sera were collected at the time of sacrifice. (a) Serum concentration of AOPP in the sera of mice. (b) Serum concentration of nitrite in the sera of mice. (c) Levels of serum anti-DNA topoisomerase 1 Abs. Values are means \pm SEM of data gained from all mice in the experimental or control groups. * $P<0.05$ and *** $P<0.001$. AU, arbitrary units; PBS, phosphate-buffered saline.

compared with PBS control mice ($P=0.0001$; Figure 6a). Treatment of HOCl-mice with (PHTe)₂NQ reduced the levels of AOPP by 40%, compared with untreated SSc animals ($P=0.0001$; Figure 6a). The level of nitrite in the sera, a marker of systemic nitrosative stress, increased in HOCl-mice compared with PBS control mice ($P=0.0006$; Figure 6b). Treatment with (PHTe)₂NQ in HOCl mice reduced the levels of serum nitrite by 18% compared with untreated SSc mice ($P=0.039$; Figure 6b).

(PHTe)₂NQ reduced serum concentration of anti-DNA topoisomerase 1 Abs

The sera of HOCl mice contained significantly higher amounts of DNA topoisomerase I Abs than the sera of mice treated with PBS ($P=0.0008$). The level of anti-DNA topoisomerase I Abs significantly reduced in HOCl mice treated with (PHTe)₂NQ compared with untreated HOCl mice ($P=0.04$; Figure 6c).

DISCUSSION

In this report, inspired by recent results obtained—by us and others—in cancer therapy using selective pro-oxidative molecules, we demonstrated that organotelluride catalysts can combine with endogenous oxidative species generated “naturally” in mouse SSc fibroblasts to selectively kill cells through a necrotic process.

Primary fibroblasts extracted from diseased skin areas display an elevated basal level of ROS, which is amplified by (PHTe)₂NQ to generate a lethal oxidative burst in contrast with healthy fibroblasts that display a normal level of endogenous ROS and resist the action of (PHTe)₂NQ. The cytotoxic effects of ROS result from an imbalance between their rate of production and the activity of various detoxification systems (Laurent *et al.*, 2005). Indeed, in SSc fibroblasts, the level of GSH is low and is not modified by (PHTe)₂NQ, whereas in normal fibroblasts this level is higher and is raised by (PHTe)₂NQ. Thus, when normal fibroblasts are exposed to (PHTe)₂NQ, the pro-oxidative activity of the compound is counterbalanced by the rise of GSH and no oxidative stress can be induced. In contrast, in diseased fibroblasts, (PHTe)₂NQ induces a huge increase in ROS that is not counterbalanced by the low level of induced GSH, and

thus reaches a lethal threshold. Because the level of endogenous ROS in SSc fibroblasts is close to that threshold, exposure to ROS-generating, redox-modulating agents, such as (PHTe)₂NQ, enhances the rate of cell death. As normal fibroblasts are not targeted by (PHTe)₂NQ, this information could have important clinical implications (Amstad *et al.*, 1991; Rodriguez *et al.*, 2000; Hussain *et al.*, 2004; Laurent *et al.*, 2005).

The depletion of GSH by BSO, and the consecutive increase of (PHTe)₂NQ toxicity in SSc and normal fibroblasts, confirms the role of the GSH pathway in mediating the cytotoxic effects of (PHTe)₂NQ. In contrast, blocking the catalase pathway or adding polyethylene glycol catalase showed that this pathway has no effect on cell survival, regardless of the considered cell type. Thus, H₂O₂-mediated (PHTe)₂NQ toxicity is controlled by the glutathione pathway and not by the catalase pathway, as already observed with several cytotoxic molecules (Jing *et al.*, 1999; Hussain *et al.*, 2004; Laurent *et al.*, 2005; Alexandre *et al.*, 2006). These findings are significant, as they seem to identify disturbances in the GSH household (and subsequent increases in ROS levels), rather than ROS generation *per se*, as the prime activity of such redox modulating agents.

In SSc, local oxidative stress is associated with a systemic oxidative state, as demonstrated by the significant increase in the serum concentrations of advanced oxidation protein products, and of nitrite, in HOCl-treated SSc mice that are compared with PBS-injected animals. Therefore, (PHTe)₂NQ induces a lethal oxidative burst in cells with increased levels of intracellular ROS, but it is not a systemic pro-oxidative molecule, as already observed in various cancer models (Fry and Jacob, 2006; Doering *et al.*, 2010; Coriat *et al.*, 2011). Several reports have linked the intracellular oxidative burst and the initiation of the immune response in human or murine models of SSc (Simonini *et al.*, 1999; Harðardo *et al.*, 2010). Indeed, local generation of HOCl or hydroxyl radicals triggers the production of anti-DNA-topoisomerase 1 auto-antibodies; consequently, the generation of peroxynitrite triggers the production of anti-centromeric protein B Abs. The mechanism through which the breach of tolerance to DNA topoisomerase 1 occurs, following exposure to HOCl or

hydroxyl radicals, is related to the oxidation and cleavage of DNA topoisomerase 1 within the cells (Servettaz *et al.*, 2009). The selective destruction of diseased fibroblasts that chronically produce high levels of intracellular ROS by (PHTe)₂NQ probably explains the decreased concentration of circulating oxidized proteins in the sera, and especially of oxidized DNA topoisomerase 1 anti-DNA-topoisomerase 1 Abs. Furthermore, oxidized topoisomerase 1 exerts a proproliferative effect on fibroblasts and increases the intracellular level of H₂O₂ in fibroblasts and endothelial cells. The decrease of circulating oxidized proteins linked to the selective destruction of diseased fibroblasts also explains the decrease in fibroblast proliferation.

One of the major consequences of oxidative stress in diseased fibroblasts is their transformation into myofibroblasts and their increased production of type I collagen (Sambo *et al.*, 2001; Toulec *et al.*, 2010). As for autoantibodies and fibroblast proliferation, the selective destruction of diseased mouse SSc fibroblasts by (PHTe)₂NQ is followed by a decrease in the number of myofibroblasts. These phenomena were associated with the inhibition of the development of mouse SSc because they were correlated with a decrease in the concentration of type I collagen in the skin of treated animals.

Altogether, our results show that the organotelluride catalyst (PHTe)₂NQ can interact with intracellular ROS generated in SSc fibroblasts to selectively kill the cells. This observation suggests a new therapeutic strategy in SSc, based on the modulation of the intracellular redox state of activated fibroblasts. Indeed, new molecules, such as (PHTe)₂NQ, could help selectively eliminate the activated cells responsible for the development of skin and visceral fibrosis and, indirectly, be used for autoimmunity. Preliminary data suggest that the molecule is not only efficient as a preventive treatment, but also as a curative treatment of SSc.

MATERIALS AND METHODS

Animals and chemicals

Specific pathogen-free, 6-week-old female BALB/c mice were used in all experiments (Harlan, Gannat, France). All mice were housed in autoclaved ventilated cages with sterile food and water *ad libitum*. They were given humane care according to the guidelines of our institution. HOCl was administered as previously described (Servettaz *et al.*, 2009). Briefly, 300 µl of HOCl was injected subcutaneously into the back of the mice 5 days per week for 6 weeks. One week after the end of the injections, the animals were killed by cervical dislocation. Serum and tissue samples were collected from each mouse and stored at -80°C until use or fixed in 10% acetic acid formol for histopathological analysis. For (PHTe)₂NQ administration, BALB/c mice treated with HOCl (*n*=10) or not treated (*n*=7) were injected intravenously with (PHTe)₂NQ (10 mg kg⁻¹ per injection diluted in PBS once per week for 6 weeks). As the control group, BALB/c mice treated with HOCl (*n*=10) and those that were not (*n*=7) were injected intravenously with sterilized PBS once per week for 6 weeks.

All cells were cultured as reported previously (Servettaz *et al.*, 2009). All chemicals were from Sigma-Aldrich (Saint Quentin Fallavier, France), except when specified. The detailed synthesis of (PHTe)₂NQ appears in Supplementary data online.

Isolation of fibroblasts from the skin of mice

HOCl or PBS was injected in the same skin area in all mice. Skin samples were then collected from that area for experimental purposes. The samples were digested with "Liver Digest Medium" (Invitrogen Life Technologies, Grand Island, NY) for 1 hour at 37°C. After three washes in complete medium, cells were seeded into sterile flasks, and isolated fibroblasts were cultured in DMEM/Glutamax-I supplemented with 10% heat-inactivated fetal calf serum and antibiotics, at 37°C in a humidified atmosphere containing 5% CO₂.

Viability assays

Isolated normal and SSc fibroblasts (4 × 10³ cells per well; Costar, Corning, NY) were incubated in 96-well plates with complete medium alone, or with 1, 2, or 4 µM of (PHTe)₂NQ for 48 hours at 37°C. The number of viable cells was evaluated by the crystal violet assay. In brief, cells were stained in 0.5% crystal violet and 30% ethanol in PBS for 30 minutes at room temperature. After two washes in PBS, the stain was dissolved in 50% ethanol and absorbance was measured at 560 nm on a microplate reader (Fusion, PerkinElmer, Wellesley, MA). Results are expressed as percentage of viable treated cells compared with untreated cells.

H₂O₂ and NO production, and levels of intracellular reduced glutathione

Isolated normal and SSc fibroblasts (2 × 10⁴ cells per well) were seeded in 96-well plates (Costar) and incubated for 24 hours at 37°C with either medium alone or with 0.5, 1, or 2 µM of (PHTe)₂NQ. Levels of H₂O₂ and NO were assessed spectrofluorometrically (Fusion, PerkinElmer) using 2',7'-dichlorodihydrofluorescein diacetate and diaminofluorescein-2 diacetate, respectively.

Cells were incubated with 200 µM of 2',7'-dichlorodihydrofluorescein diacetate or 200 µM diaminofluorescein-2 diacetate in PBS for 1 hour at 37°C. The excitation and emission wavelengths used were 490 and 535 nm for 2',7'-dichlorodihydrofluorescein diacetate and 485 and 530 nm for diaminofluorescein-2 diacetate, respectively.

The levels of intracellular glutathione were assessed spectrofluorometrically using monochlorobimane staining. Cells were then washed and incubated with 50 µM monochlorobimane for 15 minutes at 37°C. The fluorescence intensity was measured with excitation and emission wavelengths of 380 and 485 nm, respectively. The intracellular H₂O₂ and NO levels, and the intracellular glutathione level, were expressed as arbitrary units of fluorescence intensity normalized by the number of viable cells. The number of viable cells at the end of the experiments was evaluated by the crystal violet assay as described above.

Analysis of ROS metabolism of normal and SSc fibroblasts

Isolated normal or SSc fibroblasts (2 × 10⁴ cells per well) were seeded in 96-well plates and incubated for 24 hours in complete medium alone or with the following molecules: 3.2 mM N-acetylcysteine, 1.6 mM BSO, 400 µM aminotriazol, or 20 U polyethylene glycol catalase. Cells were then washed three times with PBS and incubated with 100 µl per well of 200 µM 2',7'-dichlorodihydrofluorescein diacetate for 30 minutes. Fluorescence intensity was read as described above. Intracellular H₂O₂ levels were also expressed as described above.

Synergistic effect of BSO and (PHTe)₂NQ on normal and SSc fibroblasts

Isolated normal or SSc fibroblasts (2×10^4 cells per well) were seeded in 96-well plates and incubated for 24 hours in complete medium alone or with the following molecules: 0.8 mM BSO and 0.5 μ M (PHTe)₂NQ, alone or in association. The number of viable cells at the end of the experiments was evaluated by the crystal violet assay as described above.

Analysis of cell death by fluorescence-activated cell sorting

Cell death was analyzed by fluorescence-activated cell sorting (FACS)Canto II flow cytometer (Becton Dickinson, Franklin Lakes, NJ), using the Membrane Permeability/Dead Cell Apoptosis Kit with YO-PRO-1 and propidium iodide for flow cytometry (Invitrogen), under the manufacturer's recommendations. Briefly, 1.2×10^4 normal or SSc fibroblasts isolated from the skin were incubated with 1, 2, or 4 μ M (PHTe)₂NQ for 12, 24, 36, or 48 hours. After the incubation period, the cells were collected, washed twice with PBS, stained on ice for 10 minutes with 1.5 μ M propidium iodide and 0.1 μ M YO-PRO-1, and analyzed by flow cytometry.

Dermal thickness

Skin thickness was measured 1 day before killing using a calliper and was expressed in millimeters (Servettaz *et al.*, 2010).

Collagen content in skin and lung

Skin was taken from the back region of mice with a punch (6 mm of diameter), and lung pieces from each mouse were diced using a sharp scalpel and then put into aseptic tubes, thawed, and mixed with pepsin (1:10 weight ratio) and 0.5 M acetic acid. Collagen content was assayed using the quantitative dye-binding Sircol method (Biocolor, Belfast, N. Ireland; Burdick *et al.*, 2005). The concentration values were read at 540 nm on a microplate reader (Fusion, PerkinElmer) versus a standard range of bovine collagen type I concentrations (supplied as a sterile solution in 0.5 M acetic acid).

Curative treatment

BALB/c mice were injected subcutaneously with 300 μ l HOCl 5 days per week for 5 weeks to induce mouse SSc. SSc mice were then distributed randomly into two groups. The experimental group of treated mice ($n=5$) received 10 mg kg⁻¹ of (PHTe)₂NQ administered intravenously once a week for 2 weeks. The control group ($n=5$) received intravenous saline. Dermal thickness in SSc mice was measured after 2 weeks of treatment with (PHTe)₂NQ.

Histopathological analysis

Fixed lung and skin pieces were embedded in paraffin. A 5- μ m-thick tissue section was prepared from the mid-portion of the paraffin-embedded tissue and stained with either hematoxylin/eosin or Sirius red. Slides were examined by a pathologist blinded to the animal group assignment, via standard bright-field microscopy (Olympus BX60, Tokyo, Japan).

Analysis of α -SMA expression in mouse skin

Expression of α -SMA in mouse skin was analyzed by immunohistochemistry. Tissue sections were dewaxed and then incubated with

200 mg ml⁻¹ proteinase K for 15 minutes at 37°C for antigen retrieval. Specimens were then treated with 3% hydrogen peroxide for 20 minutes at 37°C to inhibit endogenous peroxidases, and then blocked with 5% BSA for 30 minutes at 4°C. Sections were incubated with a 1:100 dilution of a monoclonal anti- α -SMA, alkaline phosphatase-conjugated Ab (Sigma-Aldrich). Antibody binding was visualized using Nitro blue tetrazolium chloride/5-bromo-4-chloro-3-indolyl phosphate (NBT/BCIP). The slides were examined by standard bright-field microscopy (Olympus BX60). Appropriate controls with irrelevant alkaline phosphatase-conjugated Ab were performed.

Determination of AOPP concentrations in sera

AOPP was measured by spectrophotometry as previously described (Servettaz *et al.*, 2009). Calibration used chloramine-T within the range of 0–100 μ mol l⁻¹. AOPP concentrations were expressed as μ mol l⁻¹ of chloramine-T equivalents.

Quantification of nitrite in mouse sera

The concentration of nitrite was determined in sera by a spectrophotometric assay using oxidation catalyzed by cadmium metal (Oxis, Portland, OR), which converts nitrate into nitrite. The total determined nitrite corresponds to NO production. The detection threshold for nitrite was 0.1 μ mol l⁻¹ (Sastry *et al.*, 2002).

Detection of serum autoantibody

Serum anti-DNA topoisomerase 1 IgG Abs were assayed by ELISA using purified calf thymus DNA topoisomerase 1 bound to the wells of a microtiter plate (Immunovision, Miami, FL). Plates were blocked with PBS-1% BSA, and 100 μ l of 1:20 mouse serum was added and allowed to react for 1 hour at room temperature. Bound Abs was detected with alkaline phosphatase-conjugated goat anti-mouse IgG Ab, and the reaction was developed by adding *p*-nitrophenyl phosphate. Optical density was measured at 405 nm using a Dynatech MR 5000 microplate reader (Dynex Technology, Chantilly, VA).

Statistical analysis

All quantitative data were expressed as means \pm SEM. Data were compared using the Mann-Whitney nonparametric test or Student's *t*-paired test.

CONFLICT OF INTEREST

The authors state no conflict of interest.

ACKNOWLEDGMENTS

This work was supported by the European Community's Seventh Framework Programme (FP7/2007-2013) under grant agreement 215009 RedCat for financial support.

SUPPLEMENTARY MATERIAL

Supplementary material is linked to the online version of the paper at <http://www.nature.com/jid>

REFERENCES

Alexandre J, Batteux F, Nicco C *et al.* (2006) Accumulation of hydrogen peroxide is an early and crucial step for paclitaxel-induced cancer cell death both *in vitro* and *in vivo*. *Int J Cancer* 119:41–8

- Allanore Y, Borderie D, Lemarechal H et al. (2004) Acute and sustained effects of dihydropyridine-type calcium channel antagonists on oxidative stress in systemic sclerosis. *Am J Med* 116:595–600
- Amstad P, Peskin A, Shah G et al. (1991) The balance between Cu,Zn-superoxide dismutase and catalase affects the sensitivity of mouse epidermal cells to oxidative stress. *Biochemistry* 30:9305–13
- Avouac J, Borderie D, Ekindjian OG et al. (2010) High DNA oxidative damage in systemic sclerosis. *J Rheumatol* 37:2540–7
- Ba LA, Doering M, Jamier V et al. (2010) Tellurium: an element with great biological potency and potential. *Org Biomol Chem* 8:4203–16
- Bellocq A, Azoulay E, Marullo S et al. (1999) Reactive oxygen and nitrogen intermediates increase transforming growth factor-beta1 release from human epithelial alveolar cells through two different mechanisms. *Am J Respir Cell Mol Biol* 21:128–36
- Burdick MD, Murray LA, Keane MP et al. (2005) CXCL11 attenuates bleomycin-induced pulmonary fibrosis via inhibition of vascular remodeling. *Am J Respir Crit Care Med* 171:261–8
- Casciola-Rosen L, Wigley F, Rosen A (1997) Scleroderma autoantigens are uniquely fragmented by metal-catalyzed oxidation reactions: implications for pathogenesis. *J Exp Med* 185:71–9
- Coriat R, Marut W, Leconte M et al. (2011) The organotelluride catalyst LAB027 prevents colon cancer growth in the mice. *Cell Death Dis* 2:e191
- Doering M, Ba LA, Lilienthal N (2010) Synthesis and selective anticancer activity of organochalcogen based redox catalysts. *J Med Chem* 14:6954–63
- Fry FH, Jacob C (2006) Sensor/effectector drug design with potential relevance to cancer. *Curr Pharm Des* 12:4479–99
- Gabrielli A, Avvedimento EV, Krieg TN (2009) Scleroderma. *Engl J Med* 360:1989–2003
- Harðardóttir H, Helvoort H, Vonk MC et al. (2010) Exercise in systemic sclerosis intensifies systemic inflammation and oxidative stress. *Scand J Rheumatol* 39:63–70
- Hussain SP, Amstad P, He P et al. (2004) p53-induced up-regulation of MnSOD and GPx but not catalase increases oxidative stress and apoptosis. *Cancer Res* 64:2350–6
- Jamier V, Ba LA, Jacob C (2010) Selenium- and tellurium-containing multifunctional redox agents as biochemical redox modulators with selective cytotoxicity. *Chemistry* 16:10920–8
- Jing Y, Dai J, Chalmers-Redman RM et al. (1999) Arsenic trioxide selectively induces acute promyelocytic leukemia cell apoptosis via a hydrogen peroxide-dependent pathway. *Blood* 94:2102–11
- Kavian N, Servettaz A, Mongaret C et al. (2010) Targeting ADAM-17/notch signaling abrogates the development of systemic sclerosis in a murine model. *Arthritis Rheum* 62:3477–87
- Laurent A, Nicco C, Chéreau C et al. (2005) Controlling tumor growth by modulating endogenous production of reactive oxygen species. *Cancer Res* 65:948–56
- LeRoy EC, Medsger TAJ (2001) Criteria for the classification of early systemic sclerosis. *J Rheumatol* 28:1573–6
- Lilienthal N, Prinz C, Peer-Zada AA et al. (2011) Targeting the disturbed redox equilibrium in chronic lymphocytic leukemia by novel reactive oxygen species-catalytic “sensor/effect” compounds. *Leuk Lymphoma* 52:1407–11
- Lonkar P, Dedon PC (2011) Reactive species and DNA damage in chronic inflammation: reconciling chemical mechanisms and biological fates. *Int J Cancer* 128:1999–2009
- Mecklenburg S, Shaaban S, Ba LA et al. (2009) Exploring synthetic avenues for the effective synthesis of selenium- and tellurium-containing multifunctional redox agents. *Org Biomol Chem* 7:4753–62
- Morgan MJ, Liu ZG (2010) Reactive oxygen species in TNF alpha-induced signaling and cell death. *Mol Cells* 30:1–12
- Ogawa F, Shimizu K, Muroi E et al. (2006) Serum levels of 8-isoprostane, a marker of oxidative stress, are elevated in patients with systemic sclerosis. *Rheumatology (Oxford)* 45:815–58
- Rodriguez AM, Carrico PM, Mazurkiewicz JE et al. (2000) Mitochondrial or cytosolic catalase reverses the MnSOD-dependent inhibition of proliferation by enhancing respiratory chain activity, net ATP production, and decreasing the steady state levels of H₂O₂. *Free Radic Biol Med* 29:801–13
- Sambo P, Baroni SS, Luchetti M et al. (2001) Oxidative stress in scleroderma: maintenance of scleroderma fibroblast phenotype by the constitutive up regulation of reactive oxygen species generation through the NADPH oxidase complex pathway. *Arthritis Rheum* 44:2653–64
- Sambo P, Jannino L, Candela M et al. (1999) Monocytes of patients with systemic sclerosis (scleroderma) spontaneously release *in vitro* increased amounts of superoxide anion. *J Invest Dermatol* 112:78–84
- Sastray KV, Moudgal RP, Mohan J et al. (2002) Spectrophotometric determination of serum nitrite and nitrate by copper-cadmium alloy. *Anal Biochem* 306:79–82
- Servettaz A, Goulvestre C, Kavian N et al. (2009) Selective oxidation of DNA topoisomerase 1 induces systemic sclerosis in the mouse. *J Immunol* 182:5855–64
- Servettaz A, Guilpain P, Goulvestre C et al. (2007) Radical oxygen species production induced by advanced oxidation protein products predicts clinical evolution and response to treatment in systemic sclerosis. *Ann Rheum Dis* 66:1202–29
- Servettaz A, Kavian N, Nicco C et al. (2010) Targeting the cannabinoid pathway limits the development of fibrosis and autoimmunity in a mouse model of systemic sclerosis. *Am J Pathol* 177:187–96
- Shabaan S, Ba LA, Abbas M et al. (2009) Multicomponent reactions for the synthesis of multifunctional agents with activity against cancer cells. *Chem Commun* 31:4702–24
- Simonini G, Cerinic MM, Generini S et al. (1999) Oxidative stress in systemic sclerosis. *Mol Cell Biochem* 196:85–91
- Svegliati Baroni S, Santillo M, Bevilacqua F et al. (2006) Stimulatory autoantibodies to the PDGF receptor in systemic sclerosis. *N Engl J Med* 354:2667–76
- Svegliati S, Cancello R, Sambo P et al. (2005) Platelet-derived growth factor and reactive oxygen species (ROS) regulate ras protein levels in primary human fibroblasts via ERK1/2. *J Biol Chem* 280:36474–82
- Toullec A, Gerald D, Despouy G et al. (2010) Oxidative stress promotes myofibroblast differentiation and tumour spreading. *EMBO Mol Med* 2:211–30

Bibliographie

- [1] Armando Gabrielli, Enrico V Avvedimento and Thomas Krieg. Scleroderma. *N Engl J Med*, 360(19):1989-2003, 2009.
- [2] E C LeRoy and T A Medsger Jr. Criteria for the classification of early systemic sclerosis. *J Rheumatol*, 28(7):1573-6, 2001.
- [3] C Lunardi, C Bason, R Navone, E Millo and G Damonte et al.. Systemic sclerosis immunoglobulin g autoantibodies bind the human cytomegalovirus late protein ul94 and induce apoptosis in human endothelial cells. *Nat Med*, 6(10):1183-6, 2000.
- [4] P J Nietert and R M Silver. Systemic sclerosis: environmental and occupational risk factors. *Curr Opin Rheumatol*, 12(6):520-6, 2000.
- [5] G Simonini, M M Cerinic, S Generini, M Zoppi and M Anichini et al.. Oxidative stress in systemic sclerosis. *Mol Cell Biochem*, 196(1-2):85-91, 1999.
- [6] A L Herrick and M Matucci Cerinic. The emerging problem of oxidative stress and the role of antioxidants in systemic sclerosis. *Clin Exp Rheumatol*, 19(1):4-8, 2001.
- [7] P Sambo, S S Baroni, M Luchetti, P Paroncini and S Dusi et al.. Oxidative stress in scleroderma: maintenance of scleroderma fibroblast phenotype by the constitutive up-regulation of reactive oxygen species generation through the nadph oxidase complex pathway. *Arthritis Rheum*, 44(11):2653-64, 2001.
- [8] P Sambo, L Jannino, M Candela, A Salvi and M Donini et al.. Monocytes of patients with systemic sclerosis (scleroderma) spontaneously release in vitro increased amounts of superoxide anion. *J Invest Dermatol*, 112(1):78-84, 1999.
- [9] A L Herrick, F Rieley, D Schofield, S Hollis and J M Braganza et al.. Micronutrient antioxidant status in patients with primary raynaud's phenomenon and systemic sclerosis. *J Rheumatol*, 21(8):1477-83, 1994.
- [10] H Ihn, K Yamane, M Kubo and K Tamaki. Blockade of endogenous transforming growth factor beta signaling prevents up-regulated collagen synthesis in scleroderma fibroblasts: association with increased expression of transforming growth factor beta receptors. *Arthritis Rheum*, 44(2):474-80, 2001.
- [11] Eugene Y Kissin, Raphael Lemaire, Joseph H Korn and Robert Lafyatis. Transforming growth factor beta induces fibroblast fibrillin-1 matrix formation. *Arthritis Rheum*, 46(11):3000-9, 2002.
- [12] G C Blobel, W P Schiemann and H F Lodish. Role of transforming growth factor beta in human disease. *N Engl J Med*, 342(18):1350-8, 2000.

- [13] Aristidis Moustakas and Carl-Henrik Heldin. Non-smad tgf-beta signals. *J Cell Sci*, 118(Pt 16):3573-84, 2005.
- [14] Yasuji Mori, Shu-Jen Chen and John Varga. Expression and regulation of intracellular smad signaling in scleroderma skin fibroblasts. *Arthritis Rheum*, 48(7):1964-78, 2003.
- [15] Chunming Dong, Shoukang Zhu, Tao Wang, Woohyun Yoon and Zhiru Li et al.. Deficient smad7 expression: a putative molecular defect in scleroderma. *Proc Natl Acad Sci U S A*, 99(6):3908-13, 2002.
- [16] Jaspreet Pannu, Yoshihide Asano, Sashidhar Nakerakanti, Edwin Smith and Stefania Jablonska et al.. Smad1 pathway is activated in systemic sclerosis fibroblasts and is targeted by imatinib mesylate. *Arthritis Rheum*, 58(8):2528-37, 2008.
- [17] T Kawakami, H Ihn, W Xu, E Smith and C LeRoy et al.. Increased expression of tgf-beta receptors by scleroderma fibroblasts: evidence for contribution of autocrine tgf-beta signaling to scleroderma phenotype. *J Invest Dermatol*, 110(1):47-51, 1998.
- [18] M Kubo, H Ihn, K Yamane and K Tamaki. Up-regulated expression of transforming growth factor beta receptors in dermal fibroblasts in skin sections from patients with localized scleroderma. *Arthritis Rheum*, 44(3):731-4, 2001.
- [19] Jaspreet Pannu, Humphrey Gardner, Jeffrey R Shearstone, Edwin Smith and Maria Trojanowska. Increased levels of transforming growth factor beta receptor type i and up-regulation of matrix gene program: A model of scleroderma. *Arthritis Rheum*, 54(9):3011-21, 2006.
- [20] B Perbal. Nov (nephroblastoma overexpressed) and the ccn family of genes: structural and functional issues. *Mol Pathol*, 54(2):57-79, 2001.
- [21] Mónica Rupérez, Oscar Lorenzo, Luis Miguel Blanco-Colio, Vanesa Esteban and Jesús Egido et al.. Connective tissue growth factor is a mediator of angiotensin ii-induced fibrosis. *Circulation*, 108(12):1499-505, 2003.
- [22] Alan Holmes, David J Abraham, Youjun Chen, Christopher Denton and Xu Shi-wen et al.. Constitutive connective tissue growth factor expression in scleroderma fibroblasts is dependent on sp1. *J Biol Chem*, 278(43):41728-33, 2003.
- [23] Swati Bhattacharyya, Minghua Wu, Feng Fang, Warren Tourtellotte and Carol Feghali-Bostwick et al.. Early growth response transcription factors: key mediators of fibrosis and novel targets for anti-fibrotic therapy. *Matrix Biol*, 30(4):235-42, 2011a.
- [24] Swati Bhattacharyya, Jennifer L Sargent, Pan Du, Simon Lin and Warren G Tourtellotte et al.. Egr-1 induces a profibrotic injury/repair gene program associated with systemic sclerosis. *PLoS One*, 6(9):e23082, 2011b.

- [25] Dmitry N Grigoryev, Stephen C Mathai, Micah R Fisher, Reda E Grgis and Ari L Zaiman et al.. Identification of candidate genes in scleroderma-related pulmonary arterial hypertension. *Transl Res*, 151(4):197-207, 2008.
- [26] M D Sternlicht and Z Werb. How matrix metalloproteinases regulate cell behavior. *Annu Rev Cell Dev Biol*, 17:463-516, 2001.
- [27] K Kuroda and H Shinkai. Gene expression of types i and iii collagen, decorin, matrix metalloproteinases and tissue inhibitors of metalloproteinases in skin fibroblasts from patients with systemic sclerosis. *Arch Dermatol Res*, 289(10):567-72, 1997.
- [28] K Holmbeck, P Bianco, J Caterina, S Yamada and M Kromer et al.. Mt1-mmp-deficient mice develop dwarfism, osteopenia, arthritis, and connective tissue disease due to inadequate collagen turnover. *Cell*, 99(1):81-92, 1999.
- [29] A Leask, D J Abraham, D R Finlay, A Holmes and D Pennington et al.. Dysregulation of transforming growth factor beta signaling in scleroderma: overexpression of endoglin in cutaneous scleroderma fibroblasts. *Arthritis Rheum*, 46(7):1857-65, 2002.
- [30] T Z Kirk, M E Mark, C C Chua, B H Chua and M D Mayes. Myofibroblasts from scleroderma skin synthesize elevated levels of collagen and tissue inhibitor of metalloproteinase (timp-1) with two forms of timp-1. *J Biol Chem*, 270(7):3423-8, 1995.
- [31] Toshiyuki Yamamoto and Kiyoshi Nishioka. Role of monocyte chemoattractant protein-1 and its receptor, ccr-2, in the pathogenesis of bleomycin-induced scleroderma. *J Invest Dermatol*, 121(3):510-6, 2003.
- [32] C P Denton, X Shi-Wen, A Sutton, D J Abraham and C M Black et al.. Scleroderma fibroblasts promote migration of mononuclear leucocytes across endothelial cell monolayers. *Clin Exp Immunol*, 114(2):293-300, 1998.
- [33] O Distler, T Pap, O Kowal-Bielecka, R Meyringer and S Guiducci et al.. Overexpression of monocyte chemoattractant protein 1 in systemic sclerosis: role of platelet-derived growth factor and effects on monocyte chemotaxis and collagen synthesis. *Arthritis Rheum*, 44(11):2665-78, 2001.
- [34] Y Kawaguchi, M Hara and T M Wright. Endogenous il-1alpha from systemic sclerosis fibroblasts induces il-6 and pdgf-a. *J Clin Invest*, 103(9):1253-60, 1999.
- [35] G Piccinini, J Golay, A Flora, S Songia and M Luchetti et al.. C-myb, but not b-myb, upregulates type i collagen gene expression in human fibroblasts. *J Invest Dermatol*, 112(2):191-6, 1999.
- [36] M Trojanowska, L T Wu and E C LeRoy. Elevated expression of c-myc proto-oncogene in scleroderma fibroblasts. *Oncogene*, 3(4):477-81, 1988.

- [37] Annemarie J van der Slot, Anne-Marie Zuurmond, Alfons F J Bardoel, Cisca Wijmenga and Hans E H Pruijs et al.. Identification of plod2 as telopeptide lysyl hydroxylase, an important enzyme in fibrosis. *J Biol Chem*, 278(42):40967-72, 2003.
- [38] A Jelaska and J H Korn. Role of apoptosis and transforming growth factor beta1 in fibroblast selection and activation in systemic sclerosis. *Arthritis Rheum*, 43(10):2230-9, 2000.
- [39] M L Biondi, B Marasini, E Bianchi and A Agostoni. Plasma free and intraplatelet serotonin in patients with raynaud's phenomenon. *Int J Cardiol*, 19(3):335-9, 1988.
- [40] David J Welsh, Margaret Harnett, Margaret MacLean and Andrew J Peacock. Proliferation and signaling in fibroblasts: role of 5-hydroxytryptamine2a receptor and transporter. *Am J Respir Crit Care Med*, 170(3):252-9, 2004.
- [41] Clara Dees, Alfiya Akhmetshina, Pawel Zerr, Nicole Reich and Katrin Palumbo et al.. Platelet-derived serotonin links vascular disease and tissue fibrosis. *J Exp Med*, 208(5):961-72, 2011.
- [42] Lorin E Olson and Philippe Soriano. Increased pdgfralpha activation disrupts connective tissue development and drives systemic fibrosis. *Dev Cell*, 16(2):303-13, 2009.
- [43] James C Bonner. Regulation of pdgf and its receptors in fibrotic diseases. *Cytokine Growth Factor Rev*, 15(4):255-73, 2004.
- [44] Silvia Svegliati, Raffaella Cancello, Paola Sambo, Michele Luchetti and Paolo Paroncini et al.. Platelet-derived growth factor and reactive oxygen species (ros) regulate ras protein levels in primary human fibroblasts via erk1/2. amplification of ros and ras in systemic sclerosis fibroblasts. *J Biol Chem*, 280(43):36474-82, 2005.
- [45] Silvia Svegliati Baroni, Mariarosaria Santillo, Federica Bevilacqua, Michele Luchetti and Tatiana Spadoni et al.. Stimulatory autoantibodies to the pdgf receptor in systemic sclerosis. *N Engl J Med*, 354(25):2667-76, 2006.
- [46] Silvia Svegliati, Attilio Olivieri, Nadia Campelli, Michele Luchetti and Antonella Poloni et al.. Stimulatory autoantibodies to pdgf receptor in patients with extensive chronic graft-versus-host disease. *Blood*, 110(1):237-41, 2007.
- [47] Jean-François Classen, Dan Henrohn, Fredrik Rorsman, Johan Lennartsson and Bernard R Lauwerys et al.. Lack of evidence of stimulatory autoantibodies to platelet-derived growth factor receptor in patients with systemic sclerosis. *Arthritis Rheum*, 60(4):1137-44, 2009.
- [48] Ralph Theo Schermuly, Eva Dony, Hossein Ardeschir Ghofrani, Soni Pullamsetti and Raj-kumar Savai et al.. Reversal of experimental pulmonary hypertension by pdgf inhibition. *J Clin Invest*, 115(10):2811-21, 2005.

- [49] Jörg H W Distler, Astrid Jüngel, Lars C Huber, Ursula Schulze-Horsel and Jochen Zwerina et al.. Imatinib mesylate reduces production of extracellular matrix and prevents development of experimental dermal fibrosis. *Arthritis Rheum*, 56(1):311-22, 2007.
- [50] Alfiya Akhmetshina, Paulius Venalis, Clara Dees, Nicole Busch and Jochen Zwerina et al.. Treatment with imatinib prevents fibrosis in different preclinical models of systemic sclerosis and induces regression of established fibrosis. *Arthritis Rheum*, 60(1):219-24, 2009.
- [51] C Doucet, D Brouty-Boyé, C Pottin-Clémenceau, G W Canonica and C Jasmin et al.. Interleukin (il) 4 and il-13 act on human lung fibroblasts. implication in asthma. *J Clin Invest*, 101(10):2129-39, 1998a.
- [52] Tracy L McGaha, Maithao Le, Takao Kodera, Cristina Stoica and Jinfang Zhu et al.. Molecular mechanisms of interleukin-4-induced up-regulation of type i collagen gene expression in murine fibroblasts. *Arthritis Rheum*, 48(8):2275-84, 2003.
- [53] C J Ong, S Ip, S J Teh, C Wong and F R Jirik et al.. A role for t helper 2 cells in mediating skin fibrosis in tight-skin mice. *Cell Immunol*, 196(1):60-8, 1999.
- [54] C Ong, C Wong, C R Roberts, H S Teh and F R Jirik. Anti-il-4 treatment prevents dermal collagen deposition in the tight-skin mouse model of scleroderma. *Eur J Immunol*, 28(9):2619-29, 1998.
- [55] T McGaha, S Saito, R G Phelps, R Gordon and N Noben-Trauth et al.. Lack of skin fibrosis in tight skin (tsk) mice with targeted mutation in the interleukin-4r alpha and transforming growth factor-beta genes. *J Invest Dermatol*, 116(1):136-43, 2001.
- [56] J Tsuji-Yamada, M Nakazawa, K Takahashi, K Iijima and S Hattori et al.. Effect of il-12 encoding plasmid administration on tight-skin mouse. *Biochem Biophys Res Commun*, 280(3):707-12, 2001.
- [57] M Hasegawa, M Fujimoto, K Kikuchi and K Takehara. Elevated serum levels of interleukin 4 (il-4), il-10, and il-13 in patients with systemic sclerosis. *J Rheumatol*, 24(2):328-32, 1997.
- [58] C Mavalia, C Scaletti, P Romagnani, A M Carossino and A Pignone et al.. Type 2 helper t-cell predominance and high cd30 expression in systemic sclerosis. *Am J Pathol*, 151(6):1751-8, 1997.
- [59] S P Atamas, V V Yurovsky, R Wise, F M Wigley and C J Goter Robinson et al.. Production of type 2 cytokines by cd8+ lung cells is associated with greater decline in pulmonary function in patients with systemic sclerosis. *Arthritis Rheum*, 42(6):1168-78, 1999.
- [60] V Salmon-Ehr, H Serpier, B Nawrocki, P Gillery and C Clavel et al.. Expression of interleukin-4 in scleroderma skin specimens and scleroderma fibroblast cultures. potential role in fibrosis. *Arch Dermatol*, 132(7):802-6, 1996.

- [61] Yann Parel, Michel Aurrand-Lions, Agneta Scheja, Jean-Michel Dayer and Eddy Roosnek et al.. Presence of cd4+cd8+ double-positive t cells with very high interleukin-4 production potential in lesional skin of patients with systemic sclerosis. *Arthritis Rheum*, 56(10):3459-67, 2007.
- [62] L I Sakkas, C Tourtellotte, S Berney, A R Myers and C D Platsoucas. Increased levels of alternatively spliced interleukin 4 (il-4delta2) transcripts in peripheral blood mononuclear cells from patients with systemic sclerosis. *Clin Diagn Lab Immunol*, 6(5):660-4, 1999.
- [63] Masatoshi Jinnin, Hironobu Ihn, Kenichi Yamane and Kunihiko Tamaki. Interleukin-13 stimulates the transcription of the human alpha2(i) collagen gene in human dermal fibroblasts. *J Biol Chem*, 279(40):41783-91, 2004.
- [64] John A Belperio, Maria Dy, Marie D Burdick, Ying Y Xue and Kewang Li et al.. Interaction of il-13 and c10 in the pathogenesis of bleomycin-induced pulmonary fibrosis. *Am J Respir Cell Mol Biol*, 27(4):419-27, 2002.
- [65] Taiji Nakashima, Masatoshi Jinnin, Keitaro Yamane, Noritoshi Honda and Ikko Kajihara et al.. Impaired il-17 signaling pathway contributes to the increased collagen expression in scleroderma fibroblasts. *J Immunol*, 188(8):3573-83, 2012.
- [66] Ayumi Yoshizaki, Koichi Yanaba, Yohei Iwata, Kazuhiro Komura and Asako Ogawa et al.. Cell adhesion molecules regulate fibrotic process via th1/th2/th17 cell balance in a bleomycin-induced scleroderma model. *J Immunol*, 185(4):2502-15, 2010.
- [67] S Morelli, C Ferri, L Di Francesco, R Baldoncini and M Carlesimo et al.. Plasma endothelin-1 levels in patients with systemic sclerosis: influence of pulmonary or systemic arterial hypertension. *Ann Rheum Dis*, 54(9):730-4, 1995b.
- [68] S Morelli, C Ferri, E Polettini, C Bellini and G F Gualdi et al.. Plasma endothelin-1 levels, pulmonary hypertension, and lung fibrosis in patients with systemic sclerosis. *Am J Med*, 99(3):255-60, 1995a.
- [69] Xu Shi-Wen, Yunliang Chen, Christopher P Denton, Mark Eastwood and Elisabetta A Renzoni et al.. Endothelin-1 promotes myofibroblast induction through the eta receptor via a rac/phosphoinositide 3-kinase/akt-dependent pathway and is essential for the enhanced contractile phenotype of fibrotic fibroblasts. *Mol Biol Cell*, 15(6):2707-19, 2004.
- [70] R A Clark, L D Nielsen, M P Welch and J M McPherson. Collagen matrices attenuate the collagen-synthetic response of cultured fibroblasts to tgf-beta. *J Cell Sci*, 108 (Pt 3):1251-61, 1995.
- [71] S A Cotton, A L Herrick, M I Jayson and A J Freemont. Tgf beta-a role in systemic sclerosis?. *J Pathol*, 184(1):4-6, 1998.
- [72] B W Needleman, J Choi, A Burrows-Mezu and J A Fontana. Secretion and binding of transforming growth factor beta by scleroderma and normal dermal fibroblasts. *Arthritis Rheum*, 33(5):650-6, 1990.

- [73] D F Poulson. Chromosomal deficiencies and the embryonic development of drosophila melanogaster. *Proc Natl Acad Sci U S A*, 23(3):133-7, 1937.
- [74] C Brou, F Logeat, N Gupta, C Bessia and O LeBail et al.. A novel proteolytic cleavage involved in notch signaling: the role of the disintegrin-metalloprotease tace. *Mol Cell*, 5(2):207-16, 2000.
- [75] Masayasu Okochi, Harald Steiner, Akio Fukumori, Hisashi Tanii and Taisuke Tomita et al.. Presenilins mediate a dual intramembranous gamma-secretase cleavage of notch-1. *EMBO J*, 21(20):5408-16, 2002.
- [76] Mark E Fortini. Gamma-secretase-mediated proteolysis in cell-surface-receptor signalling. *Nat Rev Mol Cell Biol*, 3(9):673-84, 2002.
- [77] Keiki Kumano, Shigeru Chiba, Atsushi Kunisato, Masataka Sata and Toshiki Saito et al.. Notch1 but not notch2 is essential for generating hematopoietic stem cells from endothelial cells. *Immunity*, 18(5):699-711, 2003.
- [78] F N Karanu, B Murdoch, L Gallacher, D M Wu and M Koremoto et al.. The notch ligand jagged-1 represents a novel growth factor of human hematopoietic stem cells. *J Exp Med*, 192(9):1365-72, 2000.
- [79] L M Calvi, G B Adams, K W Weibrech, J M Weber and D P Olson et al.. Osteoblastic cells regulate the haematopoietic stem cell niche. *Nature*, 425(6960):841-6, 2003.
- [80] Hua Han, Kenji Tanigaki, Norio Yamamoto, Kazuki Kuroda and Momoko Yoshimoto et al.. Inducible gene knockout of transcription factor recombination signal binding protein-j reveals its essential role in t versus b lineage decision. *Int Immunol*, 14(6):637-45, 2002.
- [81] G Anderson, J Pongracz, S Parnell and E J Jenkinson. Notch ligand-bearing thymic epithelial cells initiate and sustain notch signaling in thymocytes independently of t cell receptor signaling. *Eur J Immunol*, 31(11):3349-54, 2001.
- [82] A Wilson, I Ferrero, H R MacDonald and F Radtke. Cutting edge: an essential role for notch-1 in the development of both thymus-independent and -dependent t cells in the gut. *J Immunol*, 165(10):5397-400, 2000.
- [83] Tanapat Palaga, Lucio Miele, Todd E Golde and Barbara A Osborne. Tcr-mediated notch signaling regulates proliferation and ifn-gamma production in peripheral t cells. *J Immunol*, 171(6):3019-24, 2003.
- [84] Scott H Adler, Elise Chiffolleau, Lanwei Xu, Nicole M Dalton and Jennifer M Burg et al.. Notch signaling augments t cell responsiveness by enhancing cd25 expression. *J Immunol*, 171(6):2896-903, 2003.

- [85] Derk Amsen, J Magarian Blander, Gap Ryol Lee, Kenji Tanigaki and Tasuku Honjo et al.. Instruction of distinct cd4 t helper cell fates by different notch ligands on antigen-presenting cells. *Cell*, 117(4):515-26, 2004.
- [86] Barbara A Osborne and Lisa M Minter. Notch signalling during peripheral t-cell activation and differentiation. *Nat Rev Immunol*, 7(1):64-75, 2007.
- [87] Kazuki Kuroda, Hua Han, Shoichi Tani, Kenji Tanigaki and Tin Tun et al.. Regulation of marginal zone b cell development by mint, a suppressor of notch/rbp-j signaling pathway. *Immunity*, 18(2):301-12, 2003.
- [88] T Morimura, S Miyatani, D Kitamura and R Goitsuka. Notch signaling suppresses igh gene expression in chicken b cells: implication in spatially restricted expression of serrate2/notch1 in the bursa of fabricius. *J Immunol*, 166(5):3277-83, 2001.
- [89] Colleen M Witt, Woong-Jai Won, Vincent Hurez and Christopher A Klug. Notch2 haploinsufficiency results in diminished b1 b cells and a severe reduction in marginal zone b cells. *J Immunol*, 171(6):2783-8, 2003.
- [90] Ryuhei Okuyama, Hachiro Tagami and Setsuya Aiba. Notch signaling: its role in epidermal homeostasis and in the pathogenesis of skin diseases. *J Dermatol Sci*, 49(3):187-94, 2008.
- [91] Natsuki Hoshino, Naoyuki Katayama, Tetsunori Shibasaki, Kohshi Ohishi and Junji Nishioka et al.. A novel role for notch ligand delta-1 as a regulator of human langerhans cell development from blood monocytes. *J Leukoc Biol*, 78(4):921-9, 2005.
- [92] Tianju Liu, Biao Hu, Yoon Young Choi, Myoungja Chung and Matthew Ullenbruch et al.. Notch1 signaling in fizz1 induction of myofibroblast differentiation. *Am J Pathol*, 174(5):1745-55, 2009.
- [93] Laura S Harrington, Richard C A Sainson, Cassin Kimmel Williams, Jennifer M Taylor and Wen Shi et al.. Regulation of multiple angiogenic pathways by dll4 and notch in human umbilical vein endothelial cells. *Microvasc Res*, 75(2):144-54, 2008.
- [94] Thomas Gridley. Notch signaling in vascular development and physiology. *Development*, 134(15):2709-18, 2007.
- [95] Richard C A Sainson and Adrian L Harris. Anti-dll4 therapy: can we block tumour growth by increasing angiogenesis?. *Trends Mol Med*, 13(9):389-95, 2007.
- [96] V Lindner, C Booth, I Prudovsky, D Small and T Maciag et al.. Members of the jagged/notch gene families are expressed in injured arteries and regulate cell phenotype via alterations in cell matrix and cell-cell interaction. *Am J Pathol*, 159(3):875-83, 2001.
- [97] H Uyttendaele, V Closson, G Wu, F Roux and G Weinmaster et al.. Notch4 and jagged-1 induce microvessel differentiation of rat brain endothelial cells. *Microvasc Res*, 60(2):91-103, 2000.

- [98] Richard C A Sainson, Jason Aoto, Martin N Nakatsu, Matthew Holderfield and Erin Conn et al.. Cell-autonomous notch signaling regulates endothelial cell branching and proliferation during vascular tubulogenesis. *FASEB J*, 19(8):1027-9, 2005.
- [99] Eric J Allenspach, Ivan Maillard, Jon C Aster and Warren S Pear. Notch signaling in cancer. *Cancer Biol Ther*, 1(5):466-76, 2002.
- [100] L W Ellisen, J Bird, D C West, A L Soreng and T C Reynolds et al.. Tan-1, the human homolog of the drosophila notch gene, is broken by chromosomal translocations in t lymphoblastic neoplasms. *Cell*, 66(4):649-61, 1991.
- [101] R G Pertwee, A C Howlett, M E Abood, S P H Alexander and V Di Marzo et al.. International union of basic and clinical pharmacology. Ixxix. cannabinoid receptors and their ligands: beyond cb₁ and cb₂. *Pharmacol Rev*, 62(4):588-631, 2010.
- [102] Béla Horváth, Partha Mukhopadhyay, György Haskó and Pál Pacher. The endocannabinoid system and plant-derived cannabinoids in diabetes and diabetic complications. *Am J Pathol*, 180(2):432-42, 2012.
- [103] Natsuo Ueda, Kazuhito Tsuboi, Toru Uyama and Taira Ohnishi. Biosynthesis and degradation of the endocannabinoid 2-arachidonoylglycerol. *Biofactors*, 37(1):1-7, 2011.
- [104] Federica Barutta, Fabiana Piscitelli, Silvia Pinach, Graziella Bruno and Roberto Gambino et al.. Protective role of cannabinoid receptor type 2 in a mouse model of diabetic nephropathy. *Diabetes*, 60(9):2386-96, 2011.
- [105] Yan Zhao, Yan Liu, Weiping Zhang, Jiahong Xue and Yue Z Wu et al.. Win55212-2 ameliorates atherosclerosis associated with suppression of pro-inflammatory responses in apoe-knockout mice. *Eur J Pharmacol*, 649(1-3):285-92, 2010.
- [106] Sandeep Singla, Rajesh Sachdeva and Jawahar L Mehta. Cannabinoids and atherosclerotic coronary heart disease. *Clin Cardiol*, 2012.
- [107] Antonia Sophocleous, Euphémie Landao-Bassonga, Robert J Van't Hof, Aymen I Idris and Stuart H Ralston. The type 2 cannabinoid receptor regulates bone mass and ovariectomy-induced bone loss by affecting osteoblast differentiation and bone formation. *Endocrinology*, 152(6):2141-9, 2011.
- [108] A Mallat and S Lotersztajn. Endocannabinoids and their role in fatty liver disease. *Dig Dis*, 28(1):261-6, 2010.
- [109] A Mallat, F Teixeira-Clerc, V Deveaux, S Manin and S Lotersztajn. The endocannabinoid system as a key mediator during liver diseases: new insights and therapeutic openings. *Br J Pharmacol*, 163(7):1432-40, 2011.
- [110] Vedrana Reichenbach, Josefa Ros, Guillermo Fernández-Varo, Gregori Casals and Pedro Melgar-Lesmes et al.. Prevention of fibrosis progression in ccl4-treated rats: role of the hepatic endocannabinoid and apelin systems. *J Pharmacol Exp Ther*, 340(3):629-37, 2012.

- [111] Boris Julien, Pascale Grenard, Fatima Teixeira-Clerc, Jeanne Tran Van Nhieu and Liying Li et al.. Antifibrogenic role of the cannabinoid receptor cb2 in the liver. *Gastroenterology*, 128(3):742-55, 2005.
- [112] Javier Muñoz-Luque, Josefa Ros, Guillermo Fernández-Varo, Sònia Tugues and Manuel Morales-Ruiz et al.. Regression of fibrosis after chronic stimulation of cannabinoid cb2 receptor in cirrhotic rats. *J Pharmacol Exp Ther*, 324(2):475-83, 2008.
- [113] Amélie Servettaz, Niloufar Kavian, Carole Nicco, Vanessa Deveaux and Christiane Chéreau et al.. Targeting the cannabinoid pathway limits the development of fibrosis and autoimmunity in a mouse model of systemic sclerosis. *Am J Pathol*, 177(1):187-96, 2010.
- [114] Alfiya Akhmetshina, Clara Dees, Nicole Busch, Jürgen Beer and Kerstin Sarter et al.. The cannabinoid receptor cb2 exerts antifibrotic effects in experimental dermal fibrosis. *Arthritis Rheum*, 60(4):1129-36, 2009.
- [115] Estrella Garcia-Gonzalez, Enrico Selvi, Epifania Balistreri, Sauro Lorenzini and Roberta Maggio et al.. Cannabinoids inhibit fibrogenesis in diffuse systemic sclerosis fibroblasts. *Rheumatology (Oxford)*, 48(9):1050-6, 2009.
- [116] Maria Trojanowska. Cellular and molecular aspects of vascular dysfunction in systemic sclerosis. *Nat Rev Rheumatol*, 6(8):453-60, 2010.
- [117] U Anderegg, A Saalbach and U F Haustein. Chemokine release from activated human dermal microvascular endothelial cells—implications for the pathophysiology of scleroderma?. *Arch Dermatol Res*, 292(7):341-7, 2000.
- [118] Marco Matucci Cerinic, G Valentini, G G Sorano, S D'Angelo and G Cuomo et al.. Blood coagulation, fibrinolysis, and markers of endothelial dysfunction in systemic sclerosis. *Semin Arthritis Rheum*, 32(5):285-95, 2003.
- [119] M Matucci Cerinic and M B Kahaleh. Beauty and the beast. the nitric oxide paradox in systemic sclerosis. *Rheumatology (Oxford)*, 41(8):843-7, 2002.
- [120] Grethe Neumann Andersen, Lucia Mincheva-Nilsson, Elsadig Kazzam, Gunnar Nyberg and Natalia Klintland et al.. Assessment of vascular function in systemic sclerosis: indications of the development of nitrate tolerance as a result of enhanced endothelial nitric oxide production. *Arthritis Rheum*, 46(5):1324-32, 2002.
- [121] R Vancheeswaran, T Magoulas, G Efrat, C Wheeler-Jones and I Olsen et al.. Circulating endothelin-1 levels in systemic sclerosis subsets—a marker of fibrosis or vascular dysfunction?. *J Rheumatol*, 21(10):1838-44, 1994.
- [122] Maureen D Mayes. Endothelin and endothelin receptor antagonists in systemic rheumatic disease. *Arthritis Rheum*, 48(5):1190-9, 2003.
- [123] Jin-Jung Choi, Do-June Min, Mi-La Cho, So-Youn Min and Seon-Joon Kim et al.. Elevated vascular endothelial growth factor in systemic sclerosis. *J Rheumatol*, 30(7):1529-33, 2003.

- [124] Laura K Hummers, Amy Hall, Fredrick M Wigley and Michael Simons. Abnormalities in the regulators of angiogenesis in patients with scleroderma. *J Rheumatol*, 36(3):576-82, 2009.
- [125] Oliver Distler, Angela Del Rosso, Roberto Giacomelli, Paola Cipriani and Maria L Conforti et al.. Angiogenic and angiostatic factors in systemic sclerosis: increased levels of vascular endothelial growth factor are a feature of the earliest disease stages and are associated with the absence of fingertip ulcers. *Arthritis Res*, 4(6):R11, 2002.
- [126] Mary Jo Mulligan-Kehoe, Mary C Drinane, Jessica Mollmark, Livia Casciola-Rosen and Laura K Hummers et al.. Antiangiogenic plasma activity in patients with systemic sclerosis. *Arthritis Rheum*, 56(10):3448-58, 2007.
- [127] Nicoletta Del Papa, Nadia Quirici, Davide Soligo, Cinzia Scavullo and Michela Cortiana et al.. Bone marrow endothelial progenitors are defective in systemic sclerosis. *Arthritis Rheum*, 54(8):2605-15, 2006.
- [128] B M Kräling, G G Maul and S A Jimenez. Mononuclear cellular infiltrates in clinically involved skin from patients with systemic sclerosis of recent onset predominantly consist of monocytes/macrophages. *Pathobiology*, 63(1):48-56, 1995.
- [129] O Ishikawa and H Ishikawa. Macrophage infiltration in the skin of patients with systemic sclerosis. *J Rheumatol*, 19(8):1202-6, 1992.
- [130] Melanie C Ruzek, Sharda Jha, Steve Ledbetter, Susan M Richards and Richard D Garman. A modified model of graft-versus-host-induced systemic sclerosis (scleroderma) exhibits all major aspects of the human disease. *Arthritis Rheum*, 50(4):1319-31, 2004.
- [131] J R Seibold, R C Giorno and H N Claman. Dermal mast cell degranulation in systemic sclerosis. *Arthritis Rheum*, 33(11):1702-9, 1990.
- [132] T Yamamoto, Y Takahashi, S Takagawa, I Katayama and K Nishioka. Animal model of sclerotic skin. ii. bleomycin induced scleroderma in genetically mast cell deficient wbb6f1-w/w(v) mice. *J Rheumatol*, 26(12):2628-34, 1999.
- [133] A D Roumm, T L Whiteside, T A Medsger Jr and G P Rodnan. Lymphocytes in the skin of patients with progressive systemic sclerosis. quantification, subtyping, and clinical correlations. *Arthritis Rheum*, 27(6):645-53, 1984.
- [134] C Querfeld, B Eckes, C Huerkamp, T Krieg and S Sollberg. Expression of tgf-beta 1, -beta 2 and -beta 3 in localized and systemic scleroderma. *J Dermatol Sci*, 21(1):13-22, 1999.
- [135] John Varga and David Abraham. Systemic sclerosis: a prototypic multisystem fibrotic disorder. *J Clin Invest*, 117(3):557-67, 2007.
- [136] Carol M Artlett. Immunology of systemic sclerosis. *Front Biosci*, 10:1707-19, 2005.

- [137] Hideaki Ishikawa, Kozue Takeda, Akira Okamoto, Sei-ichi Matsuo and Ken-ichi Isobe. Induction of autoimmunity in a bleomycin-induced murine model of experimental systemic sclerosis: an important role for cd4+ t cells. *J Invest Dermatol*, 129(7):1688-95, 2009.
- [138] Francesca Ingegnoli, Daria Trabattoni, Marina Saresella, Flavio Fantini and Mario Clerici. Distinct immune profiles characterize patients with diffuse or limited systemic sclerosis. *Clin Immunol*, 108(1):21-8, 2003.
- [139] Paola Rottoli, Barbara Magi, Maria Grazia Perari, Sabrina Liberatori and Nikolaos Nikiforakis et al.. Cytokine profile and proteome analysis in bronchoalveolar lavage of patients with sarcoidosis, pulmonary fibrosis associated with systemic sclerosis and idiopathic pulmonary fibrosis. *Proteomics*, 5(5):1423-30, 2005.
- [140] Gabriella Lakos, Denisa Melichian, Minghua Wu and John Varga. Increased bleomycin-induced skin fibrosis in mice lacking the th1-specific transcription factor t-bet. *Pathobiology*, 73(5):224-37, 2006.
- [141] G Valentini, A Baroni, K Esposito, C Naclerio and E Buommino et al.. Peripheral blood t lymphocytes from systemic sclerosis patients show both th1 and th2 activation. *J Clin Immunol*, 21(3):210-7, 2001.
- [142] Chihiro Tanaka, Manabu Fujimoto, Yasuhito Hamaguchi, Shinichi Sato and Kazuhiko Takehara et al.. Inducible costimulator ligand regulates bleomycin-induced lung and skin fibrosis in a mouse model independently of the inducible costimulator/inducible costimulator ligand pathway. *Arthritis Rheum*, 62(6):1723-32, 2010.
- [143] C Chizzolini, R Rezzonico, C Ribbens, D Burger and F A Wollheim et al.. Inhibition of type i collagen production by dermal fibroblasts upon contact with activated t cells: different sensitivity to inhibition between systemic sclerosis and control fibroblasts. *Arthritis Rheum*, 41(11):2039-47, 1998.
- [144] Carlo Chizzolini, Yann Parel, Carmelina De Luca, Alan Tyndall and Anita Akesson et al.. Systemic sclerosis th2 cells inhibit collagen production by dermal fibroblasts via membrane-associated tumor necrosis factor alpha. *Arthritis Rheum*, 48(9):2593-604, 2003.
- [145] C M Artlett, J B Smith and S A Jimenez. Identification of fetal dna and cells in skin lesions from women with systemic sclerosis. *N Engl J Med*, 338(17):1186-91, 1998.
- [146] David J Abraham and John Varga. Scleroderma: from cell and molecular mechanisms to disease models. *Trends Immunol*, 26(11):587-95, 2005.
- [147] S Sato, M Hasegawa, M Fujimoto, T F Tedder and K Takehara. Quantitative genetic variation in cd19 expression correlates with autoimmunity. *J Immunol*, 165(11):6635-43, 2000.
- [148] Eriko Saito, Manabu Fujimoto, Minoru Hasegawa, Kazuhiro Komura and Yasuhito Hamaguchi et al.. Cd19-dependent b lymphocyte signaling thresholds influence skin fibrosis and autoimmunity in the tight-skin mouse. *J Clin Invest*, 109(11):1453-62, 2002.

- [149] Ayumi Yoshizaki, Yohei Iwata, Kazuhiro Komura, Fumihide Ogawa and Toshihide Hara et al.. Cd19 regulates skin and lung fibrosis via toll-like receptor signaling in a model of bleomycin-induced scleroderma. *Am J Pathol*, 172(6):1650-63, 2008.
- [150] Takashi Matsushita, Minoru Hasegawa, Koichi Yanaba, Masanari Kodera and Kazuhiko Takehara et al.. Elevated serum baff levels in patients with systemic sclerosis: enhanced baff signaling in systemic sclerosis b lymphocytes. *Arthritis Rheum*, 54(1):192-201, 2006.
- [151] J Zhang, V Roschke, K P Baker, Z Wang and G S Alarcón et al.. Cutting edge: a role for b lymphocyte stimulator in systemic lupus erythematosus. *J Immunol*, 166(1):6-10, 2001.
- [152] Joanna Groom, Susan L Kalled, Anne H Cutler, Carl Olson and Stephen A Woodcock et al.. Association of baff/blys overexpression and altered b cell differentiation with sjögren's syndrome. *J Clin Invest*, 109(1):59-68, 2002.
- [153] E Scala, S Pallotta, A Frezzolini, D Abeni and C Barbieri et al.. Cytokine and chemokine levels in systemic sclerosis: relationship with cutaneous and internal organ involvement. *Clin Exp Immunol*, 138(3):540-6, 2004.
- [154] Thomas A Wynn. Fibrotic disease and the t(h)1/t(h)2 paradigm. *Nat Rev Immunol*, 4(8):583-94, 2004.
- [155] L Casciola-Rosen, F Wigley and A Rosen. Scleroderma autoantigens are uniquely fragmented by metal-catalyzed oxidation reactions: implications for pathogenesis. *J Exp Med*, 185(1):71-9, 1997.
- [156] S Sohail Ahmed, Filemon K Tan, Frank C Arnett, Li Jin and Yong-Jian Geng. Induction of apoptosis and fibrillin 1 expression in human dermal endothelial cells by scleroderma sera containing anti-endothelial cell antibodies. *Arthritis Rheum*, 54(7):2250-62, 2006.
- [157] Khanh T Ho and John D Reveille. The clinical relevance of autoantibodies in scleroderma. *Arthritis Res Ther*, 5(2):80-93, 2003.
- [158] Jill Hénault, Mélanie Tremblay, Isabelle Clément, Yves Raymond and Jean-Luc Senécal. Direct binding of anti-dna topoisomerase i autoantibodies to the cell surface of fibroblasts in patients with systemic sclerosis. *Arthritis Rheum*, 50(10):3265-74, 2004.
- [159] Jill Hénault, Geneviève Robitaille, Jean-Luc Senécal and Yves Raymond. Dna topoisomerase i binding to fibroblasts induces monocyte adhesion and activation in the presence of anti-topoisomerase i autoantibodies from systemic sclerosis patients. *Arthritis Rheum*, 54(3):963-73, 2006.
- [160] Shinichi Sato, Ikuko Hayakawa, Minoru Hasegawa, Manabu Fujimoto and Kazuhiko Takehara. Function blocking autoantibodies against matrix metalloproteinase-1 in patients with systemic sclerosis. *J Invest Dermatol*, 120(4):542-7, 2003.

- [161] K V Salojin, M Le Tonquèze, A Saraux, E L Nassonov and M Dueymes et al.. Antien-dothelial cell antibodies: useful markers of systemic sclerosis. *Am J Med*, 102(2):178-85, 1997.
- [162] M B Hill, J L Phipps, R J Cartwright, A Milford Ward and M Greaves et al.. Antibodies to membranes of endothelial cells and fibroblasts in scleroderma. *Clin Exp Immunol*, 106(3):491-7, 1996.
- [163] D Carvalho, C O Savage, C M Black and J D Pearson. IgG antiendothelial cell autoantibodies from scleroderma patients induce leukocyte adhesion to human vascular endothelial cells in vitro. induction of adhesion molecule expression and involvement of endothelium-derived cytokines. *J Clin Invest*, 97(1):111-9, 1996.
- [164] F Alderuccio, D Witherden, B H Toh and A Barnett. Autoantibody to gp50, a glycoprotein shared in common between fibroblasts and lymphocytes, in progressive systemic sclerosis. *Clin Exp Immunol*, 78(1):26-30, 1989.
- [165] Nicoletta Ronda, Rita Gatti, Roberto Giacosa, Elena Raschi and Cinzia Testoni et al.. Antifibroblast antibodies from systemic sclerosis patients are internalized by fibroblasts via a caveolin-linked pathway. *Arthritis Rheum*, 46(6):1595-601, 2002.
- [166] Carlo Chizzolini, Elena Raschi, Roger Rezzonico, Cinzia Testoni and Roberto Mallone et al.. Autoantibodies to fibroblasts induce a proadhesive and proinflammatory fibroblast phenotype in patients with systemic sclerosis. *Arthritis Rheum*, 46(6):1602-13, 2002.
- [167] F K Tan, F C Arnett, S Antohi, S Saito and A Mirarchi et al.. Autoantibodies to the extracellular matrix microfibrillar protein, fibrillin-1, in patients with scleroderma and other connective tissue diseases. *J Immunol*, 163(2):1066-72, 1999.
- [168] V Smith, J T Van Praet, B Vandooren, B Van der Cruyssen and J-M Naeyaert et al.. Rituximab in diffuse cutaneous systemic sclerosis: an open-label clinical and histopathological study. *Ann Rheum Dis*, 69(1):193-7, 2010.
- [169] Robert Lafyatis, Eugene Kissin, Michael York, Giuseppina Farina and Kerry Viger et al.. B cell depletion with rituximab in patients with diffuse cutaneous systemic sclerosis. *Arthritis Rheum*, 60(2):578-83, 2009.
- [170] Silvia Bosello, Maria De Santis, Gina Lama, Cristina Spanò and Cristiana Angelucci et al.. B cell depletion in diffuse progressive systemic sclerosis: safety, skin score modification and IL-6 modulation in an up to thirty-six months follow-up open-label trial. *Arthritis Res Ther*, 12(2):R54, 2010.
- [171] Dimitrios Daoussis, Stamatis-Nick C Liossis, Athanassios C Tsamandas, Christina Kalogeropoulou and Alexandra Kazantzi et al.. Experience with rituximab in scleroderma: results from a 1-year, proof-of-principle study. *Rheumatology (Oxford)*, 49(2):271-80, 2010.
- [172] Ariane L Herrick and Jane Worthington. Genetic epidemiology: systemic sclerosis. *Arthritis Res*, 4(3):165-8, 2002.

- [173] Carol Feghali-Bostwick, Thomas A Medsger Jr and Timothy M Wright. Analysis of systemic sclerosis in twins reveals low concordance for disease and high concordance for the presence of antinuclear antibodies. *Arthritis Rheum*, 48(7):1956-63, 2003.
- [174] F K Tan, D N Stivers, M W Foster, R Chakraborty and R F Howard et al.. Association of microsatellite markers near the fibrillin 1 gene on human chromosome 15q with scleroderma in a native american population. *Arthritis Rheum*, 41(10):1729-37, 1998.
- [175] M C Green, H O Sweet and L E Bunker. Tight-skin, a new mutation of the mouse causing excessive growth of connective tissue and skeleton. *Am J Pathol*, 82(3):493-512, 1976.
- [176] R E Harrison, J A Flanagan, M Sankelo, S A Abdalla and J Rowell et al.. Molecular and functional analysis identifies alk-1 as the predominant cause of pulmonary hypertension related to hereditary haemorrhagic telangiectasia. *J Med Genet*, 40(12):865-71, 2003.
- [177] Carmen Fonseca, Gisela E Lindahl, Markella Ponticos, Piersante Sestini and Elisabetta A Renzoni et al.. A polymorphism in the ctgf promoter region associated with systemic sclerosis. *N Engl J Med*, 357(12):1210-20, 2007.
- [178] S Krishnan, V G Warke, M P Nambiar, H K Wong and G C Tsokos et al.. Generation and biochemical analysis of human effector cd4 t cells: alterations in tyrosine phosphorylation and loss of cd3zeta expression. *Blood*, 97(12):3851-9, 2001.
- [179] Roozbeh Sharif, Maureen D Mayes, Filemon K Tan, Olga Y Gorlova and Laura Kathleen Hummers et al.. Irf5 polymorphism predicts prognosis in patients with systemic sclerosis. *Ann Rheum Dis*, 2012.
- [180] E Diot, V Lesire, J L Guilmot, M D Metzger and R Pilore et al.. Systemic sclerosis and occupational risk factors: a case-control study. *Occup Environ Med*, 59(8):545-9, 2002.
- [181] Clodoveo Ferri, Dilia Giuggioli, Marco Sebastiani, Susi Panfilo and Giovanni Abatangelo et al.. Parvovirus b19 infection of cultured skin fibroblasts from systemic sclerosis patients: comment on the article by ray et al. *Arthritis Rheum*, 46(8):2262-3; author reply 2263-4, 2002.
- [182] Claudio Lunardi, Marzia Dolcino, Dimitri Peterlana, Caterina Bason and Riccardo Navone et al.. Antibodies against human cytomegalovirus in the pathogenesis of systemic sclerosis: a gene array approach. *PLoS Med*, 3(1):e2, 2006.
- [183] M E Gershwin, H Abplanalp, J J Castles, R M Ikeda and J van der Water et al.. Characterization of a spontaneous disease of white leghorn chickens resembling progressive systemic sclerosis (scleroderma). *J Exp Med*, 153(6):1640-59, 1981.
- [184] P J Christner, J Peters, D Hawkins, L D Siracusa and S A Jiménez. The tight skin 2 mouse. an animal model of scleroderma displaying cutaneous fibrosis and mononuclear cell infiltration. *Arthritis Rheum*, 38(12):1791-8, 1995.

- [185] L L McCormick, Y Zhang, E Tootell and A C Gilliam. Anti-tgf-beta treatment prevents skin and lung fibrosis in murine sclerodermatous graft-versus-host disease: a model for human scleroderma. *J Immunol*, 163(10):5693-9, 1999.
- [186] P J Christner, C M Artlett, R F Conway and S A Jiménez. Increased numbers of microchimeric cells of fetal origin are associated with dermal fibrosis in mice following injection of vinyl chloride. *Arthritis Rheum*, 43(11):2598-605, 2000.
- [187] M Le Hir, M Martin and C Haas. A syndrome resembling human systemic sclerosis (scleroderma) in mrl/lpr mice lacking interferon-gamma (ifn-gamma) receptor (mrl/lprgamma/-/-). *Clin Exp Immunol*, 115(2):281-7, 1999.
- [188] Britta Maurer, Nicole Busch, Astrid Jüngel, Margarita Pileckyte and Renate E Gay et al.. Transcription factor fos-related antigen-2 induces progressive peripheral vasculopathy in mice closely resembling human systemic sclerosis. *Circulation*, 120(23):2367-76, 2009.
- [189] Yoshihide Asano, Lukasz Stawski, Faye Hant, Kristin Highland and Richard Silver et al.. Endothelial fli1 deficiency impairs vascular homeostasis: a role in scleroderma vasculopathy. *Am J Pathol*, 176(4):1983-98, 2010.
- [190] Jun Wei, Denisa Melichian, Kazuhiko Komura, Monique Hinchcliff and Anna P Lam et al.. Canonical wnt signaling induces skin fibrosis and subcutaneous lipoatrophy: a novel mouse model for scleroderma?. *Arthritis Rheum*, 63(6):1707-17, 2011.
- [191] Emma C Derrett-Smith, Audrey Dooley, Korsa Khan, Xu Shi-wen and David Abraham et al.. Systemic vasculopathy with altered vasoreactivity in a transgenic mouse model of scleroderma. *Arthritis Res Ther*, 12(2):R69, 2010.
- [192] E Cadenas and K J Davies. Mitochondrial free radical generation, oxidative stress, and aging. *Free Radic Biol Med*, 29(3-4):222-30, 2000.
- [193] R L Slaughter and D J Edwards. Recent advances: the cytochrome p450 enzymes. *Ann Pharmacother*, 29(6):619-24, 1995.
- [194] Miklós Geiszt and Thomas L Leto. The nox family of nad(p)h oxidases: host defense and beyond. *J Biol Chem*, 279(50):51715-8, 2004.
- [195] Igor N Zelko, Thomas J Mariani and Rodney J Folz. Superoxide dismutase multigene family: a comparison of the cuzn-sod (sod1), mn-sod (sod2), and ec-sod (sod3) gene structures, evolution, and expression. *Free Radic Biol Med*, 33(3):337-49, 2002.
- [196] I Dalle-Donne, R Rossi, D Giustarini, N Gagliano and L Lusini et al.. Actin carbonylation: from a simple marker of protein oxidation to relevant signs of severe functional impairment. *Free Radic Biol Med*, 31(9):1075-83, 2001.
- [197] B M Babior, R S Kipnes and J T Curnutte. Biological defense mechanisms. the production by leukocytes of superoxide, a potential bactericidal agent. *J Clin Invest*, 52(3):741-4, 1973.

- [198] Matthew B Grisham. Reactive oxygen species in immune responses. *Free Radic Biol Med*, 36(12):1479-80, 2004.
- [199] Alexis Laurent, Carole Nicco, Christiane Chéreau, Claire Goulvestre and Jérôme Alexandre et al.. Controlling tumor growth by modulating endogenous production of reactive oxygen species. *Cancer Res*, 65(3):948-56, 2005.
- [200] M J Robinson and M H Cobb. Mitogen-activated protein kinase pathways. *Curr Opin Cell Biol*, 9(2):180-6, 1997.
- [201] R J Davis. Signal transduction by the jnk group of map kinases. *Cell*, 103(2):239-52, 2000.
- [202] G N Rao, B Lasségue, K K Griendlung, R W Alexander and B C Berk. Hydrogen peroxide-induced c-fos expression is mediated by arachidonic acid release: role of protein kinase c. *Nucleic Acids Res*, 21(5):1259-63, 1993.
- [203] Masuko Ushio-Fukai and R Wayne Alexander. Reactive oxygen species as mediators of angiogenesis signaling: role of nad(p)h oxidase. *Mol Cell Biochem*, 264(1-2):85-97, 2004.
- [204] M E Percy. Catalase: an old enzyme with a new role?. *Can J Biochem Cell Biol*, 62(10):1006-14, 1984.
- [205] A Meister. Glutathione metabolism. *Methods Enzymol*, 251:3-7, 1995.
- [206] Ariel Savina, Carolina Jancic, Stephanie Hugues, Pierre Guermonprez and Pablo Vargas et al.. Nox2 controls phagosomal ph to regulate antigen processing during crosspresentation by dendritic cells. *Cell*, 126(1):205-18, 2006.
- [207] Malin Hultqvist, Lina M Olsson, Kyra A Gelderman and Rikard Holmdahl. The protective role of ros in autoimmune disease. *Trends Immunol*, 30(5):201-8, 2009.
- [208] David A Hildeman. Regulation of t-cell apoptosis by reactive oxygen species. *Free Radic Biol Med*, 36(12):1496-504, 2004.
- [209] T Lehtimäki, S Lehtinen, T Solakivi, M Nikkilä and O Jaakkola et al.. Autoantibodies against oxidized low density lipoprotein in patients with angiographically verified coronary artery disease. *Arterioscler Thromb Vasc Biol*, 19(1):23-7, 1999.
- [210] Elisa Mottaran, Stephen F Stewart, Roberta Rolla, Daria Vay and Valentina Cipriani et al.. Lipid peroxidation contributes to immune reactions associated with alcoholic liver disease. *Free Radic Biol Med*, 32(1):38-45, 2002.
- [211] S Túri, I Németh, A Torkos, L Sághy and I Varga et al.. Oxidative stress and antioxidant defense mechanism in glomerular diseases. *Free Radic Biol Med*, 22(1-2):161-8, 1997.
- [212] Carlo Perricone, Caterina De Carolis and Roberto Perricone. Glutathione: a key player in autoimmunity. *Autoimmun Rev*, 8(8):697-701, 2009.
- [213] M R Namazi. Cytochrome-p450 enzymes and autoimmunity: expansion of the relationship and introduction of free radicals as the link. *J Autoimmune Dis*, 6:4, 2009.

- [214] Andras Perl. Emerging new pathways of pathogenesis and targets for treatment in systemic lupus erythematosus and sjogren's syndrome. *Curr Opin Rheumatol*, 21(5):443-7, 2009.
- [215] J M McCord, R S Roy and S W Schaffer. Free radicals and myocardial ischemia. the role of xanthine oxidase. *Adv Myocardiol*, 5:183-9, 1985.
- [216] Kamal D Srivastava, William N Rom, Jaishree Jagirdar, Ting-An Yie and Terry Gordon et al.. Crucial role of interleukin-1beta and nitric oxide synthase in silica-induced inflammation and apoptosis in mice. *Am J Respir Crit Care Med*, 165(4):527-33, 2002.
- [217] S Gossart, C Cambon, C Orfila, M H Séguélas and J C Lepert et al.. Reactive oxygen intermediates as regulators of tnf-alpha production in rat lung inflammation induced by silica. *J Immunol*, 156(4):1540-8, 1996.
- [218] T Yamamoto, S Takagawa, I Katayama, Y Mizushima and K Nishioka. Effect of superoxide dismutase on bleomycin-induced dermal sclerosis: implications for the treatment of systemic sclerosis. *J Invest Dermatol*, 113(5):843-7, 1999.
- [219] A Cárdenas, J Abián, O Bulbena, J Roselló and E Gelpi. Determination of oxidation products of n-phenyllinoleamide: Spanish toxic oil syndrome studies. *J Chromatogr*, 426(1):83-91, 1988.
- [220] Mohammed Tikly, Sara E Marshall, Neil A Haldar, Mary Gulumian and Paul Wordsworth et al.. Oxygen free radical scavenger enzyme polymorphisms in systemic sclerosis. *Free Radic Biol Med*, 36(11):1403-7, 2004.
- [221] Yannick Allanore, Didier Borderie, Hervé Lemaréchal, Ohvanesse Garabed Ekindjian and André Kahan. Acute and sustained effects of dihydropyridine-type calcium channel antagonists on oxidative stress in systemic sclerosis. *Am J Med*, 116(9):595-600, 2004.
- [222] R Solans, C Motta, R Solá, A E La Ville and J Lima et al.. Abnormalities of erythrocyte membrane fluidity, lipid composition, and lipid peroxidation in systemic sclerosis: evidence of free radical-mediated injury. *Arthritis Rheum*, 43(4):894-900, 2000.
- [223] A Rosen, L Casciola-Rosen and F Wigley. Role of metal-catalyzed oxidation reactions in the early pathogenesis of scleroderma. *Curr Opin Rheumatol*, 9(6):538-43, 1997.
- [224] S A Cotton, A L Herrick, M I Jayson and A J Freemont. Endothelial expression of nitric oxide synthases and nitrotyrosine in systemic sclerosis skin. *J Pathol*, 189(2):273-8, 1999.
- [225] A Servettaz, P Guilpain, C Goulvestre, C Chéreau and C Hercend et al.. Radical oxygen species production induced by advanced oxidation protein products predicts clinical evolution and response to treatment in systemic sclerosis. *Ann Rheum Dis*, 66(9):1202-9, 2007.

- [226] Clara Dees, Pawel Zerr, Michal Tomcik, Christian Beyer and Angelika Horn et al.. Inhibition of notch signaling prevents experimental fibrosis and induces regression of established fibrosis. *Arthritis Rheum*, 63(5):1396-404, 2011b.
- [227] Clara Dees, Michal Tomcik, Pawel Zerr, Alfiya Akhmetshina and Angelika Horn et al.. Notch signalling regulates fibroblast activation and collagen release in systemic sclerosis. *Ann Rheum Dis*, 70(7):1304-10, 2011a.
- [228] Epifania Balistreri, Estrella Garcia-Gonzalez, Enrico Selvi, Alfiya Akhmetshina and Katrin Palumbo et al.. The cannabinoid win55, 212-2 abrogates dermal fibrosis in scleroderma bleomycin model. *Ann Rheum Dis*, 70(4):695-9, 2011.
- [229] V Witko-Sarsat, M Friedlander, C Capeillère-Blandin, T Nguyen-Khoa and A T Nguyen et al.. Advanced oxidation protein products as a novel marker of oxidative stress in uremia. *Kidney Int*, 49(5):1304-13, 1996.
- [230] Véronique Witko-Sarsat, Valérie Gausson, Anh-Thu Nguyen, Malik Touam and Tilman Drüeke et al.. Aopp-induced activation of human neutrophil and monocyte oxidative metabolism: a potential target for n-acetylcysteine treatment in dialysis patients. *Kidney Int*, 64(1):82-91, 2003.
- [231] V Witko-Sarsat, M Friedlander, T Nguyen Khoa, C Capeillère-Blandin and A T Nguyen et al.. Advanced oxidation protein products as novel mediators of inflammation and monocyte activation in chronic renal failure. *J Immunol*, 161(5):2524-32, 1998.
- [232] Hong Yan Li, Fan Fan Hou, Xun Zhang, Ping Yan Chen and Shang Xi Liu et al.. Advanced oxidation protein products accelerate renal fibrosis in a remnant kidney model. *J Am Soc Nephrol*, 18(2):528-38, 2007.
- [233] Paul Q Hu, Arthur A Hurwitz and Joost J Oppenheim. Immunization with dna topoisomerase i induces autoimmune responses but not scleroderma-like pathologies in mice. *J Rheumatol*, 34(11):2243-52, 2007.
- [234] T Muryoi, K N Kasturi, M J Kafina, D S Cram and L C Harrison et al.. Antitopoisomerase i monoclonal autoantibodies from scleroderma patients and tight skin mouse interact with similar epitopes. *J Exp Med*, 175(4):1103-9, 1992.
- [235] L Casciola-Rosen, F Andrade, D Ulanet, W B Wong and A Rosen. Cleavage by granzyme b is strongly predictive of autoantigen status: implications for initiation of autoimmunity. *J Exp Med*, 190(6):815-26, 1999.
- [236] Biji T Kurien, Kenneth Hensley, Michael Bachmann and R Hal Scofield. Oxidatively modified autoantigens in autoimmune diseases. *Free Radic Biol Med*, 41(4):549-56, 2006.
- [237] O Vaarala, G Alfthan, M Jauhainen, M Leirisalo-Repo and K Aho et al.. Crossreaction between antibodies to oxidised low-density lipoprotein and to cardiolipin in systemic lupus erythematosus. *Lancet*, 341(8850):923-5, 1993.

- [238] R Hal Scofield, Biji T Kurien, Samantha Ganick, Micah T McClain and Quentin Pye et al.. Modification of lupus-associated 60-kda ro protein with the lipid oxidation product 4-hydroxy-2-nonenal increases antigenicity and facilitates epitope spreading. *Free Radic Biol Med*, 38(6):719-28, 2005.
- [239] Jeremiah Morrissey, Guangjie Guo, Kazuaki Moridaira, Melanie Fitzgerald and Ruth McCracken et al.. Transforming growth factor-beta induces renal epithelial jagged-1 expression in fibrotic disease. *J Am Soc Nephrol*, 13(6):1499-508, 2002.
- [240] S Artavanis-Tsakonas, M D Rand and R J Lake. Notch signaling: cell fate control and signal integration in development. *Science*, 284(5415):770-6, 1999.
- [241] Sanne Weijzen, Paola Rizzo, Mike Braid, Radhika Vaishnav and Suzanne M Jonkheer et al.. Activation of notch-1 signaling maintains the neoplastic phenotype in human ras-transformed cells. *Nat Med*, 8(9):979-86, 2002.
- [242] Srinivasulu Chigurupati, Thiruma V Arumugam, Tae Gen Son, Justin D Lathia and Shafaq Jameel et al.. Involvement of notch signaling in wound healing. *PLoS One*, 2(11):e1167, 2007.
- [243] Luca Fabris, Massimiliano Cadamuro, Maria Guido, Carlo Spirli and Romina Fiorotto et al.. Analysis of liver repair mechanisms in alagille syndrome and biliary atresia reveals a role for notch signaling. *Am J Pathol*, 171(2):641-53, 2007.
- [244] Tanapat Palaga, Chayanit Buranaruk, Sirirat Rengpipat, Abdul H Fauq and Todd E Golde et al.. Notch signaling is activated by tlr stimulation and regulates macrophage functions. *Eur J Immunol*, 38(1):174-83, 2008.
- [245] J C Pui, D Allman, L Xu, S DeRocco and F G Karnell et al.. Notch1 expression in early lymphopoiesis influences b versus t lineage determination. *Immunity*, 11(3):299-308, 1999.
- [246] Toshiki Saito, Shigeru Chiba, Motoshi Ichikawa, Atsushi Kunisato and Takashi Asai et al.. Notch2 is preferentially expressed in mature b cells and indispensable for marginal zone b lineage development. *Immunity*, 18(5):675-85, 2003.
- [247] C M Grimaldi, D J Michael and B Diamond. Cutting edge: expansion and activation of a population of autoreactive marginal zone b cells in a model of estrogen-induced lupus. *J Immunol*, 167(4):1886-90, 2001.
- [248] Z Zhang, P Oliver, J R Lancaster Jr, P O Schwarzenberger and M S Joshi et al.. Reactive oxygen species mediate tumor necrosis factor alpha-converting, enzyme-dependent ectodomain shedding induced by phorbol myristate acetate. *FASEB J*, 15(2):303-5, 2001.
- [249] Barbara Bedogni, James A Warneke, Brian J Nickoloff, Amato J Giaccia and Marianne Broome Powell. Notch1 is an effector of akt and hypoxia in melanoma development. *J Clin Invest*, 118(11):3660-70, 2008.

- [250] Fatima Teixeira-Clerc, Boris Julien, Pascale Grenard, Jeanne Tran Van Nhieu and Vanessa Deveaux et al.. Cb1 cannabinoid receptor antagonism: a new strategy for the treatment of liver fibrosis. *Nat Med*, 12(6):671-6, 2006.
- [251] T W Klein, C Newton and H Friedman. Cannabinoid receptors and the cytokine network. *Adv Exp Med Biol*, 437:215-22, 1998.
- [252] T W Klein, C Newton and H Friedman. Cannabinoids and immunity to legionella pneumophila infection. *Adv Exp Med Biol*, 402:103-9, 1996.
- [253] Angel Arévalo-Martín, José Miguel Vela, Eduardo Molina-Holgado, José Borrell and Carmen Guaza. Therapeutic action of cannabinoids in a murine model of multiple sclerosis. *J Neurosci*, 23(7):2511-6, 2003.
- [254] Sándor Bátkai, Douglas Osei-Hyiaman, Hao Pan, Osama El-Assal and Mohanraj Rajesh et al.. Cannabinoid-2 receptor mediates protection against hepatic ischemia/reperfusion injury. *FASEB J*, 21(8):1788-800, 2007.
- [255] Mohanraj Rajesh, Partha Mukhopadhyay, Sándor Bátkai, György Haskó and Lucas Liaudet et al.. Cb2-receptor stimulation attenuates tnf-alpha-induced human endothelial cell activation, transendothelial migration of monocytes, and monocyte-endothelial adhesion. *Am J Physiol Heart Circ Physiol*, 293(4):H2210-8, 2007.
- [256] Lorinda Chung, David F Fiorentino, Maya J Benbarak, Adam S Adler and Melissa M Mariano et al.. Molecular framework for response to imatinib mesylate in systemic sclerosis. *Arthritis Rheum*, 60(2):584-91, 2009.
- [257] A Yamakage, K Kikuchi, E A Smith, E C LeRoy and M Trojanowska. Selective upregulation of platelet-derived growth factor alpha receptors by transforming growth factor beta in scleroderma fibroblasts. *J Exp Med*, 175(5):1227-34, 1992.
- [258] Yan Wang, Juncha Gao, Di Zhang, Jian Zhang and Junji Ma et al.. New insights into the antifibrotic effects of sorafenib on hepatic stellate cells and liver fibrosis. *J Hepatol*, 53(1):132-44, 2010.
- [259] Sabine Mumprecht, Matthias Matter, Viktor Pavelic and Adrian F Ochsenbein. Imatinib mesylate selectively impairs expansion of memory cytotoxic t cells without affecting the control of primary viral infections. *Blood*, 108(10):3406-13, 2006.
- [260] You-Sun Kim, Sung-Wook Hong, Jun-Pyo Choi, Tae-Seop Shin and Hyung-Geun Moon et al.. Vascular endothelial growth factor is a key mediator in the development of t cell priming and its polarization to type 1 and type 17 t helper cells in the airways. *J Immunol*, 183(8):5113-20, 2009.
- [261] B Barleon, S Sozzani, D Zhou, H A Weich and A Mantovani et al.. Migration of human monocytes in response to vascular endothelial growth factor (vegf) is mediated via the vegf receptor flt-1. *Blood*, 87(8):3336-43, 1996.

- [262] Masato Murakami, Shinobu Iwai, Sachie Hiratsuka, Mai Yamauchi and Kazuhide Nakamura et al.. Signaling of vascular endothelial growth factor receptor-1 tyrosine kinase promotes rheumatoid arthritis through activation of monocytes/macrophages. *Blood*, 108(6):1849-56, 2006.
- [263] M Jinnin, T Makino, I Kajihara, N Honda and K Makino et al.. Serum levels of soluble vascular endothelial growth factor receptor-2 in patients with systemic sclerosis. *Br J Dermatol*, 162(4):751-8, 2010.
- [264] K Davison, S Côté, S Mader and W H Miller. Glutathione depletion overcomes resistance to arsenic trioxide in arsenic-resistant cell lines. *Leukemia*, 17(5):931-40, 2003.
- [265] N Scott, K M Hatlelid, N E MacKenzie and D E Carter. Reactions of arsenic(iii) and arsenic(v) species with glutathione. *Chem Res Toxicol*, 6(1):102-6, 1993.
- [266] Yoshihide Asano, Hironobu Ihn, Kenichi Yamane, Masahide Kubo and Kunihiko Tamaki. Impaired smad7-smurf-mediated negative regulation of tgf-beta signaling in scleroderma fibroblasts. *J Clin Invest*, 113(2):253-64, 2004.
- [267] B W Needleman, F M Wigley and R W Stair. Interleukin-1, interleukin-2, interleukin-4, interleukin-6, tumor necrosis factor alpha, and interferon-gamma levels in sera from patients with scleroderma. *Arthritis Rheum*, 35(1):67-72, 1992.
- [268] Hartmut Döhner, Elihu H Estey, Sergio Amadori, Frederick R Appelbaum and Thomas Büchner et al.. Diagnosis and management of acute myeloid leukemia in adults: recommendations from an international expert panel, on behalf of the european leukemianet. *Blood*, 115(3):453-74, 2010.
- [269] Wilson H Miller Jr, Hyman M Schipper, Janet S Lee, Jack Singer and Samuel Waxman. Mechanisms of action of arsenic trioxide. *Cancer Res*, 62(14):3893-903, 2002.
- [270] Pierre Bobé, Danielle Bonardelle, Karim Benihoud, Paule Opolon and Mounira K Chelbi-Alix. Arsenic trioxide: A promising novel therapeutic agent for lymphoproliferative and autoimmune syndromes in mrl/lpr mice. *Blood*, 108(13):3967-75, 2006.
- [271] R Korngold and J Sprent. Lethal graft-versus-host disease after bone marrow transplantation across minor histocompatibility barriers in mice. prevention by removing mature t cells from marrow. *J Exp Med*, 148(6):1687-98, 1978.
- [272] Yu-Waye Chu and Ronald E Gress. Murine models of chronic graft-versus-host disease: insights and unresolved issues. *Biol Blood Marrow Transplant*, 14(4):365-78, 2008.
- [273] Warren D Shlomchik. Graft-versus-host disease. *Nat Rev Immunol*, 7(5):340-52, 2007.
- [274] Lucy W Kappel, Gabrielle L Goldberg, Christopher G King, David Y Suh and Odette M Smith et al.. Il-17 contributes to cd4-mediated graft-versus-host disease. *Blood*, 113(4):945-52, 2009.

- [275] Emin Kansu. The pathophysiology of chronic graft-versus-host disease. *Int J Hematol*, 79(3):209-15, 2004.
- [276] Geoffrey R Hill, Stuart D Olver, Rachel D Kuns, Antiopi Varelias and Neil C Raffelt et al.. Stem cell mobilization with g-csf induces type 17 differentiation and promotes scleroderma. *Blood*, 116(5):819-28, 2010.
- [277] Hisakazu Nishimori, Yoshinobu Maeda, Takanori Teshima, Haruko Sugiyama and Koichiro Kobayashi et al.. Synthetic retinoid am80 ameliorates chronic graft-versus-host disease by down-regulating th1 and th17. *Blood*, 119(1):285-95, 2012.
- [278] Lixin Zhou, David Askew, Caiyun Wu and Anita C Gilliam. Cutaneous gene expression by dna microarray in murine sclerodermatous graft-versus-host disease, a model for human scleroderma. *J Invest Dermatol*, 127(2):281-92, 2007.
- [279] Britt E Anderson, Jennifer M McNiff, Dhanpat Jain, Bruce R Blazar and Warren D Shlomchik et al.. Distinct roles for donor- and host-derived antigen-presenting cells and costimulatory molecules in murine chronic graft-versus-host disease: requirements depend on target organ. *Blood*, 105(5):2227-34, 2005.
- [280] Motoko Koyama, Daigo Hashimoto, Kazutoshi Aoyama, Ken-ichi Matsuoka and Kennosuke Karube et al.. Plasmacytoid dendritic cells prime alloreactive t cells to mediate graft-versus-host disease as antigen-presenting cells. *Blood*, 113(9):2088-95, 2009.
- [281] Kelli P A MacDonald, Vanessa Rowe, Cheryl Philippich, Ranjeny Thomas and Andrew D Clouston et al.. Donor pretreatment with progenipoitin-1 is superior to granulocyte colony-stimulating factor in preventing graft-versus-host disease after allogeneic stem cell transplantation. *Blood*, 101(5):2033-42, 2003.
- [282] Tatjana Banovic, Kate A Markey, Rachel D Kuns, Stuart D Olver and Neil C Raffelt et al.. Graft-versus-host disease prevents the maturation of plasmacytoid dendritic cells. *J Immunol*, 182(2):912-20, 2009.
- [283] C C Mok and C S Lau. Pathogenesis of systemic lupus erythematosus. *J Clin Pathol*, 56(7):481-90, 2003.
- [284] F Batteux, P Palmer, M Daëron, B Weill and P Lebon. Fcgammarii (cd32)-dependent induction of interferon-alpha by serum from patients with lupus erythematosus. *Eur Cytokine Netw*, 10(4):509-14, 1999.

Résumé

Nous soutenons la thèse que le stress oxydant joue un rôle majeur dans le déclenchement et le développement de la sclérodermie systémique (ScS). Afin de démontrer cette thèse, nous avons mis au point un modèle murin où la maladie est déclenchée par divers types de stress oxydant, puis nous avons exploré les différentes voies d'activation des fibroblastes sous l'effet des formes réactives de l'oxygène, afin de déterminer d'éventuelles cibles thérapeutiques. Pour apprécier les effets d'un stress oxydant chronique, des solutions contenant différents oxydants ont été injectées dans la peau de souris BALB/c et BALB/c SCID. Les solutions contenant le radical hydroxyl OH[•] ou HOCl ont induit une maladie caractérisée, comme la ScS diffuse, par une fibrose cutanée et viscérale, et des auto-anticorps anti-ADN topoisomérase-1. Les sérum de ces souris contenaient de grandes quantités de dérivés oxydés des protéines et induisaient la prolifération des fibroblastes et la production de formes réactives de l'oxygène par les cellules endothéliales. Une fibrose pulmonaire de moindre importance était induite chez les souris BALB/c SCID. Grâce à ce nouveau modèle murin de ScS, nous avons démontré que le stress oxydant était directement responsable des anomalies observées dans les fibroblastes, les cellules endothéliales et le système immunitaire.

Nous avons ensuite utilisé ce modèle pour analyser les voies d'activation fibroblastique dans la ScS. Dans les fibroblastes des souris exposées à HOCl, on observe une dérégulation des voies des récepteurs Notch, des récepteurs aux cannabinoïdes, et des récepteurs au PDGF. On observe les mêmes dérégulations ex vivo dans les fibroblastes de patients atteints de ScS diffuse.

L'implication de ces différentes voies dans les processus fibrosants nous ont conduits à tester de nouvelles approches thérapeutiques dans la ScS grâce à la modulation des trois voies cellulaires étudiées par des agents pharmacologiques. Nous avons ainsi observé une amélioration clinique significative chez les souris sclérodermiques traitées avec un inhibiteur de l'activation de Notch, avec un agoniste des récepteurs aux cannabinoïdes, et avec des inhibiteurs de tyrosine-kinase ciblant le récepteur au PDGF.

Puisque les fibroblastes sclérodermiques ont un phénotype activé et produisent de forts taux de formes réactives de l'oxygène, nous avons enfin mis à profit cette particularité pour induire l'apoptose sélective de ces cellules dans le derme des souris. Le trioxyde d'arsenic, molécule cytotoxique utilisée en thérapie humaine, augmente la production cellulaire de formes réactives de l'oxygène au-delà d'un seuil létal et induit ainsi l'apoptose des fibroblastes sclérodermiques. L'utilisation in vivo de cette molécule dans notre modèle murin prévient la fibrose cutanée et viscérale, et les anomalies endothéliales. Le trioxyde d'arsenic a un effet comparable dans le modèle murin de ScS associée à la réaction du greffon contre l'hôte en détruisant les lymphocytes T CD4+ alloréactifs activés et les cellules dendritiques plasmacytoides responsables de l'activation du système immunitaire.

Les formes réactives de l'oxygène sont donc impliquées dans l'induction des lésions observées au cours de la ScS. Dans notre modèle, le rôle du système immunitaire intervient dans l'auto-entretien et l'extension systémique de la maladie. Le stress oxydant contribue à la dérégulation de diverses voies de signalisation dont les voies des récepteurs Notch, des récepteurs aux cannabinoïdes et du PDGF dans les fibroblastes. La modulation de ces voies permet d'obtenir une amélioration clinique chez les souris sclérodermiques, tout comme l'utilisation du trioxyde d'arsenic qui entraîne la délétion spécifique des fibroblastes sclérodermiques surpoudrant des formes réactives de l'oxygène. Le trioxyde d'arsenic montre également une efficacité intéressante dans le modèle de sclérodermie associée à la maladie du greffon contre l'hôte via la délétion des lymphocytes T CD4+ alloréactifs.

Mots clés : sclérodermie systémique, formes réactives de l'oxygène, fibroblastes, modèle murin, ADN topoisomérase-1, Notch, récepteurs aux cannabinoïdes, récepteurs au PDGF, arsenic trioxyde, sclérodermie associée à la réaction du greffon contre l'hôte.